UAB
Universitat Autònoma de Barcelona

Advanced Characterization of Alpha-galactosidase Nanoliposomal Formulations for Fabry Disease Treatment

Aida Carreño Fibla

ADVERTIMENT. L'accés als continguts d'aquesta tesi doctoral i la seva utilització ha de respectar els drets de la persona autora. Pot ser utilitzada per a consulta o estudi personal, així com en activitats o materials d'investigació i docència en els termes establerts a l'art. 32 del Text Refós de la Llei de Propietat Intel·lectual (RDL 1/1996). Per altres utilitzacions es requereix l'autorització prèvia i expressa de la persona autora. En qualsevol cas, en la utilització dels seus continguts caldrà indicar de forma clara el nom i cognoms de la persona autora i el títol de la tesi doctoral. No s'autoritza la seva reproducció o altres formes d'explotació efectuades amb finalitats de lucre ni la seva comunicació pública des d'un lloc aliè al servei TDX. Tampoc s'autoritza la presentació del seu contingut en una finestra o marc aliè a TDX (framing). Aquesta reserva de drets afecta tant als continguts de la tesi com als seus resums i índexs.

ADVERTENCIA. El acceso a los contenidos de esta tesis doctoral y su utilización debe respetar los derechos de la persona autora. Puede ser utilizada para consulta o estudio personal, así como en actividades o materiales de investigación y docencia en los términos establecidos en el art. 32 del Texto Refundido de la Ley de Propiedad Intelectual (RDL 1/1996). Para otros usos se requiere la autorización previa y expresa de la persona autora. En cualquier caso, en la utilización de sus contenidos se deberá indicar de forma clara el nombre y apellidos de la persona autora y el título de la tesis doctoral. No se autoriza su reproducción u otras formas de explotación efectuadas con fines lucrativos ni su comunicación pública desde un sitio ajeno al servicio TDR. Tampoco se autoriza la presentación de su contenido en una ventana o marco ajeno a TDR (framing). Esta reserva de derechos afecta tanto al contenido de la tesis como a sus resúmenes e índices.

WARNING. The access to the contents of this doctoral thesis and its use must respect the rights of the author. It can be used for reference or private study, as well as research and learning activities or materials in the terms established by the 32nd article of the Spanish Consolidated Copyright Act (RDL 1/1996). Express and previous authorization of the author is required for any other uses. In any case, when using its content, full name of the author and title of the thesis must be clearly indicated. Reproduction or other forms of for profit use or public communication from outside TDX service is not allowed. Presentation of its content in a window or frame external to TDX (framing) is not authorized either. These rights affect both the content of the thesis and its abstracts and indexes.

Advanced Characterization of Alpha-galactosidase Nanoliposomal Formulations for Fabry Disease Treatment

Aida Carreño Fibla

Tesi Doctoral

Programa de Doctorat en Ciència dels Materials

Directors

Dr. José Luis Corchero Nieto

Dr. Elisabet González Mira

Dr. Nora Ventosa Rull

Tutora

Dr. Nora Ventosa Rull

Departament de Física, Química i Geologia

Facultat de Ciències

2024

UNIVERSITAT AUTÒNOMA DE BARCELONA

FACULTAT DE CIÈNCIES

PROGRAMA DE DOCTORAT EN CIÈNCIA DELS MATERIALS

Advanced Characterization of Alpha-galactosidase Nanoliposomal Formulations for Fabry Disease Treatment

Memòria presentada per Aida Carreño Fibla per optar al grau de Doctor en Ciència dels Materials per la Universitat Autònoma de Barcelona

Aida Carreño Fibla

Vist i plau:

Dr. José Luis Corchero Nieto	**Dr. Elisabet González Mira**	**Dr. Nora Ventosa Rull**

Bellaterra, gener de 2024

JOSÉ LUIS CORCHERO NIETO, Scientific Researcher at the Biotechnology and Biomedicine Institute of the Autonomous University of Barcelona (IBB-UAB), **ELISABET GONZÁLEZ MIRA**, Researcher of the Spanish National Research Council at the Institute of Materials Science of Barcelona (ICMAB-CSIC), and **NORA VENTOSA RULL**, Scientific Researcher of the Spanish National Research Council at the Institute of Materials Science of Barcelona (ICMAB-CSIC),

CERTIFY:

That **Aida Carreño Fibla**, Master's Degree in Advanced Biotechnology and Bachelor's Degree in Biotechnology, has performed, under their management, the research work entitled "**Advanced Characterization of Alpha-galactosidase Nanoliposomal Formulations for Fabry Disease Treatment**". This work has been performed under the frame of the Materials Science PhD program of the Physics and Chemistry Department of the Autonomous University of Barcelona.

And in witness whereof this is signed by:

Directors

Dr. José Luis Corchero Nieto **Dr. Elisabet González Mira** **Dr. Nora Ventosa Rull**

Barcelona, January 2024

“What we know is a drop, what we don’t know is an ocean” – Isaac Newton

“Si una persona es perseverante, aunque sea dura de entendimiento, se hará inteligente; y aunque sea débil se transformará en fuerte” – Leonardo Da Vinci

“Sic Parvis Magna” – Sir Francis Drake

A *Polaris* amb la que sempre he trobat el nord, a tots vosaltres,

A *Polaris* con la que siempre he encontrado el norte, a todos vosotros,

To *Polaris* by which I have always found the north, to all of you,

PREAMBLE

Great part of the present Ph.D. thesis was conducted under the framework of collaborative projects. Hence, besides the results obtained by the author, it has been decided to include some experiments performed in a collaborative manner together with scientists from other institutions, which complete and reinforce the work presented in this thesis.

ACKNOWLEDGEMENTS

Amb això es tanca una important etapa, que al cap i la fi forma part d'una aventura molt més gran. Arribat a aquest punt, m'agradaria destacar que en sou vosaltres els protagonistes que heu estat capaços de fer-la possible, tota aquella gent que he tingut la sort de conèixer durant aquest viatge i m'ha fet créixer tant com a científica, com a persona. No mentiré dient que d'aquesta manera el camí ha sigut menys costós. Han hagut mil entrebancs i molts cops he trobat motius per rendir-me i canviar a un altre recorregut més fàcil. En aquests moments, allà hi ha hagut sempre algú de vosaltres, recordant-me el que m'atrau d'aquest món i proporcionant-me les forces per continuar. És per aquest motiu que us vull expressar el meu agraïment a cadascú de vosaltres.

Nora i **Pepe**, els meus directors de tesi des de l'inici d'aquesta etapa. M'agradaria agrair-vos la oportunitat que m'heu donat de formar part de dos famílies científiques molt competents, la del grup Nanomol i la del grup de Nanobiotecnologia (NBT). Nora gràcies per la confiança depositada en mi deixant-me participar en tasques de gran responsabilitat d'ambiciosos projectes com el *Phoenix*, així com la opció a formar part de col·laboracions multidisciplinàries amb grups d'altres institucions. Valoro la teva constància, professionalitat i els teus consells que m'ha guiat i desenvolupat professionalment al llarg d'aquest camí. Pepe, el meu recorregut científic va començar amb tu com a supervisor molt abans de l'inici d'aquesta tesi doctoral. Em quedo amb tot el que he après de tu, com també amb el teu suport, ajuda, consell i bon humor que han fet més fàcil i divertit el dia a dia. Aquesta part no queda completa sense la **Eli**, que tot i ser la última directora en incorporar-se oficialment al seguiment del meu treball, sempre ha estat allà per donar-me suport i empentes quan ha estat necessari. També, corregint-me sempre per millorar la qualitat del meu treball. Gràcies Eli, per les converses que han alleugerit els moments més difícils.

També m'agradaria agrair a la resta d'investigadors principals d'ambdós grups que han estat allà en algun moment. Al **Jaume Veciana** i la **Concepció Rovira** per formar un grup tan ben avingut com el de Nanomol. A la **Imma Ratera** per escoltar els meus interessos sobre la nanociència i proposar-me contactar amb Nora per valorar l'oportunitat de formar part del seu equip. Al **Toni**, per haver reunit el conjunt de persones meravelloses que formen el grup de NBT, i cuidar de cadascun del seus integrants. A la **Esther** i la **Neus**, dues grans professionals que sempre s'han preocupat per mi, m'han dedicat un bon consell quan ha estat necessari, i m'han fet sentir valorat el meu treball.

Voldria expressar la meva gratitud pel finançament rebut per part de la beca FPI-MEC del Ministerio de Ciencia, Innovación y Universidades, y de la Agencia Estatal de Investigación y del Fondo Social Europeo, amb la qual se m'ha permès realitzar aquesta tesi doctoral.

Seguidament voldria dedicar unes paraules a aquelles persones que han col·laborat amb aquesta recerca i l'han enriquit. Enviar un agraïment especial al grup de la **Dr. Miriam Royo** per la bona feina de síntesi i subministrament del chol-PEG_{400}-RGD que ha permès la producció de la majoria de mostres utilitzades en aquesta tesi. De la mateixa manera, agrair a l'equip de **Leanbio SL** per la producció i subministrament de la proteïna GLA-S que ha jugat un gran paper en aquesta recerca. Thank you for the work and scientific discussions with all the partners from the European Phoenix project. I would like to specially thank to **Dr. Ivana Vinković** from Institute for Medical Research and Occupational Health (IMI) to accept my stay abroad in her group and share with me interesting scientific discussions and knowledge about Croatian culture. Also to **Nikolina Kalčec**, who has been an incredible office mate, and my essential teacher, guide and support with the FFF-MALS technique during my stay in Zagreb. And of course to **Nikolina Peranić**, my other appreciated office mate that complete my long hours of work "between Nikolinas". Thank you for all the conversations that we had together, and to cheer up the laboratory by singing with your incredible voice! Besides, I would highlight my gratitude to the great collaboration with SPARTA Biodiscovery, in special the easy and beneficial contact with **Jelle Penders**, which has allowed the accurate measurements of liposomal formulations through Single Particle Automated Raman Trapping Analysis (SPARTA®). I would also acknowledge the constant collaboration with the team of **Prof. Dganit Danino** from Technion which have allowed the acquirement of highly detailed cryoTEM images, as well as, the initiation of accurate Isothermal Titration Calorimetry (ITC) analysis with liposomes and GLA.

A més, cal destacar el suport que he rebut dels grans professionals que formen part dels serveis cientificotècnics de la UAB, en especial a l'**Òscar** i la **Mònica** del Servei d'Anàlisi Química (SAQ), que m'han ensenyat bona part del coneixement bàsic per treballar amb tècniques analítiques basades en HPLC, però sobretot pels moments alegres i les rialles que em tingut en les instal·lacions del SAQ. També destacar al servei Laboratori de Luminescència i Espectroscòpia de Biomolècules (LLEB) de la UAB, en concret al **Salvador Bartolomé**, a les seves instruccions detallades per obtenir bones mesures de qualitat amb el fluorímetre, les divertides xerrades compartides en les llargues sessions viscudes, i el moment de pànic al descobrir un niu de vespa asiàtica just al costat de les instal·lacions, fent de tot plegat un agradable i habitual tercer laboratori de treball per a mi. També agrair a en **Martí de Cabo** del Servei de Microscopia de la UAB per les excel·lents imatges que hem obtingut durant les sessions de cryoTEM, i del riure per fer símils absurds amb les vesícules més curioses observades. D'altra banda, voldria mostrar el meu agraïment a la **Dr. Irene Fernández** de la Unitat d'Espectrometria de Masses de Caracterització Molecular ubicada als Centres Científics i Tecnològics de la Universitat de Barcelona (CCiTUB), per

realitzar els anàlisis corresponents de MALDI-TOF dels diferents enzims de GLA utilitzades en aquest treball. Com oblidar a la **Olga** i el **Fran** del Servei de Cultius Cel·lulars, Producció d'Anticossos i Citometria (SCAC) de la UAB. Olga moltíssimes gràcies per la teva ajuda i paciència amb les èpoques d'elevada tassa de contaminació cel·lular. Molts cops ens em desesperat juntes després de netejar tants cops l'incubador. Eres una gran professional de la que he après tot el necessari per poder treballar delicadament en un laboratori de nivell 2 de bioseguretat. Fran, vaig tenir la sort de rebre les primeres ensenyances per treballar amb cultius cel·lulars de la teva mà. La teva personalitat tant alegre i maca em fa ganes sempre de tornar a cultius a petar la xerrada amb tu i contar-nos anècdotes diverses, amb les quals m'has animat i apujat l'autoestima mil cops. Sense dubte has estat una de les millors persones amb les que he coincidit en aquesta part del meu viatge, no canviïs mai!

M'agradaria mostrar el meu agraïment a la Protein Production Platform (PPP) corresponent a la unitat U1 de NANBIOSIS situada a l'Institut de Biotecnologia i Biomedicina de la UAB (IBB-UAB) on he pogut purificar totes les versions de GLA que contenen cues d'histidines en aquest treball. De la mateixa manera, agrair al Soft Materials Service vinculat a la unitat U6 Biomaterial Processing and Nanostructuring, que es troba situat al centre de recerca Institut de Ciència de Materials de Barcelona (ICMAB-CSIC), on se m'ha permès sintetitzar i purificat totes les formulacions liposomals.

Com no, fer una especial menció als companys de Nanomol Technologies, on m'he pogut recolzar sobre cadascun de vosaltres quan ho he necessitat. **Santi** i **Alba** moltes gràcies per deixar-me col·laborar amb el vostre equip format per persones de qualitat científica i personal. Agrair a la **Lídia Ferrer** per tota la guia que m'ha proporcionat relacionada amb la posada a punt del mètode d'HPLC-ELSD. **Arnau** i **Josep**, simplement no sé com expressar en paraules el que ha significat el vostre gran suport. Heu estat dos dels pilars més importants que han fet possible aquest treball. Arnau, mil gràcies per la paciència i temps dedicat a escoltar tots els problemes que m'he anat trobant amb el treball relacionat amb l'HPLC. Sempre disposat a ajudar, i com aquell qui sempre sembla tenir la resposta adequada preparada, t'has convertit en el meu company d'equip analític de confiança. Josep, una persona de paraules sinceres sempre disposada a donar un cop de mà amb tot el que pot. Quantes mostres d'aquest treball i de quins volums has degut processar tu? Només el nostre equip ho sap! Moltes gràcies per facilitar-me el material que s'ha requerit per avançar amb el projecte *Phoenix*, així com per compartir amb mi l'estrès i alegries que han anat sorgint en el procés. Un plaer el col·laborar amb vosaltres, si ho pogués seguir fent en un futur, no ho dubtaria.

Voldria continuar amb aquelles persones que formen part de la família Nanomol o hi han estat integrades d'alguna manera. Ha estat tanta gent que probablement em deixi algú per esmentar, però si heu estat allà, us asseguro que heu contribuït en el meu creixement com a persona. Gràcies **Carme G, Amable, Soraya, Jorge, Mariana, Ramon, Teresa, Dolores, Judit T, Nerea, Marc, Sara R, Sara G, Sara B, Guillem, Miquel, Xavi, Edu,**

Lamia, David, Rubén, Adri, Laia, Júlia, Lídia B, Karla M, Carla, Marta, Albert G, Fabião, Judit M, Songbai, Ángel, Paula, Maria, Jamila, Carme M, Sol, Angélica, Giovanni, Ehsan, Betta, Francesca, Tina, Jose i **Lluís**. A tots vosaltres m'heu donat suport, ajuda i escalf, m'heu ensenyat i fet divertir durant aquesta etapa, espero poder seguir coincidint i passant estones plegats. Carme Gimeno, que n'hagués estat de mi sense tu al grup? Sempre amb un somriure, tot i els mils problemes que t'ocasionàvem diàriament, gestionant de la manera més òptima tota la burocràcia. Sempre donant els bons dies amb alegria, fent petar la xerrada sobre els assumptes més interessants, i amb útils consells ben preparats per als dilemes que et proposàvem. El grup ha tingut una gran pèrdua amb la teva marxa. Et trobaré molt a faltar! Soraya, una incorporación "reciente" al grupo, pero tan eficiente que para mí es como si llevaras toda la vida trabajando con nosotros. Te has convertido en una compañera con la que gestionar las cuestiones de laboratorio de la mano. Humilde, constante y de ideas claras, sin duda la mejor compañera que hubiera podido elegir. Jorge, gracias por ser una persona tan eficiente y agradable, por estar ahí compartiendo siempre una buena charla conmigo, ya sea en MATGAS, en la oficina o durante la comida, alegrando esos días de duro trabajo. David, merci per tota l'ajuda professional que m'has proporcionat, ja fos en el DELOS-susp o dia filtració, però sobretot destacar l'alegria i tranquil·litat que transmets i et fan sentir com a casa. Marc, el meu company oficial de cafès al que sempre li acabava robant alguna galeta de xocolata, i se'ns anaven les estones divagant en conversacions varies. Edu, després de 4 anys amb la guàrdia sempre en alt, un dia vas aconseguir agafar-me per sorpresa i em vas espantar al laboratori, i just va ser un dia que no en tenies intenció! Gràcies per alegrar-me el dia a dia constantment. Des de que vas marxar el BioLab no és el mateix! Judit T, merci per totes les mostres que has preparat, per reunir-te amb mi i guiar-me amb dubtes relacionats amb la nanoGLA. Definitivament tu i el Josep sou els seus papis i la coneixeu millor que ningú! Nerea, me quedo con nuestras charlas y la gran ayuda que has sido siempre para mi. Mariana, gracias por mostrar siempre interès, preguntar como estoy y estar siempre dispuesta a ayudar. Un gusto haber coincidido contigo! Guillem, una meravellosa persona amb la que sempre he pogut confiar i m'ha animat quan més ho he necessitat. Ramon, el maestro que me dejó el "legado maldito". Una llàstima no haver coincidit més temps amb tu, els dies que em vas fer de profe van ser dels més divertits que he tingut a l'ICMAB! Francesca and Tina, to be the best lab mates with whom I have shared more than one thousand smiles! Sara Garrido, mi compañera de locura en cuánto a pasar largos días de trabajo en MATGAS. Sin ti, el ambiente en el laboratorio habría sido desolador, ¡más sin una ventana por la que ver cómo transcurre el día! Lídia Ballel, com enyoro el teu sentit de l'humor que sempre m'alegrava el dia i tots els dolços que ens portaves per omplir-nos la panxa. Karla Mayolo, por confiar más en mi de lo que yo misma hago, pedirme consejo o dármelo tú, y considerarme una compañera y aliada en tu día a día. ¡Espero que vaya todo genial por México! Sol y Angélica, mis niñas recién conocidas. Gracias por las risas compartidas (así como la comida "exquisita" de máquina expendedora). Espero que os siga yendo estupendo en el viaje que os queda y que consigáis vuestros objetivos. Rubén, el genio del abanico. Gracias por

alegrarme siempre esos días que estoy de paseo por el ICMAB. Laia i Júlia, sempre juntes, fins i tot els vostres ordenadors en el despatx. Per totes les estones viscudes, llargues divagacions mantingudes, per escoltar-me i aguantar-me sempre que m'he necessitat desfogar. Y como no, mi Adri, ese chico que intenta echarme del BioLab desde el día que empezó su experimental de tesis, ¿o puede que incluso antes? No puedo decir nada más que no sepas ya, mejoraste el ambiente de trabajo desde tu incorporación, y dejé de escuchar únicamente por largos períodos el ritmo de mi querido HPLC, para pasar magníficos ratos contigo y tus chismoteos. Por esos karaokes improvisados que nos hemos montado más de una vez con esas canciones que parecían estar programadas en la radio solamente para cuando ambos estábamos presentes en el lab, *Nochentera* y *Bizarrap*, ¡Clara-mente, vamos para artistas! (aunque a veces se nos resistan los microchips).

Bé, crec que ja arriba l'esperat torn de la meva família NBT, de la qual n'he format part des d'abans d'aquesta tesi doctoral. Per les bones i per les dolentes, sempre heu estat allà quan us ho he demanat, i quan no, però ho heu cregut convenient. Més que els millors companys de feina que hagués pogut demanar mai, els meus grans amics, aliats i confidents. Tot i estar llargues temporades fora de la nostra casa, el "innovador zulo del IBB", sempre m'he sentit part de NBT essent ben integrada i valorada. Per tot això i mil coses més que ara no sabria ni com expressar, vull agrair a totes i cadascuna de les persones que en formen part o n'han estat relacionades d'alguna manera:

Podria començar per la **Rosa** i la **Mercé**, sense les quals el laboratori no estaria tant organitzat ni seria tant eficient la feina del grup. Rosa, quan em vaig incorporar al grup farà 10 anys per fer les pràctiques curriculars del grau, vaig aprendre la meitat del que en sé avui dia del Pepe, però de l'altra part en vas ser tu la que em va transmetre el coneixement. Agrair-te tot el suport amb les comandes, indicacions del lloc d'emmagatzematge de tot el material de laboratori, per l'ajuda amb els cultius, però especialment pel suport que m'has aportat en temes personals.

A aquella persona que va marxar del grup ja fa uns anys, però en seguirà formant part per sempre, la **Olivia**. Va ser a través teu que vaig establir contacte amb el grup. Vas ser la meva professora de pràctiques el meu últim any de grau, tímidament et vaig preguntar per NBT, i amb un somriure em vas acollir, explicar sobre la recerca del grup, i aconsellar per a contactar al Toni. Fins i tot vaig aprendre a preparar mostres per al MALDI amb tu! Valoro moltíssim la sinceritat amb la que m'has dirigit les paraules en tot moment. Gràcies per ser de les primeres persones en valorar les meves capacitats professionals, inclús ara que estem una mica més separades.

A **Naroa**, la chica que estaba acabando su Ph.D. recién cuando me incorporé al grupo. La tuya fue la primera de muchas defensas de tesis que presencié. Gran profesional que siempre ha sabido separar perfectamente los momentos de trabajo de los de amistad. ¡Tu optimismo y alegría le dan vida al laboratorio! Gracias por ser una

amiga en la que puedo apoyarme con total confianza y con la que poder compartir una buena copa de vino. Por las mil aventuras vividas durante estos años, ¡y las que nos quedan por disfrutar!

Pero no hay Naroa sin **Laura**, ya que os conocí a la vez y siempre juntas. Lauri, una altra gran amiga amb la que vaig tenir molta sort de poder coincidir durant uns quants anyets al *labo*, i de la que vaig aprendre moltes coses a nivell personal. Per totes les rialles que ens hem pegat juntes, els entrenaments devastadors al SAF als que hem vas arribar a sotmetre, les nostres xerradetes i berenars al *despachito*, i ensenyar-me a ser zen en els moments de dificultats! Et trobo molt a faltar durant el dia a dia, però sempre que ens reunim m'encanta veure que segueixes sent la de sempre. Merci per seguir aquí!

També a l'**Hèctor**, l'autoproclamat *jefazo de despachito Sir Hectaldo* sota el domini del qual vaig tenir la fortuna de compartir gairebé tota la estada al IBB. Gràcies per escoltar totes les meves penúries, per acompanyar-me durant la meva evolució científica i personal, per descobrir-me la meva passió per les arts marcials, per generar-me sempre un somriure, per les preguntes filosòfiques amb les que m'has socarrimat el cervell més d'un cop, i per convertir-te en el meu primer *senpai* durant la època de tortura que ens vas dedicar. Encara que estiguis bastant boig, tots t'estimem. No canviïs, *badabronx*.

A aquell jove que quan em vaig incorporar al grup era el noi de màster, **JoseVi**, i poc després va resultar ser el predoc més vell de tots, però això sí, el més ben conservat. Eres una de les persones que ha mostrat més tenacitat per aconseguir els seus objectius professionals, i potser una mica m'ho has transmès a través de *las palmaditas en la espalda*. Gràcies pel suport que m'has donat durant la tesis! Aprecio que estiguis inclús més boig que l'Hèctor, així tampoc em fa falta aparentar ser normal. Como tu ya sabes: "*Meow*".

A l'**Eric**, la única persona que he conegut que és capaç de viure la vida amb més velocitat que el AVE, però sempre *en lo cor a la mà* (especial dedicació del meu preciós dialecte), preocupant-se i disposat a ajudar als altres. M'emporto tots els bons moments que ens has fet passar tant dintre com fora del laboratori, perquè amb tu l'*olivella* i la rauxa està assegurada.

No ens podem oblidar de l'**Ugutz**, que tot i ser d'*Euskal Herria* parla el català millor que molts natius de Catalunya. Et podríem considerar l'arrel principal de NBT. T'agraeixo que sempre estiguis atent de tots nosaltres, donant-nos suport quan ho necessitem. Mil gràcies per deixar-me recolzar en tu i animar-me en els moments més difícils. A més, ningú em prepara el gintònic amb tanta qualitat com ho fas tu!

Tampoco me puedo dejar a **Paolo**, ese hombre que me enseñó todo lo referente a cromatografías, a documentar correctamente todo el experimental para alcanzar un laboratorio de calidad, y a valorarme a mí misma como profesional. Desde que te marchaste algo de esencia se ha perdido en el grupo, como el olor diario a café en el

despachito o el buen uso dado al *puff*. Me quedo con esos bailes salseros que nos marcamos por Barcelona, ¡sin duda la mejor pareja de baile en NBT!

¿Y qué voy a decir de ti **Julieta**? Eres una profesional increíble que además siempre transmite felicidad, alegría y confianza. Con tu ayuda ha sido mucho más fácil aprender sobre biofísica. Gracias por estar siempre dispuesta a ayudarme, y también por compartir tan interesantes charlas dentro y fuera del trabajo. Una alegría compartir la GLA (aunque un poquito distinta) en nuestras respectivas investigaciones.

Ara li toca al pou de saviesa de l'**Eloi**, del qui mai em canso d'amarar-me de coneixement. El meu company de moltes matinades al lab que més d'un cop m'ha espantat en trobar-me'l a fosques al *despachito*. Potser per això tant d'interès en preguntar: "*és de nit? I ara, és de nit?*". També el primer integrant del grup amb el que he compartit grans conversacions *frikis* d'anime, jocs de taula i videojocs. Aprecio el teu bon gust musical que ens ha alegrat tants viatges i estones al lab. Mil gràcies per tot el suport que m'has aportat sempre, per animar-nos sempre la gresca a tots plegats, i per dissenyar-nos els uniformes NBT amb tant bon estil!

Continuaré amb el **Carlos**, a qui li podria atorgar el títol a *profeta Gasdermina* de NBT, qui diàriament després d'arribar al laboratori i donar-me els bon dies amb amabilitat, m'ha predit encertadament la següent profecia: "*Hoy tampoco te va a salir nada; eso funciona así Aida, todo sale MAL SIEMPRE*". Jo sé que realment eres un geni, i simplement has volgut mantenir la teva ratio d'experiments èxit versus fracàs comparable a la meva per fer-me suport durant els meus darrers anys de tesis. Bromes a part, Carlititos moltíssimes gràcies per tots els moments estúpids però divertits dintre i fora la feina, per les ampolles de Baileys compartides, i per estar al meu costat sempre que ho he necessitat!

Y con esto sigue **Jara**, gran fichaje que reactivó el consumo de cafeína en el grupo. Jarita me encanta tu carácter alegre y el buen ambiente que generas a tu alrededor en el laboratorio. Sin duda, desde tu incorporación al grupo, las comidas se han vuelto mucho más interesantes gracias a tus interminables anécdotas. ¡Merci por sacarme una sonrisa en el día a día!

A esa persona con la que me ha tocado negociar sobre el hielo seco en más de una ocasión... ¿Qué paciencia conmigo, verdad **Tutty**? Valoro muchísimo tu sinceridad y voluntad de ayudar siempre a los demás. Eres de las mejores compañeras actuales con las que comparto el *despachito* que hacen de esa caverna sin ventanas, un agradable lugar en el que no se puede parar de reír. ¡Gracias por estar siempre ahí para apoyarme!

A l'altra predoc que com jo està dividida en dos grups de recerca, l'**Ari**. A pesar del "plantón" inconscient que et vaig donar el dia que em vas venir a visitar a l'ICMAB, gràcies per ser una bona amiga amb la qui poder compartir els assumptes personals. Merci per tot el suport, ara et toca a tu enfrontar la recta final de la tesis amb motivació. Sé que ho aconseguiràs!

Li arriba el torn al meu apreciat kōhai, el **Roger**, a qui li confio tant el meu lloc original al *despachito*, com la continuïtat del primer projecte de recerca en el que vaig tenir la sort d'estar involucrada. Rubén... ai vull dir Roger, ets un amic simplement genial amb el que es pot confiar cegament, parlar tranquil·lament de qualsevol assumpte i xafarderia. Ha estat un plaer treballar en poyata contigua a la teva, ja fos explicant-nos acudits realment dolents (hem quedo amb el pollastre i la gallina), o bé cantant *openings* de *One Piece* o d'altres que se'ns passen pel cap en aquells moments. ¡Sense dubte ets una de les persones que m'alegren més el dia a dia! No puc parar de riure al pensar que malgrat la competència per mantenir el nostre respectiu espai de treball més digne que el de l'altre, sempre el deixem fet un espectacle en acabar la feina (encara que creguis que el teu queda millor). Sempre estarem vinculats a través dels *eppendorfs*. A més, per mitjà teu he conegut una espectacular persona com n'és la **Chari**, que tot i ser de fora NBT, s'ha convertit en una peça indispensable en les nostres trobades. Sou una parella fantàstica i divertida amb la que comparteixo aficions molt similars, i amb la que no em canso mai de compartir el meu temps. ¡Mil gràcies per la vostra amistat!

L'altre predoc que forma part de l'actual *despachito*, el **Jan**, qui afirma tenir menys edat que jo, però tinc els meus dubtes que no es tracti d'un quarantanyer camuflat d'estudiant. Persona amb rècord anual de viatges en avió, de la qual admiro la capacitat de gestió simultània de varis projectes. Redueix ritme de vida i deixa el mòbil fora de cobertura per no envellir encara més ràpidament, t'ho recomano. Ànims amb el que et queda de tesi, i quan algun problema es concentri, afegeix un regalim d'aigua per a diluir-lo! Hahaha.

A la brasileña con la que más de una vez he competido por ver quién tenía más tubos de reacción en poyata, **Marianna**. Te odio un poquito por haberme metido miedo en el cuerpo con las historias de maletas facturadas con mala identificación en los aeropuertos. Pero supongo que te quiero demasiado por todos los buenos ratos y risas que nos hemos pegado juntas. Eres una gran amiga con la que me encanta tener largas charlas. ¡Muchísimas gracias por tu apoyo desde siempre!

To **Angela**, the nicest and kindest Italian with whom I have shared an office. I miss those little moments sharing smiles, and taking about culture, sleep schedules, how problematic the proteins are and so on. You were a wonderful lab partner!

To **Elijah**, the boy who has always had and will have nicer and longer hair than mine. It was a pity not finding an opportunity to perform the Ph.D. with us. My English pronunciation has worsened considerably since you left. I appreciate all the jokes, conversations and support you gave me, but I definitely treasure your guacamole recipe!

A aquells amb els que hem compartit IP i projectes: **Marilla, Estera, Agus, Fernando, Rubén, Andrea Sánchez, Andrea Modrego, Kika, Jessica, Sara** y **Amanda**. Special mention for Marilla, Estera and Agus, with whom I shared work days in the laboratory, classes at the gym, and unforgettable parties (including the trip to Poland). Even the

distance, we have kept in touch, sharing our lives and taking care of our friendship. Do not change girls! También a Fer, el gallego más atlético que he conocido, con la marcha del cual NBT sufrió una gran pérdida. Enviar una abraçada a Andrea S. Mai hagués imaginat tenir a algú del poble com alumne! M'ho vaig passar molt bé amb tu com a compi de labo. Recuerdos a Andrea M. que no pudo precisamente disfrutar del todo de sus prácticas por culpa del COVID. Aun así, persona indispensable para animar las casas rurales con juegos como la *mímica* o el *vickings*, y gran compañera para el ping-pong. Otro especial agradecimiento a Amanda, con la que compartí mi primer proyecto de investigación. Al final ninguna de las dos tuvo la oportunidad de seguir con eso, pero hoy día sigues siendo una gran amiga con la que compartir entretenidas charlas. Tu foto seguirá estando en los microondas del *despachito* para recordar tu aportación en el grupo. Quiero acabar con ese fenómeno de ex-vecino, Rubén, que aún hoy en día sigue sorprendiéndome con sus anécdotas. Sin duda has sido de los que más han marcado en el grupo. Además, gracias a ti he conocido a personas estupendas como Andreu, Andy, Manu y Laura, con las que siempre acabamos pasando ratos geniales cuando nos juntamos. ¡Todos vosotros chicos sois geniales, no cambiéis nunca!

Y aunque directamente no forme parte del grupo NBT, no me quisiera dejar a **Miguel**, el mejor conserje jamás conocido. Muchas gracias por recoger esos mil paquetes que llegan a diario en el grupo (ya sean reactivos para el laboratorio como otros personales), así como por solucionarme siempre con rapidez todos los problemas relacionados con la tarjeta para acceder al IBB.

Però aquests anys no han estat només feina. També he tingut la sort de conèixer el gran equip de guerrers del Dojo Gaman que sempre m'ha fet suport i ajudat a desconnectar quan més ho he necessitat. Voldria fer una especial menció a aquelles persones que, a banda de compartir duels de nivell dintre del dojo, també s'han convertit en grans amics dintre i fora d'aquestes instal·lacions: **Eli, Neus, Irina, Jesús** y **Òscar**. Cadascú amb la seva aportació: pels esmorzars, birres, balls i cafès compartits. Hem quedo amb la inoblidable nit del campament de kyokushinkai en la que la majoria de nosaltres vam coincidir. Sense dubte de les més divertides que he viscut. Allí vàrem descobrir l'habilitat de la Eli per al futbol, que el Jesús no és capaç d'obrir una ampolla de vi sense obridor, que la Neus prefereix accedir a les cases per les finestres que per les portes, així com la meva capacitat de fer el ridícul immortalitzada en certes gravacions. Almenys, tot plegat ens va portar a salvar la vida d'un pobre ratolinet que s'havia quedat atrapat a la piscina (malgrat el vol inesperat d'últim moment). Com bé diu el meu senpai: "*si te lo quedas, te envenenas*"; així que també faré esment als fabulosos roncs que ens van acompanyar durant el cap de setmana, que a pesar no deixar-nos descansar, ens van divertir incondicionalment l'estada. ¡Ens veiem al tatami per seguir millorant plegats!

No em voldria deixar als millors amics que he conegut al llarg de la vida, i sempre m'han acompanyat, tant en els bons moments com en els més dolents: **Aida, Iván, Raúl, Marina, Tere, Anna, Núria, Marta** i **Andrés**. Aideta,

Iván, Raúl i Marina, el meu estrambòtic riure de hiena només apareix quan m'ajunto amb vosaltres. Amb això ja us ho diria tot. Des de que vaig arribar a Barcelona heu estat al meu costat. Aideta, la meva altra jo caiguda d'un món paral·lel. Creus que si no ens haguéssim bifurcat laboralment, seguiríem firmant la feina conjunta com a Aida[2]? Iván, mi confidente. ¿Cuántas pelis, cenas y fiestas hemos compartido? ¡No me imagino una Barcelona sin ti! Raúl, el toque mágico y pícaro del grupo, la chispa, la vidilla y los chismoteos. Es una lástima el poder verte tan poco ahora que estás entre dos países, pero sin duda, nuestro Raúl será siempre nuestro Raúl en cada encuentro (aunque decida llevar ese bigote haha). Marina, la meva companya de ball en les millors cançons randoms que se'ns han presentat a la disco. Malgrat la distància que ens separa ara mateix, sempre et portaré al cor. Per més càmpings, excursions i escapadetes amb vosaltres. Tere i Anna, mil anècdotes compartides, tardes de guitarra, salons del manga, riures, pelis, sèries, sushi (i tallades de meló amb palets), festes i mitja vida més. Aneu preparant el sofà de Bèlgica, Menorca i Tortosa per continuar sumant experiències plegades. Núria, mira que he tingut companyes de pis, però has estat la única que ha matinat per veure Pokémon mentre esmorzava el seu tassó de llet amb cereals. Després d'un dia dur de feina, s'agraïa arribar a casa i trobar-se amb una persona alegre i esbojarrada, que és capaç de fer-te oblidar els problemes amb una bona amanida guarnida amb melmelada de fresa. A través teu vaig conèixer la Marta, una persona excel·lent, a la qui considero la millor amfitriona i guia turística que he tingut mai. Vaig gaudir moltíssim de Gènova amb vosaltres, sobretot dels croissants bomba als que em vau sotmetre sense previ avís. Per més aventures com aquesta al vostre costat. Andrés, el chico que en acabar el máster me dijo que nunca más nos volveríamos a ver, pero sigue ahí contradiciéndose. He aprendido tantas cosas de ti, que puedo asegurar con certeza que aun te quedan muchas más por enseñarme. Gracias por tu constante apoyo a pesar de la distancia. También por las charlas interminables que hemos mantenido más de una vez. Por todas las experiencias vividas junto a ti, y las que nos esperan. ¡A tots vosaltres se us estima moltíssim!

Tampoc oblidar aquells que m'han acompanyat durant tota la vida. Sou un bon grapat que podria agrupar en les **quatre colles de Tom, Manolo, Pepe** i **Leo**. Heu estat els que més m'heu evadit de la realitat per fer-me oblidar els problemes del dia a dia. Sempre que estic amb vosaltres els riures i la gresca estan assegurades, sigui quin sigui el tema de conversació al que ens dirigim. Gràcies per ser com sou!

Per acabar, voldria mostrar els meus sincers agraïments a les persones més importants de la meva vida, a la família que sempre m'ha valorat, cuidat, confiat en mi, i m'ha donat el seu afecte, suport i consell en totes les etapes viscudes. Al **papa** i la **mama**, per haver-me educat en la persona qui sóc avui dia, i haver-me permès estudiar allò que m'agrada sense dubtar del que podria aconseguir. Més d'un cop us he avasallat amb les meves històries sobre les proteïnes i els liposomes, i malgrat entendre poc del que parlava, m'heu escoltat fins el final, sentint-vos orgullosos de la meva feina. Aquesta confiança que m'heu transmès sempre, m'ha permès superar

tots els entrebancs que m'he anat trobant al llarg del meu camí. Als meus germans, **Josep** i **Judit**, els que segurament han aguantat més cops els meus mals humors generats per l'estrès. Gràcies per estar al meu costat cada dia i fer-me sentir imparable. Xep, gràcies per cuidar sempre de mi i guiar-me pel millor camí. Judit, gràcies per convertir-te en la meva companya de vida, en el meu *vino tinto*, i estar sempre atenta de les meves anades d'olla com si fossis tu la germana gran. Vaja feinada et porto, eh? Crec que tot el que t'havia d'expressar, ja ho vaig fer una nit de cel estrellat, mentre se'ns creuava Mesier pel davant. Encara que em tragueu de polleguera, sense vosaltres dos la meitat de la meva vida no tindria sentit. Sou el tot! A la meva germaneta peludeta, la **Neila**, que tot i no ser conscient de la seva aportació, és la alegria i la vida de la casa. No s'ha perdut ni una reunió de feina durant el confinament, tot i que sempre s'ha queixat de la seva durada, i que l'haguessin fet esperar per poder jugar o baixar a passejar. La seva companyia és irreemplaçable. Per tot això, si a dia d'avui sóc una persona capaç d'enfrontar grans reptes amb un somriure i optimisme és gràcies a vosaltres. Us estimo!

A TOTES aquestes persones que m'heu convertit en qui sóc avui dia, us dedico aquest treball que heu fet possible.

ABSTRACT

Nanopharmaceuticals have the potential to address the biological and therapeutic limitations of conventional drugs, offering great clinical and socio-economic benefits. Pharmaceuticals can be of two types: i) those where the therapeutic molecules are administered in their "naked" form, without the help of any nanovehicle, ii) those where the therapeutic molecules are coupled (functionalized, entrapped, or coated) to a carrier or "drug delivey system" (DDS). The use of DDS for drug delivery offers many advantages thanks to their size and tuneability, and they can be designed to improve the half-life of the drug, control the biodistribution and the release profile, eventually providing an overall clinical benefit to patients. However, the translation of nanopharmaceuticals from lab bench to an advanced stage of pharmaceutical development faces significant challenges. Among others, the high-quality that these novel nanoformulations must meet for the preclinical (and further clinical) testing is a major challenge, taking into account that most of the nanopharmaceuticals display complex multicomponent nature.

In this thesis, an advanced characterization effort was carried out to understand, guarantee and control the quality of a novel, under development, nanoliposomal formulation for Fabry disease treatment. Fabry disease is an X-linked rare disease belonging to the lysosomal storage disorders (LSDs) group in which the lack/deficiency of α-galactosidase (GLA) enzyme causes the lysosomal accumulation of neutral glycosphingolipids (mostly globotriaosylceramide, Gb3), that results in a multisystemic pathology, with the progressive damage of relevant organs such as kidneys, heart, and brain, and the premature death. Although there is not a definitive cure, enzyme replacement therapy (ERT) through the intravenous administration of the missing enzyme is the main treatment option for Fabry patients. However, ERT treatments show limitations such as poor biodistribution, poor capacity to cross biological membranes, high immunogenicity, and limited efficacy. The use of nanocarriers capable to encapsulate proteins is currently being explored and exploited as an alternative strategy to overcome the handicaps of the traditional ERTs.

RGD-targeted nanoliposomes entrapping the GLA enzyme and prepared by the green-scalable depressurization of an expanded liquid organic solution-suspension (DELOS-susp) methodology yielded a patented product more effective at preclinical level than traditional marketed ERTs. The significant benefit that this novel treatment could offer to Fabry patients was recognized by the European Medicines Agency (EMA) by means of the Orphan Drug Designation. In this context, in order to support the advancement on the development of this novel

nanoformulation to become a potential intravenous drug product candidate, further understanding and control of the molecular and supramolecular interaction between the liposomal nanocarrier and the GLA drug substance was achieved.

Four recombinant GLA enzymes differing in purification tags and expression systems were produced and explored in this thesis, using human embryonic kidney (HEK) or Chinese hamster ovary (CHO) mammalian expression systems, in order to investigate which GLA properties are the most favorable to generate stable, efficient and robust liposome-based nanoconjugates for Fabry therapy. The use of GLA protein without purification tags and expressed in CHO cells demonstrated to be the most promising prototype of drug substance to obtain GLA-entrapped liposomes with enhanced properties, in terms of higher protein entrapment efficiency and increased enzymatic activity.

Moreover, due to the complexity of these liposome-based nanosystems, small changes in their composition, media, concentration or pharmaceutical form can severely impact on their *in vivo* performance and, thus, on their safety and efficiency profile. A suitable characterization and control to ensure that the critical quality attributes (CQAs) are within an appropriate limit, range, or distribution to ensure the desired product quality is crucial prior the cGMP production batch to entry the clinical phase. Therefore, despite the advanced stage of the pharmaceutical development of the GLA-loaded nanoliposomal formulation, there were still pending the development, optimization and/or validation of analytical methods for the characterization and control of this nanopharmaceutical, taking into account the requirements from the regulatory agencies.

To address this important need, in this thesis the following methodologies were investigated and developed: i) a reverse phase-high performance liquid chromatography-evaporative light scattering detector (RP-HPLC-ELSD) methodology for the proper determination of the chemical membrane composition of the GLA-loaded nanovesicular formulations; ii) new methods based on Luria Broth (LB) agar plates and Gel clot-based Limulus Amebocyte Lysate (LAL) for the control of the microbiological contamination and bacteria endotoxin content, respectively; iii) a filtration-centrifugation-based methodology for the assessment of the GLA release kinetics in physiologically/clinically relevant media and for the GLA leakage rate from the nanoliposomes throughout shelf-life; and iv) the establishment of an *in vitro* trypsinization assay for the evaluation of the protective capacity of the liposomal nanocarriers.

Additionally, it was explored the feasibility of characterizing the targeting ligand on the surface of the nanoliposomes by a novel advanced method named SPARTA® (Single Particle Automated Raman Trapping Analysis), as well as the use of the field-flow fractionation-multi-angle light scattering (FFF-MALS) as an alternative technique to monitor the released GLA molecules from liposomes in a near future.

In summary, the results achieved in this thesis are an important contribution to advance in the Chemistry, Manufacturing and Control (CMC) development of the GLA-loaded nanoliposomal formulation for Fabry disease treatment.

CONTENT

PREAMBLE.....i

ACKNOWLEDGEMENTS.....iii

ABSTRACT.....xv

CONTENT.....xix

VOCABULARY LIST.....xxix

CHAPTER 1. INTRODUCTION: BIOMOLECULE-BASED NANOPHARMACEUTICALS.....1

1.1. Biomolecules for therapeutic applications.....1

1.1.1. Mammalian cell factories for the biosynthesis of high-quality recombinant proteins.....3

1.2. Nanocarriers in nanopharmaceutical development.....5

1.2.1. Challenges in the development of nanopharmaceuticals.....7

1.2.1.1. Quality.....8

1.2.1.1.1. Regulatory compliance requirements.....8

1.2.1.1.2. Quality by design approach as a systematic tool for the development of nanopharmaceuticals.....8

1.2.1.2. Definition of the CQAs of nanopharmaceuticals.....10

1.2.2. Road of a nanopharmaceutical from the bench to the market.....12

1.2.3. Therapeutic nanopharmaceuticals currently on the market or in clinical translation stages.....14

1.3. Lipid-based vesicles as promising molecular self-assembled structures for drug delivery.....15

1.3.1. Progression of liposomal vesicles for therapeutic applications: current state in medicine.....18

1.3.2. Methodologies for vesicle manufacturing.....21

1.3.2.1. DELOS-susp as green and scalable compressed fluid-based technology for liposomes' preparation……23

1.3.3. Methodologies for liposomes' purification……25

1.3.3.1. Filtration-based procedures for liposomes' purification.……26

1.4. Rare disease: lysosomal storage disorders……28

1.4.1. Fabry disease and the current state of treatments (approved and under development)……30

1.4.2. Nanotechnology-based treatments for Fabry disease in preclinical development……34

1.4.2.1. GLA-loaded nanoliposomal formulation as nanopharmaceutical candidate for the treatment of Fabry disease……35

1.5. References……37

CHAPTER 2. OBJECTIVES……49

CHAPTER 3. PRODUCTION, PURIFICATION, CHARACTERIZATION AND COMPARISON OF DIFFERENT ALPHA-GALACTOSIDASE A (GLA) ENZYMES……53

3.1. Introduction……53

3.1.1. Most common mammalian cell lines used as expression systems……53

3.1.2. Transfection procedures for transient expression……55

3.1.3. Stable clone for recombinant protein expression……57

3.1.4. Histidine-tag and c-myc-tag: popular affinity tags for downstream processing and detection of recombinant proteins……58

3.1.5. Recombinant GLA enzyme versions of study……60

3.2. Optimization of the transient transfection protocol to enhance the yield of recombinant protein production……62

3.3. Impact of metal ions on IMAC procedures for GLA purification……66

3.4. Impact of purification tag, expression system and storage buffer on GLA characteristics……67

3.4.1. Protein solubility, purity and specific enzymatic activity of GLA enzymes……68

3.4.2. Protein identity and molecular mass determination of GLA enzymes……..70

3.4.3. Protein size distribution and ζ-potential of GLA enzymes……72

3.4.4. Thermal-dependent structural stability of GLA enzymes……74

3.5. Summary and conclusions……79

3.6. References……80

CHAPTER 4. IMPACT OF GLA ENZYME PHYSICOCHEMICAL PROPERTIES ON ITS INTEGRATION ON RGD-TARGETED NANOLIPOSOMES……..85

4.1. Introduction……85

4.1.1. GLA-loaded nanoliposomal formulations for Fabry ERT……85

4.1.2. Framework of the study……90

4.2. Impact of GLA characteristics on physicochemical and biological features of GLA-loaded nanoliposomal formulations……92

4.2.1. Production and characterization of GLA-loaded nanoliposomal formulations used for the study...92

4.2.2. Impact of GLA characteristics on the enzyme entrapment efficiency in nanoliposomes……97

4.2.3. Impact of GLA characteristics on the GLA leakage rate of nanoliposomes……98

4.2.4. Impact of GLA characteristics on the enzymatic activity of nanoliposomes……99

4.2.4.1. Suitability of the *in vitro* fluorimetric assay for EA measurement of GLA-loaded nanoliposomal formulations……100

4.2.4.2. Comparison of the EA of naked GLA enzymes and GLA-loaded nanoliposomes……103

4.2.5. Impact of GLA characteristics on the colloidal stability of nanoliposomes……..106

4.2.6. Impact of GLA characteristics on the *in vitro* enzyme release from nanoliposomes……..107

4.3. Impact of GLA characteristics on the distribution of the integrated enzyme in the liposome……110

4.3.1. Production and characterization of GLA-adsorbed nanoliposomal formulations used for the study……111

4.3.2. Characterization of GLA distribution on nanoliposomes using proteases……115

4.3.2.1. Suitability of the *in vitro* trypsinization assay for nanoliposomal formulations……116

4.3.2.2. Comparison of the protective capacity of GLA-loaded and GLA-adsorbed nanoliposomes……117

4.3.3. Characterization of GLA distribution on nanoliposomes by fluorescence spectroscopy……119

4.3.3.1. Distribution of tryptophan residues on the structure of human GLA enzyme……119

4.3.3.2. Impact of GLA characteristics on the enzyme distribution on nanoliposomes……122

4.3.4. Characterization of GLA distribution on nanoliposomes by cryoTEM……125

4.4. Summary and conclusions……126

4.5. References……128

CHAPTER 5. DEVELOPING ANALYTICAL METHODS FOR QUALITY ASSESSMENT AND CONTROL OF THE CRITICAL QUALITY ATTRIBUTES OF GLA NANOLIPOSOMAL FORMULATIONS……131

5.1. Introduction……131

5.1.1. An advanced GLA-liposome nanoformulation for Fabry treatment: main achievements on TRL development……131

5.1.2. Definition of the final LP-RGD-GLA-S pharmaceutical form to reach the clinical phase: challenges to overcome in the clinical translation……132

5.1.3. Definition and control of the CQAs of GLA-loaded nanoliposomal formulations……135

5.2. Development, optimization and validation of an analytical RP-HPLC-ELSD method to quantify and control the liposomal membrane composition of GLA nanoliposomal formulations……139

5.2.1. RP-HPLC-ELSD method development: achieving molecule separation with good resolution……140

5.2.2. RP-HPLC-ELSD method optimization: reduction of time-consuming analysis and improvement of chromatographic parameters according to ICH guidelines……145

5.2.3. Sample preparation protocol optimization: ensuring proper analyte solubilization and maintenance of good quality chromatogram parameters……150

5.2.4. RP-HPLC-ELSD method validation: ensuring reliability of the analytical method……157

5.2.5. Contribution to the Certificate of Analysis (CoA) of LP-RGD-GLA-S formulations……176

5.2.6. Summary……177

5.3. Implementing and optimizing procedures to control LP-RGD-GLA-S microbiological quality……178

5.3.1. Bacterial contamination detection by Luria Broth agar plate test……178

5.3.2. Bacterial endotoxin quantification: Gel clot LAL assay optimization and verification……183

5.3.3. Summary……191

5.4. Development of an *in vitro* drug release methodology……192

5.4.1. Implementation of a procedure based on filtration-centrifugation……193

5.4.1.1. Influence of the cut-off membrane on the GLA diffusion……193

5.4.1.2. Optimizing membrane passivation conditions to avoid GLA protein binding……196

5.4.1.3. Impact of filtration-centrifugation protocol on nanoliposome stability……198

5.4.1.4. Variability of the optimized filtration-centrifugation procedure……199

5.4.1.5. Integrity of the GLA-loaded nanoliposomal formulation when simulating *in vitro* release conditions……200

5.4.2. Preliminary *in vitro* drug release study using different physiological relevant media……201

5.4.2.1. Stability of the GLA-loaded nanoliposomal formulation in different physiological media……204

5.4.3. Feasibility of using the filtration-centrifugation method to control the GLA leakage rate during storage conditions……209

5.4.4. Summary……210

5.5. General summary and conclusions……211

5.6. References……211

CHAPTER 6. GENERAL CONCLUSIONS……217

CHAPTER 7. EXPERIMENTAL SECTION……223

7.1. Materials……223

7.2. Methods for the design, production, purification and characterization of recombinant GLA enzymes……225

7.2.1. Design, synthesis and cloning of GLA proteins……225

7.2.2. Amplification, extraction and purification of plasmid DNA from *E. coli* strains……228

7.2.3. Transient expression of GLAH6-T and GLAcmycH6-T: transfection procedures……228

7.2.4. Stable expression of GLAcmycH6-S and GLA-S……229

7.2.5. Chromatographic procedures for secreted GLA purification……229

7.2.5.1. His-tagged GLA purification by affinity chromatography methodology……229

7.2.5.2. Two-step purification process for tag-free GLA-S purification……229

7.2.6. GLA detection, purity and quantification……230

7.2.6.1. Sodium dodecyl sulfate-polyacrylamide gel electrophoresis and western blot assays……230

7.2.6.2. Spectroscopy analysis by nanodrop equipment……231

7.2.6.3. Reversed-phase high-performance liquid chromatography-ultraviolet methodology for analytical GLA-S quantification……231

7.2.7. Determination of host cell DNA contamination in GLA enzymes……233

7.2.8. Integrity of GLA enzymes by mass spectrometry……233

7.2.9. *In vitro* fluorescent enzymatic assay for specific α-galactosidase activity……234

7.2.10. Particle size distribution and ζ-potential determination of GLA enzymes by dynamic and electrophoretic light scattering……235

7.2.11. Structural characterization of GLA enzymes by tryptophan fluorescence emission spectra analysis……236

7.2.12. Resistance to proteases assessment using an *in vitro* trypsinization assay……238

7.2.13. Stability studies of naked GLA enzymes……238

7.3. Methods for the synthesis, purification and characterization of the chol-PEG_{400}-RGD targeting molecular unit……239

7.4. Methods for the preparation, diafiltration and characterization of nanoliposomal formulations……240

7.4.1. Plants and experimental procedures for the preparation of nanoliposomal formulations by DELOS-susp methodology……240

7.4.1.1. Description of the small lab-scale DELOS-susp plant……240

7.4.1.2. Description of the intermediate lab-scale DELOS-susp plant……241

7.4.1.3. DELOS-susp methodology for the production of nanoliposomal formulations……243

7.4.2. Integration of GLA protein in nanoliposomal formulations by titration approaches……244

7.4.3. Diafiltration and concentration of nanoliposomal formulations by TFF……245

7.4.4. Summary of process parameters used for the preparation of nanoliposomal formulations……247

7.4.5. Physicochemical characterizations of nanoliposomal formulations……250

7.4.5.1. pH measurements of nanoliposomal formulations……250

7.4.5.2. Morphological analysis of nanoliposomal systems by cryogenic transmission electron microscopy……251

7.4.5.3. Particle size distribution and ζ-potential determination of nanoliposomal formulations by DLS and ELS……214

7.4.5.4. Particle concentration of nanoliposomal formulations by NTA……252

7.4.5.5. Determination of GLA entrapment efficiency in nanoliposomal systems……253

7.4.5.6. Quantification of liposomal membrane components by reversed-phase high-performance liquid chromatography-evaporative light scattering detector method……253

7.4.5.7. Preliminary RP-HPLC-ELSD method for the detection of liposome degradants……259

7.4.5.8. Characterization of the targeting chol-PEG_{400}-RGD ligand on the surface of nanoliposomes by Single Particle Automated Raman Trapping Analysis (SPARTA®)……260

7.4.5.9. Development of two field flow fractionation-based methods for the detection of GLA-S enzyme and RGD-targeted nanoliposomes……261

7.4.6. Filtration-centrifugation procedure for the separation of non-integrated GLA enzymes from GLA nanoliposomal formulations……263

7.4.6.1. *In vitro* GLA release study from nanoliposomal formulations……266

7.4.6.2. GLA leakage rate from nanoliposomal formulations under storage conditions……267

7.4.7. Determination of bacterial contamination in nanoliposomal formulations……267

7.4.7.1. Microbiological study: Luria Broth agar plate test……267

7.4.7.2. Bacterial endotoxins determination: Gel clot LAL test……268

7.4.8. Stability studies of nanoliposomal formulations……271

7.5. Figures and tables……271

7.6. References……272

SCIENTIFIC CONTRIBUTIONS……277

ANNEX I. STRESS TESTING OF NANOLIPOSOMAL MEMBRANE COMPONENTS…… I

I.1. Preliminary testing to identify potential nanoliposome degradants……I

I.1.1. Definition and design of stress studies……II

I.1.2. Evaluating RP-HPLC-ELSD analysis to identify potential degradation products……III

I.2. Summary……XIII

I.3. References……XIV

ANNEX II. LIPOSOMAL MEMBRANE COMPOSITION ANALYSIS BY SINGLE PARTICLE AUTOMATED RAMAN TRAPPING ANALYSIS (SPARTA®)……XVII

II.1. Importance of integration efficiency of targeting ligands as critical quality attribute of liposomes……XVII

II.2. SPARTA® methodology and applications……XVIII

II.2.1. Detection of chol-PEG_{400}-RGD functionalization and GLA-S loading in nanoliposomes prepared in water……XIX

II.2.2. The influence of glucose on SPARTA® measurements and particle properties……XXI

II.3. Summary……XXIV

II.4. References……XXIV

ANNEX III. FIELD FLOW FRACTIONATION COMBINED WITH MULTI-ANGLE LIGHT SCATTERING (FFF-MALS) FOR THE QUALITY CONTROL OF NANOPHARMACEUTICALS……XXVII

III.1. Introduction to field flow fractionation-based methodologies……XXVII

III.1.1. Operating principle of AF4 and applications……XXVIII

III.2. Development of an AF4-MALS-dRI methodology for the characterization of GLA-loaded nanoliposomal formulations……XXX

III.2.1. Development of the AF4-MALS-dRI protocol for the detection of nanoliposomes……XXXII

III.2.2. Development of the AF4-MALS-dRI protocol for the detection of GLA-S enzyme……XXXVIII

III.3. Summary……XLI

III.4. References……XLII

VOCABULARY LIST

A	**ACN**	Acetonitrile or CH_3CN.
	AcOH	Glacial acetic acid.
	ACS reagent	High quality chemical that meets the specifications of the American Chemical Society.
	ADV	Automatized depressurization valve used in DELOS-susp plants.
	Ads	Adsorbed (referring to the theoretical GLA organization on the vesicles surfaces after being integrated to the nanosystem by titration approaches.
	AEX	Anion exchange chromatography.
	AF4	Asymmetric flow field flow fractionation.
	AF4-UV/Vis-FLD	Asymmetric field flow fractionation coupled to an ultraviolet/visible detector and to a fluorescence detector.
	AF4-MALS-dRI	Asymmetric field flow fractionation coupled to a multi-angle light scattering detector and to a differential refractive index detector.
	API	Active pharmaceutical ingredient.
	Arg	Arginine aminoacid.
	Asp	Aspartic acid aminoacid.
	ASTMA	American Society for Testing and Materials.
	ATCC	American Type Culture Collection.
	atm	Standard atmosphere unit.
	A_s	Asymmetry parameter considered in analytical HPLC methods.
	ATR-FTIR	Attenuated total reflection-Fourier transform infrared spectroscopy.
	AUC	Analytical ultracentrifugation.
	A_{260}	Absorbance value at a wavelength of 260 nm.
	A_{280}	Absorbance value at a wavelength of 280 nm.
	A_{260}/A_{280}	Absorbance ratio value at 260 nm and 280 nm.
B	**BBB**	Blood brain barrier.
	BFV-001 and BFV-002	One-way valves used in DELOS-susp installations.

BHK cells	Baby Hamster Kidney cell cultures.
BSA	Bovine Serum Albumin protein.

C

C	Collector container used in DELOS-susp installations.
Ca^{2+}	Calcium divalent cation (positively charged ion).
CBA	Chicken β-actin promoter to induce protein production.
CBD	Chitin-binding domain.
CCiTUB	Scientific and Technologic Centers of the University of Barcelona.
CD	Circular dichroism.
CDMO	Contract Development and Manufacturing Organization.
CEVS	Controlled environment vitrification system used for cryoTEM.
CHO cells	Chinese hamster ovary (CHO) cell cultures.
Chol	Cholest-5-en-3β-ol or cholesterol.
Chol-PEG_{400}-RGD	Cholesterol pegylated with arginyl–glycyl–aspartic acid peptide.
CIBER-BBN	Centro de Investigación Biomédica en Red – Bioingeniería, Biomateriales y Nanomedicina.
C_{Fc}	Concentration factor.
CFs	Compressed fluids.
CFU	Colony Forming Units = number of live bacteria cells in a sample.
cGMP	Compliant Good Manufacturing Practices.
cIEF	Capillary isoelectric focusing.
Cl^-	Chloride anion (negatively charged ion).
CMC guidelines	Chemistry, Manufacturing and Controls guidelines.
CMO company	Contract Manufacturing Organization company.
CMV	Cytomegalovirus immediate-early enhancer for protein expression.
c-myc tag	Polypeptide protein tag (EQKLISEEDL) derived from the c-myc gene product useful for protein purification and detection purposes.
cm^2	Square centimeter = a square with each side of 1 centimeter long.
CoA	Certificate of analysis.
CO_2	Carbon dioxide.
Co^{2+}	Cobalt divalent cation (positively charged ion).
CPPs	Critical process parameters.
CQA	Critical quality attribute.

	c-RGDfk	Cyclo pentapeptide Arginine-Glycine-Aspartic acid-D-phenylalanine-Lysine with cyclic structuration.
	cryoTEM	Cryogenic transmission electron microscopy.
	Cryo1	Cryoprotectant composition for freeze-dried prototypes of nanoliposomes, containing glycine 7.5 mg/mL, trehalose 50 mg/mL and sucrose 30 mg/mL.
	Cryo2	Cryoprotectant composition for freeze-dried prototypes of nanoliposomes, containing glycine 50 mg/mL and sucrose 80 mg/mL.
	Cs	Concentrated sample.
	CSE	Control standard endotoxin.
	CSIC	Consejo Superior de Investigaciones Científicas.
	CSM	Center of spectral mass.
	C-terminus	End of an aminoacid chain from a protein or polypeptide, which encodes a free carboxyl group (-COOH).
	C_2H_6	Ethane.
	C4 or C14	4 or 14 carbon chain length, respectively.
D	**Da**	Daltons.
	DDS	Drug delivery system.
	DELOS	Depressurization of an expanded organic solution.
	DELOS-susp	Depressurization of an expanded organic solution-suspension.
	DF	Dilution factor.
	DFF	Direct flow filtration.
	DHFR- cells	Cells deficient in dihydrofolate reductase activity.
	DLS	Dynamic light scattering.
	DMSO	Dimethyl sulfoxide.
	DNA	Deoxyribonucleic acid molecule containing genetic information.
	dn/dc term	The specific refractive index increment of a molecule.
	DoE	Design of experiments.
	DPPC	1,2-dipalmitoyl-sn-glycero-3-phosphocholine.
	dRI	Differential refractive index.
	D_s	Diluted sample.
E	**EA**	Enzymatic activity.
	EC	European Commission.
	E. coli	*Escherichia coli* (gram negative bacteria).

	EE %	Enzyme entrapment efficiency.
	e.g.	Latin phrase "*exempli gratia"* meaning "for example".
	eGFP	Enhanced green fluorescent protein.
	ElFFF	Electrical field flow fractionation
	ELS	Electrophoretic light scattering.
	ELSD	Evaporative light scattering detector.
	EM	Electron microscopy.
	EMA	The European Medicines Agency.
	Empty nanoformulations	Nanoliposomal formulations without GLA presence.
	EPR effect	Enhanced permeability and retention effect.
	Eq.	Equation.
	ERT	Enzyme replacement therapy.
	et. al.	Latin phrase "*et alia"* meaning "and others".
	EtOH	Ethanol.
	EU	European Union.
	EU/mL	Endotoxin units per milliliter of solution.
	EU Phoenix project	European Pharmaceutical Open Innovation Test Bed for Enabling Nano-pharmaceutical Innovative Products project.
	EU Smart4Fabry project	European Smart multifunctional GLA-nanoformulation for Fabry disease project.
F	**FCS**	Fluorescence correlation spectroscopy.
	FDA	United States Food and Drug Administration.
	FFF	Field flow fractionation.
	FFF-MALS	Field flow fractionation-multi-angle light scattering detector.
	FLD	Fluorescence detector.
	FlFFF	Flow field flow fractionation.
	FRET	Fluorescence resonance energy transfer.
	FTO	Free-of-operate status.
G	**G**	Gauge of a needle; or the size of the hole. The higher the gauge, the smaller the hole.
	g	Gram (as weight unit); or g-force (as acceleration force during centrifugation procedures).
	Gb3	Globotriaoslyceramide.

GC-MS/MS	Gas chromatography-mass spectrometry.
GFP	Green fluorescent protein.
GLA	α-galactosidase A enzyme.
GLAcmycH6-S	Recombinant GLA version encoding both, c-myc and 6-His purification tags, and produced using stable expression procedures and CHO DG44 cells.
GLAcmycH6-T	Recombinant GLA version encoding both, c-myc and 6-His purification tags, and produced using transient gene expression procedures and HEK 293F cells.
GLAH6-T	Recombinant GLA version encoding the 6-His purification tag, and produced using transient gene expression procedures and HEK 293F cells.
GLA-adsorbed nanoformulations	Nanoliposomal formulations containing GLA added by titration procedures.
GLA-free nanoformulations	Nanoliposomal formulations without GLA presence.
GLA-loaded nanoformulations	Nanoliposomal formulations containing GLA added in the aqueous phase of the DELOS-susp methodology.
GLA-S	Recombinant GLA version without purification tags, and produced using stable expression procedures and CHO K1 cells.
GLP	Good laboratory practices.
gluc	D-(+)-glucose or glucose.
Gly	Glycine aminoacid.
GMP	Good manufacturing practices.
GST	Glutathione S-transferase protein.
GT	Gene therapy.
GUV	Giant unilamellar vesicle.

H

h	Hour.
HA	Hemagglutinin.
HCl	Hydrochloric acid.
HCOOH	Formic acid.
HCO_3	Bicarbonate.
HEK cells	Human embryonic kydney cell cultures.
He-Ne laser	Helium-Neon laser.
HF5	Hollow fiber flow field flow fractionation.
HIC	Hydrophobic interaction chromatography.
His	Histidine aminoacid.

	His-tag	Protein polyhistidine tag for purification and detection purposes.
	HPLC	High Performance Liquid Chromatography.
	HPLC-HILIC	High-performance liquid chromatography-hydrophilic interaction liquid chromatography.
	HPLC-PDA-MS	High-performance liquid chromatography with photodiode array detection coupled to a mass spectrometer.
	HPLC-UV/Vis-FLD	High-performance liquid chromatography coupled to an ultraviolet/visible and to a fluorescence detector.
	HPV	High pressure vessel used in the DELOS-susp installation.
	HR-ESI-MS	High-resolution electrospray ionization mass spectrometry.
	HSCT	Hematopoietic stem cell transplantation.
	Hz	Hertz.
	H_2O	Water.
	H_2O_2	Hydrogen peroxide.
I	**IBB**	Institut de Biotecnologia i Biomedicina de la UAB.
	ICAM-1	Intercellular adhesion molecule 1.
	ICH	The International Council for Harmonization of Technical Requirements for Pharmaceuticals for Human Use.
	ICMAB	Institut de Ciència de Materials de Barcelona.
	ID	Identification.
	i.e.	Latin phrase "*id est"* meaning "that is".
	IMAC	Immobilized metal affinity chromatography.
	IMI	Institut za medicinska istraživanja i medicinu rada (translated in English as Institute for Medical Research and Occupational Health).
	Int	Intermediate prototype of nanovesicular formulations.
	IQAC	Institut de Química Avançada de Catalunya.
	IR	Infrared.
	ISO	International Organization for Standardization.
	ITC	Isothermal titration calorimetry.
	IV	Intravenous.
K	**kDa**	KiloDaltons = 10^3 Daltons.
	kg	Kilogram = 10^3 grams.
	KO mouse	Knockout mouse, with inactivated genes by biotechnological processes.

kV Kilovolt = 10^3 volts.

K^+ Potassium cation (positively charged ion).

L

L Liter.

LAL Limulus amebocyte lysate.

LB Luria Broth media.

LC-MS/MS Liquid chromatography-mass spectrometry.

LOD Limit of detection.

LOQ Limit of quantification.

LP Liposomes (composed of DPPC and chol).

$LP_{(gluc)}$ Liposomes diafiltrated and 7.5-fold concentrated by TFF in glucose 5 % (w/v).

$LP_{(w)}$ Liposomes diafiltrated and 7.5-fold concentrated by TFF in water.

LP-RGD RGD-targeted liposomes (composed of DPPC, chol, chol-PEG_{400}-RGD (3 % mol) and MKC (5 % mol)).

$LP\text{-}RGD_{(gluc)}$ RGD-targeted liposomes diafiltrated and 7.5-fold concentrated by TFF in glucose 5 % (w/v).

$LP\text{-}RGD_{(w)}$ RGD-targeted liposomes diafiltrated and 7.5- or 16-fold concentrated by TFF in water.

LP-RGD_int RGD-targeted liposomes in 5 % EtOH + 1.2 % DMSO (v/v; intermediate prototypes).

LP-RGD-GLA RGD-targeted liposomes (composed of DPPC, chol, chol-PEG_{400}-RGD (3 % mol) and MKC (5 % mol)), with loaded GLA enzymes (added during DELOS-susp process).

LP-RGD-GLA_Ads RGD-targeted liposomes (composed of DPPC, chol, chol-PEG_{400}-RGD (3 % mol) and MKC (5 % mol)), with adsorbed GLA enzymes (added by titration).

LP-RGD-GLA-S RGD-targeted liposomes (containing loaded GLA-S enzyme).

$LP\text{-}RGD\text{-}GLAcmycH6\text{-}S_{(w)}$ RGD-targeted liposomes (containing loaded GLAcmycH6-S enzyme) diafiltrated and 7.5-fold concentrated by TFF in water.

$LP\text{-}RGD\text{-}GLAcmycH6\text{-}S_{(w)}_Ads$ RGD-targeted liposomes (containing adsorbed GLAcmycH6-S enzyme) diafiltrated and 7.5-fold concentrated by TFF in water.

LP-RGD-GLAcmycH6-S_int RGD-targeted liposomes (containing loaded GLAcmycH6-S enzyme) in 5 % EtOH + 1.2 % DMSO (v/v; intermediate prototypes).

LP-RGD-GLAcmycH6-S_int_Ads RGD-targeted liposomes (containing adsorbed GLAcmycH6-S enzyme) in 5 % EtOH + 1.2 % DMSO (v/v; intermediate prototypes).

$LP\text{-}RGD\text{-}GLAcmycH6\text{-}T_{(w)}$ RGD-targeted liposomes (containing loaded GLAcmycH6-T enzyme) diafiltrated and 7.5-fold concentrated by TFF in water.

$LP\text{-}RGD\text{-}GLAcmycH6\text{-}T_{(w)}_Ads$ RGD-targeted liposomes (containing adsorbed GLAcmycH6-T enzyme) diafiltrated and 7.5-fold concentrated by TFF in water.

LP-RGD-GLAcmycH6-T_int RGD-targeted liposomes (containing loaded GLAcmycH6-T enzyme) in 5 % EtOH + 1.2 % DMSO (v/v; intermediate prototypes).

LP-RGD-GLAcmycH6-T_int_Ads RGD-targeted liposomes (containing adsorbed GLAcmycH6-T enzyme) in 5 % EtOH + 1.2 % DMSO (v/v; intermediate prototypes).

LP-RGD-GLAH6-T$_{(w)}$ RGD-targeted liposomes (containing loaded GLAH6-T enzyme) diafiltrated and 7.5-fold concentrated by TFF in water.

LP-RGD-GLAH6-T$_{(w)}$_Ads RGD-targeted liposomes (containing adsorbed GLAH6-T enzyme) diafiltrated and 7.5-fold concentrated by TFF in water.

LP-RGD-GLAH6-T_int RGD-targeted liposomes (containing loaded GLAH6-T enzyme) in 5 % EtOH + 1.2 % DMSO (v/v; intermediate prototypes).

LP-RGD-GLAH6-T_int_Ads RGD-targeted liposomes (containing loaded GLAH6-T enzyme) in 5 % EtOH + 1.2 % DMSO (v/v; intermediate prototypes).

LP-RGD-GLA-S_int RGD-targeted liposomes (containing loaded GLA-S enzyme) in 5 % EtOH + 1.2 % DMSO (v/v; intermediate prototypes).

LP-RGD-GLA-S_int_Ads RGD-targeted liposomes (containing adsorbed GLA-S enzyme) in 5 % EtOH + 1.2 % DMSO (v/v; intermediate prototypes).

LP-RGD-GLA-S$_{(Cryo1)}$ RGD-targeted liposomes (containing loaded GLA-S enzyme) lyophilized in presence of the cryoprotectant composition named Cryo1.

LP-RGD-GLA-S$_{(Cryo2)}$ RGD-targeted liposomes (containing loaded GLA-S enzyme) lyophilized in presence of the cryoprotectant composition named Cryo2.

LP-RGD-GLA-S$_{(gluc)}$ RGD-targeted liposomes (containing loaded GLA-S enzyme) diafiltrated and 7.5-fold concentrated by TFF in glucose 5 % (w/v).

LP-RGD-GLA-S$_{(w)}$ RGD-targeted liposomes (containing loaded GLA-S enzyme) diafiltrated and 7.5-fold concentrated by TFF in water.

LP-RGD-GLA-S$_{(w)}$_Ads RGD-targeted liposomes (containing adsorbed GLA-S enzyme) diafiltrated and 7.5-fold concentrated by TFF in water.

LP-0%MKC-RGD RGD-targeted liposomes without MKC (composed of DPPC, chol and chol-PEG$_{400}$-RGD (3 % mol)).

LP-0.5%MKC-RGD RGD-targeted liposomes with low amounts of MKC (composed of DPPC, chol, chol-PEG$_{400}$-RGD (3 % mol) and MKC (0.5 % mol)).

LP-0%RGD-GLA-S Liposomes without targeting ligand (composed of DPPC, chol and MKC (5 % mol)), but containing loaded GLA-S enzyme.

LP-0%RGD-GLA-S$_{(gluc)}$ Liposomes without targeting ligand (containing loaded GLA-S enzyme), diafiltrated and 7.5-fold concentrated by TFF in glucose 5 % (w/v).

LP-0%RGD-GLA-S_int Liposomes without targeting ligand (containing loaded GLA-S enzyme), in 5 % EtOH + 1.2 % DMSO (v/v; intermediate prototypes).

LP-6%RGD-GLA-S Liposomes with high amounts of targeting ligand (composed of DPPC, chol, chol-PEG$_{400}$-RGD (6 % mol) and MKC (5 % mol)), but containing loaded GLA-S enzyme.

LP-6%RGD-GLA-S$_{(gluc)}$ Liposomes with high amounts of targeting ligand (containing loaded GLA-S enzyme), diafiltrated and 7.5-fold concentrated by TFF in glucose 5 % (w/v).

LP-6%RGD-GLA-S_int Liposomes with high amounts of targeting ligand (containing loaded GLA-S enzyme), in 5 % EtOH + 1.2 % DMSO (v/v; intermediate prototypes).

LPS	Lipopolysaccharides.
LSD	Lysosomal storage disorder.
LUV	Large unilamellar vesicle.
Lys	Lysine aminoacid.

M

M	Molar or mol/liter.
m	Meter.
mAb	Monoclonal antibody.
MALDI-TOF	Matrix assisted laser desorption ionization time-of-flight.
MALS	Multi-angle light scattering detector.
MANTRA project	Enzyme MutANts as tools in the quest for improved TheRapies for FAbry Disease project.
MB %	Mass balance.
MBP	Maltose-binding protein.
MDV	Manual depressurization pump used in DELOS-susp plants.
MeOH	Methanol.
mEq	Milliequivalent (unit of measure for electrolytes).
mg	Milligrams = 10^{-3} grams.
MgFFF	Magnetic field flow fractionation.
MIC	Minimal inhibitory concentration.
min	Minutes.
MKC	Miristalkonium chloride.
mL	Milliliters = 10^{-3} liters.
MLV	Multilamellar vesicle.
mm	Millimeters = 10^{-3} meters.
mM	Millimolar = 10^{-3} mol/liter.
MPa	MegaPascals = 10^{6} Pascals.
MP_A	Mobile phase A (mainly aqueous solution) in HPLC methodologies.
MP_B	Mobile phase B (mainly organic solution) in HPLC methodologies.
mOsm	Milliosmole = 10^{-3} osmoles.
mPES	Modified polyethersulfone.
MS	Magnetic agitation.
MTX	Methotrexate hydrate.
mV	Millivolts = 10^{-3} volts.

MVD Maximum valid dilution.

MVP Major vault protein.

MVV Multivesicular vesicle.

mW Milliwatts = 10^{-3} watts.

MW Molecular weight as g/mol.

m/m Mass/mass.

m/z Mass-to-charge ratio in mass spectrometry.

M6P Mannose-6-phosphate moiety.

N

NaCl Sodium chloride.

Na_2HPO_4 Sodium phosphate dibasic.

$NaH_2PO_4 \cdot 2H_2O$ Sodium phosphate monobasic dihydrate.

NANBIOSIS Infraestructura Integrada de Producción y Caracterización de Nanomateriales, Biomateriales y Sistemas en Biomedicina.

Nano-GLA-v1 First version of GLA-loaded nanoliposomal formulation (membrane composition of DPPC, chol and chol-PEG_{200}-RGD; and GLAH6-T as loaded enzyme version).

Nano-GLA-v2 Second version of GLA-loaded nanoliposomal formulation (membrane composition of DPPC, chol, chol-PEG_{200}-RGD and MKC; and Replagal® as loaded enzyme version).

Nano-GLA-v3 Third version of GLA-loaded nanoliposomal formulation (membrane composition of DPPC, chol, chol-PEG_{400}-RGD and MKC; and GLAcmycH6-S as loaded enzyme version).

Nano-GLA-v4 Optimal version of GLA-loaded nanoliposomal formulation (membrane composition of DPPC, chol, chol-PEG_{400}-RGD and MKC; and GLA-S as loaded enzyme version).

NaOH Sodium hydroxide.

Na^+ Sodium cation (positively charged ion).

NBT Nanobiotechnology research group from IBB-UAB.

NCL Nanotechnology Characterization Laboratory.

NCL-NCI Nanotechnology Characterization Laboratory-National Cancer Institute.

ng Nanograms = 10^{-9} grams.

NIBS Non-invasive backscatter technology.

Ni^{2+} Niquel divalent cation (positively charged ion).

nm Nanometers = 10^{-9} meters.

NMR Nuclear magnetic resonance.

NOESY-NMR Nuclear overhauser effect spectroscopy-nuclear magnetic resonance.

nrSDS-PAGE Non-reducing-sodium dodecyl sulfate polyacrylamide gel electrophoresis.

	ns	Nanoseconds = 10^{-9} seconds.
	NTA	Nanoparticle tracking analysis.
	N/A	Do not apply.
	N/P	Ratio of nitrogen residues / pDNA phospates in polyplexes used for TGE.
	N_2	Nitrogen.
	Nº	Number
O	**ODD**	Ophan drug designation.
	Osm	Osmole.
P	**P**	Cellular pellet obtained after culture centrifugation.
	Pa	Pascals.
	PBS	Phosphate buffered saline.
	P_c	Critical pressure.
	PCR	Polymerase Chain Reaction technique to amplify specific DNA segments.
	PCT	Pharmacological chaperone therapy.
	PDB	Protein Data Bank.
	PdI	Polydispersity index of particle populations.
	pDNA	Plasmid of DNA.
	PEC	Polyelectrolyte complexes.
	PEG	Polyethylene glycol moiety.
	PEI	Polyethylenimine (a hydrophilic cationic polymer).
	PES	Polyethersulfone material.
	pH	Hydrogen potential (measure of the proton concentration in a substance).
	Ph.D.	Latin phrase "*philosophiae doctor"* meaning "Doctorate of Philosophy".
	Ph.Eur	European Pharmacopoeia.
	Phe	Phenylalanine aminoacid.
	PI	Pressure indicators.
	pI	Isoelectric point.
	P_M	Permeate fraction obtained after the filtration-centrifugation method.
	PMT	Photomultiplier tubes.
	PoC	Proof of Concept.
	Poly-Arg	Aminoacid secuences of successive arginins used as purification tags.

	Poly-Arg	Aminoacid secuences of successive arginins used as purification tags.
	ppm	Parts per million = 1 μg/mL.
	PPP	Protein Production Platform unit U1 of NANBIOSIS.
	PPPs	Production process parameters.
	PT	Potentiometry.
	PTA	Particle tracking analysis.
	PTFE	Polytetrafluoroethylene material.
	PTM	Post-translational modification.
	P_w	Working temperature.
	P7.5	Small lab-scale plant to produce nanovesicular batches of 25 – 75 mL by DELOS-susp method.
	P25 and P100	Intermediate lab-scale plant to produce nanovesicular batches of 250 – 1500 mL by DELOS-susp method.
Q	**QbD**	Quality by design.
	QC	Quality control.
	QELS	Quasi-elastic light scattering.
	qPCR	Quantitative polymerase chain reaction.
	QTTP	Quality targeted product profile.
	q.s.	Latin term "*quantum sufficit"* meaning "as much amount as is sufficient".
R	**RES**	Reticuloendothelial system.
	R_g	Radius of gyration, also denominated as root mean square radius.
	RGD	Tripeptide Arginine-Glycine-Aspartic acid.
	RGD-targeted nanoliposomes	Nanoliposomal formulations containing chol-PEG_n-RGD moiety as targeting peptide.
	RH	Relative humidity.
	R_h	Hydrodynamic radius, also denominated as Stokes radius.
	RI	Refractive index.
	RL	Ringer-Lactate solution.
	r,nr-SDS-PAGE	Reducing, non-reducing-sodium dodecyl sulfate polyacrylamide gel electrophoresis.
	rpm	Revolutions per minute.
	RP-HPLC-ELSD	Reversed-Phase High-Performance Liquid Chromatography coupled to an evaporative light scattering detector.
	RP-HPLC-UV	Reversed-Phase High-Performance Liquid Chromatography coupled to an ultraviolet

		detector.
	R_s	Theoretical geometric radius value of a solid sphere.
	RS	Remote sensing.
	RSD	Relative standard deviation.
	RT	Retention time.
	R_T	Retentate fraction obtained after the filtration-centrifugation method.
	R.T.	Room temperature.
	R^2	Correlation coefficient.
S	**S**	Stirrer.
	s	Seconds.
	SA	Sinapinic acid.
	SANS	Small angle neutron scattering.
	SAXS	Small angle x-ray scattering.
	SCAC	Servei de Cultius Cel·lulars, Producció d'Anticossos i Citometria.
	s.d.	Standard deviation.
	SDS	Sodium dodecyl sulfate.
	SDS-PAGE	Sodium dodecyl sulfate polyacrylamide gel electrophoresis.
	SEC	Size-exclusion chromatography.
	SEC-HPLC	Size-exclusion chromatography-high-performance liquid chromatography.
	SeFFF	Sedimentation field flow fractionation
	SEM	Standard error of the mean.
	SF4	Symmetric flow field flow fractionation.
	SLM	Standard liter per minute.
	SMD	Small molecule drug.
	SN	Supernatant fraction without cell content after culture centrifugation.
	SNR	Signal-to-noise ratio.
	SP	Syringe pump used in the DELOS-susp installation.
	SPARTA	Single Particle Automated Raman Trapping Analysis.
	STR	Substrate reduction therapy.
	SUV	Small unilamellar vesicle.

T	**T**	Time.
	T_c	Critical temperature.
	TEM	Transmission electron microscopy.
	TFA	Trifluoroacetic acid.
	TFF	Tangential flow filtration.
	TGE	Transient gene expression.
	TGX	Tris-Glycine-eXtended Stain-Free™ FastCast™ Acrylamide
	ThFFF	Thermal field flow fractionation.
	TI	Temperature indicator.
	T_m	Melting temperature (50 % folded protein, and 50 % unfolded protein).
	TMC	Trimethyl chitosan.
	TMP	Transmembrane pressure.
	TPP	Target product profile.
	TRL	Technology Readiness Level.
	Trp	Tryptophan aminoacid.
	TSI	Turbiscan stability index.
	T_w	Working temperature.
U	**UAB**	Universitat Autònoma de Barcelona.
	UK	The United Kingdom.
	USA	United States of America.
	USP	United States Pharmacopeia classification.
	UV	Ultraviolet light.
	UV-Vis	Ultraviolet-visible.
	U1	Platform unit one of NANBIOSIS.
	U6	Platform unit six of NANBIOSIS.
V	**V**	Volume.
	V_{AS}	Volume of aqueous solution used in DELOS-susp methodology.
	V_{AS}:V_{OS}	Volumetric ratio between the aqueous and the organic solution.
	V_f	Final volume.
	V_i	Initial or original volume.
	V_{OS}	Volume of organic solution used in DELOS-susp methodology.

	VPA	Valproic acid.
	vs	Latin word "*versus*" meaning "in opposition to".
	v/v	Volume/volume.
	V-001 to V-005	Valves used in DELOS-susp plants.
W	**w**	Water.
	WFI	Water for injection.
	w/v	Weight/volume.
	w/w	Weight/weight.
X	$\mathbf{X_{CO_2}}$	CO_2 molar fraction.
#	**º**	Degree (angle).
	ºC	Degrees Celsius.
	€	Euros.
	%	Percentage.
	µg	Micrograms = 10^{-6} grams.
	µL	Microliters = 10^{-6} liters.
	µm	Micrometers = 10^{-6} meters.
	µM	Micromolar = 10^{-6} mol/liter.
	µmol	Micromoles = 10^{-6} moles.
	ζ-potential	Superficial charge of particle populations.
	λ	Wavelength.
	λ_{Abs}	Wavelength of absorbance.
	λ_{em}	Wavelength of emission (for fluorescence spectra).
	λ_{ex}	Wavelength of excitation (to a fluorochrome).
	4-MU	4-Methylumbelliferone (fluorescent product).
	4-MUG	4-methylumbelliferyl-α-D-galactopyranoside (non-fluorescent substrate).
	6-His tag	Six-histidine (HHHHHH) tag for protein purification and detection aims.

1

INTRODUCTION: BIOMOLECULE-BASED NANOPHARMACEUTICALS

1.1. Biomolecules for therapeutic applications

Pharmacology is a medicinal-based science practiced since ancient ages to treat diseases with available natural products (e.g. plants, animals and minerals) of poor purity and concentration. The influence of this primary concept is still present nowadays, and the use of traditional natural therapies or specific diets has become popularly practiced as part of the "complementary medicine" field. However, the modern discipline of clinical pharmacology was recently born at the middle of the 19th century with the discovery and isolation of potential bioactive substances (e.g. morphine from opium by Friederich Sertürner, chloroform) and their specificity of actions (i.e. chemical properties, affinity to organs or tissues, etc.), together with the possibility of artificially synthesize organic molecules (e.g. urea synthesis by Friedrich Wöhler)[1–5]. Since then, several active substances (also known as drugs) have been investigated for biomedical purposes such as prevention, diagnosis, treatment or cure of diseases.

During the initial stages of the clinical pharmacology, the scientific community put huge effort in the screening and discovery of new small molecule drugs (SMDs). These compounds of small size (< 1000 Da), high purity and well-described chemical structure can be modified or artificially produced from organic and/or inorganic substances via chemical synthesis (e.g. aspirin, antihistamines, penicillin, ibuprofen, etc.). They high stability and easily membrane permeation capacity allow their easy administration by the oral route. Although the use of SMDs is predominant in the market (around 90 %), several conventional molecules show limitations such as non-targeting capacity, low selectivity, high toxicity and poor efficacy[6–9].

The use of biopharmaceuticals as alternative strategies to SMDs emerged in the past three decades, together with the advances in the recombinant DNA technology. As an example, the recombinant human insulin protein was the first commercially approved biopharmaceutical in 1982 by the United States Food and Drug

Administration (FDA) as a biotechnological product for the treatment of diabetes mellitus. Biopharmaceuticals are therapeutic biomolecules (e.g. enzymes, monoclonal antibodies, hormones, vaccines, nucleic acids, cytokines, etc.) produced using biotechnological approaches. These biological drugs are large and complex structures with improved efficacy in contrast to SMDs, due to their higher targeting capacity and specificity which reduce the probability of side effects. However, they also show drawbacks like higher immunogenicity issues and instability than SMDs[6–9]. Characteristics from both types of pharmaceutics, SMDs and biopharmaceuticals, are compared in ***Table 1.1***.

Table 1.1. Comparison of characteristics between SMDs and biotechnological products. Adapted from[6–9].

Characteristic	SMDs	Biopharmaceuticals
Size	Small size Low molecular weight (< 1 kDa)	Large size High molecular weight (> 1 kDa)
Chemical structure	Simple and well-defined	Complex and heterogeneous
Cell permeability	Usually good	Not good
Target selectivity	Low	High
Stability	Stable	Unstable
Immunogenicity	Mostly non-immunogenic	Immunogenic
Manufacturing process (Physicochemical properties dependance)	Chemical synthesis procedures High reproducibility (Mostly process-independent)	Living cell-based biotechnology Batch-to-batch variability (Strongly process-dependent)
Administration route	Primarily oral	Primarily intravenous

Administration routes of pharmaceuticals

Nowadays, both SMDs and/or biopharmaceuticals can be chosen as treatments depending on their bioavailability to reach the desired target. The bioavailability of a drug is determined by the fraction of administered drug capable to be distributed through the systemic circulation until its site of action without being cleared from the system. The drug permeability, stability, immunogenicity and distribution are parameters that impact on molecule bioavailability. However, the pharmaceutical efficiency is not only determined by the intrinsic characteristics of drugs, but also by the administration route used[10].

Shortly, based on the drug action site the administration routes are classified as: i) local (i.e. the action of the drug is localized to the administration site), as for instance topical administration, or ii) systemic (i.e. drugs can be distributed over the whole body). The systemic routes can be subclassified as: i) enteral (e.g. oral, sublingual, and rectal), or ii) parenteral (e.g. intravenous, intramuscular, inhalation, and subcutaneous). Enteral routes force

the “first-pass metabolism” of a drug, i.e the pass through a biological barrier toward the systemic circulation, where drugs can be eliminated by enzymes. SMDs can be orally administrated due to their high permeability across gastrointestinal tissues, and high stability against metabolic enzymes. On the contrary, bioavailability of biopharmaceuticals is substantially reduced by “first-pass metabolism”. For this reason, biopharmaceuticals are directly injected or infused into bloodstream via intravenous (IV) administration[7,8,10], which allow better drug bioavailability, and in general, quicker drug efficiency (*Figure 1.1*).

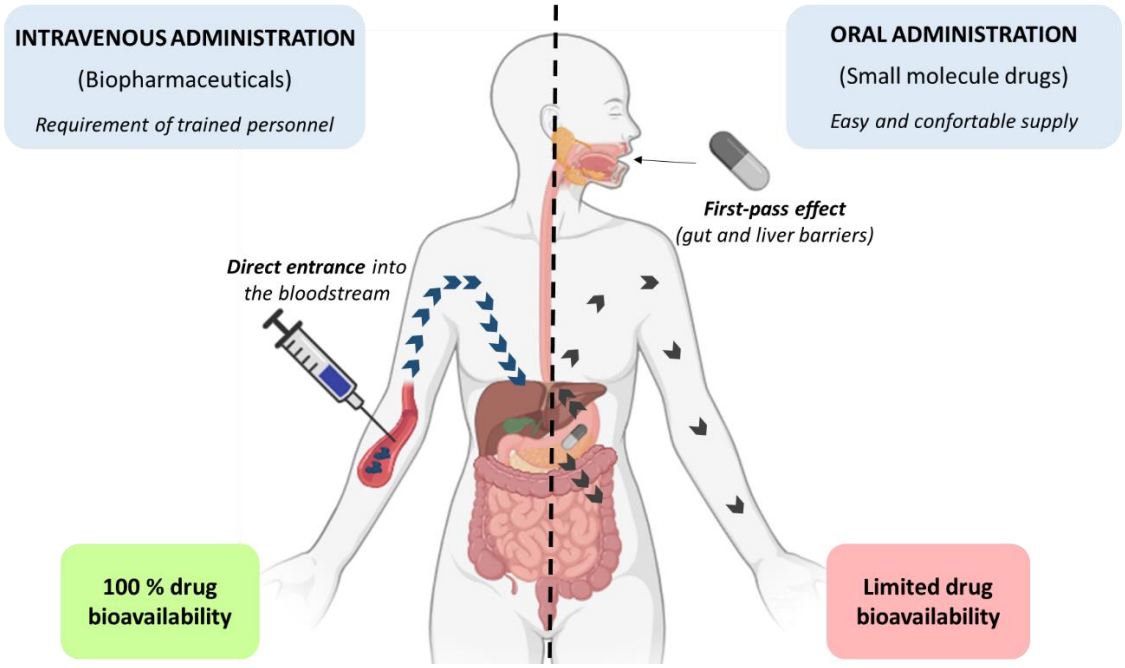


Figure 1.1. Comparison between IV and oral drug administration routes.

It is important to point out that the final drug efficiency depends on the physicochemical properties of the biomolecules (e.g. size, charge, receptor-mediated targeting, etc.) that influence their distribution and clearance from the system. For example, SMDs are habitually filtered through the kidneys due to their small molecular weight, and metabolized by liver enzymes. Meanwhile, the elimination of biopharmaceuticals is influenced by their sizes, being normally also mediated by renal clearance with biomolecules smaller than 69 kDa, or by cellular uptake and further degradation in the endo-lysosomal pathway for larger biocomplexes[8,11].

1.1.1. Mammalian cell factories for the biosynthesis of high-quality recombinant proteins

Many serious diseases are caused by the dysfunction or null synthesis of proteins in human cells. Thus, their complementation or substitution with recombinant proteins (e.g. monoclonal antibodies, enzymes, hormones, etc.) used as biopharmaceuticals is suffering an increasing demand, being recently around the 10 % of the entire drug market despite their recently discovered potential in the last three decades[12–14].

Recombinant proteins can be produced in a large variety of cellular platforms, including bacteria, yeasts, insect cells, mammalian and plant cells. Each expression system has a different impact on the protein production yield, drug development costs and scalability, as well as, in the product quality. A comparison of some production systems is represented in ***Table 1.2***.

Table 1.2. Comparison of expression systems used for the production of recombinant biopharmaceuticals. Adapted from[12–14].

Cell factory	Production time	Production yield	Production costs	Scalability	Product quality
Escherichia coli (bacteria)	Low	Medium	Low	High	Low
Yeast	Medium	High	Medium	High	Medium
Insect cells	Medium	High	Medium	High	Medium
Mammalian cells	High	Medium-high	High	Medium	High
Plant cells	Medium	High	Medium	Medium	High

The quality of a biomolecule is dictated by those physical, chemical, biological, or microbiological properties that, within a well-defined range, are capable to ensure its efficacy and safety[15,16]. These features are usually called critical quality attributes (CQAs), and the most important ones to control in proteins are listed in ***Table 1.3***.

Table 1.3. CQAs of recombinant proteins and proposed analytical methods for their control.

CQA	Analytical method
Identity:	
Molecular weight	r,nr-SDS-PAGE & MALDI-TOF
Isoelectric point	cIEF
Purity	r,nr-SDS-PAGE
Bioactivity	*In vitro* assays (specific for each case)
Product-related impurities:	
Low molecular weight forms (Degradation products)	r,nr-SDS-PAGE
High molecular weight forms (Aggregation products)	HPLC-SEC, supported by DLS and NTA
Protein glycosilation (Structural glycoform variants)	HPLC-HILIC
Process-related impurities:	
Host cell DNA	UV-Vis spectroscopy
Endotoxin presence	LAL assays
Microbiological content	Agar plates

r,nr-SDS-PAGE: reducing, non-reducing-sodium dodecyl sulfate polyacrylamide gel electrophoresis; MALDI-TOF: matrix-assisted laser desorption/ionization-time-of-flight; cIEF: capillary isoelectric focusing; HPLC-SEC: high-performance liquid chromatography- size-exclusion chromatography; DLS: dynamic light scattering; NTA: nanoparticle tracking analysis; HPLC-HILIC: high-performance liquid chromatography-hydrophilic interaction liquid chromatography; UV-Vis: ultraviolet-visible; and LAL: limulus amebocyte lysate.

The physicochemical and biological CQAs are strongly determined by the production platform of choice, which at the same time is imposed by the post-translational modification (PTM) requirements of the target protein to express. The protein glycosylation is an example of PTM involving conserved organism-dependent processes during which carbohydrates or oligosaccharides molecules are covalently attached to the target protein macromolecule, to ensure proper protein folding, targeted transport, cellular localization and functional activity[17]. A large proportion of biopharmaceuticals do not require glycosylation or other PTMs, enabling their synthesis in cheaper platforms, most commonly *Escherichia coli* (bacteria) followed by *Pichia pastoris* and *Saccharomyces cerevisae* (yeasts)[12,18]. However, some therapeutic enzymes need to be glycosylated to be biologically functional. Besides, biopharmaceuticals must be sterile if they are administered by the IV route, for example. By using mammalian cells as expression systems, the risk of product contamination with bacteria endotoxins (i.e. pyrogenic bacteria molecules) is drastically reduced. For these main reasons, mammalian cell systems are the preferred "cell factory" of choice in the industry for the expression of proteins with human-like native structure and functional activity, although they are time-consuming and expensive methods[14,18]. The 67 % of approved recombinant biopharmaceutics during the last decade have been expressed in mammalian cells such as Chinese hamster ovary (CHO), human embryonic kidney (HEK), NS0 mouse myeloma cells, or baby hamster kidney (BHK) among others[18].

Although new expression systems and biotechnological tools are continuously being tested to improve the quality of recombinant proteins, many biotherapeutics do not accomplish the required CQAs to be used as therapies due to poor stability and bioavailability. New strategies are currently being investigated in the nanopharmaceutical field to overcome the limitations of biomolecules.

1.2. Nanocarriers in nanopharmaceutical development

The nanotechnology field was originally born with the aim of manipulating materials containing at least one nanoscale dimension (from 1 – 100 nm) to develop new structures with practical application in a wide range of disciplines (e.g. energy, medicine, environmental science, optics and electronics, organic chemistry, among many others)[19–21]. In this context, nanomedicine refers to any medical application where nanotechnology is combined with biomedical sciences and pharmaceutics. As one of its main goals, nanomedicine pursue the design and development of engineered nanoscale structures to be used as drug delivery systems (DDS) capable to encapsulate active pharmaceutical ingredients (APIs) conferring protection from degradation or clearance, controlled release and specific delivery of the API to the intended site of action[22–25]. Therefore, the use of nanopharmaceuticals as DDS allows the achievement of specific drug biodistribution across the required

biological membranes, and also the increase of drug concentration only in the target tissues, leading to improved efficacy, safety and toxicological profiles than conventional drug therapies[26,27].

The most efficient route for DDS is by IV administration (parenteral route), where the drug is directly delivered into the systemic circulation in a rapid and simple method. Since DDS usually have low tissue permeation capacity, enteral routes (e.g. oral or rectal administration) are not much efficient due to therapeutics should pass through the gastrointestinal system[27–29]. Once in bloodstream, therapeutics can be eliminated or cleared from the human system by the different detoxification organs (e.g. kidneys, liver and spleen) depending on their nanometric size. Small particles (< 8 nm) are quickly eliminated by the kidneys and excreted through the urine[30]. Nanopharmaceuticals from 8 to 20 nm are removed through the biliary secretions to the gut to be excreted. Larger structures than 200 nm are retained in the reticuloendothelial system (RES) mainly located in the liver and spleen[31]. The RES is composed of phagocytic cells such as monocytes and macrophages, which are immune system cells that recognize nanopharmaceuticals as foreign substances. Thus, the optimal sizes of therapeutic nanocarriers to increase the half-life of these systems in circulation should be between 50 and 200 nm. From the bloodstream, DDS can be distributed throughout the body in two different manners: based on passive or active mechanisms. Passive targeting occurs when administering nanopharmaceuticals (between 50 – 200 nm) without any targeting ligand, and consists on their accumulation within hyper-vascularized tissues with increased permeability, which normally are generated by pathologies such as cancer tumors. This phenomenon is known as enhanced permeability and retention (EPR) effect[32,33]. To avoid an undesired systemic distribution, the active targeting of DDS can be controlled by anchoring on their surface specific ligands (e.g. antibodies, peptides, proteins, small molecules, etc.) with high affinity to cell receptors expressed in determinate tissues or organs, facilitating the cellular uptake of the nanocarriers in the desired site of action[27,33,34].

Despite the several advantages of using nanoparticulated structures, some aspects must be addressed before their IV injection to avoid side effects in tissues and organs from the whole body[35–37]. The potential toxicity of nanopharmaceuticals must be controlled by determining the biocompatibility and biodegradability of their composition. Also, the physicochemical stability of nanopharmaceuticals in physiological conditions is required to avoid the generation of bigger sized populations of nanostructures which could provoke blockages and inflammation of blood capillaries, i.e. embolism and phlebitis[35].

All the nanosystems' characteristics above can be summarized in some advantages of the intravenous use of DDS as therapeutic platforms, but also potential limitations to address when their physicochemical properties are not well-controlled (***Table 1.4***). Briefly, the size and tuneability of nanocarriers offer advantages like: i) enhanced drug protection and stability during circulation, which allows ii) increased half-life in bloodstream; iii) controlled

drug release in a sustained manner, achieving therapeutic benefits using iv) reduced dosing and/or frequency; v) possible passive accumulation by EPR (e.g. for cancer treatments); vi) targeted drug delivery given by functionalization of DDS surfaces, leading to vii) improved bioavailabity and efficacy, as well as, viii) specific biodistribution with decreased side effects and ix) reduced toxicity of healthy tissues[38–41]. In contrast, DDS can show limitations as: i) limited loading capacity that tends to be spatially reduced; ii) composition-depending toxicity; iii) nanosystem instability in physiological and storage conditions causing undesired side effects, apart from iv) drug burst release due to nanostructure breakage; v) limited efficacy due to undesired EPR or RES phenomena; vi) use of intravenous infusion as invasive method of administration, which require trained staff for the drug injection; vii) high manufacturing costs and viii) difficult scale-up under good manufacturing practices (GMP) attributable to their complex production protocols; ix) slow and arduous regulatory of DDS as a consequence of the lack of standardized guidelines[39,40,42–44].

Table 1.4. Advantages and disadvantages of nanopharmaceuticals. Adapted from[27,38–44].

Generic advantages of nanosystems	Possible limitations of nanosystems
Protection from degradation and clearance	Limited loading capacity
Longer drug circulation time	Composition-depending toxicity
Controlled drug release	Nanocarrier unstability (e.g. size, shape, charge, etc.) provoking undesired side effects
Reduced dosing and/or frequency	Drug burst release by nanosystem breakage
Enhancing drug permeability (EPR) for passive accumulation strategies	Limited efficacy due to undesired enhancing drug permeability (EPR) or reticuloendothelial system (RES) phenomena
Targeted drug delivery (moldable functionalization of the surface)	Invasive administration route (e.g. IV administration)
Improved bioavailability and efficacy	High manufacturing cost
Specific biodistribution with limited side effects	Challenging scale-up procedures under GMP
Decreased cytotoxicity of healthy tissues	Slow and arduous regulatory

1.2.1. Challenges in the development of nanopharmaceuticals

Despite the therapeutic benefits and the great potential of nanopharmaceuticals, the great progress made in the development in academia is not reflected yet in the transition to clinical practice and industrial acceptance. In most cases, failure to progress beyond the clinical phase is the norm. Some of the challenges that need to be addressed are: i) to ensure a high quality of these innovative complex nanostructures for preclinical (and further clinical) testing, ii) to use non-conventional analytical techniques for quality control (QC), iii) to meet with

pharmaceutical standards and regulations, iv) to face the increasing costs as development progresses, and v) the manufacturing methods and most of the equipment for their characterization and QC are not standard in the pharmaceutical industry[45].

1.2.1.1. Quality

The quality of these complex nanostructures must be ensured so that they can be translated into pharmaceutical products, since this has a significant impact on the safety and efficacy[46].

Since nanopharmaceuticals can be highly complex structures very linked not only to their chemical composition but also to their nanoscale properties (including the organization of the nanostructures at the supramolecular and nanoscopic level), their quality control is very challenging and requires the use of advanced non-conventional analytical techniques, as well as the compliance with the regulatory requirements.

1.2.1.1.1. Regulatory compliance requirements

The FDA and the European Medicines Agency (EMA) are responsible for ensuring the quality of medicines from a safety and efficacy perspective during the drug approval process. The US Pharmacopoeia (USP) and the European Pharmacopoeia (Ph.Eur) do not provide specific methods for nanomedicines. However, the EMA, the FDA, the International Organization for Standardization (ISO) and the American Society for Testing and Materials (ASTMA International) have published several guidelines, standardized evaluation methods, perspectives and reports specifically dedicated to the physicochemical and biological characterization of engineered nanomaterials[37,47–50]. Such guidelines also refer to the use of two important quality standards when advancing in the nanopharmaceutical development process: i) good laboratory practices (GLP) to ensure the generation of reliable data during preclinical trials[46,51], and ii) GMP to guarantee the consistent and reproducible production and characteristics of the proposed drug product[46,52].

1.2.1.1.2. Quality by design approach as a systematic tool for the development of nanopharmaceuticals

Moreover, the design and development focus on drug products must be simplified by changing the traditional formulation-driven research to an oriented clinical-driven needs and rational pattern, in order to allow the translation of the basic research into clinical applications[21,46]. In this context, the FDA and the International Council for Harmonization of Technical Requirements for Pharmaceuticals for Human Use (ICH) strongly recommend, through the ICH guidelines Q8 (R2), Q9 and Q10, the implementation of the quality by design (QbD) concept as a suitable methodology to develop robust drug manufacturing, ensure and improve the quality of

pharmaceutics, validate control methods and establish relationships between material or manufacturing variables with the product CQAs[21,53–56]. Since the initial stage of research and development, the QbD approach consists of taking into account the desired final quality that the product must have, i.e. the philosophy of this concept is to start with the end in mind taking into account the intended use, the dosage form, the administration route, and so on, what is known as defining the target product profile (TPP)[46,55,56]. During this process, the identification of CQAs and critical process parameters (CPPs) are crucial to obtain a high degree of manufacturing control and the understanding of how process parameters can impact on the quality of the nanoformulation to consistently produce a high-quality product[21,53,57,58]. The CQAs of raw material and drug products refer to that properties capable to influence on medicines characteristics at physicochemical and biological level. In order to identify which formulation variables and CPPs can potentially impact on the CQAs and define control strategies, a risk assessment analysis is performed. By using a design of experiments (DoE), a design space that ensures that the product will be obtained with the desired quality (with the CQAs within the desired specifications) can be defined. The final objective of the QbD is to produce optimal products from the quality point of view which is crucial to guarantee the efficacy and safety.

The overall process regarding QbD approach is schematized in ***Figure 1.2***.



Figure 1.2. Representation of the QbD approach.

1.2.1.2. Definition of the CQAs of nanopharmaceuticals

The CQAs of a product refer to those physical, chemical, biological, or microbiological characteristics that should be very well control within an appropriate limit, range, or distribution to ensure the desired product quality, since they can have a significant impact on the efficacy and safety of the finished product[53,59].

The CQAs of nanopharmaceuticals are related to particle size, size distribution, morphology, pH, surface charge (or ζ-potential), drug entrapment efficiency, surface functionalization (if any), among others. In general, a nanoformulation of high pharmaceutical quality should be homogeneous in size and morphology, with homogeneous drug entrapment efficiency, homogeneous distribution of the ligand on the surface of the nanoparticles for active targeting, bioactive, biocompatible and stable under storage conditions[60].

Since nanopharmaceuticals are complex structures in terms of nanoscale and supramolecular organization, they can differently impact on clinical efficacy and safety depending on their chemical composition, production parameters or intended route of administration. For these reason, in each case by case the CQAs must be well defined and evaluated.

In ***Table 1.5*** there are listed several CQAs of liposomal nanoformulations, which currently are the most advanced nanopharmaceutical products, and common techniques for their monitoring and control.

Table 1.5. Several major critical quality attributes of liposomal nanoformulations and common techniques for their monitoring[60].

	Liposome's quality attributes	Instrumental techniques
PHYSICOCHEMICAL ATTRIBUTES	**Particle size distribution**	Multiple techniques are recommended: - DLS - LD - PTA - Microscopy techniques (TEM, cryoTEM, AFM, SEM) - Fractionation techniques such as AFFF, SEC
	Morphology and/or structure	Electronic microscopy (TEM, cryoTEM, AFM) SAXS UV-vis spectroscopy Spectrofluorimetry NMR
	Surface charge (ζ-potential)	ELS
	Thermodynamic properties	DSC
	***In vitro* drug release**	Drug release monitoring in physiological/clinically relevant media using various methods: dialysis, reverse dialysis, fractional dialysis, microdialysis, ultracentrifugation, centrifugal ultrafiltration, pressure ultrafiltration, SEC, continuous flow method [61]
	Physical stability	Turbidity measurement
	Drug entrapment efficiency (drug entrapped in liposomes vs Total drug amount)	Separation of free versus entrapped drug: Solid-phase; Extraction; Size exclusion chromatography; Ultracentrifugation; Gel filtration; Dialysis Drug quantification: mass and optical spectrophotometry; HPLC; SDS-PAGE plus TGX
	Drug loading (drug-to-lipid ratio)	Lipid quantification: HPLC; Phosphorus assay Drug quantification: mass and optical spectrophotometry; HPLC; SDS-PAGE plus TGX
	Targeting ligand characterization	Quartz crystal microbalance Coating quantification as applicable – TGA, LC-CAD or ELSD SPR
	Osmolality and pH	Osmometer, pHmeter
	Degradation products	HPLC Mass and optical spectrophotometry
BIOLOGICAL ATTRIBUTES	**Bioactivity**	Appropriate methods based on the specific characteristics of the drug
	Biocompatibility	*In vitro* cytotoxicity/viability assays; hemocompatibility; immunogenicity
	Microbiological quality	Bacterial endotoxins assessment: LAL methods Mycoplasma contamination: PCR Microbial contamination: Agar plate

AFFF: asymmetrical-flow field flow fractionation; AFM: atomic force microscopy; cryo-TEM: cryogenic transmission electron microscopy; DLS: dynamic light scattering; DSC: differential scanning calorimetry; ELS: electrophoretic light scattering; HPLC: high performance liquid chromatography; LAL: limulus amebocyte lysate; LC-CAD: liquid chromatography with charged aerosol detection; LC-ELSD: liquid chromatography with evaporative light scattering detection; LD: laser diffraction; NMR: nuclear magnetic resonance; PCR: polymerase chain reaction; PTA: particle tracking analysis; SAXS: Small-angle X-ray scattering; SDS-PAGE: sodium dodecyl sulphate-polyacrylamide gel electrophoresis; SEC: size-exclusion chromatography; SEM: scanning electron microscopy; SPR: Surface Plasmon Resonance; TEM: transmission electron microscopy; TGA: thermogravimetric analysis; TGX: Tris-Glycine eXtended; MRI: magnetic resonance imaging; MS: mass spectrometry.

Regulatory challenges

From a regulatory perspective, there is a lack of standardized and common protocols for the preclinical development and physicochemical characterization steps required for translation to the clinic, and a lack of global regulatory ethics and guidelines.

Although regulatory authorities have provided of some guidelines specific for nanopharmaceuticals, due to the fact that these novel based systems are relatively new, there is still currently very little regulatory guidance in this area and still nanomedicines continue to be mostly regulated according to existing guidelines for conventional drugs. However, the properties of nanomedicines differs from those of traditional drug molecules, so nanopharmaceuticals are expected to have different pharmacokinetic and pharmacodynamic profiles. To address this problem, international regulatory agencies have convened specialized multidisciplinary groups (academics, clinicians and regulators) to work on the development of a global guideline for the evaluation and regulation of nanotechnology-based products[37,47–50,53–55,62,63].

The Nanotechnology Characterization Laboratory of the National Cancer Institute (NCL-NCI) is contributing to support the scientific community by providing standardized protocols of physical, chemical and biological characterization that help to overcome methodological gaps that exist in this field, working in coordination with the FDA.

1.2.2. Road of a nanopharmaceutical from the bench to the market

The complex process of bringing a new pharmaceutical product to the market and its correlation with Technology Readiness Level (TRL) scale applied to the field of pharmaceutical drug discovery is summarized in ***Figure 1.3***. TRL is the innovation management planning tool used in any project to evaluate and communicate the maturity and progression of the development of a new product or other technological innovation.

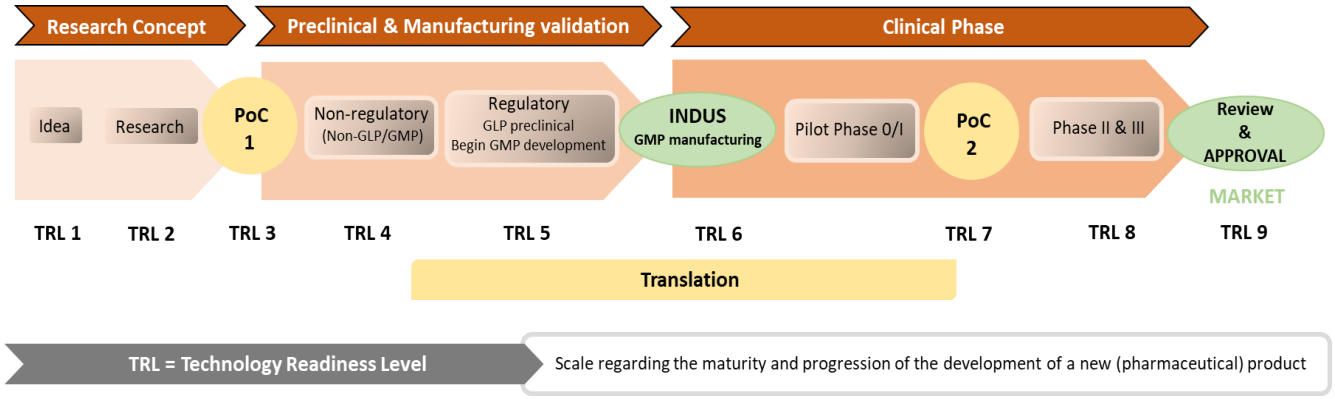


Figure 1.3. Overall process of research and development of a pharmaceutical product to reach the market. The correlation with the TRL is also represented.

Briefly, the pharmaceutical development is composed of three main phases: basic research, non-regulatory preclinical trials and regulatory preclinical trials. The initial phase of basic research and development consists on proposing a theoretical hypothesis (TRL-1), and performing preliminary studies of design, synthesis, candidate identification, technology concepts and development of methodologies (TRL-2), until a solid experimental Proof of Concept (PoC) is achieved (TRL-3)[64].

After this initial stage, the preclinical phase (TRL-4) is initiated with the validation of the prototype candidate in animal models to demonstrate efficacy and safety at non-regulatory preclinical level, as an exploratory phase. Then, regulatory preclinical phase starts (TRL-5), performing *in vivo* toxicity and safety assays mandatory under Good Laboratory Practices (GLP), which are a set of principles and guidelines that govern the conduct of non-clinical laboratory studies to ensure the quality, reliability, and integrity of non-clinical laboratory studies, and to provide confidence in the results generated from these studies. During TRL-5 phase also activities related to the scale-up of the manufacturing process from lab to pilot scale and compatibility with the Good Manufacturing Practice (GMP) regulations are carried out. GMP is a set of regulations and guidelines that govern the production and quality control of pharmaceutical products. GMP regulations ensure that these products are manufactured consistently and to a high quality. GMP are applied for products that are developed for use by human beings.

At TRL-6, the prototype is validated in an industrial environment and the clinical lots for human use are mandatory produced under GMPs. After regulatory approval, the clinical phase I, to assess the safety, and the clinical phase II, to assess the efficacy, begin (TRL-7); the clinical phase III confirms the efficacy and safety profile in a larger and more representative population (TRL-8). The last step consists of the product submission to regulatory authorities and approval for commercialization (TRL-9).

1.2.3. Therapeutic nanopharmaceuticals currently on the market or in clinical translation stages

There are many nanopharmaceuticals of distinct composition, shape, size, charge or surface functionality that have been developed to be used as potential nanocarriers for biomedical purposes. nanopharmaceuticlas such as DDS are usually associated by the nature of their material (***Figure 1.4***) and classified as inorganic nanoparticles (e.g. metallic, magnetic and silica nanoparticles, quantum dots, and carbon nanotubes), polymer-based nanoparticles (e.g. polymeric nanoparticles and micelles, dendrimers, and nanogels), lipid-based nanoparticles (e.g. liposomes, exosomes, micelles, solid-lipid nanoparticles, and other vesicles) and protein-based nanoparticles (e.g. virus-like particles, and protein conjugates)[27,65–68].

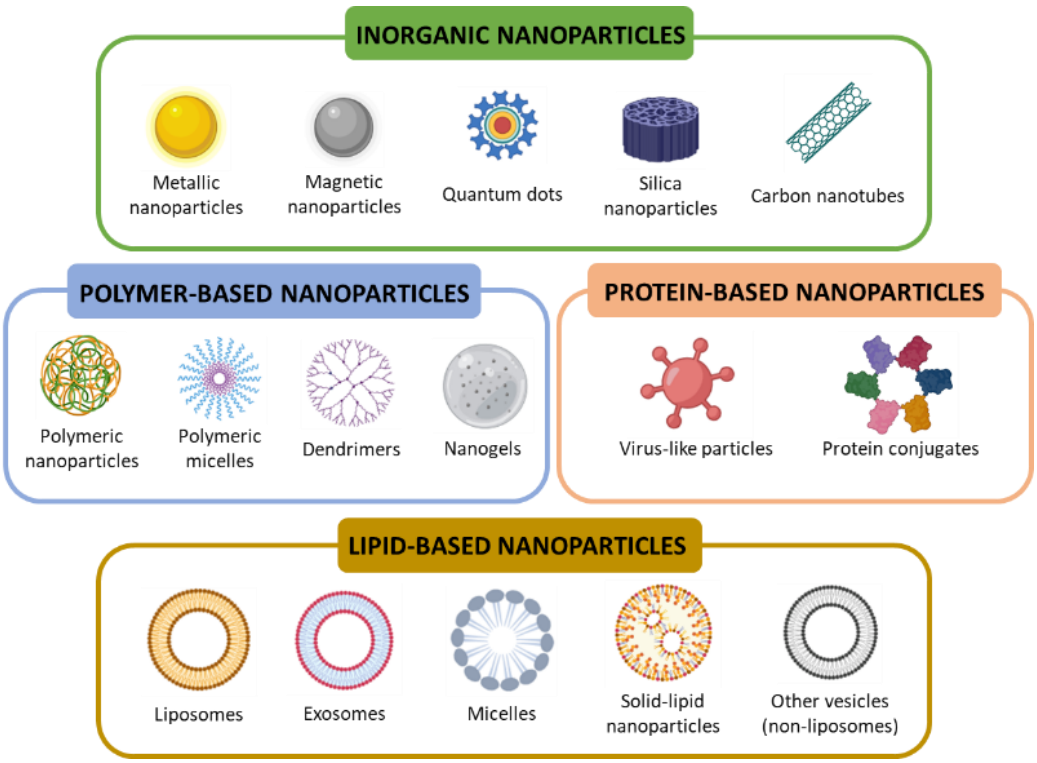


Figure 1.4. Schematized composition-based classification of distinct nanocarriers for biomedical applications. Adapted from[27,65–68].

So far, lipid-based nanoparticles (mainly liposomes) are the most widespread DDS (33 %) among the nanopharmaceuticals accessible on the market or along clinical translation, due to their outstanding advantages such as biocompatibility, biodegradability and great versatility in composition (***Figure 1.5***). Other potential competitors are: antibody-drug conjugates (15 %), polymer-drug conjugate (10 %), polymeric nanoparticles (10 %), virus-like particles (8 %), cell-derived vesicles like exosomes (4 %), inorganic nanoparticle (3 %), and other types of nanocarriers (e.g. emulsion, protein-based nanoparticle, micelle, nanocrystal, dendrimer, etc.)[21].

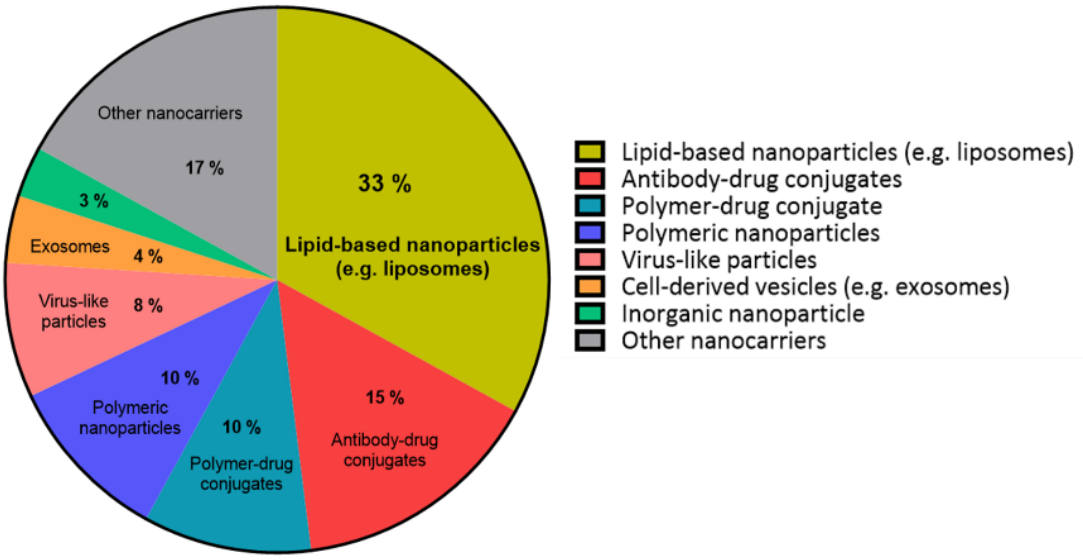


Figure 1.5. Types of nanopharmaceuticals on the market or under clinical translation during 2021. Adapted from Shan *et al.*[21].

1.3. Lipid-based vesicles as promising molecular self-assembled structures for drug delivery

Lipid-based nanovesicles are an attractive group of DDS to be administered intravenously for biomedical purposes. Lipid-based nanovesicles comprise the subgroup of lipid-based nanoparticles which are spherical-shaped bilayer vesicles constituted of amphiphilic molecules (*Figure 1.6*). The amphiphilic molecules are composed of two sections of different nature: one hydrophilic part (soluble in water) and another hydrophobic region (insoluble in water). Generally, the hydrophilic section is usually composed of a non-ionized or ionized polar head, meanwhile the hydrophobic part is constituted of non-polar tails. Once dispersed in water, these properties allow them to be self-organized as closed bilayers with an aqueous inner compartment[69–72]. In the lipid bilayer, amphiphilic molecules are oriented protecting the hydrophobic tails within the membrane and exposing their polar groups towards the aqueous phase[69,70].

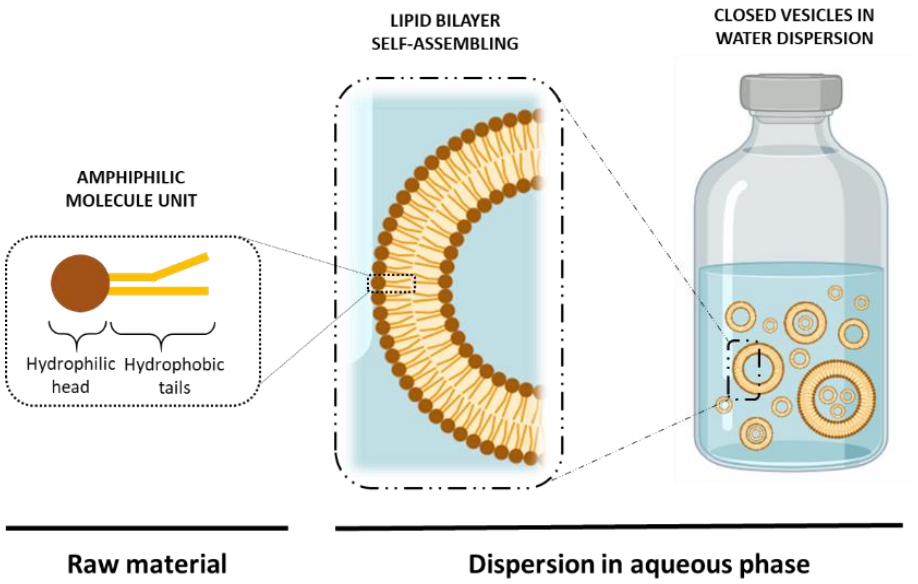


Figure 1.6. Overview of an amphiphilic molecule structure, and the vesicular self-organization of various amphiphilic units dispersed in water.

Size and lamellarity (i.e. number of bilayers) are crucial factors to take into account in order to control the performance of vesicles as drug nanocarriers[73,74]. Depending on the size of the self-assembled nanostructures, vesicles are classified as i) small (< 200 nm), ii) large (from 200 to 1000 nm) and iii) giant (> 1000 nm) vesicles; meanwhile regarding their lamellarity, they can be divided as i) unilamellar (single membrane) or ii) multilamellar (several concentric membranes). Thus, they are subgrouped in small unilamellar vesicles (SUVs), large unilamellar vesicles (LUVs), giant unilamellar vesicles (GUVs) or multilamellar vesicles (MLVs). In addition, they can be considered multivesicular vesicles (MVVs) if several small are entrapped into a larger one (***Figure 1.7***)[75,76]. SUVs have the best compromise of size for biomedical purposes, because they are large enough to avoid the rapid clearance through the kidneys, but small enough to be minimally uptake by the phagocytic cells from the reticuloendothelial system (RES), demonstrating prolonged circulation lifetime in bloodstream. Their size also favors the accumulation of SUVs within tumors through the enhanced permeability and retention (EPR) effect, and therefore, their application in cancer therapies[32,33]. Moreover, SUVs allow efficient and homogeneous surface functionalization, leading to more homogenous and sharper responses of the nanosystem to external stimulus[73,74].

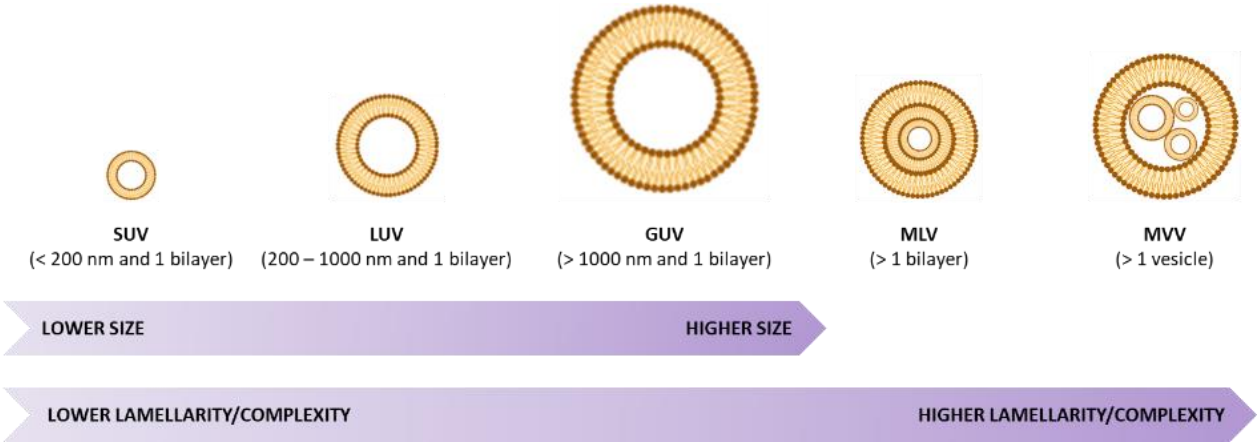


Figure 1.7. Vesicle classification regarding their size and lamellarity. SUV: small unilamellar vesicle; LUV: large unilamellar vesicle; GUV: giant unilamellar vesicle; MLV: multillamelar vesicle; and MVV: multivesicular vesicle. Adapted from Grimaldi *et al.*[73].

The grown interest of nanovesicles as DDS is the consequence of their supramolecular versatility in terms of size, surface characteristics and composition, their good biocompatibility and biodegradability, as well as, their convenient loading of hydrophilic molecules (e.g. small molecules, proteins, nucleic acids, etc.) within the internal aqueous cavity or adsorbed in membrane surfaces, but also hydrophobic substances inside the bilayer membrane[70,73,74,77]. These potential properties have led the scientific community to test nanovesicles of different compositions, of which liposomes have been the mostly investigated[73,78–81]. The predominant types of vesicles and membrane compositions studied are summarized in *Table 1.5*.

Table 1.5. Examples of nanovesicle categories with their corresponding membrane composition and main characteristics. Adapted from Grimaldi *et al.*[73].

Nanovesicle category	Membrane composition	Characteristics and specifications
Liposomes	Phospholipids (and cholesterol)	Single or multiple enclosed phospholipid bilayers with an aqueous lumen.
Transfersomes	Phospholipids Surfactants	Elastic and modelable vesicles used for transdermal delivery applications.
Virosomes	Phospholipids Viral envelope proteins	Liposomes containing viral envelope proteins to gain fusogenic capacity.
Pharmacosomes	Phospholipids Drugs	Phospolipid bilayers with covalently bound drugs to improve loading without leakage.
Ethosomes	Phospholipids Alcohols	Vesicles including elevated alcohol amounts for skin permeation purposes.
Ufasomes	Fatty acids Surfactants	Enhanced vesicle stability and drug loading. Cheap and available membrane components. Useful for topical delivery.
Sphingosomes	Cholesterol Sphingolipids	Improved drug retention and resistance to hydrolysis than liposomes.
Niosomes	Cholesterol Non-ionic surfactants	Phospolipid substitution by surfactants, which are cheaper and more stable alternatives.
Quatsomes	Cholesterol Ionic surfactants	Composed of quaternary ammonium surfactants ans sterols in specific molar ratios.

1.3.1. Progression of liposomal vesicles for therapeutic applications: current state in medicine

Liposomes have been one of the principal promising nanopharmaceuticals since their discovery in the 1960s by Alec Bangham[82,83]. Basically, liposomes are lipid-based nanovesicles composed of single or multiple enclosed phospholipid bilayers (natural or artificial) presenting an inner aqueous cavity. The initial "first-generation" of plain liposomes with simple phospholipid-based membrane composition brought to drawbacks of poor colloidal stability, quick clearance from bloodstream, increased membrane permeability and drug leakage rate[73], generally induced by the poor chemical stability of phospholipids which are easily hydrolyzed, oxidized or peroxided at high temperatures. To overcome these issues, cholesterol was incorporated as an additional membrane component to enhance the membrane rigidity, and achieve improved vesicle colloidal stability and reduced membrane permeability to prevent the leakage of the cargo molecules[73,84,85]. Also, neutral and charged phospholipids were combined to enhance drug loading and prevent their leakage[70,86]. Since then, liposomal nanostructures have drastically continued evolving (*Figure 1.8*) to be successfully used in a broad variety of fields apart from the biomedical sector (e.g. cosmetics[87], food[88], and textile[89]).

Next, the "second-generation" of liposomes appeared with the anchoring of polymeric molecules (e.g. polyethylene glycol (PEG)) to liposomal membrane compounds such as cholesterol[70,90]. PEG is a biocompatible, hydrophilic and low immunogenic polymer extensively used to enhance the protection of nanocarriers and elongating their mean lifetime in bloodstream[91]. In this way, "stealth liposomes" (i.e. PEGylated liposomes) were born as interesting DDS with reduced recognition by RES, clearance from circulation and generation of protein corona (i.e. adsorption of blood proteins to liposomes surface)[91,92]. To make liposomes more efficient, stimuli-responsive agents were also added into liposomal membranes composition to achieve controlled membrane destabilization and drug release profiles induced by the contact of the nanovesicles with endogenous (e.g. pH changes, specific biomolecules) or exogenous (e.g. temperature, magnetic field, light, ultrasound) stimulus[70].

Continuous membrane evolution was observed during the "third-generation" of liposomes, where specific ligands (e.g. peptides, antibodies, carbohydrates, etc.) were directly anchored on nanovesicle surface to selectively enhance the liposome biodistribution and drug accumulation in the targeted site. Additionally, these targeting moieties can be functionalized in liposome membranes through polymeric chains (e.g. PEG) acting as a linker. Thus, "ligand-targeted liposomes" with the protective capacities of the precursors "stealth liposomes" can be generated[93–96].

Nowadays, liposomes are in their "fourth-generation", where robust theranostic nanovesicles are capable to be used simultaneously for therapy and diagnosis purposes, due to the combination of the previous membrane modifications proposals (e.g. protection by polymeric coating, active targeting by ligand functionalization, release control by stimuli-responsive agents, etc.) with the loading of therapeutic drugs together with imaging biomolecules[70,97]. By way of summary, the overall evolution of liposomes as drug delivery platforms is schematized in ***Figure 1.8***.

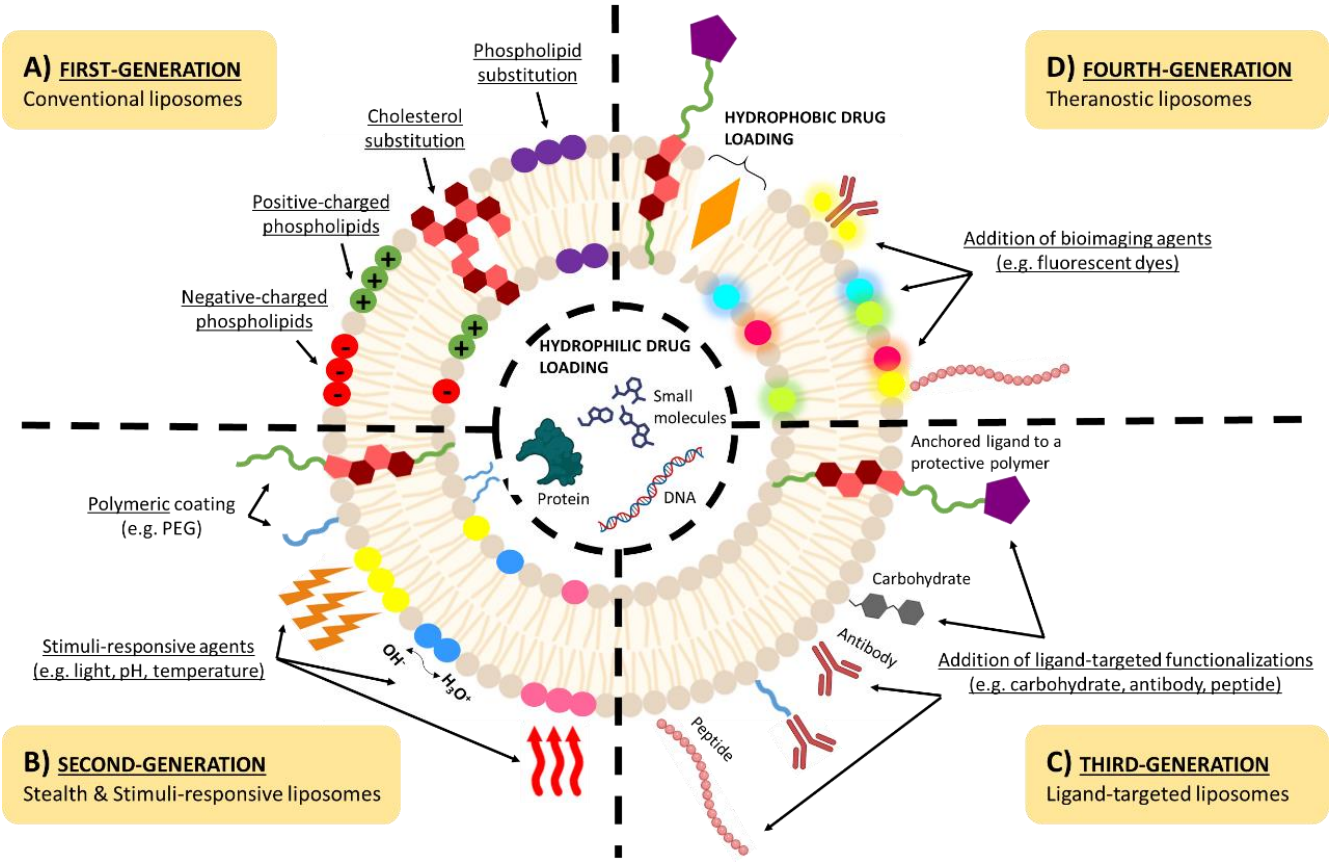


Figure 1.8. Overview of the generation evolution of liposomes. A) first-generation (conventional liposomes), B) second-generation (stealth and stimuli-responsive liposomes), C) third-generation (ligand-targeted liposomes), and D) fourth-generation (theranostic liposomes). Adapted from[60,98].

After this liposomal evolution, limitations in stability, reproducibility, loading capacity, drug leakage and release profile, have been overcome through the optimization of nanovesicle physicochemical properties (e.g. size and shape, supramolecular organization, functionalization, etc.) and the use of proper and scalable manufacturing processes[99–101]. Since liposomes are non-toxic, biodegradable and non-immunogenic nanostructures which can be synthetized as SUVs to prolong their circulation in bloodstream after being intravenously administrated, some liposomal prototypes have reached the regulatory approval and commercialization, meanwhile hundreds are currently being tested in preclinical and clinical phases[21,73,74,79,83]. The first liposome-based formulation approved by the FDA was the Doxil® in 1995 cancer therapy. Doxil® contains the doxorubicin chemotherapeutic agent integrated in liposomes for the specific treatment of ovarian cancer and AIDS-related Kaposi's sarcoma. Nowadays, there are on the market around 15 liposomal formulations, intended for other biomedical applications besides cancer therapy (*Table 1.6*). The majority of these products is intended for intravenous administration[46,79,86].

Table 1.6. Liposome products available in clinical use for biomedical applications. IV administration: intravenous administration. Adapted from[46,79,86].

Biomedical aplication	Clinical product (approval year)	Active pharmaceutical ingredients (molar ratio)	Liposome platform (molar ratio)	Administration route	Manufacturer
CANCER THERAPY	Doxil® (1995)	Doxorubicin	HSPC:Cholesterol:PEG2000-DSPE (56:38:5)	IV	Sequus Pharmaceuticals
	DaunoXome® (1996)	Daunorubicin	DSPC:Cholesterol (2:1)	IV	NeXstar Pharmaceuticals
	Depocyt® (1999)	Cytarabine	DepoFoam™	Spinal	SkyPharma Inc.
	Myocet® (2000)	Doxorubicin	Cholesterol:EPC (45:55)	IV	Elan Pharmaceuticals
	Mepact® (2004)	Mefamurtide	Multilamellar liposome DOPS:POPC (3:7)	IV	Takeda Pharmaceutical Limited
	Lipusu® (2006)	Paclitaxel	NA	IV	Luye Pharma Group
	Lipodox® (2012)	Doxorubicin	DSPC:Cholesterol:PEG2000-DSPE (56:39:5)	IV	Sun Pharma
	Marqibo® (2012)	Vincristine	SM:Cholesterol (60:40)	IV	Talon Therapeutics
	Onivyde™ (2015)	Irinotecan	DSPC:Cholesterol:MPEG2000-DSPE (3:2:0.015)	IV	Merrimack Pharmaceuticals
	Vyxeos® (2017)	Cytarabine:Daunorubicin (5:1)	DSPC:DSPG:Cholesterol (7:2:1)	IV	Jazz Pharmaceuticals
FUNGAL TREATMENT	Ambisome® (1997)	Amphotericin B	HSPC:Cholesterol:DSPG (2:1:0.8)	IV	Astellas Pharma
	Fungisome® (2003)	Amphotericin B	PC:Cholesterol (7:3)	IV	Lifecare Innovations
PHOTODYNAMIC THERAPY	Visudyne® (2000)	Verteporphin	Verteporphin:DMPC&EPG (1:8)	IV	Novartis AG
ANALGESIC	DepoDur™ (2004)	Morphine sulfate	DepoFoam™	Epidural	SkyPharma Inc.
	Exparel® (2011)	Bupivacaine	DepoFoam™	IV	Pacira Pharmaceuticals

1.3.2. Methodologies for vesicle manufacturing

The proper supramolecular structuring of nanovesicles directly influence on their optimal performance *in vivo*. Apart from the liposomal composition, component concentrations or environmental conditions (e.g. temperature, pH, ionic strength), the production method itself has been shown to have a huge impact on the homogeneity of molecular self-assembly[86,102], and thus, on the physicochemical features of liposomes (e.g. size, shape, lamellarity, etc.).

Liposomes are usually manufactured following bottom-up strategies, which imply the assembling of molecular units (i.e. the membrane components and drugs to encapsulate) into larger vesicular structures. Conventional fabrication procedures of liposomes result in high structural heterogeneity between vesicles due to a poor control of the self-assembling of the components constituting the nanostructure[73,84,102]. Some of the commonest conventional strategies used are:

- Thin-film hydration: dissolution of lipid compounds in organic solvents, followed by the evaporation of the organic solvents to obtain a thin film that is finally rehydrated in aqueous media to allow the vesicle formation.
- Reverse-phase evaporation: generation of inverted micelles through the dispersion of membrane compounds in mixtures of aqueous solution and water-immiscible solvents, and the subsequent organic solvent removal in vacuum conditions to generate vesicular structures.
- Ethanol injection: solubilization of hydrophobic molecules into an organic phase which is then injected into an aqueous solution to induce vesicle self-assembly.

After the use of conventional techniques, additional post-formation steps such as freeze-thawing, sonication, extrusion or high-pressure homogenization, are required to homogenize the size and lamellarity of liposomal vesicles[84,86,102]. Consequently, multi-step and time-consuming methodologies hardly scalable and with extensive handling have been developed for liposome manufacturing. These procedures can endanger the vesicular membrane compounds or the functionality of bioactive molecules, and even increase the probability of material losing[103]. These issues together with process-related limitations from conventional methods (e.g. low drug entrapment efficiencies, or generation of poor stable cholesterol-based supramolecular entities because of the formation of cholesterol-rich domains[104], hinder the production of controlled-quality liposomal formulations. Moreover, conventional methodologies use large organic solvent content difficult to be removed during post processing at lab or large scale, remaining as a toxic residue and compromising the safety of liposome-based products[103].

For all these reasons, new one-step manufacturing procedures for the preparation of homogeneous, high quality and safety multi-molecular vesicles with well-controlled properties are required (***Figure 1.9***). These new techniques should be easily scalable and environmentally respectful, apart from allow the reduction of organic solvent presence below the allowed limits depending on the final application of the system[105]. Also, according to the regulations of the FDA in the United States and the EMA in Europe, these procedures must be compatible with GMP to guarantee the quality, safety, and traceability of the resultant products[106].

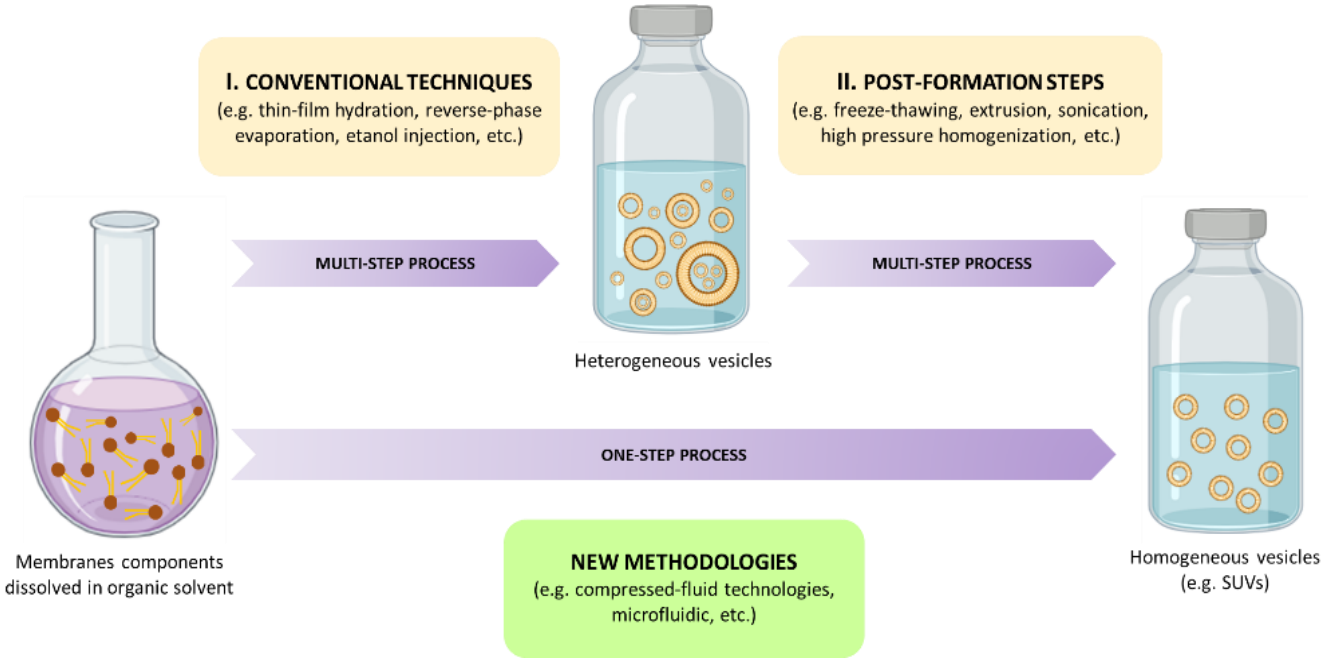


Figure 1.9. Distinct bottom-up approaches to generate homogenous vesicles.

1.3.2.1. DELOS-susp as green and scalable compressed fluid-based technology for liposomes' preparation

The use of methodologies based on compressed fluids (CFs) has gained great interest due to its alternative advantages over conventional approaches. Production methods based on compressed carbon dioxide (CO_2) avoid using organic solvents harmful for the environment, becoming safe, energy and resource efficient manufacturing processes because CO_2 presents the definitive advantages of being a 'green', abundant and cheap solvent perfectly suited for processing pharmaceuticals products at a temperature that does not disrupt the therapeutic properties of biologicals[107–109].

A novel compressed CO_2-based procedure called depressurization of an expanded liquid organic solution-suspension (DELOS-susp) was developed and patented by NANOMOL-Bio research group (ICMAB-CSIC) for the preparation of colloidal suspensions[110], becoming a promising one-step methodology for the fabrication of homogeneous multifunctional cholesterol-rich nanovesicles (e.g. liposomes or quatsomes) conjugating active biomolecules if necessary[99,100,107,111]. Moreover, DELOS-susp meets with essential requirements for the clinical translation of vesicle-based products like high batch-to-batch reproducibility and feasible scalability[58,99,100]. In fact, this technology has been scale-up and is currently exploited by Nanomol Technologies SL. A GMP compliant DELOS pilot equipment has been designed and built by engineers of this company in the frame of the European

(EU) project H2020 Phoenix (ID 953110; 2021 – 2025), which has represented a significant milestone achieved for the translation of nanopharmaceuticals to the clinics.

To point out, all the liposomal vesicles used in this thesis have been prepared by DELOS-susp according the protocol summarized in ***Figure 1.10***, and detailed below. Briefly, the DELOS-susp methodology involves three process steps:

i. The loading of the hydrophobic membrane compounds dissolved in an organic solution into a high-pressure vessel configured at a working temperature (T_w) of 35 ºC and atmospheric pressure.
ii. Pressurization of the high-pressure vessel until the working pressure (P_w) of 10 MPa by the addition of liquid compressed CO_2, and the subsequent origination of a CO_2-expanded solution containing the dissolved membrane molecules at T_w =35 ºC and P_w = 10 MPa. The CO_2-expanded solution is maintained until reaching a complete homogenization and thermic equilibration of the system.
iii. Depressurization of the CO_2-expanded solution over an aqueous solution (often water), where hydrophilic membrane substances or active biomolecules can be dissolved to induce their encapsulation during the vesicle self-assembling process. The high-pressure vessel depressurization is provoked by a flow of nitrogen (N_2) at P_w = 11 MPa capable to work as a plunger of the CO_2-expanded solution meanwhile the P_w within the vessel remains stable.

During the DELOS-susp depressurization step, the expanded organic solution suffers a quick, large and homogeneous temperature decrease produced by the CO_2 evaporation from the expanded solution, likewise the one in DELOS process. This fact might explain the high vesicle-to-vesicle homogeneity (in terms of size, lamellarity, and morphology) provided by the DELOS-susp process[107,112].

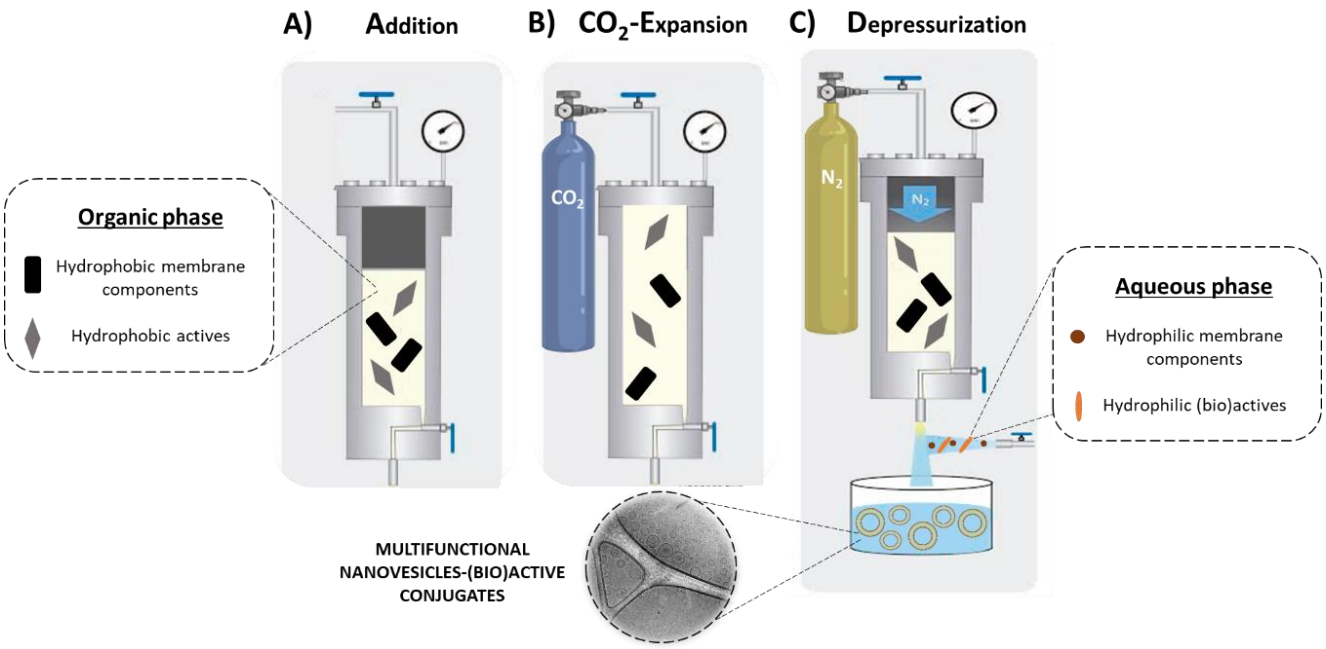


Figure 1.10. Schematized representation of the three main process steps of the DELOS-susp tehnology employed for nanovesicle manufacturing, involving: A) addition of dissolved hydrophobic components in organic solvents, B) addition of compressed CO_2 as co-solvent to expand and homogenize the solution, and C) addition of N_2 to depressurize of the CO_2-expanded solution over an aqueous solution with or without containing hydrophilic compounds. More information is detailed in *Chapter 7, Section 7.4*.

Hereby, DELOS-susp has demonstrated to be a robust green-scalable one-step procedure for the fabrication of multifunctional nanovesicles-(bio)actives conjugates with high structural homogeneity under controlled process parameters, which can easily fulfill pharmaceutical quality requirements[58,100,107].

1.3.3. Methodologies for liposomes' purification

After the preparation of liposomes, to remove the remaining organic solvent used during the manufacturing process (e.g. DELOS-susp), as well as the non-integrated components (e.g. free enzymes and other non-incorporated components) to prevent the destabilization of the supramolecular entities purification techniques can be used[61,113].

The commonest methodologies tested by the research community (e.g. dialysis, tangential flow filtration (TFF), ultracentrifugation, centrifugal ultrafiltration, pressure ultracentrifugation, and size exclusion chromatography, among others) to remove free, non-integrated components present some important limitations, so their conditions must be adapted and validated for each type of nanoformulation to be tested[61,113]. Some examples of advantages and drawbacks are listed in *Table 1.7*.

Table 1.7. Examples of common separation techniques used to isolate encapsulated molecules in nanovesicles from the non-integrated ones. Characteristics from each methodology are detailed. Adapted from[61,113].

Separation technique	Potential liposome damage	Advantages	Limitations
Dialysis	No	Simple & economic	Slow perfusion of big molecules Large solvent quantities required Difficult to scale-up
Tangential flow filtration (TFF)	No	Low probability of filter clogging Well-preservation of vesicle integrity at low transmembrane pressures (TMP) Sample concentration (if required) Easy scalability & reproducibility	Large amounts of sample required Higher operational complexity than conventional filtration systems High invesment: specialized equipment and membranes
Ultracentrifugation	Yes	Similar-sized particle separation based on small variability of mass and density Simultaneous processing of various samples Sample concentration (if required)	High probability of liposome damage Cross-contaminations among fractions Low reproducibility Difficult to scale-up
Centrifugal ultrafiltration	Yes	Simple procedure Simultaneous processing of various samples Preservation of vesicle integrity at low centrifugal forces	Probability of liposome deformation High probability of filter plugging Loss of sample Difficult to scale-up
Pressure ultrafiltration	Yes	Simple procedure Gentle separation at low pressure Non-limitations on sample volume	Probability of liposome deformation High probability of filter plugging Loss of sample
Size exclusion chromatography	No	Reproducibility & purity & scalability Well-preservation of vesicle integrity Hish sensitivity	Limitations on sample volumes to process High operational complexity High invesment: specialized equipment and chromatographic columns

1.3.3.1. Filtration-based procedures for liposomes' purification

Working with liposomes, porous-walled membranes from 0.1 – 10 µm have been broadly employed as a size-based separation technique, to remove the remaining organic solvent used during the manufacturing process or the non-integrated components from nanovesicles, but also for sterilization purposes. The filtrated-based methods for liposomes' purification are usually used together with external forces to improve their efficiency. In general, samples can be filtrated across membranes through two main *modus operandi*[114,115], which are schematized in ***Figure 1.11*** and explained below:

i. Direct flow filtration (DFF): otherwise known as dead-end filtration. It exerts a specific flow perpendicular to the membrane face to pursuit the pass of the 100 % of fluid sample across the membrane.
ii. Tangential flow filtration (TFF): also called crossflow filtration. It applies a flow parallel to the membrane face, allowing the pass across the membrane of only some fraction of the fluid sample, meanwhile the remaining one is recirculated into the system.

In both filtration modes, the transmembrane pressure (TMP) force allow the sample permeation across membranes. TMP refers to the pressure difference between the inflow and outflow of a membrane. Nevertheless, the use of TFF instead of DFF approach has been extensively implemented for the size-based separation of biomolecules in the biological sectors. The main reason is the use of crossflow which prevents the membrane fouling (i.e. accumulation of molecules causing pore obstruction), and the subsequent sample loss. This TFF characteristic allow to work with a more stable flow rate (without the abrupt declining observed in DFF), process higher sample volumes and concentrations, and prevent the deformation or breakage of nanovesicles (e.g. liposomes).

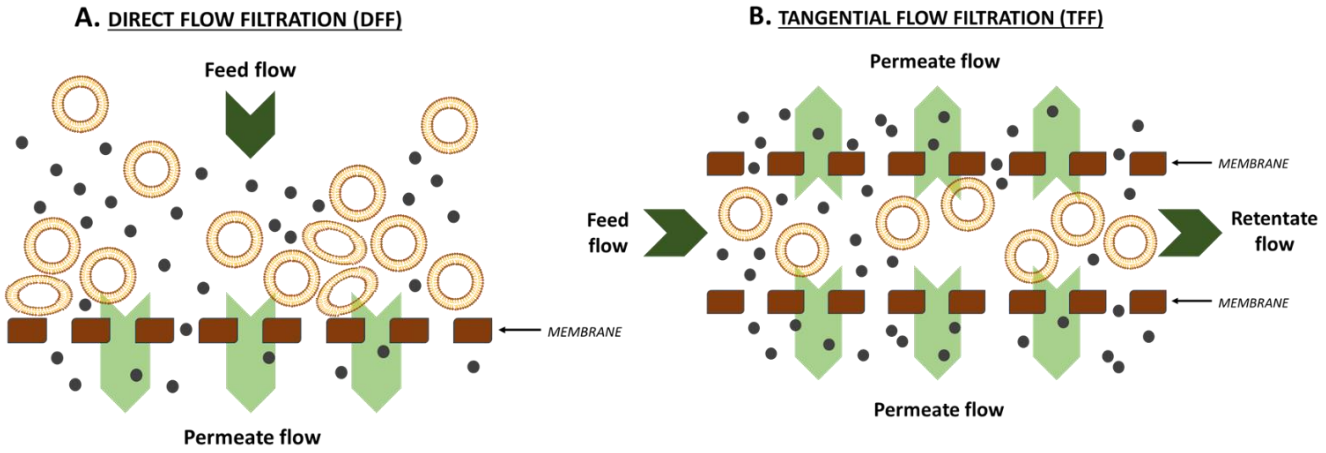


Figure 1.11. Schematic comparison between A) a DFF process, and B) a TFF process of a liposomal formulation. Adapted from Herterich *et al.*[114].

In this thesis, both filtration approaches have been used with different purposes. On the one hand, after DELOS-susp production, nanovesicles were submitted to a TFF-based procedure using a KrosFlo® Research IIi TFF System (Repligen, Waltham, USA) to simultaneously remove non-incorporated molecules, remaining organic solvents (EtOH and DMSO from DELOS-susp production) and/or concentrate sample when necessary (see *Chapter 7, Section 7.4.3*). Basically, the liposome TFF protocol can comprise three steps:

i. Diafiltration: purification step involving the use of TMP as driving force to recirculate a constant sample volume through a porous column. The same amount of removed permeate volume (containing organic solvents and probable non-encapsulated molecules) is instantaneously replaced by new aqueous media from the buffer reservoir (often pure water).
ii. Buffer exchange: the operating mode similar to the diafiltration step, but here the sample solvent is exchanged for another one, which is placed in the buffer reservoir (e.g. pure water or glucose 5 % (w/v) media in this thesis).

iii. Sample concentration: concentration step including similar operating conditions to the diafiltration step, but recycling the sample along the system without replacing the eliminated permeate volume. The concentration factor (C_{Fc}) refers to the original sample volume (V_i) divided into the final one (V_f): $C_{Fc} = V_i/V_f$.

TFF used as a part of the liposome manufacturing process has allowed the diafiltration and concentration of large sample batches without compromising vesicle integrity, with the aim to have the required drug-loaded nanoliposomal concentration for *in vivo* dosing.

On the other hand, other separation techniques such as the filtration-centrifugation (using Vivaspin® 20 polyethersulfone (PES) centrifugation Amicon® units (Sartorius, Germany)) have been developed and implemented in this thesis for the separation of the drug released from the liposomes to determine the *in vitro* drug release kinetic profile and the drug leakage rate, since TFF requires large sample volumes (more details are explained in ***Chapter 5, Section 5.4***, but also in ***Chapter 7, Section 7.4.6***). The use of minimal volumes of complex nanoformulations containing biomolecules is crucial to perform an economically affordable quality control of samples.

1.4. Rare disease: lysosomal storage disorders

Lysosomal storage disorders (LSDs) consist of a set of over 50 distinct genetic disorders characterized by lysosomal dysfunctions which are mainly induced by the deficiency of the activity in a specific enzyme implicated in the metabolism of macromolecules (e.g. sugars, proteins, nucleic acids, lipids or mucopolysaccharides)[60,116,117]. The accumulation of undegraded substrates progressively impair the lysosome functions usually resulting on severe multisystemic disease manifestations and early death[118,119]. The lack of an active specific enzyme in LSDs cases is typically inherited as monogenic autosomal recessive or X-linked diseases[60,116]. LSDs are considered rare diseases due to their low individual incidence (between 1:50,000 and 1:250,000 live births). However, the overall incidence of LSDs as a collective group is estimated to affect around 1:5,000 live births, representing a serious global health concern[116,119].

Lysosomes organelles are spherical single-membrane vesicles located in the cytoplasm of eukaryotic cells. A large variety of proteins has been found within lysosomal vesicles, of which approximately 60 are hydrolytic enzymes named hydrolases[60,120]. They allow the intracellular digestion of macromolecules such as glycosphingolipids, oligosaccharides, glycogen, glycoproteins, mucopolysaccharides, or even foreign substances, being a fundamental lysosomal function among the multiple cellular processes in which these organelles are involved[60,116,118]. Extracellular compounds can also be degraded in lysosomes after their introduction into

eukaryotic cells by receptor-mediated endocytosis, and the originated vesicles finally fused to lysosomal compartments[116,121]. Hydrolases are active glycosylated enzymes able to properly catalyze substrates in the acidic pH (around 4.5 – 5) of the lysosomal lumen, which is maintained thanks to a continuous pumping of protons through the vacuolar channel V-type ATPase across the lysosomal membrane[116]. Glycosylation post-modifications of hydrolases are essential to guarantee the proper enzyme conformation, activity, solubility, stability and transport to lysosomes[122,123]. Glycosylated hydrolases are synthetized in the endoplasmic reticulum organelle, and then mostly modified with the addition of mannose-6-phosphate (M6P) recognition targets in the Golgi apparatus. From there, an enzyme fraction can be directly packed into secretory vesicles and further delivered into lysosomes vesicles through membrane fusion, meanwhile the other enzyme fraction can be extracellularly secreted to be finally incorporated in lysosomes through membrane M6P receptor-recognition after endocytosis procedures which allow the enzyme entrance to the cellular cytosol[60,121,124].

The lack of a single lysosomal hydrolase inabilities the digestion of specific substrates leading to the progressive storage of macromolecules inside lysosomes, and therefore, in LSDs pathologies. There exist several ways to sort the distinct LSDs, but the commonest clinical classification used is according to the major accumulated substrate. Representative categories of LSDs regarding this classification include: sphingolipidosis (e.g. Gaucher abd Fabry diseases), mucopolysaccharidosis (e.g. Hunter and Sanfilippo diseases), glycogenosis (e.g. Pompe disease), oligosaccharidosis (e.g. Schindler disease) and glycoproteinoses[60,125].

Since a definitive cure for LSDs is not available due to the broad variety of genetic causes, supportive therapy is provided to LSDs patients (e.g. ventilator and nutritional support, physical therapy and even surgical interventions) to improve their living standard. Besides, several specific treatments have been developed to correct the metabolic defect of particular LSD, reducing the pathophysiological effects provoked by the compound accumulation into lysosomes (***Figure 1.12***)[126–128]. The standard treatment for several LSDs consists in the enzyme replacement therapy (ERT), i.e. the exogenous administration of the inactive or deficient lysosomal enzyme. Another used therapeutic strategy named substrate reduction therapy (STR), inhibits the enzyme responsible for the synthesis of a particular substance with the aim to reduce their accumulation within lysosome vesicles. For mutant enzymes with remaining residual activity, the pharmacological chaperone therapy (PCT) is another feasible therapeutic approximation which uses small molecule drugs to correct the conformation of defective hydrolases, improving their activity and stability. Hematopoietic stem cell transplantation (HSCT) is an alternative approach to treat LSDs with a sustained therapeutic protein delivery throughout the body, similarly to gene-therapy based treatment[120,126,129–132]. However, most of new therapeutic approaches based on gene therapy are still in development and testing in clinical trials[133].

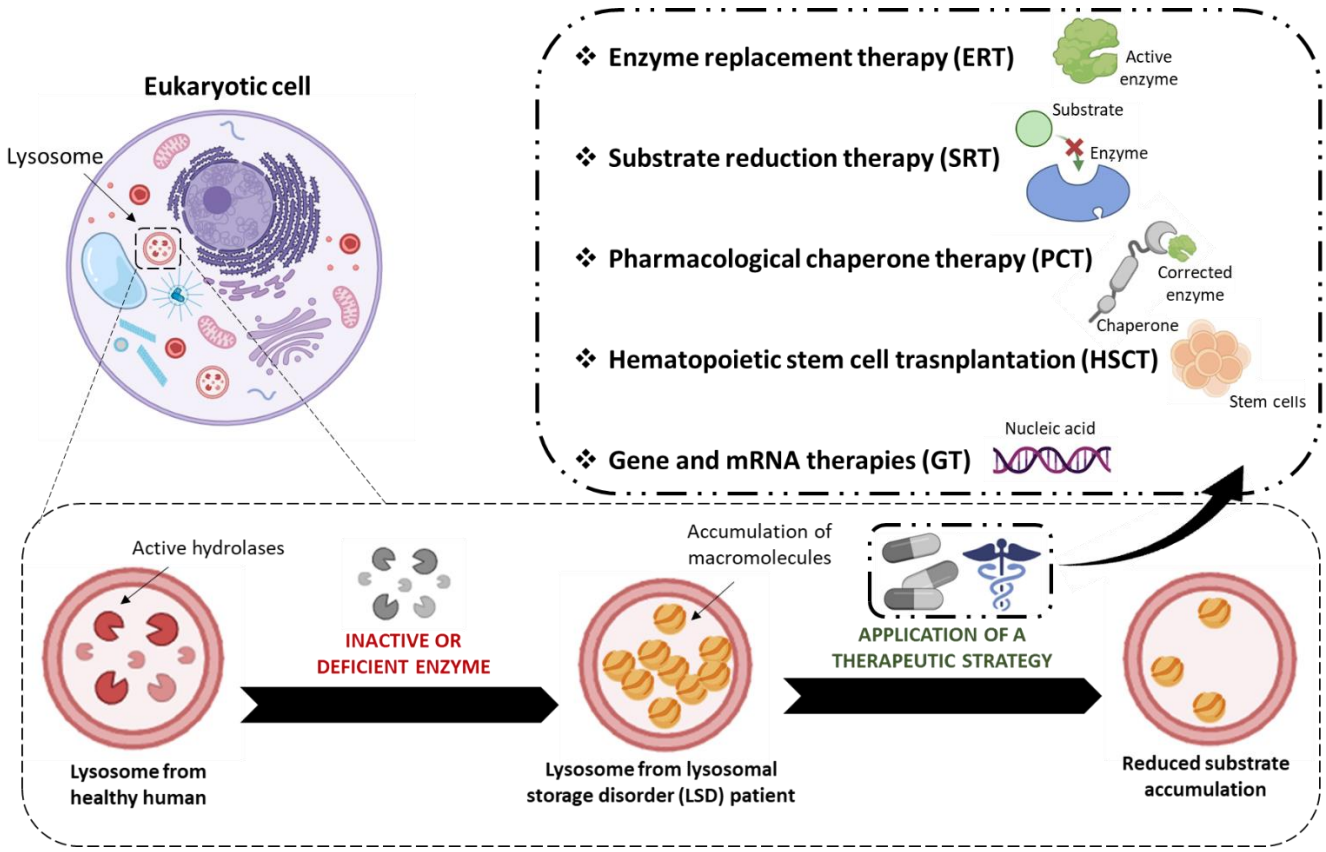


Figure 1.12. Therapeutic strategies for LSDs. Adapted from Tomsen-Melero *et al.*[60].

1.4.1. Fabry disease and the current state of treatments (approved and under development)

One of the most prevalent LSD is the Fabry disease, caused by a genetic mutation in the X-chromosome resulting on the deficiency of the α-galactosidase A (GLA) lysosomal enzyme or the missing of its activity. Fabry disease can affect both, men and women, with a wide range of approximated prevalence from 1:40,000 to 1:117,000 live births[134,135].

The glycosylated hydrolase named GLA is synthetized in the endoplasmic reticulum of human cells, then modified in the Golgi apparatus acquiring M6P moieties on its N-linked oligosaccharidic chains, after loaded into secretory vesicles, and finally delivered to the late endosomes/lysosomes. Since some fraction of the glycosylated GLA can be extracellularly secreted posterior to the pathway along Golgi, secreted GLA molecules can be recaptured by endocytosis after their interaction with M6P receptors located in cell membranes, and eventually transported to the lysosomes of neighboring cells[124,127,136].

In healthy humans, the mature GLA glycoprotein present in lysosomes is a homodimer formed by two identical subunits, each one composed of two domains. The N-terminal domain extends from residue 32 to 330 forming a (β/α)8-barrel structure containing the active site in its center, meanwhile the C-terminal domain from residue 331 to 429 forming an antiparallel β domain (***Figure 1.13***). Each monomer or subunit contains three N-linked carbohydrate sites. GLA theoretical isoelectric point (pI) value is near to pH 5.1, converting the enzyme in a negatively charged molecule around neutral pH[136–139]. As generally explained before for hydrolases, glycosylation post-modifications are also essential in the case of GLA enzyme to guarantee its proper conformation, activity, solubility, stability and transport to lysosomes[122,123]. There exist four potential N-glycosylation sites in GLA residues N139, N192, N215, and N408. From these, the huge impact on enzyme solubility and its transport from the endoplasmic reticulum to the lysosomes rests on the potential N-glycosylation of site three (N215)[123,136].

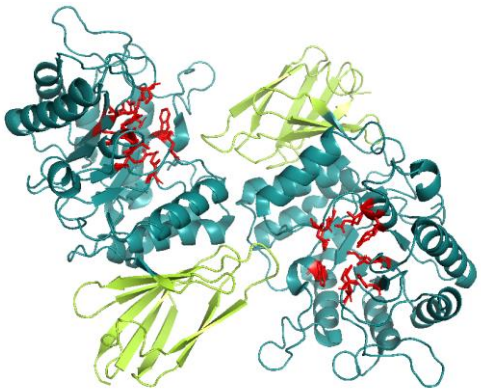


Figure 1.13. Structure of GLA homodimer, showing in blue color the N-terminal domain and in green color the C-terminal domain. The 14 residues involved in the active side (W47, D92, D93, Y134, C142, K168, D170, E203, L206, Y207, R227, D231, D266, and M267) are highlighted in red color. Visualization obtained using PyMOL software, based on PDB: 1R47[140].

Due to the absence of GLA activity, neutral glycosphingolipids, as mostly globotriaoslyceramide (Gb3), are accumulated inside lysosomes of a broad variety of Fabry's patient cells. Gb3 is the main substrate of GLA which is composed by a ceramide group directly attached to a sugar chain with one glucose and two galactoses. The main affected cellular types include endothelial cells, cardio-myocytes, renal cells and nerve cells, generating multi-systemic clinical symptoms (***Figure 1.14***)[134,141]. Among them vascular endothelial cells are the ones more impaired by substrate accumulation, leading to dysfunction of multiple cellular activities (e.g. cellular metabolism, oxidative stress reactions and ion-transport across channels). During childhood and adolescence, it can appear early manifestations of the disease pathophysiology including skin injures (e.g. angiokeratoma), gastrointestinal and neuropathic pain. Continuing into adulthood serious manifestations gain impact such as cardiac symptoms, renal dysfunction and cerebrovascular events (e.g. ischemic attacks and stroke), resulting on pathologies involving multiple organs and causing the early death of untreated patients[142–146].

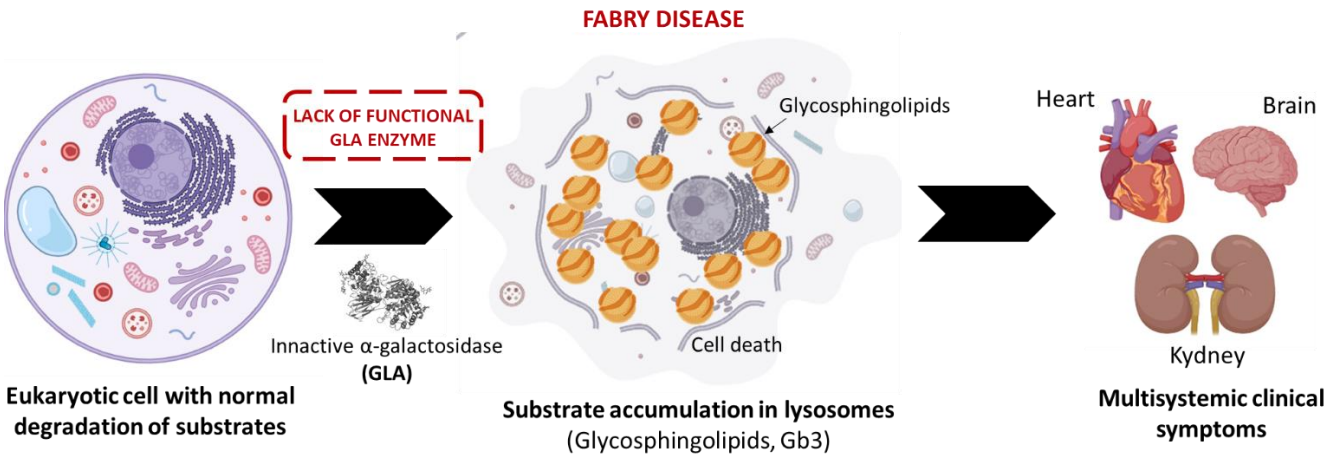


Figure 1.14. Progressive accumulation of non-degraded glycosphingolipids, mainly Gb3, within lysosomes of Fabry's patient cells caused by the absence of GLA, and the subsequently multisystemic pathophysiology developed.

Since 2001, the most relevant treatment for Fabry patients has been based on ERT, i.e. biweekly intravenous infusion of exogenous recombinant GLA[147,148], with the authorization of two products: Replagal® from Shire-Takeda (agalsidase alfa, commercialized in Europe), expressed in a human fibroblast cell line of undisclosed origin, and Fabrazyme® from Sanofi-Genzyme (agalsidase beta, commercialized in Europe and also since 2003 in USA) produced in CHO cell cultures. Both products were designated as ophan drug at the same time in 2000, meaning a stimulation for the development of drugs for rare diseases, and once these are approved, the orphan drug designation (ODD) offers benefits such as protection from competition. Nevertheless, their orphan status has already expired. Both ERT medicinal products consist of the recombinant human GLA hydrolase demonstrating identical biochemical properties, with only slight differences in their glycosylation pattern and mannose-6-phosphate receptor mediated cellular uptake, since they are related to the distinct production cell line employed[147,149,150]. These properties might be the responsible for the distinct administration dose and pharmaceutical form between Replagal® (0.2 mg/kg, and storage as a concentrated aqueous solution) and Fabrazyme® (1 mg/kg, and storage as freeze-dried product). Despite their capacity on reducing the Gb3 accumulation, reducing the progression of Fabry disease and improving the life-quality of patients, neither treatment is capable to completely reverse the disease, specifically in advanced stages[151]. In order to enhance the contribution to the Fabry treatment, the Fabrazyme®-biosimilar agalsidase beta BS or JR-051 from JCR Pharmaceuticals was approved to be marketed in Japan in 2018 under agreement, which presented identical quality, effectiveness and safety than the already approved Fabrazyme®[152,153]. Nowadays, a new promising alternative ERT have been recently approved in 2023, which is the pegunigalsidase alfa from Chiesi Global Rare Diseases called Elfabrio®. It contains a PEGylated agalsidase alfa expressed in plant tobacco cell-based expression system ProCellEx®, with stabilized pharmacokinetic after the chemical cross-linking of short PEG moieties to

covalently bound the protein subunits[154]. In comparison with others, this ERT has demonstrated higher half-life (78.9 ± 10.3 hours) and tolerance, inducing less generation of anti-GLA antibodies, being also administrated every two-weeks. Therefore, it has been established as a long-term safety up to 6 years using a dosing of 1 mg/kg[155,156].

However, extensive information from Replagal® and Fabrazyme® has evidenced several limitations (***Figure 1.15***) such as i) disability to cross the biological blood brain barrier (BBB) hindering the treatment of brain tissues, ii) low enzyme stability with a subsequent rapid degradation and short circulation half-life, iii) poor biodistribution and iv) the generation of neutralizing anti-GLA antibodies, v) required frequent intravenous administration (every other week), causing vi) high immunogenicity issues, and resulting in vii) expensive treatments (280,000 €/patient year). These disadvantages as a whole lead to viii) limited efficacy[130,142,150].

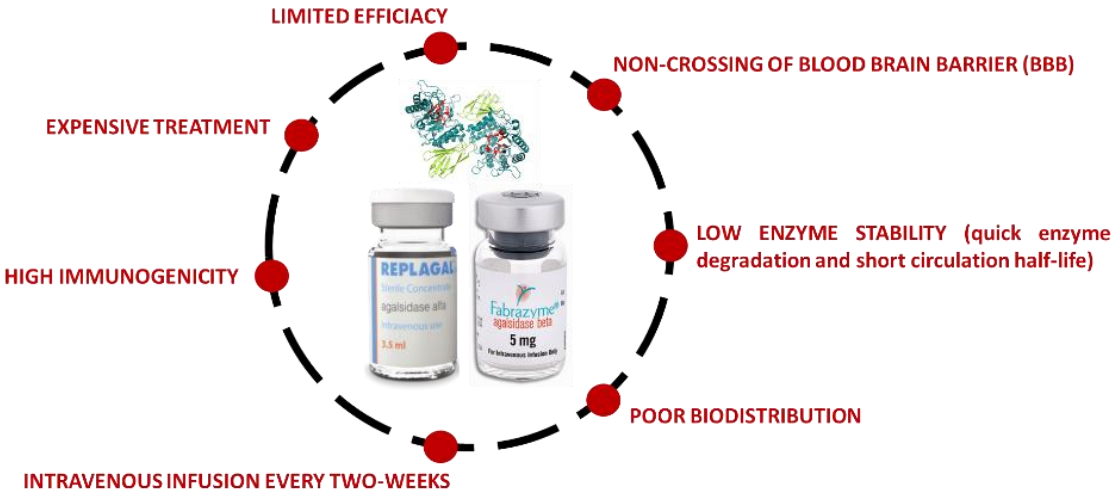


Figure 1.15. Handicaps of Replagal® and Fabrazyme® treatments based on ERT for Fabry disease.

Alternatively to ERT, the migalastat hydrochloride from Amicus Therapeutics named as Galafold® was approved as a PCT in 2016 as a product for the unique usage in Fabry patients with GLA mutants susceptible to regain activity after chaperone-induced structural conformational changes. Chaperones are small molecules capable to assist in the proper folding maturation of proteins improving their stability and trafficking to the correct functional site, e.g. the lysosomes[129,142]. Although Galafold® is only useful for Fabry patients with residual GLA activity, it presents some potential advantages such as an oral administration, non-immunogenic response, and potentiality to cross the BBB. Galafold® together with the Elfabrio® are marketed with the ODD status for Fabry disease. Several other strategies based on SRT and genetic therapy are currently under investigation, in clinical trials, with the aim of proportioning improved efficacy than the traditional ERT[150]. The strategies mentioned in this section, approved and under development in clinical trials, are compiled in ***Table 1.8***.

Table 1.8. Products approved and in clinical trials for the treatment of Fabry disease.

PRODUCT	THERAPEUTIC STRATEGY	DEVELOPMENT STAGE	USE OF NANOTECHNOLOGY
Replagal® (agalsidase alfa)	ERT	Commercialized in Europe and Japan	No
Fabrazyme® (agalsidase beta)	ERT	Commercialized in Europe, USA and Japan	No
Elfabrio® (pegunigalsidase alfa)	ERT	Recently approved by EMA and FDA	No
Agalsidase beta BS or JR-051 (Fabrazyme biosimilar)	ERT	Commercialized in Japan	No
Galafold® (migalastat hydrochloride)	PCT	Commercialized in Europe, USA and Japan (non-inferiority drug vs ERT)	No
Migalastat hydrochloride	PCT	Under development	No
Lucerastat (glucosylceramide synthase (GCS) inhibitor)	SRT	Phase III trial in USA and Japan	No
4D-310 (adeno-associated virus (AAV) gene therapy)	GT	Phase 1/2 trials	No
AVR-RD-01 (*ex vivo* lentiviral-based gene therapy)	GT	Discontinued (lack of efficacy in phase II trial)	No
ST-920 (ASV vector-mediated gene transfer)	GT	Phase II trial	No

ERT: enzyme replacement therapy; PCT: pharmacological chaperone therapy; SRT: substrate reduction therapy; GT: gene therapy.

The use of the nanotechnology to bring to the market a more effective version of ERT, with an enhanced enzyme cellular internalization, BBB crossing capacity, enzyme protection from degradation, and subsequently reduced enzyme immunogenicity, opens the door to new possibilities to continue with the improvement of ERT formulations for Fabry disease, but also for other LSDs[157–159].

1.4.2. Nanotechnology-based treatments for Fabry disease in preclinical development

As explained above, DDS are engineered nanoscale platforms used in the field of nanomedicine to encapsulate therapeutic agents reducing their potential adverse effects and improving their efficacy by means of targeted delivery and controlled release of the drug substance[27,79,160–163]. In this context, GLA enzymes have been integrated in polymeric nanoparticles of polystyrene targeted with antibodies against the intercellular adhesion molecule 1 (anti-ICAM-1), which is a protein expressed on the gastrointestinal epithelium apart from in other

tissues. As a result, enhanced enzyme targeted-delivery and Gb3 reduction levels were achieved in organs of the whole body[164,165]. Following the same direction, the use of stable polyelectrolyte complexes (PEC) containing ionically cross-linked trimethyl chitosan (TMC) with GLA molecules have also demonstrated augmented *in vitro* efficacy and delivery to lysosomal organelles of human endothelial cells[130,166]. Additionally, several vesicular systems have been developed evidencing promising efficacy and safety to be used for diverse drug delivery applications in the nanopharmaceutical field[79,162].

1.4.2.1. GLA-loaded nanoliposomal formulation as nanopharmaceutical candidate for the treatment of Fabry disease

A new patent protected nanoliposomal formulation containing a novel recombinant human GLA has been developed and optimized within the frame of multidisciplinary projects (as shown in ***Figure 1.16***) as a more effective ERT for Fabry disease[167]. The surface of these nanoliposomes is functionalized by a targeting peptide, an arginine-glycine-aspartate (RGD) derivative (i.e. c-RGDfk), by incorporating the synthetic cholesterol-PEG_{400}-RGD (chol-PEG_{400}-RGD) moiety to the liposomal membrane[168]. RGD targeting peptide leads the GLA-loaded nanoliposomes towards endothelial cells, which are one of the most predominantly affected cell type in Fabry disease and play a relevant role in disease pathophysiology[169]. This promising nanoformulation is produced using the compressed-CO_2 DELOS-susp technology followed by a TFF procedure described in the previous ***Section 1.3.3.1***.

With this GLA-loaded nanoliposomal formulation promising results have been obtained, in terms of excellent physicochemical properties, bioactivity, and high entrapment efficiency[100]. *In vivo* preclinical results also have shown superior efficacy of the nanoformulated GLA when compared to naked enzymes (included the commercially available agalsidase alpha or Replagal®), since these GLA-loaded nanoliposomes induce higher reduction of Gb3 in mice tissues and efficacy in brain, observed and published for the first time in a ERT for Fabry treatment. The significant benefit this novel treatment could offer to Fabry patients has been recognized by the EMA by means of the ODD[167,170].

In ***Figure 1.16*** the progressive drug product maturity reached with the diverse multidisciplinary projects until nowadays is summarized. Initially, national projects funding permitted to obtain a solid experimental PoC of this nanoformulation. With the EU project H2020 Smart4Fabry funding (ID 720942; 2017 – 2020), this PoC was brought to an advanced stage of preclinical development (first GLP-toxicology in rats included; TRL-3 to TRL-5) and the ODD obtained, which has important implications for the translation of the new therapeutic product from bench to bedside. Following the completion of Smart4Fabry project, the scalability of the GLA-loaded

nanoliposomal formulation compatible with GMP regulations and further Chemistry, Manufacturing, and Controls (CMC) development is being performed under the already funded EU project H2020 Phoenix (ID 953110; 2021 – 2025), since it pursues the transfer of this new nanoformulation to the clinical phase, covering the GMP clinical lot production. Very recently, a new project has been granted to NANOMOL-Bio research group (ICMAB-CSIC), named Nano4Rare, to allow the preclinical phase completion.

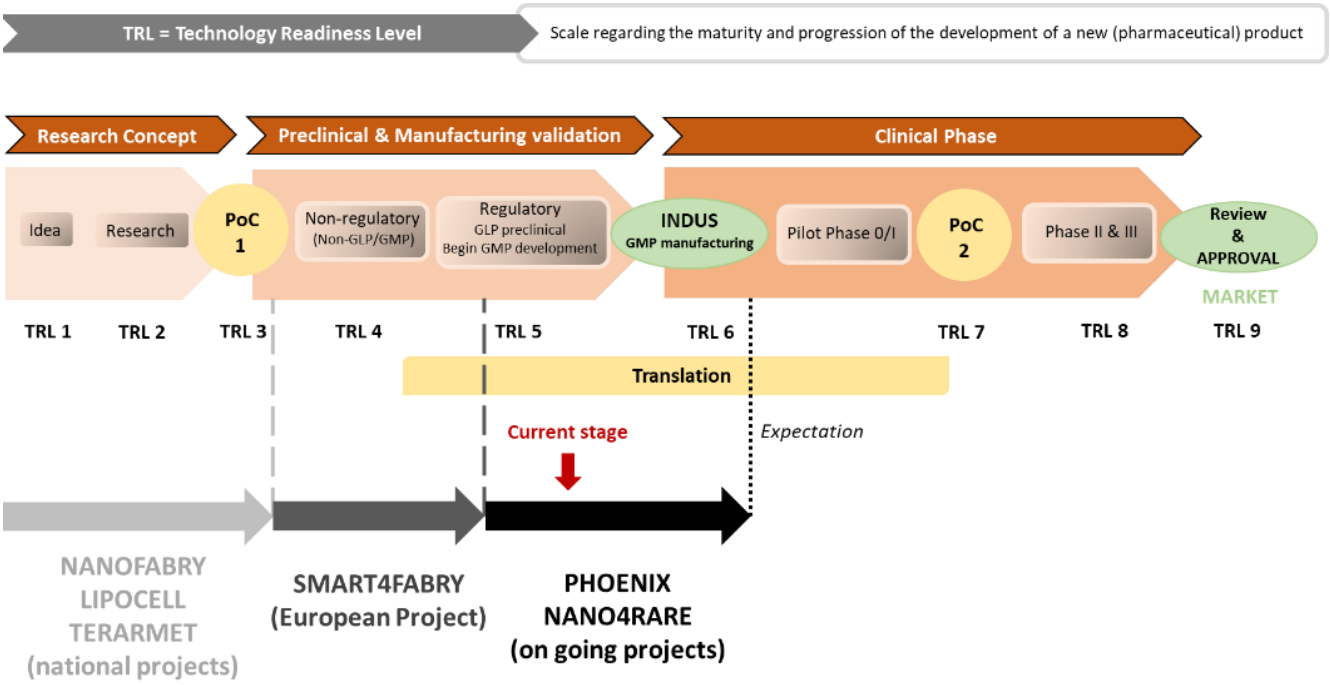


Figure 1.16. Achieved maturity development state of targeted liposomal pharmaceuticals intended for the treatment of Fabry disease, at the end of the distinct projects that contributed funding.

Despite the huge advanced state of this nanoformulation, deeper understanding and control of GLA-loaded nanoliposomes at nanoscale and supramolecular level is required to facilitate, support and guarantee that a high-quality product is translated to the clinical phase. During the development of the GLA-loaded nanoliposomes up to now, it has been observed, on different occasions, the impact that the characteristics of the GLA enzyme can have on the properties of the nanoformulation. However, at the beginning of the present doctoral project, no systematic and planned study existed to elucidate the relationship between the production process parameters and the CQAs of the drug substance, i.e. the GLA enzyme, that can impact on the nanoconjugate physicochemical and biological quality.

It is likewise crucial to perform an advanced characterization to understand, guarantee and control the quality of the drug product, i.e. the whole GLA-loaded nanoliposomal formulation, which is a challenge taking into account the high complexity of this nanoformulation.

All these issues have been addressed in this thesis to contribute to advance in the CMC development of the GLA nanoliposomal formulation for Fabry Disease Treatment.

1.5. References

1 Hollinger MA. Introduction to Pharmacology, Second Edition, Second Edition. Taylor & Francis Group, 2003.

2 Hacker M. History of Pharmacology—From Antiquity to the Twentieth Century. In: Pharmacology: Principles and Practice. Elsevier, 2009: 1–7.

3 Rang HP, Dales MM, Ritter JM, *et al.* Rang and Dale's Pharmacology, Ninth Edition. Elsevier, 2020.

4 Maehle AH, Prüll CR, Halliwell RF. The emergence of the drug receptor theory. *Nat Rev Drug Discov* 2002; **1**: 637–41.

5 Rang HP. The receptor concept: pharmacology's big idea. *Br J Pharmacol* 2006; **147 Suppl 1**: S9–16.

6 Reynolds T, de Zafra C, Kim A, Gelzleichter TR. Overview of Biopharmaceuticals and Comparison with Small-molecule Drug Development. In: Nonclinical Development of Novel Biologics, Biosimilars, Vaccines and Specialty Biologics. Elsevier Inc., 2013: 3–33.

7 Makurvet FD. Biologics vs. small molecules: Drug costs and patient access. *Med Drug Discov* 2021; **9**: 100075.

8 Zhao L, Ren TH, Wang DD. Clinical pharmacology considerations in biologics development. *Acta Pharmacol Sin* 2012; **33**: 1339–47.

9 Samanen J. Similarities and differences in the discovery and use of biopharmaceuticals and small-molecule chemotherapeutics. In: Introduction to Biological and Small Molecule Drug Research and Development: Theory and Case Studies. Elsevier, 2013: 161–203.

10 Homayun B, Lin X, Choi H-J. Challenges and recent progress in oral drug delivery systems for biopharmaceuticals. *Pharmaceutics* 2019; **11**: 129.

11 Poduval P, Parsekar S, Meena SN. Small molecules vs biologics. In: New Horizons in Natural Compound Research: Progress in Biochemistry and Biotechnology. Academic Press, 2023: 179–99.

12 Owczarek B, Gerszberg A, Hnatuszko-Konka K. A Brief Reminder of Systems of Production and Chromatography-Based Recovery of Recombinant Protein Biopharmaceuticals. *Biomed Res Int* 2019; **2019**. DOI:10.1155/2019/4216060.

13 Martins AC, Oshiro MY, Albericio F, de la Torre BG, Pereira GJ V., Gonzaga R V. Trends and Perspectives of Biological Drug Approvals by the FDA: A Review from 2015 to 2021. *Biomedicines* 2022; **10**: 2325.

14 Tripathi NK, Shrivastava A. Recent Developments in Bioprocessing of Recombinant Proteins: Expression Hosts and Process Development. *Front Bioeng Biotechnol* 2019; **7**. DOI:10.3389/fbioe.2019.00420.

15 Eon-Duval A, Broly H, Gleixner R. Quality attributes of recombinant therapeutic proteins: An assessment of impact on safety and efficacy as part of a quality by design development approach. *Biotechnol Prog* 2012; **28**: 608–22.

16 van Beers MMC, Bardor M. Minimizing immunogenicity of biopharmaceuticals by controlling critical quality attributes of proteins. *Biotechnol J* 2012; **7**: 1473–84.

17 Lin B, Qing X, Liao J, Zhuo K. Role of Protein Glycosylation in Host-Pathogen Interaction. *Cells* 2020; **9**: 1022.

18 Walsh G, Walsh E. Biopharmaceutical benchmarks 2022. *Nat Biotechnol* 2022; **40**: 1722–60.

19 Bayda S, Adeel M, Tuccinardi T, Cordani M, Rizzolio F. The history of nanoscience and nanotechnology: From chemical-physical applications to nanomedicine. *Molecules* 2020; **25**: 112.

20 Malik S, Muhammad K, Waheed Y. Nanotechnology: A Revolution in Modern Industry. *Molecules* 2023; **28**: 661.

21 Shan X, Gong X, Li J, Wen J, Li Y, Zhang Z. Current approaches of nanomedicines in the market and various stage of clinical translation. *Acta Pharm Sin B* 2022; **12**: 3028–48.

22 Albanese A, Tang PS, Chan WCW. The effect of nanoparticle size, shape, and surface chemistry on biological systems. *Annu Rev Biomed Eng* 2012; **14**: 1–16.

23 Khodabandehloo H, Zahednasab H, Ashrafi Hafez A. Nanocarriers Usage for Drug Delivery in Cancer Therapy. *Iran J Cancer Prev* 2016; **9**: e3966.

24 Barenholz Y. Doxil®--the first FDA-approved nano-drug: lessons learned. *J Control Release* 2012; **160**: 117–34.

25 Flühmann B, Ntai I, Borchard G, Simoens S, Mühlebach S. Nanomedicines: The magic bullets reaching their target? *Eur J Pharm Sci* 2019; **128**: 73–80.

26 Zeb A, Rana I, Choi HI, *et al.* Potential and Applications of Nanocarriers for Efficient Delivery of Biopharmaceuticals. *Pharmaceutics* 2020; **12**: 1–37.

27 Adepu S, Ramakrishna S. Controlled drug delivery systems: Current status and future directions. *Molecules* 2021; **26**: 5905.

28 Verma P, Thakur AS, Deshmukh K, Jha AK, Verma S. Routes of drug administration. *Int J Pharm Stud Res* 2010; **1**: 54–9.

29 Anselmo AC, Mitragotri S. Nanoparticles in the clinic. *Bioeng Transl Med* 2016; **1**: 10–29.

30 Soo Choi H, Liu W, Misra P, *et al.* Renal clearance of quantum dots. *Nat Biotechnol* 2007; **25**: 1165–70.

31 Nel AE, Mädler L, Velegol D, *et al.* Understanding biophysicochemical interactions at the nano-bio interface. *Nat Mater* 2009; **8**: 543–57.

32 Ngoune R, Peters A, von Elverfeldt D, Winkler K, Pütz G. Accumulating nanoparticles by EPR: A route of no return. *J Control Release* 2016; **238**: 58–70.

33 Attia MF, Anton N, Wallyn J, Omran Z, Vandamme TF. An overview of active and passive targeting strategies to improve the nanocarriers efficiency to tumour sites. *J Pharm Pharmacol* 2019; **71**: 1185–98.

34 Amin M, Mansourian M, Koning GA, Badiee A, Jaafari MR, Ten Hagen TLM. Development of a novel cyclic RGD peptide for multiple targeting approaches of liposomes to tumor region. *J Control Release* 2015; **220**: 308–15.

35 Wong J, Brugger A, Khare A, *et al.* Suspensions for intravenous (IV) injection: a review of development, preclinical and clinical aspects. *Adv Drug Deliv Rev* 2008; **60**: 939–54.

36 Bobo D, Robinson KJ, Islam J, Thurecht KJ, Corrie SR. Nanoparticle-Based Medicines: A Review of FDA-Approved Materials and Clinical Trials to Date. *Pharm Res* 2016; **33**: 2373–87.

37 European Medicines Agency. Reflection paper on the data requirements for intravenous liposomal products developed with reference to an innovator liposomal product. Comm. Hum. Med. Prod. EMA/CHMP/806058/2009/Rev. 02. 2013. https://www.ema.europa.eu/en/documents/scientific-guideline/reflection-paper-data-requirements-intravenous-liposomal-products-developed-reference-innovator_en.pdf (accessed March 3, 2022).

38 Alshawwa SZ, Kassem AA, Farid RM, Mostafa SK, Labib GS. Nanocarrier Drug Delivery Systems: Characterization, Limitations, Future Perspectives and Implementation of Artificial Intelligence. *Pharmaceutics* 2022; **14**. DOI:10.3390/PHARMACEUTICS14040883.

39 Chariou PL, Ortega-Rivera OA, Steinmetz NF. Nanocarriers for the Delivery of Medical, Veterinary, and Agricultural Active Ingredients. *ACS Nano* 2020; **14**: 2678–701.

40 Shen J, Burgess DJ. In Vitro Dissolution Testing Strategies for Nanoparticulate Drug Delivery Systems: Recent Developments and Challenges. *Drug Deliv Transl Res* 2013; **3**: 409–15.

41 Zhao Y, Wang Y, Ran F, *et al.* A comparison between sphere and rod nanoparticles regarding their in vivo biological behavior and pharmacokinetics. *Sci Rep* 2017; **7**: 1–11.

42 Bednarski M, Dudek M, Knutelska J, *et al.* The influence of the route of administration of gold nanoparticles on their tissue distribution and basic biochemical parameters: In vivo studies. *Pharmacol reports* 2015; **67**: 405–9.

43 Guerrini L, Alvarez-Puebla RA, Pazos-Perez N. Surface Modifications of Nanoparticles for Stability in Biological Fluids. *Materials (Basel)* 2018; **11**. DOI:10.3390/MA11071154.

44 Danaei M, Dehghankhold M, Ataei S, *et al.* Impact of Particle Size and Polydispersity Index on the Clinical Applications of Lipidic Nanocarrier Systems. *Pharmaceutics* 2018; **10**. DOI:10.3390/PHARMACEUTICS10020057.

45 Butler D. Translational research: crossing the valley of death. *Nature* 2008; **453**: 840–2.

46 Đorđević S, Gonzalez MM, Conejos-Sánchez I, *et al.* Current hurdles to the translation of nanomedicines from bench to the clinic. *Drug Deliv Transl Res* 2022; **12**: 500–25.

47 US Food and Drug Administration. Guidance for Industry on Drug Products, Including Biological Products, that Contain Nanomaterials. FDA-2017-D-0759. 2022. https://www.fda.gov/Drugs/GuidanceComplianceRegulatoryInformation/Guidances/default.htmand/or (accessed Feb 22, 2023).

48 US Food and Drug Administration. Guidance for Industry on Liposome Drug Products Chemistry, Manufacturing, and Controls; Human Pharmacokinetics and Bioavailability; and Labeling Documentation. FDA-2016-D-2817. 2018. http://www.fda.gov/Drugs/GuidanceComplianceRegulatoryInformation/Guidances/default.htm (accessed Feb 18, 2023).

49 International Standards Organization. Nanotechnologies — Measurement technique matrix for the characterization of nano-objects. ISO/TR 18196:2016 . 2016. https://www.iso.org/obp/ui/en/#iso:std:iso:tr:18196:ed-1:v1:en (accessed Nov 30, 2020).

50 European Medicines Agency. ICH guideline Q1A (R2) on Stability Testing of new Drug Substances and Products - Step 5. Comm. Hum. Med. Prod. CPMP/ICH/2736/99. 2003. https://www.ema.europa.eu/en/documents/scientific-guideline/ich-q-1-r2-stability-testing-new-drug-substances-products-step-5_en.pdf (accessed Feb 9, 2021).

51 European Medicines Agency. Good laboratory practice compliance. https://www.ema.europa.eu/en/human-regulatory/research-development/compliance/good-laboratory-practice-compliance (accessed Jan 31, 2023).

52 European Medicines Agency. Good manufacturing practice. https://www.ema.europa.eu/en/human-regulatory/research-development/compliance/good-manufacturing-practice (accessed March 22, 2023).

53 European Medicines Agency. ICH guideline Q8 (R2) on pharmaceutical development - Step 5. Comm. Hum. Med. Prod. EMA/CHMP/ICH/167068/2004. 2017. https://www.ema.europa.eu/en/documents/scientific-guideline/international-conference-harmonisation-technical-requirements-registration-pharmaceuticals-human-use_en-11.pdf (accessed Sept 20, 2022).

54 European Medicines Agency. ICH guideline Q9 on quality risk management - Step 5. Comm. Hum. Med. Prod. EMA/CHMP/ICH/24235/2006. 2015. https://www.ema.europa.eu/en/documents/scientific-guideline/international-conference-harmonisation-technical-requirements-registration-pharmaceuticals-human-use_en-3.pdf (accessed May 30, 2022).

55 European Medicines Agency. ICH guideline Q10 on pharmaceutical quality system - Step 5. Comm. Hum. Med. Prod. . 2015. https://www.ema.europa.eu/en/documents/scientific-guideline/international-conference-harmonisation-technical-requirements-registration-pharmaceuticals-human_en.pdf (accessed May 27, 2022).

56 Porfire A, Muntean DM, Rus L, Sylvester B, Tomuță I. A quality by design approach for the development of lyophilized liposomes with simvastatin. *Saudi Pharm J Off Publ Saudi Pharm Soc* 2017; **25**: 981–92.

57 Fisher AC, Lee SL, Harris DP, *et al.* Advancing pharmaceutical quality: An overview of science and research in the U.S. FDA's Office of Pharmaceutical Quality. *Int J Pharm* 2016; **515**: 390–402.

58 Merlo-Mas J, Tomsen-Melero J, Corchero JL, *et al.* Application of Quality by Design to the robust preparation of a liposomal GLA formulation by DELOS-susp method. *J Supercrit Fluids* 2021; **173**: 105204.

59 Kapoor M, Lee SL, Tyner KM. Liposomal Drug Product Development and Quality: Current US Experience and Perspective. *AAPS J* 2017; **19**: 632–41.

60 Tomsen-Melero J, Merlo-Mas J, Carreño A, *et al.* Liposomal formulations for treating lysosomal storage disorders q. *Adv Drug Deliv Rev* 2022; **190**: 114531.

61 Solomon D, Gupta N, Mulla NS, Shukla S, Guerrero YA, Gupta V. Role of In Vitro Release Methods in Liposomal Formulation Development: Challenges and Regulatory Perspective. *AAPS J* 2017; **19**: 1669–81.

62 European Medicines Agency. Joint MHLW/EMA reflection paper on the development of block copolymer micelle medicinal products. Comm. Hum. Med. Prod. EMA/CHMP/13099/2013. 2013. https://www.ema.europa.eu/en/documents/scientific-

guideline/joint-mhlwema-reflection-paper-development-block-copolymer-micelle-medicinal-products_en.pdf (accessed Sept 10, 2021).

63 European Medicines Agency. Reflection paper on the data requirements for intravenous iron-based nano-colloidal products developed with reference to an innovator medicinal product. Comm. Hum. Med. Prod. EMA/CHMP/SWP/620008/2012. 2015. https://www.ema.europa.eu/en/documents/scientific-guideline/reflection-paper-data-requirements-intravenous-iron-based-nano-colloidal-products-developed-reference-innovator-medicinal-product_en.pdf (accessed Oct 11, 2021).

64 Souto EB, Silva GF, Dias-ferreira J, *et al.* Nanopharmaceutics: Part II—Production Scales and Clinically Compliant Production Methods. *Nanomaterials* 2020; **10**. DOI:10.3390/NANO10030455.

65 Qin X, Yu C, Wei J, *et al.* Rational Design of Nanocarriers for Intracellular Protein Delivery. *Adv Mater* 2019; **31**: 1902791–823.

66 Chamundeeswari M, Jeslin J, Verma ML. Nanocarriers for drug delivery applications. *Environ Chem Lett* 2019; **17**: 849–65.

67 Sánchez-García L, Serna N, Álamo P, *et al*. Self-assembling toxin-based nanoparticles as self-delivered antitumoral drugs. *J Control release Off J Control Release Soc* 2018; **274**: 81–92.

68 Aljabali AAA, Rezigue M, Alsharedeh RH, *et al.* Protein-based nanomaterials: a new tool for targeted drug delivery. *Ther Deliv* 2022; **13**: 321–38.

69 Elizondo E, Moreno E, Cabrera I, *et al.* Liposomes and other vesicular systems: structural characteristics, methods of preparation, and use in nanomedicine. *Prog Mol Biol Transl Sci* 2011; **104**: 1–52.

70 Islam Shishir MR, Karim N, Gowd V, Zheng X, Chen W. Liposomal delivery of natural product: A promising approach in health research. *Trends Food Sci Technol* 2019; **85**: 177–200.

71 Soltani F, Parhiz H, Mokhtarzadeh A, Ramezani M. Synthetic and Biological Vesicular Nano-Carriers Designed for Gene Delivery. *Curr Pharm Des* 2015; **21**: 6214–35.

72 Shen J, Wang Y, Fan P, *et al.* Self-assembled vesicles formed by C18 unsaturated fatty acids and sodium dodecyl sulfate as a drug delivery system. *Colloids Surfaces A Physicochem Eng Asp* 2019; **568**: 66–74.

73 Grimaldi N, Andrade F, Segovia N, *et al.* Lipid-based nanovesicles for nanomedicine. *Chem Soc Rev* 2016; **45**: 6520–45.

74 Petros RA, Desimone JM. Strategies in the design of nanoparticles for therapeutic applications. *Nat Rev Drug Discov* 2010; **9**: 615–27.

75 Guida V. Thermodynamics and kinetics of vesicles formation processes. *Adv Colloid Interface Sci* 2010; **161**: 77–88.

76 Malam Y, Loizidou M, Seifalian AM. Liposomes and nanoparticles: nanosized vehicles for drug delivery in cancer. *Trends Pharmacol Sci* 2009; **30**: 592–9.

77 Sawant RR, Torchilin VP. Liposomes as 'smart' pharmaceutical nanocarriers. *Soft Matter* 2010; **6**: 4026–44.

78 Xing H, Hwang K, Lu Y. Recent Developments of Liposomes as Nanocarriers for Theranostic Applications. *Theranostics* 2016; **6**: 1336–52.

79 Bulbake U, Doppalapudi S, Kommineni N, Khan W. Liposomal Formulations in Clinical Use: An Updated Review. *Pharmaceutics* 2017; **9**: 1–33.

80 Musacchio T, Torchilin VP. Recent developments in lipid-based pharmaceutical nanocarriers. *Front Biosci* 2011; **16**: 1388–412.

81 Ferrer-Tasies L, Moreno-Calvo E, Cano-Sarabia M, *et al.* Quatsomes: vesicles formed by self-assembly of sterols and quaternary ammonium surfactants. *Langmuir ACS J surfaces colloids* 2013; **29**: 6519–28.

82 Dua JS, Rana AC, Bhandari AK. Liposome: Methods of preparation and applications. *Int J Pharm Stud Res* 2012.

83 Sharma VK, Agrawal MK. A historical perspective of liposomes-a bio nanomaterial. *Mater Today Proc* 2021; **45**: 2963–6.

84 Bozzuto G, Molinari A. Liposomes as nanomedical devices. *Int J Nanomedicine* 2015; **10**: 975–99.

85 Ulrich AS. Biophysical aspects of using liposomes as delivery vehicles. *Biosci Rep* 2002; **22**: 129–50.

86 Nsairat H, Khater D, Sayed U, Odeh F, Al Bawab A, Alshaer W. Liposomes: structure, composition, types, and clinical applications. *Heliyon* 2022; **8**: e09394.

87 Papakostas D, Rancan F, Sterry W, Blume-Peytavi U, Vogt A. Nanoparticles in dermatology. *Arch Dermatol Res* 2011; **303**: 533–50.

88 Fathi M, Mozafari MR, Mohebbi M. Nanoencapsulation of food ingredients using lipid based delivery systems. *Trends Food Sci Technol* 2012; **23**: 13–27.

89 Barani H, Montazer M. A review on applications of liposomes in textile processing. *J Liposome Res* 2008; **18**: 249–62.

90 Nag OK, Awasthi V. Surface engineering of liposomes for stealth behavior. *Pharmaceutics* 2013; **5**: 542–69.

91 Bangale GS, Rajesh KS, Shinde GV. Stealth Liposomes:A Novel Approach of Targeted Drug Delivery In Cancer Therapy. *Int J Pharma Sci Res* 2014; **5**: 750–9.

92 Moghimi SM, Szebeni J. Stealth liposomes and long circulating nanoparticles: Critical issues in pharmacokinetics, opsonization and protein-binding properties. *Prog Lipid Res* 2003; **42**: 463–78.

93 Belfiore L, Saunders DN, Ranson M, Thurecht KJ, Storm G, Vine KL. Towards clinical translation of ligand-functionalized liposomes in targeted cancer therapy: Challenges and opportunities. *J Control Release* 2018; **277**: 1–13.

94 Jain SK, Jain A. Ligand mediated drug targeted liposomes. In: Liposomal Delivery Systems: Advances and Challenges. 2015: 144–58.

95 Nobs L, Buchegger F, Gurny R, Allémann E. Current methods for attaching targeting ligands to liposomes and nanoparticles. *J Pharm Sci* 2004; **93**: 1980–92.

96 Trapani G, Denora N, Trapani A, Laquintana V. Recent advances in ligand targeted therapy. *J Drug Target* 2012; **20**: 1–22.

97 Lamichhane N, Udayakumar TS, D'Souza WD, *et al.* Liposomes: Clinical applications and potential for image-guided drug delivery. *Molecules* 2018; **23**: 288.

98 Li Y, Cong H, Wang S, Yu B, Shen Y. Liposomes modified with bio-substances for cancer treatment. *Biomater Sci* 2020; **8**: 6442–68.

99 Cabrera I, Abasolo I, Corchero JL, *et al.* α-Galactosidase-A Loaded-Nanoliposomes with Enhanced Enzymatic Activity and Intracellular Penetration. *Adv Healthc Mater* 2016; **5**: 829–40.

100 Tomsen-Melero J, Passemard S, García-Aranda N, *et al.* Impact of chemical composition on the nanostructure and biological activity of α-galactosidase-loaded nanovesicles for Fabry disease treatment. *ACS Appl Mater Interfaces* 2021; **13**: 7825–38.

101 Farokhzad OC, Langer R. Impact of nanotechnology on drug delivery. *ACS Nano* 2009; **3**: 16–20.

102 Lombardo D, Kiselev MA. Methods of Liposomes Preparation: Formation and Control Factors of Versatile Nanocarriers for Biomedical and Nanomedicine Application. *Pharmaceutics* 2022; **14**: 543.

103 Meure LA, Foster NR, Dehghani F. Conventional and dense gas techniques for the production of liposomes: a review. *AAPS PharmSciTech* 2008; **9**: 798–809.

104 Elizondo E, Larsen J, Hatzakis NS, *et al.* Influence of the preparation route on the supramolecular organization of lipids in a vesicular system. *J Am Chem Soc* 2012; **134**: 1918–21.

105 Teasdale A, Elder D, Nims RW. ICH Quality Guidelines: An Implementation Guide, First Edition. Wiley, 2017.

106 Haleem RM, Salem MY, Fatahallah FA, Abdelfattah LE. Quality in the pharmaceutical industry – A literature review. *Saudi Pharm J* 2015; **23**: 463–9.

107 Cabrera I, Elizondo E, Esteban O, *et al.* Multifunctional nanovesicle-bioactive conjugates prepared by a one-step scalable method using CO2-expanded solvents. *Nano Lett* 2013; **13**: 3766–74.

108 Soh SH, Lee LY. Microencapsulation and Nanoencapsulation Using Supercritical Fluid (SCF) Techniques. *Pharmaceutics* 2019; **11**: 21–38.

109 Maja L, Željko K, Mateja P. Sustainable technologies for liposome preparation. *J Supercrit Fluids* 2020; **165**: 104984.

110 Ventosa N, Veciana J, Sala S, Cano M. Method for obtaining micro- and nano-disperse systems. Patent WO2006/079889. 2005. https://patentimages.storage.googleapis.com/bd/b5/b7/0cd7d2abda1230/WO2006079889A1.pdf (accessed June 10, 2022).

111 Cano-Sarabia M, Ventosa N, Sala S, Patiño C, Arranz R, Veciana J. Preparation of uniform rich cholesterol unilamellar nanovesicles using CO2-expanded solvents. *Langmuir ACS J surfaces colloids* 2008; **24**: 2433–7.

112 Elizondo E, Veciana J, Ventosa N. Nanostructuring molecular materials as particles and vesicles for drug delivery, using compressed and supercritical fluids. *Nanomedicine* 2012; **7**: 1391–408.

113 Gray V, Cady S, Curran D, *et al.* In vitro release test methods for drug formulations for parenteral applications. *Dissolution Technol* 2018; **25**: 8–13.

114 Herterich JG, Xu Q, Field RW, Vella D, Griffiths IM. Optimizing the operation of a direct-flow filtration device. *J Eng Math* 2017; **104**: 195–211.

115 Spectrum Laboratories. New KrosFlo Research IIi TFF System: Product Information and Operating Instructions. 2015. https://www.yumpu.com/en/document/read/34480183/new-krosflo-research-iii-tff-system-spectrum-laboratories-inc (accessed Feb 14, 2019).

116 Scerra G, De Pasquale V, Scarcella M, Caporaso MG, Pavone LM, D'Agostino M. Lysosomal positioning diseases: Beyond substrate storage. *Open Biol* 2022; **12**. DOI:10.1098/rsob.220155.

117 Sun A. Lysosomal storage disease overview. *Ann Transl Med* 2018; **6**: 476–476.

118 Nair V, Belanger EC, Veinot JP. Lysosomal storage disorders affecting the heart: a review. *Cardiovasc Pathol Off J Soc Cardiovasc Pathol* 2019; **39**: 12–24.

119 Platt FM, d'Azzo A, Davidson BL, Neufeld EF, Tifft CJ. Lysosomal storage diseases. *Nat Rev Dis Prim* 2018; **4**. DOI:10.1038/s41572-018-0025-4.

120 Parenti G, Medina DL, Ballabio A. The rapidly evolving view of lysosomal storage diseases. *EMBO Mol Med* 2021; **13**: e12836.

121 Ferreira CR, Gahl WA. Lysosomal storage disease. *Transl Sci Rare Dis* 2017; **2**: 1–71.

122 Böhm E, Seyfried BK, Dockal M, *et al.* Differences in N-glycosylation of recombinant human coagulation factor VII derived from BHK, CHO, and HEK293 cells. *BMC Biotechnol* 2015; **15**. DOI:10.1186/s12896-015-0205-1.

123 Ioannou YA, Zeidner KM, Grace ME, Desnick RJ. Human alpha-galactosidase A: glycosylation site 3 is essential for enzyme solubility. *Biochem J* 1998; **332**: 789–97.

124 Coutinho MF, Prata MJ, Alves S. Mannose-6-phosphate pathway: A review on its role in lysosomal function and dysfunction. *Mol Genet Metab* 2012; **105**: 542–50.

125 Rajkumar V, Dumpa V. Lysosomal Storage Disease. StatPearls [Internet], 2023.

126 Leal AF, Espejo-Mojica AJ, Sánchez OF, *et al.* Lysosomal storage diseases: current therapies and future alternatives. *J Mol Med* 2020; **98**: 931–46.

127 Beck M. New therapeutic options for lysosomal storage disorders: enzyme replacement, small molecules and gene therapy. *Hum Genet* 2007; **121**: 1–22.

128 Beck M. Therapy for lysosomal storage disorders. *IUBMB Life* 2010; **62**: 33–40.

129 van der Veen SJ, Hollak CEM, van Kuilenburg ABP, Langeveld M. Developments in the treatment of Fabry disease. *J Inherit Metab Dis* 2020; **43**: 908–21.

130 Abasolo I, Seras-Franzoso J, Moltó-Abad M, *et al.* Nanotechnology-based approaches for treating lysosomal storage disorders, a focus on Fabry disease. *Wiley Interdiscip Rev Nanomed Nanobiotechnol* 2021; **13**: e1684.

131 Poletto E, Silva AO, Weinlich R, *et al.* Ex vivo gene therapy for lysosomal storage disorders: future perspectives. *Expert Opin Biol Ther* 2023; **23**: 353–64.

132 Ellison S, Parker H, Bigger B. Advances in therapies for neurological lysosomal storage disorders. *J Inherit Metab Dis* 2023; **46**:

874–905.

133 Kido J, Sugawara K, Nakamura K. Gene therapy for lysosomal storage diseases: Current clinical trial prospects. *Front Genet* 2023; **14**: 1064924.

134 Pisani A, Visciano B, Roux GD, *et al.* Enzyme replacement therapy in patients with Fabry disease: state of the art and review of the literature. *Mol Genet Metab* 2012; **107**: 267–75.

135 Bokhari SRA, Zulfiqar H, Hariz A. Fabry Disease. StatPearls [Internet], 2023.

136 Modrego A, Amaranto M, Godino A, Mendoza R, Barra JL, Corchero JL. Human α-galactosidase A mutants: Priceless tools to develop novel therapies for fabry disease. *Int J Mol Sci* 2021; **22**: 6518.

137 Garman SC, Garboczi DN. The molecular defect leading to fabry disease: Structure of human α-galactosidase. *J Mol Biol* 2004; **337**: 319–35.

138 Garman SC. Structure-function relationships in α-galactosidase A. *Acta Paediatr Int J Paediatr* 2007; **96**: 6–16.

139 Guce AI, Clark NE, Salgado EN, *et al.* Catalytic mechanism of human alpha-galactosidase. *J Biol Chem* 2010; **285**: 3625–32.

140 Research Collaboratory for Structural Bioinformatics Protein Data Bank (RCSB PDB). 1R47: Structure of human alpha-galactosidase. RCSB PDB. 2004. https://www.rcsb.org/structure/1R47 (accessed Dec 1, 2023).

141 Schaefer RM, Tylki-Szymańska A, Hilz MJ. Enzyme replacement therapy for Fabry disease: a systematic review of available evidence. *Drugs* 2009; **69**: 2179–205.

142 Miller JJ, Kanack AJ, Dahms NM. Progress in the understanding and treatment of Fabry disease. *Biochim Biophys Acta - Gen Subj* 2020; **1864**: 129437.

143 Viana-Baptista M. Stroke and Fabry disease. *J Neurol* 2012; **259**: 1019–28.

144 Bersano A, Lanfranconi S, Valcarenghi C, Bresolin N, Micieli G, Baron P. Neurological features of Fabry disease: clinical, pathophysiological aspects and therapy. *Acta Neurol Scand* 2012; **126**: 77–97.

145 Fernandez J, Sigurdsson G, Farivar RS. Cardiac surgery in patients with Fabry's disease: review of literature. *J Card Surg* 2012; **27**: 478–80.

146 West M, Nicholls K, Mehta A, *et al.* Agalsidase Alfa and Kidney Dysfunction in Fabry Disease. *J Am Soc Nephrol* 2009; **20**: 1132–9.

147 Alipourfetrati S, Saeed A, Norris JM, Rastogi A. A Review of Current and Future Treatment Strategies for Fabry Disease: A Model for Treating Lysosomal Storage Diseases. *J Pharmacol Clin Toxicol* 2015; **3**: 1051.

148 Solomon M, Muro S. Lysosomal enzyme replacement therapies: Historical development, clinical outcomes, and future perspectives. *Adv Drug Deliv Rev* 2017; **118**: 109–34.

149 Lee K, Jin X, Zhang K, *et al.* A biochemical and pharmacological comparison of enzyme replacement therapies for the glycolipid storage disorder Fabry disease. *Glycobiology* 2003; **13**: 305–13.

150 Azevedo O, Gago MF, Miltenberger-Miltenyi G, Sousa N, Cunha D. Fabry Disease Therapy: State-of-the-Art and Current

Challenges. *Int J Mol Sci* 2020; **22**: 1–16.

151 Fervenza FC, Torra R, Warnock DG. Safety and efficacy of enzyme replacement therapy in the nephropathy of Fabry disease. *Biol Ther* 2008; **2**: 823–43.

152 Morimoto H, Ito Y, Yoden E, *et al.* Non-clinical evaluation of JR-051 as a biosimilar to agalsidase beta for the treatment of Fabry disease. *Mol Genet Metab* 2018; **125**: 153–60.

153 Nakamura K, Kawashima S, Tozawa H, *et al.* Pharmacokinetics and pharmacodynamics of JR-051, a biosimilar of agalsidase beta, in healthy adults and patients with Fabry disease: Phase I and II/III clinical studies. *Mol Genet Metab* 2020; **130**: 215–24.

154 Ruderfer I, Shulman A, Kizhner T, *et al.* Development and Analytical Characterization of Pegunigalsidase Alfa, a Chemically Cross-Linked Plant Recombinant Human α-Galactosidase-A for Treatment of Fabry Disease. *Bioconjug Chem* 2018; **29**: 1630–9.

155 Hughes D, Gonzalez D, Maegawa G, *et al.* Long-term safety and efficacy of pegunigalsidase alfa: A multicenter 6-year study in adult patients with Fabry disease. *Genet Med* 2023; **25**. DOI:10.1016/j.gim.2023.100968.

156 Lenders M, Pollmann S, Terlinden M, Brand E. Pre-existing anti-drug antibodies in Fabry disease show less affinity for pegunigalsidase alfa. *Mol Ther Methods Clin Dev* 2022; **26**: 323–30.

157 Del Grosso A, Parlanti G, Mezzena R, Cecchini M. Current treatment options and novel nanotechnology-driven enzyme replacement strategies for lysosomal storage disorders. *Adv Drug Deliv Rev* 2022; **188**: 114464.

158 Lu B, Ku J, Flojo R, Olson C, Bengford D, Marriott G. Exosome- and extracellular vesicle-based approaches for the treatment of lysosomal storage disorders. *Adv Drug Deliv Rev* 2022; **188**: 114465.

159 Pardridge WM. Blood-brain barrier delivery for lysosomal storage disorders with IgG-lysosomal enzyme fusion proteins. *Adv Drug Deliv Rev* 2022; **184**: 114234.

160 Wilczewska AZ, Niemirowicz K, Markiewicz KH, Car H. Nanoparticles as drug delivery systems. *Pharmacol Reports* 2012; **64**: 1020–37.

161 Yetisgin AA, Cetinel S, Zuvin M, Kosar A, Kutlu O. Therapeutic Nanoparticles and Their Targeted Delivery Applications. *Molecules* 2020; **25**: 2193.

162 Liu P, Chen G, Zhang J. A Review of Liposomes as a Drug Delivery System: Current Status of Approved Products, Regulatory Environments, and Future Perspectives. *Molecules* 2022; **27**: 1372.

163 Ardizzone A, Kurhuzenkau S, Illa-Tuset S, *et al.* Nanostructuring Lipophilic Dyes in Water Using Stable Vesicles, Quatsomes, as Scaffolds and Their Use as Probes for Bioimaging. *Small* 2018; **14**: e1703851.

164 Hsu J, Serrano D, Bhowmick T, *et al.* Enhanced endothelial delivery and biochemical effects of α-galactosidase by ICAM-1-targeted nanocarriers for Fabry disease. *J Control release Off J Control Release Soc* 2011; **149**: 323–31.

165 Hsu J, Bhowmick T, Burks SR, Kao JPY, Muro S. Enhancing Biodistribution of Therapeutic Enzymes In Vivo by Modulating Surface Coating and Concentration of ICAM-1-Targeted Nanocarriers. *J Biomed Nanotechnol* 2014; **10**: 345–54.

166 Giannotti MI, Abasolo I, Oliva M, *et al.* Highly Versatile Polyelectrolyte Complexes for Improving the Enzyme Replacement

Therapy of Lysosomal Storage Disorders. *ACS Appl Mater Interfaces* 2016; **8**: 25741–52.

167 Ventosa L, Veciana J, Royo M, *et al.* Liposomes and its use for enzyme delivery. Patent EP 21382062.4-1112. 2021. http://hdl.handle.net/10261/289055 (accessed June 10, 2022).

168 Cristóbal-Lecina E, Pulido D, Martin-Malpartida P, Macias MJ, Albericio F, Royo M. Synthesis of Stable Cholesteryl-Polyethylene Glycol-Peptide Conjugates with Non-Disperse Polyethylene Glycol Lengths. *ACS Omega* 2020; **5**: 5508–19.

169 Bodary PF, Shayman JA, Eitzman DT. α-Galactosidase A in Vascular Disease. *Trends Cardiovasc Med* 2007; **17**: 129–33.

170 European Medicines Agency (EMA), European Comission (EC). Orphan drug designation (Designation number EU/3/20/2396). Orphan condition: Alpha galactosidase A for treatment of Fabry disease. Sponsor: Consejo Superior de Investigaciones Científicas (CSIC) . 2021.

2

OBJECTIVES

For the development of high-quality nanopharmaceuticals based on the coupling between a therapeutic biomolecule and a nanocarrier, it is necessary to perform a profound physicochemical characterization of both components, and their molecular and supramolecular interactions. This knowledge is a must to efficiently speed up the arduous translation of this type of nanopharmaceuticals towards clinical applications.

In this scenario, the present thesis was focused on the deep physicochemical characterization of a new nanopharmaceutical under development for Fabry disease treatment, based on the coupling of a recombinant human α-galactosidase A (GLA) enzyme with RGD-targeted nanoliposomes. In particular, the following three objectives have been addressed to contribute to this relevant goal:

1. Study of the impact of specific GLA production process parameters (PPPs) on the physicochemical and biological characteristics of the produced GLA enzyme. Specifically, the impact of the following PPPs has been explored:

   a) Presence or absence of purification tags in the GLA sequences.

   b) Type of cell line (human embryonic kidney (HEK) or Chinese hamster ovary (CHO) cells) used for GLA expression.

   c) Strategy (transient gene expression or stable clone) used for GLA expression.

   d) Type of immobilized metal affinity chromatography (IMAC) resin (charged with Ni^{2+} or Co^{2+} metal ions) used for GLA purification.

   e) Buffer and pH (acetic buffer 0.01 M at pH 4.5 or 5.5, or Fabrazyme-like buffer at pH 7) used for GLA storage.

2. Study of the impact of GLA characteristics over the following physicochemical and biological features of GLA nanoliposomal formulations:
    a) Enzyme entrapment efficiency (EE %).
    b) GLA leakage rate from liposome-based nanoformulations.
    c) Enzymatic activity (EA) of the integrated GLA in the nanoliposomal formulations.
    d) Colloidal stability of GLA nanoliposomal formulations.
    e) GLA release from liposome-based nanoformulations.
    f) GLA distribution on liposomal nanostructure.
    g) Protective capacity of nanoliposomes against the GLA degradation.

3. Development and validation of new analytical techniques to characterize and control the quality attributes of the optimal RGD-targeted nanoliposomal formulation which contains the GLA obtained from CHO K1 cells by stable expression production method, in order to push the advancement of this nanopharmaceutical from the non-regulatory preclinical to the early clinical phase.

3

PRODUCTION, PURIFICATION, CHARACTERIZATION AND COMPARISON OF DIFFERENT ALPHA-GALACTOSIDASE A (GLA) ENZYMES

3.1. Introduction

As previously explained in ***Chapter 1***, recombinant biopharmaceutics can be produced in a large variety of cellular expression systems (e.g. bacteria, yeasts, insect cells, mammalian and plant cells), which directly impact differently on the protein characteristics, and therefore, on the biopharmaceutical critical quality attributes (CQAs). As aforementioned, GLA enzymes are glycoproteins that can be produced through biotechnological processes to be used as enzyme replacement therapy (ERT) for Fabry disease. The use of mammalian cell lines has been extensively investigated to obtain mature and active GLA biopharmaceuticals such as Replagal® and Fabrazyme®. This chapter describes the impact of specific GLA production process parameters (PPPs) on the physicochemical and biological characteristics of four versions of recombinant GLA enzymes differing on their aminoacid sequence and expression system. The knowledge obtained contributes to the development of new biopharmaceuticals or nanopharmaceuticals based on GLA enzymes to be used as ERT for Fabry disease.

3.1.1. Most common mammalian cell lines used as expression systems

Regarding the latest survey of approved recombinant biopharmaceutical (period January 2018 – June 2022), the 67 % of them are produced in mammalian cell-based protein expression systems, being the preferred "cell factories" of choice in the industry to produce therapeutic proteins intended for human usage[1,2]. Mammalian expression systems, which allow post-translational processing of proteins, are essential to obtain biopharmaceutics presenting human-like native structure and functional activity[3]. Lately, most recombinant

therapeutics for biomedical applications (89 %) are expressed in Chinese hamster ovary (CHO) cells due to their capacity to perform similar post-translational modifications of human proteins, and their easy scalability which allow productions of protein up to g/L yields[2]. Besides, other mammalian "cell factories" has also been used for the development of approved therapeutic proteins, including human embryonic kidney (HEK), NS0 mouse myeloma cells, or baby hamster kidney (BHK) among others.

The mammalian expression system of choice for recombinant protein expression has a significant impact on the product CQAs, which may be related to slight differences on the post-translational processing responsible to protein glycosylation[4]. This consists in a well conserved organism-dependent process during which carbohydrates or oligosaccharides molecules are covalently attached to the target protein macromolecule, acting as an internal quality control mechanism to ensure proper protein folding, targeted transport, cellular localization and activity[5]. Differences between glycosylation moieties when producing the same recombinant protein sequences in CHO or HEK cells has been reported, containing respectively higher degree of sialylation or N-glycans, and directly impacting on case-by-case product quality and productivity[4]. Interestingly, the two recombinant GLA biotherapeutics approved for ERT in Europe (Fabrazyme® and Replagal®) encode the same α-galactosidase A human enzyme, but are expressed by different mammalian "cell factories"[6,7]. Replagal® is produced in a human cell line of undisclosed origin, meanwhile Fabrazyme® is produced in a CHO cell line capable to promote higher levels of sialylation and phosphorylation, which enhance the protein uptake into cells because of an increased binding to mannose-6-phospate receptors[8]. Both enzymes differ in their pharmaceutical form (Fabrazyme® being a lyophilized product, and Replagal® a concentrated solution), but also in their administration dose, suggesting that the product CQAs and protein stability are influenced by the different post-translational modifications dependent on the "cell factory" of choice.

The introduction of a gene encoding the therapeutic protein of interest into mammalian cells is required to induce its expression. This process is known as cell transfection, and can be achieved by several delivery methods of different nature: physical (e.g. electroporation), biological (e.g. viral transduction with recombinant viruses), or chemical (e.g. cationic polymer, phosphate or lipid reagents)[9]. Although the use of cationic polymer as chemical-mediated transfection is widely used in research, the choice of the delivery method is depending on the host cell and purpose. High amounts of recombinant protein (in the scale of milligrams to grams) are required for biochemical and biophysical research during the development of a biopharmaceutical, but also to test promising prototypes in pre-clinical assays. Depending on the purpose, protein expression can be performed either transiently or through stable cell lines through the following procedures: stable expression or transient gene expression (TGE). The preferred "cell factory" for each procedure is indicated on ***Table 3.1***. In this thesis,

both approaches were employed to produce different GLA enzymes in CHO or HEK cells, in order to compare their CQAs and understand the biochemical basis behind them.

Table 3.1. Habitual expression system of choice according to the intended recombinant protein expression approach to use.

Mammalian expression system	
HEK 293 cells	**CHO cells**
Human Embryonic Kidney cells	Chinese Hamster Ovary cells
Predominant cell line used for transient production	The most commonly cell line used for stable protein expression
It is not frequently used for therapeutic protein production	Predominant cell line for therapeutic protein production
Conserved post-translational modifications from human	Post-translational modifications preferred for quality of biopharmaceutics
Easy to transfect	Less easily transfectable
Adaptable for suspension culture	Adaptable for suspension culture
Transient expression	Transient and stable expression

3.1.2. Transfection procedures for transient expression

Cell transfection and further TGE approaches typically allow the production of significant amount of protein (in a range of milligrams per liter) within 1 – 2 weeks[10,11]. This is, the preferred option at early stages of the development of a new biopharmaceutical, when several prototypes must be quickly explored to demonstrate the fulfillment of required specifications to be considered potential as biotherapeutics. The basics of transient procedures consist in the introduction of a foreign genetic material (such as a plasmid DNA, pDNA) encoding the protein of interest, resulting in a heterogeneous population of transfected and non-transfected cells. Successfully transfected cells can express, for a limited period of time, the foreign gene episomally, which means that is not integrated into the cell genome (***Figure 3.1***). Consequently, the production of recombinant protein is stopped few days post-transfection due to the loss of the foreign genetic material over time due to environmental factors and dilution in each cell division[9,12]. To accomplish cell transfection, standard processes habitually condenses negatively charged pDNA molecules with polycationic reagents such as polyethylenimine (PEI), forming nanostructures called polyplexes capable to be uptaken in cells via endocytosis, which release the plasmid from endosomal vesicles to the cytoplasm after osmotic swelling, allowing the further pDNA diffusion to the cell nucleus[13,14]. Linear and low molecular weight PEI is a cost-effective transfection chemical reagent containing ethylenimine motifs responsible for its main properties (positive net charge, moderate cytotoxicity and non-biodegradable polymer), which has successfully transfected several mammalian cells[15–17]. The positively charged

amino nitrogen atoms in its polymeric structure are the responsible to bind the phosphate atoms from negatively charged pDNA molecules, subsequently generating stable pDNA:PEI complexes. It was previously described that pDNA:PEI ratio of 1:3 (w/w) which correspond to a nitrogen residues/pDNA phosphates (N/P) ratio of 23, is the one resulting in the highest transfection efficiencies for HEK cells[18,19].

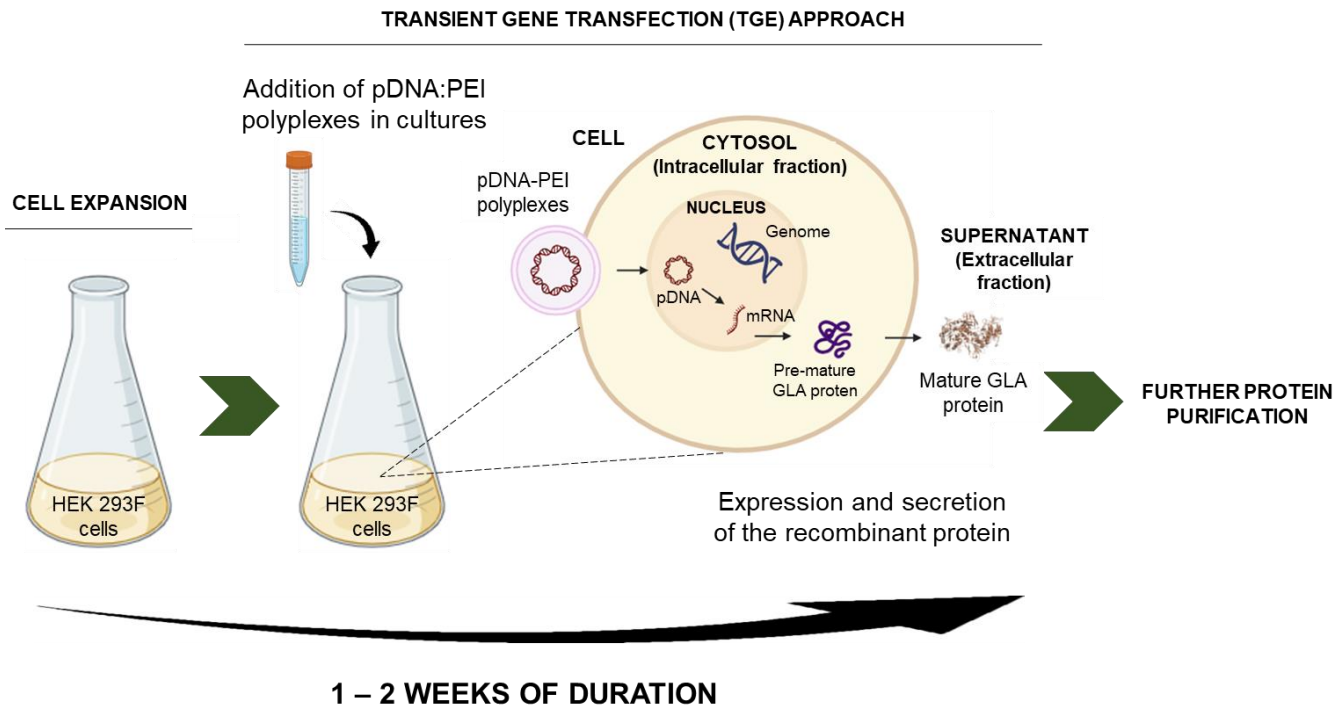


Figure 3.1. Schematic diagram representing the TGE procedure for the expression of GLA enzymes in HEK 293F cells, where a foreign non-integrated pDNA within the host genome is expressed episomally.

TGE procedures are widely performed in HEK 293 cells because of their easy growth in serum-free medium and transfection in suspension-adapted cultures[20–22], as well as their extensive usage in the production of biopharmaceuticals which achieved regulatory approval. High volumetric yields of secreted recombinant proteins are usually achieved by using HEK 293 cells[23], being serum-free suspension-adapted HEK 293F cultures widely used in industry. Furthermore, the use of a serum-free medium increases the efficiency and allow reduced steps and time for further downstream process of secreted products, by reducing the amount of impurities coming from media. For these reasons, TGE in industry has been successfully scale-up to volumes of 100 L commonly using large stirred-tank bioreactors[24–26].

Although the feasibility of TGE scalability, the recombinant protein yield reached may vary depending on the host cell of choice, cell density, composition of the culture medium, or other parameters such as culture temperature or pDNA:PEI ratio, among others[27]. The presence of non-complexed PEI may alter pDNA uptake and intracellular trafficking, as well as cause cytotoxicity[14,16,28–30]. Another important matter regarding cost-

effectiveness of TGE for industrial purposes is the amount of pDNA necessary per liter of transfection (frequently 1 mg or more), constituting a large proportion of the overall process cost. Therefore, the lowest concentrations of pDNA and PEI should be optimized case-by-case in order to reach proper cell viability, protein expression levels, and reasonable economic cost. Moreover, decreasing amounts of pDNA in TGE approaches may result on the reduced addition of probable contaminants from pDNA purification (e.g. bacterial RNA or endotoxin which may alter the purification processing of recombinant proteins[31–33]. In this scenario, some works have reported the possibility of replacing certain amounts of coding pDNA by cheaper non-specific DNA (named as "filler" DNA) in PEI-mediated TGE of mammalian cultures without provoking a significant decrease on the recombinant protein production yield[34,35]. However, in this thesis the pDNA:PEI ratio of 1:3 was maintained, and then both, codifying pDNA and PEI concentration (without any replacement using filler DNA), was directly decreased as alternative to improve the overall productivity of our TGE reduced handling-process. More efforts to achieve an even higher optimized TGE product yield are still required to become TGE in a competitive technology at industry scale in future.

3.1.3. Stable clone for recombinant protein expression

In contrast to TGE procedures, stable expression is achieved by the establishment of a stable clone, i.e. the integration of a foreign genetic material into the host genome, allowing the persistent expression of recombinant protein over several divisions of the cell line (***Figure 3.2***). After the transfection process, a mixture of transfected and non-transfected cells is obtained. Then, a time-consuming step lasting several months is conducted to select, identify and characterize individually the best clones in terms of productivity and protein quality[36–39]. This procedure can be performed thanks to a selection marker, such as an antibiotic resistance gene encoded by the pDNA construct. At the end, the best clone is cryopreserved in cryovials being stored in vapor phase of liquid nitrogen, and only expanded in large cultures for production purposes.

Therefore, the main drawback of this approach is the extensive time required to obtain the desired stable clone. For this reason, this approach is of choice for industry only when a promising biopharmaceutical needs to be produced in large quantities, since stable gene expression has demonstrated to reach higher productivities in several cases compared with TGE processes[11,23,37]. For this purpose, CHO cells are extensively used for the production of biopharmaceutics, since they are cells able to indefinitely growth into bioreactor systems on large volumetric scale, and capable of expressing and secreting bioproducts with post-translational processing similar to human[40].

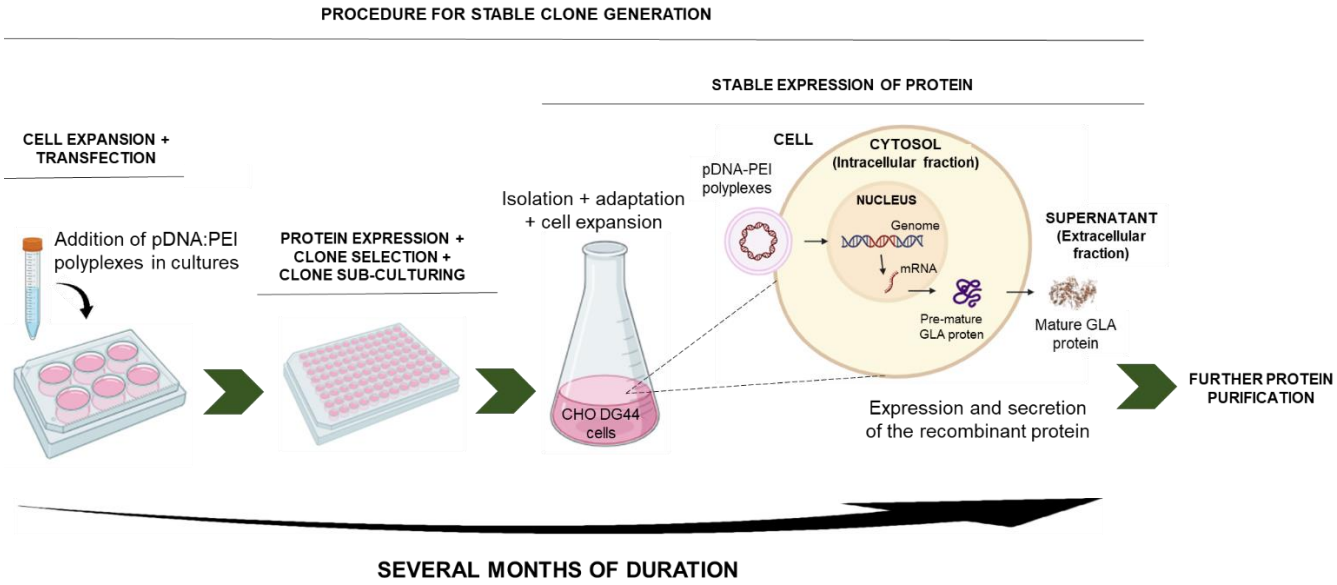


Figure 3.2. Schematic diagram representing the time-consuming procedure for the obtaining of a stable clone capable to constitutively express GLA enzymes in CHO DG44 cells, where a foreign pDNA is integrated into the host genome.

3.1.4. Histidine-tag and c-myc-tag: popular affinity tags for downstream processing and detection of recombinant proteins

After their expression, recombinant proteins need to be purified, i.e. to be separated from cellular debris and the other endogenous proteins coming from the "cell factory". Recombinant proteins can be purified by successive chromatographic steps according some parameters of the molecule (e.g. surface charge, size or hydrophobicity). The fusion of specific tags to the N-terminus or C-terminus of protein sequences is widely used to simplify downstream processing and generate standard protocols based on affinity procedures. Therefore, the fusion of some purification tags in recombinant proteins may improve the reachable protein yield after the downstream processing, the protein purity, solubility and detection in western blot[41,42]. Some of the most common affinity tags used in biotechnological procedures are compiled in *Table 3.2*. Tags with larger sizes, such as glutathione S-transferase (GST) and maltose-binding protein (MBP), usually enhance protein solubility and expression yield, but present higher immunogenicity. Meanwhile, smaller tags are widely employed due to their reduced probability to alter the protein structure and activity.

Table 3.2. Affinity tags commonly used for purification or recombinant proteins. Adapted from[41,42]. Legend: mAb means monoclonal antibody.

Affinity tag	Length (number of residues)	Size (kDa)	Sequence	Binding matrix	Elution conditions
Poly-Arg (5-Arg)	5 – 6 (usually 5)	0.80	RRRRR	Cation-exchange resin	0 to 400 mM NaCl (liniar gradient at pH > 8
Poly-His (Hexahistidine or 6-His)	2 – 10 (usually 6)	0.84	HHHHHH	Metal ions (Ni^{2+}, Co^{2+}, Cu^{2+}, Zn^{2+}, Fe^{3+})	20 – 250mM Imidazole or low pH
FLAG	8	1.01	DYKDDDDK	Anti-FLAG mAb	2 – 5mM EDTA or pH 3
Strep-tag II	8	1.06	WSHPQFEK	Strep-Tactin (modified streptavidin)	2.5 mM desthiobiotin
HA	9	1.10	YPYDVPDYA	Anti-HA epitope mAb	Low pH
c-myc	11	1.20	EQKLISEEDL	Anti-Myc epitope mAb	Low pH
S	15	1.75	KETAAAKFERQHMDS	S-protein of RNase A	0.2 M citrate at pH 2, or 3 M guanidine thiocyanate, or 3 M magnesium chloride
Calmodulin-binding peptide (CBP)	26	2.96	KRRWKKNFIAVSAAN RFKKISSSGAL	Calmodulin	EGTA with ot without 1 M NaCl
Streptavidin-binding peptide (SBP)	38	4.03	MDEKTTGWRGGHV VEGLAGELEQLRARL EHHPQGQREP	Streptavidin	2 mM biotin
Chitin-binding domain (CBD)	51	5.59	TNPGVSAWQVNTAY TAGQLVTYNGKTYKC LQPHTSLAGWEPSNV PALWQLQ	Chitin	Fused with intein: 30 – 50 mM dithiothreitol, β-mercaptoethanol or cysteine
Glutathione S-transferase (GST)	211	26.00	Protein	Glutathione	5 – 10 mM reduced glutathione
Maltose-binding protein (MBP)	396	42.00	Protein	Amylose	10 mM maltose

In general, the most frequently affinity tag used for protein purification is the hexahistidine (6-His) tag, composed by six residues of histidine in tandem, aminoacid capable to bind immobilized divalent cations such as Ni^{2+} or Co^{2+} in physiologic conditions, and extensively used to purify proteins through immobilized metal affinity chromatography (IMAC) procedures. The advantages of 6-His tag are to be non-toxic and have small size which hardly modify the physicochemical properties or immunogenicity of the fused protein[41,42]. In some commercial vectors this 6-His tag is encoded together with other purification tags like the c-myc tag (encoding the EQKLISEEDL sequence of eleven residues). Some works have reported that their combination apparently do not alter the enzymatic activity or their optimal pH of storage of enzymes produced by *Pichia Pastoris*[43], but also is capable to improve the production of soluble antibodies when are encoded in the specific order c-myc/6-His tag in contrast to other constructs with fused 6-His/c-myc tag[44]. On the other hand, c-myc tag can be useful for protein purification due to its high affinity with the 9E10 antibody, although is highly used for protein detection by western blot. However, it is described that c-myc tag can impair protein secretion to extracellular media by interfering in the translocation process if it is fused directly behind the signal peptide[41,42].

In this thesis some recombinant versions of GLA were designed with the presence of none, one or both 6-His and c-myc tags for purification purposes. As GLA enzymes encode a signal peptide on their N-terminus to be secreted to the extracellular media, the purification tags were always fused to the C-terminus of GLA sequences. Also both tags were designed to be encoded in the specific order c-myc/6-His tag to avoid solubility problems.

3.1.5. Recombinant GLA enzyme versions of study

With the aim to investigate which are the relevant GLA enzyme features to develop well-controlled manufacturing methodologies to obtain high-quality degree biopharmaceuticals intended for ERT of Fabry disease, part of the efforts of this thesis, summarized in the present chapter, were focused on the study of the impact of the following specific GLA PPPs on the physicochemical and biological characteristics of the produced recombinant GLA enzyme versions:

1. Presence or absence of purification tags in the GLA sequences.
2. Type of cell line (HEK or CHO cells) used for GLA expression.
3. Strategy (TGE or stable clone) used for GLA expression.
4. Type of IMAC resin (charged with Ni^{2+} or Co^{2+} metal ions) used for GLA purification.
5. Buffer and pH (acetic buffer 0.01M at pH 4.5 or 5.5, or Fabrazyme-like buffer at pH 7) used for GLA storage.

Briefly, different versions of recombinant GLA (described on ***Chapter 7, Section 7.2***) were produced, characterized and compared in this chapter. The four constructs differ on their gene sequence by containing or not 6-His and/or c-myc purification tags fused to their C-terminus, and were produced using different production procedures and different mammalian expression systems. The rationale behind the constructs design is to correlate the physicochemical and biological properties of GLA enzymes with the presence or absence of purification tag sequences, or with the glycosylation pattern related to the "cell factory" of choice. The main characteristics of the four GLA constructs are detailed below and schematized in ***Table 3.3***.

- **GLAH6-T:** this GLA contains the 6-His purification tag in its sequence. It is produced by TGE procedures in HEK 293F cell cultures. Gene construct developed previously to this thesis by Dr. José Luis Corchero from IBB-UAB (Barcelona)[45,46].
- **GLAcmycH6-T:** this GLA contains both c-myc and 6-His purification tags in its sequence. It is produced by TGE procedures in HEK 293F cell cultures. This gene construct was designed *de novo* in this thesis.
- **GLAcmycH6-S:** this GLA contains both c-myc and 6-His purification tags in its sequence. It is produced by a CHO DG44-based stable clone. Gene construct developed previously to this thesis by Dr. José Luis Corchero from IBB-UAB[47].

- **GLA-S**: this GLA does not contain any purification tag. It is produced by a CHO K1-based stable clone. Gene construct developed previously to this thesis by Dr. José Luis Corchero from IBB-UAB in collaboration with LeanBio SL (Barcelona)[48,49]. The protein amounts required for this thesis has been provided by LeanBio SL.

Table 3.3. Characteristics of the GLA constructs described in this chapter, and their comparison with some approved recombinant GLA products already available in the market.

Enzyme ID and supplier	Production cell line	Transfection method	Encoding purification tags	Storage media	Storage conditions
GLAH6-T [45] (NBT group from IBB-UAB, Barcelona)	Human Embyonic Kidney (HEK 293F)	Transient	6-His	Acetic acid (0.01 M, pH 4.5 or 5.5)	Liquid solution (Frozen)
GLAcmycH6-T (NBT group from IBB-UAB, Barcelona)	Human Embyonic Kidney (HEK 293F)	Transient	c-myc + 6-His	Acetic acid (0.01 M, pH 4.5 or 5.5)	Liquid solution (Frozen)
GLAcmycH6-S [47] (NBT group from IBB-UAB, Barcelona)	Chinese Hamster Ovary (CHO DG44)	Stable	c-myc + 6-His	Acetic acid (0.01 M, pH 4.5 or 5.5)	Liquid solution (Frozen)
GLA-S* (LeanBio SL, Barcelona)	Chinese Hamster Ovary (CHO K1)	Stable	None	Mannitol, sodium phosphate monobasic monohydrate, sodium phosphate dibasic heptahydrate	Liquid solution (Frozen)
Replagal® ₮ [7] (Shire, USA)	Human cells from undisclosed origin	Stable	None	Sodium phosphate, monobasic monohydrate, polysorbate 20, sodium chloride, sodium hydroxide	Liquid solution (2 – 8 ºC)
Fabrazyme® ₮ [6] (Genzyme, USA)	Chinese Hamster Ovary (CHO)	Stable	None	Mannitol, sodium phosphate monobasic monohydrate, sodium phosphate dibasic heptahydrate	Lyophilized cake (2 – 8 ºC)

*Produced and supplied by LeanBio SL as explained in *Chapter 7, Section 7.2*.

As explained before in *Chapter 1*, and in the frame of several collaborative and interdisciplinary projects, three of these GLA constructs (GLAH6-T, GLAcmycH6-S and GLA-S) were used as protein models for the development of a new liposome-based nanopharmaceutical capable to entrap GLA as drug substance for the ERT of Fabry disease. There is a need to produce high-quality degree proteins in order to avoid the destabilization of the nano and supramolecular structure of nanopharmaceuticals after their association. The identified CQAs of GLA enzymes to ensure the desired biopharmaceutical quality are summarized in *Table 3.4*. The GLA constructs produced in this chapter that reached such CQAs were integrated in liposomal nanoformulations and further investigated in *Chapter 4*.

Table 3.4. Identified CQAs for recombinant GLA enzymes intended to be nanoformulated.

CQA		Specification range
	Macroscopic Appearance	Homogeneous aqueous solution without sediment
	Mean homodimer size	7 – 15 nm
	Polydispersity index (PdI)	< 0.7
	ζ-potential	< + 2 mV
	Solubility in aqueous buffers	0.2 – 4.0 mg/mL
	Identity	40 – 65 kDa
	Purity	≥ 90 % (m/m)
	Specific enzymatic activity (EA)	Bioactive (≥ 1500 µmol/h·mg, according previous results on Corchero *et al.* [45])
	pH of storage	4.0 – 7.5
Product-related impurities	**Low molecular weight forms (degradation products)**	< 5 % (m/m)
	High molecular weight forms (aggregation products)	Conformational stability in a temperature range of 2 – 40 ºC (if possible sizes < 30 nm by DLS, and values of CSM < 353 nm by intrinsic Trp fluorescence spectra)
Process-related impurities	**Host Cell DNA**	< 5 % (m/m) nucleic acid
	Endotoxins	< 1 EU/mL*

*Parameter being only considered for the GLA-S version used in the frame of the European Phoenix project (H2020, ID 953110), and determined by LeanBio SL.

3.2. Optimization of the transient transfection protocol to enhance the yield of recombinant protein production

Previous to this thesis and as explained in ***Chapter 7, Section 7.2***, the stable clone procedures using CHO cells for the expression of GLAcmycH6-S and GLA-S were developed and optimized by Dr. José Luis Corchero from IBB-UAB and LeanBio SL, respectively[47,49]. These stable clones yielded protein productivities amounts larger than 50 mg/L. The TGE procedures using HEK 293F cells to obtain the GLAH6-T enzyme was also developed by Dr. José Luis Corchero from IBB-UAB, but yielding lower protein productivities of around 30 mg/L[45].

Several mg of GLA are necessary to perform the purposed studies in this thesis about the GLA characterization (explained in this chapter) and the ones loading GLA in nanovesicular formulations (summarized in ***Chapter 4***). Problems related of batch-to-batch reproducibility are usual when producing proteins by TGE. To avoid them, the TGE procedure previously described on Corchero *et al.*[45] was optimized in order to produce enough amounts

of GLAH6-T and GLAcmcyH6-T enzymes in unique large productions, and to carry out the aforementioned studies using the same protein batches.

Briefly, the original protocol consisted of the mixing and incubation of pDNA-PEI polyplexes (ratio pDNA:PEI of 1:3 (w/w)) in sterile medium (volume of 10 % the total volume of culture to be transfected) during 10 min at room temperature. Then, HEK 293F cells were transfected by the addition of pDNA-PEI polyplexes, at 1 µg pDNA/million cells. Finally, valproic acid (VPA) was added to cells 4 hours after transfection at a final concentration of 4 mM to enhance recombinant protein expression. The mature GLA enzymes secreted to the extracellular media were harvested at 5-day post-transfection. To optimize this original TGE protocol, plasmid encoding for GLAH6-T protein was used for the better comparison with previous results obtained by Corchero *et al.*[45]. All optimization studies were performed in transfection volumes of 2 mL in 6-well plates.

The effect of the culture medium used for cell growth and pDNA-PEI formation, but also the addition of few DMSO concentrations in cell cultures to permeabilize cell membranes and promote increased TGE efficiency are usual approaches explored during the optimization of TGE procedures[18,50–52]. However, in this thesis the GLAH6-T expression in HEK 293F cultures was not improved by implementing these proposals on the TGE procedure established by Corchero *et al.*[45] (data not shown).

Influence of decreasing pDNA-PEI amounts on recombinant GLAH6-T expression

In an attempt to reduce economical costs related to TGE procedures, the impact of using decreasing pDNA-PEI amounts for transfecting HEK 293F cells was also investigated in this thesis. The original conditions of 1 µg pDNA/mL cell has been compared with 2-fold decreased pDNA amounts, but maintaining the original ratio 1:3 of pDNA:PEI. The purpose of this study was to explore how the recombinant GLAH6-T expression is affected depending on the amount of the coding pDNA. Results shown in ***Figure 3.3*** confirmed a 2-fold increased GLAH6-T expression in both, secreted and intracellular HEK 293F cell fractions, when transfecting HEK 293F cultures at 0.5 µg pDNA/mL cell (being considered the optimal transfected condition tested). However, GLAH6-T expression levels decreased when using even lower amounts of pDNA. Interestingly, GLAH6-T solubility and secretion levels were not affected by amounts of pDNA, since values of secreted enzyme to the medium was maintained in all cases (around 60 %), evidencing that GLAH6-T enzyme was better expressed, but not better secreted. The cell viability after transfection was monitored in parallel because it is well known the PEI toxicity on eukaryotic cells. Since pDNA:PEI ratio of 1:3 was maintained in all TGE conditions tested, higher PEI amounts were used in the original TGE condition of 1 µg pDNA/mL cell compared to those newly explored in this work. Results suggested that the PEI amounts present in the original TGE condition of 1 µg pDNA/mL cell impaired the cell viability, and subsequently the GLA expression yield, unlike the new conditions investigated in this study.

Similar experiments demonstrating same results were carried out also testing the green fluorescent protein (GFP) and the His-tagged version of the human "major vault protein" (MVP; the main component of the intracellular organelle known as "vault")[53–56] as examples of recombinant proteins differing greatly in structure and functionality. Control experiments reproducing the TGE protocol when transfecting HEK 293F cultures at 0.5 µg pDNA/mL cell, but using only pDNA or only PEI reagent, supported the hypothesis of reduced PEI concentrations improve the HEK 293F cell viability, and therefore, the protein expression levels result increased. These findings were compiled in Carreño *et al.*[57].

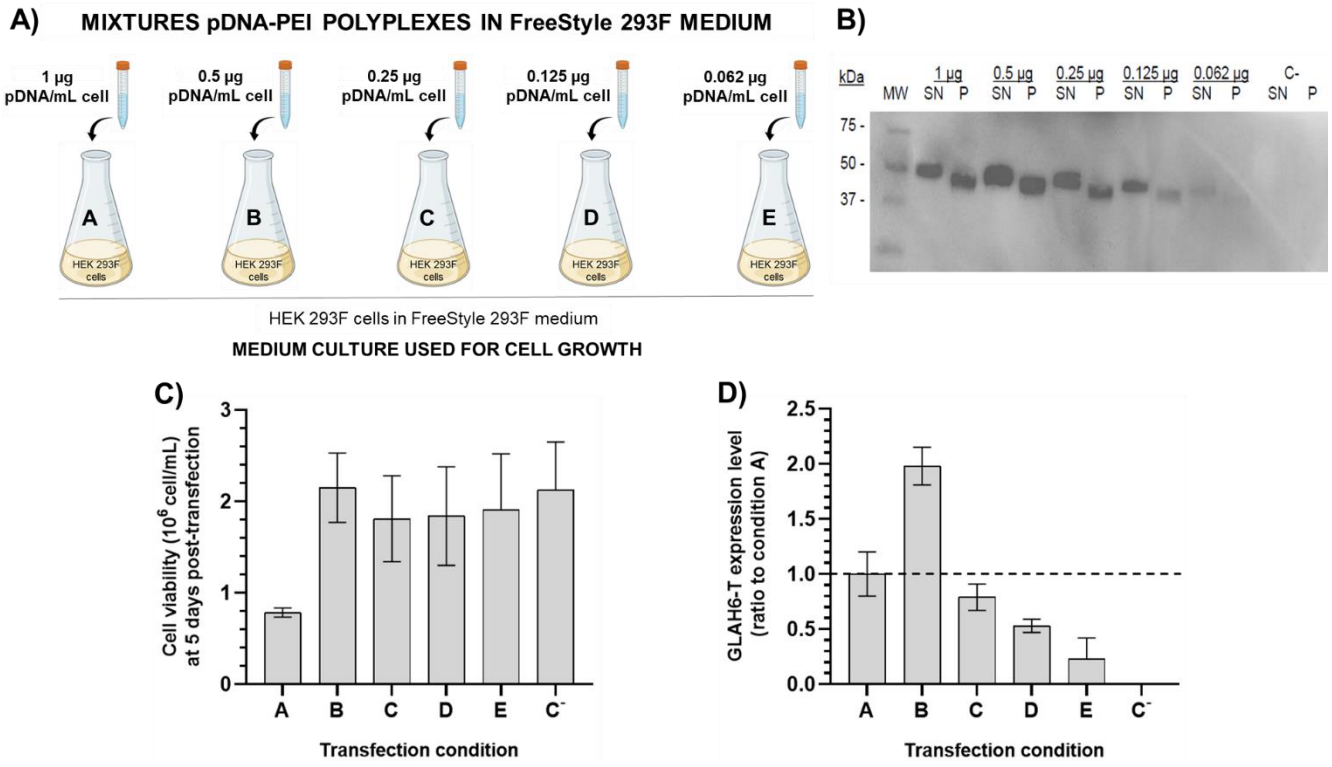


Figure 3.3. Effect of using reduced pDNA amounts in GLAH6-T expression levels by TGE procedures at 5-day post-transfection. A) Transfection conditions tested to evaluate the impact of coding pDNA concentration in TGE procedures using HEK 293F cells. B) Comparison of GLAH6-T expression levels on secreted and intercellular HEK 293F cell fractions (corresponding to supernatants (SN) and cell pellets (P) respectively) using decreasing coding pDNA amounts in TGE procedures. Legend: C- indicates negative controls from non-transfected cells, and MW means molecular weight marker C) Assessment of HEK 293F cell viability by Trypan blue. D) Comparison of GLAH6-T expression level of the different transfection conditions tested respect to the original condition A, determined by sodium dodecyl sulfate-polyacrylamide gel electrophoresis (SDS-PAGE) and further Tris-Glycine-eXtended (TGX) analysis. Duplicates of each transfection condition were measured.

As conclusion, the original TGE protocol proposed by Corchero *et al.*[45] was optimized by reducing the amount of encoding plasmid from 1 µg pDNA/mL cell to 0.5 µg pDNA/mL cell, and decreasing the overall cost of the resulting

TGE process. This new TGE protocol (detailed *Chapter 7, Section 7.2.3*) was further employed to produce the GLAH6-T and GLAcmycH6-T enzymes studied in this thesis.

Cell culture harvesting day selection depending on the amount of secreted mature GLA enzymes

Once the transfection conditions for TGE were optimized, two independent batches of GLAH6-T and GLAcmycH6-T proteins were produced in scaled-up volumes of HEK 293F cultures around 1 – 3 L. The idea was to explore if the new optimized transfection condition (at 0.5 µg pDNA/mL cell) when producing GLA enzymes in cultures of large volume (1 – 3 L) had an impact on the optimal harvesting day, in which the higher amount of secreted mature GLA enzymes can be collected from HEK 293F cultures.

Cell viability and percentages of protein secreted were checked from day 4 to 7 after transfection. Equal volumes from transfected cultures were taken at 4-, 5-, 6- and 7-day post-transfection, then centrifuged to obtain their clarified supernatant, and finally analyzed by SDS-PAGE and further western blot (*Figure 3.4*). Cell viability was found to be highly impaired after 6-day post-transfection, meanwhile the amount of secreted mature GLA version was not significantly increased after day 4 in any of both GLA. Therefore, future productions intended for the extensively enzyme characterization were stopped at time 5-day post-transfection (selected as optimal harvesting day) as previously described in Corchero *et al.*[45].

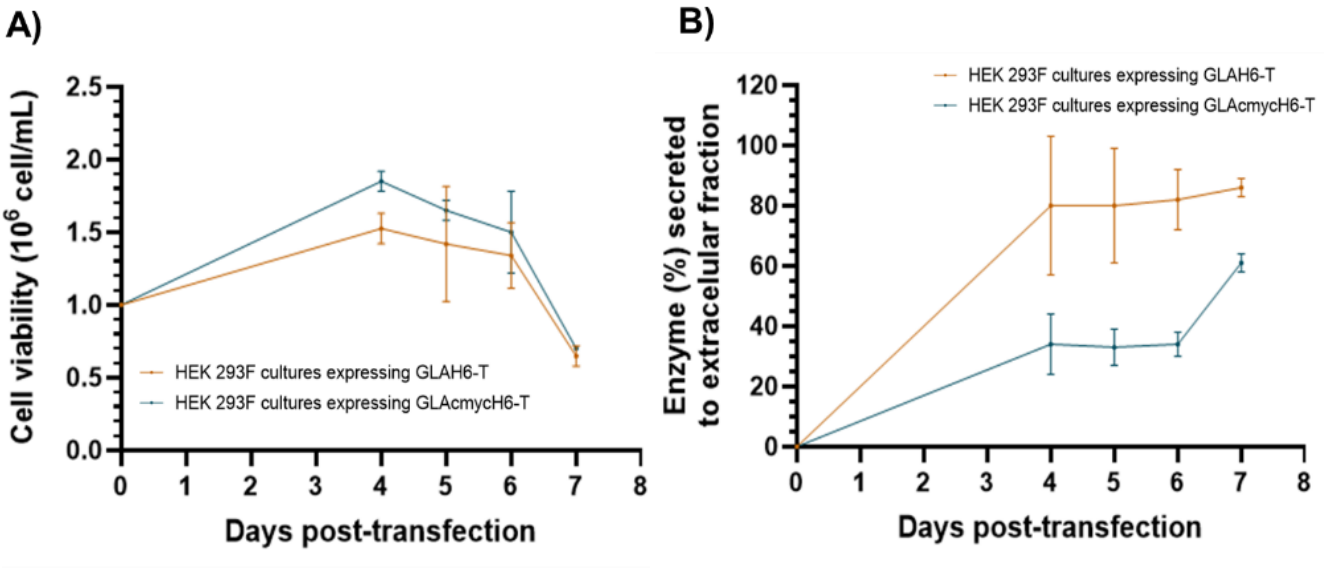


Figure 3.4. Scaling-up effects on the production of GLAH6-T and GLacmycH6-T enzymes by TGE procedures transfecting at 0.5 µg pDNA/mL cell condition. Assessment of A) cell viability by Trypan blue approach, and B) GLA secretion by SDS-PAGE and further western blot densitometry analysis, from transfected HEK 293F cultures expressing GLAH6-T or GLAcmycH6-T proteins. Two independent production batches were tested for each enzyme.

Based on the results, it can be concluded that GLAcmycH6-T enzyme is lower secreted than GLAH6-T protein to the extracellular fraction, suggesting that c-myc tag presence may be slowing down some post-translation modification such as the protein glycosylation, taking more time to have the mature version of the GLA capable to be secreted outside the cell membrane. This fact results on the obtaining of less production yields of GLAcmycH6-T than GLAH6-T protein when producing them using the same TGE procedure.

3.3. Impact of metal ions on IMAC procedures for GLA purification

High purity degree (> 90 %, or > 95 % if possible) is required for proper protein characterization and its further encapsulation in nanopharmaceuticals. For that, IMAC procedure is a well-know and widely used methodology to purify different recombinant proteins.

GLAH6-T and GLAcmycH6-S were successfully purified directly from the supernatant of cell cultures by Ni^{2+}-based IMAC resins in previous works[45,47]. After being submitted to a similar purification protocol, GLAH6-T demonstrated to be soluble and active after being dialyzed against 0.01 M acetic acid at pH 4.5[45], but GLAcmycH6-S demonstrated to be more stable when stored in 0.01 M acetic acid at pH 5.5[47]. Moreover, the GLAH6-T was obtained with high purity > 95 %, meanwhile the GLAcmycH6-S presented purities around 85 %.

In an attempt to reach improved purity of the different His-tagged versions of study in this thesis (GLAH6-T, GLAcmycH6-T and GLAcmycH6-S), an alternative Co^{2+}-based IMAC resin (TALON Superflow; Cytiva, ref. 28957502) packed into chromatography columns was explored. For this purpose, two batches of each His-tagged GLA version (50 – 150 mL of supernatant) were used. After capture and washing steps, eluted enzymes were dialyzed against 0.01 M acetic acid at pH 4.5 or at pH 5.5 in order to check the influence of the storage buffer pH on GLA properties after being submitted to Co^{2+}-based IMAC purification procedures. Results compiled in ***Table 3.5 A*** pointed out that both enzymes produced in HEK cells, GLAH6-T and GLAcmycH6-T, were more soluble at pH 4.5, while GLAcmcyH6-S (produced in CHO cells) was again more soluble at pH 5.5. However, some limitations were found when using this approach as affinity-based purification: i) lower enzymatic activity than the previous described on Corchero *et al*[45]. for GLAH6-T was found, ii) low GLAcmycH6-T purity (< 75 %), and iii) very low amounts of eluted protein (< 40 %), ending in a poor final yield. These results suggested that physicochemical and biological properties of GLA might be influenced by the divalent cations used in the purification step.

In parallel, same investigation but using HisTrap Excel column (GE Healthcare, ref. 17-3712-06) containing Ni^{2+}-based resin were carried out for each His-tagged GLA version (purification protocol is detailed in ***Chapter 7, Section 7.2.5.1***). As shown in ***Table 3.5 B*** and next in ***Section 3.4***, purified GLA enzymes with high quality properties can be obtained using Ni^{2+}-based IMAC resin.

Table 3.5. Characteristics of the His-tagged GLA versions after being purified by affinity procedures using A) Co^{2+}-based resin, and B) Ni^{2+}-based resin. After the purification step, all GLA enzymes were dialyzed against 0.01 M acetic acid buffers adjusted at pH 4.5 or pH 5.5.

A)

		GLA enzyme features after Co^{2+}-based IMAC procedures			
GLA enzyme version	Buffer pH	Solubility (%)	Enzymatic activity (μM 4MU/mg/h)	Eluted protein (%) from Co^{2+} resin	Purity (%)
GLAH6-T	4.5	104 ± 16	299 ± 4	35 ± 2	> 90
	5.5	83 ± 3	207 ± 3		
GLAcmycH6-T	4.5	93 ± 16	395 ± 38	37 ± 2	< 75
	5.5	81 ± 1	285 ± 113		
GLAcmycH6-S	4.5	44 ± 20	1149 ± 461	27 ± 1	> 90
	5.5	75 ± 5	1964 ± 194		

B)

		GLA enzyme features after Ni^{2+}-based IMAC procedures			
GLA enzyme version	Buffer pH	Solubility (%)	Enzymatic activity (μM 4MU/mg/h)	Eluted protein (%) from Ni^{2+} resin	Purity (%)
GLAH6-T	4.5	91 ± 1	2222 ± 135	79 ± 2	> 90
	5.5	90 ± 4	1586 ± 144		
GLAcmycH6-T	4.5	41 ± 1	2467 ± 38	77 ± 2	≤ 90
	5.5	75 ± 3	2873 ± 203		
GLAcmycH6-S	4.5	21 ± 10	626 ± 279	90 ± 1	≤ 89
	5.5	97 ± 3	1797 ± 250		

3.4. Impact of purification tag, expression system and storage buffer on GLA characteristics

As aforementioned in *Section 3.1*, one of the main purposes of this thesis was to investigate the correlation between the properties of recombinant GLA enzymes with some specific PPPs explored for their manufacturing, such as the fusion of purification tags in the GLA sequences, the buffer and pH of protein storage, or the use of HEK or CHO cells as expression systems (capable to confer well conserved organism-dependent glycosylation pattern to proteins).

For this purpose, home-made His-tagged GLA enzymes (GLAH6-T, GLAcmycH6-T and GLAcmcyH6-S) were obtained from two independent batches of scaled-up productions (1 – 3 L) and purified by Ni^{2+}-based IMAC resin, and stored in 0.01 M acetic buffer at pH 4.5 and pH 5.5 (as explained in *Chapter 7, Section 7.2*). In this section, it is explained their characterization and comparison with the free-tagged GLA-S version stored in Fabrazyme-like buffer prepared with neutral pH, which was provided by LeanBio SL. In order to fulfill the main objective of this chapter, the following GLA characteristics of the four constructs were examined:

- Protein solubility.
- Protein purity.
- Enzymatic activity of the recombinant enzymes.

- Protein identity and molecular mass.
- Protein size, polydispersity and ζ-potential.
- Thermal-dependent structural stability of GLA enzymes.

3.4.1. Protein solubility, purity and specific enzymatic activity of GLA enzymes

After protein purification by Ni^{2+}-based affinity chromatography, GLAH6-T, GLAcmycH6-T and GLAcmycH6-S were dialyzed again against 0.01 M acetic acid buffers adjusted at pH 4.5 or pH 5.5 to determine the optimal pH for each enzyme is terms of protein solubility and purity (parameters assessed by SDS-PAGE analysis according to the procedure described in ***Chapter 7, Section 7.2.6.1***). Summarized results in ***Figure 3.5*** and ***Table 3.6*** indicated that proteins containing the c-myc tag were more soluble in pH 5.5, meanwhile GLAH6-T only encoding the 6-His tag demonstrate similar solubility in both pHs tested. Another interesting point to highlight comparing both, GLAcmycH6-T and GLAcmycH6-S proteins, was that the expression system seemed to have an impact on their solubility, suggesting that enzymes produced using CHO cells may be slightly less soluble at lower pH than when produced in HEK 293F cells. This fact was probably related to differences in their glycosylation pattern, which was reported to be crucial for enzyme solubility, singularly the ones at site 3[58]. To better understand the impact of glycosylation on the enzyme solubility, the complete glycosylation pattern of His-tagged GLA versions should be evaluated in future studies. In contrast, the purity of the GLA-S protein was directly assessed from the purified batches provided by LeanBio SL, which were already dialyzed and stored in Fabrazyme-like buffer with neutral pH.

Moreover, differences on the protein purity were observed between the different GLA enzymes studied. Leaving aside the good purity of the GLA-S purified extensively with consecutive AEX and HIC chromatography by LeanBio SL (see ***Chapter 7, Section 7.2.5.2***), all the His-tagged GLA enzymes purified in a single step presented a correlation between its solubility and purity. It is clear that higher protein solubility ended in higher GLA concentration in sample, and for instance, higher purity. Besides, the detection of a single band in western blot analysis by using anti-GLA polyclonal antibodies (***Figure 3.5***) suggested that only the mature form is able to reach the extracellular medium without being degraded during its processing and transportation to the supernatant. Also, it was determined by absorbance measurements (see ***Chapter 7, Section 7.2.7***) that all samples analyzed content less than a 5 % of host cell DNA (m/m) in spite of sequence and/or expression system differences between them. Large content of host cell DNA was not found in recombinant GLA versions probably as a result of being extracellular proteins which do not present a high positively net surface charge.

The specific enzymatic activity of each GLA was also measured using the 4-MUG fluorimetric method (see ***Chapter 7, Section 7.2.9***). Both GLAcmycH6-T and GLAcmycH6-S enzymes, containing c-myc tag demonstrated

enhanced activity when storage in acetic buffer at pH 5.5, being correlated with their higher solubility at this condition. In contrast, GLAH6-T without c-myc tag presence, showed higher enzymatic activity when stored in acetic buffer at pH 4.5. As conclusion of comparing the different His-tagged versions, GLA enzymes produced by TGE protocols in HEK 293F cells seemed to show higher biological activity. As an exception, GLA-S protein demonstrated the highest enzymatic activity (near to the one described for Replagal®)[8], probably related to being stored in a basic buffer containing excipients.

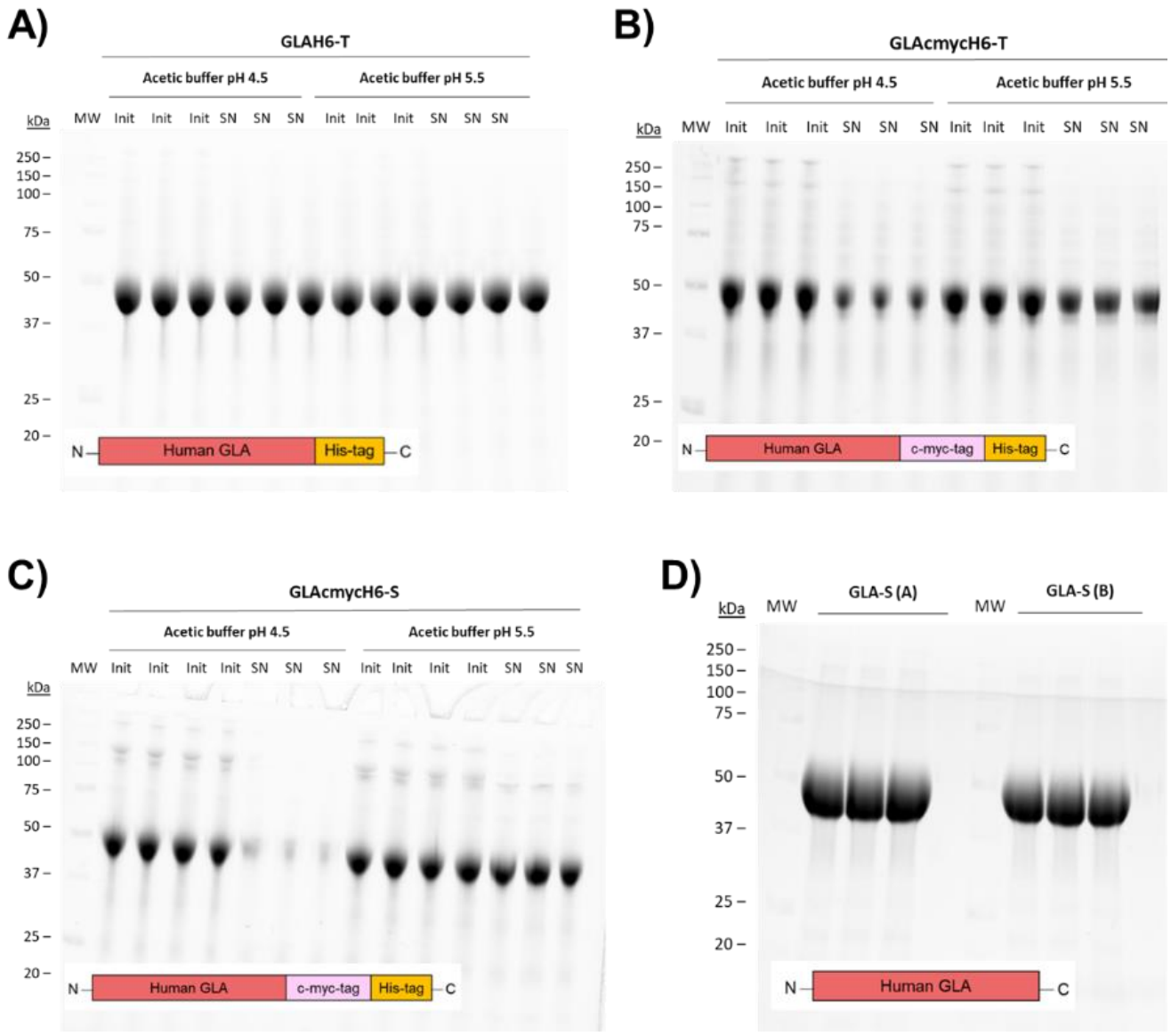


Figure 3.5. Identity, purity and solubility determination by SDS-PAGE and further TGX densitometry analysis from A) GLAH6-T, B) GLAcmycH6-T and C) GLAcmycH6-S enzymes once purified and dialyzed against 0.01 M acetic acid buffer adjusted at pH 4.5 or 5.5. Same analysis for the assessment of identity and purity of D) GLA-S enzyme were performed in two different batches (A and B). Values (presented on *Table 3.6*) correspond to measures of triplicates from two independent batches.

Table 3.6. Physicochemical and biological characterization summary of the different recombinant GLA enzymes. Values obtained from two independent production batches of each protein.

GLA enzyme version	Expression system	Buffer pH	Mean GLA concentration (mg/mL)	Solubility (%)	Purity (%)	DNA (%) containing	MW (kDa)	Size (nm)	PdI	ζ-potential (mV)	Specific EA (µM 4MU/mg/h)
GLAH6-T	HEK	4.5	1.1 ± 0.7	91 ± 1	96 ± 4	< 5	51.6 ± 0.3	14.5 ± 1.4	0.51 ± 0.05	15.7 ± 1.5	2222 ± 135
		5.5	1.0 ± 0.6	90 ± 4	97 ± 1	< 5	51.7 ± 0.1	11.8 ± 1.1	0.58 ± 0.08	-0.6 ± 0.8	1586 ± 144
GLAcmycH6-T	HEK	4.5	0.2 ± 0.1	41 ± 1	80 ± 1	< 5	52.9 ± 0.5	16.1 ± 0.6	0.52 ± 0.08	9.2 ± 6.2	2467 ± 38
		5.5	0.5 ± 0.1	75 ± 3	90 ± 3	< 5	53.5 ± 0.3	12.9 ± 0.6	0.55 ± 0.03	1.1 ± 0.5	2873 ± 203
GLAcmycH6-S	CHO	4.5	0.02 ± 0.01	21 ± 10	75 ± 11	< 5	LOD	13.1 ± 2.2	0.41 ± 0.14	2.6 ± 1.6	626 ± 279
		5.5	1.3 ± 0.2	97 ± 3	89 ± 4	< 5	53.8 ± 0.1	11.3 ± 1.0	0.47 ± 0.01	-3.0 ± 1.0	1797 ± 250
GLA-S	CHO	7	3.8 ± 0.4	N.D.	94 ± 0	< 5	42.4 ± 0.4 51.8 ± 0.5 62.3 ± 0.2	9.4 ± 3.1	0.26 ± 0.09	-0.6 ± 0.2	3556 ± 75

GLA concentration, purity and solubility were assessed by SDS-PAGE and TGX densitometry. The MW of GLA monomers was obtained by mass spectrometry. The ζ-potential measured by ELS shows the surface net charge of GLA molecules at the pH of study. The enzymatic activity of GLA was assessed by an *in vitro* fluorescence assay. Legend: LOD means limit of detection.

3.4.2. Protein identity and molecular mass determination of GLA enzymes

As previously explained in ***Chapter 1***, GLA is a homodimer glycoprotein formed by two identical monomers[59]. The molecular mass of GLA enzymes can be assessed by mass spectrometry following the protocol detailed in ***Chapter 7, Section 7.2.8***. As both GLA monomers are non-covalently bonded, they are separated during mass spectrometry analysis conducted with matrix assisted laser desorption ionization-time-of-flight (MALDI-TOF) instruments, because of the protein ionization provoked during this measurement. For this reason, the molecular weight (MW) values presented in this section by mass spectrometry correspond to the GLA monomer. As shown in ***Figure 3.6***, similar molecular weights with slightly mass variations (52 – 54 kDa) were obtained for the different His-tagged GLA versions.

After comparing these experimental values with other theoretical ones (calculated using the Expasy ProtParam tool according the human GLA sequence P06280 from UniProt database with or without incorporating the c-myc and 6-His tags)[60–62], it was suggested that the presence of some purification tag (c-myc or 6-His tag) in the aminoacid sequence of GLA proteins could increase their MW in 1 kDa (see ***Table 3.7***). Additionally, both GLAcmycH6-T and GLAcmycH6-S encodes the same aminoacid sequence with an approximated theoretical MW of 51 kDa. However, mass spectrometry results seemed to indicate a higher molecular mass of GLAcmycH6-S monomers (54 kDa) than the obtained from GLAcmycH6-T monomers (53 kDa). These slight variations were probably caused by structural differences in the N-linked glycosylation pattern and terminal sialylation already described between both HEK and CHO mammalian cells used as expression systems[4,8].

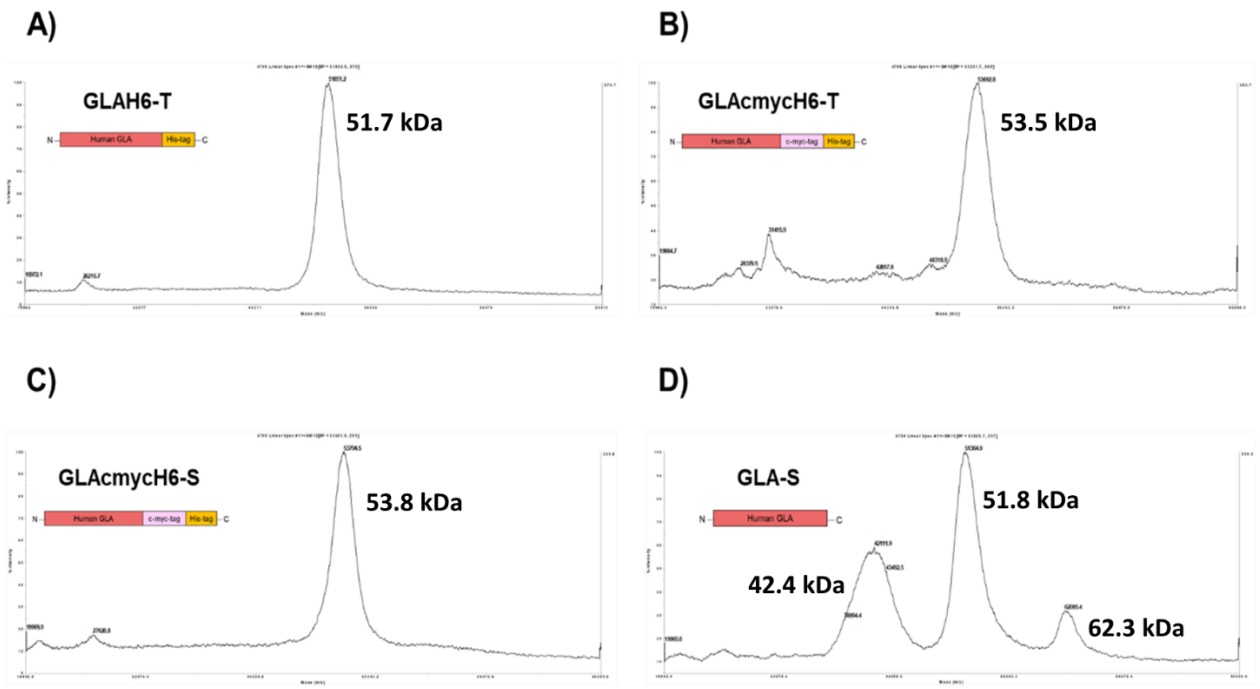


Figure 3.6. MALDI-TOF/TOF analysis to assess the molecular weight of monomers conforming the home-made enzymes A) GLAH6-T, B) GLAcmycH6-T, and C) GLAcmycH6-S dialyzed on acetic/acetate buffer pH 5.5; and the enzyme provided by LeanBio SL, D) the GLA-S dialyzed on Fabrazyme-like buffer.

Table 3.7. Comparison of experimental molecular weight values obtained by mass spectrometry analysis versus theoretical molecular weight values calculated by Expasy ProtParam tool[60] from two independent batches of the recombinant GLA enzymes studied in this work (GLAH6-T, GLAcmycH6-T, GLAcmycH6-S and GLA-S) which were produced using different expression systems, purification tags and storage buffers. In all cases, the molecular weight corresponds to the monomer of the different GLA proteins.

GLA enzyme version	Expression system	Buffer pH	Glycosilated monomer MW (kDa) by MALDI-TOF/TOF	Monomer MW (kDa) calculated by Expasy ProtParam tool ₮	Approximated mass addition by glycosilated domains (kDa)
GLAH6-T	HEK	4.5	51.6 ± 0.3	50	+ 2
		5.5	51.7 ± 0.1		+ 2
GLAcmycH6-T	HEK	4.5	52.9 ± 0.5	51	+ 2
		5.5	53.5 ± 0.3		+ 2
GLAcmycH6-S	CHO	4.5	LOD	51	LOD
		5.5	53.8 ± 0.1		+ 3
GLA-S	CHO	7	42.4 ± 0.4 51.8 ± 0.5 62.3 ± 0.2	49	- 7 + 3 + 13

The mass spectra of GLAcmycH6-S dialyzed in acetic buffer at pH 4.5 could not be detected due to concentration limitations of the protein. Legend: LOD meaning limit of detection. ₮ Theoretical MW of the GLA monomer according the overall aminoacid mass, without considering the glycosylated domains.

Curiously, heterogeneous monomers in MW were found in the mass spectra of the free-tagged GLA-S enzyme (see ***Figure 3.6*** and ***Table 3.7***). The monomer of 62 kDa might correspond to an overglycosylated population of GLA-S. In contrast, the monomer of 42 kDa (lower than the expected value of 49 kDa theoretically calculated) might represent another GLA-S population lacking some aminoacids. This finding was similarly found for Fabrazyme® and Replagal® biophamaceutics, which demonstrated slight lower MW than expected (around 51 kDa) due to the lack of one or two residues in their C-terminus[8]. However, this hypothesis should be further investigated by sequencing our GLA-S enzyme.

On the other hand, results demonstrated that pH of storage did not alter the protein integrity or its glycosylation pattern after protein production and purification in terms of protein MW, as expected.

3.4.3. Protein size distribution and ζ-potential of GLA enzymes

According to the X-ray crystallographic results published in Garman *et al.*[59], the homodimer of human GLA has a total size of around 7 – 8 nm. Therefore, recombinant enzymes encoding the same human aminoacid sequence (with or without slight modifications), and produced in mammalian cell lines, were expected to present similar protein sizes.

Herein, the different GLA constructs studied in this thesis were analyzed by dynamic light scattering (DLS) according to the procedures explained in ***Chapter 7, Section 7.2.10*** to determine if the presence of the c-myc and/or the 6-His tags, the protein nature (i.e. the glycosylation pattern), or the storage buffer could impact on the structuring of these enzymes. Apparently, the aforementioned factors do not have a significant impact on protein size according to the results shown in ***Table 3.6*** and ***Figure 3.7***, where it was evidenced that all purified enzymes show a predominant population corresponding to the homodimer conformation of approximately 10 nm at 25 ºC (with slight increased sizes for GLA versions encoding purification tags).

Same DLS analysis provided polydispersity values (or PdI values) as detailed in ***Table 3.6***. PdI values larger than 0.3 indicate that hetereogeneous particle populations in terms of size are present in the measured sample. For the all the recombinant GLA constructs analyzed, PdI values around 0.5 were found. However, peaks corresponding to higher sized GLA populations were not observed in the size distribution analysis by DLS (***Figure 3.7.***). As all the studied GLA constructs had purities lower than 98 %, one explanation of these results, could be the presence of very low percentages of remaining impurities of big protein populations present in samples, which were observed in the previous SDS-PAGE analysis (see ***Section 3.4.1***).

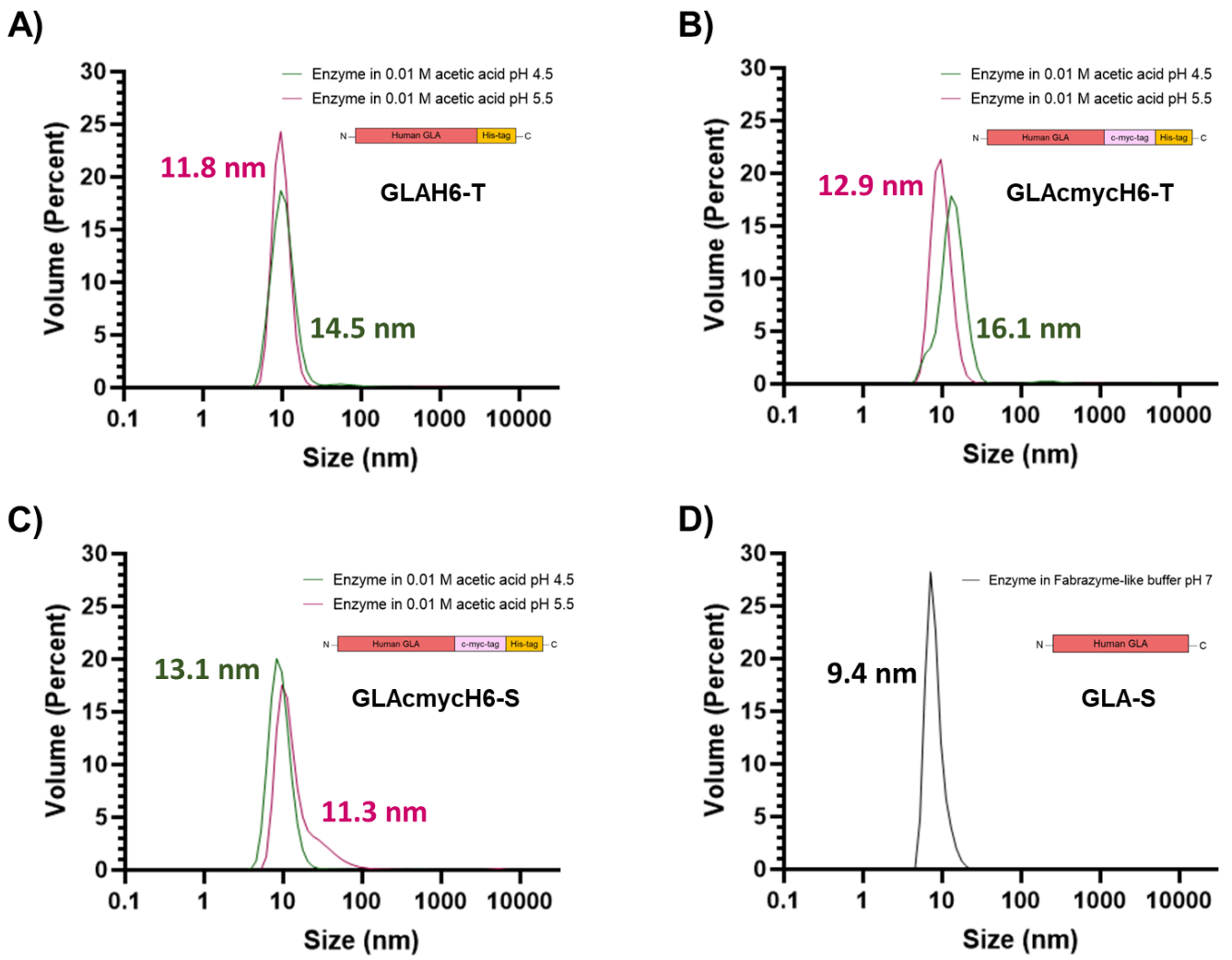


Figure 3.7. Average size distribution analysis by DLS at 25 ºC of predominant protein populations from two independent batches of A) GLAH6-T, B) GLAcmycH6-T, C) GLAcmycH6-S and D) GLA-S enzymes being storage in 0.01 M acetic acid buffer adjusted at pH 4.5 or pH 5.5.

Then, same GLA constructs were analyzed by electrophoretic light scattering (ELS) according to the procedures explained in ***Chapter 7, Section 7.2.10*** to determine the ζ-potential (i.e. the surface charge) of the different recombinant GLA molecules (results on ***Table 3.6***). As expected, GLA enzymes stored in acetic buffer at pH 5.5 showed almost neutral net charges since their theoretical isoelectric point (pI) value is near to the pH 5.1[59]. Specifically, the theoretical pI values of our recombinant GLA constructs calculated using the Expasy Protparam tool[60] vary a bit due to their differences on aminoacid sequence, being near pH 5.77 for GLAH6-T, pH 5.53 for both GLAcmycH6-T and GLAcmycH6-S, or pH 5.35 for GLA-S (see ***Figure 7.2***, in ***Chapter 7***, ***Section 7.2.***). Experimentally, GLAcmycH6-S presented a slightly negative net charge in comparison with GLAcmycH6-T despite having the same aminoacid sequence. When GLA constructs were stored at pH 4.5, in general they showed increased positive net charge correlative to their solubility, being GLAcmycH6-S the less soluble in acetic buffer

at pH 4.5. Those results indicated that differences in glycosylation moieties of GLA might modify the net charge of the protein molecule recombinantly expressed. Following this hypothesis, GLA-S also produced in CHO cells showed a little negative net charge despite to be stored in a buffer with a more basic pH of 7. These differences may be caused by the lack of purification tags on its C-terminus, but also by the presence of excipients in its formulation.

3.4.4. Thermal-dependent structural stability of GLA enzymes

The tendencies to generate protein aggregates or suffer protein conformational changes induced by temperature of GLA enzymes, i.e. the thermal-dependent structural stability of the enzymes, were explored by both DLS and fluorescence spectroscopic analysis. These measurements were carried out by exposing the GLAH6-T, GLAcmycH6-T, GLAcmycH6-S and GLA-S enzymes to a range of temperatures from 4 to 70 ºC (in DLS studies), or from 4 to 95 ºC (in fluorescence spectroscopic studies).

Thermal-dependent aggregation of GLA enzymes

In a first instance, the probable aggregation tendency of the different GLA constructs induced by temperature changes was followed by DLS. In general, in ***Figure 3.8*** is shown how all the studied GLA enzymes were highly aggregated in larger structures at temperatures above 50 ºC. One hypothesis to these results may be that GLA proteins were unstructured and unfolded, facilitating the molecule-to-molecule interaction due to the exposition of new aminoacid groups and hydrophobic patches to the aqueous medium and generating disorganized protein aggregates.

Moreover, these DLS results demonstrated that GLA-S protein was the most stable between a temperature range of 4 – 50 ºC with a constant size around 10 nm. Regardless the c-myc tag presence, analysis with GLA proteins produced in HEK 293F mammalian cells exhibited higher reproducibility when stored in acetic buffer at pH 5.5 than at pH 4.5, pH in which enzymes were sometimes less soluble. When cooling down the GLAH6-T and GLAcmycH6-T enzymes until 4 ºC, their sizes generally tended to 20 nm (probably obtaining trimer or tetramer populations), but their original homodimer size around 10 nm could be recovered after returning at 25 ºC. These results suggested that the aggregation states of GLAH6-T and GLAcmycH6-T found in the temperature range 4 – 25 ºC may be reversible.

On the other hand, despite GLAcmycH6-S protein has identical sequence than GLAcmycH6-T, the first one presented higher variability between batch productions. Also for GLAcmycH6-S at pH 5.5, at least a 2-fold increased size than for GLAcmycH6-T was detected between a temperature range of 4 – 37 ºC, probably due to their varying glycosylation pattern as a consequence of the different expression system used for their production.

Nevertheless, this effect was not reflected in GLA-S case, which is probably more stabilized by the excipient content in its formulation.

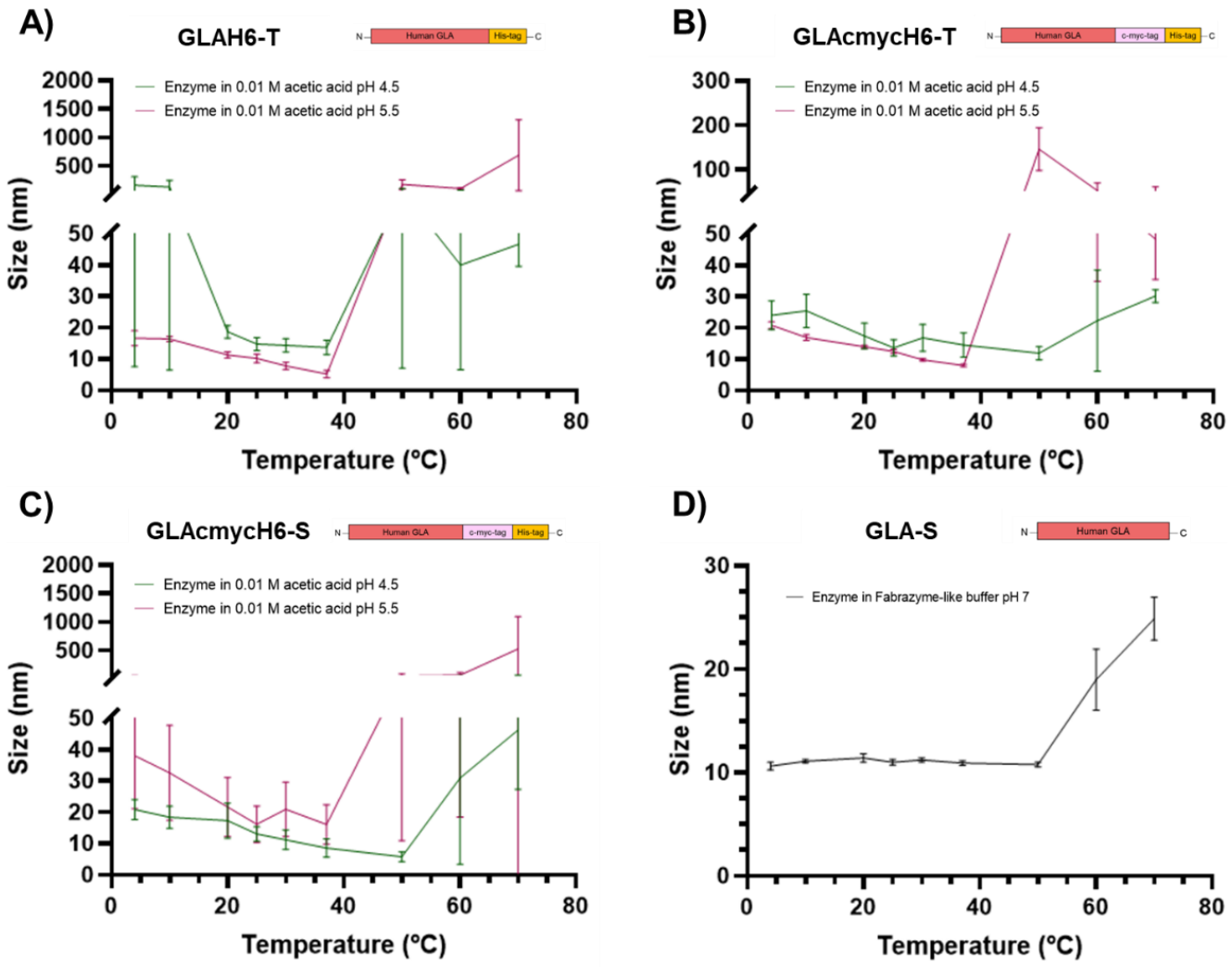


Figure 3.8. Size distribution analysis by DLS at a temperature range of 4 – 70 ºC from two independent scale-up productions of A) GLAH6-T, B) GLAcmycH6-T, C) GLAcmycH6-S and D) GLA-S enzymes prepared in their respective storage buffer.

Thermal-dependent conformational structure of GLA enzymes

The recombinant GLA enzymes studied in this thesis are homodimers containing 34 tryptophan (Trp) residues in the aminoacid sequence (17 Trp per monomer). Aromatic aminoacids in proteins such as tryptophan or tyrosin, can act as biochemical fluorophores absorbing light near 280 nm and having their emission spectra peak near 350 nm or 300 nm respectively. Usually only the Trp spectra is monitored during the fluorescence analysis of protein by exciting biomolecules at the Trp-specific wavelength of 295 nm (this photoselection avoid the interferences due to the contribution of other aromatic residues), (see *Figure 3.9*).

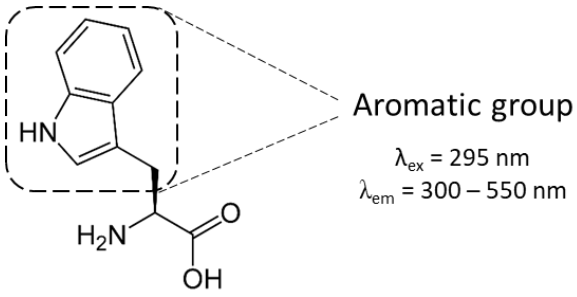


Figure 3.9. Chemical structure of tryptophan (Trp) residue. The aromatic group useful as biochemical fluorophore reported is highlighted. Specific excitation and emission conditions to monitor the intrinsic fluorescence spectra from Trp aminoacid are also indicated.

Conformational changes of proteins can be monitored by following the changes of the maximal wavelength of the Trp fluorescence emission spectra caused by changes of the Trp average exposure to the surrounding environment[63]. Such maximal wavelength of the Trp fluorescence spectra can be calculated as values of the center of spectral mass (CSM) using the equation detailed in ***Eq. 3.1***, and in ***Chapter 7, Section 7.2.11***. In ***Eq. 3.1***, λ_i and F_i correspond respectively to each wavelength and emitted fluorescence values from the emission spectra recorded between 310 and 450 nm in this thesis work.

$$CSM = \frac{\sum \lambda_i F_i}{F_i}$$

(***Eq. 4.1***)

Usually, Trp residues are more present in an apolar environment when proteins have a compact folded conformation, but they can end exposed to a more polar environment due to protein unfolding, resulting on a red-shifted CSM value of the fluorescence emission spectra (see ***Figure 3.10***).

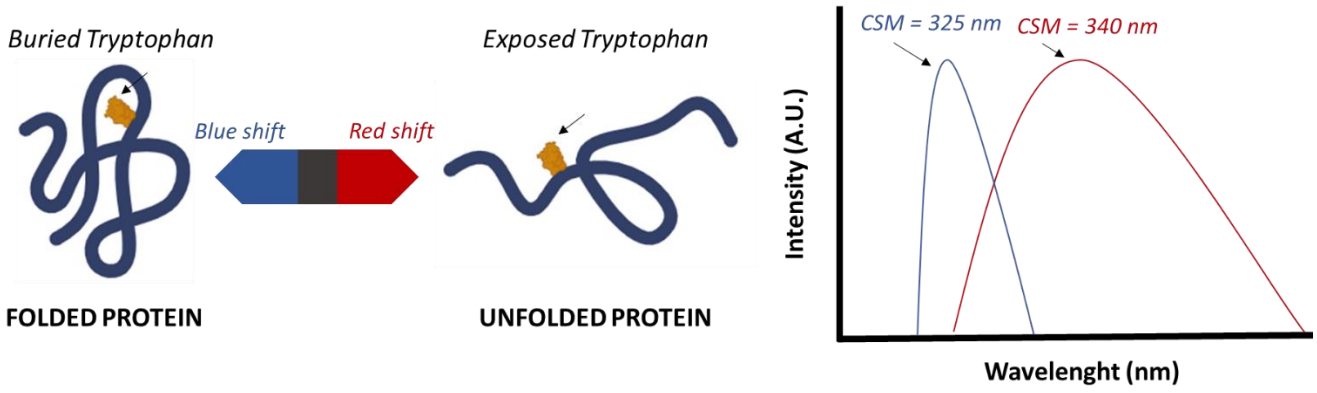


Figure 3.10. Changes of the maximal wavelength of the Trp fluorescence emission spectra (or CSM values) caused by conformational changes of proteins that modify the Trp exposure to the surrounding environment.

Therefore, the influence of the temperature on the unfolding of GLA enzymes was studied by following the CSM values obtained by fluorescence spectroscopy. In general, results shown in ***Figure 3.11*** demonstrated the conformational stability of all the recombinant GLA studied in a range of temperature of 4 – 50 ºC. However, in all cases, protein destabilization and unfolding was initiated at temperatures over 50 ºC, which probably ended inducing protein aggregation in a disorganized manner supporting the previous DLS results. Despite the described differences, in general, GLA enzymes at 25 ºC and 37 ºC presented similar average CSM values of 351 nm, excepting the GLA-S with a lower value of 350 nm, which indicated more compactness on the enzyme structural conformation.

Apparently, the pH of the buffer had no significant impact over the GLAcmycH6-S enzyme unfolding, unlike GLAH6-T and GLAcmycH6-T enzymes produced in HEK cells, where acetic buffer pH 5.5 used as storage solution was slightly delaying the unfolding process. This situation is clearly evidenced by the melting temperature (T_m) values detailed in ***Table 3.8***. The T_m value refers to that temperature at which the 50 % of the enzyme is unfolded.

Besides, together with previous DLS results, all the GLA versions demonstrated high thermal stability in terms of structural properties, without presenting great modifications until temperatures larger than 40 – 50 ºC.

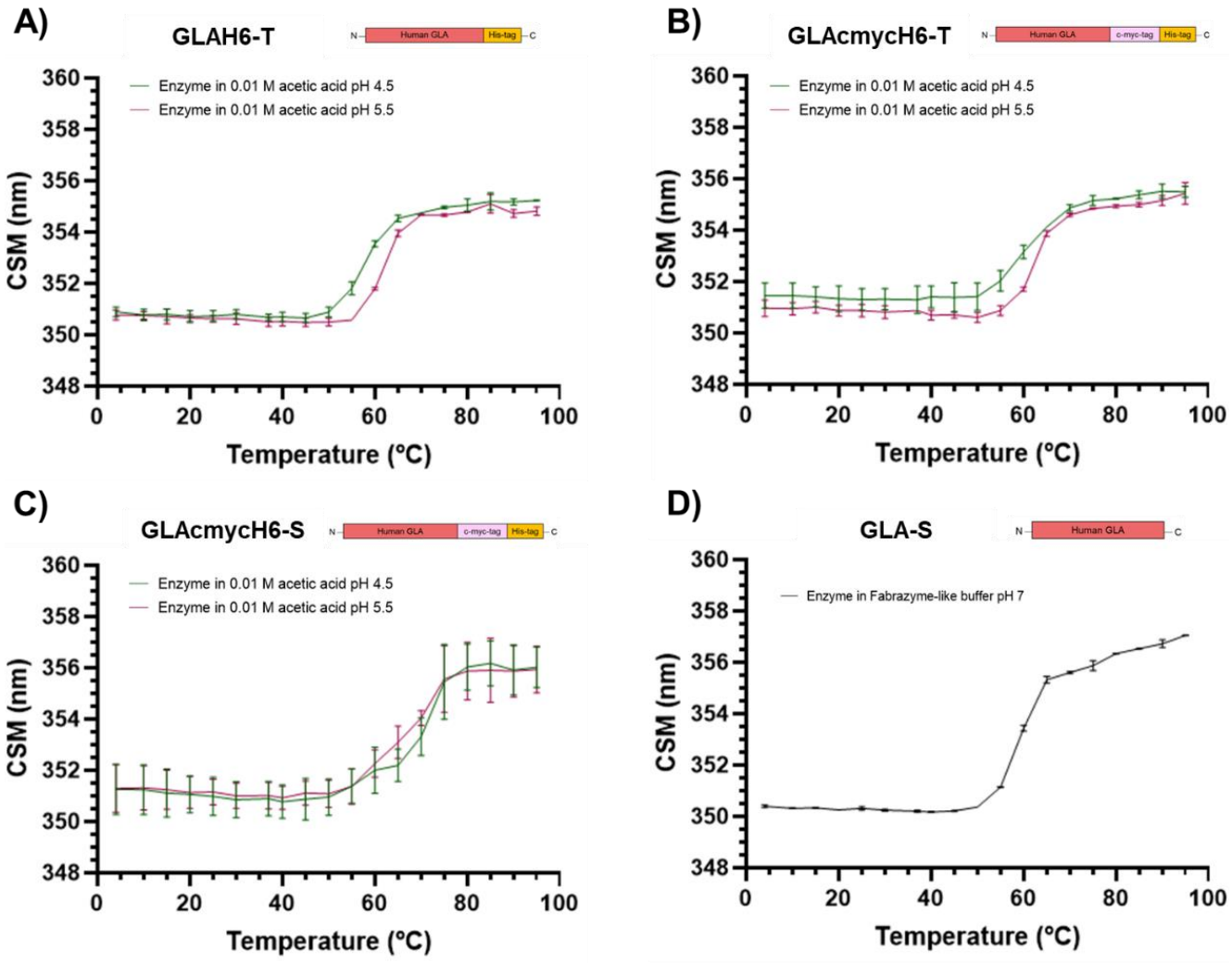


Figure 3.11. Thermal-dependent variations in CSM values from two independent scaled-up batches of purified A) GLAH6-T, B) GLAcmycH6-T, C) GLAcmycH6-S and D) GLA-S proteins prepared in their respective storage buffer.

Table 3.8. T_m value and their R squared value from non-linear sigmoidal model fitting of different recombinant GLA enzymes.

GLA enzyme version	Expression system	Buffer pH	T_m (ºC)	Fitting (R^2)
GLAH6-T	**HEK**	4.5	58.5 ± 0.1	0.994 ± 0.005
		5.5	62.1 ± 0.6	0.996 ± 0.003
GLAcmycH6-T	**HEK**	4.5	61.5 ± 0.8	0.997 ± 0.001
		5.5	63.0 ± 0.6	0.992 ± 0,006
GLAcmycH6-S	**CHO**	4.5	69.8 ± 0.1	0.986 ± 0.009
		5.5	66.6 ± 4.4	0.988 ± 0.012
GLA-S	**CHO**	7	60.3 ± 0.3	0.992 ± 0.002

3.5. Summary and conclusions

As summary, different manufacturing conditions tested in this chapter to produce and purify recombinant GLA enzymes ended in the following findings:

- Regarding GLA expression by TGE procedures, the previous protocol established by Corchero *et al.*[45] was optimized reducing the amount of pDNA-PEI polyplexes required to transfect HEK 293F cultures (from 1 to 0.5 µg pDNA/mL cell), resulting on less cell toxicity, and therefore, on 2-fold higher recombinant protein expression.
- Regarding the purification of His-tagged GLA enzymes by IMAC procedures, the metal ion used in the purification step could impact on the GLA characteristics, since improved enzymatic activity, purity and solubility were obtained in general when Ni^{2+}-based affinity chromatography was used instead of using Co^{2+}-based affinity chromatography.

Additionally, some specific PPPs for the manufacturing of GLA enzymes were correlated with their characteristics. These results can be summarized in the following conclusions:

- The presence of purification tags, specifically the c-myc tag, impaired the solubility of GLA enzymes at pH 4.5. Moreover, after being purified by IMAC procedures, slightly lower protein purities were obtained for the GLA constructs encoding the c-myc tag (GLAcmycH6-T and GLAcmycH6-S) than for GLAH6-T protein (without the presence of c-myc tag).
- The production of GLA enzymes in different mammalian cell lines (HEK or CHO) principally impacted on the protein solubility and enzymatic activity, probably due to the different organism-dependent PTMs given by each cell expression system. In general, GLA enzymes produced by TGE in HEK 293F cells presented higher enzymatic activity and protein solubility. In contrast, GLAcmycH6-S produced by stable clone in CHO cells demonstrated less structural stability at pH 5.5 and higher tendency to aggregate.
- The buffer and pH of storage for GLA enzymes impacted on the GLA characteristics. The GLA-S version provided by LeanBio SL demonstrated the most promising CQAs presumably due to being storage in a buffer containing excipients at neutral pH, being the enzyme with higher specific enzymatic activity and lower aggregation tendency.

As main conclusion of this chapter, the selection of appropriate PPPs for the manufacturing of GLA enzymes is crucial to produce high-quality biopharmaceuticals intended for ERT of Fabry disease.

3.6. References

1 Walsh G. Biopharmaceutical benchmarks 2018. *Nat Biotechnol 2018 3612* 2018; **36**: 1136–45.

2 Walsh G, Walsh E. Biopharmaceutical benchmarks 2022. *Nat Biotechnol* 2022; **40**: 1722–60.

3 Ferrer-Miralles N, Domingo-Espín J, Corchero J, Vázquez E, Villaverde A. Microbial factories for recombinant pharmaceuticals. *Microb Cell Fact* 2009; **8**: 1–8.

4 Böhm E, Seyfried BK, Dockal M, *et al.* Differences in N-glycosylation of recombinant human coagulation factor VII derived from BHK, CHO, and HEK293 cells. *BMC Biotechnol* 2015; **15**. DOI:10.1186/s12896-015-0205-1.

5 Lin B, Qing X, Liao J, Zhuo K. Role of Protein Glycosylation in Host-Pathogen Interaction. *Cells* 2020; **9**: 1022.

6 European Medicines Agency. Fabrazyme - EMEA/H/C/000370 - II/0116. https://www.ema.europa.eu/en/medicines/human/EPAR/fabrazyme (accessed Jan 21, 2021).

7 European Medicines Agency. Replagal - EMEA/H/C/000369 - IAIN/0096. https://www.ema.europa.eu/en/medicines/human/EPAR/replagal#product-information-section (accessed Dec 21, 2023).

8 Lee K, Jin X, Zhang K, *et al.* A biochemical and pharmacological comparison of enzyme replacement therapies for the glycolipid storage disorder Fabry disease. *Glycobiology* 2003; **13**: 305–13.

9 Kim TK, Eberwine JH. Mammalian cell transfection: The present and the future. *Anal Bioanal Chem* 2010; **397**: 3173–8.

10 Wurm F, Bernard A. Large-scale transient expression in mammalian cells for recombinant protein production. *Curr Opin Biotechnol* 1999; **10**: 156–9.

11 Pham PL, Kamen A, Durocher Y. Large-Scale transfection of mammalian cells for the fast production of recombinant protein. *Mol Biotechnol 2006 342* 2006; **34**: 225–37.

12 Wade-Martins R, Frampton J, James MR. Long-term stability of large insert genomic DNA episomal shuttle vectors in human cells. *Nucleic Acids Res* 1999; **27**: 1674–82.

13 Wightman L, Kircheis R, Rössler V, *et al.* Different behavior of branched and linear polyethylenimine for gene delivery in vitro and in vivo. *J Gene Med* 2001; **3**: 362–72.

14 Kircheis R, Wightman L, Wagner E. Design and gene delivery activity of modified polyethylenimines. *Adv Drug Deliv Rev* 2001; **53**: 341–58.

15 Boussif O, LezoualC'H F, Zanta MA, *et al.* A versatile vector for gene and oligonucleotide transfer into cells in culture and in vivo: polyethylenimine. *Proc Natl Acad Sci* 1995; **92**: 7297–301.

16 Boeckle S, von Gersdorff K, van der Piepen S, Culmsee C, Wagner E, Ogris M. Purification of polyethylenimine polyplexes highlights the role of free polycations in gene transfer. *J Gene Med* 2004; **6**: 1102–11.

17 Reed SE, Staley EM, Mayginnes JP, Pintel DJ, Tullis GE. Transfection of mammalian cells using linear polyethylenimine is a simple and effective means of producing recombinant adeno-associated virus vectors. *J Virol Methods* 2006; **138**: 85–98.

18 De Los Milagros Bassani Molinas M, Beer C, Hesse F, Wirth M, Wagner R. Optimizing the transient transfection process of HEK-293 suspension cells for protein production by nucleotide ratio monitoring. *Cytotechnology* 2014; **66**: 493–514.

19 Baldi L, Muller N, Picasso S, *et al.* Transient Gene Expression in Suspension HEK-293 Cells: Application to Large-Scale Protein Production. *Biotechnol Prog* 2005; **21**: 148–53.

20 Derouazi M, Girard P, Van Tilborgh F, *et al.* Serum-free large-scale transient transfection of CHO cells. *Biotechnol Bioeng* 2004; **87**: 537–45.

21 Rosser MP, Xia W, Hartsell S, *et al.* Transient transfection of CHO-K1-S using serum-free medium in suspension: a rapid mammalian protein expression system. *Protein Expr Purif* 2005; **40**: 237–43.

22 Durocher Y, Perret S, Kamen A. High-level and high-throughput recombinant protein production by transient transfection of suspension-growing human 293-EBNA1 cells. *Nucleic Acids Res* 2002; **30**: e9–e9.

23 Baldi L, Hacker DL, Adam M, Wurm FM. Recombinant protein production by large-scale transient gene expression in mammalian cells: State of the art and future perspectives. *Biotechnol Lett* 2007; **29**: 677–84.

24 Geisse S, Jordan M, Wurm FM. Large-scale transient expression of therapeutic proteins in mammalian cells. *Methods Mol Biol* 2005; **308**: 87–98.

25 Girard P, Derouazi M, Baumgartner G, *et al.* 100-Liter transient transfection. *Cytotechnology* 2002; **38**: 15–21.

26 Tuvesson O, Uhe C, Rozkov A, Lüllau E. Development of a generic transient transfection process at 100 L scale. *Cytotechnology* 2008; **56**: 123–36.

27 Kuroda H, Kutner RH, Bazan NG, Reiser J. Simplified lentivirus vector production in protein-free media using polyethylenimine-mediated transfection. *J Virol Methods* 2009; **157**: 113–21.

28 Bieber T, Meissner W, Kostin S, Niemann A, Elsasser HP. Intracellular route and transcriptional competence of polyethylenimine–DNA complexes. *J Control Release* 2002; **82**: 441–54.

29 Honoré I, Grosse S, Frison N, Favatier F, Monsigny M, Fajac I. Transcription of plasmid DNA: Influence of plasmid DNA/polyethylenimine complex formation. *J Control Release* 2005; **107**: 537–46.

30 Ketola TM, Hanzlíková M, Urtti A, Lemmetyinen H, Yliperttula M, Vuorimaa E. Role of polyplex intermediate species on gene transfer efficiency: Polyethylenimine-DNA complexes and time-resolved fluorescence spectroscopy. *J Phys Chem B* 2011; **115**: 1895–902.

31 Stadler J, Lemmens R, Nyhammar T. Plasmid DNA purification. *J Gene Med* 2004; **6**: S54–66.

32 Wright JL, Jordan M, Wurm FM. Transfection of partially purified plasmid DNA for high level transient protein expression in HEK293-EBNA cells. *J Biotechnol* 2003; **102**: 211–21.

33 Wakelin SJ, Sabroe I, Gregory CD, *et al.* "Dirty little secrets"—Endotoxin contamination of recombinant proteins. *Immunol Lett* 2006; **106**: 1–7.

34 Kichler A, Leborgne C, Danos O. Dilution of reporter gene with stuffer DNA does not alter the transfection efficiency of

polyethylenimines. *J Gene Med* 2005; **7**: 1459–67.

35 Rajendra Y, Kiseljak D, Manoli S, Baldi L, Hacker DL, Wurm FM. Role of non-specific DNA in reducing coding DNA requirement for transient gene expression with CHO and HEK-293E cells. *Biotechnol Bioeng* 2012; **109**: 2271–8.

36 Gray D. Overview of Protein Expression by Mammalian Cells. *Curr Protoc Protein Sci* 1997; **10**: 5.9.1-5.9.18.

37 Wurm FM. Production of recombinant protein therapeutics in cultivated mammalian cells. *Nat Biotechnol 2004 2211* 2004; **22**: 1393–8.

38 Balasubramanian S, Wurm FM, Hacker DL. Multigene expression in stable CHO cell pools generated with the piggyBac transposon system. *Biotechnol Prog* 2016; **32**: 1308–17.

39 Maltais JS, Lord-Dufour S, Morasse A, Stuible M, Loignon M, Durocher Y. Repressing expression of difficult-to-express recombinant proteins during the selection process increases productivity of CHO stable pools. *Biotechnol Bioeng* 2023; **120**: 2840–52.

40 Harcum SW, Lee KH. Previews CHO Cells Can Make More Protein A new comprehensive genome-scale metabolic model of Chinese hamster ovary cells identifies pathways for improving biopharmaceutical protein production. *Cell Syst* 2016; **3**: 412–3.

41 Zhao X, Li G, Liang S. Several affinity tags commonly used in chromatographic purification. *J Anal Methods Chem* 2013; **2013**: 1–8.

42 Terpe K. Overview of tag protein fusions: From molecular and biochemical fundamentals to commercial systems. *Appl Microbiol Biotechnol* 2003; **60**: 523–33.

43 Birchfield AS, McIntosh CA. The effect of recombinant tags on citrus paradisi flavonol-specific 3-o glucosyltransferase activity. *Plants* 2020; **9**: 402.

44 Kügler J, Wilke S, Meier D, *et al.* Generation and analysis of the improved human HAL9/10 antibody phage display libraries. *BMC Biotechnol* 2015; **15**: 10.

45 Corchero JL, Mendoza R, Lorenzo J, *et al.* Integrated approach to produce a recombinant, His-tagged human α-galactosidase a in mammalian cells. *Biotechnol Prog* 2011; **27**: 1206–17.

46 Cabrera I, Abasolo I, Corchero JL, *et al.* α-Galactosidase-A Loaded-Nanoliposomes with Enhanced Enzymatic Activity and Intracellular Penetration. *Adv Healthc Mater* 2016; **5**: 829–40.

47 Merlo-Mas J, Tomsen-Melero J, Corchero JL, *et al.* Application of Quality by Design to the robust preparation of a liposomal GLA formulation by DELOS-susp method. *J Supercrit Fluids* 2021; **173**: 105204.

48 Tomsen-Melero J. Study of New Liposomes for the Delivery of Enzymes through Biological Membranes. 2021. http://hdl.handle.net/10803/673786 (accessed Oct 30, 2021).

49 Ventosa L, Veciana J, Royo M, *et al.* Liposomes and its use for enzyme delivery. Patent EP 21382062.4-1112. 2021. http://hdl.handle.net/10261/289055 (accessed June 10, 2022).

50 Hildinger M, Baldi L, Stettler M, Wurm FM. High-titer, serum-free production of adeno-associated virus vectors by

polyethyleneimine-mediated plasmid transfection in mammalian suspension cells. *Biotechnol Lett* 2007; **29**: 1713–21.

51 Cervera L, Fuenmayor J, González-Domínguez I, Gutiérrez-Granados S, Segura MM, Gòdia F. Selection and optimization of transfection enhancer additives for increased virus-like particle production in HEK293 suspension cell cultures. *Appl Microbiol Biotechnol* 2015; **99**: 9935–49.

52 Ye J, Kober V, Tellers M, Naji Z, Salmon P, Markusen JF. High-level protein expression in scalable CHO transient transfection. *Biotechnol Bioeng* 2009; **103**: 542–51.

53 Anderson DH, Kickhoefer VA, Sievers SA, Rome LH, Eisenberg D. Draft Crystal Structure of the Vault Shell at 9-Å Resolution. *PLoS Biol* 2007; **5**: e318.

54 Tanaka H, Kato K, Yamashita E, *et al.* The Structure of Rat Liver Vault at 3.5 Angstrom Resolution. *Science (80-)* 2009; **323**: 384–8.

55 Querol-Audí J, Casañas A, Usón I, *et al.* The mechanism of vault opening from the high resolution structure of the N-terminal repeats of MVP. *EMBO J* 2009; **28**: 3450–7.

56 Woodward CL, Mendonça LM, Jensen GJ. Direct visualization of vaults within intact cells by electron cryo-tomography. *Cell Mol Life Sci* 2015; **72**: 3401–9.

57 Carreño A, Guerrero-Yagüe R, Casal E, Mendoza R, Corchero JL. Tuning plasmid DNA amounts for cost-effective transfections of mammalian cells: when less is more. *Appl Microbiol Biotechnol* 2024; **108**: 0.

58 Ioannou YA, Zeidner KM, Grace ME, Desnick RJ. Human alpha-galactosidase A: glycosylation site 3 is essential for enzyme solubility. *Biochem J* 1998; **332**: 789–97.

59 Garman SC, Garboczi DN. The molecular defect leading to fabry disease: Structure of human α-galactosidase. *J Mol Biol* 2004; **337**: 319–35.

60 SIB Swiss Institute of Bioinformatics. Expasy ProtParam tool. https://web.expasy.org/protparam/ (accessed Dec 27, 2018).

61 The UniProt Consortium. Alpha-galactosidase A (GLA) - Homo sapiens (Human) - P06280 | UniProtKB | UniProt. https://www.uniprot.org/uniprotkb/P06280/entry (accessed Dec 27, 2018).

62 Bateman A, Martin MJ, Orchard S, *et al.* UniProt: the Universal Protein Knowledgebase in 2023. *Nucleic Acids Res* 2023; **51**: D523–31.

63 Lakowicz JR. Principles of fluorescence spectroscopy, Third Edition. Springer, 2006.

4

IMPACT OF GLA ENZYME PHYSICOCHEMICAL PROPERTIES ON ITS INTEGRATION ON RGD-TARGETED NANOLIPOSOMES

4.1. Introduction

The knowledge of biomolecular interactions, responsible of the nano and supramolecular structure of many nanoformulations, is of huge importance for the development and continuous improvement of nanopharmaceuticals critical quality attributes (CQAs) through the establishment of well-controlled methodologies for their manufacturing. In this chapter is described the formulation of different versions of α-galactosidase A (GLA) enzymes, with different CQAs (e.g. solubility, molecular weight, net surface charge and enzymatic activity) regarding different nature and aminoacid sequence, in arginine-glycine-aspartate (RGD)-targeted nanoliposomes developed by the NANOMOL-Bio research group (ICMAB-CSIC); and the impact of GLA features on several physicochemical and biological features of GLA-loaded formulations. These GLA-loaded nanoliposomal formulations have been and are explored, in the frame of several collaborative and interdisciplinary projects, for the development of a new nanopharmaceutical for the enzyme replacement therapy (ERT) of Fabry disease (see ***Figure 1.16***). The studies reported in this chapter endeavor to contribute to a better understanding of the interaction between GLA enzyme and liposomal membrane and to the successful development of GLA-loaded nanoliposomal formulations towards their clinical use.

4.1.1. GLA-loaded nanoliposomal formulations for Fabry ERT

Composition of GLA-loaded nanoliposmal formulations for Fabry ERT has significantly changed since the first proof of concept (PoC)[1], to the actual prototype, designed as orphan drug by the European Medicines Agency (EMA) and the European Commission (EC) on 2021[2], and currently being developed, under Phoenix (H2020, ID 953110) and Nano4Rare (Horizon, ID 101136772) projects, for its entrance to clinical phases (see ***Figure 4.1***).

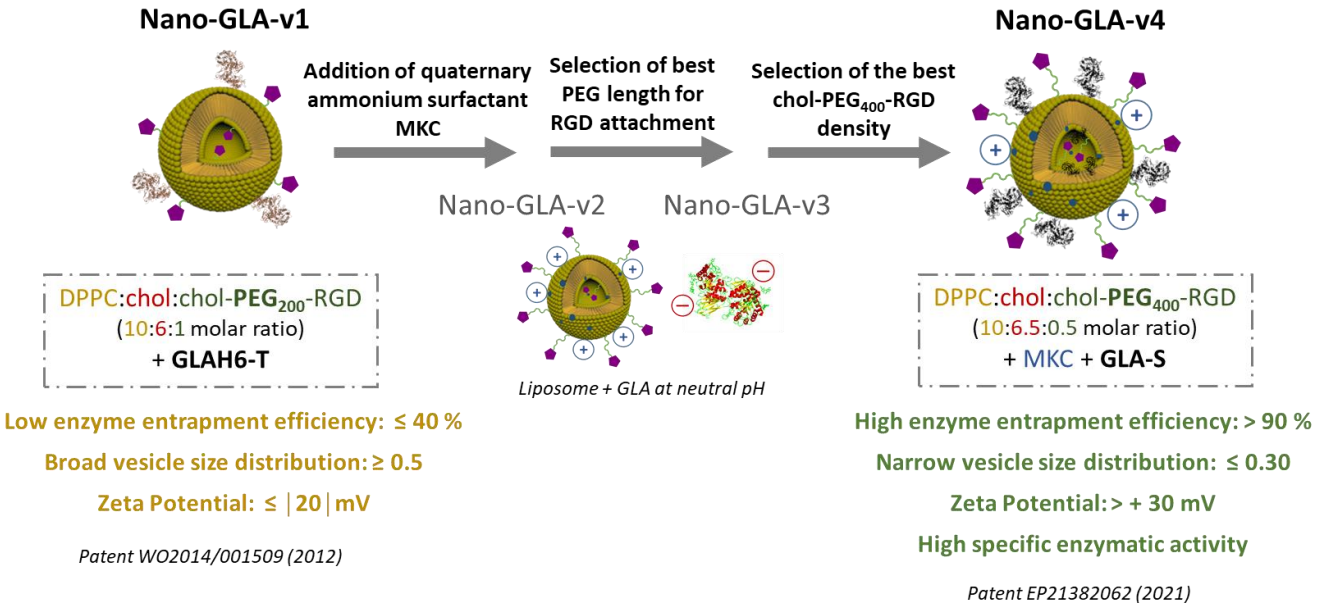
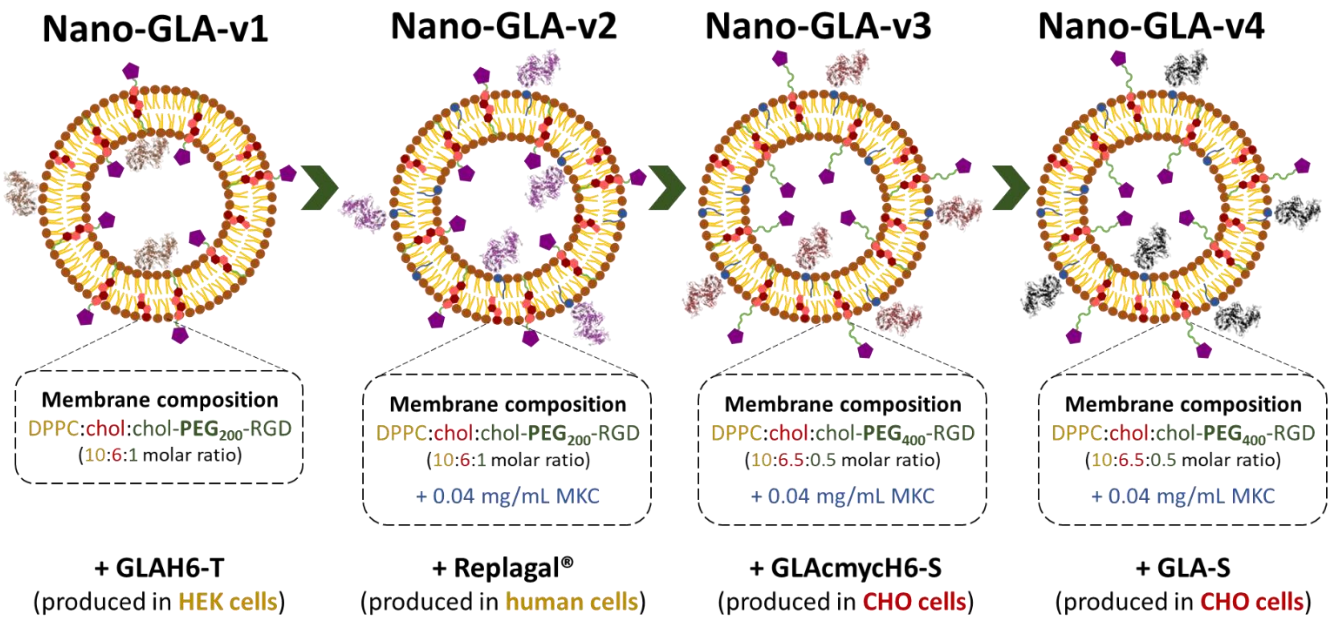


Figure 4.1. Optimization of the GLA-loaded nanoliposomal formulation to achieve requested physicochemical and biological properties for the development of a nanopharmaceutical for Fabry ERT.

First version of GLA-loaded nanoliposomal formulation, named Nano-GLA-v1, contained the tagged GLA enzyme produced by transient expression using HEK cells, named GLAH6-T, and the liposomal membrane was composed by 1,2-dipalmitoyl-sn-glycero-3-phosphocholine (DPPC), cholesterol (chol), cholesterol-polyethylene glycol $(PEG)_{200}$-RGD[1]. This nanoliposomal formulation, produced by the green and scalable depressurization of an expanded organic solution-suspension (DELOS-susp) methodology, had limited GLA entrapment efficiency (of around 40 %) and low stability upon storage, which hindered their translation to the clinical use, more over tagged GLAH6-T cannot be used in clinical testing.

Extensive development of this initial GLA formulation was done during the EU Smart4Fabry project (H2020, ID 720942) to achieve the GLA-loaded nanoliposomal formulation, named Nano-GLA-v4, currently under preclinical development for Fabry ERT to achieve first in human authorization. Nano-GLA-v4, contains the non-tagged GLA enzyme produced by stable expression using Chinese hamster ovary (CHO) cells, named GLA-S, and the liposomal membrane is composed by DPPC, chol, chol-PEG_{400}-RGD, and positive surfactant miristalkonium chloride (MKC). NanoGLA-v4, produced by DELOS-susp, has a much larger GLA entrapment efficiency and colloidal stability than Nano-GLA-v1, more over GLA-S can be used at clinical level. Nano-GLA-v4 formulation, which gained the orphan drug designation (ODD), demonstrated improved efficacy at preclinical level compared to traditional authorized ERT to treat Fabry disease, and showed for the first-time efficacy in brain tissues.

In *Figure 4.2*, are schematized the different version of GLA-loaded nanoformulations from Nano-GLA-v1 to Nano-GLA-v4, and are given details on the nature of GLA, the composition of the nanoliposomal membrane, and a qualitative description of some of the properties of these GLA-loaded liposomal nanoformulations.



Nanoliposomal prototype ID	Enzyme version	Change in membrane composition	Intended purpose	Improved nanopharmaceutical properties
Nano-GLA-v1	GLAH6-T	Addition of chol-PEG_{200}-RGD unit	Targeting of vascular endothelial cells by αvβ3 integrin recognition	↑ colloidal stability ↑ cellular internalization ↑ enzymatic activity
Nano-GLA-v2	Replagal®	Addition of MKC surfactant	Improvement of GLA encapsulation efficiencies	↑↑ colloidal stability ↑ cellular internalization ↑↑ enzymatic activity ↑↑↑ enzyme entrapment efficiency
Nano-GLA-v3	GLAcmycH6-S	Change of chol-PEG_{200}-RGD unit for the chol-PEG_{400}-RGD moiety	Enhancement of integration efficiencies of targeting peptides	↑↑↑ colloidal stability ↑↑↑ cellular internalization ↑↑ enzymatic activity ↑↑↑ enzyme entrapment efficiency ↑↑ chol-PEG_{400}-RGD entrapment efficiency
Nano-GLA-v4	GLA-S	None	Sustitution of GLAcmycH6-S enzyme by another with probable less immunogenic capacity	↑↑↑ colloidal stability ↑↑↑ cellular internalization ↑↑↑ enzymatic activity ↑↑↑ enzyme entrapment efficiency ↑↑ chol-PEG_{400}-RGD entrapment efficiency

CONTINUOUS IMPROVEMENT

Figure 4.2. Continuously development of RGD-targeted liposomal formulations intended for the treatment of Fabry disease. GLA enzymes versions used during each development step are indicated. Changes on membrane composition together with their achieved goals are detailed on the corresponding table.

Human GLA enzyme is a homodimer which contain one active site in each monomer of 48.8 kDa (see *Figure 4.3*). Since its theoretical isoelectric point (pI) is around 5.1, GLA molecules have a negative net charge close to neutral pH[3].

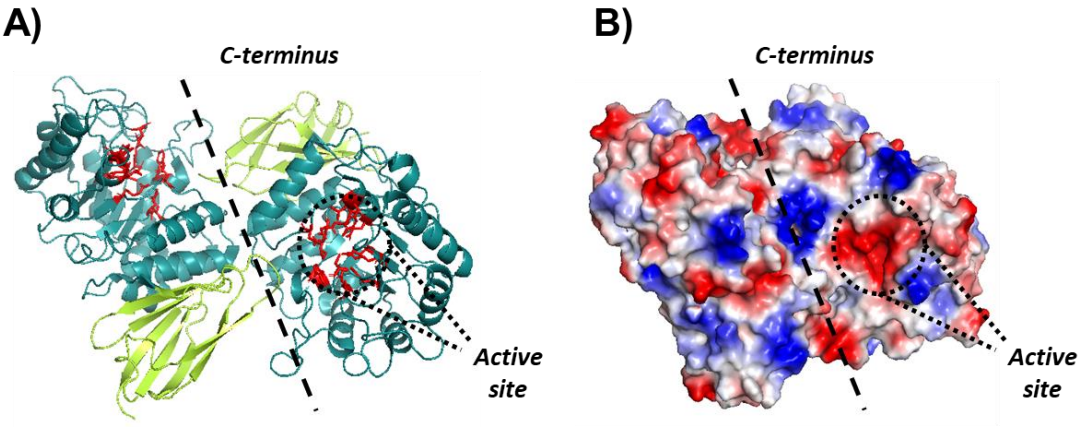


Figure 4.3. Visualizations of human GLA enzyme (PDB sequence: 1R47) using PyMOL software[4]. The GLA monomers are represented as blocks separated by a dashed line A) Secondary structure of the GLA where each monomer has represented the N-terminal domain in blue color, the C-terminal domain in green color, and the residues involved in the active site highlighted in red color. B) Theoretically estimated surface net charge of the GLA homodimer at pH 7. Surface charges are represented in legend color as red (negative charges), blue (positive charge) and white (neutral charge).

Protein charge is an important parameter strongly impacting on protein interaction with membranes[5–7]. Taking into account that GLA-loaded nanoliposomal formulations, prepared by DELOS-susp, have an aqueous phase close to neutral pH, at which GLA molecules have a negative net charge, the cationic character of liposome membranes was slightly increased by the incorporation of low amounts of positively charged surfactant MKC, which is the C14 homolog of the benzalkonium chloride, to increase the GLA entrapment efficiency of the nanoliposomal membrane. As reported in Tomsen-Melero *et al.*[8], in this version of GLA-loaded nanoformulation, named Nano-GLA-v2, the presence of MKC in targeted-liposomal nanovesicular formulations drastically improved the encapsulation efficiency of Replagal® (GLA model used in this work) as expected, but also the enzymatic activity of the encapsulated enzyme, as well as, the physicochemical stability of these nanoconjugates. However, it was also evidenced that large amounts of surfactant, for example in quatsome nanovesicular formulations cancelled the enzymatic activity of Replagal®. Therefore, MKC concentration in nanoliposomal membranes has a limit, above which integrated GLA molecules lost their activity. Cationic surfactant MKC was selected because it is present, as antimicrobial preservative, on a wide variety of already approved therapeutically products, for distinct administration routes. Representative examples of approved products containing MKC, are the parenteral formulations Celestone®, Soluspan® and Schering-Plough, with MKC concentration around 0.02 % (w/v), as well as the enteral formulation Lorazepam®[9,10].

Chol-PEG_{200}-RGD is one of the molecular components of Nano-GLA-v1 and Nano-GLA-v2 nanoformulations. Chol-PEG_{200}-RGD molecule contains RGD peptide (tripeptide Arg-Gly-Asp) linked to a cholesterol moiety through a polyethylenglycol chain of 200 Da of MW and composed by 4 units of ethylene oxide $(O–CH_2–CH_2)_4$.

Chol-PEG_{200}-RGD has a low solubility in ethanol and this is a problematic issue for the manufacturing, by DELOS-susp methodology, of nanoliposomal formulations containing this component (see DELOS-susp description in ***Chapter 7, Section 7.4.1.3***). This limitation was overcome in Nano-GLA-v3 nanoformulation (see ***Figure 4.2***), where chol-PEG_{400}-RGD, with appropriate solubility in ethanol, is used instead of Chol-PEG_{200}-RGD[11]. Nano-GLA-v3 contained the tagged GLAcmycH6-S as enzyme model instead of GLAH6-T, produced by stable expression using CHO cells.

In parallel with the development and optimization of the nanoliposomal carrier, summarized above, and in the context of the EU Smart4Fabry project, CHO-based stable clones for the production of GLAcmycH6-S (developed by Dr. José Luis Corchero, IBB-UAB) and GLA-S (developed by Dr. José Luis Corchero, IBB-UAB, in collaboration with LeanBio SL) were established, with freedom-of-operate (FTO) status, as a requirement for commercialization. As explained in ***Chapter 3***, a stable expression in CHO cells usually allows the obtaining of higher protein production yields. The presence of affinity tags in the GLAcmycH6-S protein allowed to purify the enzyme by one-step immobilized metal affinity chromatography (IMAC) procedures, obtaining large amount of the enzyme with acceptable purity level (≥ 85 %). This methodology made it possible to provide the required quantities for the advancement of the preclinical studies of the GLA-loaded nanoliposomal formulation[12,13].

GLAcmycH6-S enzyme version lacks the FTO status due to limitations related to intellectual property, as well as immunogenic issues due to the presence of purification tags[14]. To minimize immunogenic possible effects and ensure acceptance by regulatory agencies, GLAcmycH6-S was substituted by the tag-free GLA-S enzyme in Nano-GLA-v4 nanoformulation (see ***Figure 4.2***). The outstanding pre-clinical efficacy results (TRL-4) achieved with Nano-GLA-v4, where recognized by EMA and the EC with the ODD to this GLA nanoformulation for Fabry treatment. It should be mentioned, that this doctoral thesis and Judit Tomsen doctoral thesis[13] have strongly contributed to this success.

Nowadays, further development of the quality of the Nano-GLA-v4 formulation is being done in the frame of the EU Phoenix project with the aim to boost their translation to the early clinical phase (TRL-6).

4.1.2. Framework of the study

With the purpose to contribute to the development of this innovative nanopharmaceutical, part of the efforts of this thesis, summarized in the present chapter, were focused on the study of the impact of GLA characteristics on the following physicochemical and biological features of GLA-loaded RGD-targeted nanoliposomal formulations:

1. Enzyme entrapment efficiency.
2. GLA leakage rate from liposome-based nanoformulations.
3. Enzymatic activity of the encapsulated GLA in the nanoliposomal formulations.
4. Colloidal stability of GLA-loaded nanoliposomes.
5. GLA release from liposome-based nanoformulations.
6. GLA distribution on nanoliposomes.
7. Protective capacity of nanoliposomes against the GLA degradation.

As depicted in ***Figure 4.4*** and summarized in ***Table 4.1***, a single nanoliposomal membrane composition and the four GLA enzyme versions, previously described in ***Chapter 3***, were used to study the impact of GLA characteristics on the physicochemical and biological features of GLA-loaded nanoliposomal formulations. The nanoliposomal membrane composition for all the studies described in this chapter corresponds to the one of Nano-GLA-v4, also named GLA nanoliposomal formulation and LP-RGD-GLA-$S_{(gluc)}$ in this thesis, currently being scaled-up and tested under Phoenix and Nano4rare EU projects.

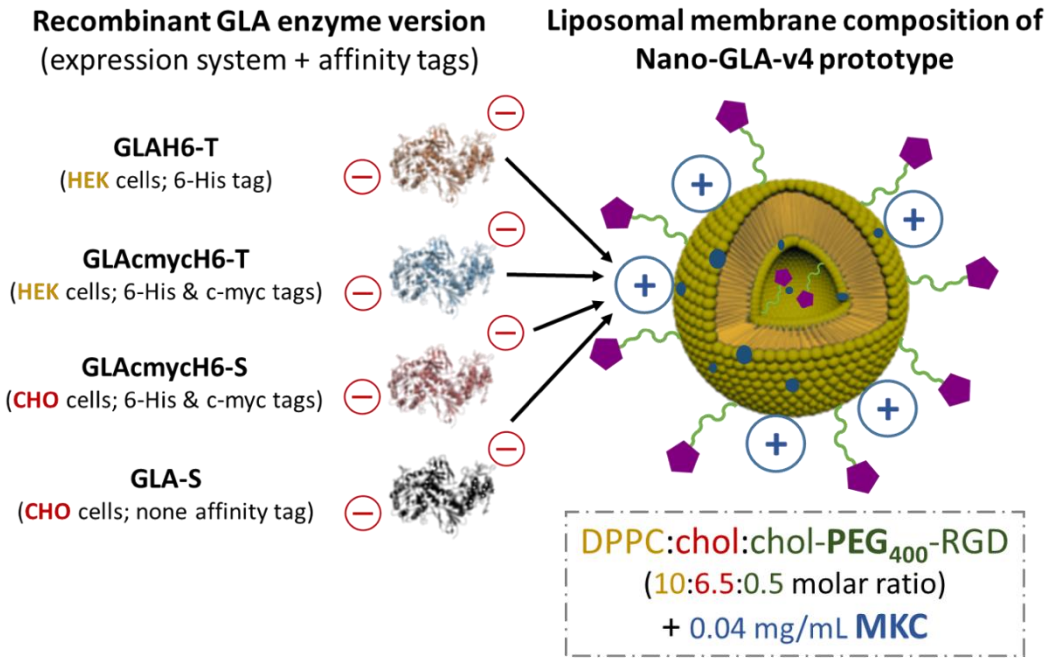


Figure 4.4. Representation of the liposomal membrane composition and the four recombinant GLA versions (GLAH6-T, GLAcmycH6-T, GLAcmycH6-S and GLA-S) used in this chapter to study the impact of GLA characteristics on the physicochemical and biological features of GLA-loaded nanoliposomal formulations.

Table 4.1. Characteristics of the different GLA versions used as enzyme models to be encapsulated in nanoliposomal formulations in this chapter. Average values from two independent batches of each GLA version. The error is expressed as their standard deviation (s.d.).

Enzyme version (cell factory)	Protein concentration (mg/mL)	Purity (%)	MW per monomer (kDa)	Solubility (%)	Theoretical pI	ζ-potential (mV)	Specific EA (μM 4MU/mg/h)	CSM (nm)
GLAH6-T (HEK)	1.0 ± 0.6	97 ± 1	51.7 ± 0.1	91 ± 1 (pH 4.5) 90 ± 4 (pH 5.5)	5.77	15.7 ± 1.5 (pH 4.5) -0.6 ± 0.8 (pH 5.5)	1586 ± 144 (pH 4.5)	350.7 ± 0.2 (pH 4.5) 350.6 ± 0.1 (pH 5.5) 350.6 ± 0.1 (pH 7)
GLAcmycH6-T (HEK)	0.5 ± 0.1	90 ± 3	53.5 ± 0.3	41 ± 1 (pH 4.5) 75 ± 3 (pH 5.5)	5.53	9.2 ± 6.2 (pH 4.5) 1.1 ± 0.5 (pH 5.5)	2873 ± 203 (pH 4.5)	350.9 ± 0.2 (pH 4.5) 350.9 ± 0.2 (pH 5.5) 352.1 ± 0.1 (pH 7)
GLAcmycH6-S (CHO)	1.3 ± 0.2	89 ± 4	53.8 ± 0.1	21 ± 10 (pH 4.5) 97 ± 3 (pH 5.5)	5.53	2.6 ± 1.6 (pH 4.5) -3.0 ± 1.0 (pH 5.5)	1797 ± 250 (pH 4.5)	351.0 ± 0.7 (pH 4.5) 351.0 ± 0.7 (pH 5.5) 350.6 ± 0.1 (pH 7)
GLA-S (CHO)	3.8 ± 0.4	94 ± 1	42.4 ± 0.4 51.8 ± 0.5 62.3 ± 0.2	N.D.	5.35	-0.6 ± 0.2 (pH 7)	3556 ± 75 (pH 4.5)	350.3 ± 0.1 (pH 7)

GLA concentration, purity and solubility were assessed by SDS-PAGE and TGX densitometry. The molecular weight (MW) of GLA monomers was obtained by mass spectrometry. Theoretical pI values, meaning that pH at which the protein should have a neutral net charge, were calculated using the Expasy ProtParam tool[15]. The surface charge (ζ-potential) was measured by ELS. The enzymatic activity (EA) of GLA was assessed by an *in vitro* fluorescence assay. Center of spectral mass (CSM) values of GLA enzymes at different pHs measured by fluorescence spectroscopy allow the monitoring of GLA conformational changes that modify the tryptophan (Trp) exposure to the surrounding environment (higher CSM values mean higher Trp exposure to the media, and usually, more unfolded protein structures). All the enzymes versions demonstrated sizes around 10 nm by DLS in a pH range of 4.5 – 7; and a host cell DNA contamination < 5 % (m/m).

4.2. Impact of GLA characteristics on physicochemical and biological features of GLA-loaded nanoliposomal formulations

The main objective of this section is to investigate the impact of GLA nature and characteristics on the production and properties of GLA-loaded RGD-targeted nanoliposomal formulations (LP-RGD-GLA).

4.2.1. Production and characterization of GLA-loaded nanoliposomal formulations used for the study

Following this aim, different LP-RGD-GLA were produced using the four different versions of GLA described in ***Table 4.1***. Liposomal membrane of these nanoformulations was composed by DPPC, cholesterol and chol-PEG_{400}-RGD (10:6.5:0.5 theoretical molar ratio), and contained a small amount of MKC (5 % molar of the total membrane components) as depicted above in ***Figure 4.4***. As explained, MKC surfactant is used to enhance nanoliposomes stability and GLA entrapment capacity due to its cationic character at neutral pH, where GLA enzymes are negatively charged (theoretical pI between 5.1 – 5.8)[3,8]. The chol-PEG_{400}-RGD molecules act as targeting units, since RGD peptide is able to recognize $\alpha_v\beta_3$-integrins overexpressed in endothelial cells[1,16]. RGD-targeted liposomes (LP-RGD) free of GLA were also synthesized as control.

GLA-loaded and GLA-free nanoliposomal formulations used to perform the present study are described in ***Table 4.2***. These nanoformulations were produced by the DELOS-susp methodology (see ***Figure 1.10*** and ***Figure 4.5 A***) using a lab-scale installation and the protocol described in ***Chapter 7, Section 7.4.1***. Briefly, the four liposomal membrane components (DPPC, cholesterol, chol-PEG_{400}-RGD and MKC) were solubilized in a mixture of ethanol (EtOH) and dimethyl sulfoxide (DMSO) (4:1 v:v), due to the low solubility of chol-PEG_{400}-RGD in pure EtOH. EtOH and DMSO are Class 3 solvents of the ICH guideline Q3C (R6) Impurities: guideline for residual solvents from the EMA, which means that both solvents can be used for the manufacturing of pharmaceutical formulations[17]. This solution was placed into a high-pressure vessel, and then compressed CO_2 was added to produce a CO_2-expanded solution at 10 MPa and 35 ºC. This pressurized solution was depressurized into a water solution containing the desired version of GLA enzyme, to produce in a one-step GLA-loaded nanoliposomes.

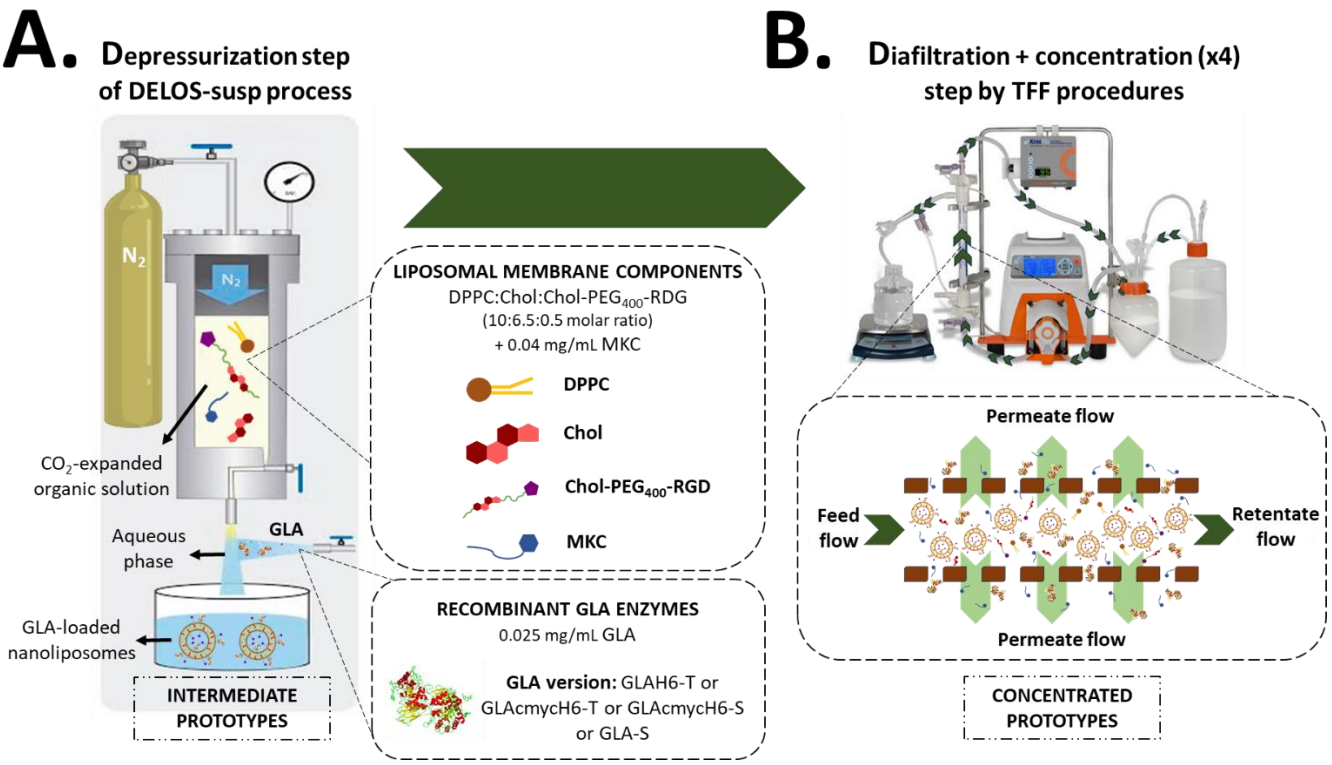


Figure 4.5. Manufacturing process of intermediate and concentrated GLA-loaded nanoliposomal formulations. A) DELOS-susp methodology for production of nanoliposomal formulations. Production of GLA-loaded nanoliposomes during the depressurization step of a CO_2-expanded organic solution of nanoliposomal membrane components, over an aqueous solution of GLA enzyme. B) Tangential flow filtration (TFF) procedure for the purification and concentration of nanoliposomal formulations produced by DELOS-susp.

Free GLA molecules, non-integrated in nanoliposomes during their production by DELOS-susp, were separated from the GLA-loaded liposomes by diafiltration through TFF procedure (see ***Figure 4.5 B***), and in some cases subsequently 4-fold concentrated until a theoretical lipid concentration of 5 mg/mL using also TFF process (apparatus and protocols described in ***Chapter 7, Section 7.4.3***). Empty liposomes (GLA-free systems named LP-$RGD_{(w)}$) were produced as controls and 7.5- or 20-fold concentrated during TFF procedures.

Details on the production of all nanoliposomal formulations used for the present study are described in ***Table 4.2*** and can be found in ***Chapter 7, Table 7.5***.

Table 4.2. Description of GLA-loaded and GLA-free nanoliposomal formulations used for the study described in *Section 4.2* and *4.3*.

Nanoliposomal formulation ID	Loaded GLA version	[A] $[lipid]_{theoric}$ (mg/mL)	[B] $[GLA]_{TGX}$ (µg/mL)	GLA:lipid mass ratio (m/m)	Size (nm)	PdI	ζ-potential (mV)	Formulation pH	Nanovesicle storage solvent
LP-RGD_int *	**None**	1.2	0	-	167 ± 15	0.199 ± 0.02	62 ± 6	4.3 ± 0.2	5 % EtOH + 1.2 % DMSO (v/v) in water
LP-RGD$_{(w)}$	**None**	9 or 20	0	-	175 ± 9	0.248 ± 0.01	61 ± 3	6.7 ± 0.1	Pure water
LP-RGD-GLAH6-T_int	**GLAH6-T**	1.2	25 ± 1	1:48	183 ± 20	0.228 ± 0.04	66 ± 5	4.4 ± 0.3	5 % EtOH + 1.2 % DMSO (v/v) in water
LP-RGD-GLAH6-T$_{(w)}$	**GLAH6-T**	5	67 ± 3	1:75	217 ± 5	0.266 ± 0.02	50 ± 3	6.9 ± 0.2	Pure water
LP-RGD-GLAcmycH6-T_int	**GLAcmycH6-T**	1.2	26 ± 1	1:46	166 ± 11	0.196 ± 0.03	50 ± 2	4.3 ± 0.1	5 % EtOH + 1.2 % DMSO (v/v) in water
LP-RGD-GLAcmycH6-T$_{(w)}$	**GLAcmycH6-T**	5	33 ± 4	1:152	204 ± 3	0.151 ± 0.03	47 ± 3	6.5 ± 0.2	Pure water
LP-RGD-GLAcmycH6-S_int	**GLAcmycH6-S**	1.2	25 ± 1	1:48	164 ± 10	0.212 ± 0.02	57 ± 1	4.3 ± 0.1	5 % EtOH + 1.2 % DMSO (v/v) in water
LP-RGD-GLAcmycH6-S$_{(w)}$	**GLAcmycH6-S**	5	103 ± 6	1:49	189 ± 13	0.244 ± 0.02	47 ± 2	6.3 ± 0.1	Pure water
LP-RGD-GLA-S_int	**GLA-S**	1.2	27 ± 1	1:44	159 ± 13	0.206 ± 0.01	54 ± 1	4.6 ± 0.1	5 % EtOH + 1.2 % DMSO (v/v) in water
LP-RGD-GLA-S$_{(w)}$	**GLA-S**	5	110 ± 1	1:45	176 ± 18	0.229 ± 0.03	39 ± 2	7.0 ± 0.1	Pure water

[A] Lipid concentration of all nanoliposomal formulations refers to the theoretical total amount of membrane components added to the DELOS-susp high pressure vessel (HPV). [B] GLA concentration of already prepared liposomal nanoformulations was assessed by SDS-PAGE and TGX densitometry. Results are shown as the average of 2 independent batches produced for each nanoliposomal system, * except for LP-RGD_int, where 8 independent batches were measured. The error is represented as the s.d. between measurements. All nanoliposomal formulations have the same membrane composition: DPPC:chol:chol-PEG_{400}-RGD (10:6.5:0.5 theoretical molar ratio) and presence of MKC (5 % molar of the total membrane components).

Physicochemical properties of all nanoformulations used for the present study are described in *Table 4.2*, and were measured next day after their production. Particle size distribution was measured by DLS/ELS (see procedures in *Chapter 7, Section 7.4.5.3*), GLA concentration was determined by SDS-PAGE and further TGX densitometry analysis (see procedures in *Chapter 7, Section 7.2.6.1*), and vesicle morphology observed by cryoTEM imaging (see procedures in *Chapter 7, Section 7.4.5.2*). The results of these characterizations are gathered in *Table 4.2* and *Figure 4.6*. The different properties of the GLA versions encapsulated seemed to have none impact on the size and shape of the liposomes. In general, highly monodisperse unilamellar liposome populations (PdI < 0.3) were obtained in all cases, confirming that GLA enzyme not destabilize the positively charged lipid systems. Both, the empty and GLA-loaded nanoliposomal formulations, showed average sizes around 170 nm and surface charges of 55 – 60 mV. However, the liposome size increased and the ζ-potential values decreased after diafiltration by TFF, possibly due to the change of dispersant media, the CO_2 removal and consequently, the pH increase. By comparing the GLA-free nanoliposomal formulations (LP-RGD_int and LP-RGD$_{(w)}$) with the formulations containing GLA, it was evidenced that variations on ζ-potential were caused by

GLA presence and/or buffer exchange. It is important to highlight that all formulations were analyzed by DLS/ELS at the same theoretical lipid concentration of 1.2 mg/mL in water as explained in ***Chapter 7, Section 7.4.5.3***.

Nanoliposomal formulations of ***Table 4.2*** were observed by cryoTEM microscopy in the Servei de Microscopia of the UAB (Barcelona), following the procedure described in ***Chapter 7, Section 7.4.5.2***. As it can be observed in ***Figure 4.6***, "Dense stick-like nanostructures" (pointed with yellow arrows) were found in the cryoTEM images of GLA-loaded nanoformulations diafiltrated by TFF in water. Interestingly, lower presence of these "dense stick-like nanostructures" were found in nanoliposomal formulations with lower GLA concentration, such as LP-RGD-GLAcmycH6-$T_{(w)}$. This observation suggests that the presence of GLA in the nanoliposomal formulations, at a concentration above a certain value, might induce that some membrane components organize themselves into "dense stick-like nanostructures" other than vesicles. Probable contamination coming from the DELOS-susp reactor or TFF procedure was discarded by processing controls containing only water and further examining them by cryoTEM (data not shown).

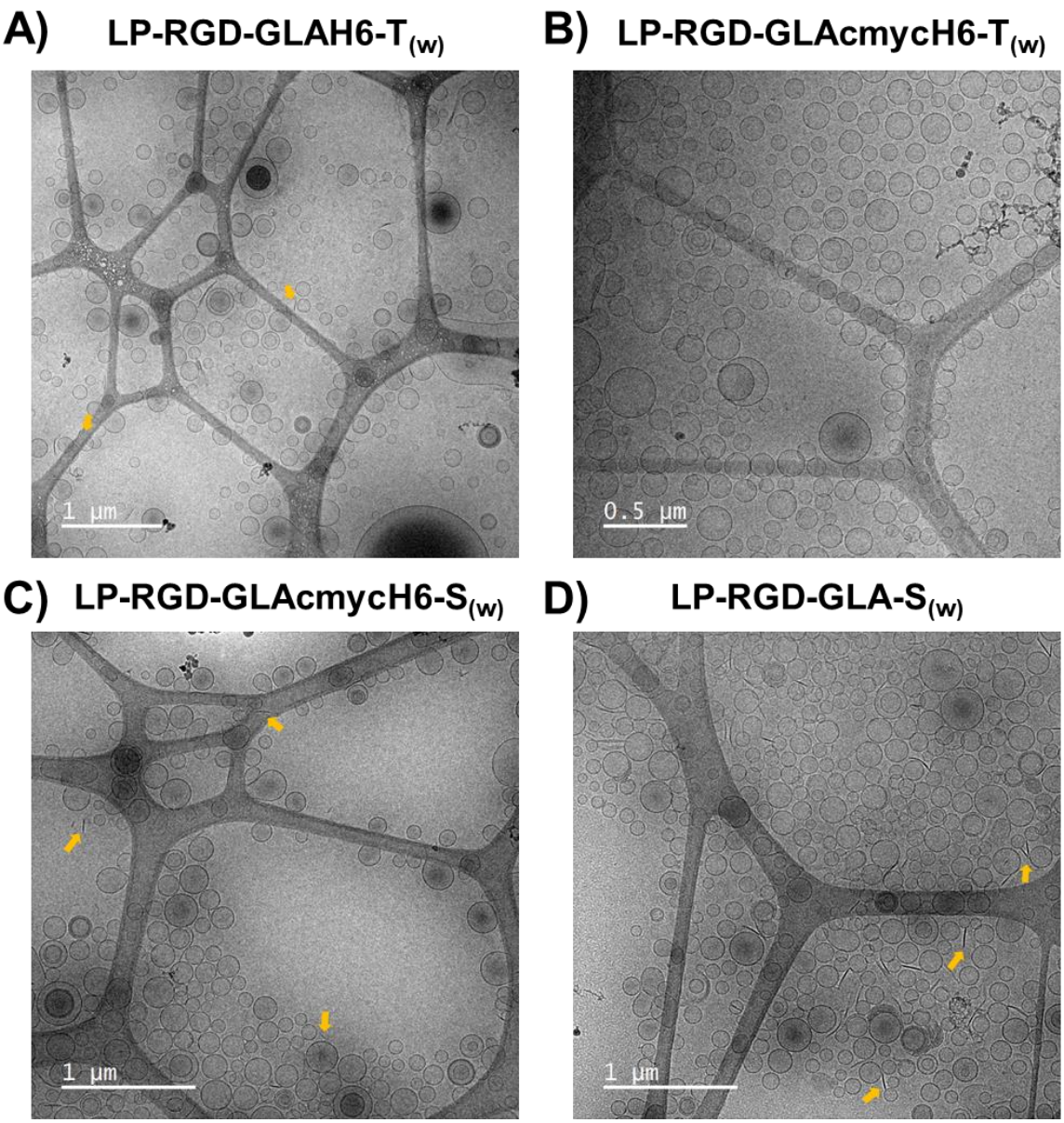


Figure 4.6. CryoTEM images of GLA-loaded liposomes two months after their production: A) LP-RGD-GLAH6-$T_{(w)}$, containing the GLAH6-T, B) LP-RGD-GLAcmycH6-$T_{(w)}$, containing the GLAcmycH6-T, C) LP-RGD-GLAcmycH6-$S_{(w)}$, containing the GLAcmycH6-S, or D) LP-RGD-GLA-$S_{(w)}$, containing the GLA-S as integrated GLA enzyme version. Yellow arrow point out "dense sticks" nanostructures probable composed by DPPC, chol, chol-PEG_{400}-RGD and/or MKC non-integrated in nanoliposomal membrane.

4.2.2. Impact of GLA characteristics on the enzyme entrapment efficiency in nanoliposomes

GLA enzyme entrapment efficiency (EE %) of GLA-loaded nanoliposomal formulations, describes the relationship in molar ratio between GLA entrapped in nanoliposomal nanostructures and GLA free. GLA EE % of GLA-loaded nanoliposomal formulations gathered in ***Table 4.2*** was calculated according to the ***Eq. 7.2*** explained in ***Chapter 7, Section 7.4.5.5***.

All the nanoliposomal formulations compared in this study, LP-RGD-GLAH6-$T_{(w)}$, LP-RGD-GLAcmycH6-$T_{(w)}$, LP-RGD-GLAcmycH6-$S_{(w)}$ and LP-RGD-GLA-$S_{(w)}$, were equally produced with the same theoretical lipid concentration (5 mg/mL) and media (pure water), but differing on the GLA version encapsulated. Results presented in ***Figure 4.7***, indicated a lower EE % of the enzymes produced by transient expression in HEK 293F cell cultures (GLAH6-T and GLAcmcyH6-T) in nanoliposomes than the other produced by stable expression in CHO cells (GLAcmycH6-S and GLA-S), which present a more negative character closer to neutral pH. This fact evidenced the importance of the GLA surface net charge, strongly related with the GLA nature, to favor protein integration in liposomes. Moreover, among the enzymes expressed in HEK cells, GLAcmycH6-T is entrapped in nanoliposomes with lower efficiency than GLAH6-T. This is probably due the lower solubility of GLAcmycH6-T than GLAH6-T described in ***Chapter 3***.

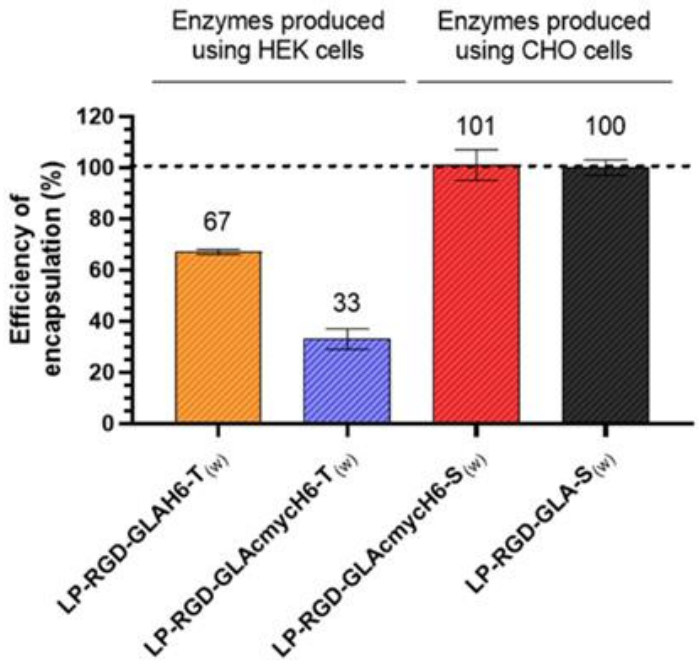


Figure 4.7. Determination of the GLA entrapment efficiency in RGD-targeted liposomal nanoformulations at three days after production. Results are shown as the average of two independent batches produced for nanovesicle systems. The error is represented as the s.d. between measurements.

In conclusion, the GLA nature impacts on the GLA entrapment efficiency in nanoliposomal formulations composed by DPPC, chol, chol-PEG_{400}-RGD and MKC prepared in pure water.

4.2.3. Impact of GLA characteristics on the GLA leakage rate of nanoliposomes

GLA leakage rate throughout shelf-life of GLA-loaded nanoliposomal formulations, describes the variations of the GLA EE % in nanoliposomes over time. GLA leakage rate of GLA-loaded nanoliposomal formulations gathered in ***Table 4.2*** was determined according to the filtration-centrifugation protocol explained in ***Chapter 7, Section 7.4.6.2***.

All the nanoliposomal formulations compared in this study, LP-RGD-GLAH6-$T_{(w)}$, LP-RGD-GLAcmycH6-$T_{(w)}$, LP-RGD-GLAcmycH6-$S_{(w)}$ and LP-RGD-GLA-$S_{(w)}$, were equally produced with the same theoretical lipid concentration (5 mg/mL) and media (pure water), but differing on the GLA version encapsulated. As shown in ***Figure 4.8***, the GLA leakage rate from these nanoformulations was monitored under storage conditions (2 – 8 ºC) during 3 months. Results indicated a continuous increased GLA leakage from nanoliposomes over time in the tested conditions, ending in a similar amount of leaked GLA (around 60 %) for all nanoformulations at time 90 days. The similar protein sizes found by DLS for all the GLA enzyme versions (around 10 nm) could be related with their same leakage rate. Interestingly, the leakage of GLAH6-T enzyme (produced in HEK cells) from LP-RGD-GLAH6-$T_{(w)}$ nanoliposomes started one month later compared to the other prototypes tested, probably influenced by the higher purity and the slightly lower molecular weight obtained for this GLA enzyme version. Additionally, the quicker leakage observed for the GLAcmycH6-S enzyme (produced in CHO) could be associated to the higher size destabilization found by DLS for this enzyme at low temperatures of 4 ºC (results described in ***Chapter 3***).

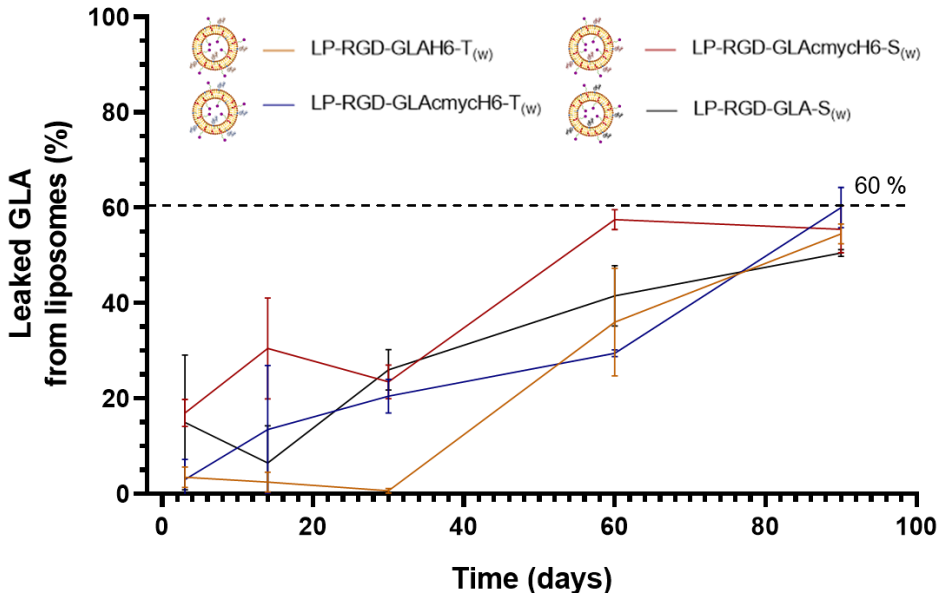


Figure 4.8. GLA leakage rate of GLA-loaded nanoliposomal formulations differing on the entrapped GLA enzyme version and stored at 2 – 8 ºC during 3 months. Leaked GLA enzymes were separated from nanoliposomes by filtration-centrifugation procedures, and then quantified by SDS-PAGE and TGX densitometry analysis. Triplicates from two independent production batches of each nanovesicular system were tested.

As summary, the GLA leakage rate from nanoliposomal formulations composed by DPPC, chol, chol-PEG_{400}-RGD and MKC, it seems that the GLA nature influence on the leakage kinetics. At the current state of these studies it is not possible to withdraw any correlation between GLA characteristics and the enzyme leakage behavior.

4.2.4. Impact of GLA characteristics on the enzymatic activity of nanoliposomes

The specific enzymatic activity (EA) of non-encapsulated GLA versions and GLA-loaded nanoliposomal formulations was measured by the *in vitro* fluorometric assay described in ***Chapter 7, Section 7.2.9***. This protocol was set-up to determine the activity of naked GLA proteins in acidic pH conditions similar to those of cell lysosomes[18,19], where GLA enzymes conduct their enzymatic catalysis[3]. As schematized in ***Figure 4.9***, this assay measures the conversion of a non-fluorescent substrate (4-MUG) into a fluorescent product (4-MU) promoted by the catalytic activity of GLA enzymes.

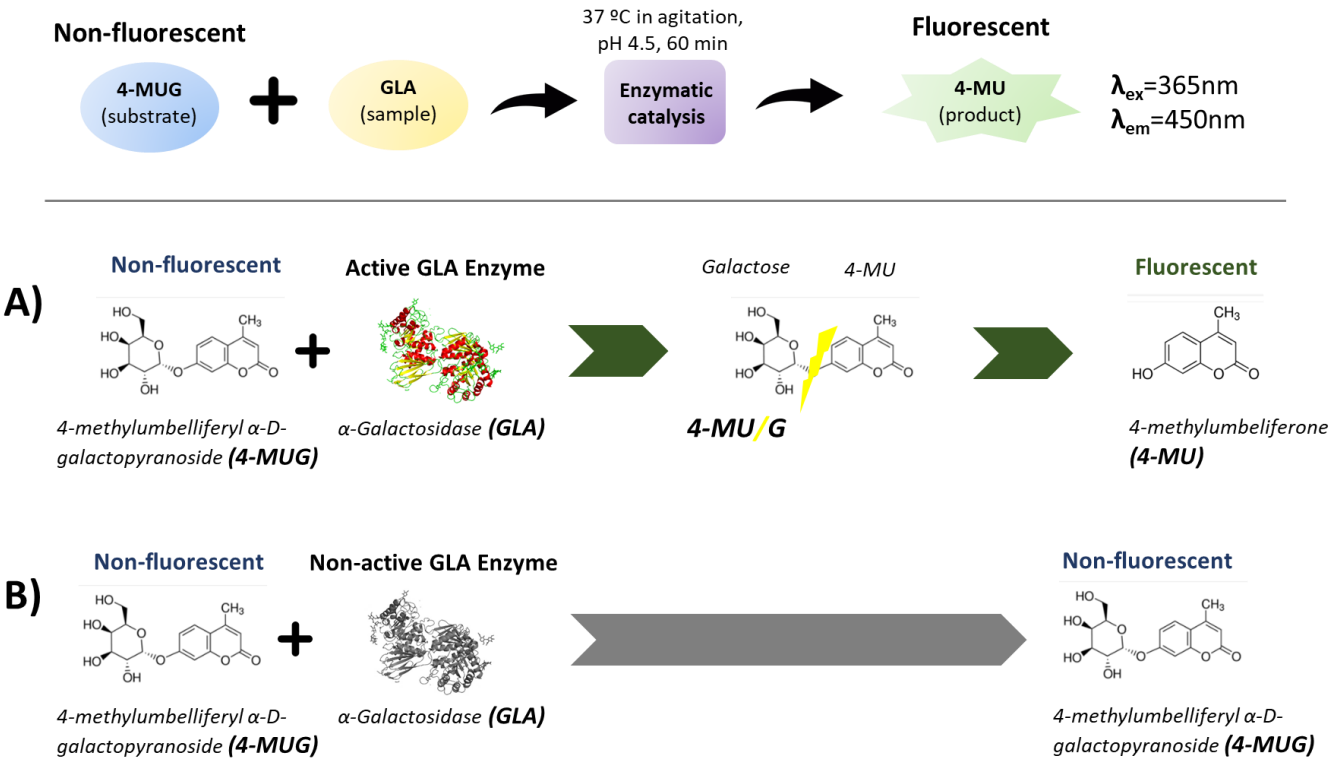


Figure 4.9. Schematization of the *in vitro* fluorescent assay to assess the EA of naked GLA enzymes conversing the 4-MUG substrate into the fluorescent 4-MU product in the presence of A) active GLA enzymes; B) no signal is obtained when inactive GLA enzymes are assayed. The detailed protocol is available on *Chapter 7, Section 7.2.9*.

The suitability of this *in vitro* assay for the characterization of the EA of GLA enzymes loaded into nanovesicular systems was evaluated during this thesis project[8]. For this purpose, empty and GLA-loaded nanoformulations diafiltrated by TFF (LP-RGD$_{(w)}$ and LP-RGD-GLAcmycH6-S$_{(w)}$, respectively) were tested.

4.2.4.1. Suitability of the *in vitro* fluorimetric assay for EA measurement of GLA-loaded nanoliposomal formulations

Nanoliposomal formulations were incubated into the assay conditions (presence of 4-MUG, 0.01 M acetic acid buffer, pH 4.5, 100 rpm and 37 ºC during 60 min), and then analyzed. As shown in *Figure 4.10*, the size distribution and particle concentration were maintained prior and after sample incubation, demonstrating the stability of the liposomal vesicles at the conditions of the *in vitro* assay. The integrity and stability of liposomes was studied by DLS and NTA measurements, following the procedures detailed in *Chapter 7, Sections 7.4.5.3* and *7.4.5.4*.

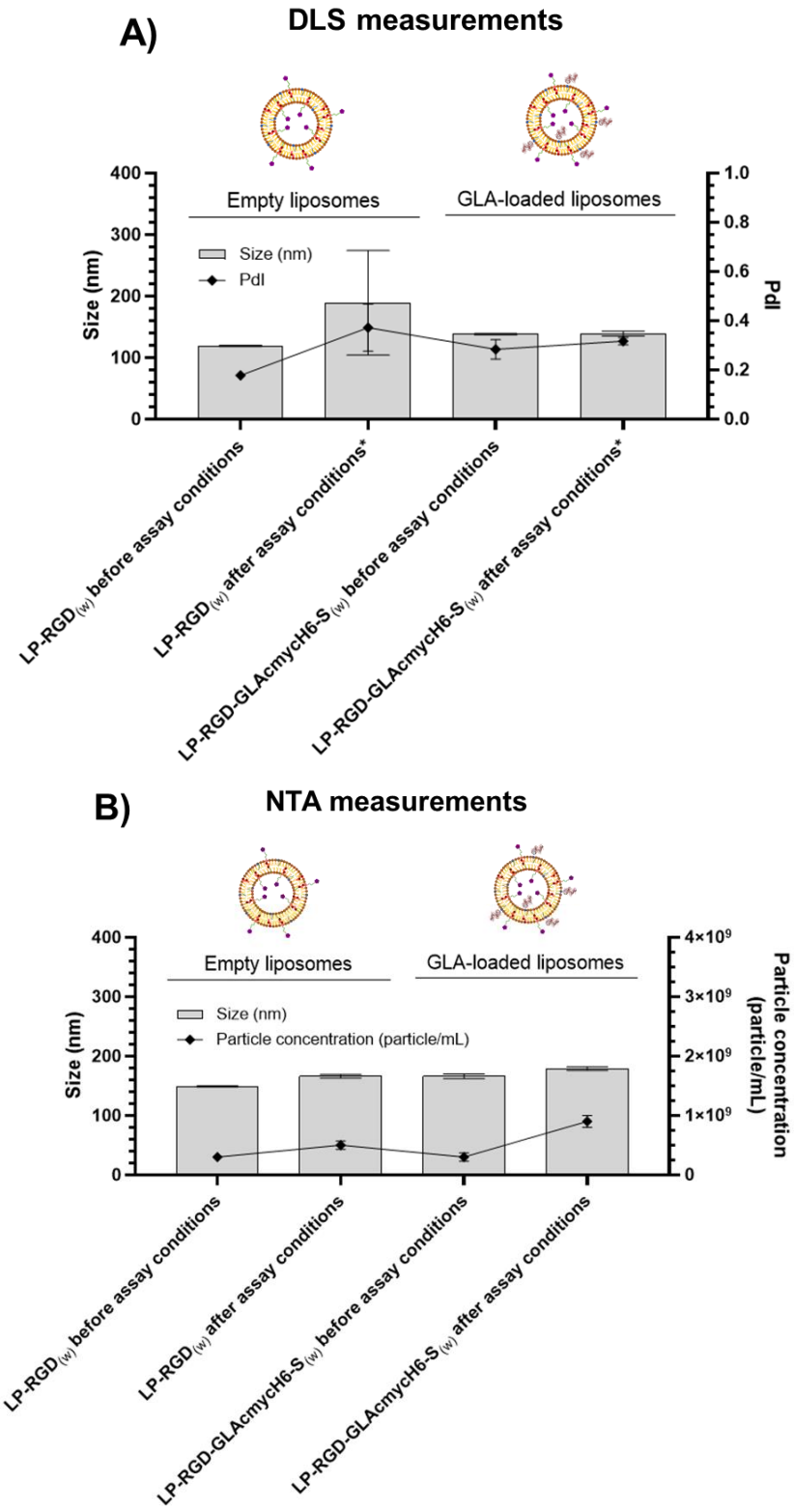
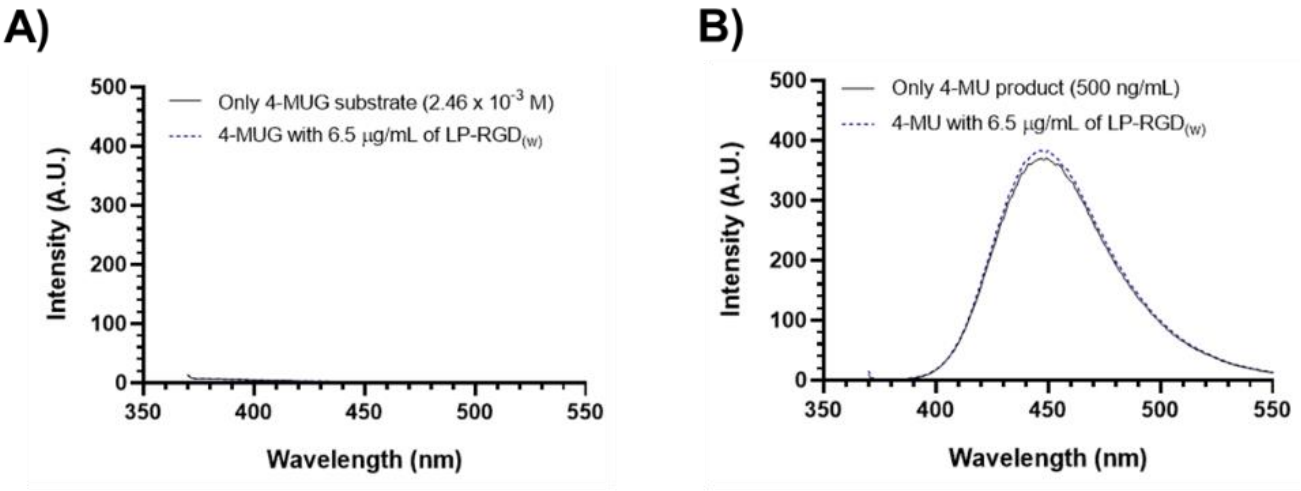
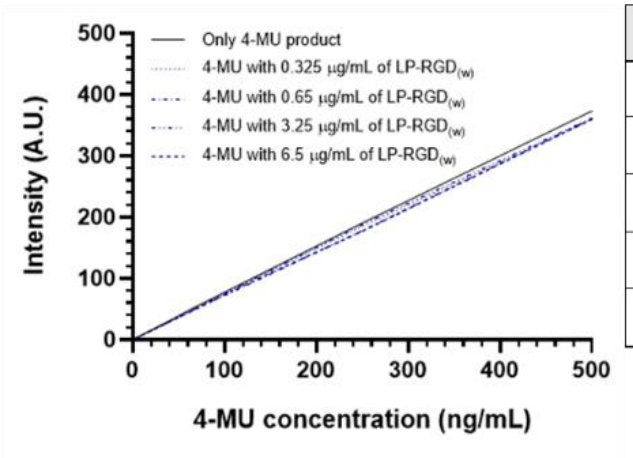


Figure 4.10. Integrity comparison of empty and GLA-loaded liposomes (LP-RGD$_{(w)}$ and LP-RGD-GLAcmycH6-S$_{(w)}$, respectively), before and after being submitted to the EA assay conditions. Nanovesicle stability was determined by A) DLS and B) NTA measurements. *Samples analyzed by DLS did not contain the 4-MUG substrate due to its interference with the measurements.

On the other hand, in the present thesis it was also studied possible matrix effects over fluorescence emission caused by lipid presence, coming from nanoliposomes. To discard these matrix effects, the fluorescence spectra of 4-MUG substrate and 4-MU substrates was recorded in the presence and absence of GLA-free nanoliposomes (LP-RGD$_{(w)}$) (see ***Figure 4.11***).



C)



Calibration curve composition	Slope
Only 4-MU product	0.7480
4-MU + LP-RGD$_{(w)}$ (0.325 µg/mL)	0.7214
4-MU + LP-RGD$_{(w)}$ (0.65 µg/mL)	0.7193
4-MU + LP-RGD$_{(w)}$ (3.25 µg/mL)	0.7274
4-MU + LP-RGD$_{(w)}$ (6.5 µg/mL)	0.7184

Figure 4.11. Fluorescence emission spectra measurements (at λ_{ex} = 365 nm, λ_{em} = 450 nm conditions) of A) 4-MUG substrate and B) 4-MU product in absence or presence of empty nanoliposomes (LP-RGD$_{(w)}$). C) Confirmation of non-matrix effects caused by nanoliposomal composition after the slope comparison of calibration curves prepared containing only the 4-MU product, or additional increasing concentrations of LP-RGD$_{(w)}$ formulation.

The results presented in ***Figure 4.11*** discard any effects of nanoliposomes over fluorescence emission of 4-MUG substrate and 4-MU product, at the usual concentrations assayed. The recorded fluorescence spectra signals were not modified due to nanovesicle presence. These results confirmed the reliability of using the same fluorimetric assay in nanostructured GLA enzyme to assess their specific EA.

4.2.4.2. Comparison of the EA of naked GLA enzymes and GLA-loaded nanoliposomes

Once determined the feasibility of using the same *in vitro* fluorometric assay for both, non-encapsulated GLA enzymes and GLA-loaded nanoliposomal formulations, the EA of some GLA-loaded nanoliposomal formulations gathered in ***Table 4.2*** was evaluated following the procedure detailed in ***Chapter 7, Section 7.2.9***.

All the nanoliposomal formulations compared in this study, LP-RGD-GLAH6-$T_{(w)}$, LP-RGD-GLAcmycH6-$T_{(w)}$, LP-RGD-GLAcmycH6-$S_{(w)}$ and LP-RGD-GLA-$S_{(w)}$, were equally produced with the same theoretical lipid concentration (5 mg/mL) and media (pure water), but differing on the GLA version encapsulated. The results presented in ***Figure 4.12***, evidenced that the specific EA of GLA enzymes once integrated in liposomal formulations was modified following a tendency correlated with the GLA nature, independently on the specific EA of each GLA enzyme in its naked form. Curiously, the GLAcmycH6-S enzyme produced in CHO cells was the unique that increased their EA once integrated in nanoliposomes. Surprisingly, despite the fact that in naked GLA versions there was no correlation between GLA nature (production in HEK or CHO cells) and their EA, it was clearly observed that once the enzymes were encapsulated, that nanoformulations containing GLA enzymes produced in CHO cells demonstrated higher EA than others prepared with GLA enzymes produced in HEK cells. As further demonstrated with the studies of Trp fluorescence (see ***Section 4.3.3.2***), the protein conformation and distribution on lipid bilayers seems to be also influenced by the GLA nature (such as the glycosylation pattern), explaining the differences between the specific EA around 3000 µM 4MU/mg/h obtained when encapsulating GLA versions produced in CHO cells, or EA < 1000 µM 4MU/mg/h for GLA versions expressed in HEK 293F cells. These results together with the previous ones of ***Section 4.2.2***, pointed out better efficiencies of GLA enzyme immobilization in lipid interfaces by using GLA versions expressed in CHO cultures.

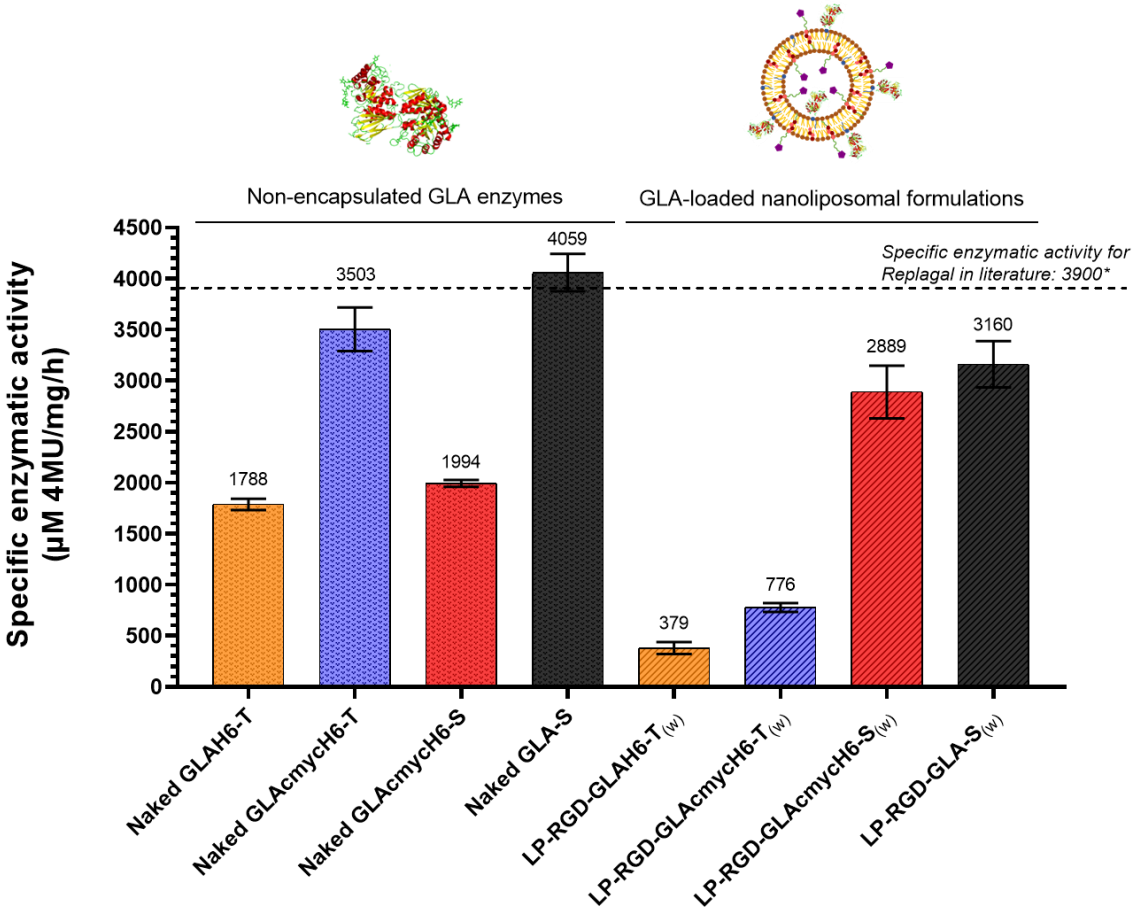


Figure 4.12. Determination of the enzymatic activity of GLA-loaded liposomal nanoformulations (LP-RGD-GLAH6-$T_{(w)}$, LP-RGD-GLAcmycH6-$T_{(w)}$, LP-RGD-GLAcmycH6-$S_{(w)}$, and LP-RGD-GLA-$S_{(w)}$) at three days after production. Non-encapsulated GLA enzymes were also measured as controls. Results are shown as the average of two independent batches produced for each nanovesicular system, but from one of each naked GLA enzyme version. The error is represented as the s.d. between measurements. *Data for Replagal obtained from Lee *et al.*[20].

Then, the EA stability of both, naked and GLA-loaded nanoliposomal formulations was also monitored in time under the storage conditions (2 – 8 ºC). All naked GLA versions studied were stored in 0.01 M acetic acid buffer at pH 5.5; except for GLA-S, which is stored in aqueous media with excipients (mannitol, sodium phosphate monobasic monohydrate, and sodium phosphate dibasic heptahydrate) previously described as Fabrazyme-like buffer in *Chapter 3*.

Results summarized in *Figure 4.13*, indicated decrease of EA since 30 days for most cases, except for naked GLAH6-T enzyme. This evidenced that the EA of GLA enzymes is not better conserved in nanoliposomal formulations when these are stored as aqueous dispersions at 2 – 8 ºC. For this reason, a great effort is being done under EU Phoenix project to develop a new prototype of GLA-loaded nanoliposomal formulation as a lyophilized nanopharmaceutical product.

Furthermore, the EA from GLA-loaded nanoliposomal formulations prepared with GLA enzymes produced using CHO cultures (LP-RGD-GLAcmycH6-$S_{(w)}$ and LP-RGD-GLA-$S_{(w)}$ prototypes) lost quicker their EA in comparison with the other ones (see ***Figure 4.13 B***). This fact might be strongly related with the GLA nature (such as the glycosylation pattern), in the same manner than the approved ERTs Replagal® (expressed in a human cell line of undisclosed origin) and Fabrazyme® (expressed in CHO cultures) need different storage conditions to maintain their stability: Replagal® is stored as a concentrated solution, but Fabrazyme® as a lyophilized product[20–22].

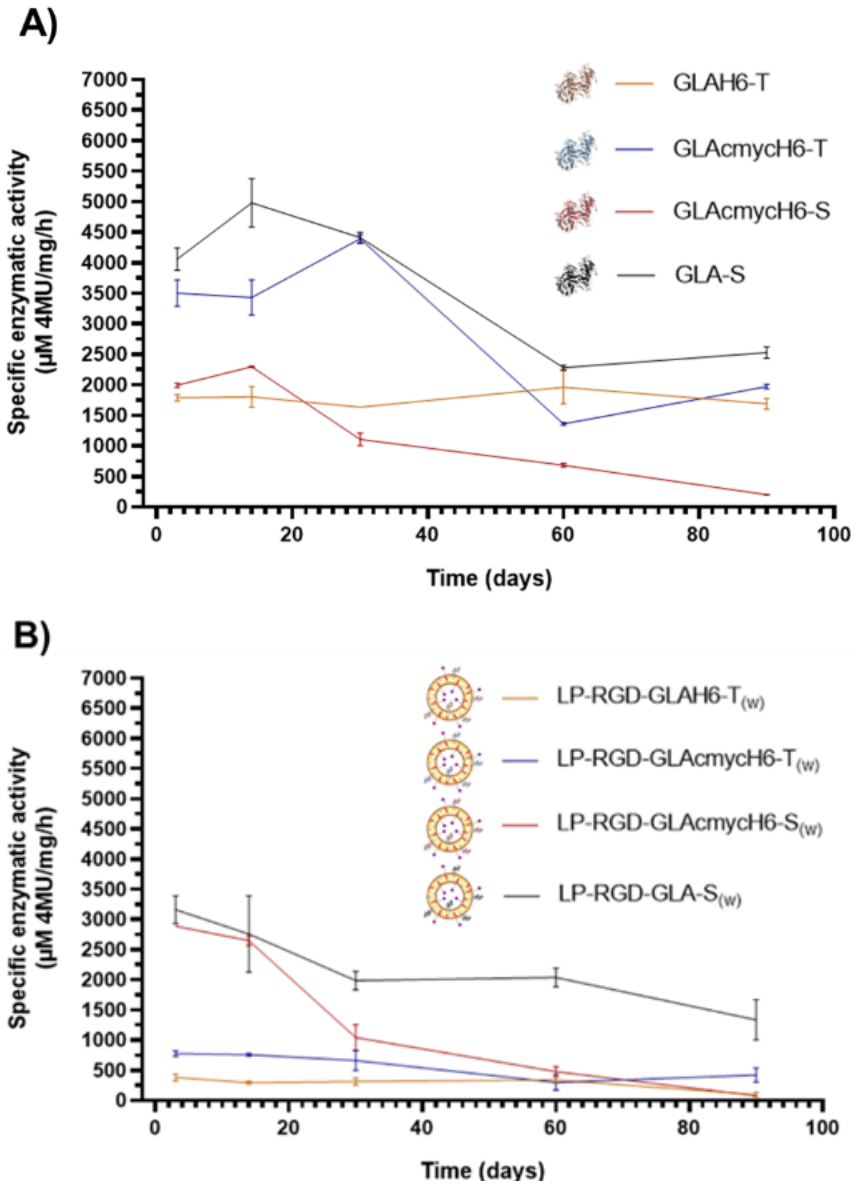


Figure 4.13. EA stability of samples stored in aqueous phase at 2 – 8 ºC in time. A) Comparison of the EA maintenance between the different naked GLA enzyme versions. The same independent production batch used during the manufacturing of LP-RGD-GLA prototypes was analyzed by triplicate. B) Comparison of the EA maintenance between the different LP-RGD-GLAH6-$T_{(w)}$, LP-RGD-GLAcmycH6-$T_{(w)}$, LP-RGD-GLAcmycH6-$S_{(w)}$, and LP-RGD-GLA-$S_{(w)}$ nanoliposomal formulations. Here, results are shown as the average of two independent batches produced for each nanovesicular system. In all cases, the error is represented as the s.d. between measurements.

In conclusion, the GLA nature impacts on the EA of GLA-loaded nanoliposomal formulations composed by DPPC, chol, chol-PEG_{400}-RGD and MKC prepared in pure water, as well as in the stability of this parameter in time.

4.2.5. Impact of GLA characteristics on the colloidal stability of nanoliposomes

Knowledge and monitoring of colloidal stability of nanoliposomal formulations is of great importance for their acceptance as medicinal products. Furthermore, the physicochemical properties of a biomolecule such as GLA enzyme can impact on this colloidal stability. Herein, the particle size distribution and ζ-potential of GLA-loaded nanoliposomal formulations gathered in ***Table 4.2*** was monitored along time by DLS/ELS measurements, as detailed in ***Chapter 7, Section 7.4.5.3***, to characterize their colloidal stability. Same measurements for the naked GLA versions were also studied as controls of the protein stability. Again, all naked GLA versions studied were stored in 0.01 M acetic acid buffer at pH 5.5; except for GLA-S, which is stored in the Fabrazyme-like buffer.

All the nanoliposomal formulations compared in this study, LP-RGD-GLAH6-$T_{(w)}$, LP-RGD-GLAcmycH6-$T_{(w)}$, LP-RGD-GLAcmycH6-$S_{(w)}$ and LP-RGD-GLA-$S_{(w)}$, were equally produced with the same theoretical lipid concentration (5 mg/mL) and media (pure water), but differing on the GLA version encapsulated. As shown in ***Figure 4.14***, the colloidal stability of these nanoformulations was monitored under storage conditions (dispersion form, 2 – 8 ºC) during 3 months.

Results presented in ***Figure 4.14 A*** and ***Figure 4.14 B***, demonstrated maintained colloidal stability (mean size, PdI and ζ-potential) of all the GLA-loaded nanoformulations tested until 3 months. ζ-potential values > 30 mV are indicative of low probability of nanoparticle aggregation. In this manner, it was suggested that any GLA feature was able to modify the colloidal stability of nanoliposomes in the conditions studied.

In contrast, results compiled in ***Figure 4.14 C***, indicated increased polydispersity of naked GLA enzymes in time under their storage conditions, and therefore, increasing protein aggregation is suggested. Although GLAcmycH6-S enzyme (produced in CHO cells and containing both, c-myc and 6-His tags) did not influence the colloidal stability of nanoliposomes once entrapped, the naked enzyme evidenced the higher protein destabilization when stored at 4 ºC (as previously commented in ***Chapter 3***).

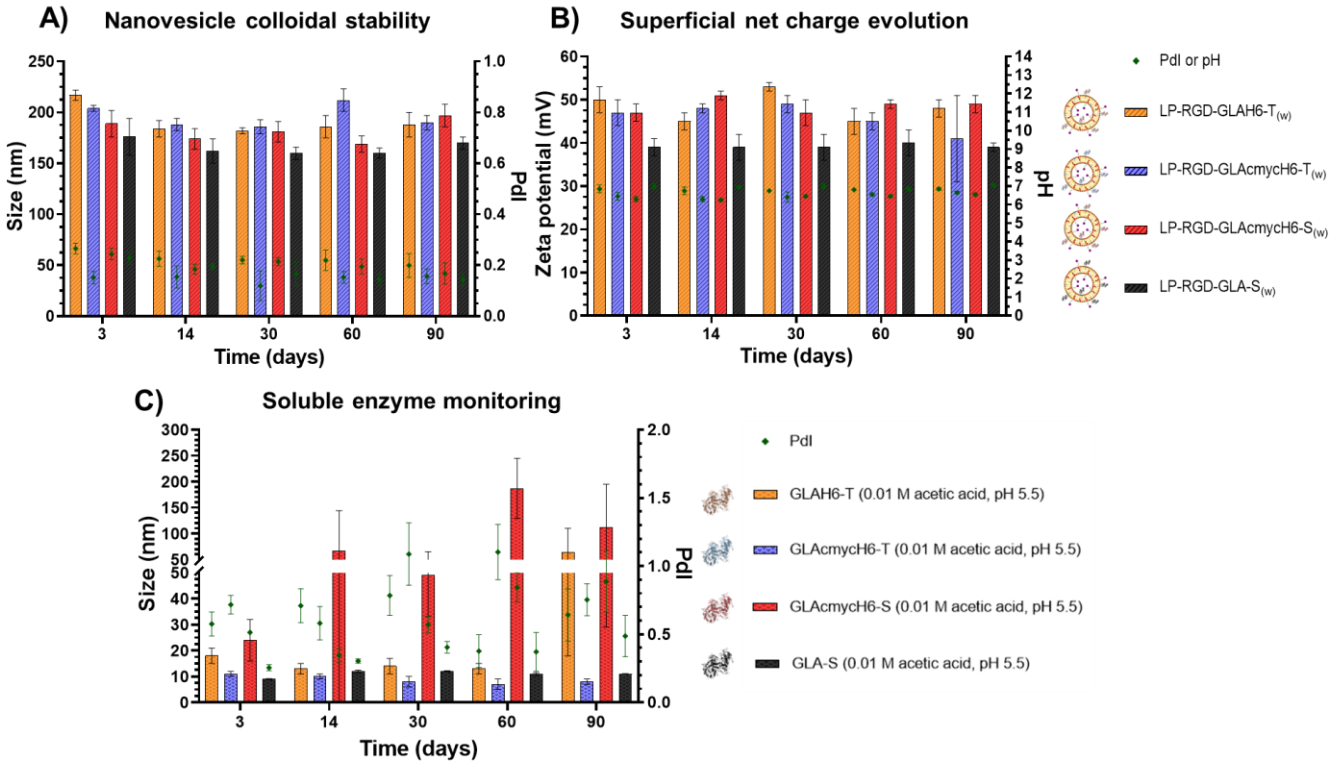


Figure 4.14. Physicochemical stability of GLA-loaded nanoliposomal formulations and naked GLA versions in their corresponding storage buffers at 2 – 8 ºC over time. Particle size distribution analysis and ζ-potential of LP-RGD-GLAH6-$T_{(w)}$, LP-RGD-GLAcmycH6-$T_{(w)}$, LP-RGD-GLAcmycH6-$S_{(w)}$, and LP-RGD-GLA-$S_{(w)}$ nanoliposomal formulations were measured by A) DLS analysis or B) ELS analysis; and results shown as the average of two independent batches produced for each nanovesicular system. B) Particle size distribution measurements by DLS of naked GLA enzyme versions as quality control analyses, and their corresponding results from the batch used during the manufacturing of LP-RGD-GLA prototypes. In all cases, the error is represented as the s.d. between measurements.

As summary, these results suggest that the different features between GLA versions do not have an impact on the colloidal stability of GLA-loaded nanoliposomal formulations composed by DPPC, chol, chol-PEG_{400}-RGD and MKC, and prepared in pure water. Furthermore, these results point out that the entrapment of GLA molecules in nanoliposomes increase protein stability in comparison to naked GLA formulations.

4.2.6. Impact of GLA characteristics on the *in vitro* enzyme release from nanoliposomes

The release rate of the active substance from nanovesicles is a relevant CQA that allows to differentiate the nanoliposomal formulation from the non-liposomal commercial products, and ensure batch-to-batch reproducibility. In ***Chapter 5, Section 5.4***, is well described the development of a methodology based on filtration-centrifugation procedures to characterize the *in vitro* GLA release from nanoliposomes. In this section, the impact of GLA characteristics on the *in vitro* enzyme release rate from nanoliposomes was investigated by using this methodology based on filtration-centrifugation (procedure detailed in ***Chapter 7, Section 7.4.6***). For

this purpose, some GLA-loaded nanoliposomal formulations gathered above in ***Table 4.2*** were studied, specifically LP-RGD-GLAH6-$T_{(w)}$, LP-RGD-GLAcmycH6-$T_{(w)}$, LP-RGD-GLAcmycH6-$S_{(w)}$ and LP-RGD-GLA-$S_{(w)}$. All these nanoformulations were equally produced with the same theoretical lipid concentration (5 mg/mL) and media (pure water), but differing on the GLA version encapsulated.

According to the Guidance for Industry from the FDA entitled "Liposome Drug Products Chemistry, Manufacturing, and Controls; Human Pharmacokinetics and Bioavailability; and Labeling Documentation", it is recommended to characterize *in vitro* release rates by using an appropriate physiological medium with suitable agitation[23]. Herein, glucose 5 % (w/v) and Ringer-Lactate solution were tested as injection solutions differing in their content of salt. Glucose 5% (w/v) does not contain any salt, meanwhile Ringer-Lactate solution has similar salt containing to human plasma. To study the *in vitro* GLA release, all nanoformulations were 4-fold diluted in both injection solutions, incubated at 37 ºC and agitated at 100 rpm, and then withdrawn at the pre-established time-points to be quantified by SDS-PAGE and TGX analysis (as explained in ***Chapter 7, Section 7.4.6***).

Different *in vitro* GLA release profiles were obtained depending on the receptor media tested, clearly influenced by salt concentration (see ***Figure 4.15***). Regardless the GLA characteristics, when GLA-loaded nanoliposomes were incubated in Ringer-Lactate solution (containing high salt concentration), more than the 50 % of the total enzyme amount in samples was suddenly released from liposomes in general, reaching a plateau without further significant increase over at least 72 h (see ***Figure 4.15 A***).

On the other hand, when GLA-loaded nanoliposomes were incubated in glucose 5 % (w/v) media (with none content of salt), the release of all GLA enzyme versions from nanoliposomes was continuously increased up to the 72 h that lasts the assay (see ***Figure 4.15 B***). Curiously, in this case, the *in vitro* release profile of GLAH6-T (enzyme produced in HEK cells) from LP-RGD-GLAH6-$T_{(w)}$ formulations was found to be quicker and higher than others.

According to these results, the quicker and higher GLA release observed during the *in vitro* release assay when GLA-loaded nanoformulations were incubated in rich salt contained media, might occur due to a salt-induced impairing of the electrostatic interaction between GLA molecules and the positively charged membranes, causing the burst release of the absorbed enzymes on the liposomal surfaces. This hypothesis suggests that the principal force of protein-membrane interactions is established by electrostatic forces. Nevertheless, results obtained by incubating the LP-RGD-GLAH6-$T_{(w)}$ in glucose 5 % (w/v) suggest that other weak attractive forces based on hydrophobic interactions, such as Van der Waals interactions, might be present in the interaction of GLAH6-T protein and RDG-targeted liposomes, which might be disturbed by osmotic changes in the environment (caused by the presence of glucose molecules).

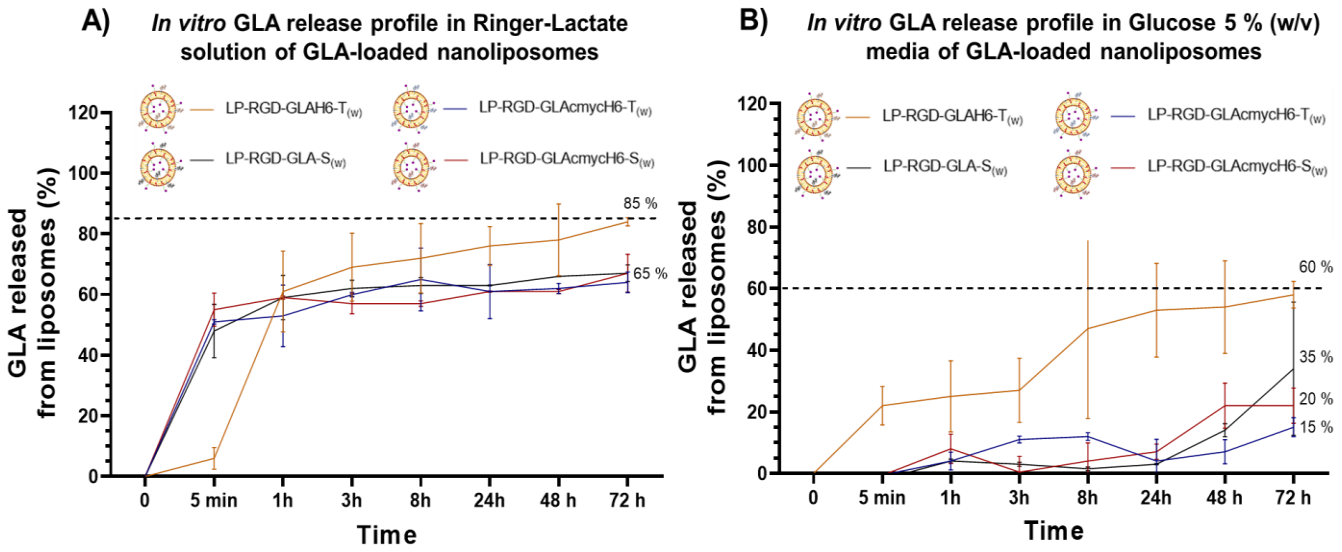


Figure 4.15. *In vitro* GLA release rate GLA from GLA-loaded nanoliposomal formulations differing on the encapsulated GLA enzyme version. All nanoformulations (LP-RGD-GLAH6-$T_{(w)}$, LP-RGD-GLAcmycH6-$T_{(w)}$, LP-RGD-GLAcmycH6-$S_{(w)}$ and LP-RGD-GLA-$S_{(w)}$) were diluted up to 1.2 mg/mL of lipid in selected receptor media, incubated at 37 ºC and 100 rpm, and further filtrated-centrifuged at the predefined time intervals. Then, GLA quantification was determined by SDS-PAGE and TGX densitometry analysis. Both receptor media selected were: A) Ringer-Lactate solution, or B) glucose 5 % (w/v) media. Two independent batch productions of each nanoformulation were tested by triplicate.

As conclusion, GLA enzymes are immediately released from nanoliposomes when GLA-loaded formulations composed by DPPC, chol, chol-PEG_{400}-RGD and MKC are incubated in Ringer-Lactate solution (rich-salt media). In this case, it is not possible to withdraw any correlation between GLA characteristics and the enzyme release behavior.

In contrast, when GLA-loaded formulations composed by DPPC, chol, chol-PEG_{400}-RGD and MKC are incubated in glucose 5 % (w/v) media (without salt presence), GLA enzymes are less released and in a slower profile. Interestingly, the GLAH6-T enzyme (produced in HEK cells and encoding the 6-His purification tag) demonstrated to be easier diffused from nanoliposomes than the other GLA enzymes in this conditions. Therefore, the combination of the GLA nature and aminoacid sequence has an impact on the *in vitro* GLA release profile in media without any content of salts.

4.3. Impact of GLA characteristics on the distribution of the integrated enzyme in the liposome

The main objective of this section is to investigate the impact of GLA nature on its distribution on the liposome. It is hypothesized that GLA-loaded nanoliposomal formulations, produced by DELOS-susp, could contain some amount of GLA molecules encapsulated into the inner space of the vesicles, and the rest in the outside membrane surface. In order to study the impact of GLA nature on the organization of the enzyme in the nanoliposomes, different GLA-containing nanoliposomal formulations, produced by two different production protocols, were compared. In particular, there were compared GLA-free and GLA-loaded RGD-targeted nanoliposomal formulations produced by DELOS-susp (LP-RGD and LP-RGD-GLA described in ***Table 4.2*** above), which might have GLA enzyme inside and outside the nanoliposome; with GLA-adsorbed RGD-targeted nanoliposomal formulations (LP-RGD-GLA_Ads described in ***Table 4.3*** below), prepared by the methodology schematized in ***Figure 4.16***, which should only have GLA enzyme attached to the nanoliposome outside.

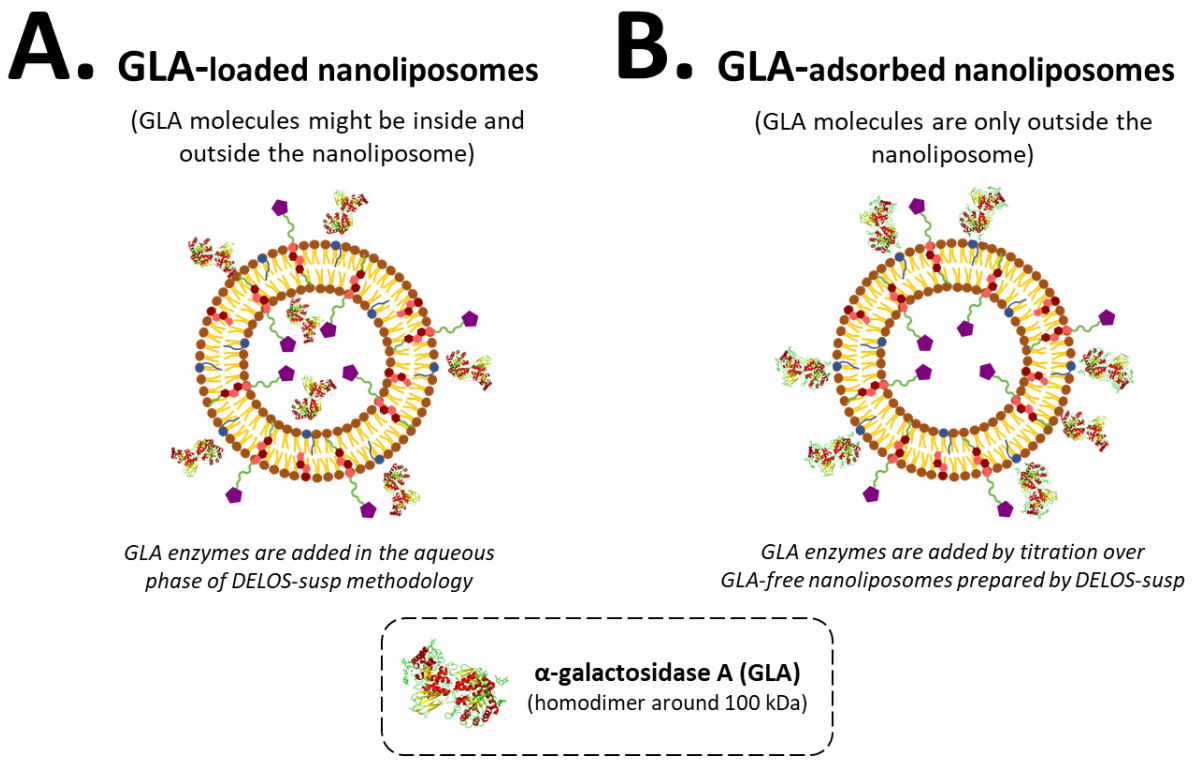


Figure 4.16. Representation of the theoretical distribution of GLA enzymes on RGD-targeted nanoliposomes regarding the method used for the addition of GLA molecules in nanoliposomal formulations. A) GLA-loaded nanoliposomes prepared by DELOS-susp. B) GLA-adsorbed nanoliposomes prepared by titration procedures.

4.3.1. Production and characterization of GLA-adsorbed nanoliposomal formulations used for the study

Different LP-RGD-GLA_Ads were produced using the four different versions of GLA described in ***Table 4.1***. As previous described for LP-RGD-GLA nanoformulations, liposomal membrane of these new GLA-adsorbed nanoliposomes was also composed by DPPC, cholesterol and chol-PEG_{400}-RGD (10:6.5:0.5 theoretical molar ratio), and contained a small amount of MKC (5 % molar of the total membrane components) as depicted above in ***Figure 4.4***.

GLA-loaded and GLA-adsorbed nanoliposomal formulations used to perform the present study are described in ***Table 4.2*** and in ***Table 4.3***, respectively. GLA-adsorbed nanoformulations were prepared following the procedure described in ***Chapter 7, Section 7.4.2***. Briefly, GLA-free nanoliposomes composed of DPPC, cholesterol, chol-PEG_{400}-RGD and MKC were prepared by DELOS-susp procedures (see ***Figure 4.17 A***). Then, a volume of aqueous solution (V_{AS}) containing known amounts of GLA enzyme was dropwise titrated over the GLA-free nanoliposomes under gentle manual agitation, and then incubated at 25 ºC during 30 min to allow the adsorption of the enzyme on the liposomal membrane, and to obtain the GLA-adsorbed nanoliposomes (see ***Figure 4.17 B***).

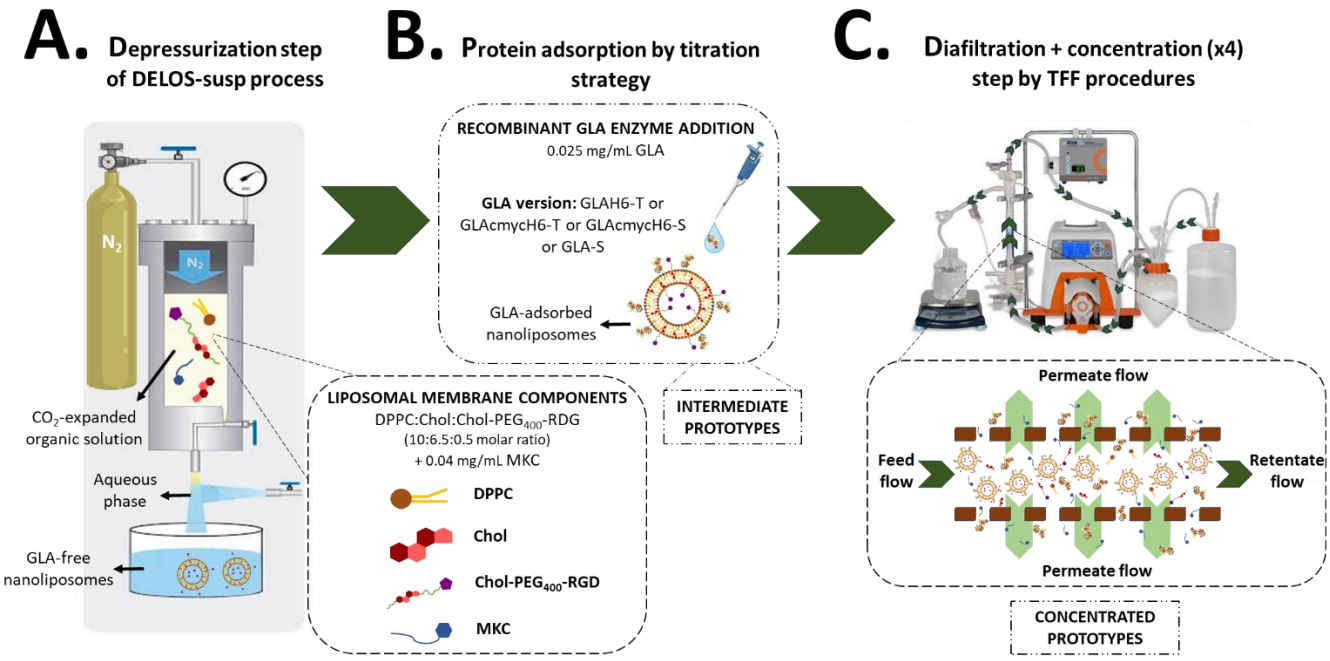


Figure 4.17. Manufacturing process of intermediate and concentrated GLA-adsorbed nanoliposomal formulations. A) DELOS-susp methodology for production of GLA-free nanoliposomal formulations. B) Addition of known amounts of GLA enzyme over GLA-free nanoliposomes to prepare GLA-adsorbed nanoliposomal formulations. C) TFF diafiltration procedure for the purification and concentration of nanoliposomal formulations with adsorbed GLA. Details on this production protocol can be found in ***Chapter 7, Section 7.4.2***.

Non-integrated GLA molecules were separated from the GLA-adsorbed liposomes by diafiltration through TFF procedure (see ***Figure 4.17 C***), and in some cases subsequently 4-fold concentrated until a theoretical lipid concentration of 5 mg/mL using also TFF process (apparatus and protocols described in ***Chapter 7, Section 7.4.3***).

Details on the production of the GLA-adsorbed nanoliposomal formulations used for the present study are described in ***Table 4.3*** and can be found in ***Chapter 7, Table 7.5***.

Table 4.3. Description of GLA-adsorbed nanoliposomal formulations used for the study described in ***Section 4.3***.

Nanoliposomal formulation ID	Loaded GLA version	[A] $[lipid]_{theoric}$ (mg/mL)	[B] $[GLA]_{TGX}$ (µg/mL)	GLA:lipid mass ratio (m/m)	Size (nm)	PdI	ζ-potential (mV)	Formulation pH	Nanovesicle storage solvent
LP-RGD-GLAH6-T_int_Ads	**GLAH6-T**	1.2	26 ± 1.3	1:46	176 ± 12	0.192 ± 0.01	64 ± 4	4.3 ± 0.1	5 % EtOH + 1.2 % DMSO (v/v) in water
LP-RGD-GLAH6-$T_{(w)}$_Ads	**GLAH6-T**	5	72 ± 19	1:69	205 ± 14	0.224 ± 0.02	49 ± 1	6.8 ± 0.1	Pure water
LP-RGD-GLAcmycH6-T_int_Ads	**GLAcmycH6-T**	1.2	26 ± 1.7	1:46	164 ± 6	0.161 ± 0.02	57 ± 7	4.3 ± 0.1	5 % EtOH + 1.2 % DMSO (v/v) in water
LP-RGD-GLAcmycH6-$T_{(w)}$_Ads	**GLAcmycH6-T**	5	51 ± 5	1:98	184 ± 8	0.138 ± 0.02	47 ± 6	6.6 ± 0.1	Pure water
LP-RGD-GLAcmycH6-S_int_Ads	**GLAcmycH6-S**	1.2	26 ± 0.6	1:46	163 ± 7	0.225 ± 0.02	46 ± 2	4.3 ± 0.1	5 % EtOH + 1.2 % DMSO (v/v) in water
LP-RGD-GLAcmycH6-$S_{(w)}$_Ads	**GLAcmycH6-S**	5	89 ± 16	1:56	178 ± 7	0.258 ± 0.02	40 ± 1	6.3 ± 0.1	Pure water
LP-RGD-GLA-S_int_Ads	**GLA-S**	1.2	26 ± 0.7	1:46	181 ± 15	0.299 ± 0.06	39 ± 2	4.5 ± 0.1	5 % EtOH + 1.2 % DMSO (v/v) in water
LP-RGD-GLA-$S_{(w)}$_Ads	**GLA-S**	5	114 ± 4	1:44	184 ± 16	0.308 ± 0.03	35 ± 2	6.7 ± 0.1	Pure water

[A] Lipid concentration of all nanoliposomal formulations refers to the theoretical total amount of membrane components added to the DELOS-susp high pressure vessel (HPV). [B] GLA concentration of already prepared liposomal nanoformulations was assessed by SDS-PAGE and TGX densitometry. Results are shown as the average of 2 independent batches produced for each nanoliposomal system. The error is represented as the s.d. between measurements. All nanoliposomal formulations have the same membrane composition: DPPC:chol:chol-PEG_{400}-RGD (10:6.5:0.5 theoretical molar ratio) and presence of MKC (5 % molar of the total membrane components).

Physicochemical properties of all GLA-adsorbed nanoformulations used in the present study are gathered in ***Table 4.3*** and ***Figure 4.18***, and were measured next day after their production. Particle size distribution was measured by DLS/ELS (see procedures in ***Chapter 7, Section 7.4.5.3***), GLA concentration was determined by SDS-PAGE and further TGX densitometry analysis (see procedures in ***Chapter 7, Section 7.2.6.1***). Nanoliposomes morphology was observed by cryoTEM microscopy at the Servei de Microscopia of the UAB (see procedures in ***Chapter 7, Section 7.4.5.2***). GLA-adsorbed nanoliposomal formulations were compared to GLA-loaded formulations prepared by DELOS-susp and described in ***Table 4.2*** and ***Figure 4.6*** (cryoTEM images). In general, similar results of size (around 170 nm) and shape of liposomes were obtained by comparing GLA-loaded and GLA-adsorbed systems with equivalent composition (in terms of membrane composition and GLA version integrated). This indicates, that for all GLA versions, there is no significant impact of the production methodology

on GLA formulations, GLA-adsorbed or GLA-loaded nanoliposomal formulations. Equally to GLA-loaded nanoformulations, GLA-adsorbed liposomes are also highly monodisperse unilamellar liposome populations (PdI < 0.3), confirming that GLA enzyme not destabilize the positively charged lipid systems at the concentration tested. Interestingly, the GLA nature seemed to impact slightly differently on the ζ-potential values of liposomes depending on the method of GLA addition employed to prepare nanoliposomal formulations. GLA-adsorbed nanoformulations prepared with GLAcmycH6-S and GLA-S enzymes (produced in CHO cells) evidenced lower ζ-potential values (35 – 45 mV) than the GLA-loaded nanoformulations containing the same GLA versions (40 – 55 mV). These results suggested larger amounts of adsorbed GLA molecules in the outer lipid membrane surface of liposomes due to protein addition by titration approach. Slightly more polydisperse populations were obtained in these cases (reaching PdI near 0.3), probably as consequence of little vesicle destabilization caused by protein excess with respect to the surface available for its interaction. In these cases, multilamellar vesicles with various non-closed lamellae layers attached to their surfaces (pointed out in yellow arrows in ***Figure 4.18***) were observed by cryoTEM in both LP-RGD-GLA-$S_{(w)}$_Ads and LP-RGD-GLAcmycH6-$S_{(w)}$_Ads. On the other hand, no differences in the ζ-potential values or morphology of the distinct GLA-loaded and GLA-adsorbed nanoformulations were observed when working with GLAH6-T and GLAcmycH6-T enzymes (produced in HEK cells).

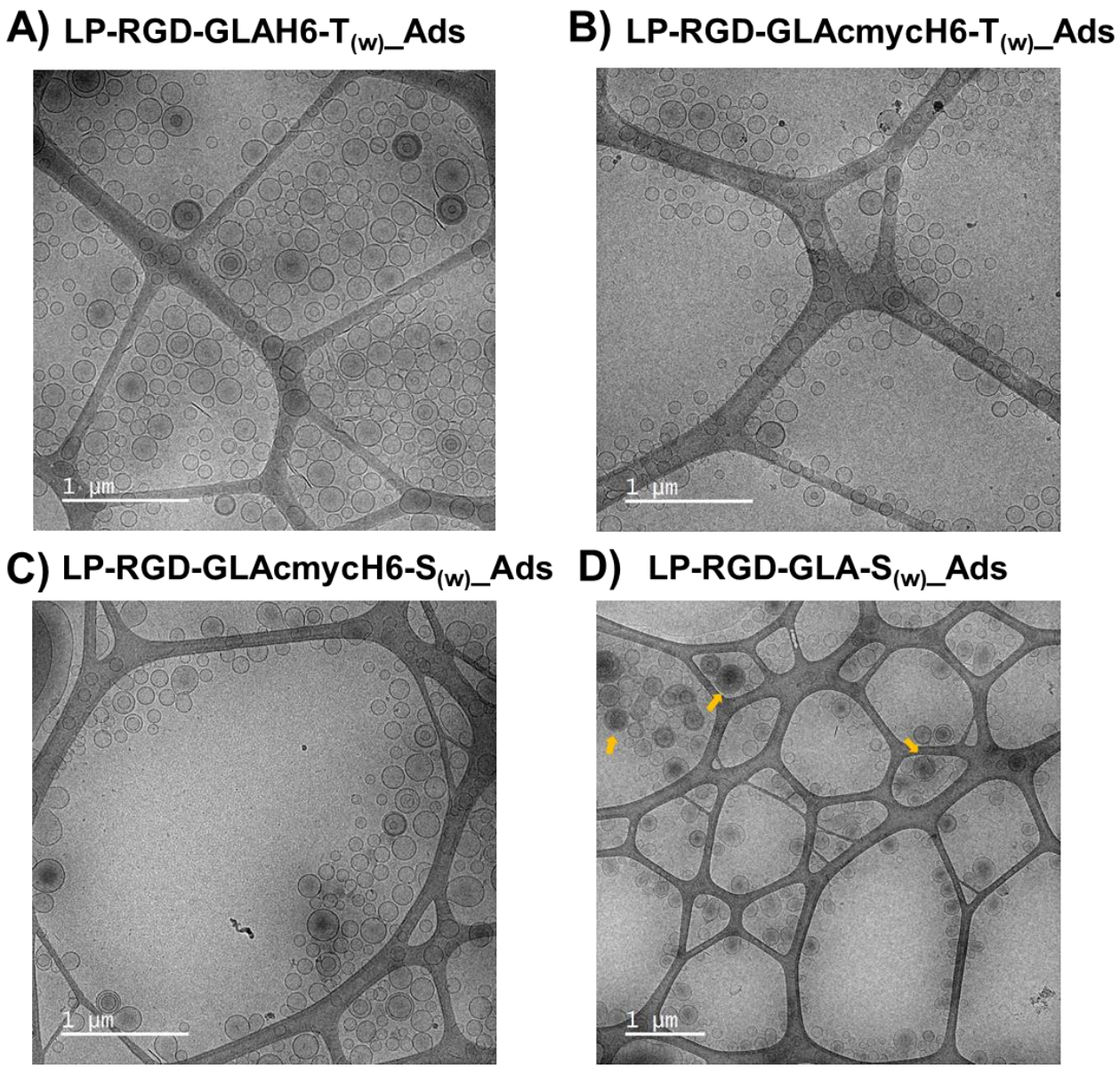


Figure 4.18. CryoTEM images of GLA-loaded liposomes two months after their production: A) LP-RGD-GLAH6-$T_{(w)}$, containing the GLAH6-T, B) LP-RGD-GLAcmycH6-$T_{(w)}$, containing the GLAcmycH6-T, C) LP-RGD-GLAcmycH6-$S_{(w)}$, containing the GLAcmycH6-S, or D) LP-RGD-GLA-$S_{(w)}$, containing the GLA-S as integrated GLA enzyme version. The GLA versions were added to nanoformulations by titration procedures. Yellow arrow pointed to highly multilamellar nanostructures.

The impact of GLA characteristics on the enzyme EE%, leakage rate, enzymatic activity, colloidal stability and *in vitro* GLA release of GLA-adsorbed nanoliposomal formulations were measured using the same procedures previously described for the characterization of GLA-loaded nanoformulations and explained in ***Sections 4.2.2, 4.2.3, 4.2.4***, ***4.2.5*** and ***4.2.6***. Very similar or even same physicochemical and biological results were obtained for GLA-adsorbed nanoformulations, prepared by the methodology schematized in ***Figure 4.1***, in comparison to the GLA-loaded nanoformulation containing the same GLA version and prepared by DELOS-susp (see ***Table 4.4***). This

high similarity between both type of GLA formulations, differently prepared, points out that most of GLA molecules of GLA-loaded nanoliposomal formulations, prepared by DELOS-sups, are adsorbed in the outer membrane of the nanoliposomes and that there are only few GLA molecules entrapped inside the nanoliposome. To reinforce this hypothesis further studies, described below, were performed.

Table 4.4. Comparison of the physicochemical and biological features of GLA-loaded and GLA-adsorbed nanoliposomal formulations prepared in pure water, but differing in the GLA addition method.

Nanoliposomal formulation ID	Loaded GLA version	EE (%)	Specific EA (μM 4MU/mg/h)	Leaked GLA (%) [§]	Released GLA (%) in glucose [ᵀ]	Released GLA (%) in RL [*]	Size variability along time (%) [Ж]
LP-RGD-GLAH6-T$_{(w)}$	**GLAH6-T**	67 ± 1	379 ± 58	55 ± 2	54 ± 15	78 ± 12	2 ± 9
LP-RGD-GLAH6-T$_{(w)}$_Ads	**GLAH6-T**	69 ± 15	450 ± 12	48 ± 6	50 ± 7	77 ± 4	-3 ± 10
LP-RGD-GLAcmycH6-T$_{(w)}$	**GLAcmycH6-T**	33 ± 4	776 ± 44	60 ± 4	7 ± 4	62 ± 2	1 ± 1
LP-RGD-GLAcmycH6-T$_{(w)}$_Ads	**GLAcmycH6-T**	49 ± 8	384 ± 64	59 ± 4	10 ± 16	51 ± 6	1 ± 2
LP-RGD-GLAcmycH6-S$_{(w)}$	**GLAcmycH6-S**	101 ± 6	2889 ± 257	56 ± 5	22 ± 7	61 ± 1	14 ± 10
LP-RGD-GLAcmycH6-S$_{(w)}$_Ads	**GLAcmycH6-S**	86 ± 14	3591 ± 1696	53 ± 6	22 ± 5	72 ± 5	15 ± 3
LP-RGD-GLA-S$_{(w)}$	**GLA-S**	100 ± 3	3160 ± 228	51 ± 1	14 ± 2	66 ± 1	5 ± 8
LP-RGD-GLA-S$_{(w)}$_Ads	**GLA-S**	110 ± 4	3994 ± 2346	62 ± 1	26 ± 6	61 ± 1	3 ± 3

* The EE (%) of all nanoformulations was assessed by SDS-PAGE and TGX densitometry, and [ı] the EA using the *in vitro* fluorimetric assay presented above. [§] The values of leaked GLA (%) of nanoformulations stored at 4 – 8 ºC correspond to the time-point of 90 days. The values of released GLA (%) of nanoformulations incubated at 37 ºC and 100 rpm, in [ᵀ] glucose 5 % (w/v) media or [*] Ringer-Lactate solution (RL), correspond to the time-point of 48 h. [Ж] Mean particle size was measured by DLS analysis. Size variability along time (%) was used as a parameter to monitor the colloidal stability of nanoformulations, and it was calculated according to the following equation: ((Size at time 90 days – Size at time 14 days)/(Size at time 14 days))*100.

4.3.2. Characterization of GLA distribution on nanoliposomes using proteases

The proteolytic environment can affect the bioavailability and stability of protein-based drugs used during treatments. This issue can be overcome by coupling proteins to nanocarriers such as liposomes, whose protective capacity is related to the protein distribution on their lipid bilayers, i.e. proteins adsorbed on liposome surfaces should be quicker degraded than others encapsulated in the inner aqueous cavity of liposomes. In this section, an *in vitro* protocol selecting trypsin as a protease model is carried out to test the protective capacity of nanoliposomes against the degradation of GLA enzymes, and to have additional insights on the GLA distribution on nanoliposomes.

4.3.2.1. Suitability of the *in vitro* trypsinization assay for nanoliposomal formulations

The suitability of this *in vitro* assay for the characterization of the nanoliposomal protective capacity against GLA degradation was evaluated during this thesis project. For this purpose, the naked GLA-S version and the GLA-free nanoformulation prepared at 9 mg/mL lipid in pure water (LP-RGD$_{(w)}$) were tested (samples characteristics described in ***Table 4.1*** and ***Table 4.2***).

As first step, different molar ratios of trypsin:GLA were tested over the naked GLA-S version (diluted at 2.25 µM in pure water) in order to observe GLA degradation kinetic without disturbing the stability of nanovesicular formulations (data not shown). The molar ratio typsin:GLA 1:20 was defined as the optimal one and used in all the *in vitro* trypsinization assays of this thesis (see protocol details in ***Chapter 7, Section 7.2.12***). Briefly, samples were incubated with presence of trypsin at 37 ºC and 100 rpm, and then withdrawn at the pre-established time-points to be quantified by SDS-PAGE and TGX analysis.

Next, LP-RGD$_{(w)}$ nanoformulation was incubated with same amounts of trypsin and assay conditions (37 ºC and 100 rpm), and then, the colloidal stability of liposomes monitored by DLS and ELS analysis. Results presented in ***Figure 4.19*** demonstrated a good maintenance of the size distribution and ζ-potential of nanoliposomes submitted to the *in vitro* assay, and therefore, discarded destabilization issues of liposomes due to the addition of the trypsin amounts tested (0.11 µM of trypsin per each theoretical lipid concentration of 9 mg/mL; simulating the trypsin:GLA 1:20 molar ratio when testing GLA-loaded nanoliposomes containing the GLA-S enzyme).

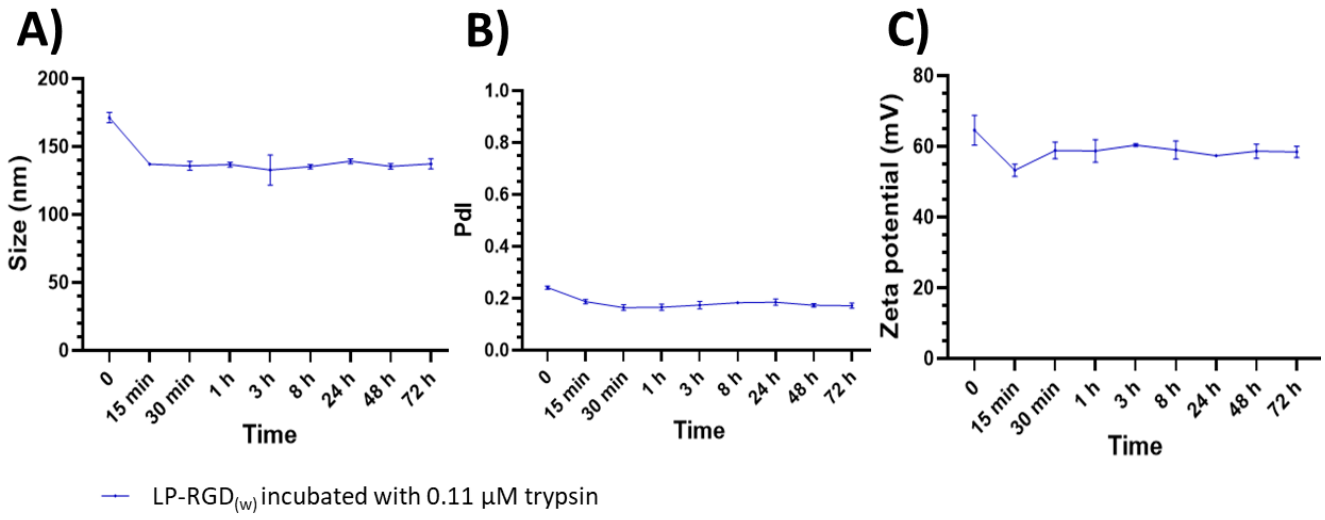


Figure 4.19. Colloidal stability by DLS/ELS analysis in time of the LP-RGD$_{(w)}$ formulation (prepared at theoretical lipid concentration of 9 mg/mL) after being incubated with trypsin molecules (0.11 µM) at 37 ºC and 100 rpm. T = 0 refers to the initial conditions of LP-RGD$_{(w)}$ sample before the addition of trypsin protease. One batch of LP-RGD$_{(w)}$ was tested.

4.3.2.2. Comparison of the protective capacity of GLA-loaded and GLA-adsorbed nanoliposomes

Once demonstrated the feasibility of using the *in vitro* trypsinization assay without impairing the stability of liposomes, some GLA-loaded nanoliposomes (LP-RGD-GLAH6-$T_{(w)}$, LP-RGD-GLAcmycH6-$T_{(w)}$, LP-RGD-GLAcmycH6-$S_{(w)}$ and LP-RGD-GLA-$S_{(w)}$) and some GLA-adsorbed nanoformulations (LP-RGD-GLAH6-$T_{(w)}$_Ads, LP-RGD-GLAcmycH6-$T_{(w)}$_Ads, LP-RGD-GLAcmycH6-$S_{(w)}$_Ads and LP-RGD-GLA-$S_{(w)}$_Ads) which differ on the GLA addition method, and are respectively gathered in ***Table 4.2*** and ***Table 4.3*** were assayed and compared (protocol details can be found in ***Chapter 7, Section 7.2.12***). All these nanoformulations were prepared with the same theoretical lipid concentration (5 mg/mL) and media (pure water), but differing on the GLA version encapsulated. All samples were evaluated at three days after production. Moreover, the four naked GLA versions (GLAH6-T, GLAcmycH6-T, GLAcmycH6-S and GLA-S) were also assayed in parallel to the *in vitro* assay as controls. Each naked GLA enzyme was diluted in pure water at the same protein concentration found in their comparative nanoformulations.

The results compiled in ***Figure 4.20*** evidenced protective capacity of liposomes against GLA degradation. In general, it was found lower GLA degradation when GLA enzymes are coupled to nanoliposomes than when assayed in their naked form (e.g. after 30 min of trypsin incubation, around 60 – 80 % of naked GLA enzymes were degraded, meanwhile around 20 – 40 % of GLA degradation is observed in nanoliposomal systems). By comparing the results obtained from GLA-loaded and GLA adsorbed nanoformulations containing the same GLA versions, non-significant differences of the GLA degradation kinetics were observed (see ***Figure 4.20 B and C***). These findings suggest that regarding the GLA addition method to nanoliposomal formulations, most of the GLA molecules might be adsorbed on the outer liposomal membranes. However, when comparing formulations containing distinct GLA nature, different behavior is found at the last time-point studied of 72 h. The totality of GLA amount was degraded at 72 h in all nanoformulations prepared with GLAH6-T and GLAcmycH6-T enzymes (produced in HEK cells), indicating that their totally amount might probably be exposed to the outside membrane of liposomes. On the other hand, around 20 % of GLA amount remained protected at 72 h in all nanoformulations prepared with GLAcmycH6-S and GLA-S enzymes (produced in CHO cells); except for the LP-RGD-GLAcmycH6-$S_{(w)}$_Ads (formulation with adsorbed GLAcmycH6-S enzyme) were this amount is lower (around 10 %).

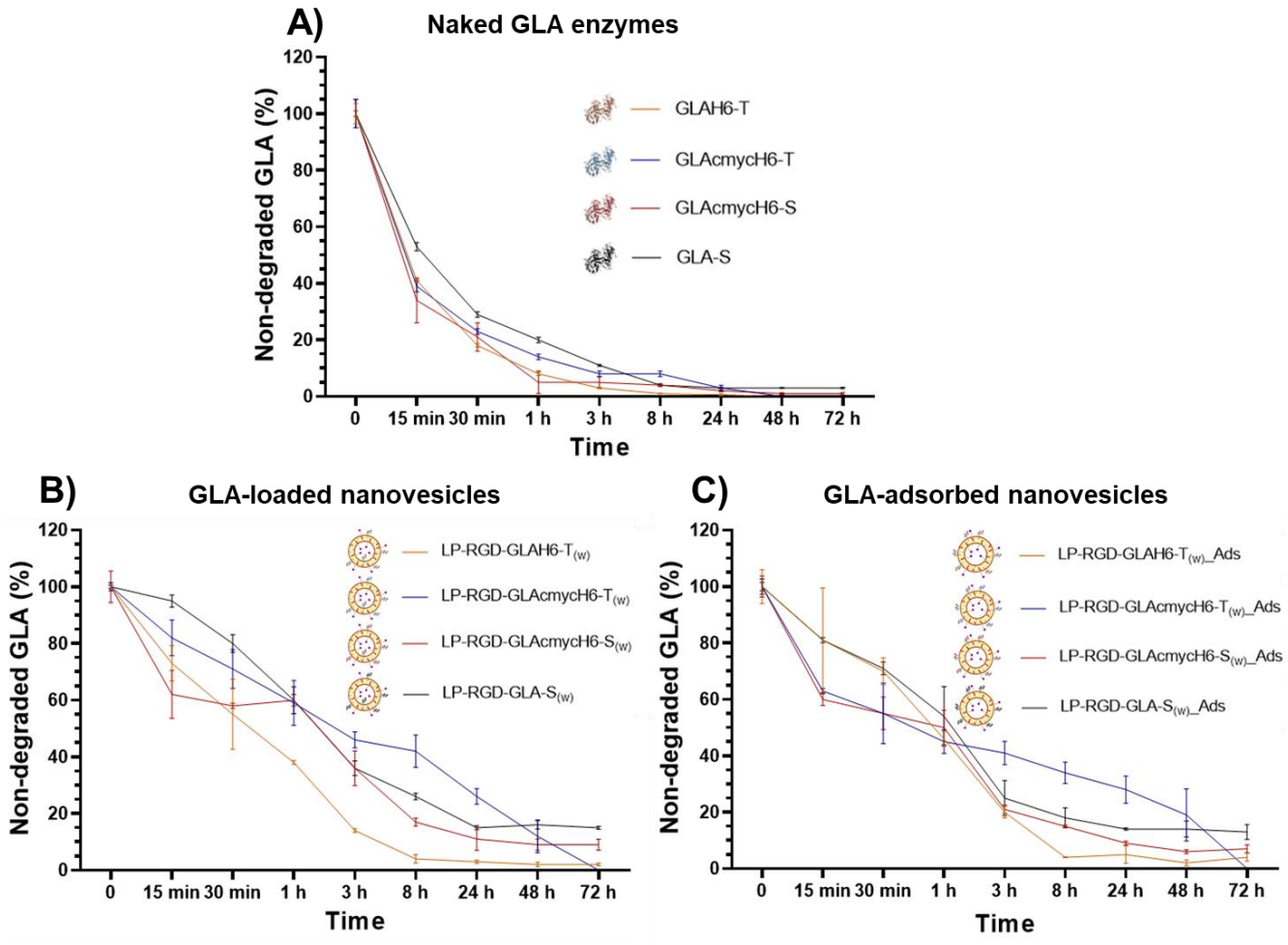


Figure 4.20. Incubation of A) soluble GLA enzymes, B) GLA-loaded liposomal nanoformulations, or C) GLA-adsorbed nanovesicular formulations in the presence of trypsin protease (condition of trypsin:GLA molar ratio 1:20) at 37 ºC and 100 rpm. Two independent production batches of each nanoliposomal systems, but only one of naked GLA enzyme versions were analyzed by triplicate in each predefined time intervals. GLA amounts were quantified by SDS-PAGE and TGX analysis.

In conclusion, the results reported in this subsection evidenced that all the liposome-based nanoformulations tested has significant protective capacity against GLA degradation.

Curiously, similar protective profiles are observed for both, GLA-loaded and GLA-adsorbed nanoformulations. This results are the first confirmatory indication that regardless of the production method, in both types of nanoformulations, GLA enzyme it is in the same way mostly exposed on the surface of the nanoliposomes.

4.3.3. Characterization of GLA distribution on nanoliposomes by fluorescence spectroscopy

4.3.3.1. Distribution of tryptophan residues on the structure of human GLA enzyme

As shortly explained in ***Chapter 3, Section 3.4.4***, conformational changes on the tertiary structure of proteins can be followed by intrinsic fluorescence emission studies. As shown in ***Figure 3.9***, tryptophan (Trp) aminoacid can be specifically excited at wavelength of 295 nm. Since the emission spectra of Trp is sensitive to the surrounding environment, changes on the maximal wavelength of the fluorescence spectra and/or their intensity values are often used to determine Trp localization on protein structures[24]. Following situations can occur related to modified conditions of the surrounding environment of a specific Trp aminoacid:

- Spectral shifts of emission spectra: are a clear indicators of the protein folding. They can be monitored by calculating the center of spectral mass (CSM) using the equation detailed in ***Eq. 3.1***, and in ***Chapter 7, Section 7.2.11***), which refer to the precise wavelength whereabouts the spectra emission of a protein is maximum according the average exposure of their Trp to the aqueous phase[25,26]. After some protein conformational change, in ***Figure 4.21 A*** it is reflected how CSM values may shift to lower wavelengths (blue shift) when a Trp residue become buried in the inner structure of the biomolecule, or may shift to longer ones (red shift) when unfolding of the protein is occurring.
- Changes on the fluorescence intensity: it can increase or decrease according to the subsequent exposure of the Trp residue to the aqueous phase but also to the interactions with aminoacids in the surroundings. For example, such changes on the fluorescence intensity can occur after the interaction of a protein with a lipid bilayer, as schematized in ***Figure 4.21 B***.

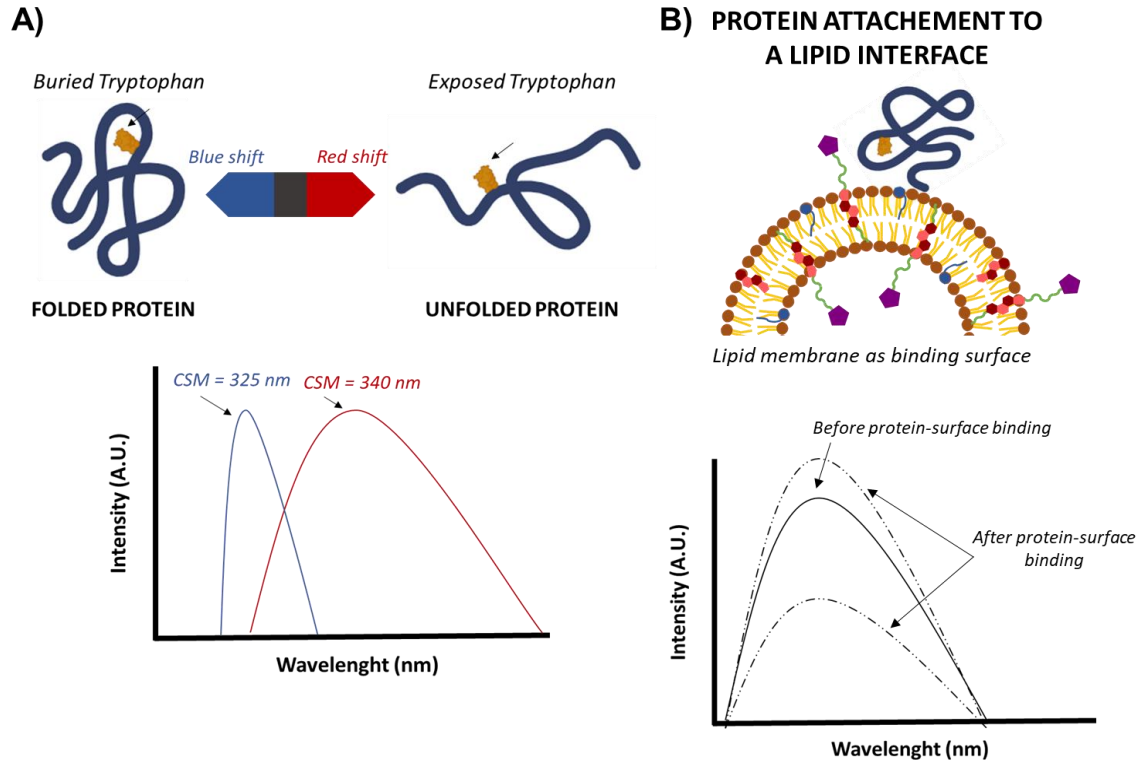
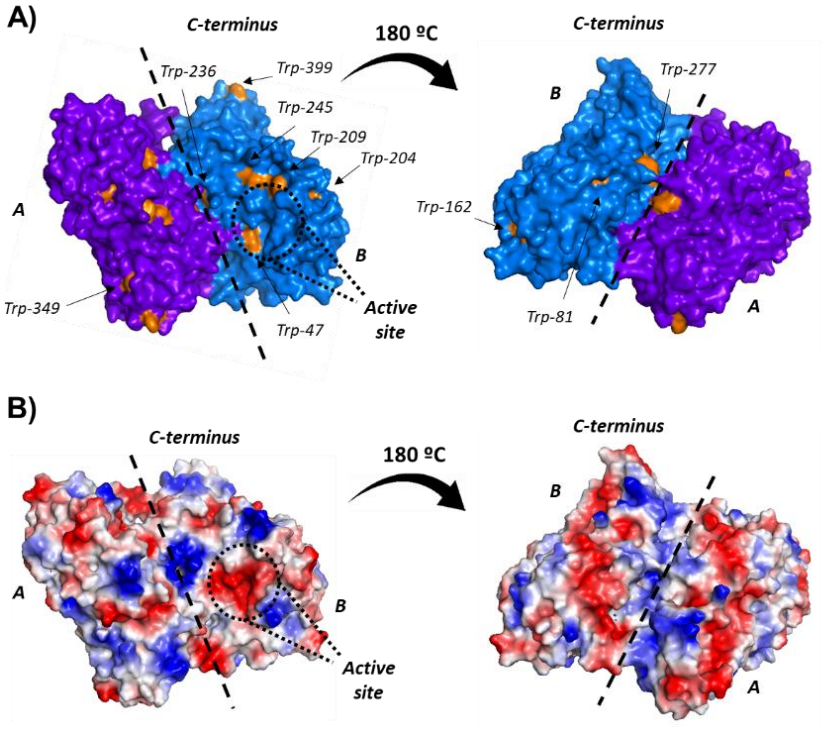


Figure 4.21. Changes of the intrinsic fluorescence spectra and/or intensity often used to determine Trp localization on protein structures. A) Shifts of a Trp emission spectra caused by conformational changes. They can be monitored following CSM values. B) Modification of the protein fluorescence intensity induced by binding interactions with lipid membranes.

Since the overall emission fluorescence depends on the average contribution of all the Trp residues encoded by a protein sequence, these correlations are easier to follow for peptides or proteins containing only one Trp aminoacid. In this thesis work, the interaction of different GLA versions with liposomal membranes was explored. As mentioned before in *Section 4.1.1* and in *Chapter 3*, human GLA enzyme is a homodimer which contain one active site in each monomer of 48.8 kDa[3]. Each monomer contains 17 Trp residues, of which 10 are partially or totally exposed to aqueous phase according to the theoretical visualization of the human GLA surface using PyMOL software (*Figure 4.22 A*).



RESIDUE EXPOSITURE TO GLA SURFACE		
Poor	**Medium**	**High**
Trp-81	Trp-47 (involved with the active site)	Trp-399 (near C-terminus)
Trp-204	Trp-162	
Trp-236 (between monomer binding site)	Trp-209 (near the active site)	
	Trp-245 (near the active site)	
	Trp-277	
	Trp-349	

Figure 4.22. Visualization of human GLA enzyme (PDB sequence: 1R47) using PyMOL software[4]. A) Surface representation of each GLA monomer as a blue or purple blocks separated by a dashed line. Trp residues reaching the protein surface are colored in orange, and compiled in the corresponding table. B) Estimated net surface charge of the GLA homodimer at pH 7. Surface charges are represented in legend color as red (negative charges), blue (positive charge) and white (neutral charge).

According to the bioinformatics results published in Cabrera *et al.*[1], residues located near the C-terminus of the protein sequence may be involved in the monomer interaction with liposomal membranes composed only of DPPC and cholesterol. However, more complex liposomal membranes composed of DPPC, cholesterol, chol-PEG_{400}-RGD and MKC surfactant were explored in this thesis. Since MKC surfactant brings positive charge to the lipid bilayers, sites of the protein surface with negatively charge density might also be involved in GLA-liposome interactions. Some Trp such as Trp-47, Trp-81 or Trp-204 are near areas of negative surface charge density, and their ability to fluoresce might be particularly affected by the GLA-liposome interactions (see *Figure 4.22 B*).

4.3.3.2. Impact of GLA characteristics on the enzyme distribution on nanoliposomes

In this section the changes on the intrinsic fluorescence emission spectra of Trp caused by the interaction of GLA enzymes with lipid membranes composed of DPPC, cholesterol, chol-PEG_{400}-RGD and MKC are described. For this purpose, the four naked GLA versions (GLAH6-T, GLAcmycH6-T, GLAcmycH6-S and GLA-S) gathered in ***Table 4.1***, and the GLA-free nanoformulation prepared at 20 mg/mL lipid in pure water (LP-$RGD_{(w)}$) described in ***Table 4.2***, were used in this study.

The present experiment consisted of titrating increasing amounts of LP-$RGD_{(w)}$ liposomes over the four naked GLA versions as schematized in ***Figure 4.23***. Changes on the Trp fluorescence emission spectra (λ_{em} = 300 – 550 nm) were measured in a Varian Cary Eclipse fluorescence spectrophotometer (Agilent Technologies, Santa Clara, CA, USA) at room temperature following the procedure explained in ***Chapter 7, Section 7.2.11***. Same volumes of pure water (without liposome presence) were also titrated over naked GLA enzymes as control of probable protein conformational changes induced by the successive protein dilution in water due to the titrated volumes. Each titration condition was performed by duplicate. All naked GLA enzymes were diluted in pure water up to an initial concentration of 0.225 mg/mL.

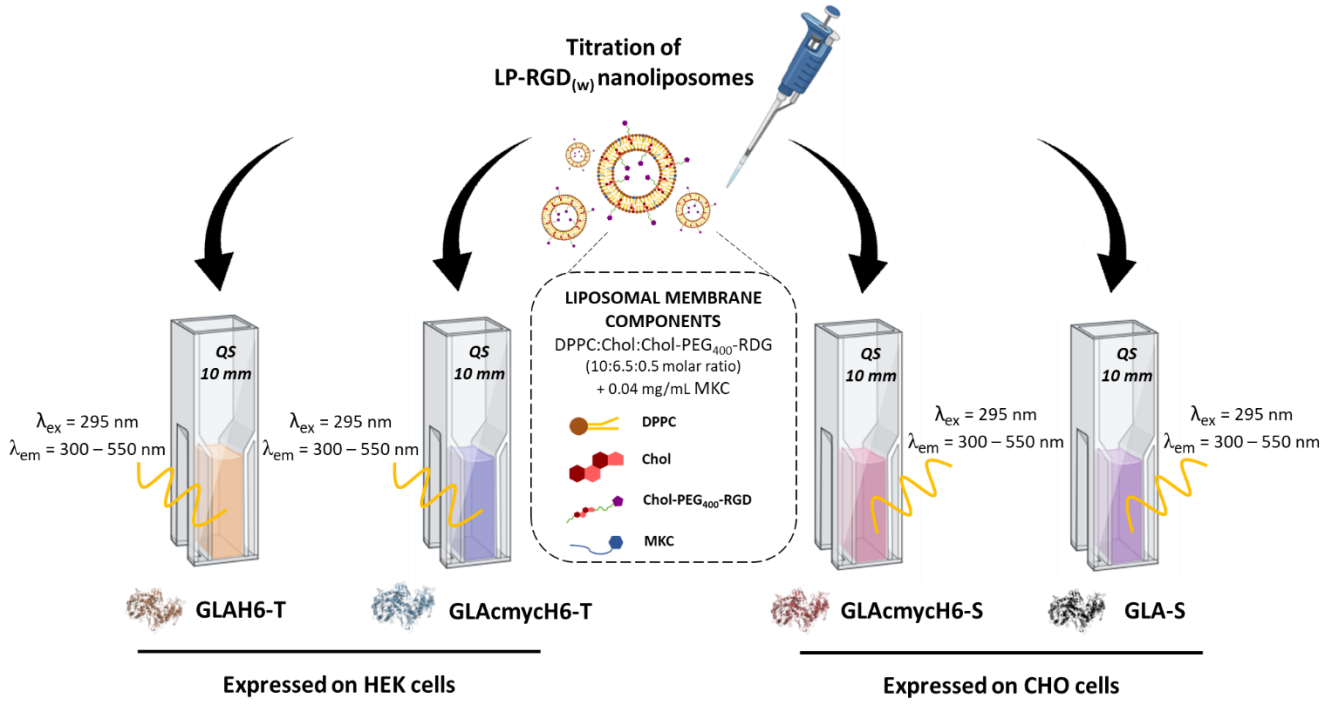


Figure 4.23. Experimental design to evaluate the capacity of LP-$RGD_{(w)}$ formulation of interacting with different GLA enzymes versions and modifying the intrinsic fluorescence emission of their Trp.

The results presented in ***Figure 4.24 A*** demonstrated the correlation of the fluorescence intensity decay with the protein concentration decrease, in agreement with the Lambert Beer's Law. The difference in the slope suggested different structuring of GLAH6-T and GLAcmycH6-S molecules respect to GLAcmycH6-T and GLA-S ones. In the case of GLAcmycH6-S is probably due to the aggregation tendency of this biomolecule described in ***Chapter 3***. It is important to mention that, in this experiment, a successive increase on the pH is caused during the protein dilution in water, capable to destabilize the macromolecule by modifying the protein surface charge from positively to neutral-negatively charged, and subsequently causing conformational changes or aggregates generation (remember that His-tagged GLA versions, GLAH6-T, GLAcmycH6-T and GLAcmycH6-S, were stored in acetic acid buffer at pH 5.5). However, the analysis of the CSM values showed that none of the proteins suffer conformational changes as the dilution increase (see ***Figure 4.24 C***) suggesting that the pH change is not affecting the conformation. Therefore, the fact that each GLA version senses this pH change in different manners supports the idea of different molecule-to-molecule distribution in each case.

In comparison, overall GLA fluorescence intensities highly decreased when LP-RGD$_{(w)}$ were titrated over soluble enzymes, evidencing protein-membrane interactions (see ***Figure 4.24 B***). Additionally, CSM values of GLA enzymes were altered after the titration with LP-RGD$_{(w)}$ nanosystems, as shown in ***Figure 4.24 D***. Depending on the GLA nature, shifts on emission spectra seem to be stabilized at different CSM values after reaching the GLA:lipid mass ratio of 1:40, suggesting that the majority of GLA molecules are already adsorbed to liposomal surfaces at this ratio. Enzymes produced in HEK 293F cells (GLAH6-T and GLAcmycH6-T) showed highly different CSM values although they converge to a similar one when they are adsorbed to liposomal membranes. Once bonded to bilayers, the last CSM values of 351 nm observed for GLAH6-T and GLAcmycH6-T (produced in HEK cells) differ from values around 350.3 nm that presented GLAcmycH6-S and GLA-S (produced in CHO cells). These differences suggested a different conformation of these biomolecules once attached to liposomal surfaces, which might be the responsible of the differences in the enzymatic activity between GLA-loaded nanoliposomal systems previously observed in ***Section 4.2.4.2***.

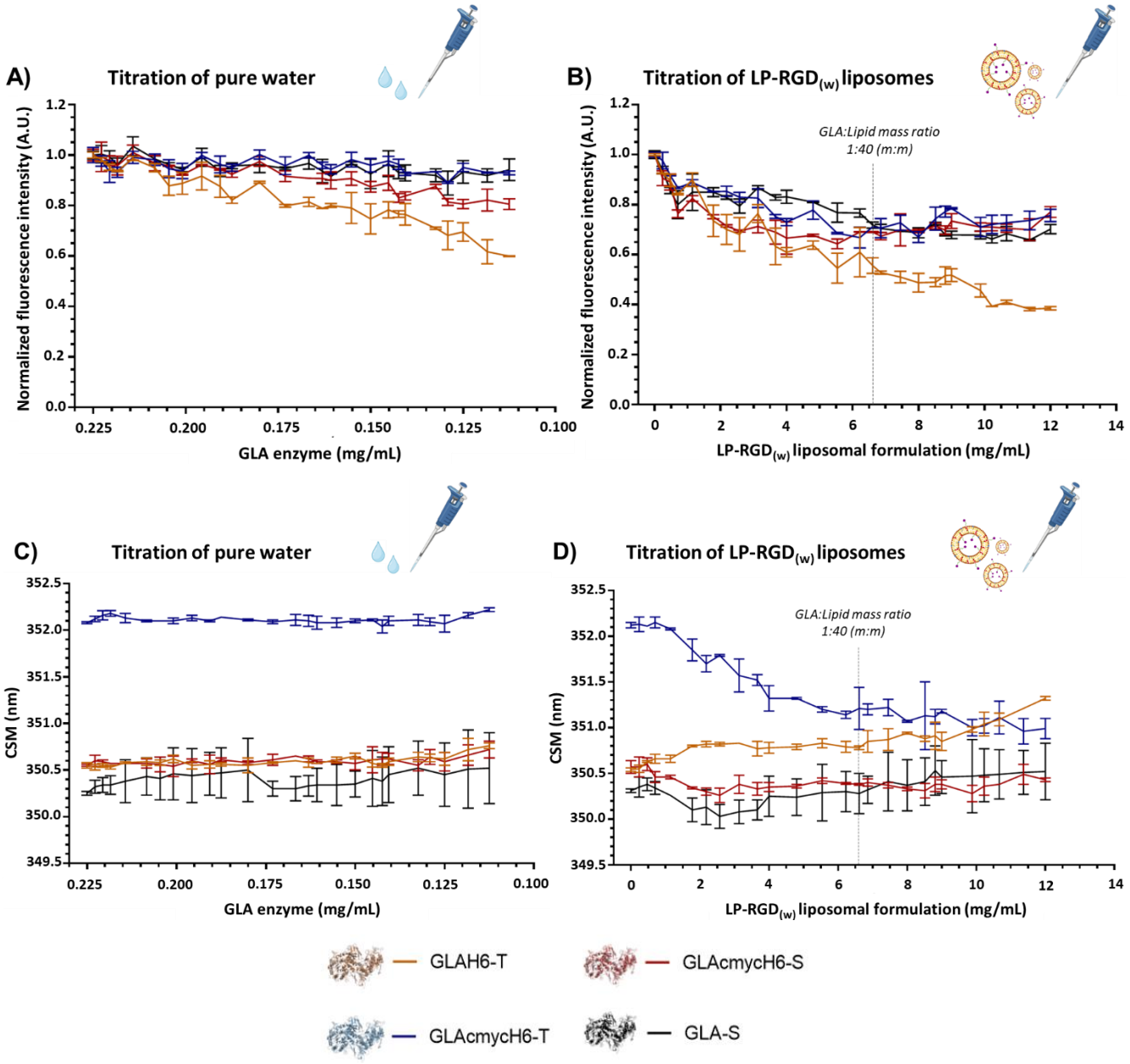


Figure 4.24. Titration experiments to monitor alterations in Trp emission spectra of GLA enzymes due to the absence or presence of LP-RGD$_{(w)}$ liposomes. Investigation of fluorescence modification after titrating GLA enzymes with A) only pure water, or with B) LP-RGD$_{(w)}$ liposomes. Displacement comparison of GLA emission spectra through the calculation of CSM values after titrating GLA enzymes with C) only pure water, or with D) LP-RGD$_{(w)}$ nanovesicular formulation. Each titration condition has been tested by duplicate with all GLA versions tested.

As summary, the GLA nature impacts on the enzyme conformation and/or distribution on nanoliposomal bilayers composed of DPPC, chol, chol-PEG$_{400}$-RGD and MKC, and prepared in pure water. Also, fluorescence results suggest that nanoliposomal surfaces might be saturated of GLA molecules near the mass ratio GLA:lipid of 1:40. Taking into account that most of the nanoformulations studied in this thesis were prepared near this mass ratio

GLA:lipid of 1:40, this finding supports the fact that the majority of GLA molecules are adsorbed to nanoliposomal surfaces regardless of the production method used to prepare the nanoformulations.

4.3.4. Characterization of GLA distribution on nanoliposomes by cryoTEM

Since cryoTEM imaging allows the preservation of water presence in samples, the morphology and size of nanoliposomes can be characterized meanwhile their vesicular structuration is preserved. In this section, the feasibility of investigating the GLA distribution on nanoliposomes by cryoTEM imaging is described.

The GLA-loaded and GLA-adsorbed nanoformulations (LP-RGD-GLAcmycH6-$S_{(w)}$ and LP-RGD-GLAcmycH6-$S_{(w)}$_Ads) used in the present study are described above in ***Table 4.2*** and ***Table 4.3***. Both of them contain the GLAcmycH6-S enzyme version (produced in CHO cells), whose characteristics are also detailed above in ***Table 4.1***. As aforementioned, both nanoformulations were prepared at 5 mg/mL of lipid in pure water, but the GLAcmycH6-S enzyme was added to nanoliposomes using a different methodology. Additionally, empty nanoliposomes (LP-$RGD_{(w)}$) prepared at 9 mg/mL in pure water, but without GLAcmycH6-S presence, were also examined as control. The liposomal membrane composition used to prepare all nanoformulations was composed by DPPC, cholesterol and chol-PEG_{400}-RGD (10:6.5:0.5 theoretical molar ratio), and contained a small amount of MKC (5 % molar of the total membrane components) as depicted above in ***Figure 4.4***.

All nanoliposomal formulations were observed by cryoTEM microscopy by Prof. D. Danino's team from Technion (Israel), following the procedure described in ***Chapter 7, Section 7.4.5.2***. As shown in ***Figure 4.25 B***, "circular-like organic nanostructures" of 20 nm of diameter, were found superposed to individual liposomal vesicles of 170 nm of diameter in both nanoformulations containing the GLAcmycH6-S enzyme. However, cryoTEM imaging does not allow to discriminate whether these nanostructures are adsorbed on the liposomal surfaces or entrapped inside the vesicles. These nanostructures were not found in empty liposomes (LP-$RGD_{(w)}$), which did not contain GLA presence (see ***Figure 25 A***). Therefore, the "circular-like organic nanostructures" observed might correspond to protein nanoparticles around 20 nm formed by several GLAcmycH6-S monomers. Besides, these organic nanostructures could not be observed either in samples of naked GLAcmycH6-S enzyme (data not shown). This finding suggest that GLAcmycH6-S monomers might generate these "circular-like organic nanostructures" due to the presence of RGD-targeted liposomes. However, more investigation is required to confirm this hypothesis.

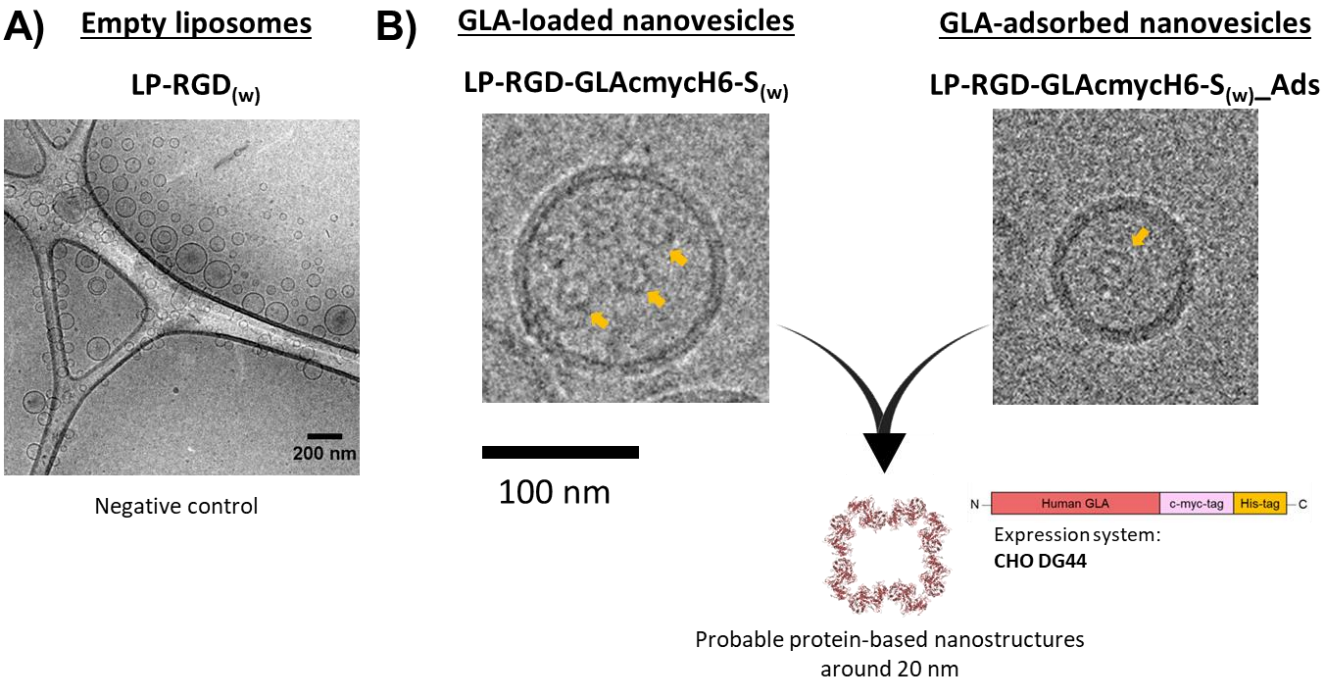


Figure 4.25. CryoTEM images taken one month after production of A) empty LP-RGD$_{(w)}$ liposomes explored as negative control, and B) both GLA-loaded and GLA-adsorbed formulations prepared with GLAcmycH6-S enzyme (LP-RGD-GLAcmycH6-S$_{(w)}$ and LP-RGD-GLAcmycH6-S$_{(w)}$_Ads). Yellow arrows pointed to "circular-like organic nanostructures" probably formed by GLAcmycH6-S molecules. Images were acquired by the research group of Prof. D. Danino from Technion.

4.4. Summary and conclusions

In this chapter, the four GLA enzyme versions (GLAH6-T, GLAcmycH6-T, GLAcmycH6-S and GLA-S) previously characterized in ***Chapter 3***, which differ in their aminoacid sequence, nature, and therefore, in their CQAs (e.g. solubility, molecular weight, net surface charge and enzymatic activity), were used to investigate the impact of GLA features on several physicochemical and biological features of RGD-targeted liposomal formulations containing GLA.

For this purpose, the four versions of GLA enzymes mentioned above were successfully integrated in RGD-targeted liposomes, either by the CO_2-based methodology, DELOS-susp, yielding GLA-loaded nanoliposomal formulations, with GLA inside and outside the nanoliposomal nanostructure, and by a titration methodology, yielding GLA-adsorbed nanoliposomal formulations, with GLA only attached to the outside nanoliposomal surface. The main GLA characteristics which demonstrated to have an impact on the physicochemical and biological features of GLA nanoliposomal formulations were given by the GLA production of the enzyme in HEK or CHO cells, which confer to the enzymes conserved and specie-related post-translational modifications (PTMs). These results can be summarized in the following conclusions:

- Higher encapsulation efficiencies were generally observed with GLAcmycH6-S or GLA-S, produced in CHO cells, in comparison with GLAH6-T and GLAcmycH6-T, produced in HEK cells. The higher negative character, at pH close to neutral, of both enzymes produced in CHO cells in comparison to the one of both enzymes produced in HEK cells, evidence the importance of the GLA surface net negative charge to favor protein integration in nanoliposomes composed by DPPC, cholesterol, chol-PEG_{400}-RGD and MKC, which have a positive character.
- Higher specific enzymatic activities were generally observed for nanoliposomal formulations prepared with GLAcmycH6-S or GLA-S (produced in CHO cells) in comparison with GLAH6-T and GLAcmycH6-T (produced in HEK cells). Tryptophan fluorescence studies suggest that GLAs produced in HEK, have a more open structural conformation at neutral pH, than GLAs produced in CHO. This different GLA conformation, might impact on the interaction mode of the enzymes with nanoliposomes composed by DPPC, cholesterol, chol-PEG_{400}-RGD and MKC, and therefore, on the enzymatic activity of GLAs nanoformulations.

In the present work it was not possible to correlate any GLA characteristic with the colloidal stability and GLA leakage rate of GLA-loaded nanoliposomal formulations. However, the comparison of *in vitro* GLA release profiles evaluated in physiological relevant media with and without salt containing (Ringer-Lactate solution and glucose 5 % (w/v) media, respectively), suggests that electrostatic forces may be predominant in the GLA binding with nanoliposomes composed by DPPC, cholesterol, chol-PEG_{400}-RGD and MKC. Interestingly, the combination of the nature and aminoacid sequence of the GLAH6-T enzyme (produced in HEK cells) allows an easier release of this enzyme from nanoliposomes incubated in salt free physiological media in comparison with the other GLA enzymes. This finding points out that other hydrophobic forces (e.g. Van der Waals interactions) might also contribute in the interaction of the GLAH6-T enzyme with nanoliposomes composed by DPPC, cholesterol, chol-PEG_{400}-RGD and MKC. Further investigation is necessary to confirm this hypothesis.

Finally, the comparison of physicochemical and biological properties of GLA-loaded and GLA-adsorbed nanoformulations described in the present chapter, points out that GLA enzyme is mainly localized in the outer surface of nanoliposomes. Indeed, although DELOS-susp methodology, based on the molecular assembling of the GLA nanoliposomal components, could yield nanoformulations with GLA enzyme inside and outside, we have observed that the big majority of enzyme molecules in the nanoliposomal formulations are localized always in the outside of the liposomal nanostructures.

Regardless the protein localization in nanoliposomes, GLA enzymes are less degraded *in vitro* by trypsin proteases when are integrated in nanoliposomes composed by DPPC, cholesterol, chol-PEG_{400}-RGD and MKC

than in their naked form. These results evidence the protective capacity and potential of RGD-targeted liposomes to be used as nanocarriers for GLA enzymes.

In summary, the results obtained in this chapter have contributed to a better understanding of the interaction between GLA enzymes and nanoliposomes composed by DPPC, cholesterol, chol-PEG_{400}-RGD and MKC, and therefore, to the continuous development of GLA-loaded nanoliposomal formulations to boost their translation to the early clinical phase (TRL-6).

4.5. References

1 Cabrera I, Abasolo I, Corchero JL, *et al.* α-Galactosidase-A Loaded-Nanoliposomes with Enhanced Enzymatic Activity and Intracellular Penetration. *Adv Healthc Mater* 2016; **5**: 829–40.

2 European Medicines Agency (EMA), European Comission (EC). Orphan drug designation (Designation number EU/3/20/2396). Orphan condition: Alpha galactosidase A for treatment of Fabry disease. Sponsor: Consejo Superior de Investigaciones Científicas (CSIC) . 2021.

3 Garman SC, Garboczi DN. The molecular defect leading to fabry disease: Structure of human α-galactosidase. *J Mol Biol* 2004; **337**: 319–35.

4 Research Collaboratory for Structural Bioinformatics Protein Data Bank (RCSB PDB). 1R47: Structure of human alpha-galactosidase. RCSB PDB. 2004. https://www.rcsb.org/structure/1R47 (accessed Dec 1, 2023).

5 Colletier JP, Chaize B, Winterhalter M, Fournier D. Protein encapsulation in liposomes: Efficiency depends on interactions between protein and phospholipid bilayer. *BMC Biotechnol* 2002; **2**: 1–8.

6 Hwang SY, Kim HK, Choo J, Seong GH, Hien TBD, Lee EK. Effects of operating parameters on the efficiency of liposomal encapsulation of enzymes. *Colloids Surfaces B Biointerfaces* 2012; **94**: 296–303.

7 Shimizu T, Mori T, Tomita M, Tsumoto K. PH switching that crosses over the isoelectric point (pI) can improve the entrapment of proteins within giant liposomes by enhancing protein-membrane interaction. *Langmuir* 2014; **30**: 554–63.

8 Tomsen-Melero J, Passemard S, García-Aranda N, *et al.* Impact of chemical composition on the nanostructure and biological activity of α- galactosidase- loaded nanovesicles for Fabry disease treatment. *ACS Appl Mater Interfaces* 2021; **13**: 7825–38.

9 European Medicines Agency. Benzalkonium Chloride Used as an Excipient. Comm. Hum. Med. Prod. EMA/CHMP/495737/2013 . 2017. https://www.ema.europa.eu/en/benzalkonium-chloride (accessed Dec 21, 2021).

10 Pramanick S, Singodia D, Chandel V. Excipient Selection In Parenteral Formulation Development. *Pharma Times* 2013; **45**: 65–77.

11 Cristóbal-Lecina E, Pulido D, Martin-Malpartida P, Macias MJ, Albericio F, Royo M. Synthesis of Stable Cholesteryl-Polyethylene Glycol-Peptide Conjugates with Non-Disperse Polyethylene Glycol Lengths. *ACS Omega* 2020; **5**: 5508–19.

12 Merlo-Mas J, Tomsen-Melero J, Corchero JL, *et al.* Application of Quality by Design to the robust preparation of a liposomal GLA formulation by DELOS-susp method. *J Supercrit Fluids* 2021; **173**: 105204.

13 Tomsen-Melero J. Study of New Liposomes for the Delivery of Enzymes through Biological Membranes. 2021. http://hdl.handle.net/10803/673786 (accessed Oct 30, 2021).

14 Khan F, Legler PM, Mease RM, Duncan EH, Bergmann-Leitner ES, Angov E. Histidine affinity tags affect MSP142 structural stability and immunodominance in mice. *Biotechnol J* 2012; **7**: 133–47.

15 SIB Swiss Institute of Bioinformatics. Expasy ProtParam tool. https://web.expasy.org/protparam/ (accessed Dec 27, 2018).

16 Cabrera I, Elizondo E, Esteban O, *et al.* Multifunctional nanovesicle-bioactive conjugates prepared by a one-step scalable method using CO2-expanded solvents. *Nano Lett* 2013; **13**: 3766–74.

17 European Medicines Agency. ICH guideline Q3C (R6) on impurities: guideline for residual solvents - Step 5. Comm. Hum. Med. Prod. EMA/CHMP/ICH/82260/2006. 2019. https://www.ema.europa.eu/en/documents/scientific-guideline/international-conference-harmonisation-technical-requirements-registration-pharmaceuticals-human-use-guideline-q3c-r6-impurities-guideline-residual-solvents-step-5_en.pdf (accessed Dec 21, 2022).

18 Desnick RJ, Allen KY, Desnick SJ, Raman MK, Bernlohr RW, Krivit W. Fabry's disease: Enzymatic diagnosis of hemizygotes and heterozygotes: α-Galactosidase activities in plasma, serum, urine, and leukocytes. *J Lab Clin Med* 1973; **81**: 157–71.

19 Mayes JS, Scheerer JB, Sifers RN, Donaldson ML. Differential assay for lysosomal alpha-galactosidases in human tissues and its application to Fabry's disease. *Clin Chim Acta* 1981; **112**: 247–51.

20 Lee K, Jin X, Zhang K, *et al.* A biochemical and pharmacological comparison of enzyme replacement therapies for the glycolipid storage disorder Fabry disease. *Glycobiology* 2003; **13**: 305–13.

21 European Medicines Agency. Replagal - EMEA/H/C/000369 - IAIN/0096. https://www.ema.europa.eu/en/medicines/human/EPAR/replagal#product-information-section (accessed Dec 21, 2023).

22 European Medicines Agency. Fabrazyme - EMEA/H/C/000370 - II/0116. https://www.ema.europa.eu/en/medicines/human/EPAR/fabrazyme (accessed Jan 21, 2021).

23 US Food and Drug Administration. Guidance for Industry on Liposome Drug Products Chemistry, Manufacturing, and Controls; Human Pharmacokinetics and Bioavailability; and Labeling Documentation. FDA-2016-D-2817. 2018. http://www.fda.gov/Drugs/GuidanceComplianceRegulatoryInformation/Guidances/default.htm (accessed Feb 18, 2023).

24 Lakowicz JR. Principles of fluorescence spectroscopy, Third Edition. Springer, 2006.

25 Sánchez JM, Sánchez-García L, Pesarrodona M, *et al.* Conformational Conversion during Controlled Oligomerization into Nonamylogenic Protein Nanoparticles. *Biomacromolecules* 2018; **19**: 3788–97.

26 Burgos MI, Ochoa A, Perillo MA. β-sheet to α-helix conversion and thermal stability of β-Galactosidase encapsulated in a nanoporous silica gel. *Biochem Biophys Res Commun* 2019; **508**: 270–4.

5

DEVELOPING ANALYTICAL METHODS FOR QUALITY ASSESSMENT AND CONTROL OF THE CRITICAL QUALITY ATTRIBUTES OF GLA NANOLIPOSOMAL FORMULATIONS

5.1. Introduction

5.1.1. An advanced GLA-liposome formulation for Fabry treatment: main achievements on TRL development

As explained in ***Chapter 1*** and ***Chapter 4***, previous work done in the frame of the European Smart4Fabry project (H2020, ID 720942) allowed the development of the robust liposome nanoformulation Nano-GLA-v4 with stable colloidal properties, enhanced targeted capacities, and meeting the requirements for injectables (being isosmotic thanks to the addition of glucose during tangential flow filtration (TFF)-based purification of samples). Various home-made recombinant α-galactosidase A (GLA) enzymes were used as protein model during the nanocarrier composition optimization, ending with the use of the GLA-S (the most optimized GLA version obtained by a stable expression–based production method using a Chinese hamster ovary (CHO) cell line to overcome the limited production yield and the inter-batch variability that the transient expression production method offers). At preclinical level, this Nano-GLA-v4, the optimized GLA-liposome nanoformulation, showed higher efficacy than traditional authorized enzyme replacement therapy (ERT) for Fabry disease treatment. This significant benefit was recognized by the European Medicines Agency (EMA), and, accordingly, in January 2021 this novel nanoformulation was designated an orphan drug by the European Commission (EC).

Furthermore, to better understand the impact of the encapsulated GLA enzyme model on the quality profile of the optimized liposomal composition, it has been firstly described in ***Chapter 3*** the characterization and

comparison of four GLA versions (GLAH6-T, GLAcmycH6-T, GLAcmycH6-S and GLA-S), and then detailed in ***Chapter 4***, their integration in the optimized liposomal carrier. Results from ***Chapter 3*** indicated modifications of the critical quality attributes (CQAs) of non-encapsulated GLA enzymes correlated with the presence of purification tags in their structure (e.g. c-myc tag can impact on the enzyme solubility and aggregation tendency), but mainly with the protein nature (i.e. the conserved glycosylation post-processing strongly related with the expression system used to produce the recombinant proteins). With this, it was found that the GLA-S version have the most promising properties, being the enzyme with higher specific enzymatic activity and lower aggregation tendency, as well as with the lack of presumable immunogenic purification tags. Once the four GLA models were integrated in the optimized liposomal membrane composition of Nano-GLA-v4 prototype reported in ***Chapter 4***, similar physicochemical properties of the different nanovesicle-bioconjugates were observed in spite of the chemical differences of the GLA enzymes used. However, in terms of biological properties, liposomes loading GLA-S showed the best enzymatic activity, entrapment efficiency, protection and so on, strongly related again with its nature provided by its stable expression in CHO cells. Due to the promising biological properties of GLA-S-loaded liposomes, together with the feasible scalability of CHO-based production procedures to obtain the required protein amounts for the late preclinical phase and the future clinical trials, the GLA-S enzyme was selected as the active pharmaceutical principle (API) of the GLA-loaded liposomal drug product. The liposome nanoformulation entrapping GLA-S protein described as Nano-GLA-v4 in ***Chapter 4***, has been named herein as LP-RGD-GLA-S.

5.1.2. Definition of the final LP-RGD-GLA-S pharmaceutical form to reach the clinical phase: challenges to overcome in the clinical translation

Nowadays, further development of the LP-RGD-GLA-S liposome formulation is being done in the frame of the European Phoenix project (H2020, ID 953110) with the aim to boost their translation to the early clinical phase (TRL-6). Nano-based biopharmaceutics can be designed in different pharmaceutical forms, such as aqueous dispersions or freeze-dried products, to be storage at specified conditions. Their choice usually plays an important role on the product stability and shelf life, becoming a critical consideration to guarantee the product quality, efficacy, and safety at clinical level.

Lyophilized-based product to enhance formulation stability

The promising GLA-loaded liposomal formulation that reached the non-regulatory preclinical phase consisted of an aqueous dispersion containing glucose as an isosmotic agent (in this chapter called as LP-RGD-GLA-$S_{(gluc)}$). In addition to the high efficacy demonstrated at this preclinical stage, the colloidal stability of LP-RGD-GLA-$S_{(gluc)}$

formulation can be guaranteed for 2 – 3 months at 2 – 8 ºC. The LP-RGD-GLA-$S_{(gluc)}$ composition and the roles of each component constituting the nanovesicular formulation are described in ***Table 5.1***.

Table 5.1. Detailed LP-RGD-GLA-$S_{(gluc)}$ composition, roles and availability of its components. Legend: q.s. means as much amount as is sufficient.

Component	Theoretical amount per mL	Role	Availability
GLA-S	0.27 mg	Active pharmaceutical ingredient (API)	Non-commercially available. Produced and provided by Leanbio SL (Spain)
DPPC	6.2 mg	Membrane component	Commercially available from CordenPharma (Switzerland)
Cholesterol	2.1 mg	Membrane component	Commercially available from Panreac AppliChem (Spain)
Cholesterol-PEG_{400}-RGD	0.59	Membrane component containing the targeting moiety	Non-commercially available. Synthetized and provided by the CDMO AmbioPharm Inc. (USA)
MKC	0.30	Stabiliser	Commercially available from US Biological Life Science (USA)
DMSO	Traces	Solubiliser of membrane components	Commercially available from Sigma-Aldrich (Spain)
EtOH	Traces	Solubiliser of membrane components	Commercially available from Sigma-Aldrich (Spain)
WFI	q.s. 1 mL	Dispersant medium	Commercially available from HyClone Laboratories (USA)
Glucose 5 % (w/v)	50 mg	Isosmotic agent	Commercially available from Braun (Germany)

It is well known that membrane components of liposomes can be destabilized over time when stored in aqueous media (e.g. phospholipid oxidation) due to temperature, pH or presence of certain components (e.g. salts or sugars) among other environmental factors[1]. This leads to the loss of the lipid bilayer colloidal stability (e.g. liposome breakage, aggregation, fusion, etc.), the decrease of the nanocarrier target capacity and efficacy, but also to the generation of degradation products form the vesicle membrane components that can potentially impair the safety of the nanoformulations in the clinics.

Most liposomal formulations are freeze-dried after their manufacturing in order to remove the water from the sample and enhance their quality and stability profiles. However, some liposomal properties can be modified during the freeze-drying process. For these reasons, protective agents or cryoprotectants are excipients usually added to the formulation in order to maintain their quality attributes.

To improve the stability of the LP-RGD-GLA-S product, two different cryoprotectant mixtures are currently being explored in the frame of the European Phoenix project. Both cryoprotectant compositions are detailed in ***Figure***

5.1. as Cryo1 and Cryo2, and the whole manufacturing process flow diagram of the freeze-dried prototypes (LP-RGD-GLA-$S_{(Cryo1)}$ and LP-RGD-GLA-$S_{(Cryo2)}$) compared with the one used for the production of the LP-RGD-GLA-$S_{(gluc)}$ liquid dispersion.

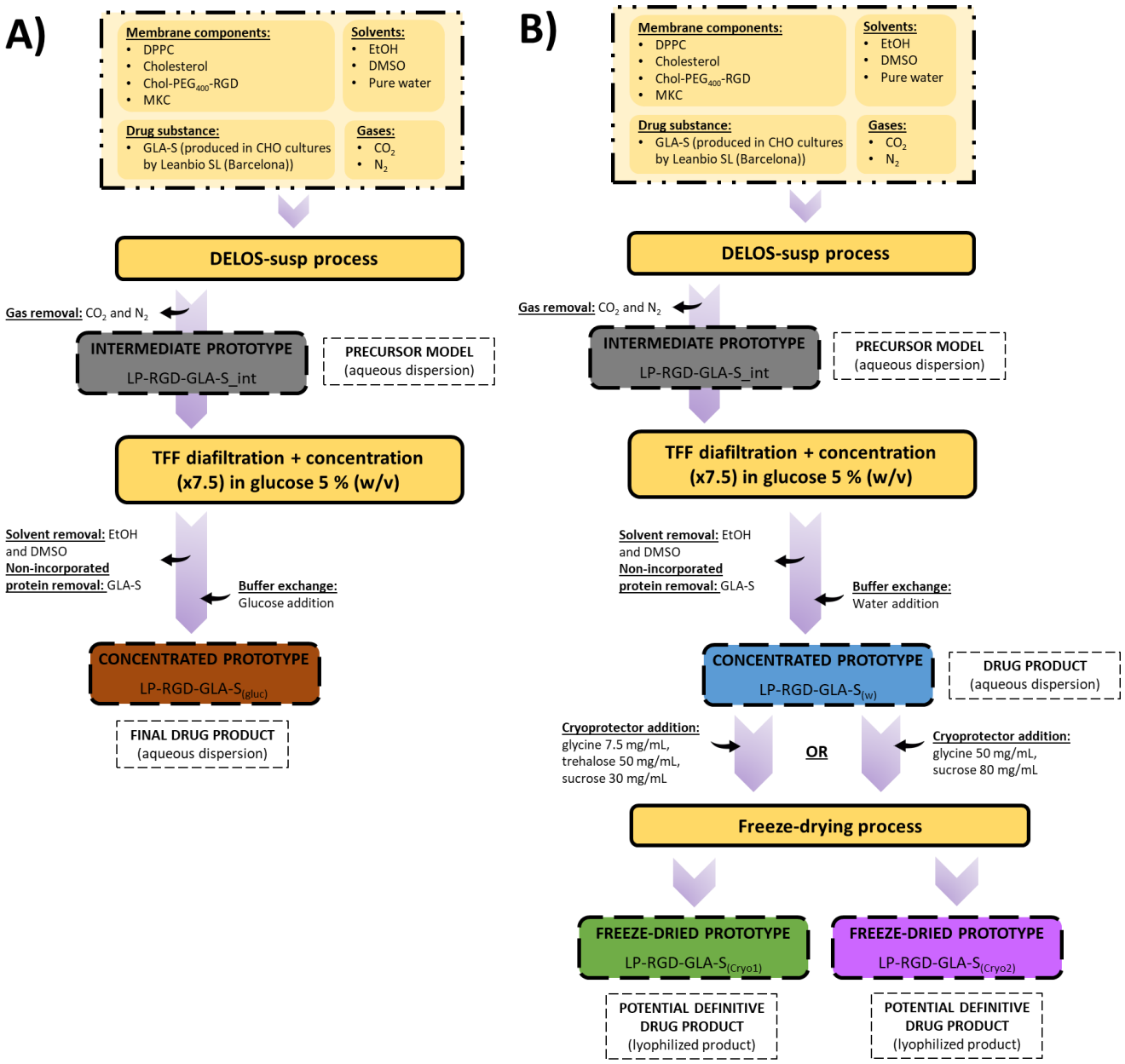


Figure 5.1. Diagrams of the whole manufacturing process of LP-RGD-GLA-S prototypes. A) Production process followed to obtain the aqueous dispersion prototype named LP-RGD-GLA-$S_{(gluc)}$. B) Production process employed to obtain the freeze-died prototypes LP-RGD-GLA-$S_{(Cryo1)}$ and LP-RGD-GLA-$S_{(Cryo2)}$. Legend: Cryo1 contains glycine 7.5 mg/mL, trehalose 50 mg/mL and sucrose 30 mg/mL; Cryo2 contains glycine 50 mg/mL and sucrose 80 mg/mL.

5.1.3. Definition and control of the CQAs of GLA-loaded nanoliposomal formulations

During the European Smart4Fabry project, a high degree of manufacturing control and the understanding of how process parameters can impact on the quality of the LP-RGD-GLA-$S_{(gluc)}$ nanoformulation to consistently produce a high-quality product were achieved by means of implementing the Quality by Design (QbD) concept[2]. Briefly, the QbD approach is a methodology recommended by the Food and Drug Administration (FDA), the EMA, the International Organization for Standardization (ISO) and the American Society for Testing and Materials (ASTMA International)[3–7], and it is based on producing optimal products taking into account from the beginning the desired final quality that the product must have, i.e. the philosophy of this concept is to start with the end in mind taking into account the intended use, the dosage form, the administration route, and so on, what is known as defining the target product profile (TPP). Then, the following key step in the QbD is the identification of the CQAs of the product (those physical, chemical, biological, or microbiological properties or characteristics that should be very well control within an appropriate limit, range, or distribution to ensure the desired product quality, since they can have a significant impact on the efficacy and safety). Next is to perform a risk assessment, in order to identify which formulation variables and process parameters can potentially impact on the CQAs and define control strategies. For example, by using a Design of Experiments (DoE) which can define a space that ensures that the product will be obtained with the desired quality (with the CQAs within the desired specifications). The final objective of the QbD is to produce optimal products from the quality point of view which is crucial to guarantee the efficacy and safety.

During these earlier stages of the development (from TRL-3 to TRL-4), the quality targeted product profile (QTPP) of the LP-RGD-GLA-$S_{(gluc)}$ was defined taking into account that it is a nanoformulation based on liposomes, designed for the intracellular targeted delivery and intended for a IV administration. Besides, its CQAs were identified (***Table 5.2***) to be characterized and controlled since these can have a significant impact on the product quality and *in vivo* performance[8,9].

Table 5.2. QTTP elements and CQAs identified for LP-RGD-GLA-$S_{(gluc)}$ nanoformulation.

QTTP elements		Target
Dosage form		**Nanoformulation**
Dosage design		**For targeted delivery**
Administration route		**Intravenous**
Quality attributes of the liposomal product	**Physicochemical properties:**	
	Macroscopic appearance	**Must meet the standards resulted from the specifications of similar approved products or from the current scientific research**
	Mean particle size and Particle size distribution (PdI)	
	Particle morphology and lamellarity	
	ζ-potential (liposome surface charge)	
	Drug entrapment efficiency / Free drug substance	
	Total drug content	
	Integration efficiency of chol-PEGn-RGD in the vesicular membrane	
	pH	
	Dispersion stability	
	Osmolality	
	Chemical composition	
	Lipid and GLA degradation products	
	Biological properties:	
	Bioactivity	**Preserve the enzymatic activity**
	Biocompatibility	**Lack of hemolytic activity and cytotoxicity**
	Protective capacity	**Drug protection from degradation**
	Drug release and drug leakage rate	**Sustained drug release and minimal drug leakage under storage conditions**
	Microbiological quality	**Sterile and free of endotoxins**

Most of the quality attributes of LP-RGD-GLA-$S_{(gluc)}$ were preliminary defined in a specific range (*Table 5.3*) previously to this thesis work, in line with relevant Chemistry, Manufacturing, and Controls (CMC) guidelines and EMA recommendations. Actually, EMA's regulatory support was requested by means of applying for a Scientific Advice procedure (Procedure No.: EMEA/H/SA/4167/1/2019/SME/III), to receive guidance and direction from EMA on specific questions regarding quality, non-clinical or clinical, and methodological issues. Despite the advanced stage of the pharmaceutical development of LP-RGD-GLA-$S_{(gluc)}$ formulation, several quality attributes still must be investigated and the analytical methods developed for their characterization and quality control in order to continue advancing in the preclinical development and prior the compliant good manufacturing practices (cGMP) production batch to entry the clinical phase. Among them, the proper control of the chemical composition, the bacterial contamination of samples, the drug release, the GLA leakage rate, or the integration efficiency of chol-PEG_{400}-RGD in the vesicular membrane were left as priority properties to characterize and control in further stages of the development of the nanoformulation. Therefore, the analytical development has been continued in this thesis with the aim to well control the aforementioned CQAs of the LP-RGD-GLA-$S_{(gluc)}$ formulation.

Table 5.3. Specification range of the CQAs of LP-RGD-GLA-$S_{(gluc)}$ formulation previously defined to this thesis work. *Investigation of new analytical techniques for the better characterization and control of the pending CQAs.

Critical quality attribute (CQA)	Specification range
Macroscopic appearance	Aqueous dispersion of homogeneous opalescent macroscopically appearance without sediment
Mean particle size	50 – 300 nm
Particle size distribution or polydispersity index (PdI)	≤ 0.45
Particle morphology and lamellarity	Spherical and mostly unilamellar vesicles
ζ-potential (liposome surface charge)	≥ + 20 mV
Drug entrapment efficiency / Free drug substance	High entrapment efficiency (≥ 70 %) and low free drug substance
Total drug content	≥ 0.2 mg/mL
Integration efficiency of chol-PEGn-RGD in the vesicular membrane*	High integration efficiency (≥ 70 %)
pH	5.0 – 6.5
Dispersion stability	Enough stability for carrying out preclinical studies (range from 2 to 8 weeks). In terms of turbidimetry stability, the turbiscan stability index (TSI) should be less than 10.0 at 24 h
Osmolality	260 – 300 mOsm/kg
Chemical composition*	Near to the theoretical molar ratio of DPPC:Chol:Chol-PEG_{400}-RGD (10:6.5:0.5) + 0.3 mg/mL MKC, i.e. recoveries of membrane component around 70 – 100%
Lipid and GLA degradation products*	Pending to be defined
Bioactivity or specific enzymatic activity (EA)	Bioactive (ratio referred to the EA of Replagal® ≥ 0.5
Biocompatibility	Lack of hemolytic activity and cytotoxicity
Drug release rate*	Pending to be defined
Drug leakage rate*	Pending to be defined
Microbiological quality*	Sterile and with endotoxin levels < 1 EU/mL

The rationale behind the necessity to characterize and control these CQAs marked with an asterisk is:

- Integration efficiency of chol-PEG_{400}-RGD targeting ligand in the vesicular membrane: the amount of targeting peptide moiety integrated in the lipid bilayer must be enough to permit the interaction of LP-RGD-GLA-$S_{(gluc)}$ with cells and facilitate the uptake by the tissue of interest, minimizing the off-targeted biodistribution of the formulation. So far, only the total concentration of chol-PEG_{400}-RGD in samples could be determined as a bulk by reversed-phase high-performance liquid chromatography-evaporative light scattering detector (RP-HPLC-ELSD). In order to corroborate the feasibility to detect the targeting moiety inside liposome membranes, distinct liposomal samples have been subjected during this thesis to an initial examination with the Single Particle Automated Raman Trapping Analysis (SPARTA®) methodology developed by the Molly Stevens' group (Stockholm, Sweden) and exploited by the Sparta Biodiscovery spin-out company (Imperial College London, UK). These results can be found in ***Annex II***.

- Liposomal chemical composition: necessary to determine the specific concentration of material injected in a defined dose at clinical level. In this thesis, the membrane composition of LP-RGD-GLA-$S_{(gluc)}$ formulation has been assessed by the development, optimization and validation of RP-HPLC-ELSD analytical method. Meanwhile, the concentration and entrapment efficiency of GLA-S in nanoliposomes is determined by Leanbio SL through a reverse phase-high-performance liquid chromatography-ultraviolet spectroscopy (RP-HPLC-UV) method developed in their facilities (described in ***Chapter 7, Section 7.2.6.3***).
- Lipid and GLA-S degradation products: the chemical stability of the lipid components and drug substance is important to maintain the physicochemical, colloidal and biological properties of liposome formulations. As drug delivery systems (DDS), liposomes should ensure a minor degradation of the encapsulated GLA-S enzyme versus their soluble pharmaceutical form. In ***Chapter 4***, good quality liposomes have been shown to have protective capacity against GLA-S degradation (API of the nanoformulation) through the use of an *in vitro* trypsinization assay. In this way, the detection of potential degradation products capable to impair the safety profile of the formulation, and the potential environmental factors capable to induce their generation are crucial to proper define the storage conditions and expiration date of drug products. During this thesis, a very preliminary study has been initiated to start with the identification of potential degradation products from the liposomal membrane components after their submission under stress conditions, by using RP-HPLC-ELSD approaches (explained on ***Annex I***). In parallel, the GLA-S degradation products will be studied through RP-HPLC-UV procedures by Leanbio SL in the frame of the European Phoenix project.
- GLA-S release profile in specific media: to ensure batch-to-batch reproducibility, GLA-S release profile from liposomal membranes must be consistent in a same media tested between production batches. Herein, a separation procedure based on filtration-centrifugation have been set-up to efficiently separate the entrapped GLA-S in liposomes from the released one. Initial characterizations diluting samples in relevant physiological media have also studied in this chapter.
- GLA-S leakage rate in storage conditions: GLA-S must remain integrated in liposomal membranes during the storage conditions, or at least minimally released to avoid the impairment of the liposomal formulation stability. Similarly, to the previous described in the GLA-S release testing, stored aliquots of nanoliposomal formulations without further manipulation have been submitted to filtration-centrifugation procedures during this thesis work to perform an initial analysis to assess the GLA-S leakage rate from liposomes.
- Microbiological contamination and bacterial endotoxins: parameter influencing the quality and safety of the drug product. As parenteral dosage form, LP-RGD-GLA-S product must be sterile and pyrogen-free.

In terms of microbiological contamination, samples must present 0 CFU/mL or be sterilized if some bacterial contamination is detected. Moreover, samples must be endotoxin-free or at least contain endotoxin levels < 1 EU/mL. In this thesis, the use of Luria Broth (LB) agar plates and Gel clot Limulus Amebocyte Lysate (LAL) assay have been explored to respectively control both parameters.

Along with the objective of the European Phoenix project to enhance the quality of LP-RGD-GLA-$S_{(gluc)}$ formulation, the main purpose of the work performed in this chapter was to develop, investigate and/or validate robust analytical methodologies for the robust characterization and quality control of the LP-RGD-GLA-$S_{(gluc)}$ nanoformulation during its development. These contributions are intended to help in the advance of the LP-RGD-GLA-$S_{(gluc)}$ product translation up to clinical phases (TRL-6 stage).

5.2. Development, optimization and validation of an analytical RP-HPLC-ELSD method to quantify and control the liposomal membrane composition of GLA nanoliposomal formulations

The analysis and control of the chemical composition regarding membrane nanovesicle components are one of the most crucial CQA to well monitor the nanoparticle batch-to-batch reproducibility, or the integration capacity of certain molecules related with slight compositional changes on a complex nanoformulation.

In this thesis, a new promising analytical RP-HPLC-ELSD method has been developed and further optimized to simultaneously detect and quantify the four membrane components of the LP-RGD-GLA-$S_{(gluc)}$ liposomal matrix formulations with high precision using a unique multi-step gradient. To ensure the reliability of the developed methodology, few validations tests following ICH Q2 (R2) and Q14 were conducted as a preliminary stage of method validation[10,11]. According to ICH guidelines the most important chromatographic and method parameters to control during method development and validation steps are:

- **Resolution:** it refers to the peak separation and the capacity to distinguish two components. Proper resolution should present values > 1.5 (or > 2 if possible).
- **Asymmetry (A_S):** it is a measure of the peak symmetry. The closer to 1.0 the more symmetric would be a chromatographic peak. Acceptable values are $0.8 \leq A_S \leq 1.5$.
- **Suitability of the equipment:** capacity to ensure a proper reproducibility of the equipment for measurements. The analysis of at least 6 injections of a standard solution is required to control retention times (RT) with variations lower than 1 % and peak symmetry (by checking values of USP tailing factor) smaller than 1.5.

- **Selectivity:** ability to distinguish unequivocally each component of study in the presence of other molecules which may be expected to be present in the matrix analyzed. The comparison of both, real sample and standard solutions, is required to confirm the complete separation of all analytes.
- **Linearity of an analytical procedure:** it is the fact of obtaining signals directly proportional to the concentration of a tested substance in a given range of concentrations. Proper linearity should have correlation coefficient (R^2) values > 0.9990. It is usually tested by preparing the calibration curve per triplicate at the usual working concentration.
- **Precision:** parameter that expresses the repeatability of a method by injecting standard solutions at different concentrations, by different analysts and/or different days of work.
- **Robustness:** capacity of a chromatogram to remain unaltered by small changes in method parameters, such as the temperature of the column, the injection volume or other modifications. This study is normally performed using triplicates of a sample.
- **Stability of the samples:** once prepared in the HPLC vials at a specific storage temperature. It helps to understand for how long the solution is stable before injecting.
- **Accuracy of an analytical method:** it refers to the degree of nearness between the "real" concentration of molecules in a sample and the experimental value determined by the method. Accuracy is often determined by measuring standards with known concentrations and comparing them with the measured values. An acceptable accuracy should have recovery values between 90-110 % (or 95-105 % if possible).

Once the RP-HPLC-ELSD method would be developed, and in parallel, the definitive pharmaceutical form of LP-RGD-GLA-S formulation would be established, in the frame of the Phoenix project this method will be first adapted to the definitive formulation composition, and then, transferred to Nanomol Technologies SL (Barcelona) and completely validated there under GMP conditions with a validated HPLC equipment.

5.2.1. RP-HPLC-ELSD method development: achieving molecule separation with good resolution

Before starting with a chromatographic method development, it is important to know well the physicochemical properties of the molecules of study to predict the solvents and column nature that would probably work properly with our formulations. As already described above and schematized in ***Figure 5.2***, the membrane of LP-RGD-GLA-S liposomal formulations are composed by 4 components: 1,2-dipalmitoyl-sn-glycero-3-phosphocholine (DPPC), cholesterol (chol), cholesterol-polyethylene glycol $(PEG)_{400}$-Arginine-Glycine-Aspartic (chol-PEG_{400}-RGD), and miristalkonium chloride (MKC).

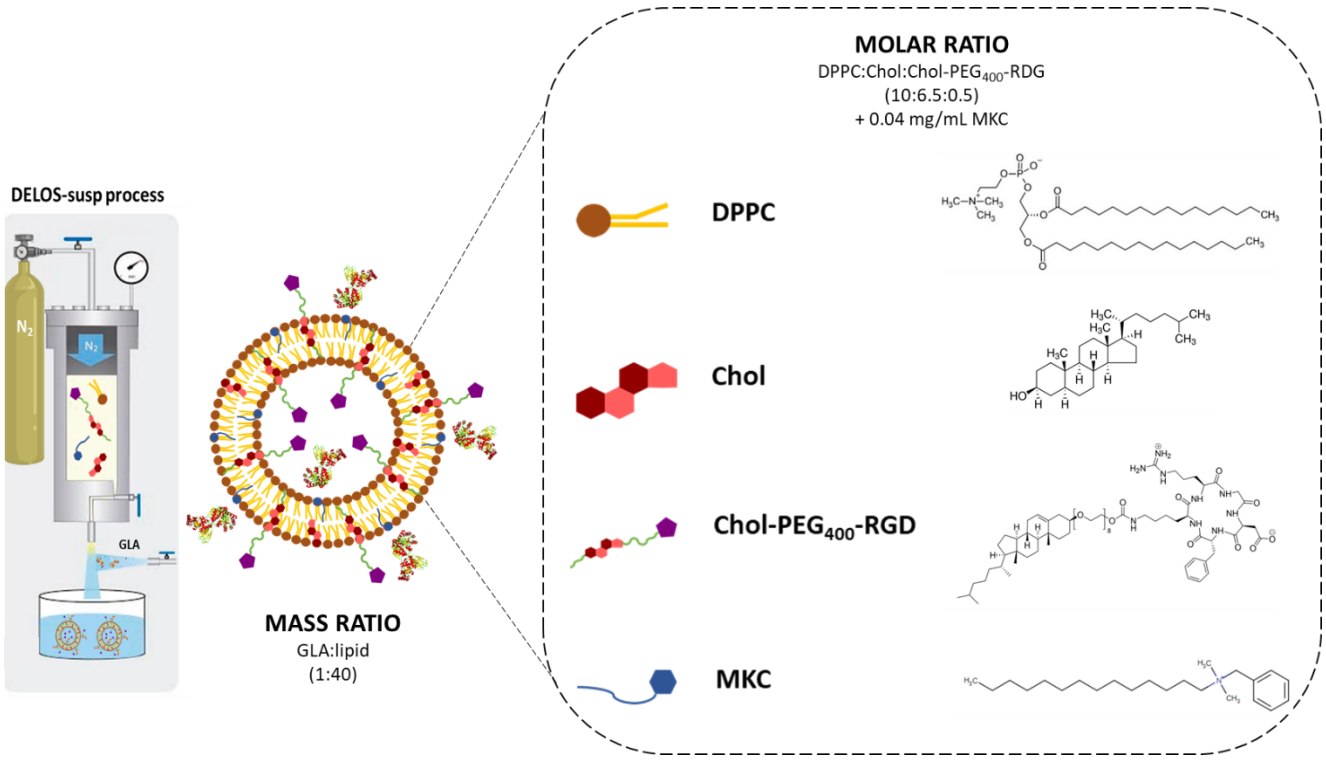


Figure 5.2. Graphic representation of LP-RGD-GLA-S liposomes. The most advanced liposomal chemical composition is shown, with highlighted GLA:lipid mass ratio, and molar ratio between membrane components.

In this thesis, reverse phase chromatography (RP-HPLC) has been chosen as a promising approach for the separation of molecules in terms of solubility. According to the hydrophobicity degree of the different membrane components (*Table 5.4* and *Figure 5.3*), DPPC and cholesterol molecules should be more retained in RP-HPLC stationary phases than chol-PEG_{400}-RGD and MKC.

Table 5.4. Solubility chemical properties to consider during a chromatographic method design[12–14]. ₸ Predicted values from public data bases; § Experimental values from literature.

PROPERTIES	MKC	Chol-PEG_{400}-RGD	Chol	DPPC
Water solubility (mg/mL)	> 1 §	Very poor solubility	0.095 §; $2.79 \cdot 10^{-5}$ ₸	Very poor solubility §; $2.4 \cdot 10^{-5}$ ₸
Log P	3.52 ₸	N.D.	7.11 ₸	8.11 ₸
pKa	18.11 ₸	N.D.	-1.4 ₸	1.86 ₸; -6 ₸
MW (g/mol)	368.05	1369	386.66	734.04

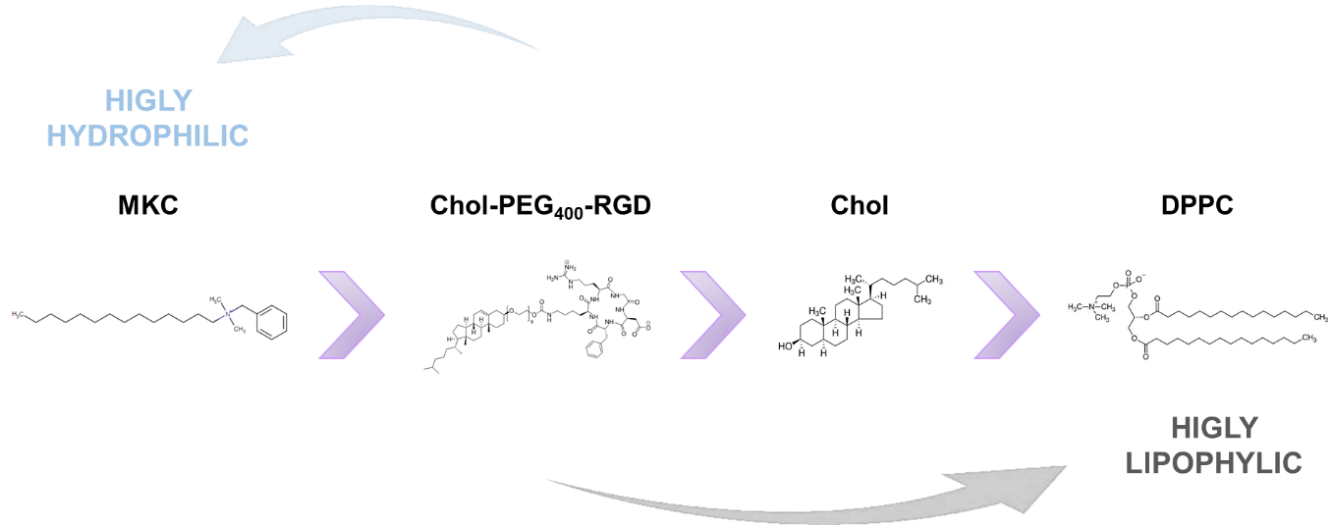


Figure 5.3. Chemical structure of the membrane compounds sorted by polarity properties.

Among the popular stationary phases usually bonded to silica gel for HPLC purposes (*Table 5.5*), the most common carbon chain bonded phase to separate small molecules is C18 (octyldecylsilane)[15,16]. However, C4 short-chain RP-HPLC columns have demonstrated to be efficient in the separation of large solutes, such as proteins or synthetic cholesterol-peptides conjugates[17]. Regarding the presence of synthetic chol-PEG_{400}-RGD conjugate and recombinant GLA enzyme in the liposomal formulations studied in the present chapter, Symmetry300 C4 HPLC columns (Agilent Technologies, USA) were chosen for the development of an RP-HPLC methodology.

Table 5.5. Compilation of the most common carbon chain bonded phase used as stationary phases in HPLC. Adapted from[15,16].

STATIONARY PHASE	Relative usage (%) in HPLC
C18 (octadecylsilane)	39
C8 (octyl)	26
Cyanopropyl	14.5
Phenyl	12
C4 (butyl)	3.7
Hydrophobic interaction	1.8
C2 (ethyl)	1.1
C1 (methyl)	0.8
Other	0.8
Polymers	0.5

The most advanced LP-RGD-GLA-$S_{(gluc)}$ nanoformulation stored as an aqueous liquid dispersion, which achieved preclinical phase (TRL-5) during the European Smart4Fabry project, was used during the RP-HPLC-ELSD method development to study the feasibility of C4 columns to resolve the liposomal components. The complete manufacturing process of LP-RGD-GLA-$S_{(gluc)}$ prototype is represented as a flow diagram in ***Figure 5.4***.

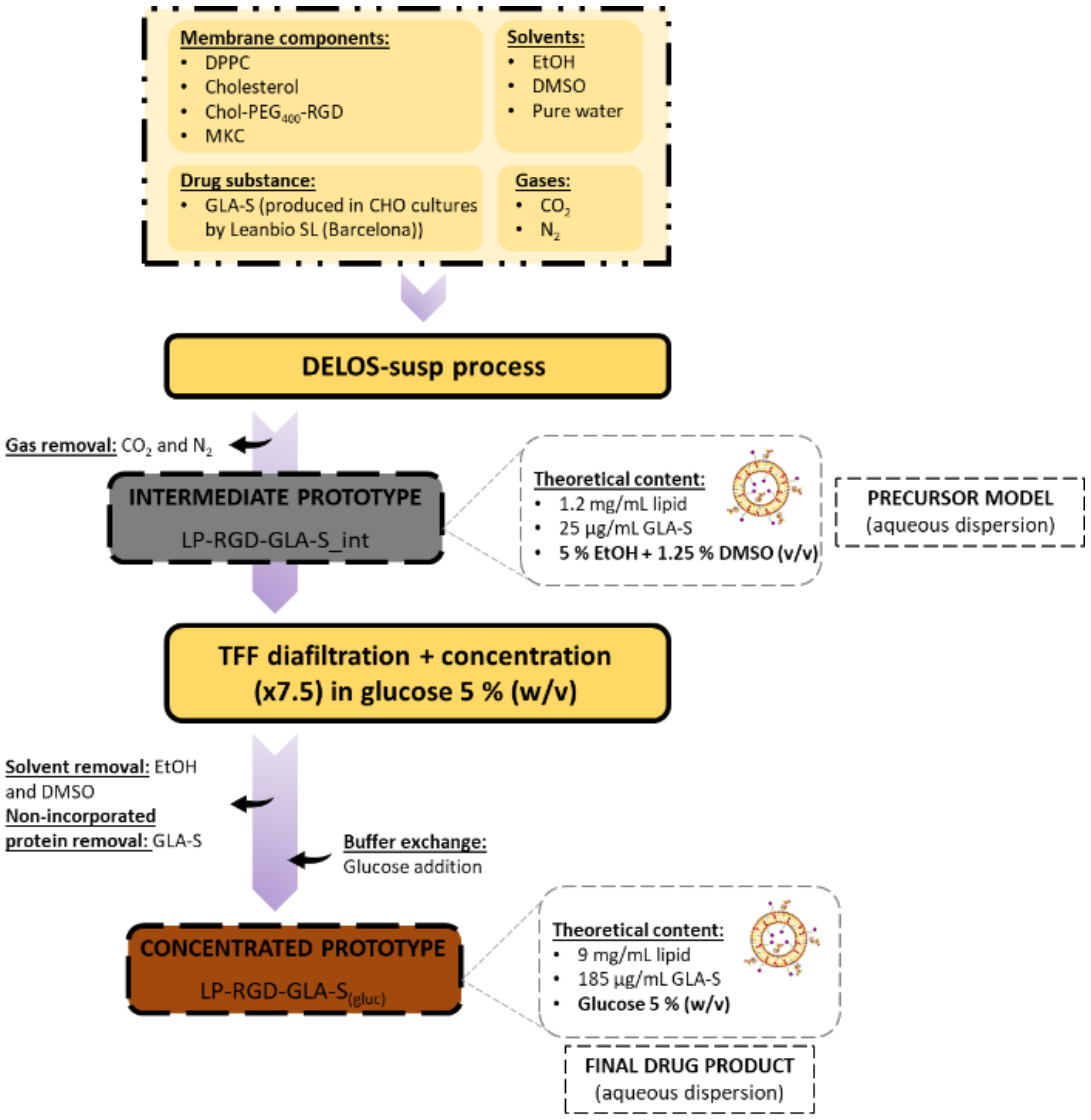


Figure 5.4. Process flow diagram to produce intermediate prototype (LP-RGD-GLA-S_int) and concentrate prototype (LP-RGD-GLA-$S_{(gluc)}$). Raw materials used and removed substances during liposome manufacturing are also indicated.

Herein, a gradient-based RP-HPLC-ELSD method capable to simultaneously separate and identify the 4 membrane components that conform LP-RGD-GLA-S liposomes, was developed as first step (described as Method_001 in ***Table 7.11, Chapter 7, Section 7.4.5.6***. As described in ***Figure 5.5***, this method used 0.01 % (v/v) formic acid (HCOOH) in water as the mobile phase A (MP_{A1}), and 0.07 % (v/v) HCOOH in acetonitrile (ACN) as the mobile phase B (MP_{B1}). The stationary phase consisted of a Symmetry300 C4 5 µm, 4.6 x 250 mm column.

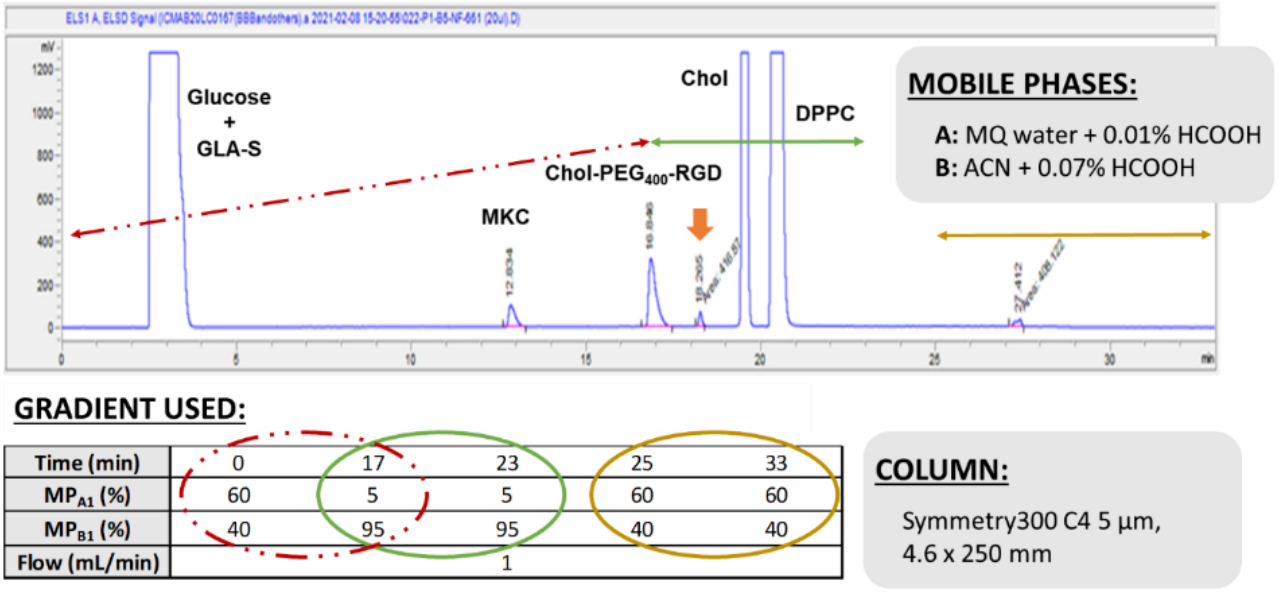


Figure 5.5. RP-HPLC-ELSD chromatogram obtained from analyzing LP-RGD-GLA-$S_{(gluc)}$ with RP-HPLC-ELSD Method_001 (33 min time of analysis, using a C4 column of 250 mm, HCOOH acid in the mobile phases, and the flow rate and gradient protocol shown in the respective table). Orange arrow represents the detection of cholesterol-related impurities. Increasing gradient is highlighted with discontinuous red lines, and isocratic phases with green and yellow straight lines. The percentage of MP_{B1} required to elute each analyte is correlated in colours code with the respective table.

In order to correlate the membrane components with each chromatograph peak, the peak selectivity was analyzed by using standards of each vesicle membrane component as controls (data not shown).

The most important limitation of Method_001 detected was the time-consuming analysis for each run (33 min). Moreover, Method_001 used an ELSD instead of a UV-vis detector to avoid probable absorbance overlap problems between the membrane components and the organic solvent used in mobile phase B, since pure MKC, chol, chol-PEG_{400}-RGD and DPPC present near UV absorbance cut-off wavelength (from 205 to 220 nm in general) to the ACN solvent (190 nm) used for their chromatographic elution[17–22]. It is important to take into account that the signal-response of an ELSD is exponential. Due to DPPC and cholesterol are present in LP-RGD-GLA-S formulations in higher molar ratios than MKC and chol-PEG_{400}-RGD, 2 different injection volumes were required to well quantify both set of components for each liposomal sample (without reaching signal saturation from the most concentrated compounds). For these reasons, further optimization of Method_001 was carried out in order to offer advantages in terms of time consuming, cost saving, and robustness.

5.2.2. RP-HPLC-ELSD method optimization: reduction of time-consuming analysis and improvement of chromatographic parameters according to ICH guidelines

To better understand the control of the RP-HPLC-ELSD parameters over the chromatographic elution of the membrane components of interest (DPPC, chol, chol-PEG_{400}-RGD and MKC), without being influenced by the glucose presence, LP-RGD-GLA-$S_{(w)}$ formulation diafiltrated by TFF in water as dispersant medium instead of glucose 5 % (w/v) was used to reduce the time of analysis of the previously developed RP-HPLC-ELSD method and optimize its chromatographic parameters. Then, the optimized parameters were extrapolated to the other aforementioned liposome matrixes used during the European Phoenix project. The complete manufacturing process of LP-RGD-GLA-$S_{(w)}$ prototype is remembered in ***Figure 5.6***.

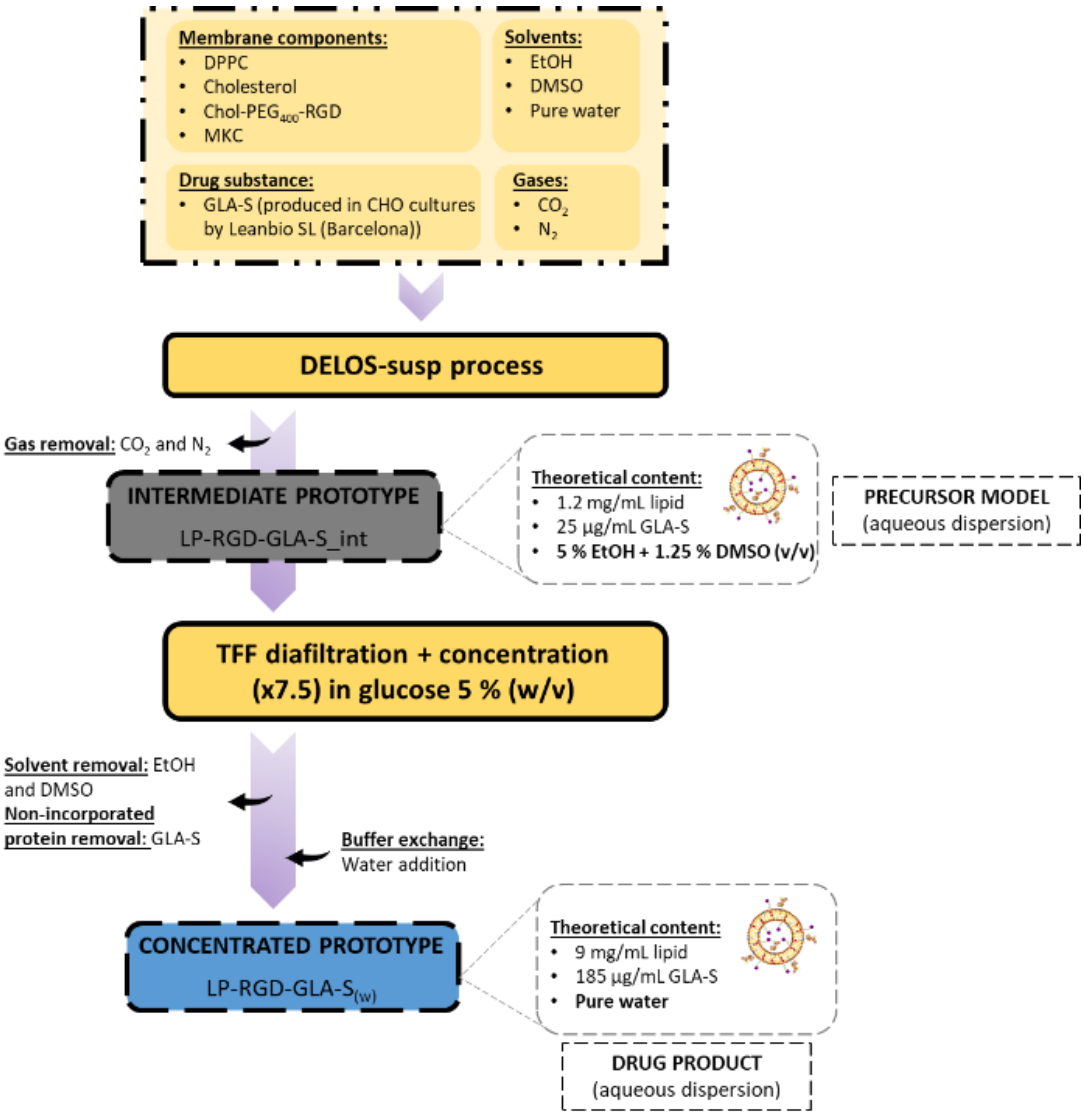


Figure 5.6. Process flow diagram to synthetize intermediate LP-RGD-GLA-S_int and concentrate LP-RGD-GLA-$S_{(w)}$ prototypes. Raw materials used and removed substances during liposome manufacturing are also indicated.

In this regard, the impact of factors such as column length, solvent flow and detector selection were investigated to reduce the analysis time of the RP-HPLC-ELSD method.

- **Length of the HPLC column:** Symmetry 300 C4 column of 250 mm used in Method_001 was substituted by a shorter Symmetry 300 C4 column of 150 mm, reducing both, time of analysis and solvent expenditure. The method was transferred from a column to another by using the Column Calculator Version 2.0 software from Waters, USA[23].
- **Solvent flow:** method flow was increased from 1 to 1.3 mL/min without modifying peak resolution, reducing the time of analysis.
- **Detector selection:** the simultaneous use of ELSD and diode array detector (DAD) was investigated for just using a unique injection volume to detect all the membrane components for each sample of study. DAD detection is based on lineal signal-response by UV-Vis absorbance of molecules. However, DPPC cannot be detected by UV-Vis absorbance (*Figure 5.7*), and 2 injections for each sample using ELSD was still required.

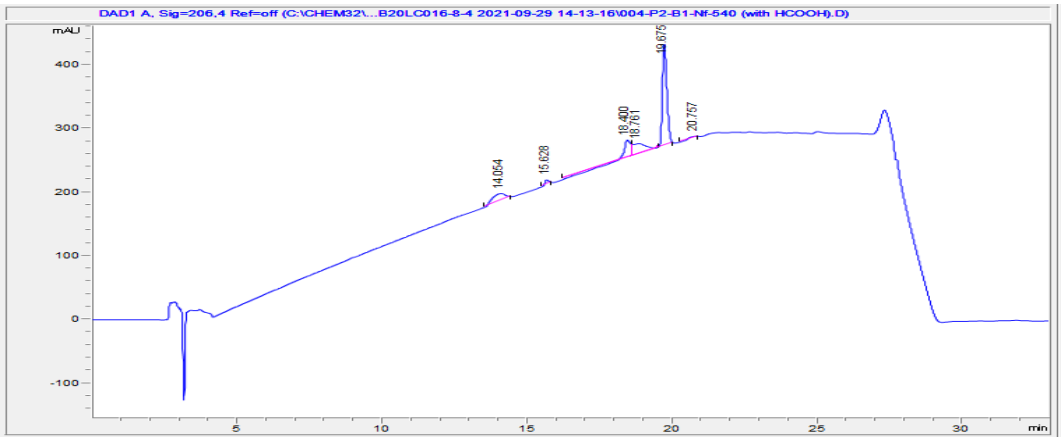


Figure 5.7. RP-HPLC-UV chromatogram obtained from analysing LP-RGD-GLA-$S_{(w)}$ with DAD using Method_001 (explained in *Chapter 7, Section 7.4.5.6*). Less quality of chromatographic peaks was obtained respect to ELSD signal, due to HCOOH absorbance at $\lambda \approx 200$ nm. Non DPPC detection by DAD.

Once optimized the method in terms of analysis time, further method optimization was carried out to achieve high quality chromatographic parameters according to ICH Q2 (R2) and Q14 guidelines[10,11]. To ensure precise, accurate and reproducible results (and fulfil some chromatographic regulations) the control of the chromatographic parameters is mandatory. According to ICH guidelines, retention time, resolution and asymmetry are the most important parameters to monitor during a method development, meanwhile others should be established during method validation procedures. During the optimization process, the overall obtained specifications for the 4 analyzed compounds (and their criteria of acceptance shown in brackets) were:

- ❖ Percentage of relative standard deviation (% RSD) of RT < 1.0 % (≤ 1.0 %).
- ❖ Peak resolution > 2.0 (≥ 2.0).
- ❖ USP tailing value for A_S evaluation of 0.8 – 1.3 (0.8 – 1.5).

Therefore, the following factors have been modified to improve chromatographic parameters according to the already described specifications:

- **Mobile phases composition:** the HCOOH used in the mobile phases from Method_001 was substituted by trifluoroacetic acid (TFA), obtaining sharper chromatographic peaks with improved symmetry. This change was also impact on the requirement of injection volume modification from Condition_1 to Condition_2 (described in ***Chapter 7, Section 7.4.5.6***). Briefly, two injection volumes were still required: one of 15 µL to quantify cholesterol, chol-PEG_{400}-RGD and MKC molecules, and another of 3 µL for DPPC analysis.
- **Gradient modifications:** a new multi-step gradient (described as Elution_2 in ***Chapter 7, Section 7.4.5.6***) to allow the elution of molecules in isocratic conditions instead of gradient conditions. This fact also played a role improving the symmetry of chromatographic peaks and their resolution.
- **Controlled temperature on HPLC column:** the controlled temperature of the stationary phase was increased from 25 to 35ºC, improving the robustness in retention times.
- **Adjustments in ELSD settings:** changes on gain, evaporator and nebulizer temperatures, gas flow rate, data rate and smoothing also enhanced resolution and peak symmetry. However, with ELSD Agilent equipment, detector parameters can be modified in accordance with few pre-established values, hindering the achievement of conditions to be capable to quantify the 4 membrane components of interest in only one injection volume. This issue will be considered in further steps in the frame of the European Phoenix project, once the method will be transferred to a GMP-compliant HPLC equipment from Nanomol Technologies SL.

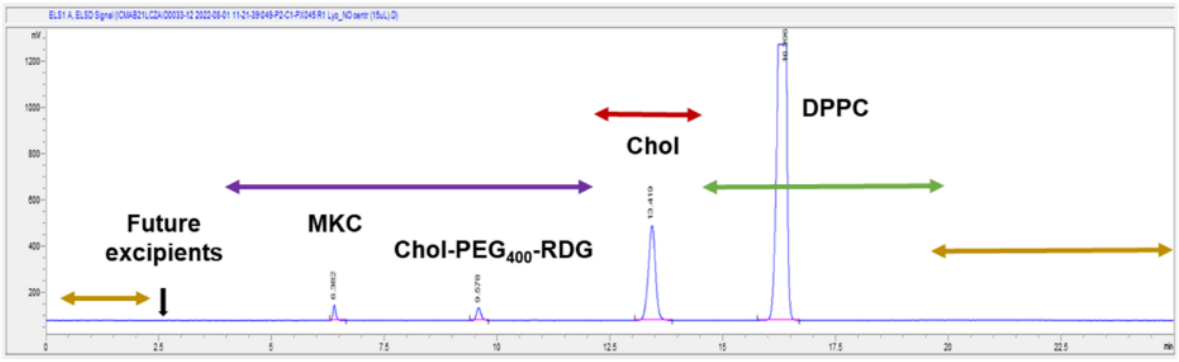
As a result of this optimization work in which various parameters were modified, the 33 min of analysis from Method_001 were reduced to a new 25 min procedure (described as Method_002 in ***Table 7.11, Chapter 7, Section 7.4.5.6***). Additionally, better chromatographic parameters were achieved meeting specifications (see ***Figure 5.8***).

COLUMN:

Symmetry300 C4 5 µm,
4.6 x 150 mm

MOBILE PHASES:

A: MQ water + 0.01% TFA
B: ACN + 0.07% TFA



GRADIENT USED:

Time (min)	0	2.5	4	12.5	12.8	17	17.01	20	21	25
MP_{A2} (%)	50	50	30	30	20	20	5	5	50	50
MP_{B2} (%)	50	50	70	70	80	80	95	95	50	50
Flow (mL/min)	1.3									

Figure 5.8. RP-HPLC-ELSD chromatogram obtained from analysing LP-RGD-GLA-$S_{(w)}$ with HPLC-ELSD Method_002 (25 min time of analysis, using a column of 150 mm, TFA acid in the mobile phases, and the flow rate and gradient protocol shown in the respective table). Black arrow represents the retention time where glucose and GLA-S molecules should be detected when analysing LP-RGD-GLA-$S_{(gluc)}$ in future. The different isocratic phases of the gradient method are highlighted with colour arrows. The percentage of MP_{B2} required to elute each analyte is correlated in colours code with the respective table. As a summary, development and optimization steps of the method chromatographic conditions were concluded with the modifications indicated in the next *Table 5.6*.

Table 5.6. Modifications of the chromatographic conditions applied during RP-HPLC-ELSD optimization procedure. *Elution conditions are detailed in previous *Figure 5.5* and *Figure 5.8*, but also in *Chapter 7, Section 7.4.5.6*. Legend: SLM means standard liter per minute; PMT means photomultiplier tubes.

CHROMATOGRAPHIC CONDITIONS	BEFORE	OPTIMIZED
Mobile phase A (MP_A)	0.01 % (v/v) HCOOH in water	0.07 % (v/v) HCOOH in ACN
Mobile phase B (MP_B)	0.01 % (v/v) TFA in water	0.07 % (v/v) TFA in ACN
Initial gradient conditions (% MP)	60 % MP_A + 40 % MP_B*	50 % MP_A + 50 % MP_B*
Solvent flow	1 mL/min	1.3 mL/min
Chromatographic column (length)	Symmetry300 C4 5 µm, 4.6 x (250 mm)	Symmetry300 C4 3.5 µm, 4.6 x (150 mm)
Column temperature	25 ºC	35 ºC
Injection volume (component detection)	20 µL (MKC and chol-PEG_{400}-RGD) 1.0 µL (Chol and DPPC)	15 µL (MKC, chol-PEG_{400}-RGD, chol) 3.0 µL (DPPC)
Analytical run time	33 min	25 min
Detector of choice	ELSD	ELSD
Detector parameters	ELSD parameters	ELSD parameters
» Evaporator temperature	» 80 ºC	» 80 ºC
» Nebulizer temperature	» 40 ºC	» 42 ºC
» Gas flow rate	» 1.00 SLM	» 1.60 SLM
» Data rate	» 40 Hz	» 10 Hz
» Smoothing	» 40	» 30
» PMT Gain	» 8	» 5
LIPOSOMAL MATRIX ANALYZED	**LP-RGD-GLA-$S_{(gluc)}$**	**LP-RGD-GLA-$S_{(w)}$**

5.2.3. Sample preparation protocol optimization: ensuring proper analyte solubilization and maintenance of good quality chromatogram parameters

Regarding sample preparation during the preceding steps of method development and optimization, liposomal formulations were lyophilized previously to their analysis following the sample preparation Strategy_2 procedure (described at ***Chapter 7, Section 7.4.5.6***) similarly to Ruiz-Garcia *et al.*[24]. The water removal has the objective to ensure a proper solubilization of the hydrophobic components with MeOH on sample preparation step. However, lyophilization process is a time consuming step for sample preparation that was explored whether it can be dispensable.

Another matter to take into account is the presence of protein in the samples. The intended liposomal LP-RGD-GLA-S formulations to be analyzed by RP-HPLC-ELSD contain the recombinant GLA-S. Concerning the hydrophobic stationary phase C4 which is bonded to a surface of silica-gel, residual silanols (***Figure 5.9***) can be present and induce probable analyte-surface interactions. Specially in short-chain C4 phases the adsorption and accumulation of protein material can occur causing column fouling[15,16]. In this section, the possibility and necessity to eliminate GLA-S presence from samples to avoid future interfering on HPLC chromatographic parameters has been also studied.

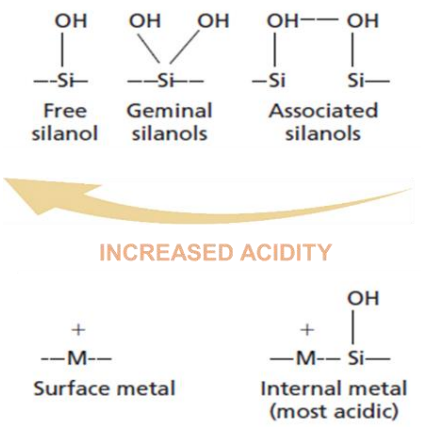


Figure 5.9. Types of silanols on the surface of silica gel where the hydrophobic stationary phase is bonded. Adapted from[15,16].

In general, sample preparation for liposomal concentrated prototypes was conducted by diluting samples in pure MeOH (or mixtures MeOH:ACN with increasing concentrations of ACN, detailed in this section when necessary). Sample:solvent ratio was precisely leveled up to 1:10 by using volumetric flasks. Then, samples were sonicated 10 min to well solubilize the vesicle membrane components.

In order to investigate the necessity of water or protein removal from samples for accurate RP-HPLC-ELSD analysis, four different strategies of sample preparation were explored in this thesis (as described in ***Chapter 7, Section 7.4.5.6***) and compared with the purpose of optimizing the original protocol (Strategy_2). The main differences between strategies were: i) to perform the sample freeze-drying before its dilution with organic solvent (for water removal), or ii) add a sample centrifugation step (30 min, 3000 g at 4 ºC, or other if indicated) after sonication (for GLA-S removal). Briefly, the four compared strategies were:

i. **Strategy_1:** Non-lyophilization, neither centrifugation of liposomal sample.
ii. **Strategy_2:** Lyophilization, but non-centrifugation of liposomal sample.
iii. **Strategy_3:** Non-lyophilization, although centrifugation of liposomal sample.
iv. **Strategy_4:** Lyophilization, and also centrifugation of liposomal sample.

The different matrixes of concentrated and lyophilized liposomal prototypes produced in the European Phoenix have been tested in this section. The complete manufacturing process of these prototypes is schematized in ***Figure 5.10***.

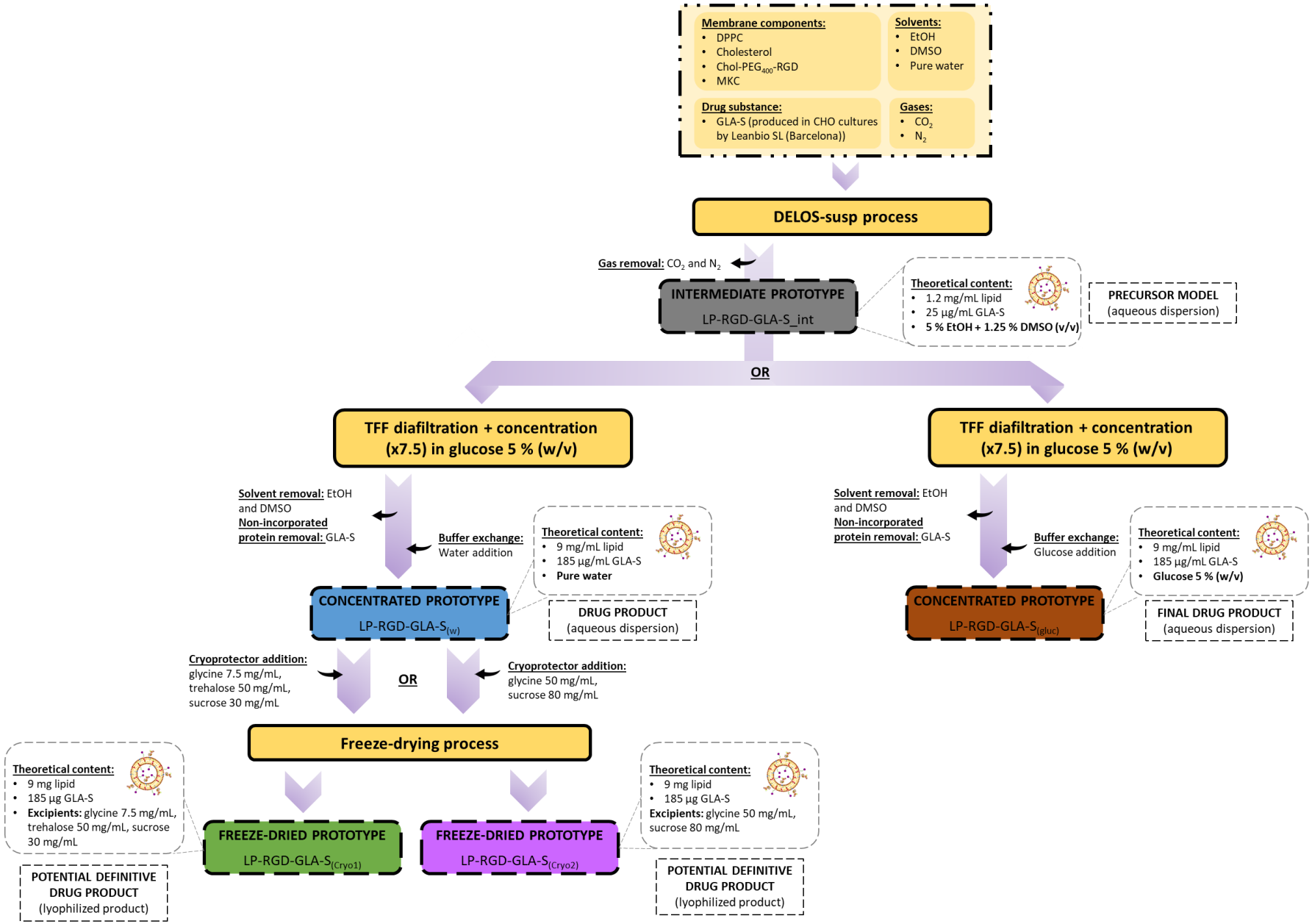


Figure 5.10. Process flow diagram to prepare the intermediate prototype (LP-RGD-GLA_int), concentrated prototypes (LP-RGD-GLA-$S_{(w)}$ and LP-RGD-GLA-$S_{(gluc)}$), or freeze-dryied prototypes (LP-RGD-GLA-$S_{(Cryo1)}$ and LP-RGD-GLA-$S_{(Cryo2)}$). Raw materials and removed substances during liposome manufacturing are also indicated.

Enzyme removal based on protein precipitation approach

Effective protein removal method based on precipitation due to presence of organic solvents is well known in literature[25–27]. ACN is found as an efficient organic solvent to induce protein precipitation.

As described on sample preparation for RP-HPLC-ELSD measurement in ***Chapter 7, Section 7.4.5.6***, normally, samples were diluted with MeOH to ensure a total solubilization of the vesicle membrane components. However, to achieve an effective GLA-S removal method based on protein precipitation, several mixtures of MeOH:ACN with increasing concentrations of ACN were tested and described in this chapter.

Starting with LP-RGD-GLA-$S_{(w)}$ samples in aqueous dispersion or previously lyophilized (to avoid the presence of water), the best working conditions for the precipitation of the GLA-S enzyme were investigated (i.e. different centrifugation conditions and percentages of organic solvents were used, as shown in ***Table 5.7***). According to the obtained results, the conditions that seem better to precipitate the GLA-S are the ones in which samples in aqueous dispersion (without being previously lyophilized) are used, and then treated with 95% of MeOH + 5% ACN (v/v) to solubilize the sample, and centrifuged at 3000 x g. These conditions allowed 86% of enzyme precipitation.

Table 5.7. Summary of different condition to precipitate the GLA-S enzyme in LP-RGD-GLA-$S_{(w)}$ samples. GLA-S quantification of each sample was measured in triplicate by SDS-PAGE and further TGX analysis.

Formulation tested	Previous sample lyophilization?	Solvent (v/v)	Sample dilution factor	Centrifugal force (x g)	Replicates analyzed	GLA-S precipitated (%)
LP-RGD-GLA-$S_{(w)}$	Yes	100 % MeOH	10	3000	2	36 ± 7
	No	100 % MeOH	10	3000	2	77 ± 20
	Yes	100 % MeOH	10	15000	2	22 ± 0
	No	100 % MeOH	10	15000	2	74 ± 12
	Yes	95 % MeOH / 5 % ACN	10	3000	2	65 ± 1
	No	95 % MeOH / 5 % ACN	10	3000	6	86 ± 9
	Yes	75 % MeOH / 25 % ACN	10	3000	2	33 ± 2
	No	75 % MeOH / 25 % ACN	10	3000	4	70 ± 7
	Yes	50 % MeOH / 50 % ACN	10	3000	0	-
	No	50 % MeOH / 50 % ACN	10	3000	3	70 ± 7

Nowadays, the main intended liposomal formulation to be analyzed by RP-HPLC-ELSD is the LP-RGD-GLA-$S_{(gluc)}$ which contains glucose 5% (w/v) as isosmotic agent, being the most advanced in formulation development. However, in the frame of the European Phoenix project this RP-HPLC-ELSD method is also intended to be adapted for the analysis of the definitive lyophilized pharmaceutical form of LP-RGD-GLA-S formulation, which still is in development. Therefore, same analysis was reproduced using the most efficient solvent mixture MeOH:ACN 95:5 (v/v) to induce GLA-S precipitation (***Table 5.8***) in LP-RGD-GLA-$S_{(gluc)}$, but also in both LP-RGD-GLA-$S_{(Cryo1)}$ and LP-RGD-GLA-$S_{(Cryo2)}$ promising formulations. Results showed that sugars present in samples are stabilizing the protein, hindering the protein precipitation capacity in both, dispersion and lyophilized samples.

Table 5.8. Summary of different conditions to precipitate the GLA-S enzyme in LP-RGD-GLA-$S_{(gluc)}$, LP-RGD-GLA-$S_{(Cryo1)}$ and LP-RGD-GLA-$S_{(Cryo2)}$ samples. GLA-S quantification of each sample was measured in triplicate by SDS-PAGE and further TGX analysis.

Formulation tested	Previous sample lyophilization?	Solvent (v/v)	Sample dilution factor	Centrifugal force (x g)	Replicates analyzed	GLA-S precipitated (%)
LP-RGD-GLA-$S_{(gluc)}$	Yes	95 % MeOH / 5 % ACN	10	3000	3	22 ± 3
	No	95 % MeOH / 5 % ACN	10	3000	3	23 ± 3
LP-RGD-GLA-$S_{(Cryo1)}$	Yes	95 % MeOH / 5 % ACN	10	3000	3	13 ± 1
	No	95 % MeOH / 5 % ACN	10	3000	3	13 ± 2
LP-RGD-GLA-$S_{(Cryo2)}$	Yes	95 % MeOH / 5 % ACN	10	3000	3	14 ± 3
	No	95 % MeOH / 5 % ACN	10	3000	3	15 ± 1

Due to the difficulties to establish a precipitation protocol for GLA-S in liposomal formulations containing sugars, a study was also performed to investigate how the GLA-S presence can influence on the system suitability, future column damage, and therefore, alterations on chromatographic parameters. With this proposal, 40 serial injections of empty liposomes LP-$RGD_{(w)}$ (without GLA-S containing), followed by 40 serial injections of GLA-loaded liposomes LP-RGD-GLA-$S_{(w)}$ (containing GLA-S protein) were analyzed (***Figure 5.11***). Results demonstrated that the presence of GLA-S enzyme was not impairing chromatographic parameters such as the peak symmetry or resolution (***Table 5.9***). Therefore, there should be no need of sample centrifugation to induce GLA-S precipitation during sample preparation for RP-HPLC-ELSD measurements, decreasing the probability of material loss by extra handling. This also facilitate the sample preparation procedure in terms of less time dedication.

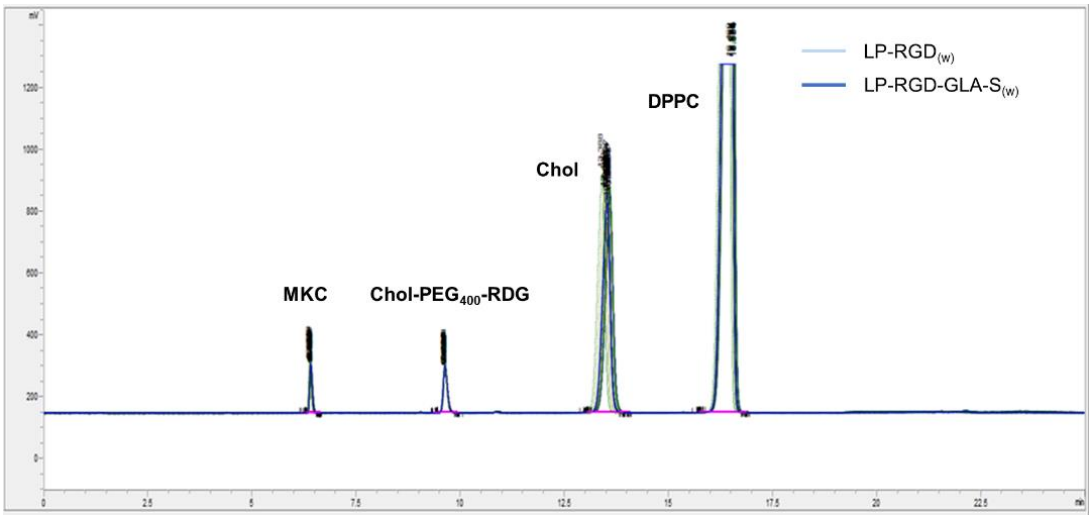


Figure 5.11. Superposition of the chromatograms obtained after the analysis of 40 successive injections of LP-RGD$_{(w)}$ and LP-RGD-GLA-S$_{(w)}$ nanoliposomal formulations, in which it is clearly observed that the GLA presence does not impact on chromatographic parameters such as selectivity, symmetry and resolution of the peaks.

Table 5.9. System suitability of retention time and symmetry values on the HPLC chromatograms obtained after the analysis of 40 successive injections of LP-RGD$_{(w)}$ and LP-RGD-GLA-S$_{(w)}$ nanoliposomal formulations, using injection volumes of 20 µL and 3.5 µL.

		Chromatogram parameters: Retention times and USP tailing of the analytes of					
		MKC			Chol-PEG$_{400}$-RGD		
Sample	Injection volume (µL)	RT (min)	RSD (%)	USP tailing	RT (min)	RSD (%)	USP tailing
LP-RGD$_{(w)}$	20	6.397	0.226	0.918	9.710	0.306	1.110
LP-RGD-GLA-S$_{(w)}$	20	6.398	0.145	1.191	9.622	0.086	1.200
		Chromatogram parameters: Retention times and USP tailing of the analytes of					
		Chol			DPPC		
Sample	Injection volume (µL)	RT (min)	RSD (%)	USP tailing	RT (min)	RSD (%)	USP tailing
LP-RGD$_{(w)}$	3.5	13.378	0.473	1.084	16.236	0.180	0.029
LP-RGD-GLA-S$_{(w)}$	3.5	13.343	0.445	1.064	16.195	0.159	0.026

Water/solvent removal by lyophilization procedure

So far, the preparation of liposomal samples included a lyophilization step to remove the water from the samples and, thus, to facilitate the solubility of all the nanovesicle components in MeOH prior to their HPLC analysis. However, latest trials comparing the recoveries obtained with and without the lyophilization step revealed that there is no need to account with this previous step. As can be seen in *Table 5.10*, in general the recoveries were even better when the sample was not undergone this extra lyophilization step probably since we minimize the error that can be induced by an extra handling. This optimization (use of Strategy_1 described in *Chapter 7, Section 7.4.5.6*) contributed to reduce the time of sample preparation prior to its HPLC analysis. Further

investigation must be done if LP-RGD-GLA-$S_{(Cryo2)}$ would be the final choice as the definitive freeze-dried pharmaceutical form in the European Phoenix project.

Table 5.10. Recoveries comparison of the different sample components when nanoliposomal formulations were lyophilized vs non-lyophilized prior to the HPLC analysis. Each condition was analyzed in triplicate.

		COMPONENTS TO BE ANALYSED							
		MKC		Chol-PEG_{400}-RGD		Chol		DPPC	
Sample	Submission to lyophilization step?	Mean recovery (%)	Difference (%)	Mean recovery (%)	Difference (%)	Mean recovery (%)	Difference (%)	Mean recovery (%)	Difference (%)
LP-RGD-GLA-$S_{(w)}$	Yes	73	4	91	5	77	2	89	2
	No	77		96		79		91	
LP-RGD-GLA-$S_{(gluc)}$	Yes	70	14	76	7	91	6	87	12
	No	84		83		97		99	
LP-RGD-GLA-$S_{(Cryo1)}$	Yes	66	1	76	-1	82	-1	91	0
	No	67		75		81		91	
LP-RGD-GLA-$S_{(Cryo2)}$	Yes	74	0	72	5	95	-7	126	-29
	No	74		77		88		97	

To summarize this section, the optimized preparation method for liposomal samples prior to HPLC analysis is compiled in the following *Table 5.11*.

Table 5.11. Sample preparation condition used before and after the optimization process.

SAMPLE PREPARATION CONDITIONS	BEFORE	OPTIMIZED
Sample pre-treatment	Freeze-drying step	None (directly use of aqueous dispersion)
Sample dilution	1:10	1:10
Solvent of dilution	Pure MeOH	Pure MeOH
Sample solubilization step (time)	Ultrasonic sonication (15 min)	Ultrasonic sonication (10 min)
LIPOSOMAL MATRIX ANALYZED	**LP-RGD-GLA-$S_{(gluc)}$**	**LP-RGD-GLA-$S_{(w)}$** **LP-RGD-GLA-$S_{(gluc)}$** **LP-RGD-GLA-$S_{(Cryo1)}$** **LP-RGD-GLA-$S_{(Cryo2)}$***

*Further sample preparation optimization must be required if LP-RGD-GLA-$S_{(Cryo2)}$ matrix composition would be chose as the definitive freeze-dried pharmaceutical form in the European Phoenix project.

5.2.4. RP-HPLC-ELSD method validation: ensuring reliability of the analytical method

After the development and optimization of a new analytical method, the parameters of the method must be validated in order to determine their specifications and ensure the reliability of its results. The studied parameters of analytical HPLC methods must be considered acceptable or inappropriate according to the criteria of acceptance of ICH Q2 (R2) and Q14[10,11]. In this thesis, chromatographic parameters such as selectivity, linearity, resolution, asymmetry and precision, but also the suitability of the equipment were evaluated.

Selectivity of the RP-HPLC-ELSD method: identifying analytes in RP-HPLC-ELSD chromatograms

One of the most important aims on the European Phoenix project is to enhance and control the quality of the proposed LP-RGD-GLA-S formulation to guarantee good physicochemical and biological properties, stability and safety. In this direction, new membrane components with higher quality grade (e.g. cholesterol of pharma grade or chol-PEG_{400}-RGD synthetized by a GMP-compliant CMO) required for further preclinical studies were used for method validation purposes. Therefore, before conducting any experiment, the selectivity of the new components was compared with the old ones and validated.

Selectivity is the ability to distinguish unequivocally a determinate component from the matrix of study. The proper selectivity determination of each analyte by using standards is essential to identify the components of interest on an RP-HPLC-ELSD chromatogram obtained from a real LP-RGD-GLA-S sample. Liposomal membrane components differing on storage time and quality degree were compared in this thesis to validate their chromatographic behaviour. Individual standard preparations of each analyte were used for the comparison of the research quality materials (used during the development and optimization steps of the present RP-HPLC-ELSD analytical method) with the higher quality grade ones (also used in further RP-HPLC-ELSD validation studies). The individual analysis of cholesterol evidences that the peak which is eluted at retention times around 10.7 min correspond to a cholesterol-related impurity. RP-HPLC-ELSD chromatograms demonstrated the maintenance of selectivity and retention times among other chromatographic parameters (see ***Figure 5.12***) despite the higher quality profile of the new materials. In conclusion, the selectivity specifications for the four membrane component were:

- Selectivity modifications cannot be caused by quality degree of materials (the peaks are well identified).
- Mean retention times of analytes = MKC around 6.2 min, chol-PEG_{400}-RGD around 9.0 min, cholesterol around 12.0 min, and DPPC around 15.2 min.

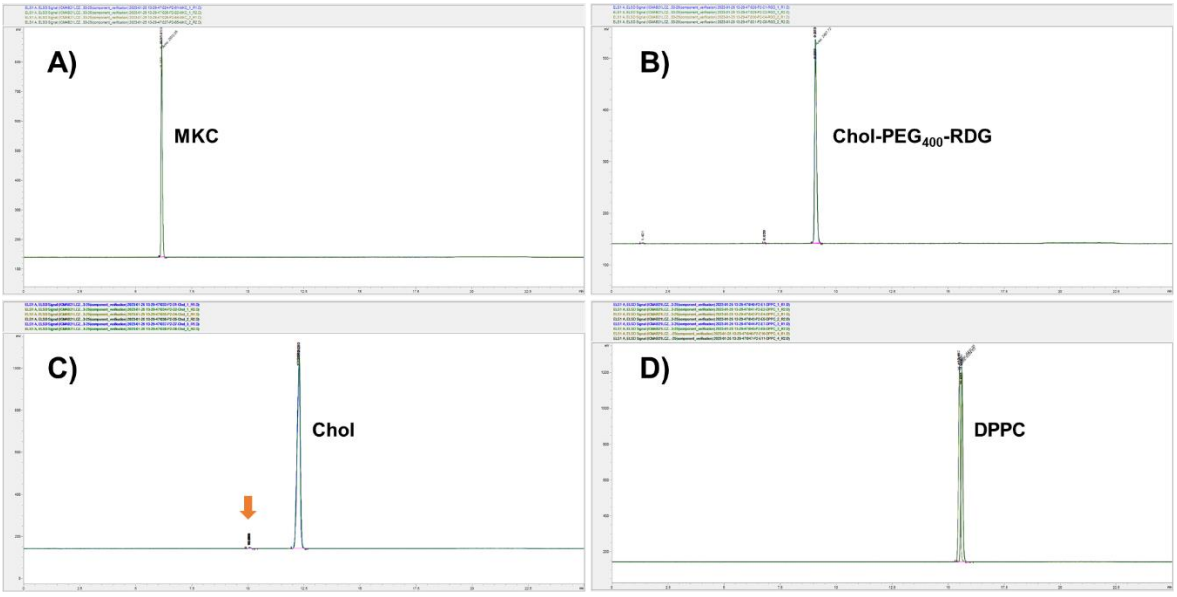


Figure 5.12. Individual RP-HPLC-ELSD chromatograms for the different analytes: A) MKC, B) chol-PEG_{400}-RGD, C) cholesterol and D) DPPC. Overlapped chromatograms of research quality materials and higher quality grade materials are compared by each analyte examination. Orange arrow corresponds to the detection of cholesterol-related impurities.

Linearity and concentration range of the analytes: matrix effects caused by excipient presence

Since the HPLC gradient and the sample preparation protocol were developed and optimized, and the selectivity of analytes controlled, next step consisted of establishing the concentration range in which each analyte had a linear signal-response, i.e. the linearity of the method. As far as liposomal samples were solubilized using MeOH, the same solvent was chosen to prepare calibration curves as explained in ***Chapter 7, Section 7.4.5.6***, according to Composition_1. Briefly, four independently stocks of the analytes to quantify (DPPC at 2000 ppm, chol at 1000 ppm, chol-PEG_{400}-RGD at 180 ppm, and MKC at 1000 ppm) were prepared in MeOH and further mixed in 5 different volumetric flasks of 2 mL to obtain the different calibration points of the curve. A different concentration range was chosen for each compound, based on the final concentration expected in LP-RGD-GLA-S samples once prepared in HPLC vials. Proper linearity was achieved for the 4 components of analysis (see ***Table 5.12***) in the concentration range examined according to the following specifications (and their criteria of acceptance shown in brackets):

- Correlation coefficient (R^2) of the calibration curve ≥ 0.9995 (≥ 0.9990).
- Precision or % RSD of linearity obtained in different days < 0.05 % (< 1.0 %).

Table 5.12. Summarized data of linearity and precision during the development of the method. Precision has been studied by injecting the calibration curve in 3 different days.

	Linearity		Precision
Components	**Concentration range (ppm)**	**Correlation coefficient (R^2)**	**Different days RSD (%)**
MKC	100 - 5	0.9995	0.044
Chol-PEG$_{400}$-RGD	140 - 10	0.9998	0.02
Chol	400 - 50	0.9997	0.021
DPPC	900 - 100	0.9995	0.035

Once ensured the linearity of the optimized method, real samples of intermediate (LP-RGD-GLA-S_int) and concentrate (LP-RGD-GLA-S$_{(w)}$ and LP-RGD-GLA-S$_{(gluc)}$) liposomal prototypes were quantified using the same calibration curve composition described above (Composition_1). The manufacturing process and sample composition of these prototypes is again remembered in ***Figure 5.13***.

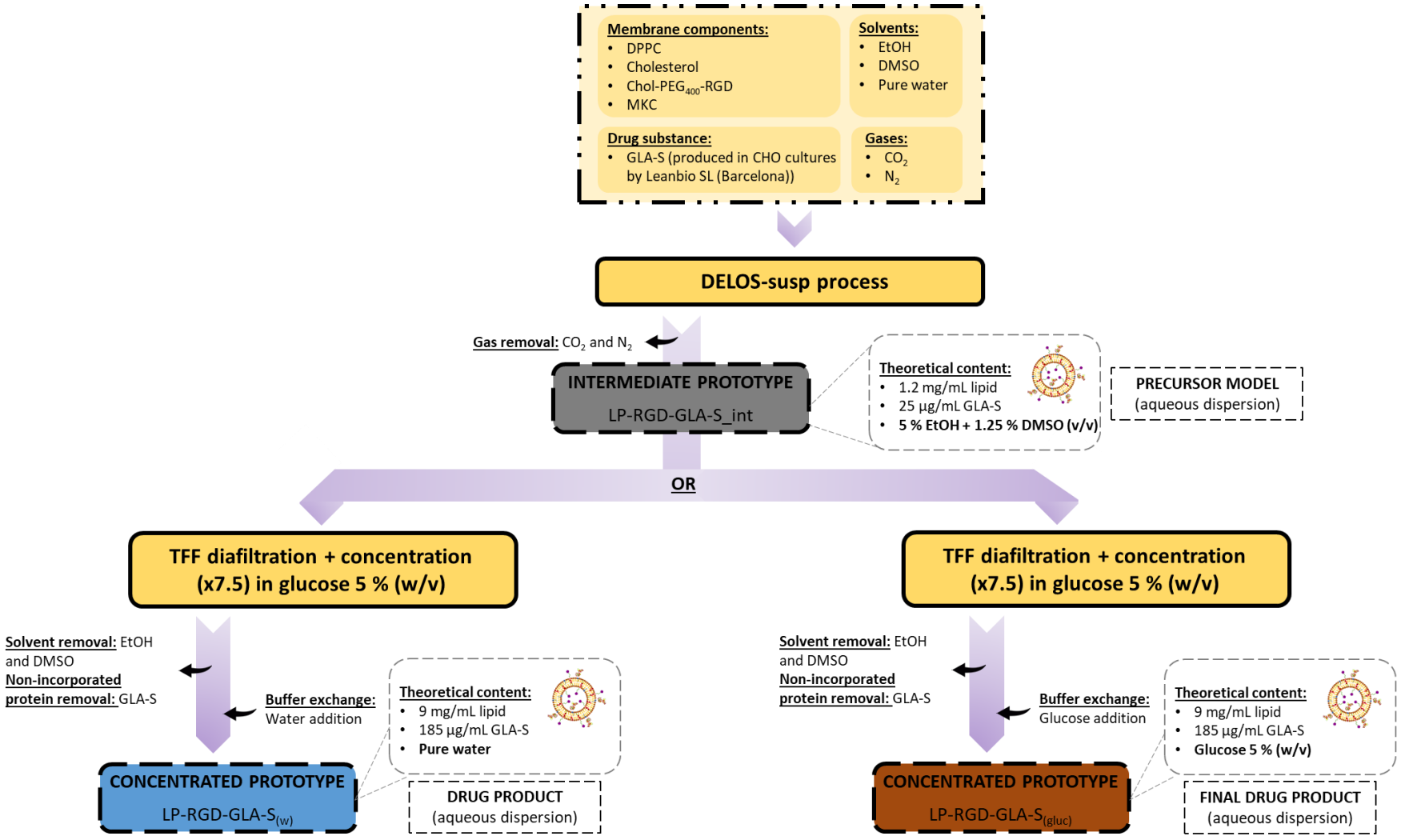


Figure 5.13. Process flow diagram to produce the intermediate prototype (LP-RGD-GLA_int), and the concentrated prototypes (LP-RGD-GLA-$S_{(w)}$ and LP-RGD-GLA-$S_{(gluc)}$). Raw materials used and removed substances during liposome manufacturing are also indicated.

Values of sample quantification are given as recovery percentages of the theoretical component concentrations obtained after DELOS-susp and TFF procedures, according to calculations of ***Eq. 5.1***. The experimental analyte concentrations were corrected with the dilution factor (FD) applied to samples during their preparation in HPLC vials.

$$Recovery\ (\%) = \frac{Experimental\ analyte\ concentration\ x\ FD}{Theoretical\ analyte\ concentration\ after\ manufacturing}\ x\ 100$$

(***Eq. 5.1***)

Briefly, for quantification purposes three different liposomal matrixes (coming from a same production batch) differing only in its buffer composition were studied in triplicate. Results on ***Table 5.13*** showed variability on recovery values of the same components between different matrixes. These differences might be related to two different hypotheses: i) material loss due to differences in the production procedure; or ii) matrix effects on recovery values due to the presence of different molecules in the dispersion media.

Table 5.13. Comparison of experimental values between replicates obtained from different liposomal matrixes prepared in a same production batch. LP-RGD-GLA-S_int was analyzed in duplicates, but LP-RGD-GLA$_{(w)}$ and LP-RGD-GLA$_{(gluc)}$ in triplicates.

		Accuracy parameters							
		MKC		Chol-PEG$_{400}$-RGD		Chol		DPPC	
Sample	Excipients	Recovery (%)	RSD (%)	Recovery (%)	RSD (%)	Recovery (%)	RSD (%)	Recovery (%)	RSD (%)
LP-RGD-GLA-S_int	5 % EtOH + 1.2 % DMSO (v/v)	95	8.31	64	6.32	81	8.36	93	9.81
LP-RGD-GLA-S$_{(w)}$	Water	70	6.90	74	8.89	81	7.47	99	13.08
LP-RGD-GLA-S$_{(gluc)}$	Glucose 5 % (w/v)	76	1.38	82	2.23	81	2.32	86	2.32

To discard or detect if discrepancies of recovery values were related to a matrix effect caused by the presence of different excipients in liposomal samples, different calibration curves containing same excipient concentrations than nanovesicular formulations were prepared (as described in ***Chapter 7, Section 7.4.5.6***) and their linearity evaluated again. Briefly, same amount of EtOH and DMSO (for the quantification of LP-RGD-GLA-S_int prototypes), or glucose (for the analysis of LP-RGD-GLA-S$_{(gluc)}$ formulations) as found in HPLC vials after sample preparation were added to all the calibration curves of the respective curves. The necessity to add GLA-S in all calibration curves was also investigated.

According to results on ***Table 5.14***, it is clear that DPPC signal reaches saturated response in presence of glucose molecules, decreasing its concentration range of linearity. To overcome this obstacle, two approaches were set up: i) concentration range in calibration curves of almost all components were narrowed to ensure linearity in presence of excipients, and ii) the injection volume when analyzing DPPC in standards and samples containing

glucose was decreased from 3 µL to 1.5 µL (see *Table 5.15*). Similar specifications (with their corresponding criteria of acceptance shown in brackets) as previous analysis were found for the 4 analytes of different liposomal matrixes, ensuring proper linearity when using the optimized concentration range and injection volumes in each case:

- R^2 of the calibration curve ≥ 0.9992 (≥ 0.9990).
- Precision or % RSD of linearity obtained in different days < 0.08 % (< 1.0 %).
- Precision or % RSD of linearity obtained by different analysts < 0.06 % (< 1.0 %).

Table 5.14. Linear signal-response values obtained by the different membrane components and their relation to the injection volume used, the excipient content in calibration curves, and the presence of GLA-S enzyme. The calibration curves were prepared by adding as excipients A) only MeOH, B) 1 % EtOH and 0.025 % DMSO (v/v) in MeOH (with or without GLA-S presence), or C) 5000 ppm of glucose in MeOH (with or without GLA-S presence).

A)

Point of calibration curve	Curve calibration containing only MeOH Mean peak area			
	MKC	Chol-PEG$_{400}$-RGD	Chol	DPPC
A	4042	4240	648	214
B	1265	2688	1368	2305
C	732	1074	6854	4853
D	99	332	9259	6282
E	25	57	9628	6776
Injection volume (µL)	15	15	15	3

B)

Point of calibration curve	Curve calibration containing EtOH + DMSO Mean peak area				Curve calibration containing EtOH + DMSO + GLA-S Mean peak area			
	MKC	Chol-PEG$_{400}$-RGD	Chol	DPPC	MKC	Chol-PEG$_{400}$-RGD	Chol	DPPC
A	3534	4276	808	219	4013	4509	819	192
B	1406	2693	13330	2416	1466	2789	1402	2240
C	610	1147	6535	4125	635	1159	6608	3869
D	87	346	8881	4990	91	360	9190	5007
E	23	58	9070	5828	29	59	9187	5238
Injection volume (µL)	15	15	15	3	15	15	15	3

C)

Point of calibration curve	Curve calibration containing Glucose Mean peak area					Curve calibration containing Glucose + GLA-S Mean peak area			
	MKC	Chol-PEG$_{400}$-RGD	Chol	DPPC		MKC	Chol-PEG$_{400}$-RGD	Chol	DPPC
A	4158	3190	756	167	44	4469	3184	660	45
B	1571	1918	2435	1896	654	1576	1906	2177	518
C	680	794	6586	3340	1226	697	812	6060	843
D	82	227	8616	3805	1482	97	236	8348	999
E	23	39	9104	4367	2220	25	40	9391	1535
Injection volume (µL)	15	15	15	3	1.5	15	15	15	1.5

SATURATED SIGNAL

OVERCOMING SATURATION BY DECREASING THE INJECTED AMOUNT OF DPPC

Table 5.15. Summarized data of linearity and precision from the calibration curves differing in composition. The new established concentration ranges of analytes (detailed in tables) and injection volumes (15 µL for MCK, chol-PEG_{400}-RGD and chol; or 1.5 µL for DPPC) were used. Precision was studied injecting calibration curves in 2 different days, but also by 2 different analysts. The calibration curves were prepared by adding as excipiets A) only MeOH, B) 1 % EtOH and 0.025 % DMSO (v/v) in MeOH (with or without GLA-S presence), or C) 5000 ppm of glucose in MeOH (with or without GLA-S presence). Legend: N.D. means non-determined.

A)

Components	Shortened concentration range (ppm)	Curve calibration containing only MeOH		
		Linearity	Precision	
		R^2	Different days RSD (%)	Different analysts RSD (%)
MKC	80 - 5	0.9993	0.014	0.01
Chol-PEG_{400}-RGD	140 - 10	0.9997	0.028	0.021
Chol	250 - 50	0.9995	0.071	0.058
DPPC	800 - 100	0.9999	0	N.D.

B)

Components	Shortened concentration range (ppm)	Curve calibration containing EtOH + DMSO			Curve calibration containing EtOH + DMSO + GLA-S		
		Linearity	Precision		Linearity	Precision	
		R^2	Different days RSD (%)	Different analysts RSD (%)	R^2	Different days RSD (%)	Different analysts RSD (%)
MKC	80 - 5	0.9994	0.035	0.039	0.9998	0.014	N.D.
Chol-PEG_{400}-RGD	140 - 10	0.9999	0.007	0.015	0.9997	0.035	N.D.
Chol	250 - 50	0.9998	0.028	0.030	0.9996	0.021	N.D.
DPPC	800 - 100	0.9997	0	0.012	0.9996	0.064	N.D.

C)

Components	Shortened concentration range (ppm)	Curve calibration containing Glucose			Curve calibration containing Glucose + GLA-S		
		Linearity	Precision		Linearity	Precision	
		R^2	Different days RSD (%)	Different analysts RSD (%)	R^2	Different days RSD (%)	Different analysts RSD (%)
MKC	80 - 5	0.9995	0.021	0.015	0.9995	0.014	N.D.
Chol-PEG_{400}-RGD	140 - 10	0.9996	0.042	0.031	0.9999	0.007	N.D.
Chol	250 - 50	0.9995	0.014	0.015	0.9993	0.014	N.D.
DPPC	800 - 100	0.9994	0.035	0.040	0.9992	0.028	N.D.

After applying the new implemented approaches, various liposomal nanoformulations differing in excipient composition were analyzed by using the different calibration curves of study. Results complied on *Table 5.16* proved modest deviations between recovery values obtained with different calibration curve composition, demonstrating the importance of having similar matrix composition on both, standards and samples, to obtain reliable measurements. To ensure the overcoming of matrix effects conducted by the addition of excipient in calibration curves, further studies to explore the method accuracy were performed as follow in this section.

Table 5.16. Effect of calibration curve composition on analytes recoveries (%) and RSD (%) between triplicates of real liposomal matrixes depending on i) excipient constitution and/or ii) GLA-S presence. Results of real A) LP-RGD-GLA-S_int (as intermediate prototype), and B) LP-RGD-GLA-$S_{(gluc)}$ (as concentrated formulation).

A)

			MKC DETERMINATION WITH CALIBRATION CURVES CONTAINING:					
			Only MeOH		EtOH + DMSO		EtOH + DMSO + GLA-S	
Sample	Production batch replicate	Excipients	Recovery (%)	RSD (%)	Recovery (%)	RSD (%)	Recovery (%)	RSD (%)
LP-RGD-GLA-S_int	R1	EtOH + DMSO + GLA-S	117	1.80	117	1.76	108	1.84
	R2	EtOH + DMSO + GLA-S	108	2.76	95	2.99	98	2.94
			CHOL-PEG_{400}-RGD DETERMINATION WITH CALIBRATION CURVES CONTAINING:					
			Only MeOH		EtOH + DMSO		EtOH + DMSO + GLA-S	
Sample	Production batch replicate	Excipients	Recovery (%)	RSD (%)	Recovery (%)	RSD (%)	Recovery (%)	RSD (%)
LP-RGD-GLA-S_int	R1	EtOH + DMSO + GLA-S	67	1.32	66	1.32	65	1.31
	R2	EtOH + DMSO + GLA-S	48	1.67	45	1.75	52	1.65
			CHOL DETERMINATION WITH CALIBRATION CURVES CONTAINING:					
			Only MeOH		EtOH + DMSO		EtOH + DMSO + GLA-S	
Sample	Production batch replicate	Excipients	Recovery (%)	RSD (%)	Recovery (%)	RSD (%)	Recovery (%)	RSD (%)
LP-RGD-GLA-S_int	R1	EtOH + DMSO + GLA-S	102	1.15	91	1.28	89	1.28
	R2	EtOH + DMSO + GLA-S	72	1.07	72	1.08	72	1.08
			DPPC DETERMINATION BY USING CALIBRATION CURVES CONTAINING:					
			Only MeOH		EtOH + DMSO		EtOH + DMSO + GLA-S	
Sample	Production batch replicate	Excipients	Recovery (%)	RSD (%)	Recovery (%)	RSD (%)	Recovery (%)	RSD (%)
LP-RGD-GLA-S_int	R1	EtOH + DMSO + GLA-S	78	2.99	78	3.21	84	3.10
	R2	EtOH + DMSO + GLA-S	78	1.34	78	1.34	83	1.30

B)

			MKC DETERMINATION WITH CALIBRATION CURVES CONTAINING:			
			Glucose		Glucose + GLA-S	
Sample	Production batch replicate	Excipients	Recovery (%)	RSD (%)	Recovery (%)	RSD (%)
LP-RGD-GLA-S$_{(gluc)}$	R1	Glucose + GLA-S	56	1.99	54	2.25
	R2	Glucose + GLA-S	54	1.13	55	1.11
			CHOL-PEG$_{400}$-RGD DETERMINATION WITH CALIBRATION CURVES CONTAINING:			
			Glucose		Glucose + GLA-S	
Sample	Production batch replicate	Excipients	Recovery (%)	RSD (%)	Recovery (%)	RSD (%)
LP-RGD-GLA-S$_{(gluc)}$	R1	Glucose + GLA-S	52	1.94	50	2.02
	R2	Glucose + GLA-S	33	1.24	32	1.26
			CHOL DETERMINATION WITH CALIBRATION CURVES CONTAINING:			
			Glucose		Glucose + GLA-S	
Sample	Production batch replicate	Excipients	Recovery (%)	RSD (%)	Recovery (%)	RSD (%)
LP-RGD-GLA-S$_{(gluc)}$	R1	Glucose + GLA-S	65	1.60	66	1.62
	R2	Glucose + GLA-S	62	0.52	63	0.52
			DPPC DETERMINATION WITH CALIBRATION CURVES CONTAINING:			
			Glucose		Glucose + GLA-S	
Sample	Production batch replicate	Excipients	Recovery (%)	RSD (%)	Recovery (%)	RSD (%)
LP-RGD-GLA-S$_{(gluc)}$	R1	Glucose + GLA-S	56	2.11	65	2.30
	R2	Glucose + GLA-S	58	0.71	64	0.71

As conclusion, these results evidenced the necessity of preparing specific calibration curves simulating the same matrix composition from each testing nanoliposomal formulation in order to avoid matrix effects caused by the presence of excipients, which were capable of deviating the signal-responses of analytes when these were only present in the sample of analysis but not in the calibration curve used. ***Table 5.17*** summarizes the slight method variations to consider based on the use of different calibration curves containing same excipient concentrations than nanoliposomal formulations of testing, as well as the injection volumes and the concentration ranges of analytes intended for the analysis of the specific liposomal composition in each case.

Table 5.17. Modified and optimized versions of the RP-HPLC-ELSD method proposed to use depending on the liposomal sample to be analysed for chemical composition quantification.

METHOD CHARACTERISTICS	OPTIMIZED RP-HPLC-ELSD METHOD VERSION				
	Method_003	**Method_004**	**Method_005**	**Method_006**	**Method_007**
Analyte concentration range (ppm)	MKC (5 – 80) Chol-PEG_{400}-RGD (10 – 140) Chol (50 – 250) DPPC (100 – 800)	MKC (5 – 80) Chol-PEG_{400}-RGD (10 – 140) Chol (50 – 250) DPPC (100 – 800)	MKC (5 – 80) Chol-PEG_{400}-RGD (10 – 140) Chol (50 – 250) DPPC (100 – 800)	MKC (5 – 80) Chol-PEG_{400}-RGD (10 – 140) Chol (50 – 250) DPPC (100 – 800)	MKC (5 – 80) Chol-PEG_{400}-RGD (10 – 140) Chol (50 – 250) DPPC (100 – 800)
Calibration points composition (Solvents and excipients)	MeOH	MeOH 1 % (v/v) EtOH 0.25 % (v/v) DMSO	MeOH 1 % (v/v) EtOH 0.25 % (v/v) DMSO 5 ppm GLA-S	MeOH 5000 ppm glucose	MeOH 5000 ppm glucose 20 ppm GLA-S
Injection volumes (component detection)	15 µL (MKC, Chol-PEG_{400}-RGD, Chol) 3.0 µL (DPPC)	15 µL (MKC, Chol-PEG_{400}-RGD, Chol) 3.0 µL (DPPC)	15 µL (MKC, Chol-PEG_{400}-RGD, Chol) 3.0 µL (DPPC)	15 µL (MKC, Chol-PEG_{400}-RGD, Chol) 1.5 µL (DPPC)	15 µL (MKC, Chol-PEG_{400}-RGD, Chol) 1.5 µL (DPPC)
Liposomal matrixes recommended for RP-HPLC-ELSD analysis	**LP-$RGD_{(w)}$**	**LP-RGD_int**	**LP-RGD-GLA-S_int**	**LP-$RGD_{(gluc)}$**	**LP-RGD-GLA-$S_{(gluc)}$**

Results showed that:

- For the intermediate products, i.e. after DELOS process, the calibration curve must contain the same solvents as the ones that contain these prototypes (EtOH + DMSO).
- For final products, i.e. after the TFF process to remove the solvents and exchange the dispersant medium for glucose 5% (w/v) and the concentration step (x7.5), glucose must be added to the calibration curve.

Accordingly, main matrix effects (mainly over DPPC component) were overcome by the appropriate selection of calibration curve composition according to the sample prototype to analyse.

Accuracy of the analytical RP-HPLC-ELSD method: analysis of artificial samples prepared with a specific analyte concentration

After the knowledge about the impact on signal-response HPLC values over liposomal components when different excipients are present in the nanoformulations (see *Section 5.2.4*), the method accuracy was evaluated to assess if this was between the recommended values by ICH guidelines, when adding excipients on calibration curve composition. The criteria of acceptance for accuracy parameters to fulfill according ICH guidelines:

- Recovery (%) values between 95 – 105 %.
- % RSD between injection replicates < 10 % (< 5 % if possible).

For these proposed studies, artificial samples (i.e. samples simulating the same matrix composition of each nanoliposomal formulation of study) by using four independently stocks standards of the analytes were

prepared, reproducing the intermediate LP-RGD-GLA-S_int prototype (containing EtOH and DMSO), concentrated empty liposomes which may be dispersed in only water or glucose 5 % (w/v) media (LP-RGD$_{(w)}$ and LP-RGD$_{(gluc)}$, respectively), or concentrated GLA-loaded LP-RGD-GLA-S$_{(gluc)}$ prototypes (with glucose as dispersant medium). Some artificial samples with small modifications on theoretical concentrations of MKC and chol-PEG$_{400}$-RGD components were also analyzed to determine if the accuracy of the method is maintained after slight modifications on liposomal membrane composition. The sample composition simulated with the artificial samples prepared is described in ***Table 5.18***.

Table 5.18. Composition of artificial samples prepared for the accuracy determination of the optimized RP-HPLC-ELSD (and its slight different versions) according to the different liposomal matrixes intended to be tested.

	Nanovesicular system ID	Membrane composition (theoretical molar ratio)	[lipid]$_{theoric}$ (mg/mL)	[GLA-S]$_{theoric}$ (µg/mL)	Theoretical % RGD (molar)	Theoretical % MKC (molar)	System prototype	Solvent and excipients
UNLOADED PROTOTYPES (WITHOUT GLA CONTAINING)	**LP$_{(w)}$**	**DPPC:Chol (10:7)**	9	-	0	5	Concentrated	Pure water
	LP-RGD$_{(w)}$	**DPPC:Chol:Chol-PEG$_{400}$-RGD (10:6.5:0.5)**	9	-	3	5	Concentrated	Pure water
	LP-6%RGD-$_{(w)}$	**DPPC:Chol:Chol-PEG$_{400}$-RGD (10:6:1)**	9	-	6	5	Concentrated	Pure water
	LP$_{(gluc)}$	**DPPC:Chol (10:7)**	9	-	0	5	Concentrated	Glucose 5 % (w/v) media
	LP-RGD$_{(gluc)}$	**DPPC:Chol:Chol-PEG$_{400}$-RGD (10:6.5:0.5)**	9	-	3	5	Concentrated	Glucose 5 % (w/v) media
	LP-6%RGD-$_{(gluc)}$	**DPPC:Chol:Chol-PEG$_{400}$-RGD (10:6:1)**	9	-	6	5	Concentrated	Glucose 5 % (w/v) media
	LP-0.5%MKC-RGD$_{(gluc)}$	**DPPC:Chol:Chol-PEG$_{400}$-RGD (10:6.5:0.5)**	9	-	3	0.5	Concentrated	Glucose 5 % (w/v) media
	LP-0%MKC-RGD$_{(gluc)}$	**DPPC:Chol:Chol-PEG$_{400}$-RGD (10:6.5:0.5)**	9	-	3	0	Concentrated	Glucose 5 % (w/v) media
GLA-LOADED PROTOTYPES	**LP-RGD-GLA-S_int**	**DPPC:Chol:Chol-PEG$_{400}$-RGD (10:6.5:0.5)**	1.2	25	3	5	Concentrated	1 % EtOH 0.25 % DMSO (both in v/v)
	LP-RGD-GLA-S$_{(gluc)}$	**DPPC:Chol:Chol-PEG$_{400}$-RGD (10:6.5:0.5)**	1.2	185	3	5	Concentrated	Glucose 5 % (w/v) media

Each kind of sample matrix composition was analyzed with its corresponding calibration curve composition. Results on ***Table 5.19*** demonstrated that matrix effects were not interfering on RP-HPLC-ELSD measurements when same matrix composition on sample and calibration curve was used for the analysis, as well as, that none of the theoretical concentrations used for the 4 components was capable to saturate RP-HPLC-ELSD detection signal. Also, these studies evidenced that the use of slightly different versions of the optimized method, which differ in excipient composition or in GLA-S presence (named as Method_003 to Method_007, and described in ***Table 7.11,*** and in ***Chapter 7, Section 7.4.5.6***), for the analysis of liposomal samples, displayed recoveries values between 95 – 105 % ensuring a proper accuracy of the analytical RP-HPLC-ELSD method employed in each case. Therefore, the accuracy specifications were fulfilled according the aforementioned ICH criteria of acceptance.

Table 5.19. Accuracy results from triplicates of artificial samples depending on i) excipient constitution and/or ii) GLA presence. [L]Component amount inferior to limit of detection (LOD), being incapable to be detected by ELSD. *Detailed information in *Chapter 7, Section 7.4.5.6*.

				MEMBRANE COMPONENT ANALYSIS							
				MKC		Chol-PEG$_{400}$-RGD		Chol		DPPC	
	Artificial sample	Reproducing prototype	Calibration curve composition	Recovery (%)	Replicate RSD (%)	Recovery (%)	Replicate RSD (%)	Recovery (%)	Replicate RSD (%)	Recovery (%)	Replicate RSD (%)
NONE GLA-S PRESENCE	LP$_{(w)}$	TFF in water	Composition_1*	98	3.25	0	0	101	1.54	100	2.32
	LP-RGD$_{(w)}$			102	2.67	100	1.88	100	1.04	97	4.02
	LP-6%RGD$_{(w)}$			99	3.71	96	1.43	103	2.58	98	4.44
	LP$_{(gluc)}$	TFF in glucose 5 % (w/v)	Composition_4*	103	1.54	0	0	101	1.35	100	2.32
	LP-RGD$_{(gluc)}$			101	3.10	104	3.32	101	2.88	97	4.02
	LP-6%RGD$_{(gluc)}$			100	0.97	97	1.92	99	1.78	96	4.38
	LP-0.5%MKC-RGD$_{(gluc)}$	TFF in glucose 5 % (w/v)	Composition_4*	Below LOD[L]		104	1.24	104	1.60	96	2.62
	LP-0%MKC-RGD$_{(gluc)}$			0	0	101	1.79	104	0.68	104	2.72
GLA-S PRESENCE	LP-RGD-GLA-S_int	DELOS-susp in 5 % EtOH + 1.2 % DMSO (v/v)	Composition_3*	98	1.71	103	0.69	98	2.16	103	0.93
	LP-RGD-GLA-S$_{(gluc)}$	TFF in glucose 5 % (w/v)	Composition_5*	102	0.46	105	1.19	101	1.20	99	3.97

DIFFERENT AMOUNTS OF MKC AND CHOL-PEG$_{400}$-RGD ON ARTIFICIAL SAMPLES DO NOT IMPAIR THE ACCURACY OF THE RP-HPLC-ELSD METHOD

In these analyses, remains of glucose from HPLC column were cleaned injecting 100 µL of pure water every 6 injections of samples containing glucose. This fact results on a critical step to achieve the great accuracy explained in this section. The necessity of implementing this column cleaning is well explained below.

Another concern to be a cause of probable matrix effects was the mismatch between the molar ratio of membrane components in real samples and the designed calibration curves (explained in *Chapter 7, Section 7.4.5.6*). However, recoveries values of the artificial samples indirectly demonstrated the non-necessity to control the molar ratio between the 4 components on the studied concentration range.

Instrumentation cleaning optimization: removal of glucose molecules from the system

Since it was demonstrated that excipient presence in samples (glucose in particular) is capable to enhance the signal-response of components (especially DPPC), the importance of cleaning steps during HPLC was investigated.

During the sample preparation procedure by MeOH solubilization, glucose precipitation cannot be observed macroscopically. For this reason, during the already explained accuracy analysis using artificial samples, a first study was conducted carrying out cleanings of the HPLC column by the injection of 100 µL of pure MeOH every

6 injections of samples or standards. These cleanings were intended to remove probable lyophilic molecules remained attached inside the column, such as high hydrophilic molecules or remaining glucose. However, using this approach, an increase between the DPPC recoveries of artificially-prepared samples containing glucose was observed (see *Table 5.20*). This fact evidences an accumulation of glucose inside the column due to an inappropriate cleaning procedure.

Table 5.20. Improvement of DPPC accuracy values after the implementation of HPLC column cleaning with pure water after 6 injections of samples containing glucose.

				MEMBRANE COMPONENT ANALYSIS							
				MKC		Chol-PEG_{400}-RGD		Chol		DPPC	
	Artificial sample	Cleanings of HPLC column during analysis	Calibration curve composition	Recovery (%)	Replicate RSD (%)	Recovery (%)	Replicate RSD (%)	Recovery (%)	Replicate RSD (%)	Recovery (%)	Replicate RSD (%)
NONE GLA-S PRESENCE	$LP_{(gluc)}$	After 6 injections: 100 µL of pure MeOH	Composition_4*	103	1.54	0	0	101	1.35	100	2.32
	$LP\text{-}RGD_{(gluc)}$			103	1.94	99	1.61	99	2.88	112	4.01
	$LP\text{-}6\%RGD_{(gluc)}$			100	0.97	97	1.92	99	1.78	109	2.49
	$LP_{(gluc)}$	After 6 injections: 100 µL of pure H_2O	Composition_4*	N.D.	N.D.	N.D.	N.D.	N.D.	N.D.	N.D.	N.D.
	$LP\text{-}RGD_{(gluc)}$			101	3.10	104	3.32	101	2.88	97	4.02
	$LP\text{-}6\%RGD_{(gluc)}$			N.D.	N.D.	N.D.	N.D.	N.D.	N.D.	N.D.	N.D.

WATER REMOVES REMAINING GLUCOSE MOLECULES FROM STATIONARY PHASE, ENSURING DPPC RECOVERY VALUES

In order to improve the accuracy of the method and to avoid matrix effects caused by the presence of glucose molecules in the RP-HPLC-ELSD system, a second study was conducted but adding a new cleaning step of the column between sample analysis: to inject 100 µL of pure water every 6 injections of samples when they contain glucose. The optimization highlighted in *Table 5.21* ended with the achievement of great accuracy values when analyzing matrixes containing glucose, as explained above.

Table 5.21. Implementation of a new cleaning step of the HPLC column after the analysis of samples containing glucose, to avoid glucose accumulation in the stationary phase.

CLEANING IMPLEMENTATION	BEFORE	OPTIMIZED
Injections of 100 µL during sample analysis	1 of pure MeOH after 6 injections of sample	1 of pure MeOH after 6 injections of sample + 1 of pure water after 6 injections of sample
Column cleaning after analysis	Solvent exchange to ACN for storage	Pure water (2 h, at 1 mL/min and 45 ºC) + Solvent exchange to ACN for storage
LIPOSOMAL MATRIX ANALYZED	**Anyone**	**LP-RGD-GLA-$S_{(gluc)}$**

Furthermore, it is well known the better solubility of glucose in hot water. To avoid the contamination of the HPLC column with glucose between analysis, an extensive cleaning with pure water was established after each sequence of samples containing glucose, setting the column temperature at 45 ºC during 2 h at 1 mL/min. This column maintenance allowed the preservation over time (at least 1 year) of the stationary phase packed inside the HPLC column, i.e. keeping constant the chromatographic parameters evaluated during the system suitability testing (e.g. resolution, A_s or RT among others).

System suitability test: appropriateness of the instrumentation and the RP-HPLC-ELSD method

Once well-established the optimized RP-HPLC-ELSD method to use for each liposomal formulation (taking into account the chromatographic conditions, gradient, sample preparation, injection volumes, calibration curve composition and even system cleanings), it is relevant to well study the system suitability of the equipment in order to demonstrate its consistency and appropriateness. The proper reproducibility of measurements conducted by the instrumental system and the reproducibility of the method itself were determined through the evaluation of the following parameters:

- Resolution of the analytes to ensure an accurate peak separation between components and their maintenance between measurements.
- Peak A_s of the analytes by measuring values of USP tailing factor.
- Maintenance of the selectivity of the analytes by studying the RT of the analytes.
- Robustness of the method: by comparing the RT of the analytes among different liposomal matrix compositions.

For this purpose, real samples of LP-RGD-GLA-S_int (as an example of intermediate prototype) and LP-RGD-GLA-$S_{(gluc)}$ (as an example of concentrate prototype) were submitted to system suitability examinations, by respectively using the previous optimized Method_5 and Method_007 (specified above in ***Table 5.17***). Both tested liposomal matrixes were evaluated through six consecutive injections from the same sample. Results on ***Table 5.21*** proved that the equipment used is in proper conditions to conduct further validation test and sample measurements. The general specifications obtained by RP-HPLC-ELSD analysis (with their corresponding criteria of acceptance shown in brackets) for the 4 liposomal components analysed were:

- Consecutive injections time % RSD < 0.08 % (≤ 1.0 %).
- Consecutive injections area % RSD < 7 % (≤ 10 %, or ≤ 5 % if possible).
- Peak resolution > 2.0. without resolution problems are observed (≥ 2.0).
- Symmetry factor of between 0.85 – 1.30 (0.80 – 1.50).
- Points per peak ≥ 100 in all cases (the peaks are well defined).

Table 5.21. System suitability test using LP-RGD-GLA-S_int (as an example of intermediate prototype) and LP-RGD-GLA-$S_{(gluc)}$ (as an example of concentrate prototype) evaluated through six consecutive injections from the same sample.

Nanovesicular system ID	Analyte	Injection volume (µL)	Mean RT (min)	Injection RSD (%)	Mean area	Injection RSD (%)	Mean resolution value to prev peak	Injection RSD (%)	Mean USP tailing factor	USP tailing range	Average points per peak	Points per peak range
LP-RGD-GLA-S_int	MKC	15	6.196	0.042	65	6.22	37.07	1.079	1.063	1 – 1.2	199	180 – 250
	Chol-PEG_{400}-RGD		8.996	0.060	67	2.99	22.53	1.671	1.135	1 – 1.3	289	270 – 310
	Chol		11.895	0.063	1033	1.12	16.18	1.564	1.043	1 – 1.1	390	350 – 420
	DPPC	3	15.216	0.026	415	1.83	18.76	2.028	1.228	1.1 – 1.3	293	270 – 320
LP-RGD-GLA-$S_{(gluc)}$	MKC	15	6.193	0.027	248	1.62	9.77	0.140	1.103	1 – 1.2	213	180 – 250
	Chol-PEG_{400}-RGD		9.000	0.032	378	1.79	22.56	0.418	1.147	1.1 – 1.2	298	270 – 320
	Chol		11.997	0.056	4811	0.46	15.60	1.067	0.915	0.85 – 1	467	430 – 510
	DPPC	1.5	15.255	0.021	540	3.12	18.79	1.747	1.192	1.1 – 1.3	341	290 – 360

Sample dissolution test: ensuring the analyte solubility after the sample preparation protocol

This test is useful to validate the sample preparation protocol for further RP-HPLC-ELSD analysis. Sample dissolution test consists of the evaluation and comparison of samples prepared in different dilution conditions to demonstrate component solubility. A sample dilution test is considered positive when obtaining recoveries between 95 – 105 % following calculations based on *Eq. 5.2*, where the experimental analyte concentration of the more diluted sample (D_S) is multiplied by the dilution factor (DF) that differs both tested samples, and divided by the experimental analyte concentration of the more concentrated sample (C_S).

$$Recovery\ (\%) = \frac{D_S(ppm)\ x\ DF}{C_S(ppm)}\ x\ 100$$

(Eq. 5.2)

In this section, the aforementioned concentrated LP-RGD-GLA-$S_{(gluc)}$ liposomal prototype containing glucose as an isosmotic agent was used in the sample dissolution test. The optimized version of RP-HPLC-ELSD method used during the analysis was the one named as Method_007 and described in *Table 5.17,* and in *Chapter 7, Section 7.4.5.6*, which uses a calibration curve with glucose content. The replicates and the LP-RGD-GLA-$S_{(gluc)}$ sample preparation protocol to be compared during the test are schematized as follows:

1 – Triplicates of samples prepared according to the sample preparation procedure established in the analytical method, i.e. triplicates of LP-RGD-GLA-$S_{(gluc)}$ sample 10-fold diluted in MeOH (described as Strategy_1 in *Chapter 7, Section 7.4.5.6*).

2 – Triplicates of samples prepared with the same sample preparation protocol but 2-fold more diluted, i.e. triplicates of LP-RGD-GLA-$S_{(gluc)}$ sample 20-fold diluted in MeOH instead of diluting samples only 10-fold in MeOH.

In this thesis, an extra study was planned to complement sample dissolution test consisting on the preparation of:

3 – Triplicates of samples prepared with the same sample preparation protocol but 2-fold more concentrated, i.e. triplicates of LP-RGD-GLA-$S_{(gluc)}$ sample 5-fold diluted in MeOH instead of using the habitual sample dilution of 10-fold in MeOH.

Recoveries between 95 – 105 % obtained in sample dissolution test (detailed on ***Table 5.22***) meant positive results, which validated that the protocol of sample preparation for further RP-HPLC-ELSD analysis following Strategy_1 (explained on ***Chapter 7, Section 7.4.5.6***) is capable to well solubilize the liposomal membrane components when diluting LP-RGD-GLA-$S_{(gluc)}$ samples at least 10-fold in MeOH. However, from the extra study, it was sure to confirm that matrix effects due to higher glucose concentration or a bad sample solubilization was occurring when samples were diluted less than 10-fold in MeOH, obtaining low material recoveries by using the RP-HPLC-ELSD analytical method named Method_007 in ***Table 7.11, Chapter 7, Section 7.4.5.6***.

Table 5.22. Summarized data of the accuracy results obtained in the sample dilution test. LP-RGD-GLA-$S_{(gluc)}$ nanoliposomal formulation was diluted using MeOH.

		MEMBRANE COMPONENT ANALYSIS							
		MKC		Chol-PEG_{400}-RGD		Chol		DPPC	
Nanovesicular system ID	Sample dilution comparison	Recovery (%)	Replicate RSD (%)	Recovery (%)	Replicate RSD (%)	Recovery (%)	Replicate RSD (%)	Recovery (%)	Replicate RSD (%)
LP-RGD-GLA-$S_{(gluc)}$	10 vs 20	95	1.91	102	1.42	101	1.05	99	1.18
	10 vs 5	101	1.91	79	1.42	50	1.05	89	1.18

Doping (accuracy) test: analysis of real samples on a certain analyte concentration range

At this point sample preparation and important method parameters (e.g. selectivity, linearity, analyte concentration range, system suitability…) were validated, and the probable matrix effects caused by the presence of some excipient overcome. However, another validation test named as doping test is suggested by ICH guidelines to fulfil the validation of the method accuracy parameter. The aim of the doping test is to investigate if some component of the liposomal matrix individually might interfere with each other. It consists of the addition of a standard solution (containing the specific analyte to investigate) over a real sample. Then, probable matrix effects caused due to deviations of the concentration presence of that specific analyte in real samples can be evaluated. Therefore, doping test is useful to corroborate that matrix effects are not occurring in real samples in the concentration range of RP-HPLC-ELSD analysis. A doping test is considered positive when obtaining recoveries between 95 – 105 % following calculations which relation the different samples analyzed following the ***Eq. 5.3***, where R_S refers to the analyte experimental value obtained with real sample, S_D to the one

obtained with the individual standards, and R_S+S_D to the one obtained with real samples in which the individual standard was added.

$$Recovery\ (\%)\ = \frac{[R_S + S_D(ppm)]\ -\ R_S(ppm)}{S_D(ppm)}\ x\ 100$$

(**Eq. 5.3**)

Herein, the same real concentrated LP-RGD-GLA-$S_{(gluc)}$ sample containing glucose as an isosmotic agent previously evaluated in the sample dissolution test was used to perform the doping test. Again, the RP-HPLC-ELSD Method_007 (detailed in ***Table 5.17,*** and in ***Chapter 7, Section 7.4.5.6***), which uses a calibration curve with glucose content, was employed for the analytical HPLC analysis of samples. The replicates and LP-RGD-GLA-$S_{(gluc)}$ sample preparation protocol to be compared during the doping test are schematized as follows:

1 – Triplicates of LP-RGD-GLA-$S_{(gluc)}$ samples prepared according to the sample preparation procedure established in the analytical method, i.e. triplicates of LP-RGD-GLA-$S_{(gluc)}$ sample 10-fold diluted in MeOH (described as Strategy_1 in ***Chapter 7, Section 7.4.5.6***).

2 – Triplicates of individual membrane component standards (on a range between 70 – 130 % the theoretical concentration of the component present in real samples). In complete validation procedures each analyte should be analyzed at different concentrations (e.g. 70 %, 100 % and 130 %). However, the scope of this thesis was to conduct only a preliminary validation and, thus, each component was analyzed only at 100 % theoretical concentration. Here, in the case of LP-RGD-GLA-$S_{(gluc)}$ formulation, the following standards were prepared in presence of glucose:

- MKC standard (27 ppm) / x3 replicates
- Chol-PEG_{400}-RGD standard (80 ppm) / x3 replicates
- Chol standard (235 ppm) / x3 replicates
- DPPC standard (651 ppm) / x3 replicates

3 – Triplicates of real LP-RGD-GLA-$S_{(gluc)}$ samples prepared as explained in point 1, but adding in each triplicate set the analyte of study at the same concentration/composition of each individual component standard analyzed before in point 2. Here, in the case of LP-RGD-GLA-$S_{(gluc)}$ formulation, the following samples were prepared also in glucose presence:

- LP-RGD-GLA-$S_{(gluc)}$ + MKC standard (27 ppm) / x3 replicates
- LP-RGD-GLA-$S_{(gluc)}$ + Chol-PEG_{400}-RGD standard (80 ppm) / x3 replicates
- LP-RGD-GLA-$S_{(gluc)}$ + Chol standard (235 ppm) / x3 replicates
- LP-RGD-GLA-$S_{(gluc)}$ + DPPC standard (651 ppm) / x3 replicates

Samples prepared in point 3 were 2-fold diluted before HPLC measurements to reach analyte concentrations inside the range of the prepared calibration curve. Then, DF was corrected during data analysis.

Recoveries between 95 – 105 % were obtained in the doping test for the evaluated concentrations of analytes (results are summarized in ***Table 5.23***). The positive results of the test robustly demonstrated that matrix effects were not occurring by standard addition and/or modification of membrane component ratios in the studied concentration ranges of the four analytes of interest (i.e. 26 – 43 ppm of MKC, 29 – 110 ppm of chol-PEG_{400}-RGD, 148 – 383 ppm of cholesterol, and 397 – 1048 ppm of DPPC). With this, the high method accuracy of 95 – 105 % demonstrated when measuring LP-RGD-GLA-$S_{(gluc)}$ formulations with the optimized RP-HPLC-ELSD Method_007 version (detailed in ***Table 5.17,*** and in ***Chapter 7, Section 7.4.5.6***).

Table 5.23. Accuracy data results obtained in the doping test analysing LP-RGD-GLA-$S_{(gluc)}$ nanoliposomal formulation.

	MEMBRANE COMPONENT ANALYSIS							
	MKC		Chol-PEG_{400}-RGD		Chol		DPPC	
Nanovesicular system ID	Recovery (%)	Replicate RSD (%)	Recovery (%)	Replicate RSD (%)	Recovery (%)	Replicate RSD (%)	Recovery (%)	Replicate RSD (%)
LP-RGD-GLA-$S_{(gluc)}$	98	5.96	105	3.89	103	2.29	104	1.11

Intermediate precision of the analytical RP-HPLC-ELSD method: intra-day analysis of real samples

Another interesting parameter to evaluate is the precision of the experimental values obtained between different days. For this aim, triplicates of a LP-RGD-GLA-$S_{(gluc)}$ formulation were prepared and analyzed using the RP-HPLC-ELSD Method_007 (detailed in ***Table 5.17***, and in ***Chapter 7, Section 7.4.5.6***) during 4 consecutive weeks of work. The results compiled on ***Table 5.24*** showed a high accurate reproducibility values for MKC and chol substances (RSD % < 5) and quite good accuracy for chol-PEG_{400}-RGD and DPPC molecules (RSD % < 10), taking into account the complexity of the liposomal nanostructures analyzed. The general specification obtained by RP-HPLC-ELSD analysis (with their corresponding criteria of acceptance shown in brackets) for the 4 liposomal components analysed in this study was:

- % RSD between injection replicates < 10 % (< 5 % if possible).

Table 5.24. Intermediate precision data of the analytical method.

		MEMBRANE COMPONENT ANALYSIS							
		MKC		Chol-PEG$_{400}$-RGD		Chol		DPPC	
Nanovesicular system ID	Calibration curve composition	Average recovery (%)	Inter-day RSD (%)	Average recovery (%)	Inter-day RSD (%)	Average recovery (%)	Inter-day RSD (%)	Average recovery (%)	Inter-day RSD (%)
LP-RGD-GLA-S$_{(gluc)}$	Composition_5*	58	2.99	36	9.13	63	2.26	61	9.11

According to all the validation tests performed in this section, the method parameters and liposomal matrix validated in this section using their corresponding version of the analytical RP-HPLC-ELSD method are summarized in ***Table 5.25***. Validation studies were carried out for each analyte of interest (MKC, chol-PEG$_{400}$-RGD, cholesterol and DPPC), but in ***Table 5.25*** only the general specifications obtained for all of them are indicated to simplify the information.

Table 5.25. Performed validation tests with their criteria of acceptance, the obtained method specifications and the liposomal matrix tested in each case.

TEST VALIDATION STUDY	GENERAL METHOD SPECIFICATION (including the 4* analytes tested)	CRITERIA OF ACCEPTACE	LIPOSOMAL MATRIX TESTED (RP-HPLC-ELSD METHOD)
Selectivity	All analytes have been well-identified	Identification of analyte peak	**Individual standards** dissolved in pure MeOH (Method_003)
Linearity (R^2) and concentration range (ppm)	≥ 0.9992 (MKC (5 – 80) Chol-PEG400-RGD (10 – 140) Chol (50 – 250) DPPC (100 – 800))	> 0.9990	**LP-RGD$_{(w)}$** (Method_003) **LP-RGD_int** (Method_004) **LP-RGD-GLA-S_int** (Method_005) **LP-RGD$_{(gluc)}$** (Method_006) **LP-RGD-GLA-S$_{(gluc)}$** (Method_007)
System suitability testing **» % RSD RT** **» % RSD area** **» Peak resolution** **» Symmetry factor** **» Points per peak**	 » < 0.08 % » < 5 (< 7 % for MKC in LP-RGD-GLA-S_int) » > 2.0 (well-resolved) » 0.85 – 1.30 » > 100 (peaks well-defined)	 » ≤ 1.0 % » ≤ 10 % » ≥ 2.0 » 0.80 – 1.50 » ≥ 100	 **LP-RGD-GLA-S_int** (Method_005) **LP-RGD-GLA-S$_{(gluc)}$** (Method_007)
Accuracy (using artificial samples)	95 – 105 %	95 – 105 %	**LP$_{(w)}$**, **LP-RGD$_{(w)}$** and **LP-6%RGD$_{(w)}$** (Method_003) **LP-RGD-GLA-S_int** (Method_005) **LP$_{(gluc)}$**, **LP-RGD$_{(gluc)}$**, **LP-6%RGD$_{(gluc)}$**, **LP-0%MKC-RGD$_{(gluc)}$** and **LP-0.5%MKC-RGD$_{(gluc)}$** (Method_006) **LP-RGD-GLA-S$_{(gluc)}$** (Method_007)
Sample dissolution test	95 – 105 %	95 – 105 %	**LP-RGD-GLA-S$_{(gluc)}$** (Method_007)
Accuracy (doping test)	95 – 105 %	95 – 105 %	**LP-RGD-GLA-S$_{(gluc)}$** (Method_007)
Intra-day intermediate precision (% RSD area)	< 5 % for MKC and Chol-PEG$_{400}$-RGD < 10 % for Chol and DPPC	< 10 %	**LP-RGD-GLA-S$_{(gluc)}$** (Method_007)

*The four analytes submitted to validation were MKC, chol-PEG$_{400}$-RGD, cholesterol and DPPC.

5.2.5. Contribution to the Certificate of Analysis (CoA) of LP-RGD-GLA-S formulations

Using the slight variations of RP-HPLC-ELSD method depending on the liposomal matrix to be analyzed (see ***Chapter 7, Section 7.4.5.6***), the chemical composition of the following formulation compositions listed on ***Table 5.26*** were assessed to support lab-scale experimentation intended to formulation development, but also to contribute to the CoA creation of samples intended to be used in important preclinical studies.

Table 5.26. Examples of nanoliposomal formulations analysed by RP-HPLC-ELSD to determine their chemical composition. Theoretical sample composition and sample contribution in lab-scale or preclinical studies is detailed.

Liposomal matrix analyzed	Membrane composition (theoretical molar ratio)	$[GLA\text{-}S]_{theoric}$ (μg/mL)	Theoretical % RGD (molar)	Theoretical % MKC (molar)	System prototype ($[lipid]_{theoric}$)	Solvent and excipients	RP-HPLC method employed	Purpose of Study
LP-RGD-GLA-S_int	**DPPC:Chol:Chol-PEG_{400}-RGD (10:6.5:0.5)**	30	3	5	Intermediate (1.2 mg/mL)	1 % EtOH 0.25 % DMSO (both in v/v)	Method_002	**Development of filtration sterilization protocol**
LP-RGD-GLA-$S_{(w)}$	**DPPC:Chol:Chol-PEG_{400}-RGD (10:6.5:0.5)**	200	3	5	Concentrated (9 mg/mL)	Pure water	Method_002	
LP-0%MKC-$RGD_{(gluc)}$	**DPPC:Chol:Chol-PEG_{400}-RGD (10:6.5:0.5)**	-	3	0	Concentrated (9 mg/mL)	Glucose 5 % (w/v) media	Method_006	**Non-GLP 28-day intravenous toxicity study in rats**
LP-0.5%MKC-$RGD_{(gluc)}$	**DPPC:Chol:Chol-PEG_{400}-RGD (10:6.5:0.5)**	-	3	0.5	Concentrated (9 mg/mL)	Glucose 5 % (w/v) media	Method_006	
LP-$RGD_{(gluc)}$	**DPPC:Chol:Chol-PEG_{400}-RGD (10:6.5:0.5)**	-	3	5	Concentrated (9 mg/mL)	Glucose 5 % (w/v) media	Method_006	
LP-RGD-GLA-$S_{(Cryo1)}$	**DPPC:Chol:Chol-PEG_{400}-RGD (10:6.5:0.5)**	200	3	5	Concentrated (9 mg/mL)	Cryo1 *	Method_003	**Development of the definitive lyophilized pharmaceutical product form**
LP-RGD-GLA-$S_{(Cryo2)}$	**DPPC:Chol:Chol-PEG_{400}-RGD (10:6.5:0.5)**	200	3	5	Concentrated (9 mg/mL)	Cryo2 *	Method_003	
LP-0%RGD-GLA-S_int	**DPPC:Chol (10:7)**	30	0	5	Intermediate (1.2 mg/mL)	1 % EtOH 0.25 % DMSO (both in v/v)	Method_005	**Preclinical biodistribution in Fabry mouse model**
LP-6%RGD-GLA-S_int	**DPPC:Chol:Chol-PEG_{400}-RGD (10:6:1)**	30	6	5	Intermediate (1.2 mg/mL)	1 % EtOH 0.25 % DMSO (both in v/v)	Method_005	
LP-0%RGD-GLA-$S_{(gluc)}$	**DPPC:Chol (10:7)**	200	0	5	Concentrated (9 mg/mL)	Glucose 5 % (w/v) media	Method_007	
LP-RGD-GLA-$S_{(gluc)}$	**DPPC:Chol:Chol-PEG_{400}-RGD (10:6.5:0.5)**	200	3	5	Concentrated (9 mg/mL)	Glucose 5 % (w/v) media	Method_007	
LP-6%RGD-GLA-$S_{(gluc)}$	**DPPC:Chol:Chol-PEG_{400}-RGD (10:6:1)**	200	6	5	Concentrated (9 mg/mL)	Glucose 5 % (w/v) media	Method_007	

* Cryo1 contained: glycine 7.5 mg/mL, trehalose 50 mg/mL and sucrose 30 mg/mL; and Cryo2: glycine 50 mg/mL and sucrose 80 mg/mL.

5.2.6. Summary

In this chapter, a RP-HPLC-ELSD analytical method capable to simultaneously analyze MKC, chol-PEG_{400}-RGD, cholesterol and DPPC molecules, was successfully developed and its chromatographic parameters optimized according to regulatory ICH guidelines. However, the RP-HPLC-ELSD method described in this chapter requires of two different inject volumes of sample to the accurate simultaneous quantification of all components due to limitations on the parameter configuration of ELSD equipment from Agilent. In future, this issue could be solved by transferring the methodology to another ELSD instrument with a more flexible configuration.

In parallel, the preparation procedure of samples for RP-HPLC-ELSD analysis was improved by avoiding the extra sample freeze-drying step, decreasing the time of dedication and reducing sample handling.

Several versions of liposomal formulations (with or without GLA-S containing) differing on excipient composition were tested with the optimized method. These results evidenced the necessity of preparing specific calibration curves simulating the same matrix composition of each nanoliposomal formulation of study in order to avoid matrix effects caused by the presence of excipients, which are capable of deviating the analytes' signal-responses when these are only present in sample of analysis but no in the used calibration curve.

Moreover, a validation was conducted to ensure the reliability of the RP-HPLC-ELSD method in various liposomal matrixes differing on membrane or excipient composition. For the accurate and reliable quantification of liposomal membrane components from each liposomal matrix, it was evidenced the necessity of using slightly different versions of the optimized RP-HPLC-ELSD analytical method (named from Method_003 to Method_007 in ***Table 5.17*** of the ***Section 5.2.4.***, and detailed in ***Chapter 7, Section 7.4.5.6***), which consisted of the same gradient, column and instrumental parameters, but using specific calibration curves of different composition (simulating the liposomal matrix to analyse). LP-RGD-GLA-$S_{(gluc)}$ was the unique formulation validated using the RP-HPLC-ELSD Method_007, allowing to consider their obtained results as quantitative values. This validation was done in the following analyte concentration range of LP-RGD-GLA-$S_{(gluc)}$ samples: 26 – 43 ppm of MKC, 29 – 110 ppm of chol-PEG_{400}-RGD, 148 – 383 ppm of cholesterol, and 397 – 1048 ppm of DPPC. The validation tests meeting the criteria of acceptance recommended for ICH guidelines and, thus, within specifications were: selectivity, linearity (≥ 0.9992), system suitability test, sample dissolution test (95 – 105 %), accuracy (95 – 105 %) and intra-day precision (RSD < 5 % for MKC and chol-PEG_{400}-RGD, and RSD < 10 % for cholesterol and DPPC). These robust results demonstrated the proper quantification of MKC, chol-PEG_{400}-RGD, cholesterol and DPPC in complex liposomal formulations with small deviation on quantification values. These promising results allowed the characterization and control of the chemical composition of liposomal samples containing glucose as isosmotic agent, which has been evaluated in preclinical studies during the European Phoenix project. RP-HPLC-

ELSD analysis of the other liposomal compositions must be considered semi-quantitative until further method validation would be performed.

Once the definitive pharmaceutical form will be defined (e.g. freeze-dried formulation), the RP-HPLC-ELSD method will be adjusted and validated due to probable slight changes in their composition (e.g. presence of cryoprotectants). In that moment, the definitive RP-HPLC-ELSD method will be transferred to Nanomol Technologies SL for its GMP-compliant validation.

5.3. Implementing and optimizing procedures to control LP-RGD-GLA-S microbiological quality

Microbiological specification for intravenous formulations is that it must be sterile and pyrogen free throughout it shelf-life[28–34]. Accordingly, for liposome product stability validation, EMA and FDA requires three studies: microbiological, physical, and chemical product stability[3,4,6,7,35].

Since the manufacturing of the nanoliposome formulations is conducted in aseptic-like conditions but not in a clean room facility, terminal sterilization by filtration was chosen as the most convenient method to sterilize the samples. In the frame of the European Phoenix project, a sterilization strategy based on nanovesicle filtration has been developed by Nanomol Technologies SL. In order to prove that the developed filtration protocol is efficient to remove bacteria from the nanoformulation and/or the absence of endotoxins in the liposomal formulations, a methodology based on Luria Broth agar plate test (for bacterial contamination assessment) and Gel clot LAL assay (for endotoxins assessment) has set up in this thesis. Nevertheless, to point out that these assays are not intended to certify the samples as sterile.

5.3.1. Bacterial contamination detection by Luria Broth agar plate test

This procedure is based on the Method STE-2.2 protocol from Nanotechnology Characterization Laboratory (NCL)[36,37], and it is well described on ***Chapter 7, Section 7.4.7.1***.

As aforementioned, the main objective of using the Luria Broth agar plate test was to prove that the developed filtration sterilization protocol is efficient to remove bacteria from the nanoformulations. With this aim, the microbiological quality assessment of samples submitted to filtration sterilization assays was tested before and after the filtration step (***Table 5.27***). Briefly, liposomal samples and the non-encapsulated GLA-S enzyme (used as control) were spread on the surface of agar plates. After 72 h of incubation at 37 ºC, the growth of bacterial colonies was monitored. As shown in ***Table 5.27*** and ***Figure 5.14***, some nanoliposomal formulations may present bacterial contamination after the manufacturing process in non-sterile conditions. However, once the

nanoformulations were filtrated, no bacterial colonies could be detected in the tested sample dilutions. Besides, contamination was neither observed for the non-encapsulated GLA-S which was used as control (*Figure 5.15*), indicating that microbial contamination was not coming from GLA-S enzyme. Taking into account these results, it seems that the developed filtration sterilization protocol is efficient to eliminate microbial contamination from nanoliposomal samples. Nevertheless, further investigation including analysis of minimal inhibitory concentration (MIC) must be performed to evaluate the nanomaterial potential to inhibit bacterial growth (testing different sample concentrations and using positive controls) to validate the methodology and verify such findings.

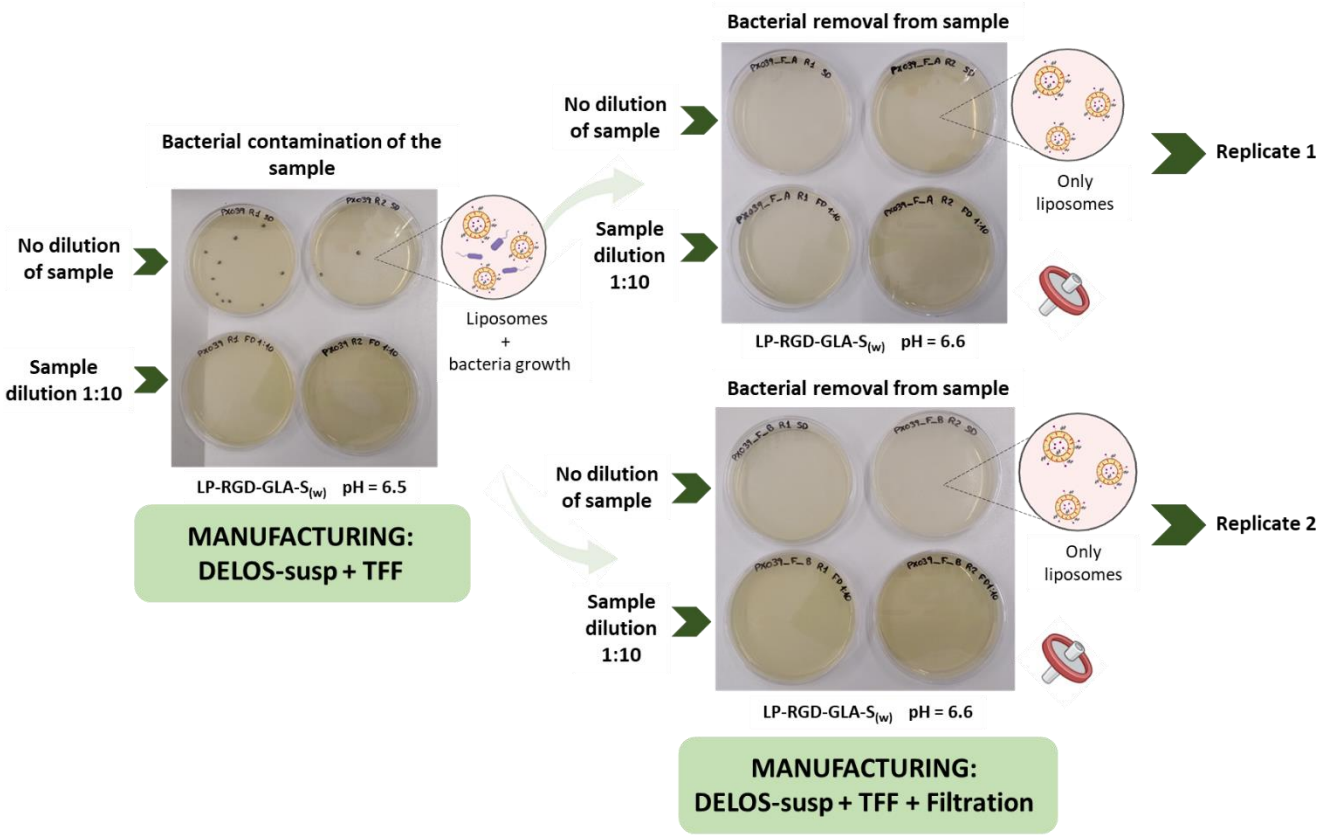


Figure 5.14. Images of Luria Broth agar plates for determining if there was bacterial contamination on LP-RGD-GLA$_{(w)}$ formulation (as a concentrated product prototype), before and after filtration sterilization process. Samples were diluted using endotoxin-free water when necessary for the test.

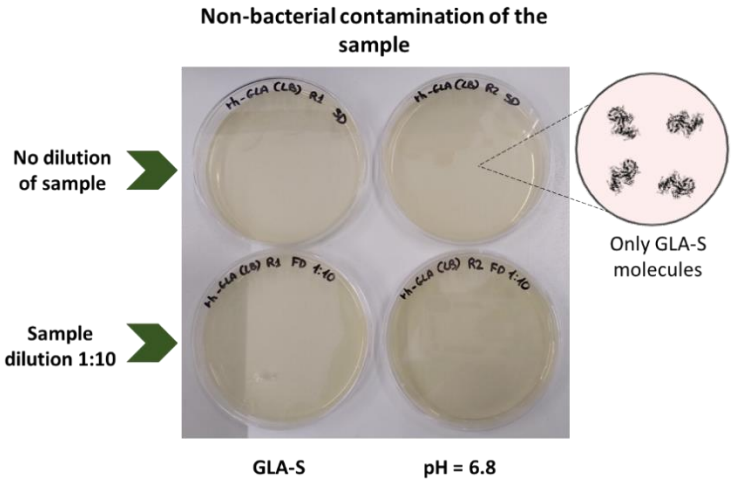


Figure 5.15. Image of Luria Broth agar plates to determine the microbiological quality of the non-encapsulated GLA-S enzyme. Sample were diluted using endotoxin-free water when necessary for the test.

Furthermore, several liposomal nanoformulations differing on composition were tested using this methodology (compiled on *Table 5.27*), and their chemical composition analyzed by RP-HPLC-ELSD method (explained on *Section 5.2*), demonstrating good recoveries of all liposomal components after filtration steps (see *Figure 5.16*). GLA-S recoveries and remaining enzymatic activity for these experiments were determined by LeanBio SL according to methods explained on *Chapter 7, Sections 7.2.6.3* and *7.2.9*).

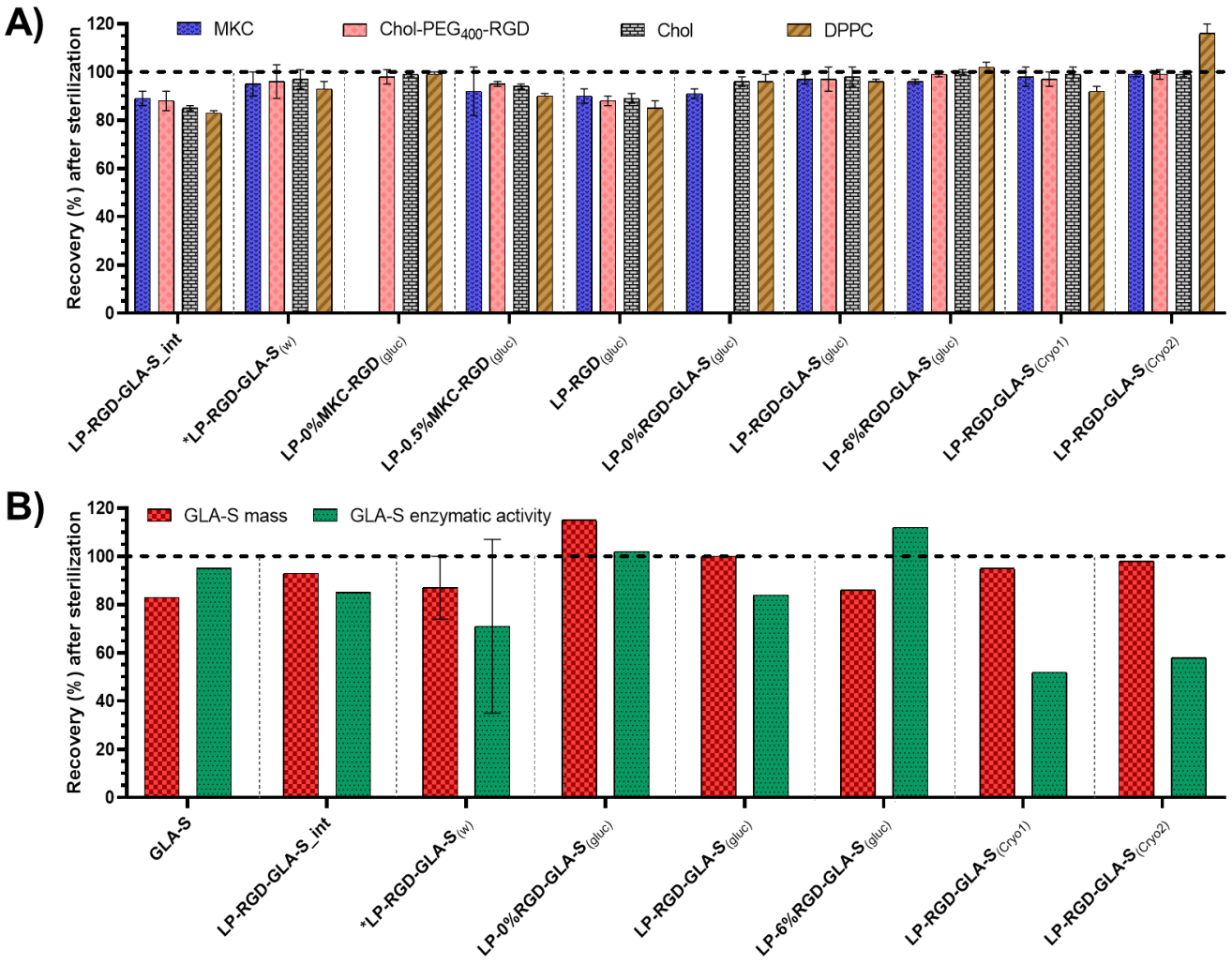


Figure 5.16. Analysis of liposomal formulation submitted to filtration-sterilization procedures for the assessment of: A) mass membrane component recoveries by RP-HPLC-ELSD measurements, and B) recoveries of GLA-S mass by HPLC-UV and remaining enzymatic activity. Only 1 batch of each formulation was measured by triplicate. * In this specific case, two batches of LP-RGD-GLA-$S_{(w)}$ were analyzed.

Table 5.27. Liposomal formulations analyzed by Luria Broth agar plate test. Relevant sample properties such as composition, pH and microbiological content before and after sterilization procedures are compiled.

	NANOFORMULATION PROPERTIES								
Nanovesicular system ID	**Theoretical lipid (mg/mL)**	**Theoretical GLA (mg/mL)**	**pH**	**Excipients**	**Filtration sterilization ?**	**pH adjustment requirement**	**Microbiological content (CFU/mL)**	**Batches analyzed**	**Purpose of Study**
GLA-S	0	4	6.8 ± 0.1	Mannitol, sodium phosphate monobasic monohydrate, sodium phosphate dibasic heptahydrate	No	No	0	2	Development of filtration sterilization protocol
LP-RGD-GLA-S_int	1.2	0.03	5.1 ± 0.2	5 % EtOH + 1.2 % DMSO (v/v)	No	Yes	0	3	
					Yes	***Yes***	***0***	***1***	
LP-RGD-GLA-$S_{(w)}$	9	0.2	6.8 ± 0.4	Pure water	No	No	1200 ± 1200	2	
					Yes	***No***	***0***	***3***	
LP-0%MKC-$RGD_{(gluc)}$	9	0	4.5	Sterile glucose 5% (w/v) from Braun	No	Yes	0	1	Non-GLP 28-day intravenous toxicity study in rats
					Yes	***Yes***	***0***	***1***	
LP-0.5%MKC-$RGD_{(gluc)}$	9	0	4.7	Sterile glucose 5% (w/v) from Braun	No	Yes	0	1	
					Yes	***Yes***	***0***	***1***	
LP-$RGD_{(gluc)}$	9	0	4.8	Sterile glucose 5% (w/v) from Braun	No	Yes	0	1	
					Yes	***Yes***	***0***	***1***	
LP-RGD-GLA-$S_{(Cryo1)}$	9	0.2	6.8	Glycine 7.5 mg/mL, Trehalose 50 mg/mL, Sucrose 30 mg/mL	No	No	1600	1	Development of the definitive lyophilized pharmaceutical product form
					Yes	***No***	***0***	***1***	
LP-RGD-GLA-$S_{(Cryo2)}$	9	0.2	6.8	Glycine 50 mg/mL, Sucrose 80 mg/mL	No	No	2400	1	
					Yes	***No***	***0***	***1***	
LP-0%RGD-GLA-S_int	1.2	0.03	4.2	5 % EtOH + 1.2 % DMSO (v/v)	No	Yes	0	1	Preclinical biodistribution in Fabry mouse model
LP-6%RGD-GLA-S_int	1.2	0.03	4.2	5 % EtOH + 1.2 % DMSO (v/v)	No	Yes	0	1	
LP-0%RGD-GLA-$S_{(gluc)}$	9	0.2	4.7	Sterile glucose 5% (w/v) from Braun	No	Yes	0	1	
					Yes	***Yes***	***0***	***1***	
LP-RGD-GLA-$S_{(gluc)}$	9	0.2	4.9	Sterile glucose 5% (w/v) from Braun	No	Yes	0	1	
					Yes	***Yes***	***0***	***1***	
LP-6%RGD-GLA-$S_{(gluc)}$	9	0.2	4.8	Sterile glucose 5% (w/v) from Braun	No	Yes	0	1	
					Yes	***Yes***	***0***	***1***	

According to NCL, complementary studies to assess bacterial contamination might also be performed by using other tests such as RPMI suspension test or Tryptic Soy Broth agar plates[38], which use other media capable to grow different kind of bacteria (e.g. autotrophic, oligotrophic…) or microorganism (e.g. yeast…) to better understand the microbiological pattern of the samples analyzed[39].

5.3.2. Bacterial endotoxin quantification: Gel clot LAL assay optimization and verification

It is important to take into account that whenever a sample is sterilized by some procedure (e.g. filtration, irradiation or others)[40,41], some bacteria material can remain on the pharmaceutical formulation. Endotoxins are lipopolysaccharides (LPS) present in gram-negative bacteria membranes capable to act as immunostimulators causing fever and septic shock in blood circulation. So, their quantity in formulations must be also controlled to avoid the health compromising of animals or humans, and therefore, the alteration of results obtained during preclinical and clinical assays[42–44]. In the NCL database, *in vitro* assays based on LAL are described as potential methodologies capable to detect and quantify endotoxin amounts in pharmaceutical products[45]. The use of LAL for endotoxin detection started from the discovering by Frederick Bang (1950), that amebocytes (blood cells) of horseshoe crab (*Limulus Polyphemus*) clot in presence of low levels of endotoxins[46]. So, a lysate from these washed amebocytes is used as a principle of an enzymatic reaction in LAL kits. They are available in three different formats:

- Gel clot method: based on gel formation.
- Chromogenic technique: based on the color formation after cleavage of a synthetic peptide-chromogen complex.
- Turbidimetric technique: based on turbidity generation after cleavage of an endogenous substrate.

In order to obtain accurate, precise and robust results, FDA regulatory strongly recommend to follow the chosen pathway schematized on ***Figure 5.17***. Briefly, endotoxins of a pharmaceutical product should be analyzed with a quantitative method such as Chromogenic LAL assay (as long as the product absorbance spectrum does not overlap the absorbance wavelength used in the assay). If it is no possible, Turbidity LAL assay can also be used as a quantitative method (unless the product consist on a turbid formulation). As last choice, Gel clot LAL assay should be tested. However, pharmaceutical products must be tested and their endotoxin content compared by two different methodologies for result verification, due to the high variability related with LAL assays especially when these are used inter-laboratory. Many nanomaterials can interfere with such assays, so only when required, different bioassays may be employed for the verification of LAL data.

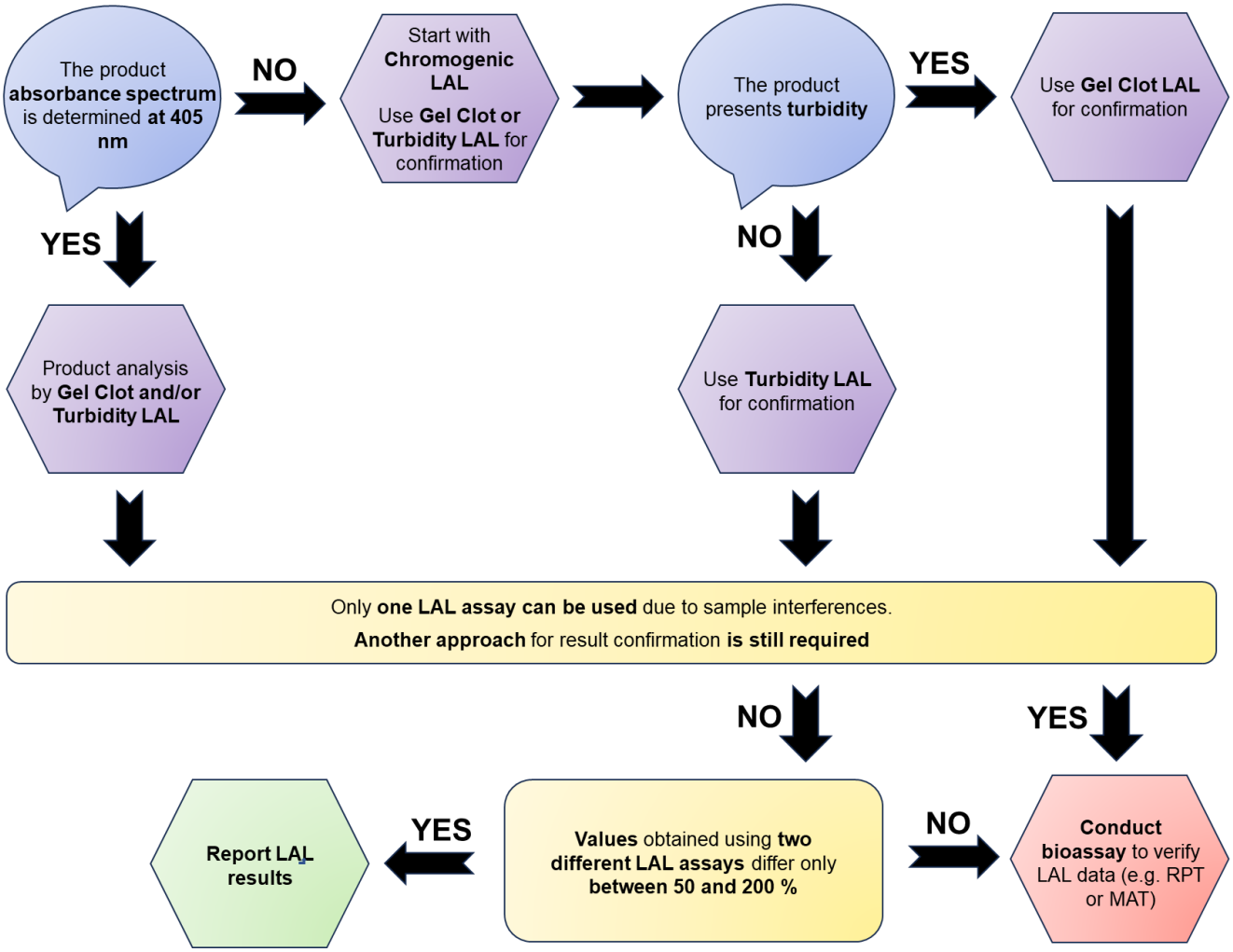


Figure 5.17. Decision tree diagram indicating methodologies to use for sample endotoxin determination, taking into account the probability of sample interferences with them. Adapted from McNeil[47]. Legend: RPT means rabbit pyrogen test, and MAT means monocyte activation test.

Herein, to control the endotoxin amount present in the liposomal samples, the Gel clot LAL assay[42–44,48,49] (PYROGENT™ Plus Gel Clot LAL Assay) was selected because, although this is a qualitative assay to be used in a qualitative manner, the turbidity of the nanoliposomal formulations interferes with LAL Chromogenic Endotoxin Quantitation Kit which is based on absorbance measurements. In the case of Gel Clot kit, the presence of gram-negative bacterial endotoxins catalyzes the activation of an enzymatic cascade, starting for a proenzyme called coagulase. When coagulase is active induce the further activation of coagulin, a clotting protein, capable to form a gelatinous clot[50].

During this thesis, the Gel clot protocol to determine endotoxins was optimized and detailed on *Chapter 7, Section 7.4.7.2*. Briefly, the most important contributions implemented over the protocol described as Method STE-1.3[48] are:

i. Use of β-glucan blocker: to avoid false-positive results by using a volume ratio of sample:blocker of 1:1. B-glucans are capable to start the same protease cascade as endotoxins, inducing false-positives in LAL assays (see *Figure 5.18*)[51].

ii. Addition of sodium dodecyl sulfate (SDS) in samples: to avoid false-negative results by solubilizing nanovesicles using a final concentration of 0.001 % (v/v) of sterile SDS, and disrupting probable electrostatic interactions between LPS and the positives charges of our liposomal membrane due to the MKC surfactant. In this manner, LPS may be accessible to LAL reaction[52,53].

iii. Heat treatment of samples: to facilitate the nanoliposomes solubilization and the disruption of electrostatic bindings between components of the product by boiling samples at 95 ºC during 30 min.

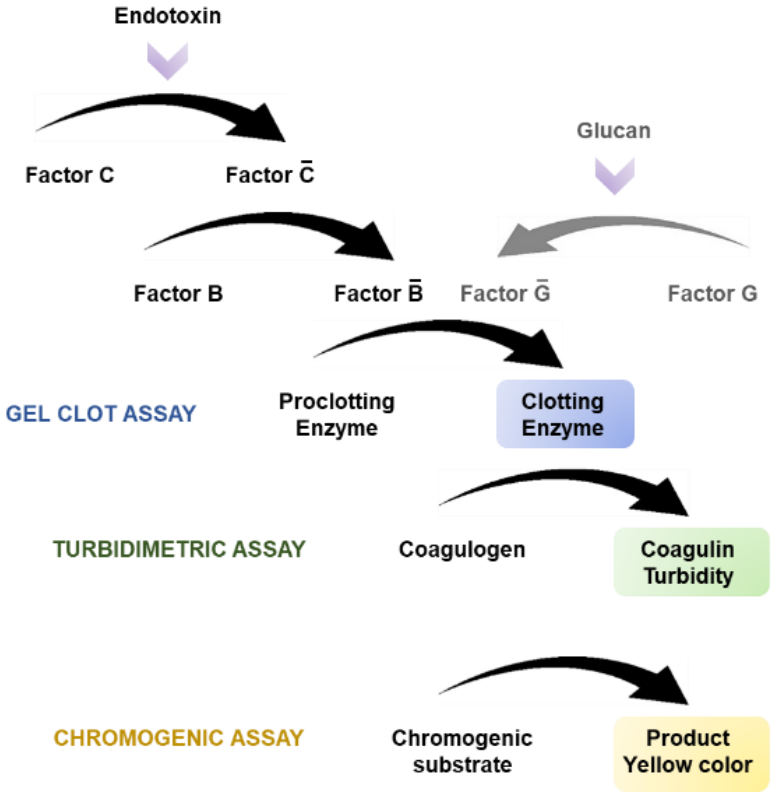


Figure 5.18. Endotoxin-induced enzymatic cascade and end-point reaction achieved by each LAL assay format. B-glucan-induced enzymatic cascade is also represented to better understand its probable interaction in LAL-based methodologies.

Once optimized the Gel clot LAL protocol to employ for liposomal formulations, the method compatibility with liposomal-based nanoformulations was tested to verify results reliability. For this purpose, three parallel studies must be conducted: i) confirmation of label claim, ii) endotoxin level testing on sample, and iii) product inhibition test. The samples deeply analyzed following this procedure were: non-encapsulated GLA-S enzyme (as control), LP-RGD-GLA-S_int (as intermediate prototype containing organic solvents) and LP-RGD$_{(gluc)}$ (as liposomal nanoformulation containing glucose to test in preclinical studies). In *Table 5.28* their composition is detailed.

Table 5.28. Summary of samples tested using Gel clot LAL assay. Legend: MVD refers to the maximum allowable dilution to be tested by LAL assays.

Sample ID	Theoretical lipid (mg/mL)	Theoretical GLA (mg/mL)	pH	pH adjustement requirement	Excipients	Batches analyzed	MVD	Endotoxin amount* (EU/mL)	Matrix validation
GLA-S	0	3.11	6.9	No	Mannitol, sodium phosphate monobasic monohydrate, sodium phosphate dibasic heptahydrate	1	25	≥ 1.25 but < 2.5	No
LP-RGD-GLA-S_int	1.2	0.025	5.1 ± 0.2	Yes	5 % EtOH (v/v) 1.2 % DMSO (v/v)	2	9	Incompatible matrix with LAL assay	No
$LP\text{-}RGD_{(gluc)}$	9	0	4.7 ± 0.1	Yes	Sterile glucose 5% (w/v) from Braun	2	72	< 0.52	Yes

* Endotoxin amounts (EU/mL) in samples were determined by Gel clot LAL assay.

Confirmation of label claim

For each new commercial Gel clot LAL kit, a confirmation of label claim test is required. This test is intended to check and calculate the sensitivity of the assay used, i.e. the minimal concentration of units of endotoxins per milliliter capable to be detected (EU/mL). In order to perform the study, calibration curves with endotoxin standard are prepared in quadruplicate using endotoxin-free water and then results analyzed according to manufacturer instructions. Since in this work, samples analyzed by Gel clot LAL procedures contain few amounts of SDS, the confirmation of label claim test was also performed using calibration curves prepared by using sterile 0.001 % SDS (v/v) previously prepared using endotoxin-free water (see *Table 5.29*). This experiment was intended to investigate if SDS presence in samples can interfere with LAL lysate reaction. Furthermore, extra calibration curves containing both glucose 5 % (w/v) and 0.001 % SDS (v/v) were analyzed to study if glucose molecules can inhibit the clotting formation. A commercial lysate with a sensitivity value ≥ 0.125 EU/mL was used to perform these experiments.

Table 5.29. Results of confirmation of label claim test comparing calibration curves of endotoxin standard prepared A) only using endotoxin-free water, B) using a sterile solution of 0.001 % SDS (v/v), or C) using sterile glucose 5 % (w/v) + 0.001 % SDS (v/v).

A)	CONFIRMATION OF LABEL CLAIM TEST Endotoxin concentration (EU/mL) on Calibration Curve points prepared only using endotoxin-free water					
Replicate tested	0.5	0.25	0.125	0.06	0.03	0
1	+	+	+	-	-	-
2	+	+	-	-	-	-
3	+	+	+	+	-	-
4	+	+	+	-	-	-

B)	CONFIRMATION OF LABEL CLAIM TEST Endotoxin concentration (EU/mL) on Calibration Curve points prepared using sterile 0.001 % SDS (v/v)					
Replicate tested	0.5	0.25	0.125	0.06	0.03	0
1	+	+	+	-	-	-
2	+	+	+	-	-	-
3	+	+	+	-	-	-
4	+	+	-	+	-	-

C)	CONFIRMATION OF LABEL CLAIM TEST Endotoxin concentration (EU/mL) on Calibration Curve points containing sterile glucose 5 % (w/v) and 0.001 % SDS (v/v)					
Replicate tested	0.5	0.25	0.125	0.06	0.03	0
1	+	+	+	-	-	-
2	+	+	+	-	-	-
3	+	+	+	-	-	-
4	+	+	+	-	-	-

Due to positive results were mainly achieved in all cases when endotoxin concentrations ≥ 0.125 EU/mL were tested, results confirmed that glucose presence or the addition of few SDS amounts in samples were not interfering with the clotting capacity or sensitivity of the lysate used.

Endotoxin level testing on sample and product inhibition test

Before conducting any sample testing, the maximum allowable dilution (MVD) of pharmaceutical formulations must be calculated, according to *Eq. 7.6.* in *Chapter 7, Section 7.4.7.2*. MVD describes the maximum sample dilution which can be tested to determine the endotoxin content to obtain reliable results. Briefly, MVD correlates the sample concentration of testing with the LAL lysate sensitivity and the endotoxin limit that must not reach a drug to be administered. Endotoxin limit is imposed by FDA and EMA, and the limit value for intravenous drug administration is 1 EU/mL[42–44]. Intermediate and final (concentrated) nanoliposomal

prototypes tested in this chapter present a respective MVD value of 9 and 72 due to their difference in lipid concentration.

Once MVD is determined, testing of endotoxin levels on successive sample dilutions can be analyzed until achieving negative results (< 0.125 EU/mL). Then, product inhibition test must be performed to verify that sample composition is not interfering with LAL lysate reaction, and determine if results are reliable. The product inhibition test consists of adding known amounts of endotoxin standard concentrations (also known as endotoxin spikes) to those dilutions with negative results in order to discard false-negative results.

Below, the compatibility of some liposomal-based nanoformulations prepared in aseptic-like conditions was investigated:

- Testing of LP-RGD-GLA-S_int formulation prototype

After DELOS-susp production, intermediate nanoliposomal prototype containing few amounts of organic solvents (5 % EtOH + 1.2 % DMSO (v/v)) in their composition are obtained. In order to study if some endotoxin contamination can occur in the reactor during nanoliposomes production, two different batches of LP-RGD-GLA-S_int were tested by Gel clot LAL assay and same results were obtained.

The results obtained from LP-RGD-GLA-S_int formulations (see ***Table 5.30***), suggested that the tested samples contained endotoxin concentration < 0.125 EU/mL. However, when these results were compared with those in which various concentrations of endotoxin spikes were added, it could be seen that the sample composition is interfering in the test, yielding false-negative results due to clotting inhibition.

Table 5.30. Result compilation from A) endotoxin level evaluation in successive LP-RGD-GLA-S_int formulation dilutions, and B) product inhibition test in LP-RGD-GLA-S_int samples tested at two different dilutions.

A)	SAMPLE TESTING BY GEL CLOT ASSAY LP-RGD-GLA-S_int formulations in 5 % EtOH + 1.2 % DMSO + 0.001 % SDS (v/v)					
Replicate tested	No dilution	Dilution 1:2	Dilution 1:4	Dilution 1/5	Dilution 1/9	Only EtOH + DMSO solvents
1	-	-	-	-	-	-
2	-	-	-	-	-	-
3	-	-	-	-	-	-
4	-	-	-	-	-	-

B)	PRODUCT INHIBITION TESTING Standard endotoxin spikes (EU/mL) in LP-RGD-GLA_int formulations containing 5 % EtOH + 1.2 % DMSO + 0.001 % SDS (v/v)						
Replicate tested	0.5	0.25	0.125	0.06	0.03	0	Sample dilution tested
1	-	-	-	-	-	-	No dilution
2	-	-	-	-	-	-	
3	-	-	-	-	-	-	
4	-	-	-	-	-	-	
1	-	-	-	-	-	-	Dilution 1:5
2	-	-	-	-	-	-	
3	-	-	-	-	-	-	
4	-	-	-	-	-	-	

In order to discard sample incompatibility with the test due to the presence of GLA-S protein, same studies were performed with one batch of GLA-S protein provided by LeanBio SL and certified to contain endotoxin levels < 2 EU/mL. The calculated MVD value for the enzyme batch is 25. Results compiled in *Table 5.31* supported that low endotoxin recoveries in LP-RGD-GLA-S_int samples were not caused by GLA-S presence. Nevertheless, Gel clot LAL assay is a qualitative assay in which there is no possible to discard false-positive results. So, further investigation with GLA-S batches, certified to contain < 0.125 EU/mL by LeanBio SL in the provided CoA using the Endosafe® nexgen-PTS™ (a method based on visible spectrophotometry)[54], should be performed in near future to verify at which specific GLA-S concentrations, the protein is not able to interfere in Gel clot testing.

Table 5.31. Comparison of two experiments run in parallel: A) endotoxin level testing of GLA-S enzyme and, B) product inhibition test of GLA-S enzyme.

A)	SAMPLE TESTING BY GEL CLOT ASSAY GLA-S enzyme in 0.001 % SDS (v/v)					
Replicate tested	No dilution	Dilution 1:2	Dilution 1:5	Dilution 1/10	Dilution 1/20	Only 0.001 % SDS (v/v)
1	+	+	+	-	-	-
2	+	+	+	+	-	-
3	+	+	-	-	-	-
4	+	+	-	+	-	-

B)	PRODUCT INHIBITION TESTING GLA-S enzyme in 0.001 % SDS (v/v)						
Replicate tested	0.5	0.25	0.125	0.06	0.03	0	Sample dilution tested
1	+	+	+	-	-	-	Dilution 1:20
2	+	+	+	+	-	-	
3	+	+	+	+	-	-	
4	+	+	+	-	-	-	
1	+	+	+	-	-	-	Dilution 1:25
2	+	+	+	-	-	-	
3	+	+	+	-	-	-	
4	+	+	+	-	-	-	

❖ Testing of LP-RGD$_{(gluc)}$ nanovesicular formulation

In the frame of the European Phoenix project, the LP-RGD$_{(gluc)}$ nanovesicular formulation containing glucose as isosmotic agent is intended to be tested in toxicology preclinical studies since it is the most advanced composition in terms of product development and quality. Before, the accurate analysis on its endotoxin content by Gel clot LAL assay must be validated. Two batches of LP-RGD$_{(gluc)}$ nanoformulation with 0 CFU/mL detected by Luria Broth agar plate test (see *Section 5.3.1*) were used for validation purposes.

According to results shown in *Table 5.32 A*, both LP-RGD$_{(gluc)}$ batches should contain endotoxin concentrations < 0.52 EU/mL, since negative results were not achieved until sample dilution 1:5. Furthermore, when testing 5- or 10-fold diluted LP-RGD$_{(gluc)}$ with the addition of various concentrations of endotoxin spikes, positive results were obtained only in replicates containing endotoxin spikes ≥ 0.125 EU/mL (see *Figure 5.32 B*). These results suggested that there are non-interferences due to neither liposomal composition nor material capacity of causing false negative-results. Interestingly, these results support that these nanoliposomal formulations produced in asceptic-like conditions can achieve the required endotoxin specification of < 1 EU/mL.

As conclusion, LP-RGD$_{(gluc)}$ nanovesicular system can be tested if it is at least 5-fold diluted obtaining reliable results. With lower sample dilutions (< 5-fold diluted) a confirmatory study to discard possible false-positive results cannot be performed due to the qualitative nature of this Gel clot LAL assay.

Table 5.32. Compilation of results from A) endotoxin level evaluation of successive dilutions of LP-RGD$_{(gluc)}$ formulation, and B) product inhibition test of LP-RGD$_{(gluc)}$ nanoformulation tested at two different dilutions (1:5 and 1:10).

A) SAMPLE TESTING BY GEL CLOT ASSAY LP-RGD$_{(gluc)}$ formulation containing sterile glucose 5 % (w/v) + 0.001 % SDS (v/v)								
Replicate tested	No dilution	Dilution 1:2	Dilution 1:4	Dilution 1/5	Dilution 1/10	Dilution 1/20	Dilution 1/50	Only Glucose 5 % (w/v) + 0.001 % SDS (v/v)
1	+	+	-	-	-	-	-	-
2	+	+	+	-	-	-	-	-
3	+	+	-	-	-	-	-	-
4	+	+	-	-	-	-	-	-

B) PRODUCT INHIBITION TESTING LP-RGD$_{(gluc)}$ formulation containing sterile glucose 5 % (w/v) + 0.001 % SDS (v/v)							
Replicate tested	0.5	0.25	0.125	0.06	0.03	0	Sample dilution tested
1	+	+	+	-	-	-	Dilution 1:5
2	+	+	+	-	-	-	
3	+	+	+	-	-	-	
4	+	+	+	-	-	-	
1	+	+	+	-	-	-	Dilution 1:10
2	+	+	+	-	-	-	
3	+	+	+	-	-	-	
4	+	+	+	-	-	-	

Regarding LP-RGD$_{(gluc)}$ nanoformulation matrixes, these were validated to be analyzed by Gel clot LAL assay, and next steps will involve the validation of this nanoformulation containing the GLA-S enzyme (LP-RGD-GLA-S$_{(gluc)}$) to discard interferences by GLA-S presence. In near future, Gel clot methodology must be validated using a GLA-S batch of high quality regarding endotoxin levels (< 0.125 EU/mL if possible) as explained above.

Nevertheless, a complementary quantitative test (e.g. LAL chromogenic assay or LAL turbidimetric assay) for the endotoxin assessment would be appropriate to use. The implementation of new sample pretreatment protocols to try to overcome material interference or the use of bioassays (e.g. rabbit pyrogen test (RPT) or monocyte activation test (MAT)) could be an alternative in future.

5.3.3. Summary

To summarize the work explained in this chapter, two tests were used and optimized to assess and control the microbiological quality of the liposomal nanoformulation under development. On the one hand, the Luria Broth agar plate test was implemented for the detection of bacterial contamination in the nanoliposomal formulations. Additionally, this methodology was contributed to prove that the filtration procedure developed by Nanomol Technologies SL for nanoliposome sterilization is efficient to remove bacteria from the nanoformulations. However, further investigation including analysis of MIC is needed to verify such results. On the other hand, Gel clot LAL assay demonstrated to be a suitable assay to determine and control the bacterial endotoxins content in

the nanoformulations. It was found to be incompatible with LP-RGD-GLA-S_int prototype due to the presence of organic solvents in the composition, but compatible with LP-RGD$_{(gluc)}$ nanoformulation containing glucose as isosmotic agent. This fact allowed to obtain a preliminary method to assess and control the endotoxin content of samples intended to be used in the *in vivo* preclinical studies. Further work is required in order to validate this method.

5.4. Development of an *in vitro* drug release methodology

Other relevant CQA to well determine and control on nanopharmaceuticals based on nanocarriers is the release rate of the active substance or drug from nanovesicles. Drug release kinetics should be investigated as it is a crucial parameter allowing to differentiate the nanoliposomal formulation from the non-liposomal commercial products. By measuring the non-encapsulated drug substance versus the encapsulated one, the *in vitro* release study characterizes liposome integrity which may significantly impact the drug product's clinical performance. As stated in FDA's draft guidance: "Ideally, the dissolution/*in vitro* release method should be able to discriminate batches that are not bioequivalent to the pivotal clinical batch, which will have demonstrated efficacy and safety"[3]. Following this objective, an *in vitro* release test must be established to ensure the consistent *in vivo* stability and drug release profile of a nanopharmaceutical. According to the Guidance for Industry from the FDA entitled "Liposome Drug Products Chemistry, Manufacturing, and Controls; Human Pharmacokinetics and Bioavailability; and Labeling Documentation", it is stated "A validated analytical procedure for *in vitro* release should be established, preferably using an appropriate physiological medium (e.g., simulated physiological medium or human plasma) with suitable agitation"[4].

Herein, efforts were focused on setting-up a methodology for an *in vitro* GLA release study from LP-RGD-GLA nanoformulations in physiologically/clinically relevant media. With this aim, different release analysis methods for liposomal products were investigated. The main challenge was to obtain a methodology efficient enough to separate the released drug substance from the liposomes. Among the most common used methods, dialysis and ultracentrifugation were discarded since the total diffusion of non-encapsulated GLA through dialysis membranes, or the maintenance of liposomes integrity and physicochemical stability, were not achieved, by using respectively both aforementioned methods. However, the filtration-centrifugation was the most appropriate method to use with the GLA-loaded nanoliposomal formulation. The development of the filtration-centrifugation methodology is explained in this section, and the final optimized protocol detailed in ***Chapter 7, Section 7.4.6***.

5.4.1. Implementation of a procedure based on filtration-centrifugation

Centrifugation using low centrifugation forces with membrane diffusion by using Amicon® centrifugation filter units was the selected method to separate the released GLA enzymes from the nanoliposomes. Basically, the idea of the experimental protocol consisted of the centrifugation of the LP-RGD-GLA liposomes in an Amicon® centrifugation filter unit, obtaining the non-encapsulated GLA protein in the Permeate fraction (P_M) and the entrapped GLA into nanovesicles in the Retentate fraction (R_T). The P_M refers to the volumetric fraction obtained in the lower part of the concentrator once the sample diffuses through the membrane during centrifugation. However, the R_T is the volumetric fraction unable to permeate through the membrane that remains in the upper part of the Amicon® membrane.

Preliminary studies to choice the better material and procedure to follow when analyzing LP-RGD-GLA formulations were performed using as protein model the following home-made GLA enzymes containing purification tags: GLAH6-T (produced in HEK 293F cells by transient expression production methods) and GLAcmycH6-S (obtained from CHO DG44 cells by stable expression based production system). The rationale behind the use of these alternative enzymes was to avoid the consume of the novel tag-free and high quality GLA-S version (obtained from CHO K1 cells also by stable expression procedures at LeanBio SL at this stage of the method development.

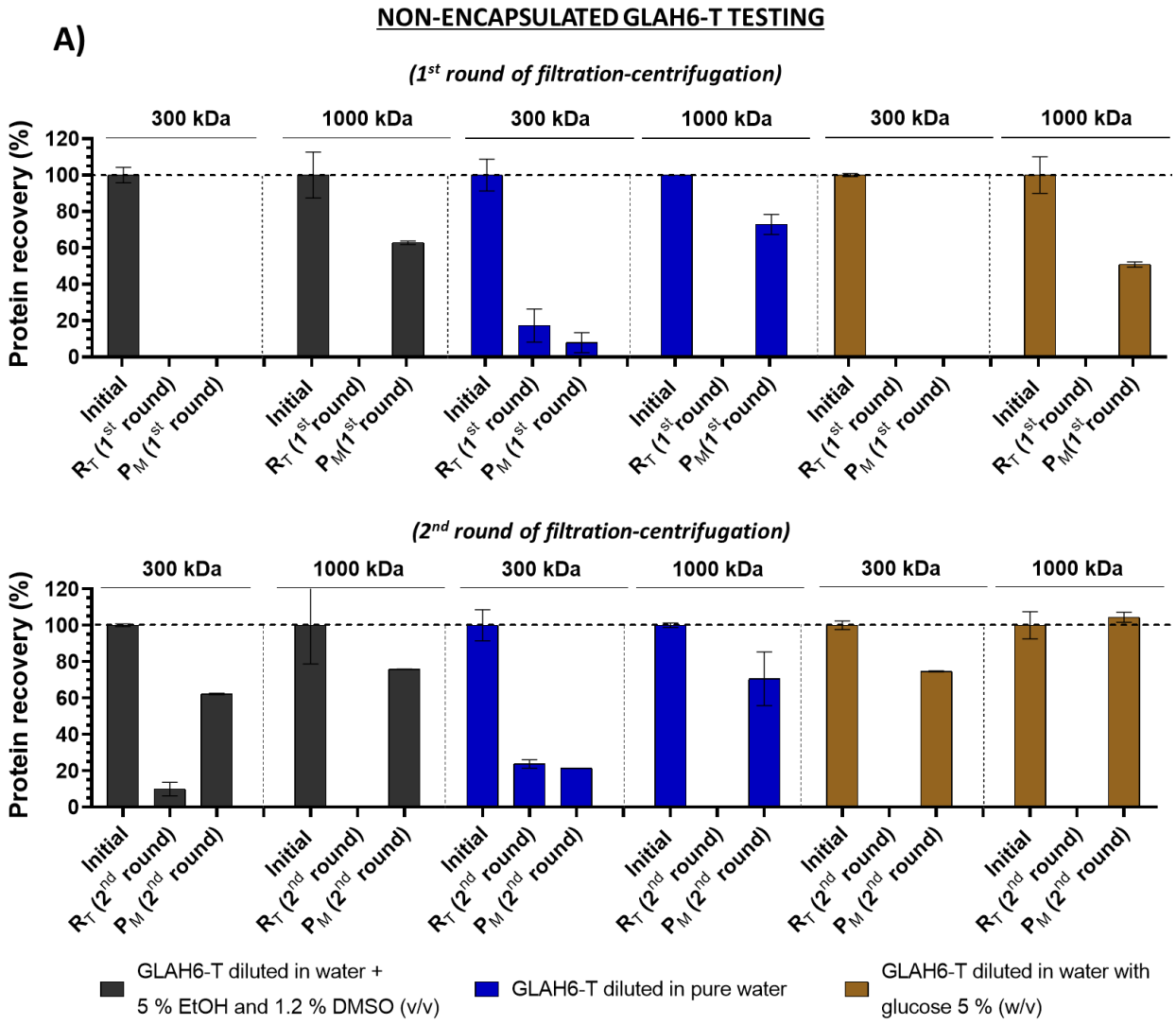
5.4.1.1. Influence of the cut-off membrane on the GLA diffusion

The effect of the cut-off membrane on the protein diffusion was investigated carrying out a set of experiments.

According to Amicon® manufacturers recommendations , two pore membranes of 300 kDa and 1000 kDa were used with the purpose to guarantee the diffusion of non-encapsulated GLA molecules through the membrane pores, but avoiding the diffusion of the nanoliposomes, since the GLA homodimer has a molecular weight of approximately 100 kDa (around 10 nm) and liposomes have mean sizes around 150 nm[55]. For these initial tests, polyethersulfone (PES) membranes and samples containing only unloaded GLA enzymes were used. These experiments allowed to determine the real percentage of unloaded protein capable to diffuse the membrane, and the percentage of enzyme retained by this.

Both home-made GLAH6-T and GLAcmycH6-S were diluted up to the concentration of 30 µg/mL in different media, i.e. those media used during liposomal manufacturing (water, glucose 5 % (w/v), and 5 % EtOH + 1.2 % DMSO (v/v)), in order to check if different media may influence the GLA diffusion through the membrane. Results showed low GLA recovery efficiencies due to the high adsorption of both proteins to the membrane in all cases, although higher adsorption was observed when GLAH6-T was used (see ***Figure 5.19***). Amicon® commercial warns

that if a specific amount of protein is adhered to membrane in a first centrifugation round, then in a second one the protein loss should be lower because of the filter should be more blocked. This hypothesis was confirmed by performing a second centrifugation round using the same GLA version. Interestingly, samples containing glucose demonstrated less protein binding to the membrane. Therefore, it was explored if a membrane "pre-treatment" previously to the centrifugation step could avoid the protein binding.



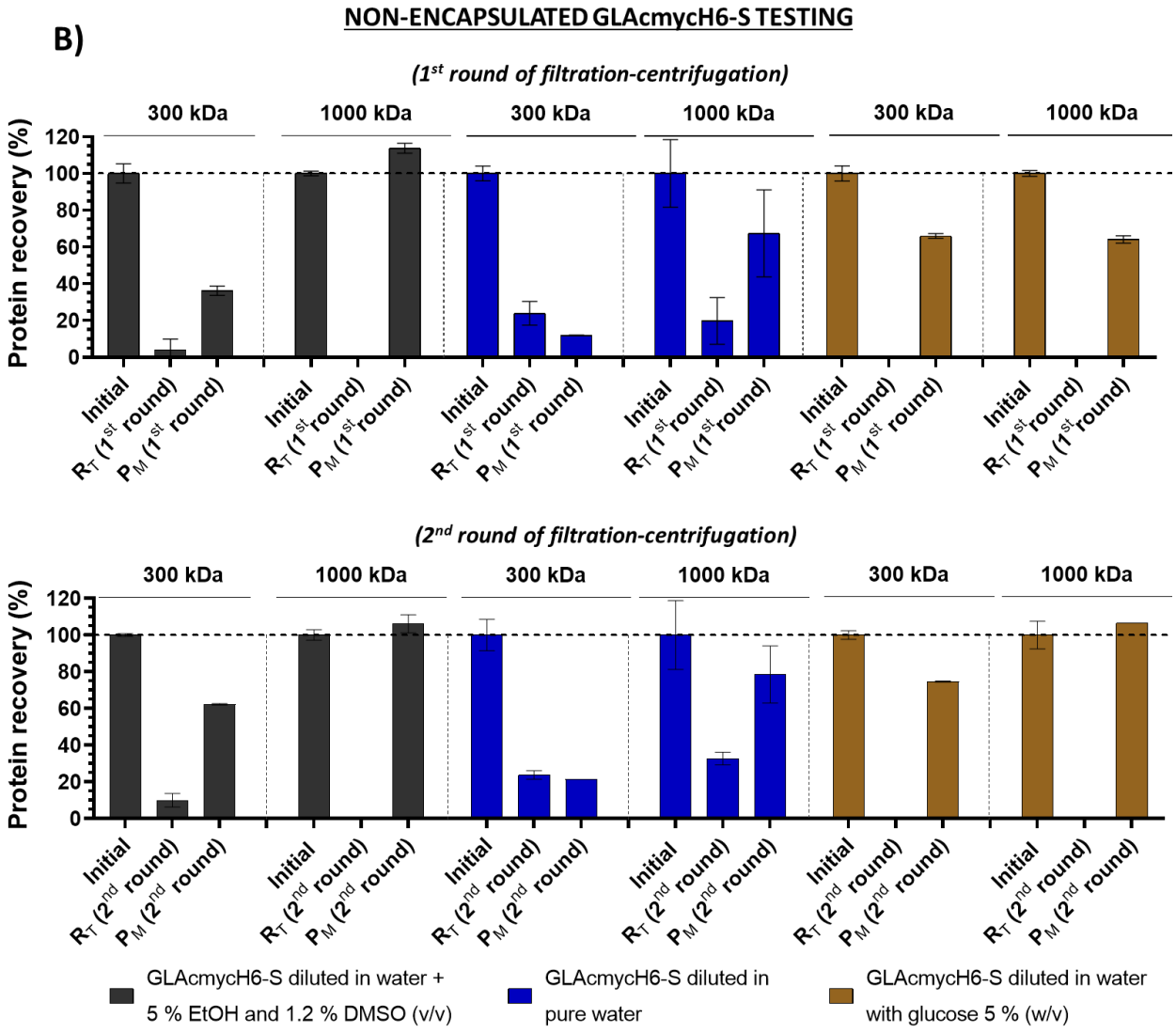


Figure 5.19. Preliminary explorative experiments to assess the permeability capacity of GLAs enzymes through PES membranes of 300 kDa and 1000 kDa. Obtained results in the first (1st) and second (2nd) centrifugation round testing A) unloaded GLAH6-T or B) unloaded GLAcmycH6-S diluted in different media (5 % EtOH + 1.2 % DMSO (v/v); pure water; or glucose 5 % (w/v)).

As both 300 kDa and 1000 kDa membranes seemed to require a previous step of membrane passivation to avoid GLA adsorption, next steps were only performed using 300 kDa membranes because of a lower cut-off membrane should be better to ensure only unloaded GLA diffusion.

5.4.1.2. Optimizing membrane passivation conditions to avoid GLA protein binding

The effect of pre-treating the membrane to avoid the protein binding was explored employing the following blocking agents:

- 2 % powdered milk in PBS (w/v).
- 5 % powdered milk in PBS (w/v).
- 5 % SDS in water (v/v).
- 1 % Tween-20 in water (v/v).
- 5 % Tween-20 in water (v/v).
- 0.25 mg/mL BSA in PBS.
- 0.5 mg/mL BSA in PBS.

Results showed that the best pre-treatment able to allow GLA diffusion through the Amicon® membrane was the option of using 1 % Tween-20 (v/v) for the analysis of GLAcmycH6-S (see in ***Table 5.33***). Nevertheless, none of the aforementioned conditions solved the problem of the protein adsorption to the membrane when GLAH6-T was used, indicating that the GLA nature has an impact on the enzyme binding with PES membranes.

The same efficient protocol pre-treating PES membranes with Tween-20, which ensures the diffusion of GLAcmycH6-S protein through the membrane, was tested with GLAcmycH6-T and the tag-free GLA-S enzyme for the further investigation about the correlation between GLA nature and the enzyme binding to the PES membrane. Although the four tested GLA versions have differences in the absence or presence of certain purification tags, when comparing results of ***Table 5.33*** and ***Table 5.34***, it is clear that both GLA enzymes produced in HEK 293F cells by transient expression procedures (GLAH6-T and GLAcmycH6-T) have higher affinity for binding PES membranes than those produced in CHO cells (GLAcmycH6-S and GLA-S). Probably, differences between their glycosylation pattern have higher impact on protein binding than the presence or absence of purification tags.

Table 5.33. Analysis of various membrane passivation conditions to avoid the attachment of GLA enzymes to PES membranes of 300 kDa by testing A) unloaded GLAH6-T or B) unloaded GLAcmycH6-S, both diluted in water up to 30 µg/mL previously to the filtration-centrifugation step. Quantifications were performed by SDS-PAGE and TGX densitometry analysis.

A) Non-encapsulated GLAH6-T testing		
Membrane passivation condition	**R_T ↑ (GLA concentration % (m/m))**	**P_M ↓ (GLA concentration % (m/m))**
Without pre-treatment	5 ± 0	16 ± 1
5 % powdered milk (w/v)	17 ± 0	0 ± 0
5 % SDS (v/v)	21 ± 1	15 ± 1
1 % Tween-20 (v/v)	0 ± 0	38 ± 0
5 % Tween-20 (v/v)	4 ± 1	34 ± 3
0.25 mg/mL BSA	2 ± 2	41 ± 2
0.5 mg/mL BSA	0 ± 0	36 ± 2

B) Non-encapsulated GLAcmycH6-S testing		
Membrane passivation condition	**R_T ↑ (GLA concentration % (m/m))**	**P_M ↓ (GLA concentration % (m/m))**
Without pre-treatment	0 ± 0	66 ± 1
2 % powdered milk (w/v)	79 ± 0	0 ± 0
5 % powdered milk (w/v)	102 ± 2	2 ± 0
5 % SDS (v/v)	11 ± 0	15 ± 1
1 % Tween-20 (v/v)	0 ± 0	102 ± 1
5 % Tween-20 (v/v)	17 ± 1	108 ± 2

Table 5.34. Confirmation of the validity of using Tween-20 for the passivation of 300 kDa PES membranes whether analyzing A) unloaded GLAcmycH6-T or B) unloaded GLA-S, both diluted in water up to 30 µg/mL previously to the filtration-centrifugation step. Quantifications were performed by SDS-PAGE and TGX densitometry analysis.

A) Non-encapsulated GLAcmycH6-T testing		
Membrane passivation condition	**R_T ↑ (GLA concentration % (m/m))**	**P_M ↓ (GLA concentration % (m/m))**
5 % Tween-20 (v/v)	0 ± 0	51 ± 4

B) Non-encapsulated GLA-S testing		
Membrane passivation condition	**R_T ↑ (GLA concentration % (m/m))**	**P_M ↓ (GLA concentration % (m/m))**
1 % Tween-20 (v/v)	0 ± 0	93 ± 3
5 % Tween-20 (v/v)	17 ± 1	97 ± 2

Additionally, the same passivation condition of PES membranes with 1 % Tween-20 (v/v) was tested with all the GLA versions once encapsulated in nanoliposomal formulations. The aim of this study was to corroborate if similar GLA binding would be occurring in presence of nanoliposomes, and if the nature of GLA could play a role as in the previous studies where non-encapsulated GLA versions were tested. The different GLA-loaded nanoliposomal formulations were diafiltrated by TFF in water to remove probable non-encapsulated enzyme from the nanoformulations and facilitate the analysis of the obtained results. After 3 days of storage at 4 ºC, all formulations were submitted to the filtration-centrifugation method. Interestingly, all loaded GLA enzymes were fully recovered at R_T regardless of the nature of the enzyme (see ***Table 5.35***). Therefore, these results demonstrated that the developed filtration-centrigufation protocol can be used to determine the entrapped concentration of any GLA enzyme in nanoliposomal formulations.

Table 5.35. GLA mass percentage (m/m) was assessed by SDS-PAGE and TGX densitometry analysis in the R_T and P_M after filtration-centrifugation with passivated 300 kDa PES membranes by using 1 % Tween-20 (v/v). Two individual production batches of LP-RGD-GLAH6-$T_{(w)}$, LP-RGD-GLAcmycH6-$T_{(w)}$, LP-RGD-GLAcmycH6-$S_{(w)}$ and LP-RGD-GLA-$S_{(w)}$ nanoliposomes were analyzed.

FILTRATION-CENTRIFUGATION PROCEDURE USING 300 kDa PES MEMBRANES PASSIVATED WITH 1 % TWEEN-20 (v/v)		
GLA-loaded nanoliposomal formulation tested	**R_T ↑ (GLA concentration % (m/m))**	**P_M ↓ (GLA concentration % (m/m))**
LP-RGD-GLAH6-$T_{(w)}$	96 ± 2	0 ± 0
LP-RGD-GLAcmycH6-$T_{(w)}$	99 ± 2	0 ± 0
LP-RGD-GLAcmycH6-$S_{(w)}$	89 ± 7	0 ± 0
LP-RGD-GLA-$S_{(w)}$	99 ± 4	0 ± 0

5.4.1.3. Impact of filtration-centrifugation protocol on nanoliposome stability

Next step consisted of checking if empty nanoliposomes (without containing GLA) were capable to permeate through 300 kDa Amicon® membrane when using the previous established filtration-centrifugation protocol. For this purpose, three different batches of LP-$RGD_{(w)}$ nanoliposomal formulations were submitted to filtration-centrifugation forces in Amicon® units with and without passivated membranes by using 1 % Tween-20 (v/v). Liposomes' stability was confirmed after the filtration-centrifugation step by DLS measurements (see ***Figure 5.20***). Lipid recovery in R_T and P_M was assessed by mass balance after freeze-drying the fractions (calculations performed according to ***Eq. 7.4*** in ***Chapter 7, Section 7.4.6***). As shown in ***Table 5.36***, nanoliposomes did not diffuse through the membrane since lipids were not recovered in the P_M. However, successive centrifugation rounds were not an option because lipid mass recovery decreased probably due to liposomal stability impairment.

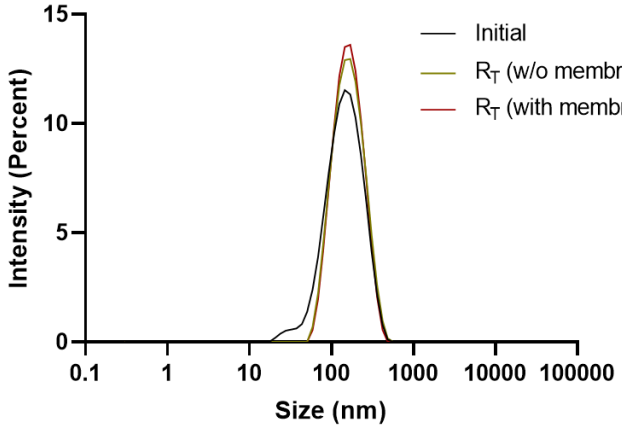


Figure 5.20. Confirmation of colloidal stability of LP-RGD$_{(w)}$ nanoliposomes submitted to filtration-centrifugation procedure. Particle size comparison of sample before filtration-centrifugation (named as Initial, black line), and after filtration-centrifugation (R_T) through 300 kDa PES membranes with (red line) or without (yellow line) passivation step using 1 % Tween-20 (v/v).

Table 5.36. Lipid mass percentage (m/m) assessed by mass balance in the R_T and P_M after filtration-centrifugation with passivated or non-passivated membrane. Three individual production batches of empty LP-RGD$_{(w)}$ nanoliposomes were tested.

	Empty LP-RGD$_{(w)}$ nanoliposomes testing			
	1x Centrifugation round		**3x Centrifugation round**	
Membrane passivation condition	**R_T ↑ (lipidic mass % (m/m))**	**P_M ↓ (lipidic mass % (m/m))**	**R_T ↑ (lipidic mass % (m/m))**	**P_M ↓ (lipidic mass % (m/m))**
Without pre-treatment	110 ± 6	0	N.D.	N.D.
1% Tween-20	102 ± 1	0	76 ± 6	3 ± 5

All these assays proved that the developed filtration-centrifugation protocol (i.e. the use of 1 % Tween-20 (v/v) to passivate the PES membrane, and the use of a unique centrifugation round) is appropriate to separate the released GLA enzyme from the GLA-loaded nanoliposomes.

5.4.1.4. Variability of the optimized filtration-centrifugation procedure

It is known that accurate sample handling is important when working with Amicon® units to reduce the error and variability between results. Besides, SDS-PAGE and further TGX densitometry, used in these experiments for GLA concentration determination, is considered a semi-quantitative method. For these reasons, before carrying out any *in vitro* release study, the variability of the developed centrifugation-filtration method was investigated. The sample used for this purpose was the nanoformulation under development in the frame of the European Phoenix project (LP-RGD-GLA-S$_{(gluc)}$) due to its higher quality and more advanced stage development. The test consisted in the filtration-centrifugation of 9 replicates from the same LP-RGD-GLA-S$_{(gluc)}$ diluted in glucose 5 % (w/v) up to 1.8 mg/mL of lipid and around 30 µg/mL of GLA-S. Enzyme quantification was assessed by SDS-PAGE

and further TGX densitometry analysis, and the quantification of lipid membrane components by RP-HPLC-ELSD. Results demonstrated high material recovery in R_T with errors (expressed as standard deviation) lower than 10 % (see ***Table 5.37***).

Table 5.37. Mass percentage of GLA and lipid membrane components (m/m) determined by SDS-PAGE and TGX densitometry and by RP-HPLC-ELSD, respectively. R_T and P_M were analyzed after sample filtration-centrifugation with passivated 300 kDa PES membranes by using 1 % Tween-20 (v/v). 9 replicates from same production batch of LP-RGD-GLA-$S_{(gluc)}$ were measured.

FILTRATION-CENTRIFUGATION OF LP-RGD-GLA-$S_{(gluc)}$ USING 300 kDa PES MEMBRANES PASSIVATED WITH 1 % TWEEN-20 (v/v)		
Component analyzed	**R_T ↑ (mass concentration % (m/m))**	**P_M ↓ (mass concentration % (m/m))**
GLA-S	100 ± 7	0 ± 0
DPPC	111 ± 5	0 ± 0
Chol	107 ± 3	0 ± 0
Chol-PEG_{400}-RGD	103 ± 1	0 ± 0
MKC	96 ± 2	0 ± 0

5.4.1.5. Integrity of the GLA-loaded nanoliposomal formulation when simulating *in vitro* release conditions

One objective of this thesis was to carry out a preliminary *in vitro* GLA-S release testing from LP-RGD-GLA-$S_{(gluc)}$ nanoliposomal formulation, which is in an advanced stage of development and investigated in the frame of the European Phoenix project. Physiological-like conditions (37 ºC) using nanoformulations diluted in specific media up to 30 µg/mL of GLA-S were chosen to perform the preliminary *in vitro* GLA-S release testing. The integrity of nanoliposomes after being incubated at such conditions and submitted to the previous developed filtration-centrifugation protocol was assessed before to conduct any analysis. The aim of this study was to ensure the efficiency of the established separation method protocol when simulating future *in vitro* release conditions. For this purpose, LP-RGD-GLA-$S_{(gluc)}$ nanoliposomes were diluted in glucose 5 % (w/v) up to 30 µg/mL, incubated at 37 ºC, and analyzed at predetermined time-points. The stability of nanovesicles' integrity after simulating the *in vitro* release assay conditions was assessed by DLS/ELS measurements and by RP-HPLC-ELSD to determine particle size and lipid mass recovery, respectively. The R_T before and after filtration-centrifugation were compared. Nanoliposomes' integrity remained unaltered and the lipid concentration constant in the R_T up to 24 h (as shown in ***Figure 5.21***), proving that nanovesicles remained stable and unable to diffuse through Amicon® filter membrane.

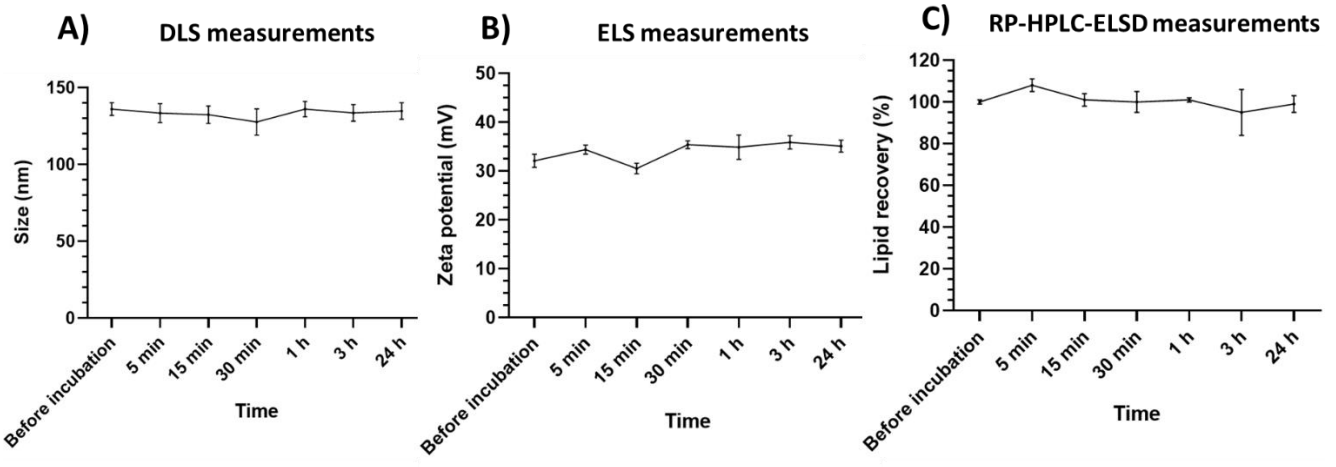


Figure 5.21. Comparison between R_T before and after being incubated in glucose 5 % (w/v) at 37 ºC, and further filtrated-centrifuged at the predefined time intervals. A) Mean particle size and B) zeta potential were assessed by DLS, and C) total lipid concentration as the sum of all liposome membrane components (DPPC, chol, chol-PEG_{400}-RGD and MKC) quantified by RP-HPLC-ELSD. Triplicates from same production batch of LP-RGD-GLA-$S_{(gluc)}$ were tested.

5.4.2. Preliminary *in vitro* drug release study using different physiological relevant media

Once an efficient methodology to separate the released GLA-S from the nanoliposomes was obtained, the *in vitro* drug release profile was investigated using the following physiological relevant media[56,57]:

- Glucose 5 % (w/v): medium used as injection solution which do not contain any salt.
- Ringer-Lactate solution: medium with similar salt content to human plasma.
- PBS 100 mM: it is not considered a physiological media at this high salt concentration. This buffer was used as positive control which ensures burst GLA release from nanoliposomes (previously described in Tomsen-Melero PhD thesis[58]).

Previously to the *in vitro* drug release study, the assessment of "sink conditions" to avoid interference from GLA-S solubility due to its saturation in the assay medium was performed by dissolving the GLA-S in each of the three proposed media, at a final volume of 6 mL and a concentration of GLA-S of 0.225 mg/mL[59]. This was a 7.5-fold concentrated GLA-S amount that the one which would be used during the *in vitro* release study. Samples were incubated at 37 ºC (simulating the conditions of the *in vitro* drug release assay) during 72 h, and then centrifuged 15 min at 13000 rpm to calculate the GLA-S amount that remained soluble. Results of this study demonstrated the solubility of GLA-S at the concentration and conditions tested, ensuring the "sink conditions" of the enzyme in further *in vitro* drug release assays (see ***Table 5.38***).

Table 5.38. Solubility test of non-encapsulated GLA-S in similar conditions to the *in vitro* release study (enzyme incubation at 37 ºC), after being diluted in glucose 5 % (w/v), Ringer-Lactate solution or PBS 100 mM buffer. Triplicates from same production batch of GLA-S were measured. GLA-S quantification was assessed by SDS-PAGE and further TGX densitometry analysis.

		Sample centrifugation at 13000 rpm during 15 min
Media of dilution	**GLA-S concentration (mg/mL)**	**Soluble GLA-S (%) after 72 h at 37 ºC**
Glucose 5 % (w/v)	0.225	95 ± 4
Ringer-Lactate solution	0.225	103 ± 5
PBS 100 mM	0.225	102 ± 8

Then, LP-RGD-GLA-$S_{(gluc)}$ formulation was submitted to a preliminary *in vitro* release assay under "sink conditions" to assess the GLA-S release from the nanovesicles, by adding 1.2 ml of sample in vials with 4.8 ml of receptor medium, to have a final total volume of 6 mL and a final GLA-S concentration around 30 µg/mL. Non-nanoformulated GLA-S enzyme was used as control group, being incubated at the same enzyme concentration of 30 µg/mL. Different glass vials were used per each time point, which were incubated at 37ºC (simulating the body temperature) and shacked at 100 rpm (see the experimental design in ***Figure 5.22***). At the predetermined time intervals, the respective vials were collected and 1.75 ml sample was withdrawn from the vial and filtered-centrifuged using the procedure detailed in ***Chapter 7, Section 7.4.6***, to separate the released GLA-S from the nanoliposomes.

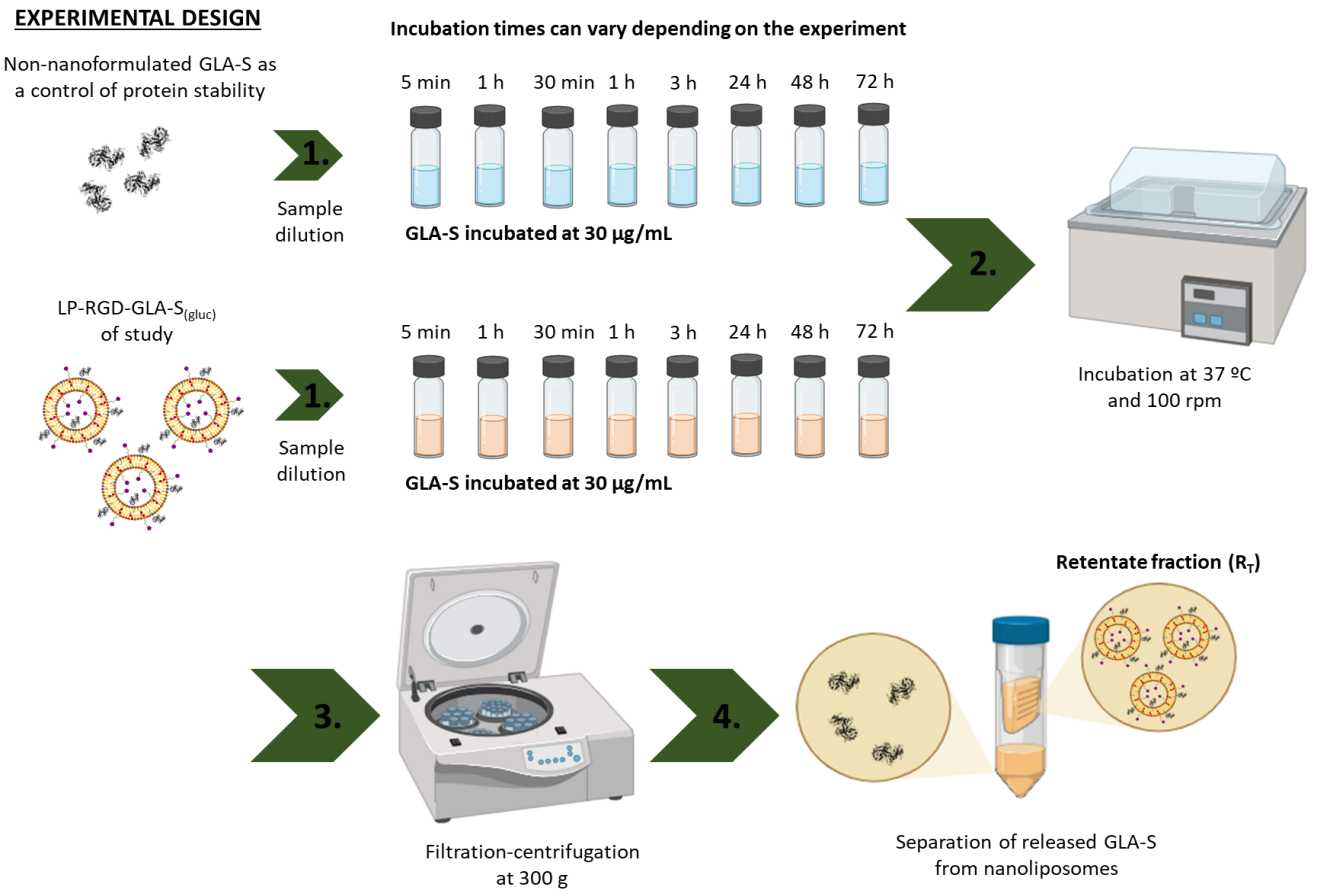


Figure 5.22. Scheme of the preliminary protocol used for the *in vitro* drug release assay.

Different receptor media (glucose 5 % (w/v), Ringer-Lactate solution or PBS 100 mM) were used for this study to evaluate the impact of the selected receptor media on the GLA-S release from LP-RGD-GLA-$S_{(gluc)}$ nanovesicles. *Figure 5.23 A* shows the results obtained with the non-nanoformulated GLA-S as control, demonstrating that GLA-S completely diffuses through Amicon® membranes from the first time point in the selected receptor media.

Interestingly, different GLA-S release profile was obtained when LP-RGD-GLA-$S_{(gluc)}$ formulation was analyzed in the different tested receptor media. When Ringer-Lactate or PBS 100 mM solution (both containing high salt concentration) were used as receptor media, more than the 50 % of the GLA-S was immediately released from the nanoliposomes, reaching a plateau where no significant increase over at least 72 h is observed (see *Figure 5.23 B*). However, when aqueous solution of glucose 5 % (w/v) was used, GLA-S release was retarded and did not start after 3 h of study initiation, having then a sustained release up to the 72 h of the assay.

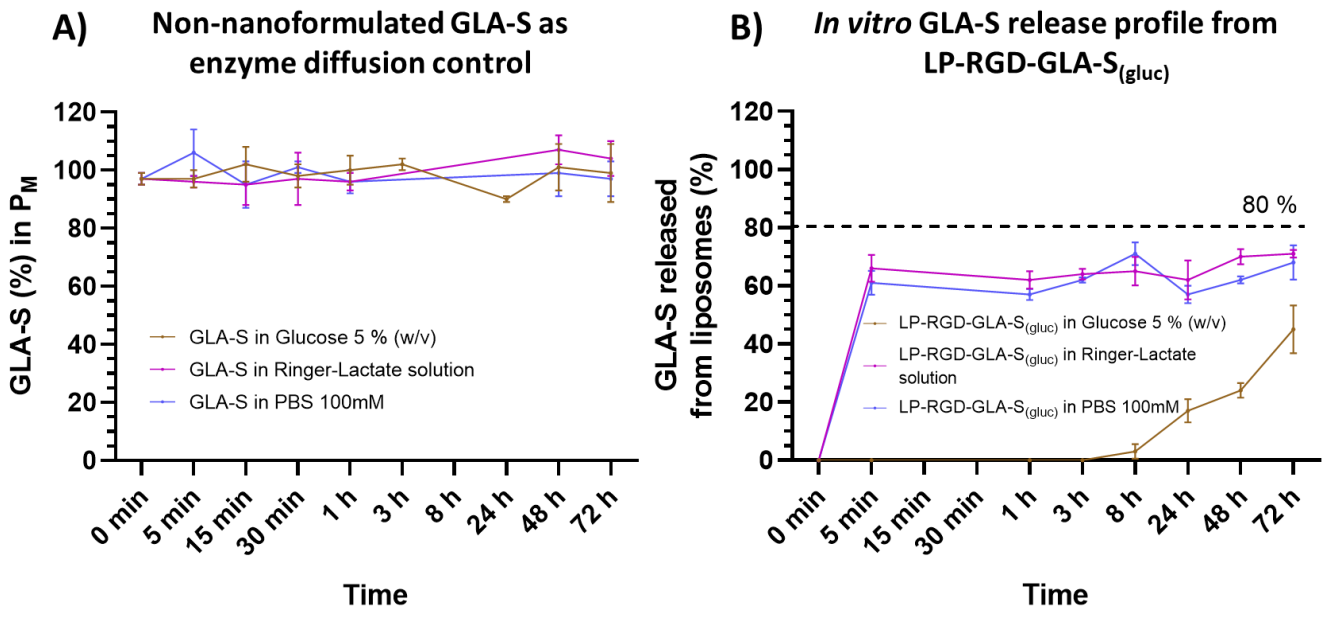


Figure 5.23. Percentage of GLA-S protein found in the P_M of the Amicon® centrifugation filter units when A) non-encapsulated GLA-S enzyme or B) LP-RGD-GLA-$S_{(gluc)}$ nanoformulations were filtered-centrifuged after their incubation at 37 ºC in selected receptor media at the predefined time intervals. Nanovesicles were diluted up to 1.8 mg/mL of lipid and 30 µg/mL of GLA-S in glucose 5 % (w/v) media, Ringer-Lactate solution or PBS 100 mM buffer. GLA-S quantification was determined by SDS-PAGE and TGX densitometry analysis.

Definitely, it was observed that the media selected for the *in vitro* release assays had a significant impact on the GLA-S release profile from nanoliposomes (clearly induced by salt concentration). Therefore, further investigation will be performed to choice the best receptor media for the quality control of this nanoformulation, that permits to discriminate batches that are not equivalent between them. Besides, correlations between *in vitro* release and *in vivo* pharmacokinetic data must be established.

5.4.2.1. Stability of the GLA-loaded nanoliposomal formulation in different physiological media

After realizing that media with high salt content induce a burst GLA release from nanoliposomes, the LP-RGD-GLA-$S_{(gluc)}$ integrity changes in response to salt concentration and pH were evaluated by DLS after incubating the nanoformulation in the different physiologically relevant media during 30 minutes at room temperature. A secondary aim of this study was also to collect preliminary data of LP-RGD-GLA-$S_{(gluc)}$ stability in media used for intravenous injections, in order to choose some media candidates for the reconstitution of the future lyophilized pharmaceutical form, which is under development in the frame of the European Phoenix project. However, once the definitive pharmaceutical form would be developed, these studies should be repeated to ensure whether changes on liposomal composition could impact on the nanovesicle physicochemical stability and GLA-S release profile.

Herein, the physiologically relevant media used to dilute LP-RGD-GLA-$S_{(gluc)}$ and study the impact of media pH or salt concentration on nanovesicle colloidal stability were:

- Aqueous solution of Glucose 5 % (w/v): do not contain any salt, only this sugar.
- PBS 100 mM: this buffer was used as positive control which ensures GLA release from nanovesicles. It contains high salt concentration.
- Ringer-Lactate solution: it was chosen due to its similarity in salt content to human plasma.
- Glucosaline solution with 3.6 % glucosa + 0.3 % NaCl (w/v): chosen as medium with intermediate salt concentration.
- Glucosaline solution with 4 % glucosa + 0.18 % NaCl (w/v): chosen as media with low salt concentration.
- 50 % Human plasma (v/v) pH 5.5: medium to simulate blood stream conditions and nanovesicle pH-dependent stability.
- 50 % Human plasma (v/v) pH 6.5: medium to simulate blood stream conditions and nanovesicle pH-dependent stability.
- 50 % Human plasma (v/v) pH 7.5: medium to simulate blood stream conditions and nanovesicle pH-dependent stability.

The integrity of LP-RGD-GLA-$S_{(gluc)}$ in response to salt concentration and pH was assessed by DLS and cryoTEM. The results compiled in ***Figure 5.24*** and ***Figure 5.25*** seem to confirm that salt presence and neutral-basic pH may induce the formation of larger multilamellar structures and the increase of the polydispersity index. The higher the salt concentration, the higher the destabilization of the sample observing the presence of bigger nanovesicles entrapping small nanovesicles. Therefore, LP-RGD-GLA-$S_{(gluc)}$ liposomes were more stable in glucosaline media (with lower salt concentration) and glucose 5 % (w/v) (without salt content), keeping most of the vesicles close to 100 nm in size. Additionaly, low liposomal polydispersity was found in 50 % human plasma (v/v) at lower pHs suggesting that maybe serum proteins might be organizing themselves as protein corona around vesicles stabilizing them.

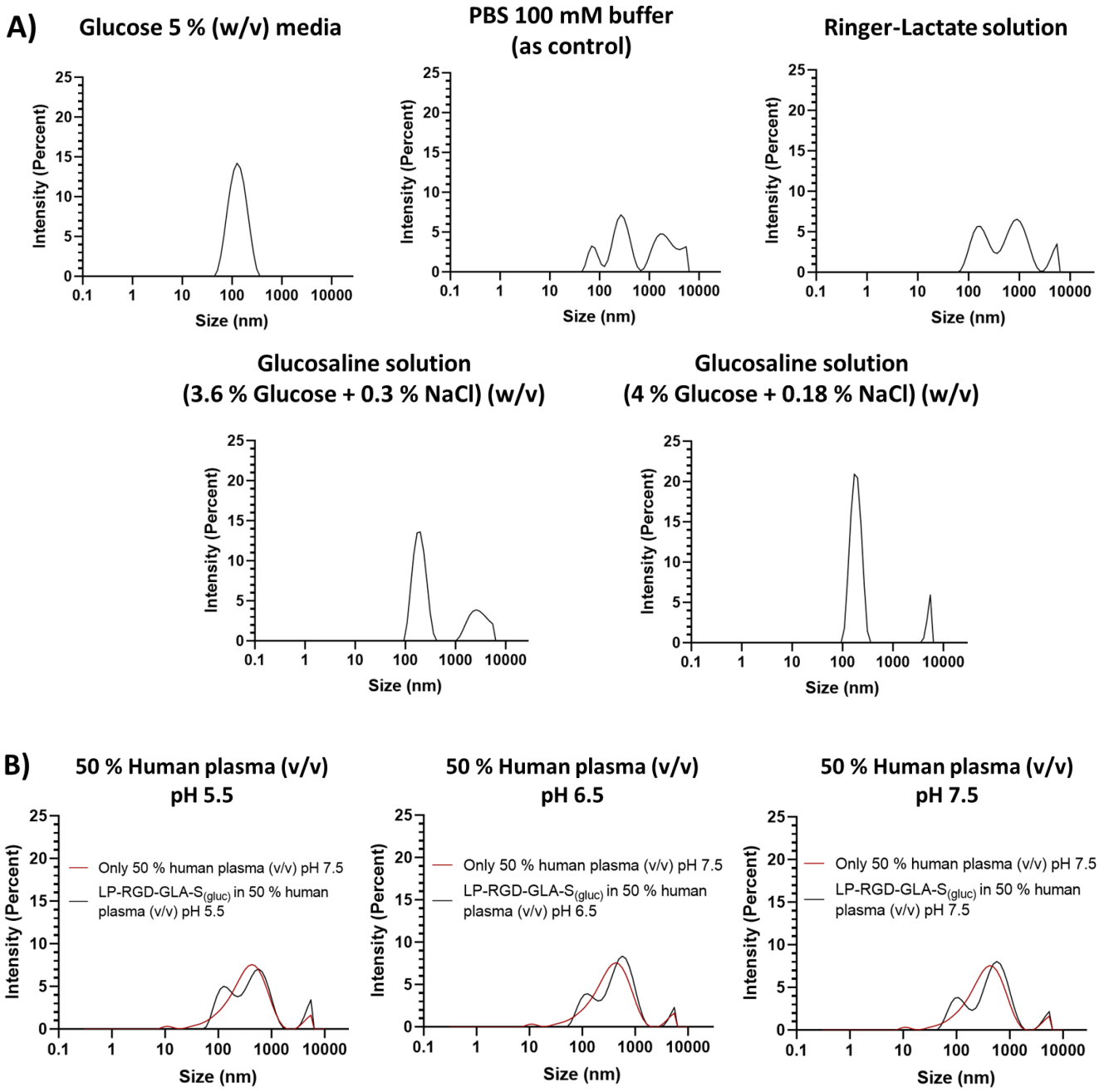


Figure 5.24. DLS measurements of the LP-RGD-GLA-$S_{(gluc)}$ formulation after 30 min of incubation at room temperature A) in PBS 100 mM buffer and various physiologically relevant media. B) DLS signals comparison between only 50% human plasma (v/v) as control, and LP-RGD-GLA-$S_{(gluc)}$ once incubated in 50% human plasma (v/v) differing on pH. DLS averages from triplicates of measures from one production batch sample.

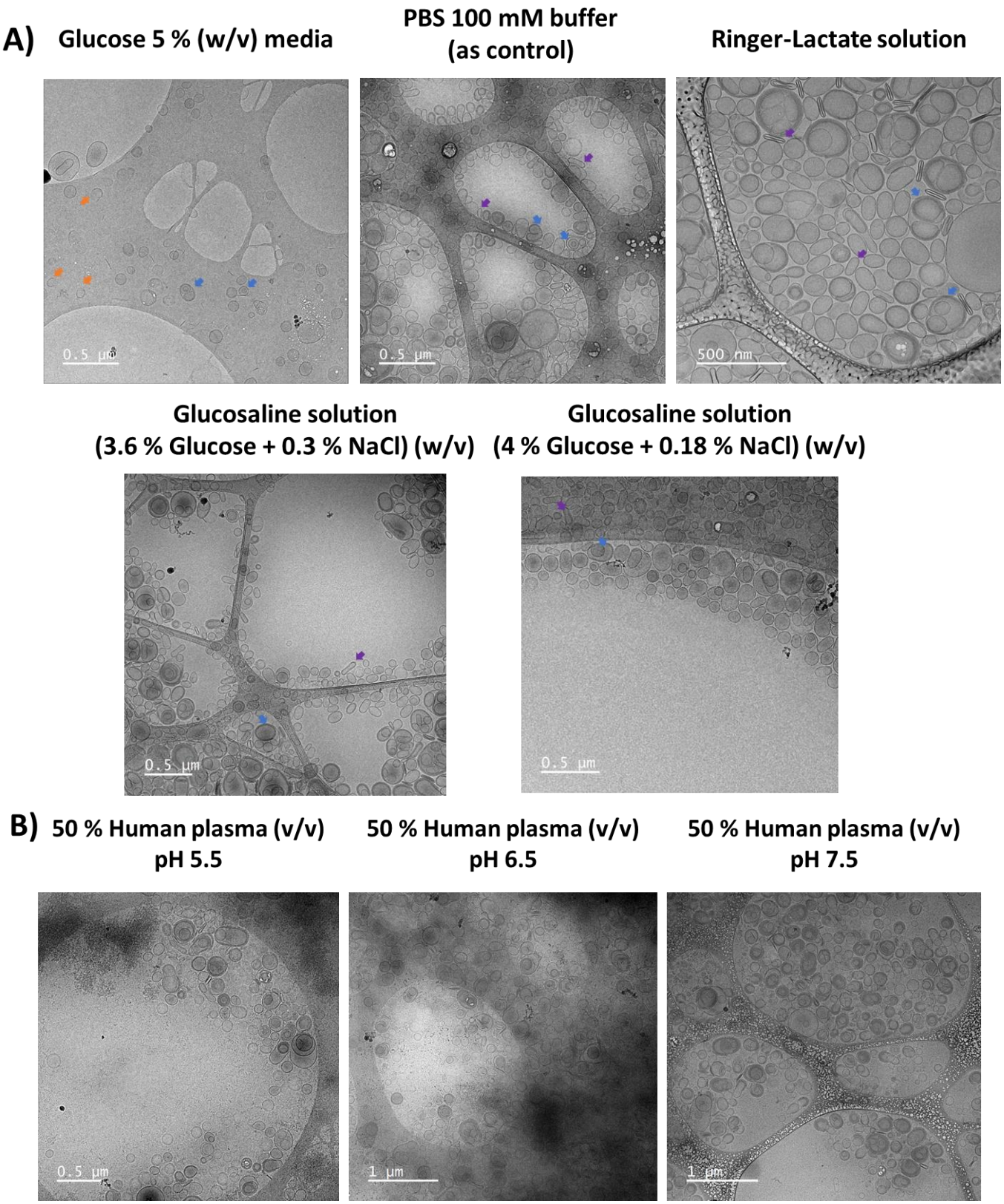


Figure 5.25. Cryo-TEM images of the LP-RGD-GLA-$S_{(gluc)}$ formulation after 30 min of incubation at room temperature A) in PBS 100 mM buffer and various physiologically relevant media, and B) in 50% human plasma (v/v) differing on pH. Blue arrows point to some multi-lamellar structures, orange arrows to opened membranes and purple arrows to oval structures.

According to these results, two hypothesis might explain the burst GLA-S release observed in the *in vitro* release study when LP-RGD-GLA-$S_{(gluc)}$ was incubated in rich salt contained media: i) the break of vesicles to form multi-lamellar structures in media containing salts may cause the GLA-S release from these vesicles; or ii) electrostatic interaction between the GLA enzyme and the positive charged liposomal membrane may be impaired by salts provoking the observed burst release of the adsorbed GLA enzyme on the nanovesicles' surface. Further investigation is ongoing to better understand these findings.

In parallel, the enzymatic activity was also assessed when LP-RGD-GLA-$S_{(gluc)}$ was incubated in the different physiological media in order to check if this was maintained. In general, the protein activity was maintained when LP-RGD-GLA-$S_{(gluc)}$ formulation was incubated in buffers containing glucose, but increased with other containing high salt concentrations (see ***Figure 5.26***). Interestingly, the higher increase of the LP-RGD-GLA-$S_{(gluc)}$ activity was observed when the nanoformulation was incubated in 50 % human plasma (v/v).

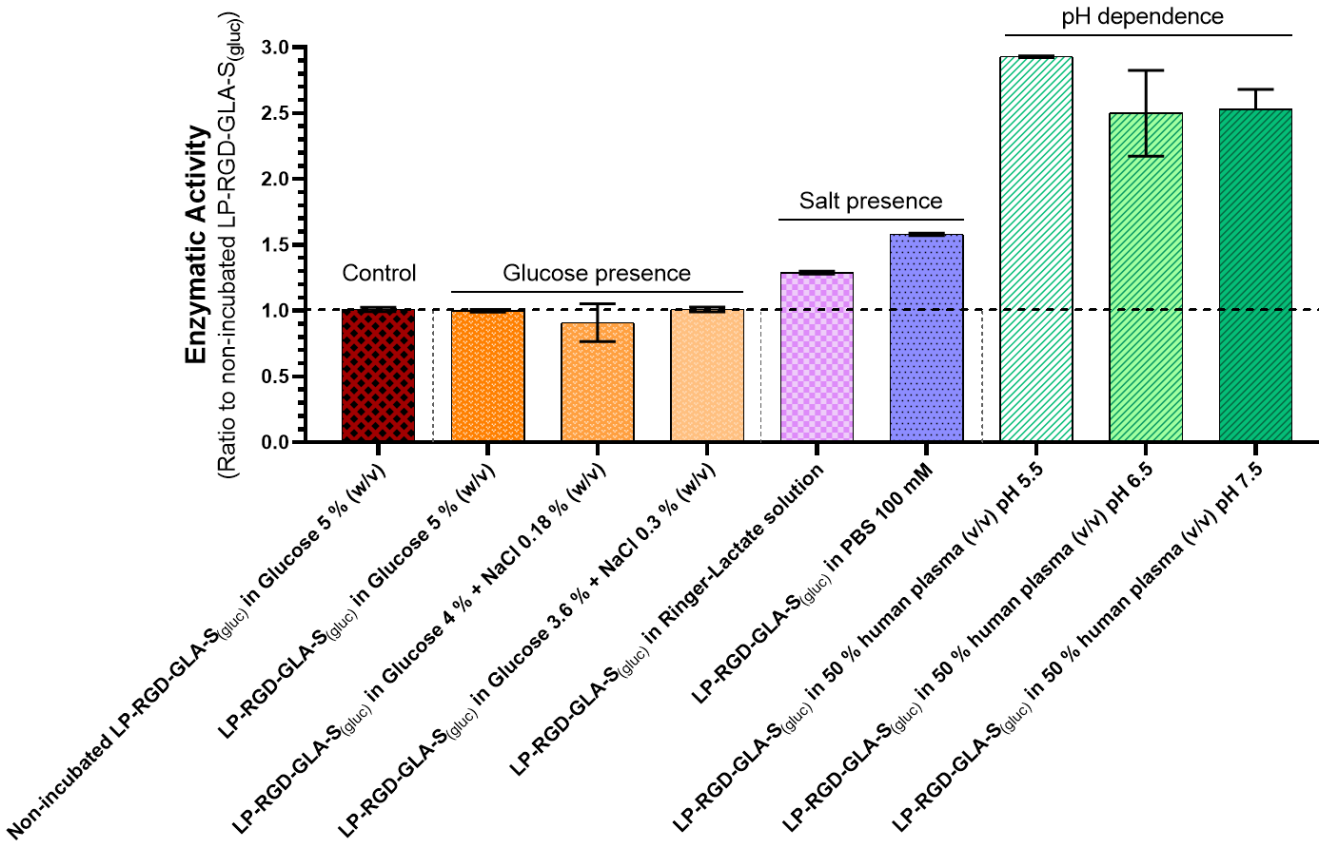


Figure 5.26. Assessment of the GLA-S enzymatic activity in LP-RGD-GLA-$S_{(gluc)}$ formulation before and after 30 min of incubation at room temperature in various physiologically relevant media, PBS 100 mM buffer and 50 % human plasma (v/v) at different pH. In all cases LP-RGD-GLA-$S_{(gluc)}$ formulation was diluted up to 30 µg/mL. Triplicates from one production batch of LP-RGD-GLA-$S_{(gluc)}$ formulation were analyzed by *in vitro* fluorescence-based assays. The enzymatic activity is referred to the one obtained for the LP-RGD-GLA-$S_{(gluc)}$ formulation diluted in glucose 5 % (w/v) previous to sample incubation.

5.4.3. Feasibility of using the filtration-centrifugation method to control the GLA leakage rate during storage conditions

Drug leakage rates from the liposomes throughout shelf-life must be determined since it is required by regulatory agencies in the stability studies of liposome drug formulations. Until now, the TFF (also known as diafiltration process) was the methodology used to separate the unloaded GLA enzyme from the entrapped one in the nanoliposomal formulations. However, TFF requires high sample volume to monitor the drug leakage rate during the stability studies. For this reason, the use of low centrifugation forces combined with membrane diffusion by using Amicon® centrifugation filter units was explored as an alternative technique of separation of released GLA-S from LP-RGD-GLA-$S_{(gluc)}$ nanoliposomes, with the aim to monitor the GLA-S leakage rate during stability studies. The established Amicon®-based separation protocol in which the blocking solution 1 % Tween-20 (v/v) is required to avoid protein binding to the filter membrane was employed (see ***Chapter 7, Section 7.4.6***).

Previous results shown in ***Table 5.35*** confirmed that filtration-centrifugation procedure was a suitable methodology to control the leakage rate. Comparable results to the TFF were obtained. As explained in ***Chapter 4***, LP-RGD-GLA-S formulations showed an enzyme entrapment efficiency (EE %) ≥ 95 % after the production, meaning that practically all the protein added to the formulation was integrated in the nanovesicles and there was no free GLA to diffuse through the 300 kDa membranes. In the preliminary test of ***Table 5.35***, it was found that GLA-loaded nanoliposomal formulations after 3 days of storage at 4 ºC do not leak GLA protein, maintaining the initial EE. Therefore, the developed filtration-centrifugation method is a suitable procedure to monitor the drug leakage rate, and requires less amount of sample for the separation of the drug substance from the nanoliposomes than TFF procedure.

By using this procedure, enzyme leakage rate from one batch of LP-RGD-GLA-$S_{(gluc)}$ (concentrated prototype) was monitored after being stored at 4 ºC for 3, 30 and 90 days. Despite the error related to the handling when using Amicon® filter membranes as separation technique, initial results ensure a GLA-S leakage lower than 20 % after 30 days of storage, and lower than 40 % after 90 days of sample storage at 4 ºC. Further investigation is required to confirm these findings.

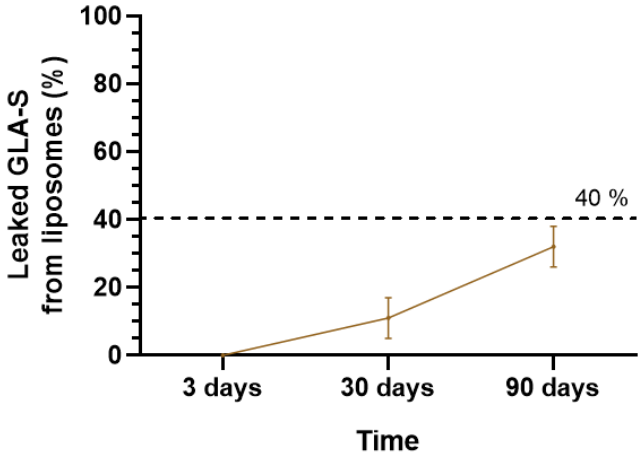


Figure 5.27. Leakage rate monitoring of LP-RGD-GLA-S$_{(gluc)}$ nanoliposomal formulation when stored at 4 ºC. GLA-S release was separated by filtration-centrifugation approaches, and then quantified by SDS-PAGE and further TGX densitometry analysis. Triplicates from one production batch were tested.

5.4.4. Summary

Briefly, an efficient methodology based on filtration- centrifugation by using Amicon® 300 kDa PES membranes was developed to allow the separation of the GLA enzyme released from nanoliposomes, without compromising the integrity of the nanovesicles. Although the GLA enzyme evidenced binding affinity to PES membrane (higher affinity when both home-made GLAH6-T and GLAcmycH6-T proteins produced by transient transfection in HEK 293F cells were tested), membrane passivation using the blocking 1 % Tween-20 (v/v) solution overcame this drawback. Filtration-centrifugation procedure demonstrated to be useful to perform *in vitro* drug release assays and leakage rate assessment.

For *in vitro* drug release profile testing, different media containing salts induced a burst release of GLA-S enzyme from nanoliposomes, probably due to the breakdown of electrostatic forces between both the enzyme and the nanocarrier. In order to prove vesicle integrity in the different media, DLS/ELS and cryoTEM techniques were used, demonstrating that high salt content can impair nanovesicle stability. However, LP-RGD-GLA$_{(gluc)}$ demonstrated to remain stable when diluted and incubated in glucose 5 % (w/v) media without salt containing. Media with 50 % human plasma was also used to check LP-RGD-GLA$_{(gluc)}$ integrity, showing good vesicle stability. The enzymatic activity was preserved in all cases and even increased in human plasma. Nevertheless, another separation methodology should be set up to carry out the *in vitro* drug release study in human plasma, since Amicon® 300 kDa PES membrane was totally blocked by protein plasma, obstructing the diffusion of the GLA-S through Amicon® membrane.

5.5. General summary and conclusions

In this chapter, analytical methods were successfully developed, optimized and, in some cases validated, for the proper quality control of the following nanoliposomes' quality attributes: chemical composition, microbiological and bacterial endotoxin content, *in vitro* drug release kinetics, and drug leakage rate. Their development has positively contributed to advance in the CMC development of the GLA-loaded nanoliposomal formulation for Fabry Disease Treatment.

Additionally, it was explored the feasibility of characterizing the targeting ligand on the surface of the nanoliposomes by a novel advanced method named SPARTA® (Single Particle Automated Raman Trapping Analysis), as well as the use of the field-flow fractionation-multi-angle light scattering (FFF-MALS) as an alternative technique to monitor the released GLA molecules from liposomes in a near future (see ***Annex II*** and ***Annex III***).

5.6. References

1 Yu JY, Chuesiang P, Shin GH, Park HJ. Post-processing techniques for the improvement of liposome stability. *Pharmaceutics* 2021; **13**. DOI:10.3390/pharmaceutics13071023.

2 Merlo-Mas J, Tomsen-Melero J, Corchero JL, *et al.* Application of Quality by Design to the robust preparation of a liposomal GLA formulation by DELOS-susp method. *J Supercrit Fluids* 2021; **173**: 105204.

3 US Food and Drug Administration. Guidance for Industry on Drug Products, Including Biological Products, that Contain Nanomaterials. FDA-2017-D-0759. 2022. https://www.fda.gov/Drugs/GuidanceComplianceRegulatoryInformation/Guidances/default.htmand/or (accessed Feb 16, 2023).

4 US Food and Drug Administration. Guidance for Industry on Liposome Drug Products Chemistry, Manufacturing, and Controls; Human Pharmacokinetics and Bioavailability; and Labeling Documentation. FDA-2016-D-2817. 2018. http://www.fda.gov/Drugs/GuidanceComplianceRegulatoryInformation/Guidances/default.htm (accessed Feb 18, 2023).

5 International Standards Organization. Nanotechnologies — Measurement technique matrix for the characterization of nano-objects. ISO/TR 18196:2016 . 2016. https://www.iso.org/obp/ui/en/#iso:std:iso:tr:18196:ed-1:v1:en (accessed Nov 30, 2020).

6 European Medicines Agency. Reflection paper on the data requirements for intravenous liposomal products developed with reference to an innovator liposomal product. Comm. Hum. Med. Prod. EMA/CHMP/806058/2009/Rev. 02. 2013. https://www.ema.europa.eu/en/documents/scientific-guideline/reflection-paper-data-requirements-intravenous-liposomal-products-developed-reference-innovator_en.pdf (accessed March 3, 2022).

7 European Medicines Agency. ICH guideline Q1A (R2) on Stability Testing of new Drug Substances and Products - Step 5. Comm. Hum. Med. Prod. CPMP/ICH/2736/99. 2003. https://www.ema.europa.eu/en/documents/scientific-guideline/ich-q-1-r2-stability-testing-new-drug-substances-products-step-5_en.pdf (accessed Feb 9, 2021).

8 European Medicines Agency. ICH guideline Q10 on pharmaceutical quality system - Step 5. Comm. Hum. Med. Prod. . 2015. https://www.ema.europa.eu/en/documents/scientific-guideline/international-conference-harmonisation-technical-requirements-registration-pharmaceuticals-human_en.pdf (accessed May 27, 2022).

9 Zhou Y, Gong XJ, Yang JB. Introduction to the guidance for industry on liposome drug products: chemistry, manufacturing, and controls; human pharmacokinetics and bioavailability; and labeling documentation issued by FDA. . *Chinese J New Drugs* 2018; **27**: 1835–40.

10 European Medicines Agency. ICH guideline Q2 (R2) on validation of analytical procedures - Step 2b. Comm. Hum. Med. Prod. EMA/CHMP/ICH/82072/2006. 2022. https://www.ema.europa.eu/en/documents/scientific-guideline/ich-guideline-q2r2-validation-analytical-procedures-step-2b_en.pdf (accessed Dec 2, 2021).

11 European Medicines Agency. ICH guideline Q14 on analytical procedure development - Step 2b. Comm. Hum. Med. Prod. EMA/CHMP/ICH/195040/2022. 2022. https://www.ema.europa.eu/en/documents/scientific-guideline/ich-guideline-q14-analytical-procedure-development-step-2b_en.pdf (accessed Dec 5, 2021).

12 DrugBank Online. Bioinformatics and cheminformatics data base. https://go.drugbank.com/drugs (accessed Oct 12, 2020).

13 PubChem chemistry data base. https://pubchem.ncbi.nlm.nih.gov/ (accessed Oct 18, 2020).

14 Chemaxon Ltd. Calculators and Predictors. https://chemaxon.com/ (accessed Oct 21, 2020).

15 Agilent Technologies Inc. The LC Handbook: Guide to LC Columns and Method Development. USA, 2016 www.agilent.com/chem/contactus.

16 Majors RE. The Cleaning andRegeneration ofReversed-Phase HPLC Columns. *Column Watch LC·GC Eur* 2003. www.lcgceurope.com.

17 Cristóbal-Lecina E, Pulido D, Martin-Malpartida P, Macias MJ, Albericio F, Royo M. Synthesis of Stable Cholesteryl-Polyethylene Glycol-Peptide Conjugates with Non-Disperse Polyethylene Glycol Lengths. *ACS Omega* 2020; **5**: 5508–19.

18 Elfaramawy SM, Rizk RA. Spectrophotometric Studies on Antioxidants-Doped Liposomes. *J Am Sci* 2011; **7**: 363–9.

19 Paulazo MA, Sodero AO. Analysis of cholesterol in mouse brain by HPLC with UV detection. *PLoS One* 2020; **15**: e0228170.

20 Ganzera M, Aberham A, Stuppner H. Development and validation of an HPLC/UV/MS method for simultaneous determination of 18 preservatives in grapefruit seed extract. *J Agric Food Chem* 2006; **54**: 3768–72.

21 Walker SE, Mowery Jr. RA, Bade RK. LC Solvents and Spectral Considerations with a New Process Liquid Chromatographic Optical Absorbance Detector. *J Chromatogr Sci* 1980; **18**: 639–49.

22 University of Toronto. UV Cutoff. https://www.utsc.utoronto.ca/~traceslab/PDFs/UV_Cutoff.pdf (accessed Aug 28, 2021).

23 Waters. Columns Calculator Version 2.0. https://www.waters.com/waters/support.htm?lid=134891632&locale=en_US (accessed Dec 11, 2020).

24 Ruiz-Garcia M, Pérez-Lozano P, Mercadé-Frutós D, *et al.* Development and Validation of a New High-Performance Liquid Chromatography Method for the Simultaneous Quantification of Coenzyme Q10, Phosphatidylserine, and Vitamin C from a

Cutting-Edge Liposomal Vehiculization. *ACS Omega* 2019; **4**: 19710–5.

25 Evans DRH, Romero JK, Westoby M. Chapter 9 Concentration of Proteins and Removal of Solutes. In: Methods in Enzymology. Academic Press Inc., 2009: 97–120.

26 Yoshikawa H, Hirano A, Arakawa T, Shiraki K. Mechanistic insights into protein precipitation by alcohol. *Int J Biol Macromol* 2012; **50**: 865–71.

27 Polson C, Sarkar P, Incledon B, Raguvaran V, Grant R. Optimization of protein precipitation based upon effectiveness of protein removal and ionization effect in liquid chromatography-tandem mass spectrometry. *J Chromatogr B* 2003; **785**: 263–75.

28 European Pharmacopoeia. Microbiological examination of non-sterile products: microbial enumeration tests. Ed. 6.3 Ref. 01/200920612. 2009. http://varban.airbase.ru/old-airbase/EPh/20612e.pdf (accessed March 13, 2022).

29 European Pharmacopoeia. Microbiological examination of non-sterile products: test for specified micro-organisms. Ed. 6.3 Ref. 01/200920613. 2009. http://varban.airbase.ru/old-airbase/EPh/20613e.pdf (accessed March 10, 2022).

30 European Medicines Agency. ICH guideline Q4B Annex 4A on evaluation and recommendation of pharmacopoeial texts for use in the ICH regions on micro enumeration - Step 5. Comm. Hum. Med. Prod. EMA/CHMP/ICH/308671/2008. 2017. https://www.ema.europa.eu/en/documents/scientific-guideline/ich-guideline-q4b-annex-4a-evaluation-and-recommendation-pharmacopoeial-texts-use-ich-regions-micro-enumeration-step-5_en.pdf (accessed Feb 26, 2022).

31 European Medicines Agency. ICH guideline Q4B Annex 4B on evaluation and recommendation of pharmacopoeial texts for use in the ICH regions on Tests for specified micro-organisms - Step 5. Comm. Hum. Med. Prod. EMEA/CHMP/ICH/308817/2008. 2017. https://www.ema.europa.eu/en/documents/scientific-guideline/ich-guideline-q4b-annex-4b-evaluation-and-recommendation-pharmacopoeial-texts-use-ich-regions-tests-specified-micro-organisms-step-5_en.pdf (accessed Feb 26, 2022).

32 European Medicines Agency. ICH guideline Q4B Annex 4C on evaluation and recommendation of pharmacopoeial texts for use in the ICH regions on acceptance criteria for pharmaceutical preparations and substances for pharmaceutical use - Step 5. Comm. Hum. Med. Prod. EMA/CHMP/ICH/308867/2008. 2017. https://www.ema.europa.eu/en/documents/scientific-guideline/ich-guideline-q4b-annex-4c-evaluation-and-recommendation-pharmacopoeial-texts-use-ich-regions-acceptance-criteria-pharmaceutical-preparations-and-substances-pharmaceutical-use-step-5_en.pdf (accessed Feb 26, 2022).

33 European Medicines Agency. ICH guideline Q4B annex 14 to note for evaluation and recommendation of pharmacopoeial texts for use in the ICH regions on bacterial endotoxins tests – general chapter - Step 5. Comm. Hum. Med. Prod. EMA/CHMP/ICH/529785/2010. 2013. https://www.ema.europa.eu/en/documents/regulatory-procedural-guideline/international-conference-harmonisation-technical-requirements-registration-pharmaceuticals-human-use-ich-guideline-q4b-annex-14-note-evaluation-and-recommendation-pharmacopoeial-texts-use_en.pdf (accessed March 30, 2022).

34 Ratajczak M, Kubicka MM, Kamin´ska DK, Sawicka P, Długaszewska J. Microbiological quality of non-sterile pharmaceutical products. *Saudi Pharm J* 2014; **23**: 303–7.

35 European Medicines Agency. ICH guideline Q1C on Stability Testing: Requirements for New Dosage Forms - Step 5. Comm. Hum. Med. Prod. CPMP/ICH/280/95 . 1998. https://www.ema.europa.eu/en/documents/scientific-guideline/ich-q-1-c-stability-testing-requirements-new-dosage-forms-step-5_en.pdf (accessed Feb 8, 2021).

36 Neun BW, Potter TM, Dobrovolskaia MA. NCL Method STE-2.2: Detection of Bacterial Contamination Using Luria Broth Agar Plates. *Mol Biol* 2018; **1628**: 19–22.

37 McNeil SE. Characterization of Nanoparticles Intended for Drug Delivery: Methods in Molecular Biology 697, Second Edition. Springer, 2011 http://www.springer.com/series/7651.

38 Neun BW, Cedrone E, Potter TM, Dobrovolskaia MA. NCL Method STE-2.4: Detection of Bacterial Contamination using Tryptic Soy Agar Plates and RPMI Suspension Tests for the Purposes of Determining Bacterial ID. 2020. DOI:10.17917/86Y9-3Y16.

39 Garrity GM. Bergey's Manual of Systematic Bacteriology, Second Edition. Springer, 2005.

40 Sakar F, Özer AY, Erdogan S, *et al.* Nano drug delivery systems and gamma radiation sterilization. *Pharm Dev Technol* 2017; **22**: 775–84.

41 Ribeiro N, Soares GC, Santos-Rosales V, *et al.* A new era for sterilization based on supercritical CO2 technology. *J Biomed Mater Res - Part B Appl Biomater* 2020; **108**: 399–428.

42 United States Pharmacopeia. United States Pharmacopeial Convention. General Chapter <85> Bacterial Endotoxin Test. *Biol Tests* 2012; : 5625–30.

43 European Pharmacopoeia. 2.6.14. Bacterial endotoxins. Ref. 01/201820614. 2018. https://www.edqm.eu/documents/52006/277487/Free+access+to+supportive+pharmacopoeial+texts+in+the+field+of+vaccines+for+human+use+during+the+coronavirus+disease+%28COVID-19%29+pandemic+Updated+package+-+October+2020.pdf/72875b16-432e-3854-36ca-51422e221d68?t=1637742526915 (accessed April 4, 2022).

44 European Pharmacopoeia. 5.1.10. Guidelines for using the test for bacterial endotoxins. Ref. 01/202150110. 2018. https://www.edqm.eu/documents/52006/277487/Free+access+to+supportive+pharmacopoeial+texts+in+the+field+of+vaccines+for+human+use+during+the+coronavirus+disease+%28COVID-19%29+pandemic+Updated+package+-+October+2020.pdf/72875b16-432e-3854-36ca-51422e221d68?t=1637742526915 (accessed April 4, 2022).

45 National Cancer Institute. Nanotechnology Characterization Laboratory (NCL) database. Nanodelivery Syst. Devices. https://www.cancer.gov/nano/research/ncl (accessed Oct 26, 2020).

46 Bang FB. A bacterial disease of Limulus polyphemus. *Bull Johns Hopkins Hosp* 1956; **98**: 325–51.

47 McNeil SE. Characterization of Nanoparticles Intended for Drug Delivery: Methods in Molecular Biology 1682, Second Edition. 2018 http://www.springer.com/series/7651.

48 Neun BW, Dobrovolskaia MA. NCL Method STE-1.3: Detection and Quantification of Gram-Negative Bacterial Endotoxin Contamination in Nanoparticle Formulations Using the Gel-Clot LAL Assay. 2020. DOI:10.17917/VRHF-5Y74.

49 Lonza Walkersville. Traditional Gel Clot Limulus Amebocyte Lysate (LAL) Assay Procedure Quick Guide. 2021. https://bioscience.lonza.com/download/content/asset/28673 (accessed April 4, 2022).

50 Young NS, Levin J, Prendergast RA. An invertebrate coagulation system activated by endotoxin: evidence for enzymatic mediation. *J Clin Invest* 1972; **51**: 1790–7.

51 Dawson ME. LAL Update: Interference with the LAL Test and How to Address It. 2005; **22**.

https://www.acciusa.com/pdfs/newsletter/LAL Update Vol 22_No3 rev 001.pdf (accessed March 10, 2022).

52 Harmon P, Cabral-Lilly D, Reed RA, Maurio FP, Franklin JC, Janoff A. The Release and Detection of Endotoxin from Liposomes. *Anal Biochem* 1997; **250**: 139–46.

53 Reich J, Lang P, Grallert H, Motschmann H. Masking of endotoxin in surfactant samples: Effects on Limulus-based detection systems. *Biologicals* 2016; **44**: 417–22.

54 Charles River. The endosafe® nexgen-pts™. https://www.criver.com/sites/default/files/resources/doc_a/Endosafe®nexgen-PTS™AssayGuide.pdf (accessed March 21, 2023).

55 Mcrae R, Naumann[2] C, Hoehne K, Zeidler R. Treatment of Vivaspin ® Concentrators For Improved Recovery of Low-Concentrated Protein Samples - Application Note. 2020. www.sartorius.com/en/products/lab-filtration-purification/ultrafiltration-devices (accessed March 14, 2020).

56 Hoorn EJ. Intravenous fluids: balancing solutions. *J Nephrol* 2017; **30**: 485–92.

57 Matt vera BSN RN. IV Fluids and Solutions Guide & Cheat Sheet (2023 Update) - Nurseslabs. 2023. https://nurseslabs.com/iv-fluids/ (accessed April 8, 2022).

58 Tomsen-Melero J. Study of New Liposomes for the Delivery of Enzymes through Biological Membranes. 2021. http://hdl.handle.net/10803/673786 (accessed Oct 30, 2021).

59 Siepmann J, Siepmann F. Sink conditions do not guarantee the absence of saturation effects. *Int J Pharm* 2020; **577**: 119009.

6

GENERAL CONCLUSIONS

From the work carried out in this Ph.D. thesis, the following conclusions can be withdrawn:

1. A new fast, straightforward and cost-efficient approach to optimize transient gene expression (TGE) methodology for recombinant protein expression was developed using human embryonic kidney (HEK) 293F cultures. This improvement optimizes (by reducing) the amount of pDNA-PEI polyplexes needed to transfect cells, both reducing cell toxicity, and hence, increasing recombinant protein expression.

2. His-tagged α-galactosidase A (GLA) enzymes named GLAH6-T, GLAcmycH6-T, and GLAcmycH6-S, were successfully expressed in HEK or Chinese hamster ovary (CHO) mammalian cells, by TGE or stable clone procedures, respectively. All the expressed versions of the enzyme could be purified by Ni^{2+}-based affinity chromatography, and exhibited the proper quality attributes for further therapeutic applications.

3. Higher GLA recoveries from the chromatographic column (> 70 %) and improved GLA characteristics (e.g. enzymatic activity, purity and solubility) were obtained in general when Ni^{2+}-based affinity chromatography was used instead of using Co^{2+}-based affinity chromatography, evidencing the impact of the divalent cation used in the purification step over the final protein properties.

4. The His-tagged GLA enzymes, GLAH6-T and GLAcmycH6-T, expressed in HEK 293F mammalian cells demonstrated increased solubility, purity and specific enzymatic activity, in general, compared to GLAcmycH6-S produced in CHO cultures. Besides, the presence of c-myc purification tag even worsens these factors at low pHs apart from reducing the production yield of TGE procedures.

5. The non-tagged GLA-S version produced by the Contract Development and Manufacturing Organization (CDMO) LeanBio SL with scaled-up CHO cultures and solubilized using a medium with excipients such as

mannitol and sodium phosphates, demonstrated the most promising quality attributes and stability properties, being the enzyme with higher specific enzymatic activity and lower aggregation capacity. The lack of presumable immunogenic purification tags turns this enzyme into an attractive and potential therapeutic drug substance to be used as enzymatic replacement therapy (ERT) for the treatment of Fabry disease.

6. All different versions of GLA enzymes mentioned above were successfully integrated in RGD-targeted liposomal formulations using the compressed CO_2-based DELOS-susp technology and purified through tangential flow filtration (TFF) procedures.

7. RGD-targeted nanovesicular systems with GLA-absorbed on the surface were successfully prepared by titrating the four types of GLA (GLAH6-T; GLAcmycH6-T; GLAcmycH6-S and GLA-S) over non-GLA loaded RGD-targeted nanoliposomes produced by DELOS-susp.

8. All nanoliposomal aqueous formulations containing GLA showed colloidal stability for at least 3 months when stored at 2 – 8 ºC. Importantly, all GLA versions increased their stability when loaded in nanoliposomes in comparison to respective naked GLA counterparts.

9. Characteristics and properties of the different versions of the GLA enzymes given by their expression cell factory, HEK or CHO, with conserved and specie-related post-translational modifications (PTMs), strongly impacts on the encapsulation efficiency and biological properties of GLA nanoliposomal formulations. Higher encapsulation efficiencies and higher specific enzymatic activities were generally observed with GLAcmycH6-S or GLA-S produced in CHO cells in comparison with GLAH6-T and GLAcmycH6-T produced in HEK cells. On the contrary, lower stabilities of the aqueous nanovesicular formulations where observed with GLA enzymes produced in CHO in comparison to those produced in HEK.

10. Tryptophan-based fluorescence measurements pointed-out that the nature of the GLA enzymes given by their expression cell factory, HEK or CHO, impacts on the GLA interaction mode with nanoliposome bilayers and, consequently, on the enzymatic activity of the different types of GLA when integrated in nanoliposomes.

11. The comparison of the physicochemical and biological characteristics of both, GLA-loaded and GLA-adsorbed nanoliposomes, suggests that GLA molecule is mainly localized in the outer bilayer surface in

all the studied GLA formulations. Nanoliposomal formulations with a percentage of enzyme molecules inside nanoliposomes were only achieved by using DELOS-susp production. Titration based procedures always yielded nanovesicular formulations with the GLA molecule absorbed in the outer nanoliposome bilayer.

12. An optimized RP-HPLC-ELSD analytical method was achieved for the simultaneous detection and quantification of MKC, chol-PEG_{400}-RGD, cholesterol and DPPC membrane components of the different prototypes of GLA-loaded RGD-targeted liposomal formulations. The method was validated for the quantitative determination of the chemical composition of the LP-RGD-GLA-$S_{(gluc)}$ nanoformulation, i.e. the GLA-nanoliposomal formulation in an advanced stage of the pharmaceutical development, which contains GLA-S protein and glucose as isosmotic agent.

13. The Luria Broth (LB) agar plate test was successfully implemented to determine and control the microbiological quality of GLA-loaded nanosystems, i.e. for the detection of bacterial contamination. Besides, this methodology contributed to prove that the developed filtration sterilization protocol was efficient to remove bacteria from the nanoformulations.

14. A methodology based on Gel clot LAL assay was optimized for the qualitative analysis and control of bacterial endotoxins content in the optimal GLA nanoliposomal formulation containing glucose in the dispersant medium. However, the LAL substrate demonstrated to be incompatible when low amounts of organic solvents are present in the intermediate liposomal prototypes.

15. An efficient filtration-centrifugation methodology to separate the released GLA enzyme, as drug substance, from the nanoliposomes was developed, optimized, and validated. This allowed to set-up an *in vitro* test to study the drug release kinetics in physiologically/clinically relevant media, as well as to assess the GLA leakage rate during storage. The burst GLA release observed in media rich of salts suggested that the electrostatic interactions are the predominant ones between the GLA and the positive charged liposomal bilayer.

16. The integrity of the nanovesicles in the different physiologically/clinically relevant media was confirmed by means of cryoTEM examination. Nevertheless, it was found that the higher the salt concentration of the media, the higher the destabilization of the nanoformulation (e.g. slight nanovesicles' morphological changes and polydispersity index increase). This could also explain the burst GLA release observed in rich

salt contained media. However, when media contained 50 % human plasma (v/v), no changes in morphology and colloidal stability were observed, suggesting that serum proteins might be organizing themselves as a protein corona around vesicles stabilizing them.

17. The protective capacity of liposomal nanovesicles against the GLA degradation by proteases was demonstrated through the establishment of an *in vitro* trypsinization assay. Nevertheless, further investigation is required to determine the assay variability, and also the batch-to-batch reproducibility.

18. The preliminary tests with SPARTA® (Single Particle Automated Raman Trapping Analysis) system, carried out in collaboration with SPARTA Biodiscovery company, suggested that this could be an appropriate technique to characterize the targeting ligand (i.e. chol-PEG_{400}-RGD) on the surface of the nanoliposomes.

Based on these global conclusions, this Ph.D. thesis has contributed to the investigation of critical properties from GLA enzymes to generate potential liposome-based drug delivery systems, as well as to the exploration of new analytical techniques to evaluate and control several critical quality attributes from GLA-loaded nanovesicular formulations intended to be used as ERT for Fabry disease. The generated knowledge is positively benefiting the optimization and progress of GLA-loaded drug products towards the regulatory preclinical and early translation to GMP development.

7

EXPERIMENTAL SECTION

7.1. Materials

Recombinant proteins

Recombinant versions of the human alpha-galactosidase A (GLA), named GLAH6-T, GLAcmycH6-T and GLAcmycH6-S, were home-made produced and purified at the Servei de Cultius Cel·lulars, Producció d'Anticossos i Citometria (SCAC, UAB) and at the NANBIOSIS Protein Production Platform (PPP) unit U1, both located at the Institut de Biotecnologia i Biomedicina (IBB-UAB, Barcelona) facilities. On the other hand, the GLA-S version was produced by LeanBio SL (Barcelona). Procedures followed were explained in ***Section 7.2***.

Membrane components of nanovesicles

For lab-scale experiments, 1,2-dipalmitoyl-sn-glycero-3-phosphocholine (DPPC; MW = 734.04 g/mol, purity 99 %, ref. #LP-R4-057) was supplied by CordenPharma (Liestal, Switzerland). Cholest-5-en-3β-ol (cholesterol, chol; MW = 386.66 g/mol, purity 95 %, ref. A0807,0100) was purchased from Panreac AppliChem (Castellar del Vallès, Spain). Miristalkonium chloride (MKC; MW = 368.05 g/mol, purity 99.2 %, ref. 262393) was obtained from US Biological Life Science (Salem, USA). Cholesterol pegylated with arginyl–glycyl–aspartic acid peptide (chol-PEG_{400}-RGD; MW = 1369 g/mol, purity 84%) was designed and synthetized by the group of Dr. Miriam Royo from the Institut de Química Avançada de Catalunya (IQAC-CSIC; Barcelona, Spain) as described in ***Section 7.3***.

For preclinical studies, chol (purity 95 %, ref. 30455-27) of Pharmaceutical grade was acquired from Fagron Ibérica (Terrassa, Barcelona), and chol-PEG_{400}-RGD (purity 83 %) was synthetized by the good manufacturing practices (GMP)-compliant contract manufacturing organization (CMO) AmbioPharm Inc company (Beech Island, USA).

Chemical structure of all nanovesicle membrane components are represented on ***Figure 7.1***.

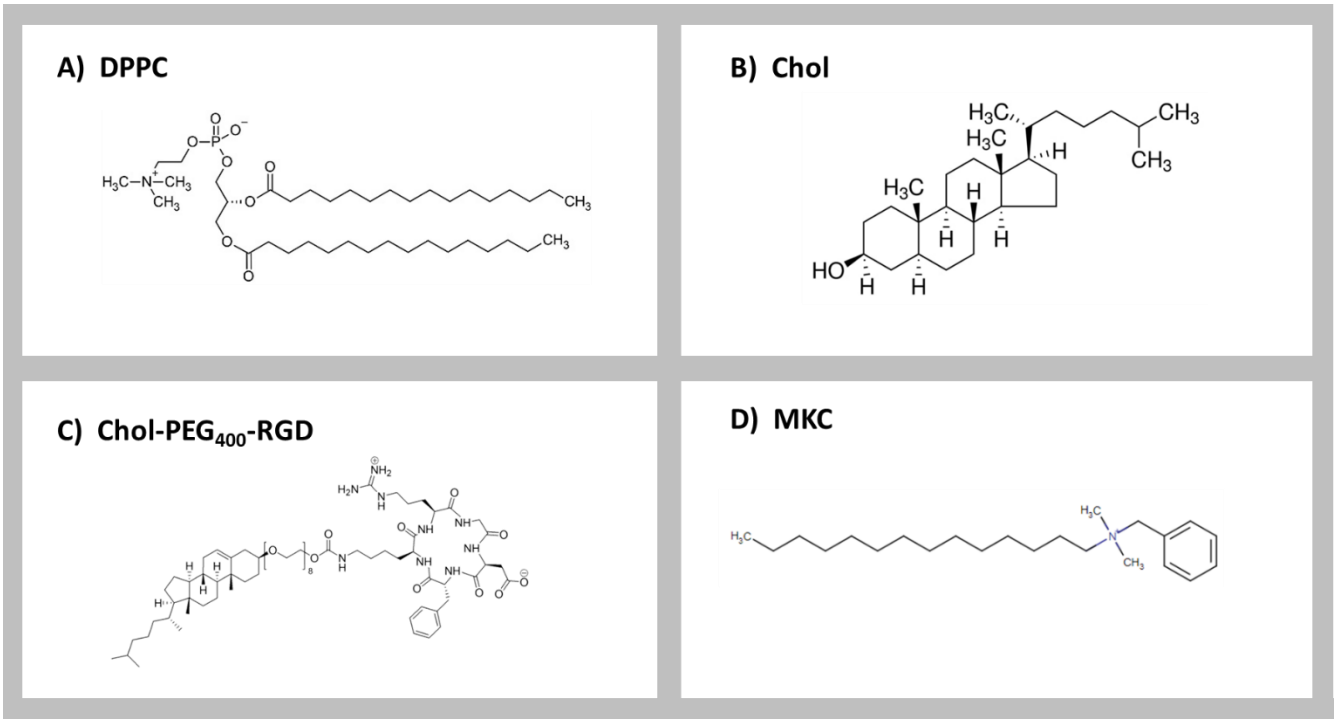


Figure 7.1. Chemical structure of A) 1,2-dipalmitoyl-sn-glycero-3-phosphocholine (DPPC), B) cholesterol (chol), C) cholesterol-PEG_{400}-cRGDfk (chol-PEG_{400}-RGD), and miristalkonium chloride (MKC).

Organic solvents and gases

Ethanol (EtOH; HPLC grade, ref. 34852-M), dimethyl sulfoxide (DMSO; ACS reagent; purity 99.9 %, ref. 276855) and trifluoroacetic acid (TFA; purity ≥ 99 %, ref. 302031) were purchased from Sigma-Aldrich (Madrid, Spain). Methanol (MeOH; LC/MS Grade, ref. 9822) was obtained from J.T. Baker (New Jersey, USA). Formic acid (HCOOH; purity 98 – 100 %, ref. 100264) was acquired from Merck Millipore (Massachusetts, USA). Acetonitrile (ACN; LC/MS Grade, ref. A955-212) and glacial acetic acid (AcOH; ref. 10384970) were provided from Fischer Scientific (Sant Cugat del Vallès, Spain). Carbon dioxide (CO_2; purity, 99.9%) and nitrogen (N_2) was supplied from Carburos Metálicos (Cornellà de Llobregat, Spain). Ultrapure Type I water (H_2O), was purified using Milli-Q® Advantage A10 water purification equipment (Millipore Ibérica, Madrid, Spain). Water for injection (WFI; ref. SH31191) was purchased from HyClone Laboratories (Utah, USA).

Chemical reagents

Bacto™ Tryptone from Pancreatic Digest of Casein (Gibco, ref. 212750), and Bacto™ Yeast Extract from an extract of autolyzed yeast cells (Gibco, ref. 212750), sodium chloride (NaCl; MW = 58.44, purity ≥ 99.5 %, ref. S/3120/60) and Select™ Agar (Invitrogen, ref. 30391049) were purchased from Thermo Fischer Scientific (Sant Cugat del Vallès, Spain). LB medium was prepared with 10 g/L tryptone, 5 g/L yeast extract, 0.5 g/L NaCl and 15 g/L agar.

Urea (ref. 1.08486) was obtained from Merck KGaA (Madrid, Spain). 2-mercaptoethanol (purity 99 %, ref. M3148) and glycerol (purity ≥ 99 %, ref. G5516) were provided from Sigma-Aldrich (Madrid, Spain). Tris base (ref. BP152-1) was acquired from Fisher Scientific (Sant Cugat del Vallès, Spain). Sodium dodecyl sulfate (SDS; ref. A2263) was purchased from Panreac AppliChem (Castellar del Vallès, Spain). Laemmli buffer was prepared with Tris 1.28 % (w/v), SDS 1.6 % (w/v), urea 9.6 % (w/v), glycerol 0.08 % (v/v) and 2-mercaptoethanol 0.04 % (v/v).

Sodium phosphate dibasic (Na_2HPO_4; MW = 141.96, purity 99 %) was supplied from Sigma-Aldrich (Madrid, Spain). Sodium phosphate monobasic dihydrate ($NaH_2PO_4 \cdot 2H_2O$, MW = 156.01, purity ≥ 99.0 %) was obtained from Honeywell (North Carolina, U.S.A.). PBS 100 mM was prepared with 5.494 mg/mL NaCl, 0.44 mg/mL Na_2HPO_4 and 0.14 mg/mL $NaH_2PO_4 \cdot 2H_2O$.

D-(+)-glucose (glucose; MW = 180.16, purity ≥ 99.5 %) and glycine (MW = 75.07, purity ≥ 99 %) were supplied from Sigma-Aldrich (Madrid, Spain). D-(+)-sucrose (sucrose; MW = 342.30, purity ≥ 99.5 %), and sodium acetate trihydrate (sodium acetate; ACS reagent, ref. 32318) were purchased from Honeywell (North Carolina, U.S.A.). D-(+)-trehalose 2-hydrate (trehalose; BioChemica, MW = 378.34, purity ≥ 98%), was acquired from PanReac AppliChem (Castellar del Vallès, Spain).

High quality isotonic clinical relevant solutions of glucose 5 % (w/v; ref. 571120) and Ringer's Lactate (ref. 622555) were purchased from Braun (Melsungen, Germany).

All the chemicals were used without further purification.

7.2. Methods for the design, production, purification and characterization of recombinant GLA enzymes

7.2.1. Design, synthesis and cloning of GLA proteins

Gene constructs encoding the different recombinant GLA proteins used in this work are shown on ***Figure 7.2***. The four constructs express the full-length human GLA gene (UniProt P06280; AGAL_HUMAN) with the c-myc and hexahistidine (6-His) tags fused to their C-terminus for further detection and purification purposes. GLAH6-T and GLAcmycH6-S constructs were designed and described previously[1,2] by Dr. José Luis Corchero from IBB-UAB; and GLA-S construct developed by both Dr. José Luis Corchero from the IBB-UAB and LeanBio SL. The GLAcmycH6-T construct was designed *de novo* in this thesis with both c-myc and 6-His tags fused to the C-terminus of the protein.

The *Escherichia coli* (*E. coli*) DH5α strain was used for the maintenance and amplification of all expression plasmids.

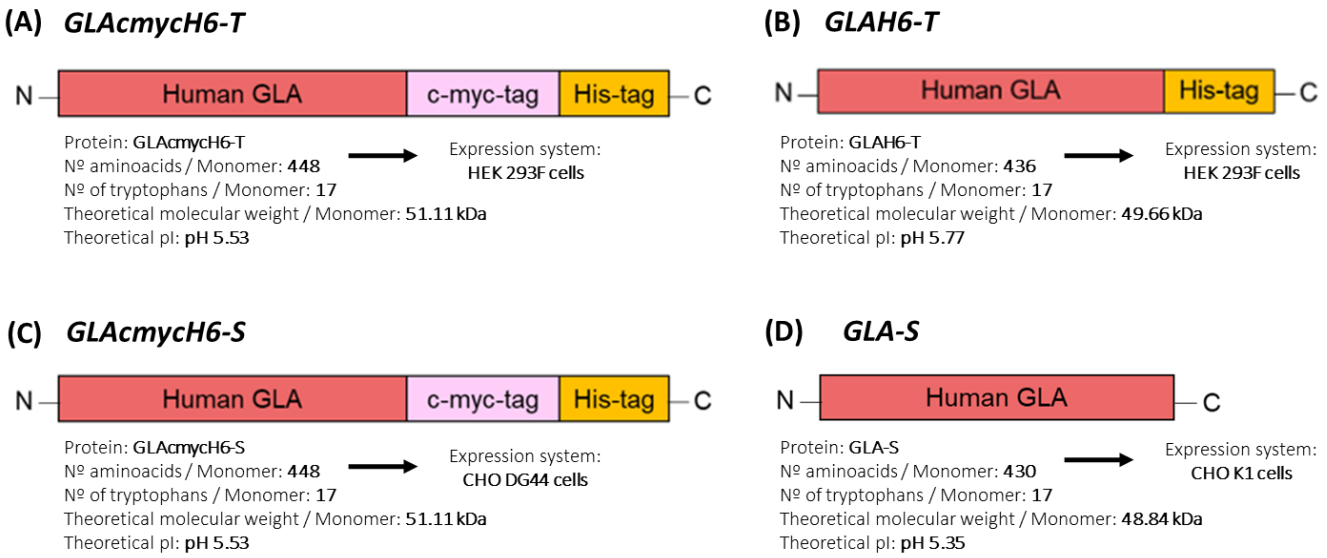


Figure 7.2. Gene constructs of the recombinant proteins A) GLAcmycH6-T, B) GLAH6-T, C) GLAcmycH6-S, and D) GLA-S used in the current work. Expasy Protparam tool was used for calculations of theoretical molecular weight (MW) and isolectric point (pI)[3].

GLAH6-T and GLAcmycH6-T plasmid constructs

Two different expression vectors encoding the GLAH6-T or GLAcmycH6-T proteins were used for transfection and further transient gene expression (TGE) of GLA in human embryonic kidney (HEK) cell cultures (HEK 293F cells). As previously described in Corchero *et al.*[1], GLAH6-T synthetic sequence was cloned by in-fusion methodology in a pTriEx-2 (Novagen, ref. 70826) derivative expression vector called pOpinE of 5534 bp[4]. The resultant expression vector pOpinE-GLA encodes the human GLA gene sequence, lacks the c-myc tag, and only contains a 6-His tag fused to its C-terminus.

In this work, the synthetic gene GLAcmycH6-T was synthesized and cloned (by GeneArt®, Life Technologies) into pTriEx1.1-Hygro vector (Novagen, cat. nº70928-9 Millipore, 6951 bp), between the restriction sites *Nco I* and *EcoR I*. As result, pTriEx1.1.-GLAcmycH6-T plasmid construct includes the human GLA gene sequence plus both c-myc and 6-His tags fused to its C-terminus.

In both, pOpine-GLA and pTriEx1.1.-GLAcmycH6-T expression vectors, GLA production is under the control of cytomegalovirus (CMV) immediate-early enhancer fused to chicken β-actin (CBA) promoter. This fact allows their use as expression plasmid in mammalian cells, ensuring high levels of target protein from a single vector copy.

GLAcmycH6-S and GLA-S plasmid constructs and selection of positive clones

Stable clone of Chinese hamster ovary (CHO) cell cultures (CHO DG44 and CHO K1 cells, respectively) were developed with new expression vectors encoding the GLAcmycH6-S or GLA-S gene sequences for further high yield production of recombinant GLA. As previously described in Merlo-Mas *et al.*[2], GLAcmycH6-S synthetic sequence was cloned in the commercial vector pReceiver-M10 (OmicsLink ORF Expression Clone, ref. EX-Q0172-M10) where the recombinant protein production is under the control of the CMV promoter. In pReceiver-M10 vector both c-myc and 6-His tags sequences are present on the plasmid. For further steps of vector maintenance and TGE procedures, the pOptiVEC™-TOPO® TA Cloning Kit (12744-017, Invitrogen) was used following the recommended commercial protocol. The PCR product was cloned into the pOptiVEC™-TOPO® plasmid, obtaining a resulting plasmid named pOptiVec-GLA, whose gene sequence codified presents a full-length version of the human GLA gene, in which both c-myc and 6-His tags are fused to its C-terminus (same content than the explained above for GLAcmycH6-T construct).

CHO DG44 cells, deficient in dihydrofolate reductase (DHFR-) activity, were used to obtain a clone stably expressing GLAcmycH6-S[5]. The detailed protocol of transfection and selection of positive clones was previously described in Merlo-Mas *et al.*[2]. Finally, the selected positive CHO DG44 clone was cryopreserved in cryovials being stored in a vapor phase of liquid nitrogen.

Also, previous to this work and in the frame of the European Smart4Fabry project, the tag-free recombinant human GLA named GLA-S was designed and developed by LeanBio SL using similar procedures[6]. Briefly, to develop a GLA stable expression based production system, a synthetic gene encoding only for human GLA enzyme (without any tag incorporated) was synthetized and cloned into a commercial vector containing specific antibiotic resistances. Such plasmid was transfected into CHO-K1 (ATCC CCL-61) cells. Two days after transfection, positive cells (resistant to the specific antibiotics) were selected. After this step, serial cell dilutions were prepared and seeded into 24-well plates. GLA production in supernatants was confirmed and estimated by western blot 10 days post-transfection, and the best clone in terms of productivity was individually expanded, isolated and cryopreserved. More detailed information cannot be specified due to trade secret in procedure.

7.2.2. Amplification, extraction and purification of plasmid DNA from *E. coli* strains

The *E. coli* strain DH5α was used for pOpinE-GLA and pTriEx1.1.-GLAcmycH6-T plasmid maintenance and amplification for further TGE experiments. DH5α strain transformations were conducted by mixing 1 ng/µL of pTriEx1.1.-Hygro derived vector with competent bacterial cells and performing a thermal shock, consisting on stepwise cell incubation of 45 s at 42 ºC and then 30 s at 4 ºC.

All plasmids encode resistance to ampicillin, which is used as a selection marker for positively transformed bacterial cells growth at 37 ºC. Then, overnight cultures (2500 mL of ampicillin resistant DH5α cells) were used to purify the expression vectors, with the EndoFreeVR Plasmid Giga Kit (Qiagen, ref. 12391). Absorbance ratio at 260 nm (A_{260}) and 280 nm (A_{280}) were measured for plasmid quantification, and only samples with ratios A_{260}/A_{280} higher than 1.75 were used for TGE experiments.

7.2.3. Transient expression of GLAH6-T and GLAcmycH6-T: transfection procedures

Recombinant GLAH6-T and GLAcmycH6-T enzymes were expressed in the suspension-adapted HEK 293F cell line (Invitrogen, Life Technologies, ref. R790-07) by polyethyleneimine (PEI)-mediated TGE procedures using pOpinE-GLA and pTriEx1.1-GLAcmycH6-T vectors, respectively. These cells were maintained and grown according to the vendor instructions, using Erlenmeyer flasks with plain bottoms and vented caps filled, in FreeStyle™ Expression medium (Thermo Fisher Scientific, ref. 12338018), at 37 ºC in an 8 % CO_2 atmosphere with gentle shaking (120 rpm).

TGE conditions used were based on a previous optimized published protocol[1]. Briefly, HEK 293F cells were transfected at 1 x 10^6 cells/mL using PEI, a 25 kDa linear molecule of transfection-grade (Polysciences, ref. 23966-100). Nanoconjugates of pDNA and PEI were mixed in sterile pre-warmed medium, in a final volume of 10 % the total volume of culture to be transfected. In this work, to optimize protein expression yield, amounts of pDNA were varied from 1 to 0.062 µg pDNA/million cells, but always maintaining the same pDNA:PEI ratio of 1:3 (w/w). The condition using 0.5 µg pDNA/million cells was found as optimal and used for large productions (1 – 3 L) of recombinant GLAH6-T and GLAcmycH6-T proteins. After mixture and incubation (10 min at room temperature) of pDNA-PEI polyplexes, nanoconjugates were added dropwise to cells. Besides, valproic acid (VPA; Merck, Sigma-Aldrich, ref. P4543) was added to cells at a final concentration of 4 mM after 4 hours post-transfection, to enhance recombinant protein expression[7]. Cell viability was estimated by using the Trypan blue exclusion assay.

7.2.4. Stable expression of GLAcmycH6-S and GLA-S

To initiate GLAcmycH6-S production, cryovials of the previously selected positive CHO DG44 clone were thawed under standard procedures, being rapidly thawed at 37 ºC and resuspended in 15 mL of pre-warmed complete CD OptiCHO medium. Cells were subcultured to be expanded up to the desired volume, diluting them into pre-warmed complete CD DG44 medium to give a final cell density of 2 x 10^6 – 3 x 10^6 viable cells/mL.

Similar procedures were used for the production of scaled-up batches of GLA-S protein at LeanBio SL facilities. Detailed information cannot be specified due to trade secret in procedure. In summary, cells were expanded until volumes up to 50 L bioreactor using standard fed-batch methodologies[8].

7.2.5. Chromatographic procedures for secreted GLA purification

Clarified supernatants of transfected cultures containing extracellular GLAH6-T, GLAcmycH6-T or GLAcmycH6-S enzymes were obtained by centrifugation (15 min at 14000 rpm). In particular, the supernatant containing extracellular GLA-S protein was further clarified by 0.22 µm filtration and then 10-fold concentrated by tangential flow filtration (TFF).

7.2.5.1. His-tagged GLA purification by affinity chromatography methodology

Firsts batches at lab-scale (50 to 150 mL of supernatant) of GLA enzymes encoding 6-His tag were purified by using gravity chromatography column (BioRad, ref. #7321010) packed with TALON Superflow resin (Cytiva, ref. 28957502). However, once production was scaled to 1 – 3 L of supernatant, recombinant GLA enzymes encoding 6-His tag were purified in an ÄKTA Pure system (GE Healthcare) by using an affinity chromatography with a HisTrap Excel column (GE Healthcare, ref. 17-3712-06) according to the manufacturer's instructions. GLA enzymes were eluted using the elution buffer (20 mM Tris pH 8, 500 mM NaCl and 500 mM Imidazol), and then, dialyzed against storage buffer (0.01 M acetic/acetate buffer at pH 4.5, or pH 5.5) into a Spectra/PorR 1 Dialysis Membrane Standard RC Tubing MWCO: 6 – 8 kDa (ref. 132650). Recombinant GLAs solubility in both storage buffers was analyzed by centrifuging dialyzed samples (15 min at 14000 rpm) and quantifying the enzyme percentage amount remained in the supernatant. At the end, purified GLA was aliquot and stored at – 20 ºC.

7.2.5.2. Two-step purification process for tag-free GLA-S purification

GLA-S tag-free protein batches were purified at LeanBio SL facilities following a two-step purification process consisting on an anion exchange chromatography (AEX) as a capture step, followed by a final polishing step using a hydrophobic interaction chromatography (HIC). Detailed information cannot be specified due to trade secret in procedure. Elution fractions containing GLA-S protein were submitted to buffer exchange and storage in a

Fabrazyme-like formulation buffer of pH 7 containing 3 % mannitol, 0.275 % $NaH_2PO_4 \cdot H_2O$ and 0.8 % $Na_2HPO_4 \cdot 7H_2O$ at – 20 ºC[9]. The test certificate of the batches provided by LeanBio SL is described in ***Table 7.1***.

Table 7.1. Test certificate of the two batches of GLA-S provided by LeanBio SL with their analytical characterization after production and purification steps.

Purpose	Quality attribute	Analytical method	Results batch R1	Results batch R2
Content	Content	Absorbance at 280 nm	3.34 mg/mL	3.00 mg/mL
Identity	Immunoidentity	Western blot	Immunoreactive band	Immunoreactive band
	Isoelectric point	cIEF	5.41	5.28
	Potency	*In vitro* activity assay	50 U/mg	40 U/mg
Purity (Product-related variants)	Molecular weight	SEC-HPLC	94.55 %	95.12 %
	Hydrophilicity	RP-HPLC	90.24 %	89.76 %
	Charge	cIEF	34.46 %	N.D.
	Purity	nrSDS-PAGE	93.47 %	96.79 %
Purity (Process-related impurities)	Host cell DNA	qPCR	< LOQ (3 pg/mg)	15.3 pg/mg
	Endotoxins	LAL	< LOQ (0.81 EU/mg)	10.27 EU/mg
	Microbial contamination	Bioburden	N.D.	< LOQ (10 CFU/mL)

cIEF: capillary isoelectric focusing; SEC-HPLC: size-exclusion chromatography-high-performance liquid chromatography; RP: reverse phase; nrSDS-PAGE: non-reducing-sodium dodecyl sulfate polyacrylamide gel electrophoresis; qPCR: quantitative polymerase chain reaction; and LAL: limulus amebocyte lysate.

7.2.6. GLA detection, purity and quantification

7.2.6.1. Sodium dodecyl sulfate-polyacrylamide gel electrophoresis and western blot assays

Sodium dodecyl sulfate-polyacrylamide gel electrophoresis (SDS-PAGE) and subsequent western blot analyses were conducted to detect and quantify recombinant GLA from crude supernatants of transfected cultures, purified GLA enzymes, or GLA present in the nanoliposomal product (results presented on ***Chapters 3, 4 and 5***). SDS-PAGE is not considered an extremely accurate analytical technique, thus, the obtained results were considered semi-quantitative but useful for research-level studies.

Samples were properly denatured by diluting them in Laemmli buffer and boiling them 10 min at 98 ºC before use. Acrylamide gels were prepared with Tris-Glycine-eXtended (TGX) Stain-Free™ FastCast™ Acrylamide 12 % (BioRad, ref. 161-0185), capable of making protein tryptophan fluorescent to allow direct protein visualization in gel after a short photoactivation time (45 s) by using a ChemiDoc™ Touch Imaging System (BioRad, U.S.A.),

without staining requirements. For GLA protein amounts estimation, known amounts (ranging from 18 to 145 ng) of a standard His-tagged GLA previously produced, purified, and quantified in-house was used as calibration curve for analysis.

After electrophoresis, SDS-PAGE proteins were blotted onto nitrocellulose membranes for western blot analysis, and further revealed by using a rabbit polyclonal anti-GLA primary antibody (Sigma, ref. HPA000237) or the anti-His monoclonal antibody (Clontech, ref. 631212) to visualize GLA immunoreactive bands.

Samples and standards to be quantitatively compared were always run in the same gel and processed as a set. Densitometric analyses of the bands were performed with ImageLab™ software (version 5.2.1, BioRad).

7.2.6.2. Spectroscopy analysis by nanodrop equipment

Purified recombinant GLA were also quantified by spectrophotometry. GLAH6-T, GLAcmycH6-T and GLAcmycH6-S were directly measured by ultraviolet (UV) absorbance (λ_{Abs} = 280 nm) without any previous sample dilution. The buffer used as control for background subtraction was the one used as storage buffer in each case (0.01 M acetic/acetate buffer at pH 4.5, or pH 5.5). Measurements were performed with a NanoDrop™ One equipment (Thermo Scientific, USA).

GLA-S produced by LeanBio SL was quantified in its facilities. The GLA-S was also diluted using its formulation buffer (mannitol 3 %, $NaH_2PO_4 \cdot H_2O$ 0.275 %, $Na_2HPO_4 \cdot 7H_2O$ 0.8 %, pH 7) at three different ratios (1:5, 1:10 and 1:20), and then directly measured by UV absorbance (λ_{Abs} = 280 nm). The same formulation buffer used in the protein was used as control for background subtraction.

7.2.6.3. Reversed-phase high-performance liquid chromatography-ultraviolet methodology for analytical GLA-S quantification

In order to quantify the GLA-S concentration in a more accurate and quantitative manner, samples of purified GLA-S, and also nanoliposomal formulations containing GLA-S, were analyzed by LeanBio SL using a reversed-phase high-performance liquid chromatography-ultraviolet (RP-HPLC-UV) method (results presented on ***Chapter 5***). The analysis was performed in an Infinity 1260 II HPLC equipment (Agilent Technologies, USA), coupled to a Zorbax 300SB-C18 3.5 µm, 4.6 x 150 mm column (Agilent Technologies, USA) with a controlled temperature at 60 ºC.

The calibration curve was prepared in a range 5.0 – 40 µg/mL of GLA (***Table 7.2***), by diluting a reference standard (soluble commercial GLA, Replagal®) in a liposomal matrix of empty liposomes (without GLA-S presence). The liposomal matrix was solubilized in a mixture of MeOH and acetic acid (AcOH, 0.010 M, pH 5.5), by using a

sample:MeOH:AcOH volume ratio of 1:1:1. All calibration points were filtered by 0.22 µm with polytetrafluoroethylene (PTFE) filter before injection.

Table 7.2. Preparation and concentration range of the calibration curve to quantify GLA amounts by RP-HPLC-UV.

Calibration point	GLA concentration (ppm)
A	40
B	25
C	15
D	10
E	5

Sample preparation by solubilizing the nanoliposomal formulations containing GLA-S was prepared by same aforementioned procedure. Nanoliposomes were disintegrated in the already explained mixture of MeOH:AcOH using the sample:MeOH:AcOH volume ratio of 1:1:1. Samples were also filtered with a 0.22 µm PTFE filter before HPLC injection. Each sample was prepared in two independent replicates to test. Notably, previously to submit samples to this solubilization process, those containing theoretical GLA-S concentration higher than 40 µg/mL (corresponding to the upper limit value of the prepared calibration curve) were previously diluted in pure water to achieve an approximate concentration around 20 – 30 µg/mL.

The elution conditions of the procedure used a mobile phase A (MP_A) composed of 0.1 % (v/v) TFA in a volumetric mixture of water:ACN 95:5 %, and a mobile phase B (MP_B) composed of 0.09 % (v/v) TFA in a volumetric mixture of water:ACN 5:95 %. Separation step used a 30 min linear gradient from 0 to 60 % MP_B, followed to a 5 min cleaning step using 100 % MP_B in a flow rate of 1 mL/min (*Table 7.3*). The injection volume was 100 µL of sample, and GLA-S was analyzed using a UV-detector at λ_{Abs} = 215 nm.

Table 7.3. Gradient elution method for GLA-S quantification with and without liposome presence.

Time (min)	0	35	40	40.5	45
MP_A (%)	100	40	0	100	100
MP_B (%)	0	60	100	0	0
Flow (mL/min)	1				

7.2.7. Determination of host cell DNA contamination in GLA enzymes

According to the methodology established by Sambrook & Russell[8], an estimated percentage of host cell DNA present in purified GLAs was determined by absorbance ratio at 260 nm (A_{260}) and 280 nm (A_{280}) following the ratio A_{260}/A_{280} (see ***Table 7.4***).

Table 7.4. Relation between absorbance of nucleic acids and proteins, and the percentage of nucleic acids and/or protein present in samples. Adapted from Sambrook & Russell[8].

Absorbance of Nucleic Acids and Proteins

% Protein	% Nucleic Acid	A_{260} / A_{280} ratio
100	0	0.57
95	5	1.06
90	10	1.32
85	15	1.48
80	20	1.59
75	25	1.67
70	30	1.73
65	35	1.78
60	40	1.81
55	45	1.84
50	50	1.87
45	55	1.89
40	60	1.91
35	65	1.93
30	70	1.94
25	75	1.95
20	80	1.96
15	85	1.97
10	90	1.98
5	95	1.99
0	100	2.00

7.2.8. Integrity of GLA enzymes by mass spectrometry

The integrity of the purified GLA enzymes was analyzed by Dra. Irene Fernández from Mass Spectromety Unity of Molecular Characterization located in Scientific and Technologic Centers of the University of Barcelona (CCiTUB). Samples were analyzed using a 4800 Plus MALDI TOF/TOF (ABSCIEX – 2010) instrument. Mass spectrometry samples were prepared in a matrix of sinapinic acid (SA) using a "Sandwich" method. The protocol consisted of depositing on a plate 1 µL of SA solution (27 mg/mL acetone:H_2O 99:1); once the aliquot was dried, 1 µL of purified enzyme was spotted above, and when it was dried, 1 µL of SA solution (10 mg/mL H_2O:CH_3CN 1:1 0.1 % TFA) was added again and left to dry before analysis.

Matrix assisted laser desorption ionization (MALDI) mass spectra were recorded in the positive ion lineal mode on the time-of-flight (TOF) instrument. It used a solid state laser (Nd:YAG) at 355 nm, 200 Hz and 3 – 7 ns pulse). The instrument was calibrated with a mixture of standards (BSA) in order to obtain the accuracy specified in the technical conditions of the instrument for the analyzed mass range: +/– 0.05 to 1 %. A mass range m/z = 20 – 80 kDa was recorded.

A Gaussian smooth filter of 15 was applied to the spectra obtained in order to improve the visualization of the result.

7.2.9. *In vitro* fluorescent enzymatic assay for specific α-galactosidase activity

Fluorimetric methodologies initially described by Desnick *et al.*[10] and further modified by Mayes *et al.*[11], were used to assay GLA enzymatic activity as previously detailed[1,12,13]. The basics of the enzymatic activity assay consists on the conversion (when active GLA is present) of a non-fluorescent substrate named 4-methylumbelliferyl-α-D-galactopyranoside (4-MUG, Sigma-Aldrich, M-7633) in the fluorescent product 4-Methylumbelliferone (4-MU). In our protocol, 25 µL of sample (either soluble purified GLA protein or GLA-encapulated in liposomal formulations) were incubated 60 min at 37 ºC in a water bath with agitation of 100 rpm with 100 µL of artificial substrate 4-MUG at an excess concentration of 2.46×10^{-3} M, diluted in assay buffer (0.01 M acetic/acetate buffer at pH 4.5). Reactions were stopped by adding 1.25 mL of 0.2 M glycine/NaOH buffer at pH 10.4. The fluorescence from the released product 4-MU was determined using fluorimetric conditions at λ_{ex} = 365 nm and λ_{em} = 450 nm. Aliquots of commercial product 4-MU (Sigma-Chemical, M-1381) ranging from 5 to 500 ng/mL in 0.2 M glycine/NaOH buffer at pH 10.4, were used to obtain a calibration curve to transform fluorescence measurements into 4-MU concentration. The specific protein activity (expressed as µmol 4-MU/h·mg) was calculated from the 4-MU regression plot, and incorporating in the equation the enzyme concentration and the reaction time used.

Assays usually corresponded to a single representative experiment, replicated in three independent assays. The error is the standard deviation of the mean (s.d.) of the three replicates.

In the experiments of ***Chapter 5, Section 5.4.2.1***, enzymatic activity values were referred to enzymatic activity of standardized LP-RGD-GLA-$S_{(gluc)}$ liposomes, in order to compare the enzymatic activity variation when incubating the formulation in different media.

Absence of matrix effects in fluorescence readings were verified by comparing fluorescent emission of 4-MUG substrate and 4-MU product with and without spiking of empty nanoliposomal formulations (without GLA). Both fluorescence spectra of 4-MUG and 4-MU molecules used in the enzymatic activity reaction were not altered by

the presence of liposomes. Vesicle colloidal stability was also confirmed by determining the particle size distribution by dynamic light scattering (DLS) and nanoparticle tracking analysis (NTA) using the same conditions as when performing the enzymatic activity assay (see ***Chapter 4, Section 4.2.3***).

7.2.10. Particle size distribution and ζ-potential determination of GLA enzymes by dynamic and electrophoretic light scattering

Recombinant proteins can be destabilized under certain conditions and generate larger-sized populations of protein aggregates with reduced enzymatic activity, homogeneity or modified native structure. The protein aggregation is more common when enzyme surfaces present neutral electrical charge. In this thesis, protein size, population polydispersity and superficial charge were used as quality criteria to evaluate the colloidal stability of recombinant GLA proteins and better understand their biological performance as enzymes.

A DLS and electrophoretic light scattering (ELS) analyzer of a Malvern Zetasizer Nano ZS and/or Zetasizer Ultra equipment (Malvern Instruments, UK) based on non-invasive backscatter technology (NIBS) were used to measure the protein size, polydispersity index (PdI) and superficial charge (ζ-potential) of recombinant GLA enzymes. Both instruments have equipped a 4 mW He-Ne laser beam (λ = 633 nm) with the detector set at 173 º for particle size distribution analysis, and at 13 º for the ζ-potential measurements. In all cases, sample measurements were performed in triplicate at 25 ºC. Then, values were expressed as the triplicate average, and the error as their s.d.. Data was recorded and analyzed by Zetasizer Software 7.13 and/or ZS Xplorer v2.01 (Malvern Panalytical, UK).

For particle size distribution determination of purified recombinant GLA proteins based on intensity and/or volume size-distribution, 50 – 75 µL of sample was dispensed in a ZEN0040 disposable plastic micro cuvette or a ZEN2112 3 mm quartz cuvette, which allow the use of lower sample volumes. In particular, for ζ-potential measurements with low volumes of purified GLA, the diffusion barrier technique was employed in a DTS1070 disposable folded capillary cell together by applying a voltage of 40 mV. This technique has the advantage of physically separate the protein molecules from the electrodes by buffer (see ***Figure 7.3***) avoiding the probable denaturation and/or aggregation damage caused by their contact[14]. Once the capillary cell was filled with the buffer used for the dissolution of GLA protein, to generate the diffusion barrier technique, only 20 – 100 µL of the sample must be directly plugged at the U-bend bottom of the cuvette with a gel loading tip (Costar, ref. 4853).

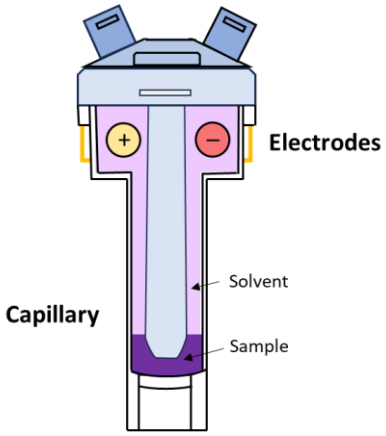


Figure 7.3. Schematic representation of the diffusion barrier technique applied in a DTS1070 disposable folded capillary cell, for the ζ-potential analysis of purified GLA enzymes. Adapted from the operating recommendations of the manufacturer[14].

In all cases, ELS data was based on Smoluchowski model. The DLS results were provided from the original scattered intensity data, which is the most robust due to the fact that it does not use additional approximated calculations with value assumptions such as volume or number size-distribution data. However, samples of purified enzyme usually contain few amount in percentage of large protein contaminants or nanoaggregates of the same protein, which could interfere in the correct detection and analysis of the main protein population (typically with lower sizes, but higher amounts in percentage). To ensure a robust and complete sample colloidal characterization, values of intensity size-distribution were used for size and PdI analysis in this work, but results based on volume size-distribution were also checked to better follow the smaller soluble GLA population together with the apparition of new aggregates.

Characterization of the thermal-dependent aggregation of GLA enzymes by DLS

Furthermore, to check the thermal dependence of protein aggregation or denaturation, the size distribution of all purified GLAs were progressively determined by quintuplicate measurements in a temperature range of 4 ºC to 70 ºC allowed for the DLS equipment.

7.2.11. Structural characterization of GLA enzymes by tryptophan fluorescence emission spectra analysis

Since tryptophan (Trp) aminoacid exists in most proteins, it can be widely employed in protein structural studies by the indirectly analysis of fluorescence emission spectra of those aromatic aminoacids contained in protein sequences[15]. For this purpose, GLA enzymes were excited at λ_{ex} = 295 nm, and the Trp fluorescence emission spectra (λ_{em} = 300 – 550 nm) was measured in a Varian Cary Eclipse fluorescence spectrophotometer (Agilent Technologies, Santa Clara, CA, USA) at 25 ºC.

The center of spectral mass (CSM) of the spectra was calculated using the equation ***Eq. 7.1***[16,17].

$$CSM = \frac{\sum \lambda_i F_i}{F_i}$$

(***Eq. 7.1***)

Where λ_i and F_i correspond respectively to each wavelength and emitted fluorescence values from the emission spectra recorded between 310 and 450 nm.

Characterization of the thermal-dependent conformational structure of GLA enzymes by fluorescence spectroscopy

Additionally, the thermal dependence of tertiary protein structure in purified GLA enzymes was also checked by following the CSM values of purified GLA enzymes in a temperature range of 4 ºC to 95 ºC, using the Varian Cary Eclipse fluorescence equipment. A Cary Eclipse Multicell Holder and Cary Temperature Controller were coupled to the fluorimeter in order to thermostat the samples. The experimental data was fitted with a non-linear sigmoidal model from GraphPad Prism 8.0.2. program to extrapolate the temperature of half completion of transition between two average macroscopic states (T_m) value.

Characterization of the binding capacity of GLA enzymes with liposomal membranes

As previously explained in ***Chapter 4***, the emission spectra of Trp is sensitive to be modified according to the subsequent exposure of the aminoacid to the aqueous phase but also to the interactions with other aminoacids in the surroundings. Therefore, variations in the local environment of Trp can be induced by the interaction of a protein with other biomolecules, or even with surfaces.

In this work, the binding capacity of GLA enzymes with nanoliposomal membranes was studied by fluorescence spectroscopy. Thereby, increasing amounts of nanoliposomes were titrated over 0.225 mg of purified GLA enzymes. Changes of Trp fluorescence emission spectra were recorded exciting samples at λ_{ex} = 295 nm, and emitting light on λ_{em} = 300 – 550 nm. CSM values were monitored to follow probable conformational changes of the GLA enzymes induced by the enzyme-liposome interactions.

7.2.12. Resistance to proteases assessment using an *in vitro* trypsinization assay

In vitro assays with trypsin as protease model are commonly performed to test protection capacity of nanoparticles over integrated peptides or proteins. Trypsin is an enzyme of 23.8 kDa from the serine protease family capable to carry out peptide cleavage on their C-terminus side on lysine and arginine residues, in an optimal pH range of 7 – 9.

To conduct the assay, a trypsin stock of 225 µM was prepared by reconstituting commercial porcine lyophilized trypsin (Sigma-Aldrich, ref. T7409) in PBS 100 mM adjusted at pH 7.4. Digestion reactions of soluble GLA and GLA-integrated liposomal formulations were performed within a trypsin:peptide ratio from 1:100 to 1:20, as recommended by the manufacturer. Mostly, samples for kinetic studies were withdrawn at 15 min, 30 min, 1 h, 3 h, 8 h, 24 h, 48 h and 72 h. For each time-point, 3 replicates of each sample were prepared in individual eppendorfs, and incubated in a water bath at 37 ºC and 100 rpm. Reactions were stopped by denaturing the trypsin enzyme by mixing 75 µL of sample with 25 µL of Laemmli buffer (composition: Tris 1.28 % (w/v), SDS 1.6 % (w/v), urea 9.6 % (w/v), glycerol 0.08 % (v/v) and β-mercaptoethanol 0.04 % (v/v)) for further SDS-PAGE analysis.

All sample time-points from the kinetic reaction and their corresponding initial samples (reaction time: T = 0) were run in the same gel and processed as a set to be quantitatively compared. Results are given in percentages of remaining GLA amount, taking the GLA amount of initial samples as the 100 %. Densitometric analyses of the bands were performed with ImageLab™ software (version 5.2.1, BioRad).

7.2.13. Stability studies of naked GLA enzymes

The stability of the purified recombinant GLA enzymes was followed in different conditions:

i. Under increasing temperatures, to follow the influence of the temperature on the denaturation and/or aggregation of the GLA proteins. For this purpose, particle size analysis of the GLA proteins by DLS was performed in a temperature range from 4 to 70 ºC (as previously explained in ***Section 7.2.10***), and the tryptophan fluorescence emission spectra of GLA enzymes were followed in a temperature range from 4 to 95 ºC (protocol detailed in ***Section 7.2.11***). The respective results are reported on ***Chapter 3***.

ii. Under storage conditions (at fridge between 2 – 8 ºC), to understand the stability of the physicochemical and biological properties of the GLA enzymes at such conditions in a short-term of 3 months. Particle size distribution and ζ-potential was followed by DLS/ELS (protocol detailed in ***Section 7.2.10***), and the GLA enzymatic activity assessed by fluorimetric methodologies (described in ***Section 7.2.9***). The respective results are reported on ***Chapter 4***.

In all cases, an aliquot was withdrawn at the established time points to perform physicochemical and biological characterizations of the different samples.

7.3. Methods for the synthesis, purification and characterization of the chol-PEG_{400}-RGD targeting molecular unit

The design and synthesis of the targeting molecule named chol-PEG_{400}-RGD (***Figure 7.4***) was in charge of the group of Dr. Miriam Royo from IQAC-CSIC. The conjugation of cyclic c-RGDfK peptide ligand (simplified here as RGD) into chol-PEG_n-OH moieties, was previously described in Cristóbal-Lecina *et al.*[18]. Briefly, it consisted of a two-step process based on the hydroxyl group transformation of chol-PEG_n-OH into the corresponding chloroformate or ester carbonate intermediates, for the further RGD peptide introduction through a carbamate bond. The excess or RGD peptide was eliminated by washing with H_2O the precipitated compound, and unreacted chol-PEG_n intermediate moieties removed by using acetonitrile (ACN; CH_3CN).

Chemical formula of chol-PEG_{400}-RGD: $C_{71}H_{117}N_9O_{17}$ (MW = 1369 g/mol).

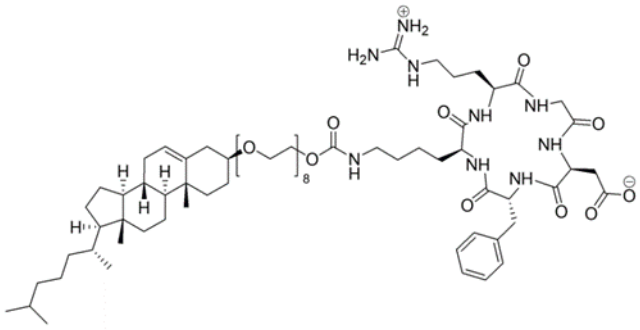


Figure 7.4. Chemical structure of cholesterol-PEG400-cRGDfk (chol-PEG_{400}-RGD).

High-resolution electrospray ionization mass spectrometry (HR-ESI-MS) was used to calculate chol-PEG_{400}-RGD mass by measuring the mass-to-charge ratio (m/z) of their ions. Values found were $[M+H]^+$: 1368.86402 and 1368.87080 g/mol.

A chemical purity of chol-PEG_{400}-RGD higher than 95 %, was determined using high-performance liquid chromatography with photodiode array detection coupled to a mass spectrometer (HPLC-PDA-MS). The procedure was based on a Symmetry300, C4, 5 µm, 4.6 x 250 mm column, using as elution solvents: A = 0.1 % HCOOH in H_2O, and B = 0.07 % HCOOH in ACN in an increasing gradient from 5 % to 100 % B using a flow of 1 mL/min. The analysis had a duration of 30 min and the RT of chol-PEG_{400}-RGD molecules was 17.7 min. The column temperature was controlled at 50 ºC and the peptide was analyzed at λ = 210 nm.

Finally, an amino acid analysis by using HPLC-UV, AccQTag Waters pre-column derivatization method ensured ≥ 85 % peptide content (Asp, Gly, Arg, Lys, Phe).

7.4. Methods for the preparation, diafiltration and characterization of nanoliposomal formulations

7.4.1. Plants and experimental procedures for the preparation of nanoliposomal formulations by DELOS-susp methodology

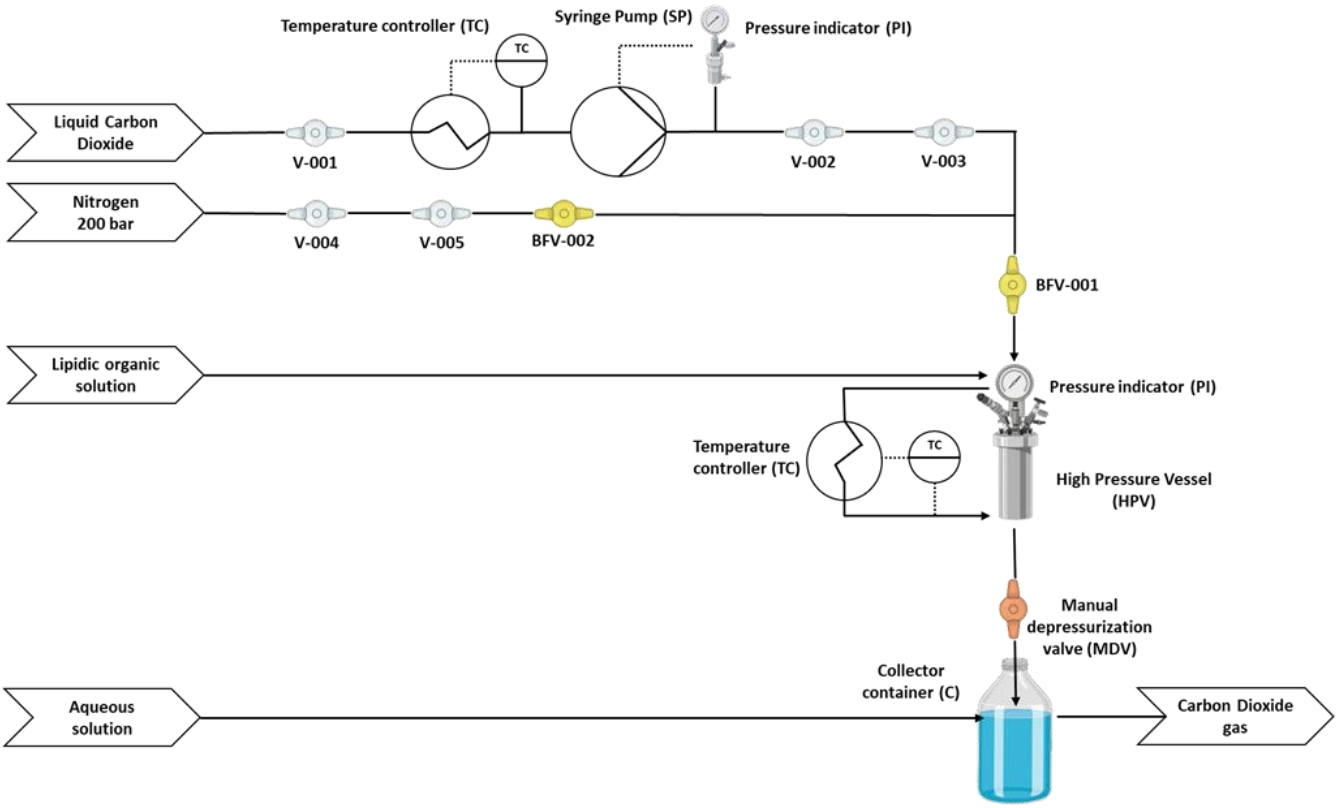
The preparation of nanoliposomal formulations was carried out using an innovative technology, based on the use of compressed CO_2, named depressurization of an expanded liquid organic solution-suspension (DELOS-susp). This is a robust and green technology developed by researchers of ICMAB-CSIC[12,19], and scaled-up and exploited by the company Nanomol Technologies SL. Besides, a GMP compliant DELOS-susp pilot equipment has been designed and built by Nanomol Technologies' engineers for future GMP compliant production.

DELOS-susp plants of different scales were used to prepare different batch size of nanoliposomal formulations. The small plant (P7.5), which consists of a 7.5 mL high-pressure vessel, was used at lab-scale for the production of batches between 25 – 75 mL). However, large plants (P25/P100), which consist of 25 mL or 100 mL high-pressure vessels, were used at intermediate lab-scale for the preparation of batches between 250 – 1500 mL. Configuration of both equipments plants is detailed and schematized in ***Section 7.4.1.1 and Section 7.4.1.2***. All the nanoformulations used in this thesis were prepared at the Soft Materials Service of ICMAB-CSIC linked to Biomaterial Processing and Nanostructuring Unit (U6) of NANBIOSIS ICTS, or at Nanomol Technologies SL facilities.

7.4.1.1. Description of the small lab-scale DELOS-susp plant

The most of the nanoliposomal formulations reported in this work were prepared by DELOS-susp technology using P7.5 plant. The configuration of the small lab-scale plant (see ***Figure 7.5***) comprises a 7.5 mL high pressure vessel (HPV), whose temperature is controlled by an external fluid heating jacket. By using a thermostatic syringe pump (SP) from model 260D (ISCO Inc., Lincoln, US), CO_2 is introduced inside the HPV passing across valves V-002 and V-003 until reaching working pressure. Subsequently, a manual depressurization valve (MDV) allows the depressurization of the expanded liquid solution contained in the HPV into an aqueous phase placed in a collector container (C) at atmospheric pressure. In parallel, pressurized nitrogen (N_2) is pumped through valve V-005 into HPV to ensure that the pressure inside HPV is kept constant during the depressurization step. To prevent contamination in CO_2 and N_2 pipelines by backflow from HPV, two one-way valves (BFV-001 and BFV-002) are

located before V-003 and V-005. To well monitor the system pressure, two pressure indicators (PI) are installed: one inside CO_2 line, and another just before HPV.



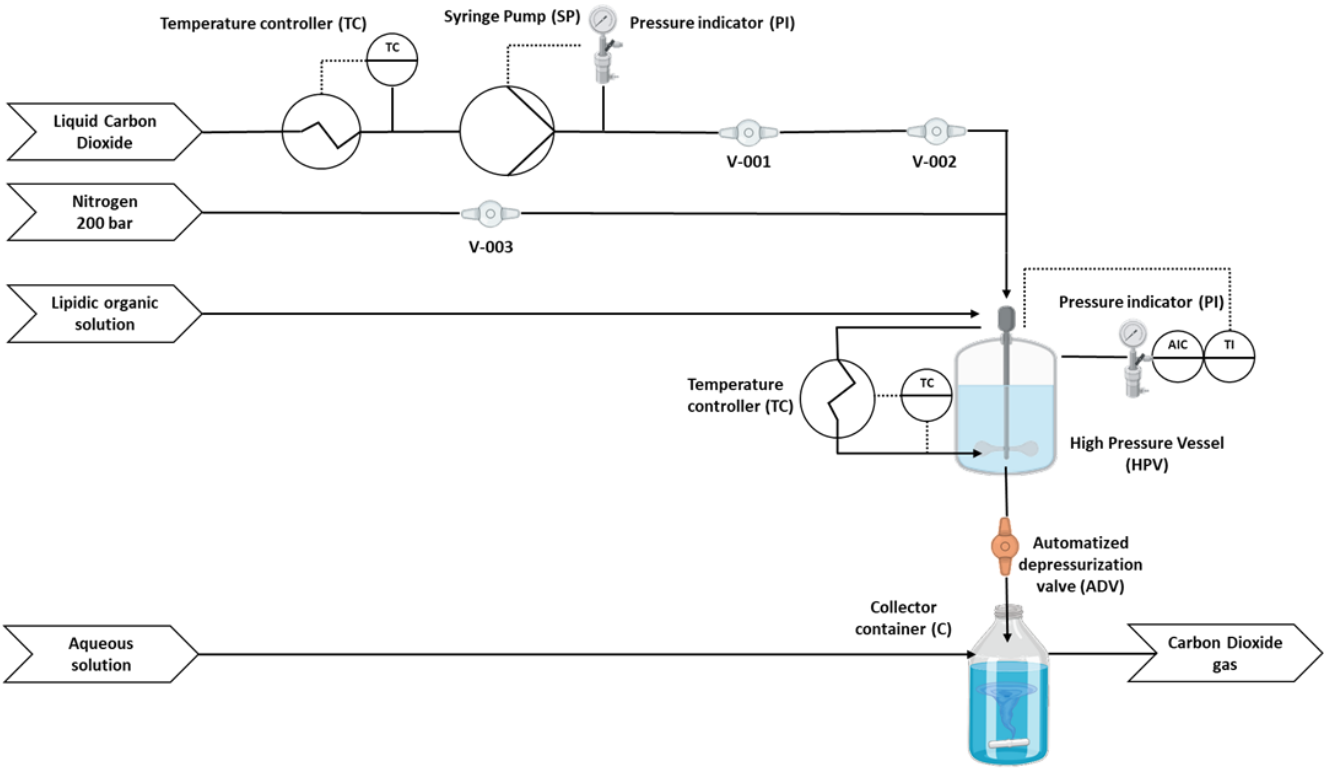
LEGEND	
V-001	CO_2 bottle valve
V-002	CO_2 feed valve
V-003	CO_2 fume hood feed valve
V-004	N_2 bottle valve
V-005	N_2 pressure regulator
BFV-001	CO_2 back flow valve
BFV-002	N_2 back flow valve

Figure 7.5. Schematic diagram of the small lab-scale plant (P7.5) used for the production of nanoliposomal formulations by DELOS-susp.

7.4.1.2. Description of the intermediate lab-scale DELOS-susp plant

Nanoliposomal formulations supplied by Nanomol Technologies SL partners were prepared by DELOS-susp using P25 or P100 plant. The intermediate lab-scale DELOS-susp plant (see *Figure 7.6*) comprises a 25 mL or 100 mL HPV, which are independent and interchangeable. Again, HPV temperature is controlled by an external fluid heating jacket, but also monitored by a temperature indicator (TI) in this case. By using a thermostatic syringe pump (SP) from model 260D (ISCO Inc., Lincoln, US), CO_2 is introduced inside the HPV passing across valves V-001 and V-002 until reaching working pressure. Interestingly, a stirrer (S) with controllable speed is present inside

HPV, ensuring the well homogeneity of the mixture in the expanded liquid phase. Subsequently, an automatized depressurization valve (ADV) allows the depressurization of the expanded liquid solution contained in the HPV into an aqueous phase placed in a collector container (C) under magnetic agitation (MS) at atmospheric pressure. In parallel, pressurized nitrogen (N_2) is pumped through valve V-003 into HPV to ensure that the pressure inside HPV is kept constant during the depressurization step. Again, to well control the system pressure, two pressure indicators (PI) are installed: one inside CO_2 line, and another inside HPV.



LEGEND	
V-001	CO_2 feed valve
V-002	CO_2 fume hood feed valve
V-003	N_2 fume hood feed valve

Figure 7.6. Schematic process diagram of the intermediate lab-scale plant (P25/P100) used for the production of nanoliposomal formulations by DELOS-susp.

7.4.1.3. DELOS-susp methodology for the production of nanoliposomal formulations

In this section the different DELOS-susp based experimental procedures used in the present thesis for the synthesis of GLA-free nanoliposomes and GLA-loaded nanoliposomes are described.

Preparation of nanoliposomal formulations by DELOS-susp

The procedure for the preparation of nanoliposomal formulations by DELOS-susp methodology is schematized in ***Figure 7.7***.

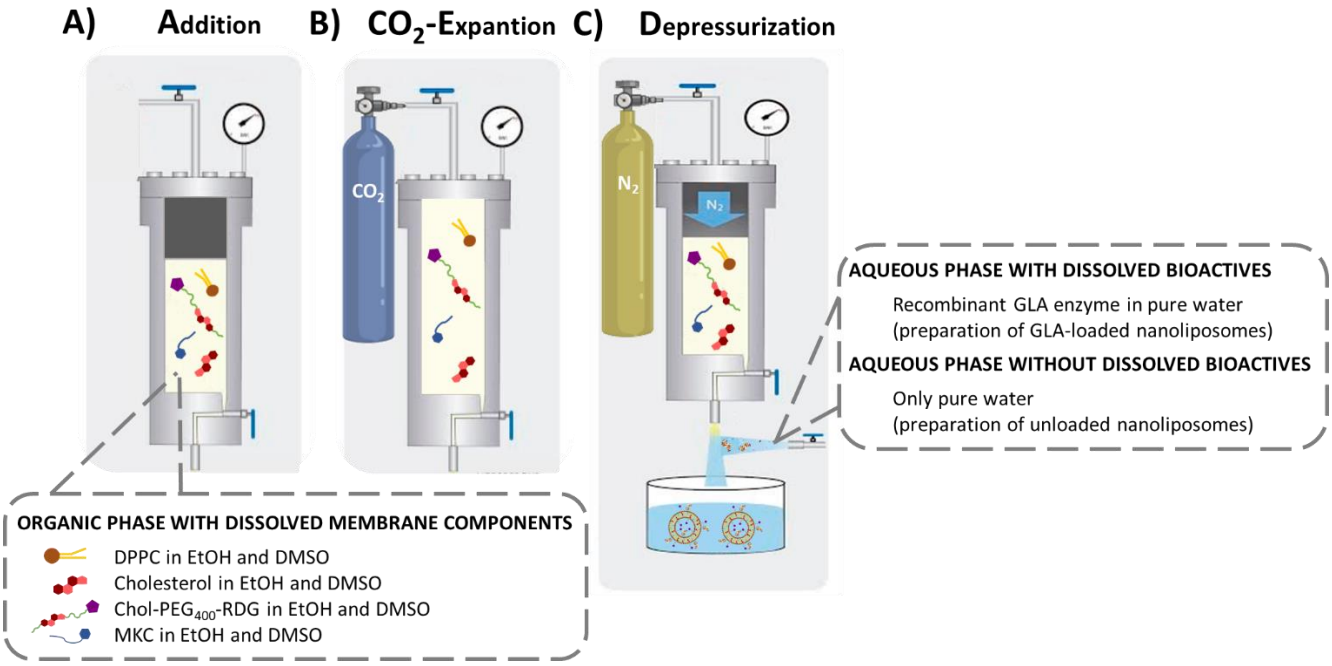


Figure 7.7. Overview of the procedure to prepare nanoliposomal formulations by DELOS-susp: A) Addition of dissolved membrane components in an organic solution into the HPV. B) Addition of compressed CO_2 to expand the solution. C) Depressurization of the organic phase on an aqueous solution with or without containing the dissolved bioactive for the preparation of GLA-loaded nanoliposomes or unloaded nanoliposomes, respectively.

Basically, known quantities of hydrophobic membrane components (DPPC, chol, and/or chol-PEG_{400}-RGD, and/or MKC) were solubilized in a volume (V_{OS}) of an organic solution (mixture of EtOH and DMSO) being sonicated 5 – 15 min at 35 – 40 ºC, and then introduced into HPV working at atmospheric pressure and a controlled temperature between 35 – 40 ºC. The organic solution was then volumetrically expanded with liquid compressed CO_2 until reaching a CO_2 molar fraction (X_{CO_2}) between 0.2 – 0.85 and a working pressure between 8.5 – 10 MPa. To ensure the thermal equilibration of the organic solution at 35 – 40 ºC and its homogenization, the CO_2-expanded solution was left to equilibrate (1 h when using the P7.5, or 15 min under 500 rpm of mechanical stirring when using P25 or P100 HPV) before its depressurization over a volume of aqueous solution (V_{AS}). Purified

water through a Milli-Q® Advantage A10 water purification system was always used to prepare the aqueous solution. For the production of unloaded nanoliposomal formulations, pure water was used as aqueous solution. For the preparation of GLA-loaded liposomal formulations, recombinant GLA enzyme was dissolved in the pure water (aqueous phase) at the desired concentration just before the depressurization of the CO_2-expanded solution. In this manner, the biomolecule integration can be achieved during the liposomes' formation. The volumetric relation between the aqueous and the organic solution was 16:1 (V_{AS}:V_{OS}, aqueous solution:organic solution). A flow of N_2 at 10 ± 1 MPa is used to plunge the CO_2-expanded solution from the reactor to maintain constant the pressure inside the HPV during the depressurization process. The average time per experiment was respectively around 2 h for P7.5 plant, or 1 h for P25/P100 installation. The obtained nanoliposomal formulations were stored at 2 – 8 ºC until further characterization and diafiltration by TFF.

7.4.2. Integration of GLA protein into a nanoliposomal formulations by titration approaches

In the present thesis, GLA-adsorbed nanoliposomes where produced by the titration of recombinant GLA enzyme in already structured unloaded nanoliposomes previously prepared by the DELOS-susp methodology explained in ***Section 7.4.1.3***. A V_{AS} containing known amounts of solubilized GLA protein was dropwise titrated over unloaded liposomes under gentle manual agitation, and then incubated at 25 ºC during 30 min to allow protein-membrane interaction (***Figure 7.8***).

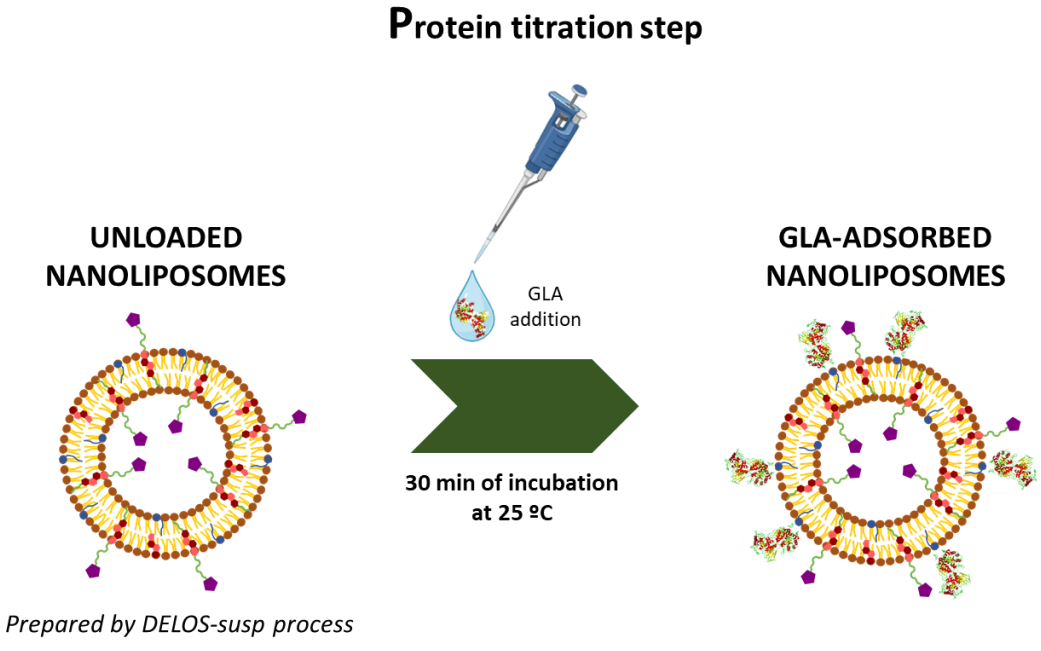
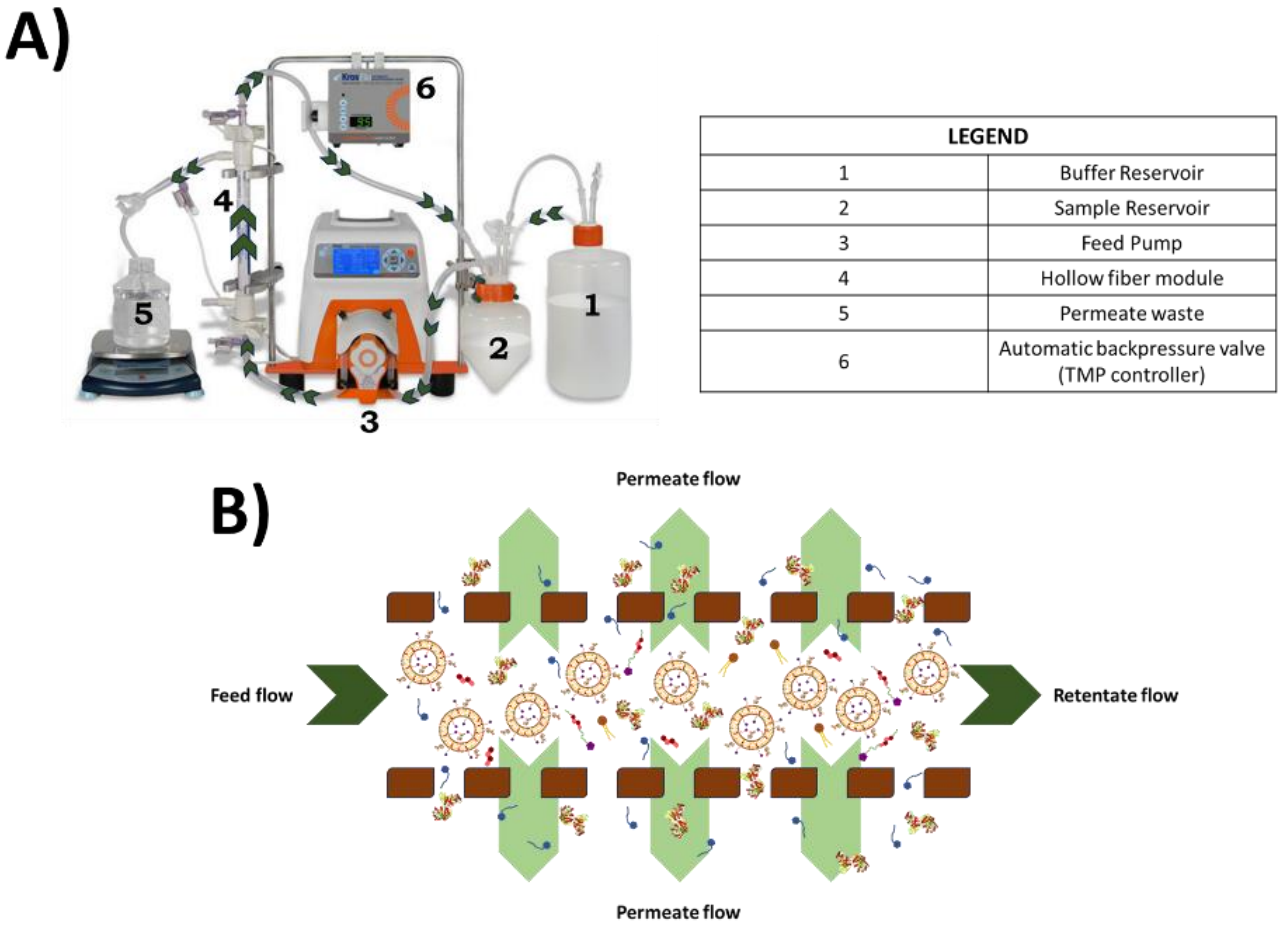


Figure 7.8. Overview of the GLA integration on nanoliposomal systems by titration approaches. GLA enzyme is titrated after the formation of unloaded nanoliposomal structures following DELOS-susp procedures.

7.4.3. Diafiltration and concentration of nanoliposomal formulations by TFF

Nanoliposomal formulations were submitted to a TFF process (see *Figure 7.9*), using a KrosFlo® Research IIi TFF System (Repligen, Waltham, USA), one day after their production, as step to simultaneously remove organic solvent molecules (EtOH and DMSO from DELOS-susp process), non-integrated membrane components and/or non-encapsulated GLA protein by dispersant medium exchange. TFF process was also employed to concentrate nanoliposomal samples when necessary[20]. TFF process was performed at the Soft Materials Service of ICMAB-CSIC linked to Biomaterial Processing and Nanostructuring Unit (U6) of NANBIOSIS, or at Nanomol Technologies SL facilities.



LEGEND	
1	Buffer Reservoir
2	Sample Reservoir
3	Feed Pump
4	Hollow fiber module
5	Permeate waste
6	Automatic backpressure valve (TMP controller)

Figure 7.9. Schematized representation of A) the KrosFlo® Research IIi TFF System equipment set-up and B) the diafiltration step of liposomes through TFF process. Adapted from the operating recommendations of the manufacturer[20].

Basically, the protocol based on TFF technique to diafiltrate the nanoliposomal formulations comprises the following steps:

i. Simultaneous diafiltration by TFF and buffer exchange: diafiltration step involves the use of transmembrane pressure (TMP) as driving force to recirculate the sample through a porous column, meanwhile new solvent is added to the system. Nanoliposomal formulations were diafiltrated by TFF by using 300 kDa cut-off hollow fibber columns made of modified poyethersulfone (mPES) with a surface area of 40 cm^2 or 235 cm^2 (C04-E300-05-N or D04-E300-05-N, respectively; Repligen, USA). C04-E300-05-N columns were used for the diafiltration by TFF of sample volumes of 25 – 60 mL, meanwhile D04-E300-05-N columns for sample volumes > 200 mL. To proceed with sample diafiltration by TFF, a specific volume of sample was added to the feed reservoir and submitted to 6 cycles of diafiltration by TFF, meantime the removed volume of the system was replaced by new media placed in the buffer reservoir to maintain constant vesicle concentration. Process parameters like system pressure, flow… were set-up depending the volume of sample to proceed and according manufacturer instructions. This allows the elimination of non-integrated components having sizes below pore size, such as recombinant GLA (over 100 kDa protein), MKC, remaining organic solvents or others. The buffer reservoir usually contained pure water (for purification purposes) or a different buffer (for buffer exchange). When processing samples containing GLA samples, the process was done in cold conditions (2 – 8 ºC) to safeguard GLA activity.

ii. Sample concentration: a volume between 10 and 5000 mL can be added to the sample container, which is only connected to the column. In this case, the sample will become more concentrated as volume is being removed. The degree of concentration (Concentration Factor, C_{Fc}) corresponds to the initial volume (V_i) divided into the final volume (V_f), $C_{Fc} = V_i / V_f$. For example, if the initial volume is 50 mL and the desired CF is 5, then the process will stop when sample volume in the sample container is 10 mL. In this thesis the CF routinely applied in samples was of 7.5-fold.

The time for the completion of the process depends on the total volume processed and the operation parameters and the expert in the field knows how to adjust it. In this work, the overall duration of this process generally took about 1 -2 h.

This TFF process step for samples intended to be used in preclinical studies was conducted in a class II laminar flow biological safety cabinet (Maxisafe 2020, Thermo Scientific). Filter hollow columns (C04-E300-05-S or D04-E300-05-S) and pressure transductors were purchased directly in a sterile packaging (Repligen, USA). All the diafiltration material employed was previously sterilized: tubes, reservoirs and volumetric glass recipients using pressurized saturated steam in an autoclave (Presoclave-III 50, J.P. Selecta) configured at 121 ºC during 20 min;

and reservoir caps, tubing connectors or other plastic pieces being submerged overnight in ethanol. During all procedure, samples were always manipulated and aliquoted in a laminar flow cabinet environment.

To point out, those nanoliposomal formulations prepared for preclinical studies at Nanomol Technologies' facilities were filtrated through Sartopore® Platinum Midicaps® (Sartorius, ref. 5495307H8--OO--A), which are heterogeneous polyethersulfone (PES) double layer filters of 0.45 to 0.22 µm pore size, as terminal sterilization procedure.

These nanoliposomal formulations were aliquoted in 50 mL sterile United States Pharmacopeia (USP) type I borosilicate glass vials assembled with butyl stoppers and aluminum seals (Thermo Scientific, ref. 15153518). USP type I glass was chosen because of its suitability for most products for parenteral and non-parenteral uses. Finally, vials were filled individually using a sterile syringe coupled to a 23 G needle (Terumo Agani, G 23, 0.6 x 25 mm), working inside a laminar flow cabinet.

7.4.4. Summary of process parameters used for the preparation of nanoliposomal formulations

Liposomal-based nanoformulations were prepared at the Soft Materials Service of ICMAB-CSIC linked to Biomaterial Processing and Nanostructuring Unit (U6) of NANBIOSIS, or in Nanomol Technologies SL (Barcelona) facilities under the frame of EU projects Smart4Fabry and Phoenix. Detailed process parameters used for the preparation of all nanoliposomal formulations using the plants and procedures described in ***Sections 7.4.1, 7.4.2 and 7.4.3*** are described in ***Tables 7.5***, ***7.6*** and ***7.7***.

Table 7.5. DELOS-susp[A,B], titration and TFF[Ŧ] process parameters used for the preparation of the nanoliposomal formulations described in *Chapter 4* of this thesis.

Nanovesicular system ID	Membrane components	V_{OS} (mL)	[ƺ] $[DPPC]_{OS}$:$[Chol]_{OS}$:$[Chol\text{-}PEG]_{OS}$:$[MKC]_{OS}$ (mg/mL)	V_{AS} (mL)	X_{CO2}	[Ж] [GLA version] – Method of addition	Post-process
LP-RGD_int [A]	DPPC:Chol:Chol-PEG_{400}-RGD:MKC	1.6	0.85:0.28:0.09:0.04	24.4	0.58	None	None
LP-$RGD_{(w)}$ [B]	DPPC:Chol:Chol-PEG_{400}-RGD:MKC	15	0.86:0.31:0.01:0.04	235	0.71	None	TFF D+C in water
LP-RGD-GLAH6-T_int [A]	DPPC:Chol:Chol-PEG_{400}-RGD:MKC	1.6	0.85:0.28:0.09:0.04	24.4	0.58	25 µg/mL GLAH6-T – AS of DELOS-susp	None
LP-RGD-GLAH6-$T_{(w)}$ [A]	DPPC:Chol:Chol-PEG_{400}-RGD:MKC	1.6	0.85:0.28:0.09:0.04	24.4	0.58	25 µg/mL GLAH6-T – AS of DELOS-susp	TFF D+C in water
LP-RGD-GLAcmycH6-T_int [A]	DPPC:Chol:Chol-PEG_{400}-RGD:MKC	1.6	0.85:0.28:0.09:0.04	24.4	0.58	25 µg/mL GLAcmycH6-T – AS of DELOS-susp	None
LP-RGD-GLAcmycH6-$T_{(w)}$ [A]	DPPC:Chol:Chol-PEG_{400}-RGD:MKC	1.6	0.85:0.28:0.09:0.04	24.4	0.58	25 µg/mL GLAcmycH6-T – AS of DELOS-susp	TFF D+C in water
LP-RGD-GLAcmycH6-S_int [A]	DPPC:Chol:Chol-PEG_{400}-RGD:MKC	1.6	0.85:0.28:0.09:0.04	24.4	0.58	25 µg/mL GLAcmycH6-S – AS of DELOS-susp	None
LP-RGD-GLAcmycH6-$S_{(w)}$ [A]	DPPC:Chol:Chol-PEG_{400}-RGD:MKC	1.6	0.85:0.28:0.09:0.04	24.4	0.58	25 µg/mL GLAcmycH6-S – AS of DELOS-susp	TFF D+C in water
LP-RGD-GLA-S_int [A]	DPPC:Chol:Chol-PEG_{400}-RGD:MKC	1.6	0.85:0.28:0.09:0.04	24.4	0.58	25 µg/mL GLA-S – AS of DELOS-susp	None
LP-RGD-GLA-$S_{(w)}$ [A]	DPPC:Chol:Chol-PEG_{400}-RGD:MKC	1.6	0.85:0.28:0.09:0.04	24.4	0.58	25 µg/mL GLA-S – AS of DELOS-susp	TFF D+C in water
LP-RGD-GLAH6-T_int_Ads [A]	DPPC:Chol:Chol-PEG_{400}-RGD:MKC	1.6	0.85:0.28:0.09:0.04	24.4	0.58	25 µg/mL GLAH6-T – Titration over vesicles	None
LP-RGD-GLAH6-$T_{(w)}$_Ads [A]	DPPC:Chol:Chol-PEG_{400}-RGD:MKC	1.6	0.85:0.28:0.09:0.04	24.4	0.58	25 µg/mL GLAH6-T – Titration over vesicles	TFF D+C in water
LP-RGD-GLAcmycH6-T_int_Ads [A]	DPPC:Chol:Chol-PEG_{400}-RGD:MKC	1.6	0.85:0.28:0.09:0.04	24.4	0.58	25 µg/mL GLAcmycH6-T – Titration over vesicles	None
LP-RGD-GLAcmycH6-$T_{(w)}$_Ads [A]	DPPC:Chol:Chol-PEG_{400}-RGD:MKC	1.6	0.85:0.28:0.09:0.04	24.4	0.58	25 µg/mL GLAcmycH6-T – Titration over vesicles	TFF D+C in water
LP-RGD-GLAcmycH6-S_int_Ads [A]	DPPC:Chol:Chol-PEG_{400}-RGD:MKC	1.6	0.85:0.28:0.09:0.04	24.4	0.58	25 µg/mL GLAcmycH6-S – Titration over vesicles	None
LP-RGD-GLAcmycH6-$S_{(w)}$_Ads [A]	DPPC:Chol:Chol-PEG_{400}-RGD:MKC	1.6	0.85:0.28:0.09:0.04	24.4	0.58	25 µg/mL GLAcmycH6-S – Titration over vesicles	TFF D+C in water
LP-RGD-GLA-S_int_Ads [A]	DPPC:Chol:Chol-PEG_{400}-RGD:MKC	1.6	0.85:0.28:0.09:0.04	24.4	0.58	25 µg/mL GLA-S – Titration over vesicles	None
LP-RGD-GLA-$S_{(w)}$_Ads [A]	DPPC:Chol:Chol-PEG_{400}-RGD:MKC	1.6	0.85:0.28:0.09:0.04	24.4	0.58	25 µg/mL GLA-S – Titration over vesicles	TFF D+C in water

[A] Nanoformulation batches of 26 mL produced using the P7.5 plant, or [B] batches of 250 mL prepared using the intermediate lab-scale P25 plant. [ƺ] All nanoliposomal formulations were prepared at 1.2 mg/mL of lipid, solubilizing all the known quantities of membrane components in a specific volume of organic solution (V_{OS}) containing 5 % EtOH and 1.2 % DMSO (v/v), and being depressurized over a determined V_{AS} consisting of pure water. [Ж] To prepare GLA formulations, known amounts of GLA enzymes (25 µg/mL) were added into nanoliposomal formulations using a specific V_{AS} consisting of pure water. [Ŧ] TFF details employed in all the post-processed nanosystems: C04-E300-05-N (for 26 mL-sized batches) or D04-E300-05-N (for 250 mL-sized batches), 27 mL/min feed flow, TMP 5 – 10, tubing #14, and D+C means diafiltration and concentration of samples by TFF.

Table 7.6. Process parameters of DELOS-susp[A,B] and TFF[Ŧ] procedures used for the synthesis of the liposome-based formulations described in *Chapter 5* of this thesis. All these formulations were provided by Nanomol Techonologies SL.

Nanovesicular system ID	Membrane components	V_{OS} (mL)	[ƺ] $[DPPC]_{OS}$:$[Chol]_{OS}$:$[Chol\text{-}PEG]_{OS}$:$[MKC]_{OS}$ (mg/mL)	V_{AS} (mL)	X_{CO2}	[Ж] [GLA version] – Method of addition	Post-process
LP-RGD-GLA-S_int [A]	DPPC:Chol:Chol-PEG_{400}-RGD:MKC	56	0.88:0.29:0.09:0.04	840	0.62	30 µg/mL GLA-S – AS of DELOS-susp	None
LP-RGD-GLA-$S_{(w)}$ [A]	DPPC:Chol:Chol-PEG_{400}-RGD:MKC	100	0.88:0.29:0.09:0.04	1500	0.27	25 µg/mL GLA-S – AS of DELOS-susp	TFF D+C in water
LP-0%MKC-$RGD_{(gluc)}$ [A]	DPPC:Chol:Chol-PEG_{400}-RGD	77.5	0.86:0.30:0.10:0	1315	0.37	None	[§] TFF D+C in glucose 5 % (w/v)
LP-0.5%MKC-$RGD_{(gluc)}$ [A]	DPPC:Chol:Chol-PEG_{400}-RGD:MKC	68.8	0.86:0.30:0.09:0.004	1030	0.51	None	[§] TFF D+C in glucose 5 % (w/v)
LP-$RGD_{(gluc)}$ [A]	DPPC:Chol:Chol-PEG_{400}-RGD:MKC	77.5	0.86:0.30:0.10:0.03	1315	0.36	None	[§] TFF D+C in glucose 5 % (w/v)
LP-RGD-GLA-$S_{(Cryo1)}$ [A]	DPPC:Chol:Chol-PEG_{400}-RGD:MKC	100	0.88:0.29:0.09:0.04	1500	0.27	25 µg/mL GLA-S – AS of DELOS-susp	TFF D+C in Cryo1 (glycine 7.5 mg/mL, trehalose 50 mg/mL, sucrose 30 mg/mL)
LP-RGD-GLA-$S_{(Cryo2)}$ [A]	DPPC:Chol:Chol-PEG_{400}-RGD:MKC	100	0.88:0.29:0.09:0.04	1500	0.27	25 µg/mL GLA-S – AS of DELOS-susp	TFF D+C in Cryo2 (glycine 50 mg/mL, sucrose 80 mg/mL)
LP-0%RGD-GLA-S_int [B]	DPPC:Chol:MKC	15	0.87:0.32:0:0.04	235	0.72	25 µg/mL GLA-S – AS of DELOS-susp	None
LP-6%RGD-GLA-S_int [B]	DPPC:Chol:Chol-PEG_{400}-RGD:MKC	15	0.80:0.25:0.18:0.04	235	0.72	25 µg/mL GLA-S – AS of DELOS-susp	None
LP-0%RGD-GLA-$S_{(gluc)}$ [B]	DPPC:Chol:MKC	15	0.87:0.32:0:0.04	235	0.72	25 µg/mL GLA-S – AS of DELOS-susp	[§] TFF D+C in glucose 5 % (w/v)
LP-RGD-GLA-$S_{(gluc)}$ [B]	DPPC:Chol:Chol-PEG_{400}-RGD:MKC	15	0.83:0.29:0.09:0.04	235	0.73	25 µg/mL GLA-S – AS of DELOS-susp	[§] TFF D+C in glucose 5 % (w/v)
LP-6%RGD-GLA-$S_{(gluc)}$ [B]	DPPC:Chol:Chol-PEG_{400}-RGD:MKC	15	0.80:0.25:0.18:0.04	235	0.72	25 µg/mL GLA-S – AS of DELOS-susp	[§] TFF D+C in glucose 5 % (w/v)

Liposomal batches from 250 to 1500 mL prepared using the intermediate lab-scale [A] P100 plant or [B] P25 plant. [ƺ] All nanoliposomal formulations were prepared at 1.2 mg/mL of lipid, solubilizing all the known quantities of membrane components in a specific V_{OS} containing 5 % EtOH and 1.2 % DMSO (v/v), and being depressurized over a determined V_{AS} consisting of pure water. [Ж] To prepare GLA formulations, known amounts of GLA enzymes (25 µg/mL) were added into nanoliposomal formulations using a specific V_{AS} consisting of pure water. [Ŧ] TFF details employed in all the post-processed nanosystems: D04-E300-05-N or sterile [§] D04-E300-05-S (for samples intended for preclinical studies), 27 mL/min feed flow, TMP 5 – 10, tubing #14, and D+C means diafiltration and concentration of samples by TFF.

Table 7.7. Operation parameters of DELOS-susp[A,B] and TFF[Ŧ] processes used for the fabrication of the nanoliposomal systems described in *Annex I*, *Annex II* and *Annex III* of this thesis.

Nanovesicular system ID	Membrane components	V_{OS} (mL)	[ƺ] $[DPPC]_{OS}$:$[Chol]_{OS}$:$[Chol\text{-}PEG]_{OS}$:$[MKC]_{OS}$ (mg/mL)	V_{AS} (mL)	X_{CO2}	[Ж] [GLA version] – Method of addition	Post-process
$LP_{(w)}$ [A]	DPPC:Chol:MKC	1.6	0.89:0.31:0:0.04	24.4	0.58	None	TFF D+C in water
$LP_{(gluc)}$ [A]	DPPC:Chol:MKC	1.6	0.89:0.31:0:0.04	24.4	0.58	None	TFF D+C in glucose
LP-$RGD_{(w)}$ [B]	DPPC:Chol:Chol-PEG_{400}-RGD:MKC	15	0.86:0.31:0.01:0.04	235	0.71	None	TFF D+C in water
LP-RGD-GLA-$S_{(w)}$ [A]	DPPC:Chol:Chol-PEG_{400}-RGD:MKC	1.6	0.85:0.28:0.09:0.04	24.4	0.58	25 µg/mL GLA-S – AS of DELOS-susp	TFF D+C in water
LP-RGD-GLA-$S_{(gluc)}$ [A]	DPPC:Chol:Chol-PEG_{400}-RGD:MKC	1.6	0.85:0.28:0.09:0.04	24.4	0.58	25 µg/mL GLA-S – AS of DELOS-susp	TFF D+C in glucose
LP-RGD_int [A]	DPPC:Chol:Chol-PEG_{400}-RGD:MKC	1.6	0.85:0.28:0.09:0.04	24.4	0.58	None	None
LP-RGD-GLA-S_int [A]	DPPC:Chol:Chol-PEG_{400}-RGD:MKC	1.6	0.85:0.28:0.09:0.04	24.4	0.58	25 µg/mL GLA-S – AS of DELOS-susp	None

[A] Nanoliposomal formulations of 26 mL produced using the small lab-scale P7.5 plant, or [B] batches of 250 mL prepared using the intermediate lab-scale P25 plant. [ƺ] All nanoliposomal formulations were prepared at 1.2 mg/mL of lipid, solubilizing all the known quantities of membrane components in a specific V_{OS} containing 5 % EtOH and 1.2 % DMSO (v/v), and being depressurized over a determined V_{AS} consisting of pure water. [Ж] To prepare GLA formulations, known amounts of GLA enzymes (25 µg/mL) were added into nanoliposomal formulations using a specific V_{AS} consisting of pure water. [Ŧ] TFF details employed in all the post-processed nanosystems: C04-E300-05-N (for 26 mL-sized batches) or D04-E300-05-N (for 250 mL-sized batches), 27 mL/min feed flow, TMP 5 – 10, tubing #14, and D+C means diafiltration and concentration of samples by TFF.

7.4.5. Physicochemical characterizations of nanoliposomal formulations

7.4.5.1. pH measurements of nanoliposomal formulations

The presence of small amounts of CO_2 in dispersions is capable to acidify the media. The pH of nanoliposomal formulations was used to monitor the content of CO_2 after their manufacturing and storage along time. Nanoliposomal formulations were tempered during 15 min until reaching room temperature before starting with pH measurements. For the analysis of each sample, triplicates were measured with a HI5221-02 pH meter (Hanna Instruments, USA), cleaning the electrode between replicates. All analyses were performed without sample stirring to avoid the alteration of nanovesicle morphology. Resultant values were expressed as the average of the different measurements, and the error as their s.d..

To have a second verification, in some cases pH range was also estimated by pH indicator strips (indicator strips pH 0 – 14, 1 x 4.8 m, Filter-Lab).

7.4.5.2. Morphological analysis of nanoliposomal systems by cryogenic transmission electron microscopy

Cryogenic transmission electron microscopy (cryoTEM) was used to examine the morphology and structure of lipid-based vesicles since this technique allows the preservation of water presence in samples and, therefore, their vesicle structures. Through a quick sample freezing using liquid ethane (C_2H_6), the water content can vitrify without ice crystals formation allowing the pass of the electron beam without interferences. Cryogenic temperatures (– 196 ºC) using liquid N_2 must be maintained during the overall process to avoid a phase transition of the vitrified water into crystalline ice and consequently sample damage.

Mainly, images were acquired in the Servei de Microscopia of the UAB (Barcelona) by using a JEOL JEM-2011 transmission electron microscope (JEOL LTD, Tokyo, Japan) operating at 200 kV under low-dose conditions. For sample vitrifying a controlled environment vitrification system (CEVS) Leica EMCPC (Leica Microsystems, Germany) was used, and 5 – 10 µL of sample were deposited in a copper grid coated with a lacey carbon film, eliminating the water excess blotting it with filter paper (Whatman® grade 1). After that, a Leica EM GP automatic plunge freezer (Leica, Wetzlar, Germany) was used to quickly plunge the grid into liquid C_2H_6 just above its freezing point (– 179 ºC) to induce immediately sample vitrifying. For sample transference and insertion into the microscope, a cryo-transfer system Gatan 626 (Gatan, Pleasanton, USA) with controlled temperature of – 196 ºC with liquid N_2 was used. Finally, images were recorded on a CCD Gatan 895 USC 4000 camera (Gatan, Pleasanton, USA) and analyzed with the Digital Micrograph 1.8 software. No image processing was applied except for background subtraction.

When specified, samples were sent to Prof. Dganit Danino's group and analyzed in the CryoEM Laboratory of Soft Matter from Technion (Israel) for deeper cryoTEM analysis. Similar procedure was followed for sample vitrifying but using perforated Ted Pella grids. Then, samples were studied using a T12 G2 Tecnai (FEI) and a Talos F200C (Thermo Fisher) microscopes under cryogenic temperatures. Images were recorded with a Gatan UltraScan 2kx2k CCD camera or a Ceta camera at low dose operation. Again, no image processing was applied except for background subtraction.

7.4.5.3. Particle size distribution and ζ-potential determination of nanoliposomal formulations by DLS and ELS

Size, PdI and ζ-potential of all samples were measured by a DLS and ELS analyzer of a Malvern Zetasizer Nano ZS and/or Zetasizer Ultra equipment (Malvern Instruments, UK) using a non-invasive backscatter technology (NIBS). Both instruments have equipped a 4 mW He-Ne laser beam (λ = 633 nm) with the detector set at 173 º for particle size distribution analysis, and at 13 º for the ζ-potential measurements. In both analyses, sample measurements were performed in triplicate at 25 ºC and values expressed as the average of the different replicates, and the error as their s.d.. Data was recorded and analyzed by Zetasizer Software 7.13 and/or ZS Xplorer v2.01 (Malvern Panalytical, UK).

These measurements were mostly performed at the Soft Materials Service at ICMAB-CSIC linked to Biomaterial Processing and Nanostructuring Unit (U6) of ICTS NANBIOSIS.

To analyze liposome-based nanovesicles based on intensity size-distribution, 1 mL of sample was deposited in a DTS0012 disposable polystyrene cuvette (for particle size distribution measurements) or in a DTS1070 disposable folded capillary cell (for ζ-potential measurements, by applying a voltage 40 mV). Before the analysis, concentrated samples by TFF procedures (as explained above in ***Section 7.4.3***) were diluted in their same solvent (water or glucose 5 % (w/v)) by considering the same dilution than the concentration factor previously applied.

In all cases, DLS values were provided from scattered intensity size-distribution data, and ELS data was based on Smoluchowski model.

7.4.5.4. Particle concentration of nanoliposomal formulations by NTA

When necessary to control the particle concentration and vesicle stability of liposome-based formulations (see ***Chapter 4, Section 4.2.3***), particle size distribution as well as particle concentration were measured using NTA with a Nanosight NS300 instrument (Malvern Panalytical, UK) coupled to a laser beam (λ = 488 nm) that impacts on nanovesicles generating scattered light capable to be recorded in a field of view of 100 µm x 80 µm x 10 µm by an optical microscope equipped with 20x objective lens and a sCMOS camera. The collected scattering signal ends in a video of particles moving under Brownian motion. Further, individual particle-to-particle analysis using the Stokes-Einstein equation for the calculation of nanovesicle hydrodynamic diameter and the particle concentration was performed by the NTA software. In this thesis, NTA results come from the average data of three independent videos, and the material preparation for the subsequent analysis consisted of sample dilution (between 1000 to 100000-fold factor) to achieve between 50 – 90 particles/frame (values recommended by

manufacturer). The solvent employed for sample dilution was the same one used for the dispersion of nanoliposomes.

These measurements were mostly performed at the Soft Materials Service at ICMAB-CSIC linked to Biomaterial Processing and Nanostructuring Unit (U6) of ICTS NANBIOSIS.

7.4.5.5. Determination of GLA entrapment efficiency in nanoliposomal systems

The calculation of the enzyme entrapment efficiency (EE %) parameter was explained beforehand in Cabrera *et al.*[12], Merlo-Mas *et al.*[2] and Tomsen-Melero *et al.*[13]. Basically, the nanoliposomal formulations containing the initial GLA amount just after their preparation were diafiltrated by the TFF procedure in order to remove the non-encapsulated GLA. Then, EE % was calculated by comparing the encapsulated GLA amount after TFF with the initial amount of GLA present in the nanoformulations obtained just after their preparation, either by DELOS-susp or by the titration procedure (see ***Eq. 7.2***).

$$EE\ (\%) = \frac{mass\ GLA\ after\ diafiltration\ by\ TFF}{initial\ GLA\ mass}\ x\ 100$$

(***Eq. 7.2***)

The incorporation of GLA into nanoliposomes was determined by SDS-PAGE or RP-HPLC-UV analysis, following the protocols and sample preparation already explained in ***Section 7.2.6.1*** and ***Section 7.2.6.3*** of this chapter. Briefly, known amounts of GLA (ranging from 18 to 145 µg/mL in the case of SDS-PAGE analyisis; or from 5 to 40 µg/mL) were used as calibration curve for analysis. In all cases, samples and standards to be quantitatively compared were processed as a set in a same experiment.

7.4.5.6 Quantification of liposomal membrane components by reversed-phase high-performance liquid chromatography-evaporative light scattering detector method

Quantitative analysis of membrane nanovesicle components was performed by reversed-phase high-performance liquid chromatography-evaporative light scattering detector (RP-HPLC-ELSD) using an HPLC equipment 1260 Infinity II from Agilent Technologies (Santa Clara, USA), composed of a quaternary pump, an automatic injector, an ELSD, and a column oven where the column was placed. The ELSD is coupled to the HPLC equipment to allow component quantification and also determination of purity degree. All modules were controlled using the OpenLab CDS ChemStation software.

To obtain the most accurate analysis from different nanoliposomal formulations, during the RP-HPLC-ELSD method development and optimization different sample preparation strategies, column length, controlled

temperature, mobile phases, elution conditions, detector parameters, injection volumes and calibration curve composition were explored, as explained below.

Sample preparation strategies for further RP-HPLC-ELSD analysis

Four different sample preparation strategies were investigated (see ***Figure 7.10***) in order to find the most efficient methodology to well solubilize the analytes of interest (MKC, chol-PEG_{400}-RGD, chol and DPPC), and avoid probable chromatographic mismatches in time caused by the presence of proteinaceous material like GLA-S enzyme.

The common steps of the proposed sample preparation strategies consisted on the solubilization of liposome components by diluting nanoliposomal formulations in pure MeOH (or mixtures MeOH:ACN with increasing concentrations of ACN, detailed when use it in the specific studies on ***Chapter 5, Section 5.2.3***). Sample:solvent ratio was precisely leveled up to 1:5 for samples containing 1.2 mg/mL lipid (intermediate prototypes), and 1:10 for others containing 9 mg/mL lipid (concentrate prototypes), by using volumetric flasks. Then, samples were sonicated 10 min to well solubilize the vesicle membrane components.

The main differences between the proposed strategies were the use of i) sample lyophilization previously to MeOH addition in order to remove water presence in matrixes, and/or ii) sample centrifugation after sonication process (30 min, 3000 g at 4 ºC) to remove GLA-S presence. The exact methodology of each proposed sample preparation strategy is detailed next and schematized in ***Figure 7.10***.

i. **Strategy_1**: Non-lyophilization, neither centrifugation of liposomal sample.
ii. **Strategy_2**: Lyophilization, but non-centrifugation of liposomal sample.
iii. **Strategy_3**: Non-lyophilization, although centrifugation of liposomal sample.
iv. **Strategy_4**: Lyophilization, and also centrifugation of liposomal sample.

After each sample preparation process, all the dissolved samples were filtered using a hydrophilic 0.2 µm PTFE Millex-LG membrane syringe filter (Merck KGaA, Darmstadt, Germany) before their injection into the HPLC system.

Specifically, for the freeze-drying of nanoliposomal formulations (required in Strategy_2 and Strategy_4), a LyoQuest™ Plus – 85 ºC (Telstar®, Terrassa, Spain) equipment was used. A sample volume of 1 mL of intermediate prototypes, or 0.5 mL of concentrated prototypes, was placed into 4 mL glass vials and then covered by aluminum foil with tiny holes made using a needle, to prevent the loss of sample mass but allowing a way out to sublimed water. As explained before, freeze-drying process (also known as lyophilization) was used in some sample preparation strategies to remove water from previously frozen formulations. Its operating mode is based on the

directly sublimation of the sample ice, allowing its phase transition from solid to gaseous state working under vacuum conditions (see *Figure 7.11*).

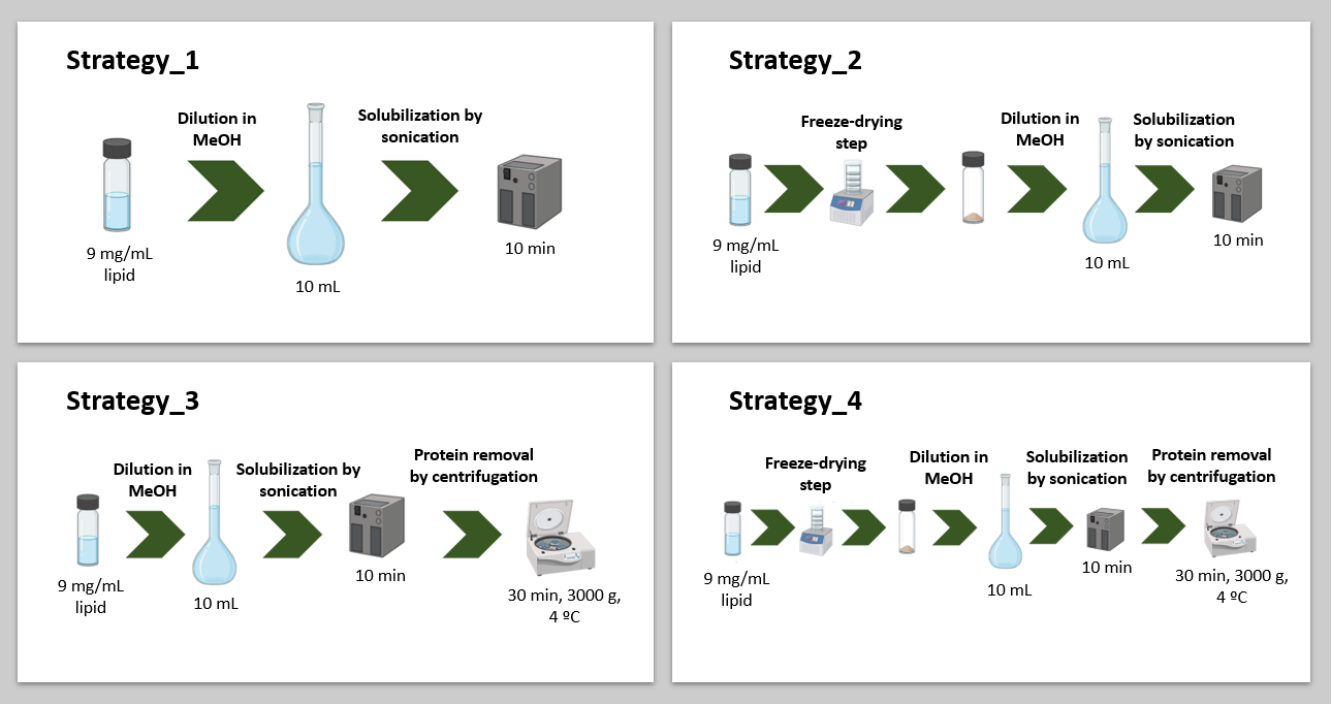


Figure 7.10. Overview of the different proposals od sample preparative strategies for concentrated liposomal formulations (9 mg/mL lipid) to achieve the solubilization of liposome components and accurate analysis by RP-HPLC-ELSD procedures.

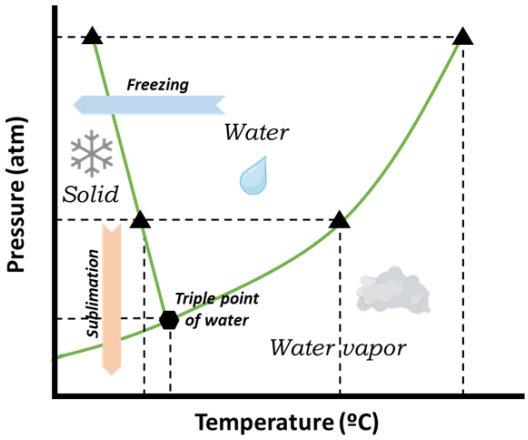


Figure 7.11. Schematic representation of the water phase diagram, where sample is frozen at atmospheric pressure, and then lyophilized through a sublimating process caused by decreasing the pressure.

Preparation of calibration curves with different compositions

Additionally, four independent stocks of the analytes to quantify (DPPC at 2000 ppm, chol at 1000 ppm, chol-PEG_{400}-RGD at 180 ppm, and MKC at 1000 ppm) were prepared in MeOH to the further obtaining of various

calibration curves. In order to obtain the different calibration points of the curves, 5 different mixtures of the stocks are prepared in 2 mL volumetric flasks (see *Table 7.8*). A different concentration range is chosen for each compound, based on the final concentration expected in LP-RGD-GLA-S samples once prepared in HPLC vials. In order to avoid matrix effects, some excipients (e.g., glucose, GLA-S and/or organic solvents) were added to calibration curves, simulating each liposomal sample composition to analyze.

i. **Composition_1**: each calibration point contains DPPC, chol, chol-PEG_{400}-RGD and MKC dissolved in MeOH.
ii. **Composition_2**: each calibration point contains DPPC, chol, chol-PEG_{400}-RGD, MKC, 1 % (v/v) EtOH and 0.25 % (v/v) DMSO dissolved in MeOH.
iii. **Composition_3**: each calibration point contains DPPC, chol, chol-PEG_{400}-RGD, MKC, 1 % (v/v) EtOH, 0.25 % (v/v) DMSO and 5 ppm GLA-S dissolved in MeOH.
iv. **Composition_4**: each calibration point contains DPPC, chol, chol-PEG_{400}-RGD, MKC and 5000 ppm glucose dissolved in MeOH.
v. **Composition_5**: each calibration point contains DPPC, chol, chol-PEG_{400}-RGD, MKC, 5000 ppm glucose and 20 ppm GLA-S dissolved in MeOH.

Table 7.8. Concentration of individual analytes (MKC, chol-PEG_{400}-RGD, cholesterol and DPPC) added in each calibration point (A to E) for the preparation of all compositions of the different calibrations curves used in this thesis.

	Analyte concentration (ppm) dissolved in MeOH			
Calibration point	**MKC**	**Chol-PEG_{400}-RGD**	**Cholesterol**	**DPPC**
A	80	135	50	800
B	50	100	70	700
C	30	60	200	600
D	10	30	250	400
E	5	10	260	100

Parameters influencing the chromatographic specifications of the RP-HPLC-ELSD method

Each liposomal sample was analyzed in three independent replicates, but regarding the high difference in concentration between components, each replicate was analyzed at two sample injection volumes. These volumes were modified depending on sample concentration and composition:

i. **Condition_1**: 1 µL for DPPC and chol quantification, and 20 µL for chol-PEG_{400}-RGD and MKC quantification.
ii. **Condition_2**: 3 µL for DPPC quantification, and 15 µL for chol, chol-PEG_{400}-RGD and MKC quantification.
iii. **Condition_3**: 1.5 µL for DPPC quantification, and 15 µL for chol, chol-PEG_{400}-RGD and MKC quantification.

Otherwise, the HPLC columns used as stationary phase at a controlled temperature of 25 ºC or 35 ºC were:

i. **Column_1**: Symmetry300 C4 5 µm, 4.6 x 250 mm.
ii. **Column_2**: Symmetry300 C4 3.5 µm, 4.6 x 150 mm.

Generally, water and ACN were used as mobile phases with the addition of distinct acid to improve chromatographic parameters:

i. **Solvents_1**: the mobile phase A (MP_{A1}) was composed by 0.01 % (v/v) HCOOH in water, and the mobile phase B (MP_{B1}) by 0.07 % (v/v) HCOOH in ACN.
ii. **Solvents_2**: the mobile phase A (MP_{A2}) was composed by 0.01 % (v/v) TFA in water, and the mobile phase B (MP_{B2}) by 0.07 % (v/v) TFA in ACN.

Elution conditions principally studied were:

i. **Elution_1**: separation performed by using the one-step gradient of 33 min detailed at *Table 7.9* in a flow rate of 1 mL/min.
ii. **Elution_2**: separation performed by using the multistep gradient of 25 min detailed at *Table 7.10* in a flow rate of 1.3 mL/min.

Table 7.9. One-step gradient Elution_1 condition for the RP-HPLC-ELSD analysis of liposomal samples.

Elution_1 condition: one-step gradient

Time (min)	0	17	23	25	33
MP_{A1} (%)	60	5	5	60	60
MP_{B1} (%)	40	95	95	40	40
Flow (mL/min)	1				

Table 7.10. Multi-step gradient Elution_2 condition for the RP-HPLC-ELSD analysis of liposomal samples.

Elution_2 condition: multi-step gradient

Time (min)	0	2.5	4	12.5	12.8	17	17.01	20	21	25
MP_{A2} (%)	50	50	30	30	20	20	5	5	50	50
MP_{B2} (%)	50	50	70	70	80	80	95	95	50	50
Flow (mL/min)	1.3									

Detector conditions of the RP-HPLC-ELSD method

Moreover, the principal ELSD parameters set-up to recover good quality signal intensities were:

i. **Configuration_1**: maintaining the respectively temperature of the evaporator and the nebulizer at 80 ºC and 40 ºC, the gas flow rate at 1 standard liter per minute (SLM), the data rate at 40 Hz, the smoothing at 40 and the photomultiplier tubes (PMT) Gain at 8.

ii. **Configuration_2**: controlling the respectively temperature of the evaporator and the nebulizer at 80 ºC and 42 ºC, the gas flow rate at 1.60 SLM, the data rate at 10 Hz, the smoothing at 30 and the PMT Gain at 5.

Proposed RP-HPLC-ELSD methods depending on the nanoliposomal formulation composition to test

Different compositions of nanovesicle matrixes were analyzed in this work, thus, the best HPLC method selected for each case is detailed in ***Table 7.11***. The HPLC-ELSD procedure to analyze the matrix containing DPPC, chol, chol-PEG_{400}-RGD, MKC and tag-free GLA-S in glucose media (referring to samples LP-RGD-GLA-$S_{(gluc)}$) was validated, so the obtained values can be considered quantitative. Nevertheless, the other similar matrixes with small changes in composition (e.g., absence of GLA-S, MKC, chol-PEG_{400}-RGD, glucose…) should be considered semi-quantitative, since the method with these matrixes was not validated.

Table 7.11. Evolution of RP-HPLC-ELSD methods investigated in this thesis. Method_001 and Method_002 are the proposed RP-HPLC-ELSD methods previous to the method optimization. The optimized methods are from Method_003 to Method_007 (with slight differences) to be used with different liposome compositions in order to avoid matrix effects during the quantification of the different analytes (MKC, chol-PEG_{400}-RGD, cholesterol and DPPC).

	Method_001	Method_002	Method_003	Method_004	Method_005	Method_006	Method_007
Sample preparation	Strategy_2	Strategy_2	Strategy_1	Strategy_1	Strategy_1	Strategy_1	Strategy_1
HPLC column	Column_1	Column_2	Column_2	Column_2	Column_2	Column_2	Column_2
Mobile phase	Solvents_1	Solvents_2	Solvents_2	Solvents_2	Solvents_2	Solvents_2	Solvents_2
Elution condition	Elution_1	Elution_2	Elution_2	Elution_2	Elution_2	Elution_2	Elution_2
ELSD parameters	Configuration_1	Configuration_2	Configuration_2	Configuration_2	Configuration_2	Configuration_2	Configuration_2
Injection volumes	Condition_1	Condition_2	Condition_2	Condition_2	Condition_2	Condition_2	Condition_2
Calibration curve	Composition_1	Composition_1	Composition_1	Composition_2	Composition_3	Composition_4	Composition_5
Liposomal matrixes recommended to analyze	LP-$RGD_{(w)}$	LP-$RGD_{(w)}$	LP-$RGD_{(w)}$	LP-RGD_int	LP-RGD-GLA-S_int	LP-$RGD_{(gluc)}$	LP-RGD-GLA-$S_{(gluc)}$
Method validation?	No	No	No	No	No	No	Yes
Measurement considerations	Semi-quantitative	Semi-quantitative	Semi-quantitative	Semi-quantitative	Semi-quantitative	Semi-quantitative	Quantitative

7.4.5.7. Preliminary RP-HPLC-ELSD method for the detection of liposome degradants

The potential product related impurities/degradants must be investigated and defined to ensure its quality level according ICH guidelines[21–25]. In this thesis, an initial stress testing of each liposome membrane components (MKC, chol-PEG_{400}-RGD, cholesterol and DPPC), which are in different states (liquid or solid), were conducted to identify the environmental factors more susceptible to impair liposome quality and stability. A liposomal formulation named $LP_{(w)}$ (containing 0 % chol-PEG_{400}-RGD or GLA-S) was chosen instead a LP-RGD-$GLA_{(w)}$ formulation (with presence of chol-PEG_{400}-RGD and GLA-S) to a better initial understanding due to less product complexity. $LP_{(w)}$ formulation was stored in aqueous dispersion during 6 months at 2 – 8 ºC, in order to detect probable membrane component instabilities due to storage conditions. Manufacturing information about $LP_{(w)}$ sample is detailed in ***Table 7.7***.

Conditions to induce sample degradation

The environmental factors with extreme conditions tested to induce the degradation of liposome components were:

- **Temperature and humidity**: sample incubation at 70 ºC and 15 % relative humidity (RH) during 24 or 72 h.
- **Oxidation**: addition of 0.3 % and 3 % H_2O_2 in samples, and incubation at 25 ºC in dark during 24 h.
- **Hydrolysis in acid media**: addition of 0.1 M and 1 M HCl in samples, and incubation at 25 ºC in dark during 24 h.
- **Hydrolysis in basic media**: addition of 0.1 M and 1 M NaOH in samples, and incubation at 25 ºC in dark during 24 h.

Preliminary RP-HPLC-ELSD method for the detection of liposome degradants

Stressed samples of individual MKC, chol-PEG_{400}-RGD, cholesterol and DPPC were analyzed by RP-HPLC-ELSD based on the procedures explained at ***Section 7.4.5.6***. In this case, the method was based on a Symmetry300, C4, 5 µm, 4.6 x 250 mm column, using as elution solvents: MP_{A2} = 0.01 % TFA in H_2O, and MP_{B2} = 0.07 % TFA in ACN. Injection volumes of 20 µL and 3 µL were used to analyze MKC and chol-PEG_{400}-RGD components, or cholesterol and DPPC analytes, respectively. The analysis lasted 65 min and the elution multi-step gradient used is described in ***Table 7.12***, controlling the flow at 1 mL/min and the column temperature at 30 ºC. The ELSD parameters were set-up at a respective temperature of the evaporator and the nebulizer at 80 ºC and 42 ºC, the gas flow rate at 1.60 SLM, the data rate at 10 Hz, the smoothing at 30 and the PMT Gain at 5. The retention time

(RT) of each non-degraded component was found: at 14.497 min for MKC, at 21.425 min for chol-PEG_{400}-RGD, at 29.117 min for cholesterol, and at 35.455 min for DPPC.

Table 7.12. Elongated RP-HPLC-ELSD multi-step gradient for the detection of potential degradation products from liposome components (MKC, chol-PEG_{400}-RGD, cholesterol and DPPC) submitted to stress conditions.

Time (min)	0	3	8	11	16	26	36	39	45	48	54	57	58	65
MP_{A2} (%)	60	60	40	40	30	30	20	20	10	10	5	5	60	60
MP_{B2} (%)	40	40	60	60	70	70	80	80	90	90	95	95	40	40
Flow (mL/min)	1.3													

The sample preparation strategy for further RP-HPLC-ELSD analysis was the same as the one optimized before (named as Strategy_1 in *Section 7.4.5.6*).

7.4.5.8. Characterization of the targeting chol-PEG_{400}-RGD ligand on the surface of nanoliposomes by Single Particle Automated Raman Trapping Analysis (SPARTA®)

In order to verify the integration of the chol-PEG_{400}-RGD targeting ligand in the liposomal membrane and assess if this is homogenously distributed on the surface of the nanoliposomes, unloaded and GLA-loaded liposomal samples were measured by Single Particle Automated Raman Trapping Analysis (SPARTA®) at SPARTA Biodiscovery facilities (London, UK). The SPARTA® approach is capable to obtain detailed particle-to-particle compositional spectra from complex nanoformulations, thanks to the simultaneous combination of a controlled laser which allows the trapping of single particles, with the confocal Raman spectroscopy capable to obtain compositional information from label-free particles. Detailed information about samples analyzed ($LP_{(w)}$, $LP_{(gluc)}$, LP-$RGD_{(w)}$, LP-RGD-GLA-$S_{(w)}$, and LP-RGD-GLA-$S_{(gluc)}$) was described in *Table 7.7*.

Dispersant measurements

For background measurements, 5 % glucose (w/v) in water and pure water were measured, to be used for corresponding samples. 20 spectral acquisitions were obtained, the mean of which was used as background subtraction as part of the SPARTA® data pre-processing.

Particle measurements

The laser disabling time was set to 2 seconds since this would allow the given size of particles (between 50 – 100 nm) to diffuse several distances away from the optical trap, whilst allowing possible bigger aggregates to diffuse away adequately as well to avoid them getting stuck in the optical trap. The acquisition time for the data acquisition was set to 10 seconds per particle, as this allows high signal-to-noise ratio spectra to be acquired for further data analysis.

Nanoliposomal samples were diluted in the appropriate diluent (water or 5 % glucose (w/v) in water) by 5 – 10x based on optimizing trapping efficiency. As a standard measurement, 200 trapping acquisitions attempts were set up for each sample. Trapping efficiencies between 72 – 100 % were achieved for the samples.

The acquired data, in the form of 2000-data point single particle Raman spectra, were pre-processed prior to analysis, as is standard practice for Raman spectra. The pre-processing includes spectral response correction (part of the system calibration), cosmic spike removal, background subtraction, baseline correction, cropping (to spectral region of interest), smoothing and normalization.

7.4.5.9. Development of two field flow fractionation-based methods for the detection of GLA-S enzyme and RGD-targeted nanoliposomes

Asymmetric flow field flow fractionation (AF4) technique is a non-destructive methodology useful for the separation of fragile particles of a wide range of sizes (1 nm – 10 µm). The determination of the particle shape and morphology of nanoparticle populations can be achieved by coupling AF4 to multi-angle light scattering (MALS) or DLS detectors, but also the analyte concentration from samples can be studied by using ultraviolet (UV), differential refractive index (dRI) or fluorescence (FLD) detectors[26,27]. In this thesis, two AF4-MALS-dRI methods have been developed (see ***Annex III***) in order to detect the free-tagged GLA-S protein and RGD-targeted nanoliposomes. The optimized elution conditions found for each case (GLA-S protein or nanoliposomes) are also described in this section.

Equipment and sample preparation for AF4-MALS-dRI measurements

The instrument used for the AF4-MALS-dRI consisted of an Eclipse separation system (Eclipse NEON FFF; Wyatt Technology Europe GmbH, Dernbach, Germany) that was connected to a degasser, isocratic pump, and an autosampler with temperature control (Agilent 1200 series; Agilent Technology, Böblingen, Germany). A dispersion-inlet channel (Wyatt Technologies, Dernbach, Germany) with a 350 µm plastic spacer was used, and a regenerated cellulose membrane with a cut-off of 10 kDa served as the accumulation wall (Wyatt Technologies, Dernbach, Germany). The channel was coupled online to a dRI detector (G7162A, Agilent Technology, Böblingen, Germany) and an 18-angle static light scattering detector MALS (DAWN HELEOS II, Wyatt Europe, laser wavelength 658 nm).

Previously to AF4-MALS-dRI analysis, all samples were filtered through PTFE-L sterile syringe filters with a pore size of 0.22 µm (Nantong FilterBio Membrane Co., Ltd., Nantong City, Jiangsu P.R China). GLA-S (5 – 10 µL), LP-RGD_int and LP-RGD-GLA-S_int liposomes (5 – 100 µL) were injected and fractionated under the different

conditions described in ***Annex III***. Detailed information about the nanoliposomal formulations analyzed (LP-RGD_int, and LP-RGD-GLA-S_int) was described in ***Table 7.7***.

The mobile phase (10 mM PBS + 0.02 % sodium azide) was filtrated through VacuCap 60 Vacuum Filtration Devices - 0.1 µm (4631, Pall Corporation, Portsmouth, UK).

Optimized elution conditions for the detection of the free-tagged GLA-S enzyme by AF4-MALS-dRI

The elution conditions of the AF4-MALS-dRI method that allowed the best identification of the homodimeric GLA-S protein of about 10 nm are summarized in ***Table 7.13***, where XF means crossflow.

Table 7.13. Optimized conditions which allow the elution and detection of both, unloaded nanoliposomes (without GLA-S) and GLA-loaded nanoliposomes, by AF4-MALS-dRI. Legend: XF means crossflow.

Injection flow (mL/min)	0.1		
Channel flow (mL/min)	1		
MODE	**STEP DURATION (min)**	**XF START (mL/min)**	**XF stop (mL/min)**
Elution	5	3	3
Elution + injection	25	3	3
Elution + injection	1	3	0
Elution + injection	10	0	0

Optimized elution conditions for the detection of RGD-targeted nanoliposomes by AF4-MALS-dRI

The elution conditions of the AF4-MALS-dRI method that allowed the best identification of both, unloaded nanoliposomes (without GLA-S) and GLA-loaded nanoliposomes, are summarized in ***Table 7.14***, where XF means crossflow.

Table 7.14. Optimized conditions which allow the elution and detection of both, unloaded nanoliposomes (without GLA-S) and GLA-loaded nanoliposomes, by AF4-MALS-dRI. Legend: XF means crossflow.

Injection flow (mL/min)	0.1		
Channel flow (mL/min)	1		
MODE	**STEP DURATION (min)**	**XF START (mL/min)**	**XF stop (mL/min)**
Elution	2	2	2
Elution + injection	2	2	2
Elution + injection	10	2	0.1
Elution + injection	35	0.1	0
Elution + injection	10	0	0

Data analysis

Root-mean square radius (R_g or rms radius) and molar mass of samples were calculated by the Astra software version 8.1.2. (Wyatt Europe, Dernbach, Germany) using the Zimm fit model for the analysis of the GLA-S enzyme and the Berry fit model for the analysis of liposomes. The light-scattering fit Zimm model is recommended to be used for molecules with an R_g smaller than 50 nm and in comparison to the Deby fit model, it often requires a lower fit degree to yield the same size molecule. However, this fit model should be avoided for particles larger than 50 nm. For larger particles such as liposomes, the light-scattering fit Berry model should be used. High-angle data with poor quality have to be deleted in order to obtain the values of R_g and molar mass more accurately.

R_g is defined by the equation ***Eq. 7.3***, where R_s is the geometric radius of a solid sphere, while molar mass can be determined if the specific refractive index increment (dn/dc) and concentrations of a solute are known. In this study, the theoretical lipid concentration of liposome samples was 1.2 mg/mL, while the concentration of GLA-S was 3.5 mg/mL. dn/dc values of 0.160 and 0.185 for phospholipids and proteins in water were used, respectively[28].

$$R_g = \sqrt{3/5} \cdot R_s$$

(***Eq. 7.3***)

7.4.6. Filtration-centrifugation procedure for the separation of non-integrated GLA enzymes from GLA nanoliposomal formulations

A methodology efficient enough to separate the released drug substance from the liposome vesicles was developed. Same process was useful to assess the leakage rate during storage, i.e. the changes of the enzyme entrapment efficiency over time.

Separation principle of filtration-centrifugation procedures combines centrifuge force and membrane diffusion. In this thesis, Vivaspin® 20 PES amicons of 300 or 1000 kDa membranes (Sartorius, ref. VS0252 or ref. VS0262, respectively) were tested using liposomal samples containing GLA enzymes with the objective to obtain the non-entrapped or free GLA protein in the Permeate fraction (P_M), and the GLA-loaded liposomes in the Retentate fraction (R_T). The P_M is the volumetric fraction recovered in the lower part of the concentrator, once the sample pass through the membrane after centrifugation, meanwhile, the R_T is the volumetric fraction remained in the upper part of the Amicon® membrane (see ***Figure 7.12***).

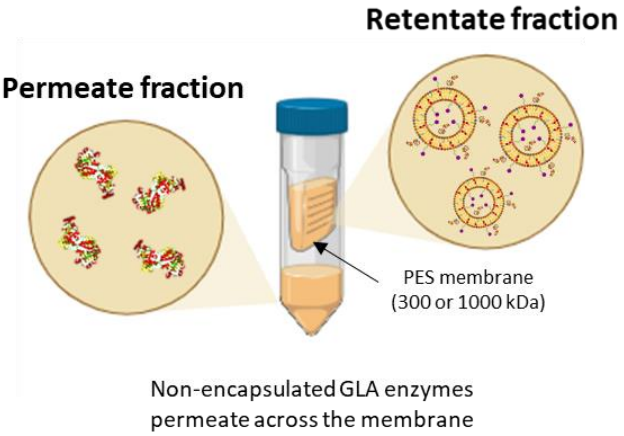


Figure 7.12. Volumetric fractions obtained after the filtration-centrifugation procedure for the separation of non-integrated GLA enzymes from GLA-loaded nanoliposomal formulations. Free or released GLA enzyme is able to cross the Amicon® membrane and pass through Permeate fraction, meanwhile GLA-loaded liposomes remain in the Retentate fraction.

The procedure followed to achieve the separation of non-encapsulated GLA from the integrated one in the nanoliposomal formulations consisted of the following steps:

i. Membrane hydration: Amicon® units were cleaned in two successive centrifugation rounds (3000 g, 2 min), using 2 mL of pure water each time. P_M was discarded in both cases.

ii. Membrane passivation to avoid GLA retention: Amicon® units were filled with 2 mL of a blocking solution composed of 1 % v/v Tween-20 and incubated rolling at room temperature during 2 hours. After, the solution was centrifuged through the membrane (3000 g, 2 min). The excess of blocking solution was rinsed in two successive centrifugation rounds (3000 g, 2 min), using 2 mL of pure water each time. P_M was discarded in all cases.

iii. Membrane equilibration: when samples to process were dispersed in buffers different from pure water (e.g. glucose media), 2 mL of that buffer were passed through membrane in one centrifugation round (3000 g, 2 min). Again P_M was discarded.

iv. Amicon® drying to reduce manipulation error: the Amicon® walls of its lower part were dried with compressed air. The remaining drops of water or buffer in the upper part of the Amicon® were removed carefully with a tip avoiding membrane damaging.

v. Sample separation: to allow protein diffusion through Amicon® membrane, 1.75 mL of sample containing between 20 to 300 µg/mL of GLA were submitted to low centrifugation forces of 300 g during 5 min, ending with P_M of 1500 µL and R_T of 250 µL, approximately. Then, buffer was carefully added to RT to precisely level up sample volume until its initial 1.75 mL to avoid protein concentration and error in sample analysis. Both, P_M and R_T were recovered for further analysis.

vi. GLA quantification: samples were analyzed by SDS-PAGE and further TGX techniques to calculate the percentage of protein in each fraction. Both, P_M and R_T fractions were run in the same gel and processed as a set together with their corresponding initial fraction (sample before centrifugation step) to be quantitatively compared. Results were given in percentages of remaining GLA amount in each fraction, taking the GLA amount of initial samples as the 100 %. Densitometric analyses of the bands were performed with ImageLab™ software (version 5.2.1, BioRad).

Three individual replicates of each sample were processed by the filtration-centrifugation procedure and then analyzed by SDS-PAGE technique. Results were expressed as their mean average, and their error as s.d..

Recombinant GLA (without presence of nanoliposomes) was also tested as control, to ensure the capacity of the enzyme to diffuse through the membrane.

Liposome diffusion assessment through Amicon® membranes by gravimetric analysis

The capacity of nanoliposomes to diffuse across Amicon® membranes during the filtration-centrifugation procedure was followed by gravimetric analysis. It consisted of measuring the mass of nanoliposomal formulations before and after being submitted to the filtration-centrifugation process (see ***Chapter 5, Section 5.4.1.3***).

The gravimetric analysis required sample lyophilization, and was performed by weighing empty vials (previously to sample lyophilization), and ended by weighing full vials containing the lyophilized sample (after to sample freeze-drying). These measurements were obtained from at least two independent replicates of each sample, and using an XA105 DualRange analytical balance (Mettler Toledo, USA).

Finally, the mass balance (MB %) was calculated by comparing the remaining mass of nanoliposomal formulations once filtered-centrifuged, with the initial mass of non-processed nanoliposomal formulation (see ***Eq. 7.4***). The loss of material in percentage was calculated according ***Eq. 7.4***.

$$MB\ (\%) = \frac{lipid\ mass\ after\ filtration - centrifugation\ procedure}{initial\ lipid\ mass}\ x\ 100$$

$$Material\ loss\ (\%) = 100 - MB\ (\%)$$

(***Eq. 7.4***)

7.4.6.1. *In vitro* GLA release study from nanoliposomal formulations

An *in vitro* study to assess GLA release from the nanoliposomes was set up by adding 1.2 mL of sample (GLA-loaded nanoliposomes containing 9 mg/mL of lipid) in vials with 4.8 mL of receptor medium, to have a final total volume of 6 mL, and a final GLA concentration around 30 µg/mL. This study was performed under "sink conditions" to avoid interference from GLA solubility in the *in vitro* release medium. A free GLA-S group was used as control group, at the same GLA concentration of 30 µg/mL GLA-S (i.e. 60 µL of free GLA-S were added in vials with 5.94 mL of receptor medium). Different vials were used per each time point, which were incubated at 37 ºC (body temperature) and shacked at 100 rpm. At the predetermined time intervals, the respective vials were collected and 1.75 ml sample was withdrawn from the vial and filtered-centrifuged using the procedure previously explained (***Section 7.4.6***), to separate the released GLA enzymes from the nanoliposomes.

As an exception, the *in vitro* GLA release studies explained in ***Chapter 4*** were carried out by adding 1.5 ml of sample (GLA-loaded nanoliposomes containing 5 mg/mL of lipid) in vials with 4.5 ml of receptor medium, to have a final total volume of 6 mL, and a final GLA concentration of 8 – 25 µg/mL.

Different receptor media were used for this study, to evaluate the impact of the selected receptor media on the GLA release from nanoliposomes:

i. Glucose 5 % (w/v) media (Braun, ref. 571120): solution containing 5 g of glucose in 100 mL of water, with an osmolarity of 252 mOsm/L and pH between 3.5 – 6.6.
ii. Ringer's Lactate (Braun, ref. 622555): solution containing similar salt composition to human plasma (see ***Table 7.15***), with an osmolarity of 277 mOsm/L and pH between 5 – 7.
iii. PBS 100 mM: home-made solution containing a mixture of NaCl and phosphates salts at a pH of 7.4. The composition tested was composed of 96 mM NaCl, 3 mM Na_2HPO_4, and 1 mM NaH_2PO_4.

Table 7.15. Composition of clinical relevant media and their comparison with the human plasma.

FLUID	Na^+ mEq/L	Cl^- mEq/L	K^+ mEq/L	Ca^{2+} mEq/L	Glucose g/L	Buffer mEq/L	Osmolarity mOsm/L	Tonicity
Normal plasma	140	100	4	2.4	0.85	HCO_3 24	290	N/A
0.9 % saline	154	154	0	0	0	0	308	Isotonic
Ringer's lactate	130	109	4	4	0	Lactate 28	273	Isotonic
Glucose 5 % (w/v) in water	0	0	0	0	50	0	252	Hypotonic

Recombinant GLA enzymes and the nanoliposomal formulation compositions studied in this work were detailed at ***Table 7.5*** and ***Table 7.6***, as well as at ***Chapters 4*** and ***5***).

7.4.6.2. GLA leakage rate from nanoliposomal formulations under storage conditions

In order to determine if the integrated GLA in liposomal membranes could be released over time due to sample storage conditions, liposomal formulations were submitted to the filtration-centrifugation procedure explained above at different time-points after being stored at 4 ºC. Samples were directly processed (without any dilution or other manipulation requirements).

7.4.7. Determination of bacterial contamination in nanoliposomal formulations

Bacterial contamination must be avoided to obtain robust preclinical results.

Besides, the presence of bacterial remains like endotoxins must be also monitored in drug products and medical devices to avoid pyrogenic response and/or septic shock in human patients receiving these treatments. Accordingly, the following tests have been carried out to characterize and control these critical quality attributes for an intravenous formulation.

7.4.7.1. Microbiological study: Luria Broth agar plate test

According the Method STE-2.2 protocol from Nanotechnology Characterization Laboratory (NCL), Luria Broth (LB) agar plates were used to detect and quantitative determine the microbial contamination in liposomal nanovesicle samples (see ***Figure 7.13***)[29,30]. LB media is normally used by American Type Culture Collection (ATCC) as a defined medium (of known chemical composition) for *E. coli* growth and maintenance in molecular biology applications[31].

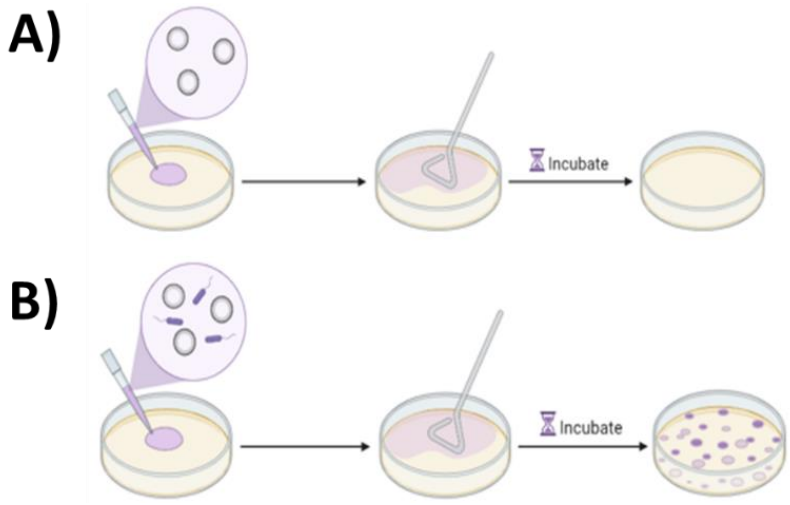


Figure 7.13. Overview of microbiological testing of liposomal samples. Examination of A) non-contaminated samples without microbiological growth observed in LB agar plates, or B) bacteria-containing samples with the respective bacteria (e.g. *E. coli*) growth in LB agar plates.

LB medium was composed of 10 g/L tryptone, 5 g/L yeast extract, 0.5 g/L NaCl and 15 g/L agar. The media was home-made elaborated by reconstituting the powdered components in water and then sterilized by autoclave 15 min at 121 ºC. LB agar plates were prepared into a flow cabinet pouring LB into Petri dishes once media was slightly cooled, and let to solidify at room temperature. LB agar plates were storage at 2 – 8 ºC until their use.

Before assay, samples were adjusted at pH range 6 – 8, if necessary, using sterile solutions of NaOH or HCl. Small aliquots of samples were removed for measuring pH to avoid sample contamination from microelectrode.

Serial 2-fold dilutions of samples were prepared using endotoxin-free Limulus Amebocyte Lysate (LAL) reagent water (Lonza, ref. W50-1000) for sample testing under sterile conditions in a flow cabinet. Each sample dilution was tested minimum in duplicates (but preferable in quadruplicates), and in parallel also negative controls containing only endotoxin-free water to ensure material quality. Once, LB agar plates warmed at room temperature, 50 µL of sample were added onto the surface of the agar and spread using sterile disposable bacterial spreader. As soon as liquid was absorbed, the Petri dish was recapped, turned it upside down to prevent condensation, placed into the incubator for 72 h at 37 ºC, and finally results reported according to equation (***Eq. 7.5***).

Nº Colonies x Dilution Factor x Sampling Factor = CFU/mL

(***Eq. 7.5***)

Where sampling factor correspond to the quotient between the total volume of the sample aliquot analyzed, and the 50 µL of sample spread on the plate. For example, the sampling factor of nanovesicle aliquots of 1 mL is 20.

7.4.7.2. Bacterial endotoxins determination: Gel clot LAL test

Gram-negative bacteria have lipopolysaccharides (LPS), also known as endotoxins, in their outer membrane, capable to act as immunostimulators causing fever and septic shock in human blood circulation (***Figure 7.14***).

To control the endotoxin content present in the liposomal formulations, the Gel clot LAL assay (PYROGENT™ Plus Gel clot LAL Assay) has been selected because, although this is a qualitative assay to be used in a qualitative manner, the turbidity of the nanovesicles interferes with LAL Chromogenic Endotoxin Quantitation Kits.

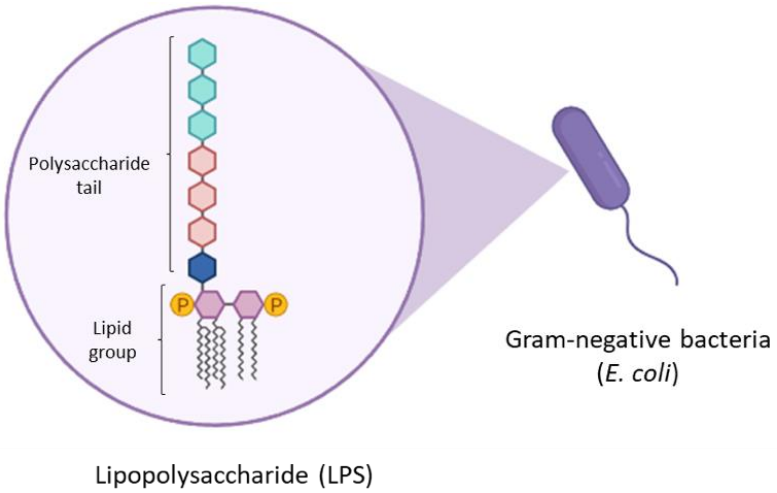


Figure 7.14. Representation of the chemical structure of endotoxin molecules found in gram-negative bacteria such as *E. coli*.

Gel clot LAL test

Liposomal formulations were analyzed using the commercial kit PYROGENT™ Plus Gel clot LAL Assay (Lonza, ref. N294-125). It contains a lyophilized preparation of purified endotoxin from *E. coli* strain 055:B5, used for two purposes:

- Preparation of a calibration curve: serial two-fold dilutions of purified endotoxin (from 0 to 1 EU/mL) were prepared with endotoxin-free LAL reagent water (Lonza, ref. W50-1000) in order to confirm the lysate sensitivity from the assay used.
- Procedure validation: known amounts of purified endotoxins were spiked over nanoliposome samples, obtaining positives results only when the total endotoxin amount in samples was higher than 0.125 EU/mL (lysate sensitivity used).

The experimental procedure consisted on the preparation of a standard curve (between 0 and 1 EU/mL) by serial two-fold dilution in sterile tubs (Lonza, ref. N207), using the control standard endotoxin (CSE) provided by the commercial kit. In parallel, the lyophilized LAL lysate was reconstituted with β-G-Blocker Kit (Lonza, ref. N190) to avoid false-positive results, since β-glucans are capable to start the same protease cascade as endotoxins, inducing false-positives in LAL assays. This was performed at 1:1 volume ratio of sample:blocker following the instructions of the manufacturer. The commercial lysate sensitivity value used was around a concentration of ≥ 0.125 EU/mL.

Before sample testing, all liposomal samples were submitted to a pre-treatment in order to ensure a better LPS detection by Gel clot kit by solubilizing lipid-based vesicles and disrupting the probable electrostatic interactions between LPS and the positives charges of our membrane[32–34]. The pre-treatment consisted on adding a final

concentration of 0.001 % (v/v) SDS (sterile solution) to samples, and the further sample boiling at 95 ºC during 30 min. Then, serial 2-fold or 5-fold dilutions of samples were prepared with endotoxin-free LAL reagent water (Lonza, ref. W50-1000) until reaching their maximum valid dilution (MVD) at which the endotoxin limit can be determined, according ***Eq. 7.6***.

$$MVD = \frac{Concentration\ of\ testing\ sample\ \left(\frac{mg}{mL}\right) x\ Endotoxin\ limit\ \left(\frac{EU}{mL}\right)}{Sensivity\ of\ assay\ used\ \left(\frac{EU}{mL}\right)}$$

(***Eq. 7.6***)

Also, to avoid reaction interferences in LAL assays and previously to be tested, samples were adjusted at pH range 6 – 8 when necessary, by using sterile solutions of NaOH or HCl.

Once all material is prepared, samples can be assayed by Gel clot procedure. To test standard and/or unknown samples, 0.1 mL from the different serial two-fold dilution series of sample were mixed thoroughly with 0.1 mL of the reconstituted lysate on individually capped tubes (Lonza, ref. N201), and incubated at 37 ºC ± 1 ºC in a non-circulating hot water bath during 60 minutes ± 2 minutes. After the indicated time, each tube was carefully removed and inverted 180 º (***Figure 7.15***). Each standard and sample dilution was tested minimum in duplicates (but preferable in quadruplicates). In each assay, a standard calibration should be assayed together with unknown samples and processed as a set to have quality control of the results. Results of each reaction/vial ought to be recorded in columns as either positive or negative. Results were considered as:

- Positive reaction: means endotoxin presence. It was characterized by the formation of a firm gel that remains intact momentarily when the tube was inverted.
- Negative reaction: it was characterized by the absence of a solid clot after inversion. The lysate could show an increased turbidity or viscosity, but it was considered a negative result.

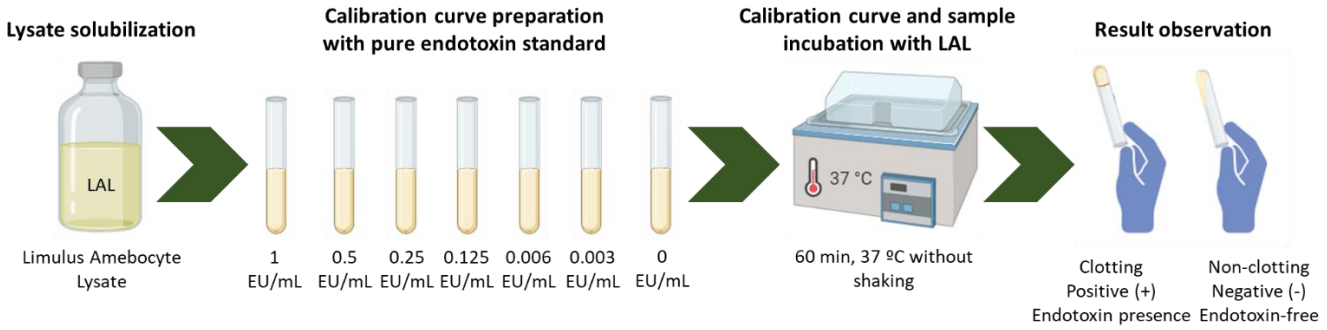


Figure 7.15. Gel clot methodology base on gel formation for the detection of endotoxin in samples. Adapted from the operating recommendations of the manufacturer[35].

Finally, test validation was performed by spiking samples with increasing amounts of endotoxins (between 0 and 0.5 EU/mL), and only obtaining positive results with the spikes ≥ 0.125 EU/mL as expected.

During the overall process, standards and samples were manipulated inside a flow cabinet (sterile conditions) and using pyrogen-free material.

7.4.8. Stability studies of nanoliposomal formulations

The stability of GLA nanoliposomal formulations was followed at different conditions:

i. Under storage conditions (at fridge between 2 – 8 ºC), to understand the stability of the physicochemical and biological properties of the GLA nanoliposomal formulations at such conditions in a short-term of 3 months. Particle size distribution and ζ-potential was followed by DLS/ELS (protocol detailed in ***Section 7.4.5.3***), liposomal morphology was monitored by cryoTEM (as explained in Section ***7.4.5.2***), and the GLA enzymatic activity assessed by fluorimetric methodologies (described in ***Section 7.2.9***). Additionally, filtration-centrifugation procedures were used to separate the leaked GLA from liposomes stored at 2 – 8 ºC (as explained in ***Section 7.4.6.2***), and the leaked GLA enzymes quantified by SDS-PAGE and TGX analysis (see ***Section 7.2.6.1***). The respective results are reported on ***Chapter 4***.

ii. Under physiological-like conditions, to investigate the stability of GLA nanoliposomal formulations in bloodstream-like conditions. For this purpose, LP-RGD-GLA-$S_{(gluc)}$ nanoformulation (i.e. the GLA nanoliposomal formulation in an advanced stage of the pharmaceutical development, which contains GLA-S protein and glucose as isosmotic agent) was incubated in physiologically relevant media such as an aqueous solution of glucose 5 % (w/v), Ringer-Lactate solution, or others reported in ***Chapter 5***. Vesicle integrity was examined by DLS and cryoTEM, and GLA enzymatic activity by fluorimetric methodologies.

In all cases, an aliquot was withdrawn at the established time points to perform physicochemical and biological characterizations of the different samples.

7.5. Figures and tables

Figures and tables designed in this thesis were created using PowerPoint (Microsoft Office), Excel (Microsoft Office), GraphPad Prism 5, PyMOL 2.4.0 and Biorender softwares.

7.6. References

1 Corchero JL, Mendoza R, Lorenzo J, *et al.* Integrated approach to produce a recombinant, His-tagged human α-galactosidase a in mammalian cells. *Biotechnol Prog* 2011; **27**: 1206–17.

2 Merlo-Mas J, Tomsen-Melero J, Corchero JL, *et al.* Application of Quality by Design to the robust preparation of a liposomal GLA formulation by DELOS-susp method. *J Supercrit Fluids* 2021; **173**: 105204.

3 SIB Swiss Institute of Bioinformatics. Expasy ProtParam tool. https://web.expasy.org/protparam/ (accessed Dec 27, 2018).

4 Berrow NS, Alderton D, Sainsbury S, *et al.* A versatile ligation-independent cloning method suitable for high-throughput expression screening applications. *Nucleic Acids Res* 2007; **35**. DOI:10.1093/nar/gkm047.

5 Urlaub G, Käs E, Carothers AM, Chasin LA. Deletion of the diploid dihydrofolate reductase locus from cultured mammalian cells. *Cell* 1983; **33**: 405–12.

6 Ventosa L, Veciana J, Royo M, *et al.* Liposomes and its use for enzyme delivery. Patent EP 21382062.4-1112. 2021. http://hdl.handle.net/10261/289055 (accessed June 10, 2022).

7 Sunley K, Butler M. Strategies for the enhancement of recombinant protein production from mammalian cells by growth arrest. *Biotechnol Adv* 2010; **28**: 385–94.

8 Sambrook JF, Russell DW. Molecular Cloning: A Laboratory Manual, Third Edition. Cold Spring Harbor Laboratory Press , 2001 https://books.google.hr/books?id=Bosc5JVxNpkC&pg=SA16-PA1&hl=ca&source=gbs_toc_r&cad=2#v=onepage&q&f=false (accessed Nov 27, 2023).

9 European Medicines Agency. ANNEX I SUMMARY OF PRODUCT CHARACTERISTICS (Fabrazyme®). 2009. https://www.ema.europa.eu/en/documents/product-information/fabrazyme-epar-product-information_en.pdf (accessed Jan 16, 2023).

10 Desnick RJ, Allen KY, Desnick SJ, Raman MK, Bernlohr RW, Krivit W. Fabry's disease: Enzymatic diagnosis of hemizygotes and heterozygotes: α-Galactosidase activities in plasma, serum, urine, and leukocytes. *J Lab Clin Med* 1973; **81**: 157–71.

11 Mayes JS, Scheerer JB, Sifers RN, Donaldson ML. Differential assay for lysosomal alpha-galactosidases in human tissues and its application to Fabry's disease. *Clin Chim Acta* 1981; **112**: 247–51.

12 Cabrera I, Abasolo I, Corchero JL, *et al.* α-Galactosidase-A Loaded-Nanoliposomes with Enhanced Enzymatic Activity and Intracellular Penetration. *Adv Healthc Mater* 2016; **5**: 829–40.

13 Tomsen-Melero J, Passemard S, García-Aranda N, *et al.* Impact of chemical composition on the nanostructure and biological activity of α- galactosidase- loaded nanovesicles for Fabry disease treatment. *ACS Appl Mater Interfaces* 2021; **13**: 7825–38.

14 Malvern Panalytical. APPLICATION NOTE: The Diffusion Barrier Technique for Accurate and Reproducible Protein Mobility Measurement. 2014 https://www.malvernpanalytical.com/en/learn/knowledge-center/application-notes/an120906diffusionbarriertechnique (accessed June 22, 2020).

15 Lakowicz JR. Principles of fluorescence spectroscopy, Third Edition. Springer, 2006.

16 Sánchez JM, Sánchez-García L, Pesarrodona M, *et al.* Conformational Conversion during Controlled Oligomerization into Nonamylogenic Protein Nanoparticles. *Biomacromolecules* 2018; **19**: 3788–97.

17 Burgos MI, Ochoa A, Perillo MA. β-sheet to α-helix conversion and thermal stability of β-Galactosidase encapsulated in a nanoporous silica gel. *Biochem Biophys Res Commun* 2019; **508**: 270–4.

18 Cristóbal-Lecina E, Pulido D, Martin-Malpartida P, Macias MJ, Albericio F, Royo M. Synthesis of Stable Cholesteryl-Polyethylene Glycol-Peptide Conjugates with Non-Disperse Polyethylene Glycol Lengths. *ACS Omega* 2020; **5**: 5508–19.

19 Ventosa N, Veciana J, Sala S, Cano M. Method for obtaining micro- and nano-disperse systems. Patent WO2006/079889. 2005. https://patentimages.storage.googleapis.com/bd/b5/b7/0cd7d2abda1230/WO2006079889A1.pdf (accessed June 10, 2022).

20 Spectrum Laboratories. New KrosFlo Research IIi TFF System: Product Information and Operating Instructions. 2015. https://www.yumpu.com/en/document/read/34480183/new-krosflo-research-iii-tff-system-spectrum-laboratories-inc (accessed Feb 14, 2019).

21 European Medicines Agency. ICH guideline Q1A (R2) on Stability Testing of new Drug Substances and Products - Step 5. Comm. Hum. Med. Prod. CPMP/ICH/2736/99. 2003. https://www.ema.europa.eu/en/documents/scientific-guideline/ich-q-1-r2-stability-testing-new-drug-substances-products-step-5_en.pdf (accessed Feb 9, 2021).

22 European Medicines Agency. ICH guideline Q1B on Photostability Testing of New Active Substances and Medicinal Products - Step 5. Comm. Hum. Med. Prod. CPMP/ICH/279/95. 1998. https://www.ema.europa.eu/en/documents/scientific-guideline/ich-q-1-b-photostability-testing-new-active-substances-medicinal-products-step-5_en.pdf (accessed April 2, 2021).

23 European Medicines Agency. ICH guideline Q1C on Stability Testing: Requirements for New Dosage Forms - Step 5. Comm. Hum. Med. Prod. CPMP/ICH/280/95 . 1998. https://www.ema.europa.eu/en/documents/scientific-guideline/ich-q-1-c-stability-testing-requirements-new-dosage-forms-step-5_en.pdf (accessed Feb 8, 2021).

24 European Medicines Agency. ICH guideline Q1D on Bracketing and Matrixing designs for Stability Testing of Drug Substances and Drug Products - Step 5. Comm. Hum. Med. Prod. CPMP/ICH/4104/00 . 2002. https://www.ema.europa.eu/en/documents/scientific-guideline/ich-q-1-d-bracketing-matrixing-designs-stability-testing-drug-substances-drug-products-step-5_en.pdf (accessed Feb 12, 2021).

25 European Medicines Agency. ICH guideline Q1E on Evaluation of Stability Data - Step 5. Comm. Hum. Med. Prod. CPMP/ICH/420/02. 2003. https://www.ema.europa.eu/en/documents/scientific-guideline/ich-q-1-e-evaluation-stability-data-step-5_en.pdf (accessed Feb 20, 2021).

26 Bian J, Gobalasingham N, Purchel A, Lin J. The Power of Field-Flow Fractionation in Characterization of Nanoparticles in Drug Delivery. *Molecules* 2023; **28**: 4169.

27 Parot J, Caputo F, Mehn D, Hackley VA, Calzolai L. Physical characterization of liposomal drug formulations using multi-detector asymmetrical-flow field flow fractionation. *J Control Release* 2020; **320**: 495–510.

28 Nobbmann U. Refractive index increment dn/dc values - Materials Talks. Malvern Panalytical. 2013. https://www.materials-talks.com/refractive-index-increment-dndc-values/ (accessed Sept 21, 2023).

29 Neun BW, Potter TM, Dobrovolskaia MA. NCL Method STE-2.2: Detection of Bacterial Contamination Using Luria Broth Agar

Plates. *Mol Biol* 2018; **1628**: 19–22.

30 McNeil SE. Characterization of Nanoparticles Intended for Drug Delivery: Methods in Molecular Biology 1682, Second Edition. 2018 http://www.springer.com/series/7651.

31 Garrity GM. Bergey's Manual of Systematic Bacteriology, Second Edition. Springer, 2005.

32 Harmon P, Cabral-Lilly D, Reed RA, Maurio FP, Franklin JC, Janoff A. The Release and Detection of Endotoxin from Liposomes. *Anal Biochem* 1997; **250**: 139–46.

33 Dawson ME. LAL Update: Interference with the LAL Test and How to Address It. 2005; **22**. https://www.acciusa.com/pdfs/newsletter/LAL Update Vol 22_No3 rev 001.pdf (accessed March 10, 2022).

34 Reich J, Lang P, Grallert H, Motschmann H. Masking of endotoxin in surfactant samples: Effects on Limulus-based detection systems. *Biologicals* 2016; **44**: 417–22.

35 Lonza Walkersville. Traditional Gel Clot Limulus Amebocyte Lysate (LAL) Assay Procedure Quick Guide. 2021. https://bioscience.lonza.com/download/content/asset/28673 (accessed April 4, 2022).

SCIENTIFIC CONTRIBUTIONS

Publications

Publications within the scope of this Ph.D. thesis

J. Tomsen-Melero, J. Merlo-Mas, A. Carreño, S. Sala, A. Córdoba, J. Veciana, E. González-Mira, and N. Ventosa. Liposomal formulations for the therapy of lysosomal storage disorders. *Advanced Drug Delivery Reviews* 190, 114531 (**2022**).

A. Carreño, R. Guerrero, E. Casal, R. Mendoza, and J.L. Corchero. Tuning plasmid DNA amounts for cost-effective transfections of mammalian cells: when less is more. *Applied Microbiology and Biotechnology* 108, 0 (**2024**).

Congresses

Participation to national or international congresses

M. Amaranto, A. Godino, A. Carreño, R. Mendoza, J.L. Corchero, and J.L. Barra. Expression, purification and characterization of recombinant human alpha-galactosidase A mutants. *Sociedad Argentina de Investigaciones en Bioquímica (SAIB)*, Cádiz, Spain, **2019**. Scope: national (Participation: poster; Presenter: M. Amaranto).

A. Carreño, E. González-Mira, J.L. Corchero, and N. Ventosa. Does nanoliposomes presence interfere in the fluorescent GLA enzymatic activity assay? *The 5th Scientific Meeting of PhD Students #JPhD2020*, Barcelona, Spain, **2020**. Scope: national (Participation: oral communication; Presenter: A. Carreño).

L. Ballell, A. Boloix, D. Bueno, A. Carreño, A. Córdoba, L. Ferrer, E. González-Mira, M. Köber, J. Merlo-Mas, J. Morlà, N. Segovia, J. Tomsen-Melero, G. Vargas, S. Sals, J. Veciana, and N. Ventosa. CO_2-expanded solvents for the preparation of high-quality nanovesicles for medical applications. *European Meeting on Supercritical fluids (EMSF2021)*, Bordeaux, France, **2021**. Scope: international (Participation: oral communication; Presenter: L. Ballell).

E. González-Mira, J. Tomsen-Melero, J. Merlo-Mas, E. Cristóbal-Lecina, V. Díaz, A. Font, M. Moltó, N. García, J.L. Corchero, A. Carreño, J.N. Pedersen, J. Lyngsø, I. Ionita, D. Pulido, S. Sala, J. Veciana, S. Schwartz, D. Danino, J.S. Pedersen, A. Soldevila, M. Royo, A. Córdoba, I. Abasolo, and N. Ventosa. Development of an effective

nanomedicine to treat Fabry disease. *Controlled Release Society (CRS2021)*, Virtual meeting, **2021**. Scope: international (Participation: oral communication; Presenter: E. González-Mira).

A. Carreño, E. González-Mira, J.L. Corchero, and N. Ventosa. Evaluating safety of liposomal-based nanovesicles. *XV Annual Ciber-BBN meeting*, virtual, Spain, **2021**. Scope: national (Participation: oral communication; Presenter: A. Carreño).

E. González-Mira, J. Tomsen-Melero, J. Merlo-Mas, E. Cristóbal-Lecina, V. Díaz, A. Font, M. Moltó, N. García, J.L. Corchero, A. Carreño, J.N. Pedersen, J. Lyngsø, I. Ionita, D. Pulido, S. Sala, J. Veciana, S. Schwartz, D. Danino, J.S. Pedersen, A. Soldevila, M. Royo, A. Córdoba, I. Abasolo, and N. Ventosa. Advancing a new nanomedicine for Fabry disease treatment towards clinical translation. *NanoBio&Med2022*, Barcelona, Spain, **2022**. Scope: national (Participation: oral communication; Presenter: E. González-Mira).

Organization of national congresses

A. Carreño declares to have collaborated on the organization of JPhD2021 scientific meeting of Barcelona Nanocluster-Bellaterra (BNC-b) which was performed in November 2021 at the Institute of Materials Science of Barcelona (ICMAB-CSIC), Spain.

Scientific projects

Contributions in scientific projects

Smart multifunctional GLA-nanoformulation for Fabry disease (**Smart4Fabry**; ID 720942) - H2020-NMBP-2016-2017 (**2017 – 2020**). Coordinator: Nora Ventosa Rull. Funding from the European Commission within the Horizon 2020 Research and Innovation program. Contribution of A. Carreño as contracted technical laboratory personnel.

Enzyme MutANts as tools in the quest for improved TheRapies for FAbry disease (**MANTRA**) – Intramural CIBER (**2021 – 2022**). Coordinator: Neus Ferrer Miralles. Funding from the Instituto de Salud Carlos III-CIBER-BBN. Contribution of A. Carreño as team member.

Pharmaceutical Open Innovation Test Bed for Enabling Nano-pharmaceutical Innovative Products (**PHOENIX**; ID 953110) - H2020-LEIT-NMBP/07650 (**2021 – 2025**). Coordinators: Tommaso Serchi (Luxembourg Institute of Science and Technology (LIST)) and Nazende Günday-Türel (MyBiotech SA company); Principal investigator (ICMAB-CSIC): Nora Ventosa Rull. Funding from the European Commission within Horizon 2020 Research and Innovation program. Contribution of A. Carreño as research laboratory personnel. The research activities presented in this manuscript have been mainly carried out in the frame of this European project.

Enzyme MutANts as tools in the quest for improved TheRapies for FAbry disease (**MANTRA**) – Intramural CIBER (**2023 – 2024**). Coordinator: Neus Ferrer Miralles. Funding from the Instituto de Salud Carlos III-CIBER-BBN. Contribution of A. Carreño as team member.

Improved drug delivery systems for enzyme replacement therapies in Fabry disease. Effect of targeting, and protein corona in the efficacy of nanosystems (**PEGLyso-2**) – Intramural CIBER (**2023 – 2024**). Coordinator: Ibane Abasolo. Funding from the Instituto de Salud Carlos III-CIBER-BBN. Contribution of A. Carreño as team member.

Local and Systemic Enzyme Replacement Therapies for Pycnodysostosis (**PYCNO-2**) – Intramural CIBER (**2023 – 2024**). Coordinator: Ibane Abasolo. Funding from the Instituto de Salud Carlos III-CIBER-BBN. Contribution of A. Carreño as team member.

Fellowships

Predoctoral fellowship

Grant Severo Ochoa - CEX2019-000917-S (**2020 – 2024**). Funding from the Agencia Estatal de Investigación, Ministerio de Ciencia e Innovación MCIN/AEI/10.13039/501100011033. The research activities presented in this manuscript have been possible thanks to A. Carreño has been supported by this predoctoral fellowship (**PRE2019-089017**).

I

STRESS TESTING OF NANOLIPOSOMAL MEMBRANE COMPONENTS

I.1. Preliminary testing to identify potential nanoliposome degradants

Nowadays, liposomes are one of the most approved carriers for drug delivery of biomolecules in the nanopharmaceutical field, despite it is well known the poor stability of phospholipids in aqueous dispersion formulations. For translation of a nanopharmaceutical towards the clinics, not only it is important to prove higher efficacy than other current treatments, but also to fulfill all the regulatory requirements that will be mandatory to reach the pharmacopeia approval. In this sense, it is crucial to identify the environmental factors more susceptible to impair on sample quality and stability, in order to guarantee proper storage conditions and expiration date of drug products to ensure their safety at clinical level.

For this reason, it is of huge importance to investigate and control the CQA of a drug product referring on its profile of potential degradation products. The stability tests required to ensure drug product quality level are described in ICH guidelines[1–5], as also recommended by FDA an EMA regulatory. The mainly targets of such studies are:

- Provide evidence about the quality of an API or a drug product under the influence of environmental factors such as temperature, humidity and light, in time.
- Define recommended storage conditions to ensure the drug product stability.
- Define re-test and expiration date, which is the date until the drug product retain its quality characteristics, being storage in proper conditions.
- Identify degradation products
- Determine pathways of degradation products generation (light, water, temperature…), degradation kinetics and stability during use.
- Select formulation and packaging material to use.

Stability studies must be performed at least in triplicates of pilot scale batches of the drug product, consisting of the same formulation, packaging and container closure system as proposed for marketing. Since, the definitive composition of LP-RGD-GLA-S formulation is still being improved in the frame of the European Phoenix project (as previously explained in ***Chapter 1, 4*** and ***5***), these analyses will be performed in later stages.

However, stress testing of the drug product must be conducted before the stability studies to identify potential degradation products of the formulation, as well as its cause of generation. These studies must be also performed using the definitive formulation, packaging and container closure system as proposed for marketing. However, in this thesis, preliminary stress testing has been carried out to advance in the development of an RP-HPLC-ELSD gradient capable to detect various degradation products or impurities related on LP-RGD-GLA-S manufacturing, but also to identify the most probable environmental factors which can influence in the quality of the liposomal membrane components. Regarding the active substance of the nanoformulation (GLA-S protein), the collaborator LeanBio SL (Barcelona) on the European Phoenix project will be in charge to determine the potential degradation products, stability and impurities related to GLA-S, as the producer company.

I.1.1. Definition and design of stress studies

Stress studies consist of submitting a drug product to controlled extreme conditions to induce between 5 – 15 % degradation of the substances present in a formulation, to identify the environmental factors more susceptible to impair sample quality and stability. These studies are also useful to control the stability of a formulation during its overall manufacturing process, as well as, to identify the better storage conditions of a drug product in order to maintain its quality. Nevertheless, stress testing must be repeated if certain changes are made to the product (e.g. formulation composition, excipients, packaging…).

The typical parameters and extreme conditions of sample submission[6] during stress studies are summarized below:

- **Temperature:** 50 ºC up to 70 ºC, in a maximum of 17 days.
- **Humidity:** 75 % relative humidity (RH) or greater. It can be studied by comparing closed and opened packaging.
- **Oxidation:** 0.3 – 3 % H_2O_2 at room temperature in dark.
- **Photolysis:** 2 to 5 times greater than the recommended for confirmation studies (1.2 million lux hour and 200 watt hours/square meter).
- **Hydrolysis:** when sample in suspension.
    - 0.1 M HCl, as acid media.
    - 0.1 M NaOH, as for basic media.

In this chapter, preliminary stress testing has been performed with the individual liposomal membrane components (DPPC, chol, chol-PEG_{400}-RGD and MKC) and the non-definitive $LP_{(w)}$ formulation (stored 6 months at 2 – 8 ºC) with the aim of identifying degradation products of liposome components. $LP_{(w)}$ formulation, composed by DPPC, chol (10:7, theoretical molar ratio) and MKC (5 % molar of the total membrane components), was prepared by DELOS-susp and TFF at 9 mg/mL lipid in pure water (see manufacturing protocols in ***Chapter 7, Sections 7.4.1*** and ***7.4.3***). The experimental procedure followed to carry out this preliminary stress testing study is explained in ***Chapter 7, Section 7.4.5.7***. The forced degradation conditions tested are compiled on ***Table I.1***.

Table I.1. Conditions of the stress testing to force the degradation of liposomal membrane components.

Parameter	Condition	Glass vial closure	Time of exposure	Sample state	Sample tested
Temperature and Humidity	70 ºC and 15 % RH	Closed vs Opened	24 h vs 72 h	Solid vs Suspension (in water)	Individual MKC, chol-PEG_{400}-RGD, cholesterol, DPPC analytes and $LP_{(w)}$ formulation
Oxidation	0.3 % and 3 % H_2O_2 (25 ºC in dark)	Closed	24 h	Solution (in H_2O/ACN/MeOH mixture) vs Suspension (in water)	
Hydrolysis	0.1 M and 1 M HCl (25 ºC in dark)	Closed	24 h	Solution (in H_2O/ACN/MeOH mixture) vs Suspension (in water)	
	0.1 M and 1 M NaOH (25 ºC in dark)	Closed	24 h	Solution (in H_2O/ACN/MeOH mixture) vs Suspension (in water)	
Photolysis	Pending for further steps. Requeriment of homologate chambers				

I.1.2. Evaluating RP-HPLC-ELSD analysis to identify potential degradation products

As explained previously in ***Chapter 5, Section 5.2.*** an accurate RP-HPLC-ELSD method which allow the simultaneously detection of MKC, chol-PEG_{400}-RGD, cholesterol and DPPC molecules has been developed during this thesis work. Based on this procedure, a new RP-HPLC-ELSD analytical method (***Figure I.1***) using the Symmetry300 C4 5 µm, 4.6 x 250 mm column (called as Column_1 in ***Chapter 7, Section 7.4.5.6***) was developed to explore the feasibility of identifying degradation products of the nanoliposomal components (protocol described in ***Chapter 7, Section 7.4.5.7***). The rationale behind using a longer column than the one used for RP-HPLC-ELSD methods previously explained in ***Chapter 5, Section 5.2***, is to explore the possibility of obtaining the complete impurity profile and/or liposomal degradations by increasing the resolution capacity of the system.

For this purpose, and prior to any stress testing, an artificial sample (i.e. sample simulating the same matrix composition of a GLA nanoliposomal formulation) was prepared by using four independently stocks standards of the membrane components, reproducing the LP-$RGD_{(w)}$ prototype. This artificial sample was prepared at 9 mg/mL in MeOH, and composed by DPPC, cholesterol and chol-PEG_{400}-RGD (10:6.5:0.5 theoretical molar ratio),

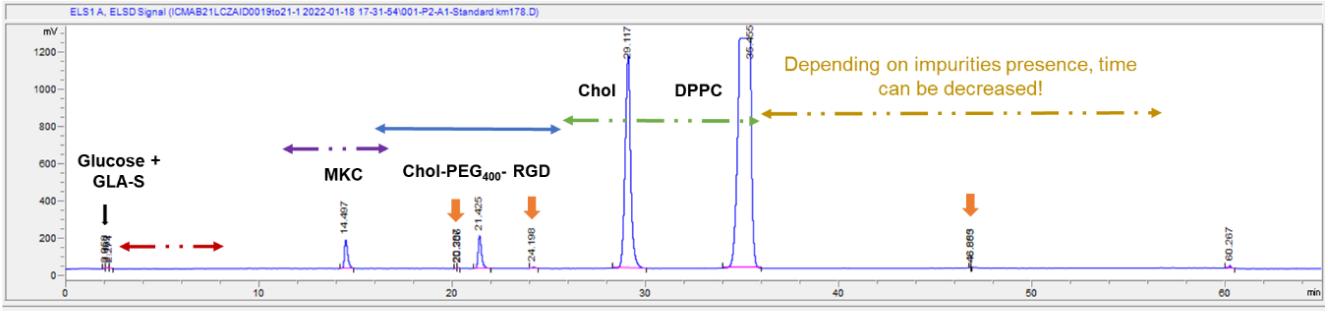
and contained a small amount of MKC (5 % molar of the total membrane components). Such artificial sample was analyzed by RP-HPLC-ELSD following the procedures explained in ***Chapter 7, Section 7.4.5.7*** (at injection volumes of 20 and 3 µL), in order to determine the elution times of the undegraded liposomal components: MKC at 14.497 min, chol-PEG_{400}-RGD at 21.425 min, cholesterol at 29.117 min and DPPC at 35.455 min. Interestingly, some probable impurities related to material might also be detected at 20.308 min, 24.198 min and 46.883 min.

COLUMN:

Symmetry300 C4 5 µm,
4.6 x 250 mm

MOBILE PHASES:

A: MQ water + 0.01% TFA
B: ACN + 0.07% TFA



GRADIENT USED:

Time (min)	0	3	8	11	16	26	36	39	45	48	54	57	58	65
MP_{A2} (%)	60	60	40	40	30	30	20	20	10	10	5	5	60	60
MP_{B2} (%)	40	40	60	60	70	70	80	80	90	90	95	95	40	40
Flow (mL/min)	1.3													

Figure I.1. Analysis of an artificial sample (reproducing the composition of the LP-$RGD_{(w)}$ nanoliposomal formulation) by RP-HPLC-ELSD (65 min time of analysis, using a column of 250 mm, TFA acid in the mobile phases, and the flow rate and gradient protocol shown in the respective table). Black arrow represents the theoretical retention time where GLA-S molecules should be detected when analysing real LP-RGD-GLA-$S_{(w)}$ nanoformulations. Orange arrows represent probable impurities of the components tested. The different gradient phases of the method are highlighted with colour arrows (discontinuous arrows indicating gradient changes, and straight arrows for isocratic phases). The percentage of MP_{B2} required to elute each analyte is correlated in colours code with the respective table.

Identifying degradation products

As explained in ***Chapter 4***, GLA nanoformulations are stored at 2 – 8 ºC as aqueous dispersions. The $LP_{(w)}$ formulation prepared by DELOS-susp, and used in this study, was stored 6 months in dark at 2 – 8 ºC as aqueous dispersion, in order to investigate the impact of these storage conditions on the stability of nanoliposomal formulations composed by DPPC, chol and MKC. As control, this nanoformulation was analyzed by RP-HPLC-ELSD to identify their components and degradants caused by the storage conditions. Chromatogram on ***Figure I.2***, shows the presence of a new peak (elution time at 10.310 min), demonstrating that $LP_{(w)}$ formulation is highly sensitive to temperature and not stable after 6 months stored at these conditions.

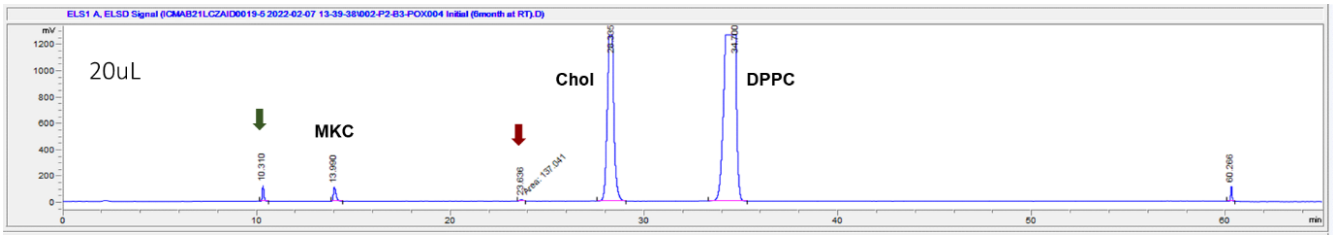


Figure I.2. RP-HPLC-ELSD analysis of a $LP_{(w)}$ formulation stored at 2 – 8 ºC in dark for 6 months. Green arrow indicates a potential degradation product from the formulation, meanwhile red arrow points out the probable cholesterol-related impurity.

Then, the four individual liposomal membrane components (DPPC, chol, chol-PEG_{400}-RGD and MKC), and the 6-month old $LP_{(w)}$ nanoliposomal formulation were submitted to the stress conditions previously explained in ***Table I.1, Section I.1.1***, and next, analyzed by RP-HPLC-ELSD in order to explore the possibility of detecting degradants from the liposomal components caused by the different stress testing conditions.

- Impact of temperature and humidity on material stability.

6-month old $LP_{(w)}$ formulation was submitted at 70 ºC and 15 % RH during 72 h being storage in two different conditions: i) using a closed glass vial (to avoid or reduce water evaporation), and ii) using an opened glass vial (to allow water evaporation). Several peaks related to degradation products were detected by RP-HPLC-ELSD (see ***Figure I.3***), confirming that $LP_{(w)}$ formulation is temperature-sensitive. The opened vial suffered totally sample evaporation ending in solid form, causing the reduction of MKC peak intensity, suggesting a probable instability of MKC in solid state at high temperature. Meanwhile, on the closed vial sample, where sample remained in dispersion form, the cholesterol peak intensity was highly reduced suggesting a lesser cholesterol stability in aqueous form at higher temperatures. In this case, several new chromatographic peaks appeared, being the bigger ones eluted at 10.3 min and 19.1 min.

To explore from which component each degradant originates, then the four individual liposomal membrane components (DPPC, chol, chol-PEG_{400}-RGD and MKC) were also submitted to the same conditions, but in solid state, and during 24 h and 72 h. As shown in ***Figure I.4***, the potential degradation peaks eluted around 10 and 19 min previously observed with $LP_{(w)}$ were not detected with any of the individual membrane components, suggesting that their stability is more impaired when stored in aqueous conditions. However, when stored in solid state, MKC seemed to be the component more unstable to high temperatures with low humidity, meanwhile chol-PEG_{400}-RGD resulted the more unstable at high temperatures with high humidity levels.

These results demonstrate that the material state (solid or solubilized in aqueous solutions), and the nanostructuring of liposomal components impact on their thermal-dependent stability.

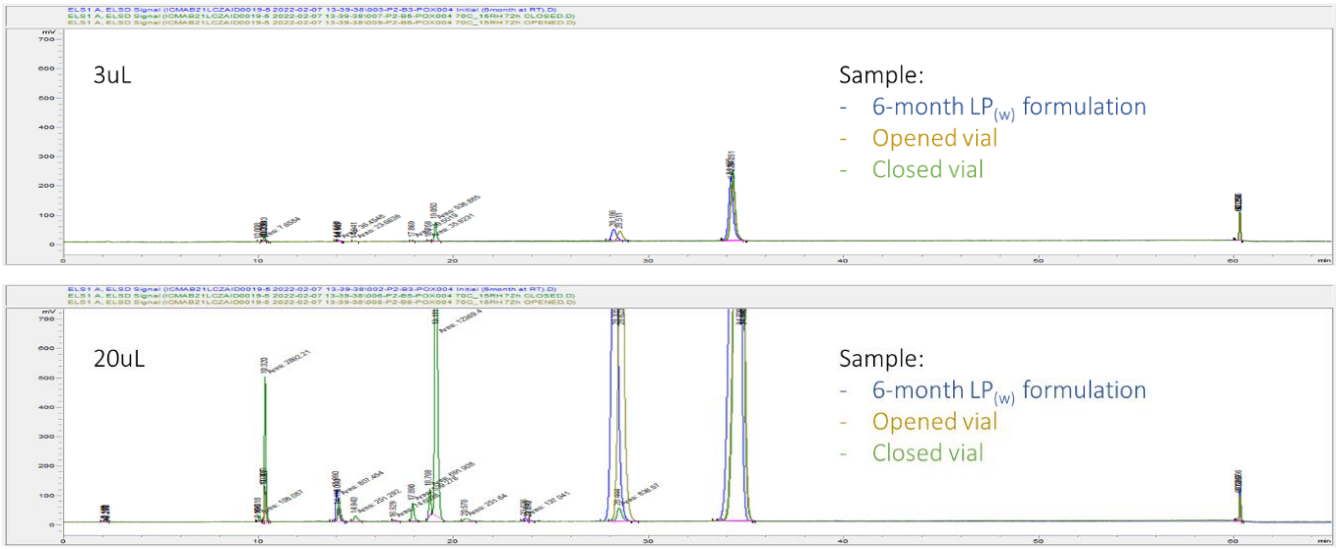


Figure I.3. RP-HPLC-ELSD analysis of a 6-month old $LP_{(w)}$ formulation in aqueous dispersion (in blue) compared with same sample after being stored 72 h at 70 ºC and 15 % RH in an opened vial (in yellow) or in a closed vial (in green).

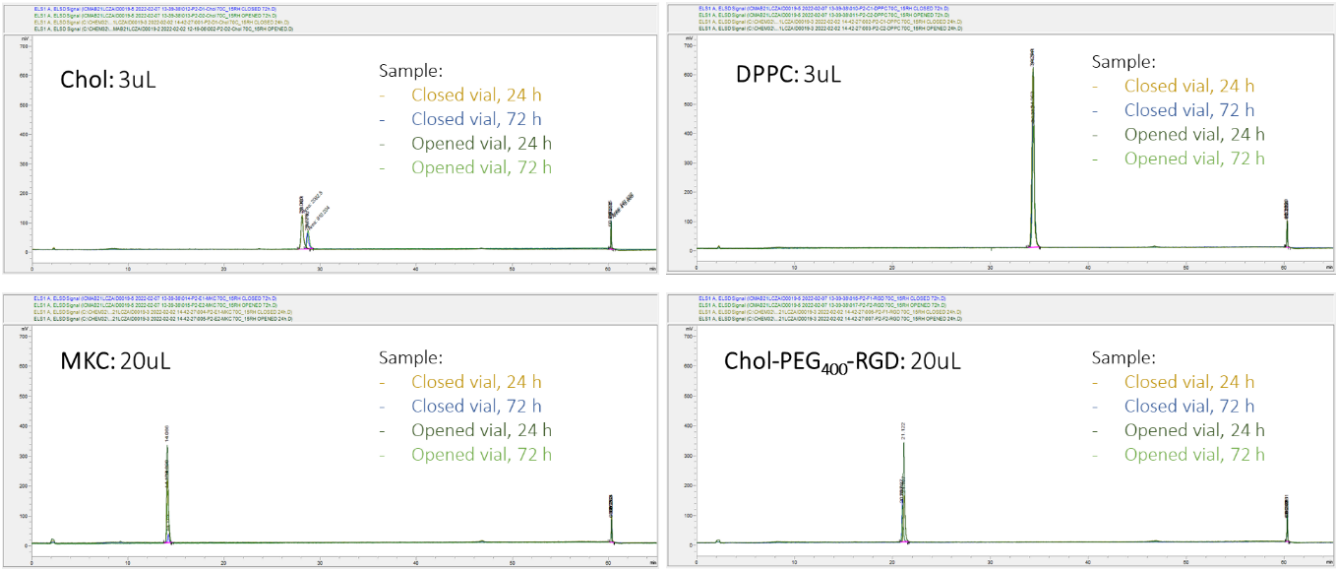


Figure I.4. RP-HPLC-ELSD chromatograms for individual liposomal membrane components (DPPC, chol, chol-PEG_{400}-RGD and MKC) stored 24h or 72 h in solid state at 70 ºC and 15 % RH in an opened vial or in a closed vial.

❖ <u>Impact of oxidation on material stability</u>.

Herein, same 6-month old $LP_{(w)}$ formulation was submitted to an oxidative treatment by adding 0.3 % or 3 % H_2O_2 and storing the sample at 25 ºC in dark during 24 h in closed vials (to avoid water evaporation). The RP-HPLC-ELSD analysis of the stressed sample indicated a general slight right-shift and decrease of chromatographic peaks (see ***Figure I.5***). These results suggest that $LP_{(w)}$ formulation is less sensitive to oxidation than temperature.

In parallel, individual liposomal membrane components (DPPC, chol, chol-PEG_{400}-RGD and MKC) were tested in same conditions to investigate the generation of new chromatographic peaks related to degradation products. However, to investigate oxidative procedures, samples should be in aqueous solution, and most of the hydrophilic liposomal components are not soluble in water. To simulate aqueous conditions, membrane components were solubilized in mixtures H_2O/ACN/MeOH (8/40/52 ratio v/v), and analyzed by RP-HPLC-ELSD after stress testing (see ***Figure I.6***). The solution H_2O/ACN/MeOH (8/40/52 ratio v/v) was also tested as control. Results suggested less stability of the liposomal components in front of oxidation when are individually solubilized than when are nanostructured as nanoliposomes.

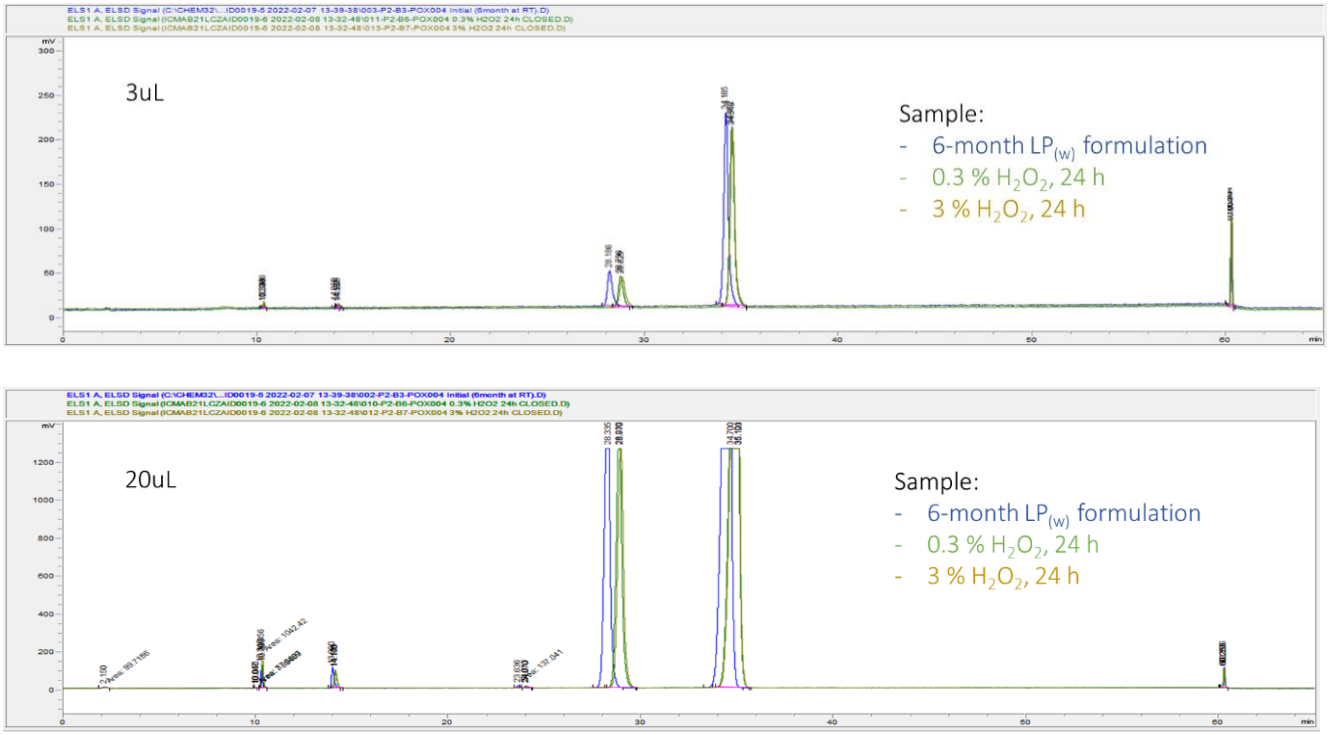


Figure I.5. RP-HPLC-ELSD analysis of a 6-month old $LP_{(w)}$ nanoformulation in aqueous dispersion (in blue) compared with same sample after being stored 24 h at 25 ºC in dark inside closed glass vials, with 0.3 % H_2O_2 (in green) or 3 % H_2O_2 (in yellow).

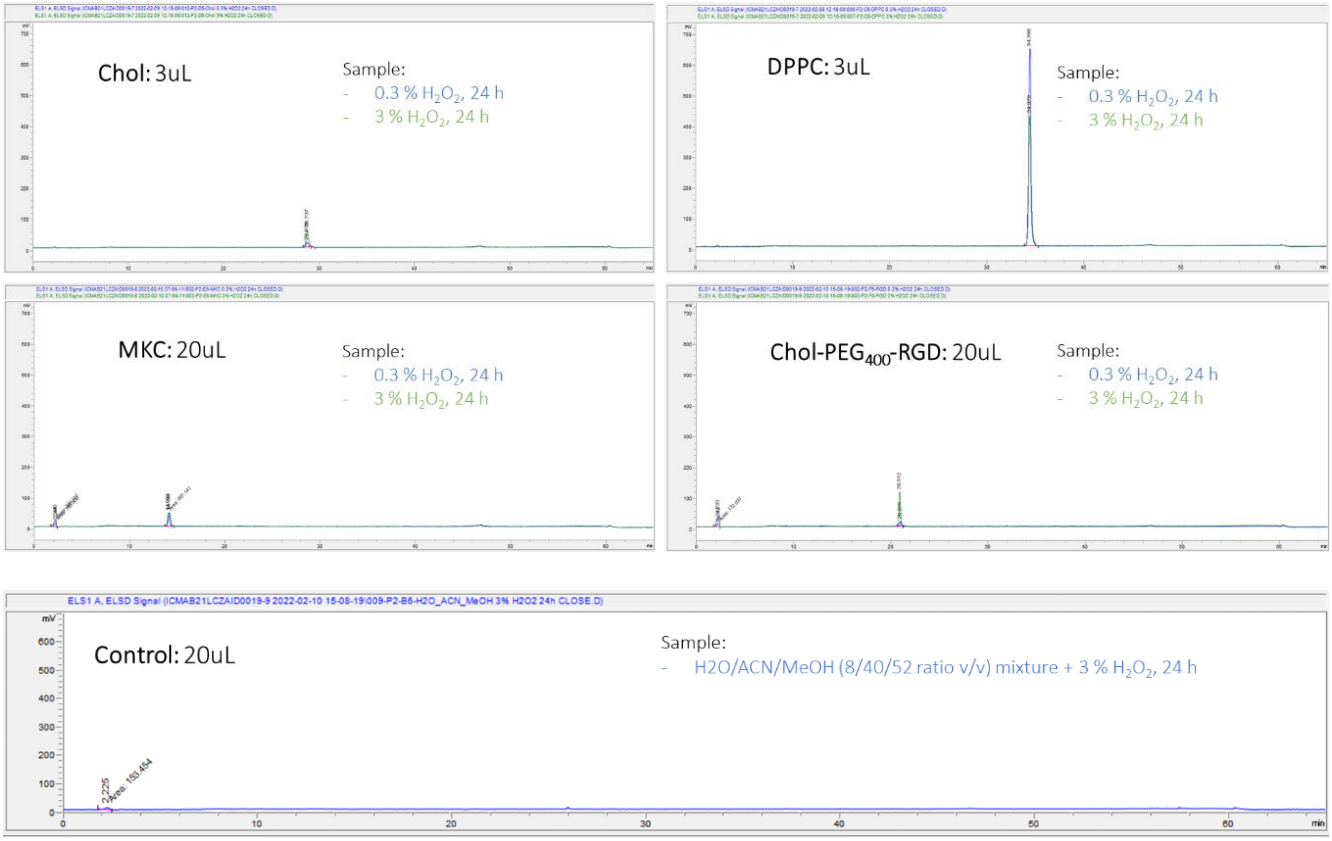


Figure I.6. RP-HPLC-ELSD chromatograms for individual liposomal membrane components (DPPC, chol, chol-PEG_{400}-RGD and MKC) solubilized in mixtures H_2O/ACN/MeOH (8/40/52 ratio v/v) and stored 24 h at 25 ºC in dark inside closed glass vials, with 0.3 % H_2O_2 (in blue) or 3 % H_2O_2 (in light green). A control containing only the H_2O/ACN/MeOH (8/40/52 ratio v/v) mixture + 3 % H_2O_2 is also represented.

- ❖ <u>Impact of hydrolysis on material stability in acid and basic media</u>.

After, possible material hydrolysis in acid and basic media was investigated. First, to reproduce acid conditions, 0.1 M or 1 M HCl were added to the 6-month old $LP_{(w)}$ formulation, and then, stored at 25 ºC in dark during 24 h in closed vials. Chromatograms on ***Figure I.7*** show a huge decrease of the DPPC peak intensity, and the generation of probable DPPC degradants (eluted around 2, 10, 12 and 18 min). These results evidence the high instability of nanostructured DPPC in nanoliposomes, stored as aqueous dispersion, induced by the presence of certain amounts of HCl.

In parallel, individual liposomal membrane components (DPPC, chol, chol-PEG_{400}-RGD and MKC) solubilized in mixtures H_2O/ACN/MeOH (8/40/52 ratio v/v) werw tested under same conditions to explore from which component each degradant originates (see ***Figure I.8***). A control containing only the H_2O/ACN/MeOH (8/40/52 ratio v/v) mixture and 1 M HCl was also tested. Results suggested high instability of solubilized DPPC and chol-PEG_{400}-RGD molecules in presence of acid media, but also slight instability of solubilized cholesterol and MKC components tested at same conditions.

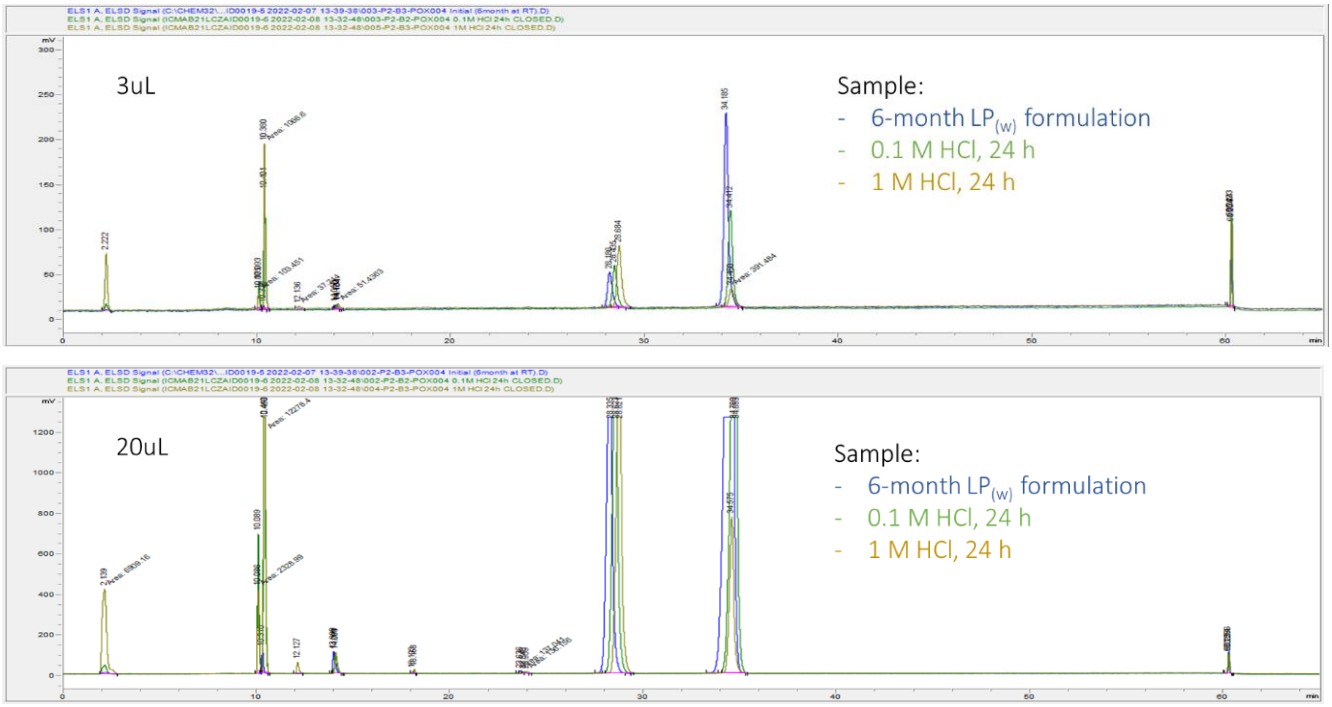


Figure I.7. RP-HPLC-ELSD analysis of a 6-month old $LP_{(w)}$ nanoformulation in aqueous dispersion (in blue) compared with same sample after being stored 24 h at 25 ºC in dark inside closed glass vials, with 0.1 M HCl (in green) or 1 M HCl (in yellow).

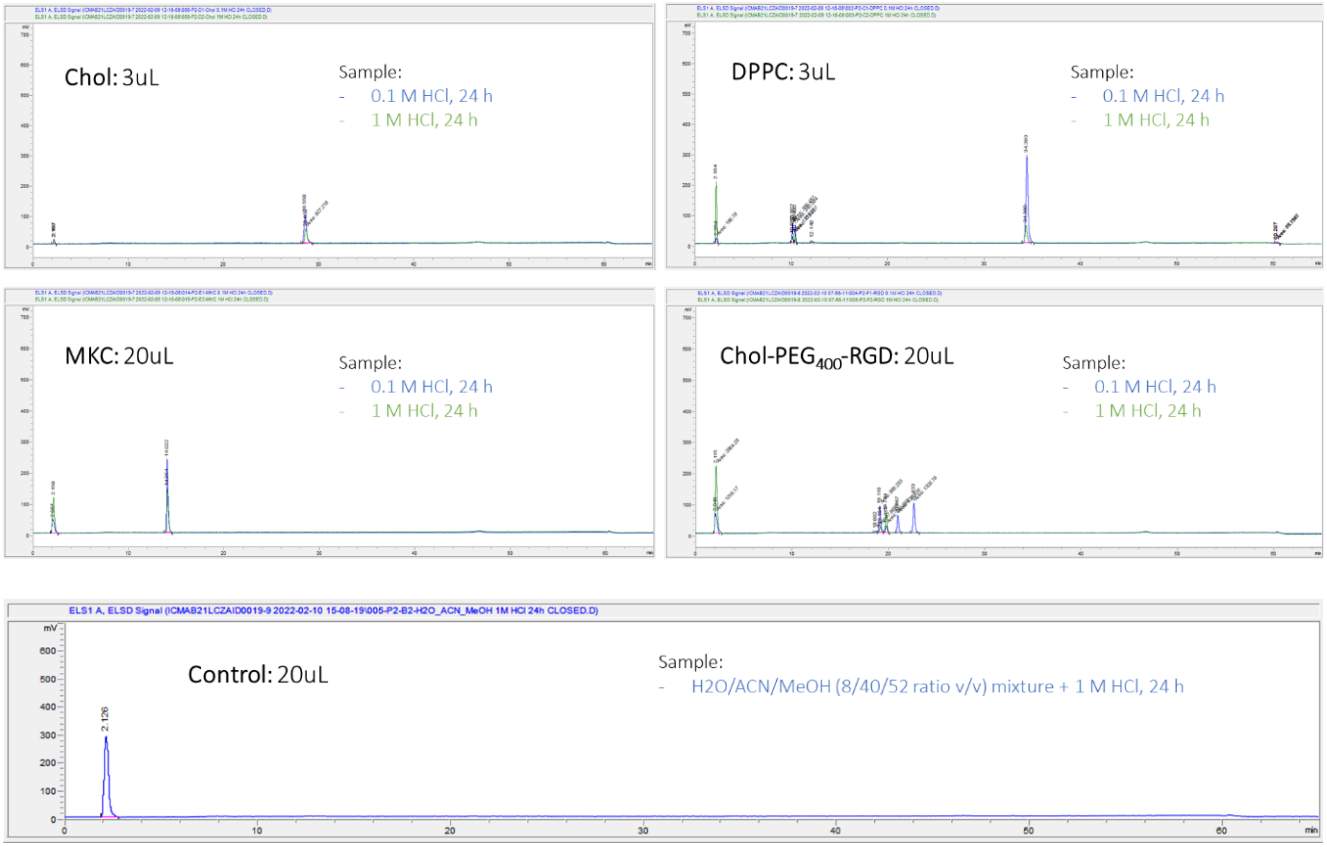


Figure I.8. RP-HPLC-ELSD chromatograms for individual liposomal membrane components (DPPC, chol, chol-PEG_{400}-RGD and MKC) solubilized in mixtures H_2O/ACN/MeOH (8/40/52 ratio v/v) and stored 24h at 25 ºC in dark inside closed glass vials, with 0.1 M HCl (in blue) or 1 M HCl (in light green). A control containing only the H_2O/ACN/MeOH (8/40/52 ratio v/v) mixture + 1 M HCl is also represented.

On the other hand, to investigate possible material hydrolysis in basic conditions, 0.1 M or 1 M NaOH was added to the 6-month old $LP_{(w)}$ formulation, and then, stored at 25 ºC in dark during 24 h in closed vials. RP-HPLC-ELSD chromatograms on ***Figure I.9*** show a total degradation of DPPC component (peak disappearance) caused by the presence of NaOH, and the generation of new chromatographic peaks (eluted around 2 and 18 min). These results suggest that the nanostructured DPPC component, in nanoliposomal formulations stored as aqueous dispersions, is highly instable in presence of certain amounts of NaOH.

In parallel, individual liposomal membrane components (DPPC, chol, chol-PEG_{400}-RGD and MKC) solubilized in mixtures H_2O/ACN/MeOH (8/40/52 ratio v/v) were tested under same conditions to investigate from which component each degradant originates (see ***Figure I.10***). A control containing only the H_2O/ACN/MeOH (8/40/52 ratio v/v) mixture and 1 M NaOH was also tested. It was observed a huge peak intensity decrease for all the solubilized components (and the total DPPC peak disappearance) induced by the presence of NaOH. These results suggested the individually solubilized liposomal membrane components are highly sensitive to hydrolysis in basic media.

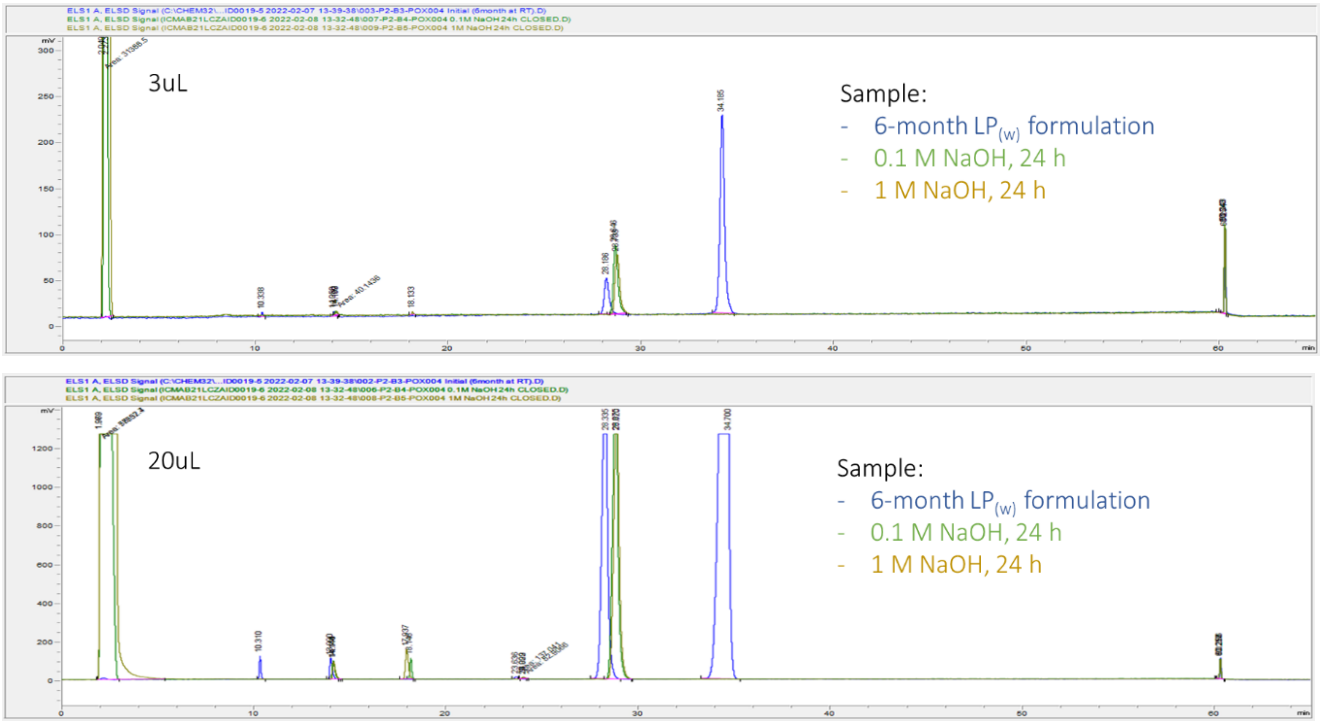


Figure I.9. RP-HPLC-ELSD analysis of a 6-month old $LP_{(w)}$ formulation in aqueous dispersion (in blue) compared with same sample after being stored 24 h at 25 ºC in dark inside closed glass vials, with 0.1 M NaOH (in green) or 1 M NaOH (in yellow).

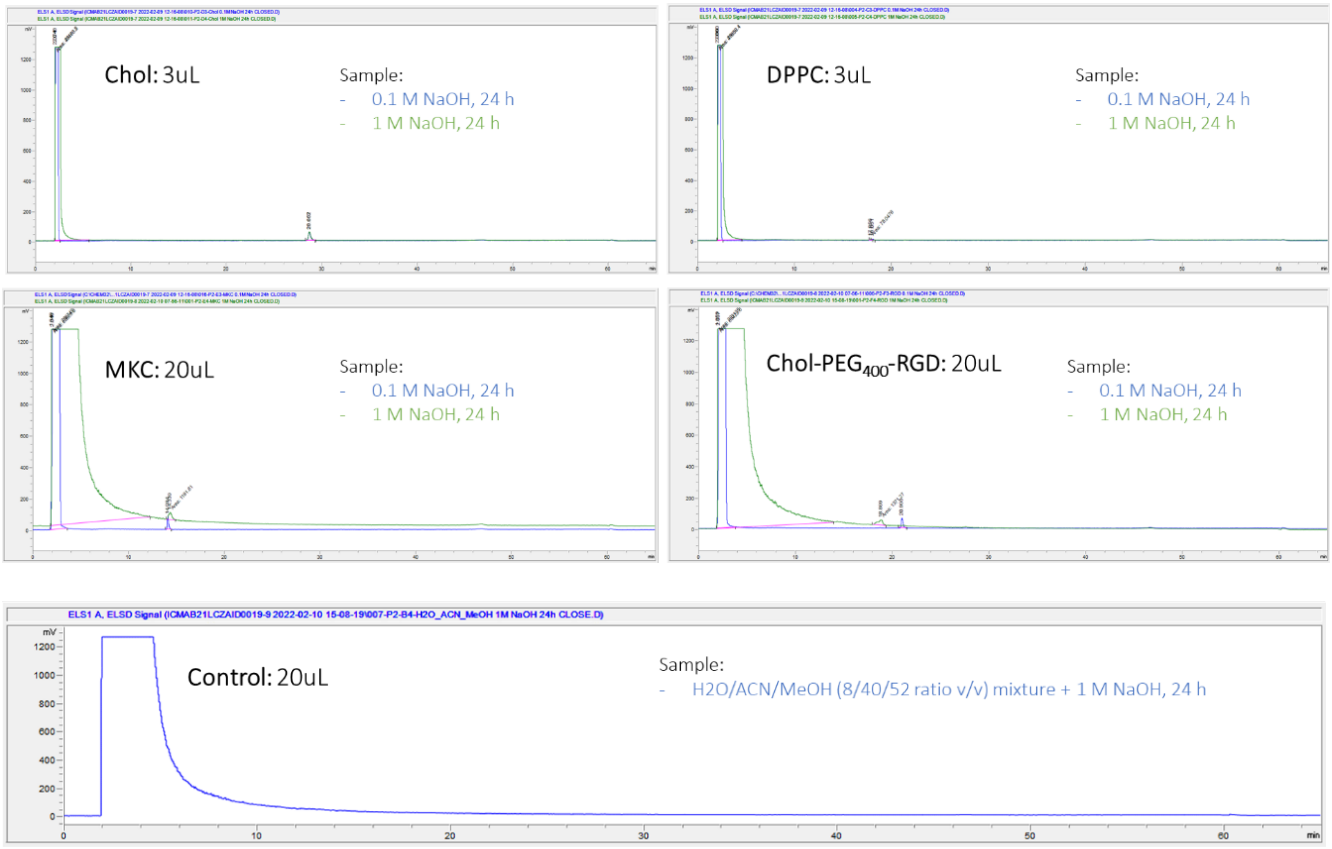


Figure I.10. RP-HPLC-ELSD chromatograms for individual liposomal membrane components (DPPC, chol, chol-PEG_{400}-RGD and MKC) solubilized in mixtures H_2O/ACN/MeOH (8/40/52 ratio v/v) and stored 24h at 25 ºC in dark inside closed glass vials, with 0.1 M NaOH (in blue) or 1 M NaOH (in light green). A control containing only the H_2O/ACN/MeOH (8/40/52 ratio v/v) mixture + 1 M NaOH is also represented.

Conclusion of the study

The results obtained in this section (summarized in *Table I.2*) suggest that the different extreme conditions investigated impacted differently on the stability of DPPC, chol, chol-PEG_{400}-RGD and MKC liposomal membrane components. Moreover, the storage of these components solubilized in an aqueous solution or in solid state impacted on a different way over the stability of DPPC, chol, chol-PEG_{400}-RGD and MKC.

After the stress testing of DPPC, chol, chol-PEG_{400}-RGD and MKC under different extreme conditions, most of the probable degradation products generated resulted on more hydrophilic molecules, i.e. molecules able to elute in RP-HPLC-ELSD gradients with lower concentrations of organic solvent or mobile phase B (MP_{B2}; mainly composed of ACN) (see *Figure I.11*). These molecules with increased hydrophilic character presented similar elution times and low resolution between their chromatographic peaks. For these reason, further optimization of the RP-HPLC-ELSD method proposed in this annex is required to improve peak resolution of the probable liposome degradants detected.

Table I.2. Summarized results about the impact of the extreme conditions of the stress testing study on liposomal membrane components.

		Impact of environmental conditions over liposomal membrane components			
Parameter	**Condition**	**MKC**	**Chol-PEG$_{400}$-RGD**	**Chol**	**DPPC**
Temperature and Humidity	70 ºC and 15 % RH	High temperature-sensitive (in Solid state)	High humidity-sensitive (in Solid state)	High temperature-sensitive (in Aqueous state)	Slight sensitive (in both states)
Oxidation	0.3 % and 3 % H_2O_2 (25 ºC in dark)	Slight sensitive (in Aqueous states)	Semi-sensitive (in Aqueous states)	Semi-sensitive (in Aqueous states)	Slight sensitive (in Aqueous states)
Hydrolysis	0.1 M and 1 M HCl (25 ºC in dark)	Slight sensitive (in Aqueous states)	High sensitive (in Aqueous states)	Slight sensitive (in Aqueous states)	High sensitive (in Aqueous states)
	0.1 M and 1 M NaOH (25 ºC in dark)	Slight sensitive (in Aqueous states)	Semi-sensitive (in Aqueous states)	Semi-sensitive (in Aqueous states)	Very high sensitive (in Aqueous states)
Probable potent degradation peaks, RT (min)		9.938	18.662, 19.118, 19.744, 22.633	10.320, 14.943, 16.929, 17.890, 18.768, 19.111, 20.578	10.086, 10.440, 12.157

I.2. Summary

In this annex, a preliminary stress testing of a nanoliposomal formulation composed of DPPC, chol and MKC (stored as an aqueous dispersion), but also of the individual liposomal components of LP-RGD nanoliposomes (DPPC, chol, chol-PEG$_{400}$-RGD and MKC; as solubilized or solid material) was carried out to investigate which environmental factors might be more susceptible to impair the stability of the liposomal membrane components, and generate liposomal degradants. The main conclusions of these studies have been:

- The material state of individual liposomal membrane components, solid or solubilized in an aqueous solution) impacts on the stability of such components exposed to certain environmental conditions (e.g. temperature, pH…).
- In comparison to the individually solubilized membrane components, the nanostructuring of these components in vesicles improve their stability against some stress conditions (e.g. oxidation and hydrolysis). However, the exposure of LP$_{(w)}$ nanoliposomal formulation at hight temperatures, suggest that liposomes composed of DPPC, chol and MKC are highly temperature-sensitive when stored as an aqueous dispersion.
- The RP-HPLC-ELSD method used in this studies allows the detection of DPPC, chol, chol-PEG$_{400}$-RGD and MKC, as well as, some probable degradants originated from these components. However, further optimization of this method is still necessary to obtain better resolutions of the chromatographic peaks

in presence of liposomal degradants, and to discriminate from which liposomal component is each degradant generated.

I.3. References

1 European Medicines Agency. ICH guideline Q1A (R2) on Stability Testing of new Drug Substances and Products - Step 5. Comm. Hum. Med. Prod. CPMP/ICH/2736/99. 2003. https://www.ema.europa.eu/en/documents/scientific-guideline/ich-q-1-r2-stability-testing-new-drug-substances-products-step-5_en.pdf (accessed Feb 9, 2021).

2 European Medicines Agency. ICH guideline Q1B on Photostability Testing of New Active Substances and Medicinal Products - Step 5. Comm. Hum. Med. Prod. CPMP/ICH/279/95. 1998. https://www.ema.europa.eu/en/documents/scientific-guideline/ich-q-1-b-photostability-testing-new-active-substances-medicinal-products-step-5_en.pdf (accessed April 2, 2021).

3 European Medicines Agency. ICH guideline Q1C on Stability Testing: Requirements for New Dosage Forms - Step 5. Comm. Hum. Med. Prod. CPMP/ICH/280/95 . 1998. https://www.ema.europa.eu/en/documents/scientific-guideline/ich-q-1-c-stability-testing-requirements-new-dosage-forms-step-5_en.pdf (accessed Feb 8, 2021).

4 European Medicines Agency. ICH guideline Q1D on Bracketing and Matrixing designs for Stability Testing of Drug Substances and Drug Products - Step 5. Comm. Hum. Med. Prod. CPMP/ICH/4104/00 . 2002. https://www.ema.europa.eu/en/documents/scientific-guideline/ich-q-1-d-bracketing-matrixing-designs-stability-testing-drug-substances-drug-products-step-5_en.pdf (accessed Feb 12, 2021).

5 European Medicines Agency. ICH guideline Q1E on Evaluation of Stability Data - Step 5. Comm. Hum. Med. Prod. CPMP/ICH/420/02. 2003. https://www.ema.europa.eu/en/documents/scientific-guideline/ich-q-1-e-evaluation-stability-data-step-5_en.pdf (accessed Feb 20, 2021).

6 Baertschi SW, Alsante KM, Reed RA. Pharmaceutical stress testing: predicting drug degradation, Second Edition. Informa Healthcare, 2011.

II

LIPOSOMAL MEMBRANE COMPOSITION ANALYSIS BY SINGLE PARTICLE AUTOMATED RAMAN TRAPPING ANALYSIS (SPARTA®)

II.1. Importance of integration efficiency of targeting ligands as critical quality attribute of liposomes

The targeting capacity of drug delivery systems such as liposomes allow the precise delivery of drug substances to the site of action, avoiding to reach unspecific tissues or organs, and the generation of subsequent side effects. Thus, it is necessary to control the integration of the targeting functionalizations into the bilayer, and to monitor their probable leakage rate during storage conditions. In the frame of this thesis, new methodologies have been explored to evaluate the integration efficiency of the chol-PEG_{400}-RGD molecule, which is the targeting ligand used in the GLA-loaded nanoliposomes intended for the treatment of Fabry disease.

So far, RP-HPLC-ELSD procedures have been employed to determine quantitatively as a bulk the amount chol-PEG_{400}-RGD present in liposomal samples. In order to specifically characterize the targeting ligand on the surface of nanovesicles, a collaboration with SPARTA Biodiscovery (London, UK) through Dr. Jelle Penders was established to perform initial analysis of liposomal samples with Single Particle Automated Raman Trapping Analysis (SPARTA®)[1]. The main objectives of these analyses were:

- Evaluate the compatibility of the composition of diverse liposomal matrixes to be measured by SPARTA®.
- Detection and investigation of the heterogeneous/homogeneous distribution of chol-PEG_{400}-RGD functionalization and GLA loading on the surface of the nanoliposomes.
- Assessment of the influence of a glucose-based buffer on SPARTA® measurements for nanoliposomes.

II.2. SPARTA® methodology and applications

SPARTA® consists of a label-free analysis of nanoparticles (from synthetic polymer particles to liposomes) based on a high-end confocal Raman spectroscopy with a simultaneously controlled laser, camera and spectroscope. The laser allows the trapping of single particles for the acquisition of their high quality Raman spectra through spectroscopy. For this reason, it is a methodology capable to perform particle-to-particle measurements with few volumes and concentrations of samples[1]. The experimental procedure for measuring particles and data analysis is described in ***Chapter 7, Section 7.4.5.8***. Briefly, SPARTA® measurements are performed in five experimental steps:

i. Set-up of the acquisition parameters such as laser disabling time, iteration acquisition time, high signal-to-noise ratio (SNR) acquisition time, iteration number and number of acquisitions.
ii. Thresholding based on the signal obtained from an initial particle trap to set the peak position and height used to determine a successful particle trap.
iii. Acquisition loop, switching off and on the laser to iteraterately carry out quick scans until a trap is recognized.
iv. Taking and saving high SNR acquisition for further data processing.
v. Laser disabling to allow the particle to diffuse away and repeated the process for the continuous analysis of other particles belonging to the sample examined.

Thanks to these properties, the main advantages from SPARTA® described are: i) high-throughput and sensitivity to resolve particle mixtures, ii) the obtaining of detailed compositional spectra of complex particles, iii) capacity to track sequential functionalizations, iv) capacity to derive particle sizes, and v) capacity to monitor dynamics of click reactions on the nanoparticle surface[1].

In this work, a first characterization of liposomes was conducted in order to determine the feasibility of SPARTA® to detect the targeting chol-PEG_{400}-RGD ligand and the GLA-S drug substance in the bilayer of nanovesicles. For these purposes, the concentrated liposomes prototypes detailed in ***Table II.1*** were prepared by DELOS-susp and further TFF (procedures described in ***Chapter 7, Sections 7.4.1*** and ***7.4.3***), and then, measured by SPARTA®. Details on the production of all nanoliposomal formulations used for the present study can be found in ***Chapter 7, Table 7.7***.

Table II.1. Description of GLA-free and GLA-loaded nanoliposomal formulations prepared to be investigated by SPARTA® methodology.

Nanoliposomal system ID	Membrane composition (theoretical molar ratio)	Loaded GLA version	[A] $[lipid]_{theoric}$ (mg/mL)	[B] $[GLA]_{theoric}$ (µg/mL)	Size (nm)	PdI	ζ-potential (mV)	Storage media
$LP_{(w)}$	**DPPC:Chol (10:7) MKC = 0.04 mg/mL**	None	9	0	141.8 ± 5.0	0.23 ± 0.01	54.1 ± 0.7	Pure water
$LP_{(gluc)}$	**DPPC:Chol (10:7) MKC = 0.04 mg/mL**	None	9	0	114.2 ± 4.4	0.18 ± 0.02	50.3 ± 0.9	Glucose 5 % (w/v) media
LP-$RGD_{(w)}$	**DPPC:Chol:Chol-PEG_{400}-RGD (10:6.5:0.5) MKC = 0.04 mg/mL**	None	20	0	117.6 ± 2.1	0.27 ± 0.01	65.9 ± 3.1	Pure water
LP-RGD-GLA-$S_{(w)}$	**DPPC:Chol:Chol-PEG_{400}-RGD (10:6.5:0.5) MKC = 0.04 mg/mL**	GLA-S	9	187	108.8 ± 0.4	0.23 ± 0.01	42.4 ± 1.4	Pure water
LP-RGD-GLA-$S_{(gluc)}$	**DPPC:Chol:Chol-PEG_{400}-RGD (10:6.5:0.5) MKC = 0.04 mg/mL**	GLA-S	9	187	96.4 ± 2.9	0.18 ± 0.01	47.4 ± 2.3	Glucose 5 % (w/v) media

[A] Lipid concentration of all nanoliposomal formulations refers to the theoretical total amount of membrane components added to the DELOS-susp HPV. [B] GLA concentration refers to the theoretical amount of GLA-S added to the aqueous phase (25 µg/mL) of the DELOS-susp process, and obtained after the 7.5-fold concentration of samples by TFF (187 µg/mL).

II.2.1. Detection of chol-PEG_{400}-RGD functionalization and GLA-S loading in nanoliposomes prepared in water

The nanoliposomal formulations used in this subsection, $LP_{(w)}$, LP-$RGD_{(w)}$, and LP-RGD-GLA-$S_{(w)}$, which are gathered in *Table II.1*, were prepared equally in pure water, but differing on the theoretical lipid concentration (9 or 20 mg/mL) and on the presence of chol-PEG_{400}-RGD and/or GLA-S. Nanoformulations were measured by SPARTA® following the procedures described on *Chapter 7, Section 7.4.5.8*, in order to determine the possibility of detection of chol-PEG_{400}-RGD and/or GLA-S in the nanovesicle surfaces.

Results of the mean Raman spectra with standard deviation (shaded region) from more than 160 single particles per nanoformulation tested, and measured from the nanoliposomes purified in water by SPARTA®, are compiled in *Figure II.1*. Sample $LP_{(w)}$ (in red) represents the unfunctionalized and unloaded nanoliposomes, LP-$RGD_{(w)}$ (in blue) represents the functionalized but unloaded nanoliposomes, and LP-RGD-GLA-$S_{(w)}$ (in yellow) represents the functionalized and GLA-S-loaded nanoliposomes. Spectral signatures from lipids and cholesterol were detected in all samples. All nanosystems presented characteristic lipid peaks around 1062, 1084, 1130 cm^{-1} and the two strong peaks at 1300 and 1440 cm^{-1} relating to C-C and CH_2 vibrations. In addition, two clear peaks on the right of the spectrum were also found around 1657 and 1733 cm^{-1}, and could be assigned to the C=O and C=C vibrations of the lipids. For cholesterol, a characteristic peak at 700 cm^{-1} was also detected. The signals were consistent between samples, indicating homogenous lipid and cholesterol content. Moreover, two main peaks could be identified for the chol-PEG_{400}-RGD targeting moiety at 1003 cm^{-1} (insert *Figure II.1*) and 1240 cm^{-1}. Using

the single particle ability of SPARTA®, the area of these two peaks were compared for each nanoliposome across the three different formulations (***Figure II.2***). A clear difference between the unfunctionalized and functionalized particles was observed, with a mean normalized peak area at 1003 cm^{-1} of 0.0074 for $LP_{(w)}$ compared to 0.0093 and 0.0096 for LP-$RGD_{(w)}$ and LP-RGD-GLA-$S_{(w)}$ respectively. This peak likely derived from the arginine amino acid. Similarly, the normalized peak area at 1240 cm^{-1} was 0.0057 for $LP_{(w)}$ compared to 0.0078 and 0.0075 for LP-$RGD_{(w)}$ and LP-RGD-GLA-$S_{(w)}$ respectively. This peak was associated with the C–N stretch and N–H bend from protein amides. Therefore, the 1003 and 1240 cm^{-1} peaks likely derived from the chol-PEG_{400}-RGD targeting moiety, and could be used to identify its presence. However, SPARTA® analysis could not detect significant differences between LP-$RGD_{(w)}$ and LP-RGD-GLA-$S_{(w)}$, which suggested that the tested GLA-S concentration in sample was too low to be detected with the measurement conditions employed. All the assigned peaks detected are summarized in ***Table II.2***.

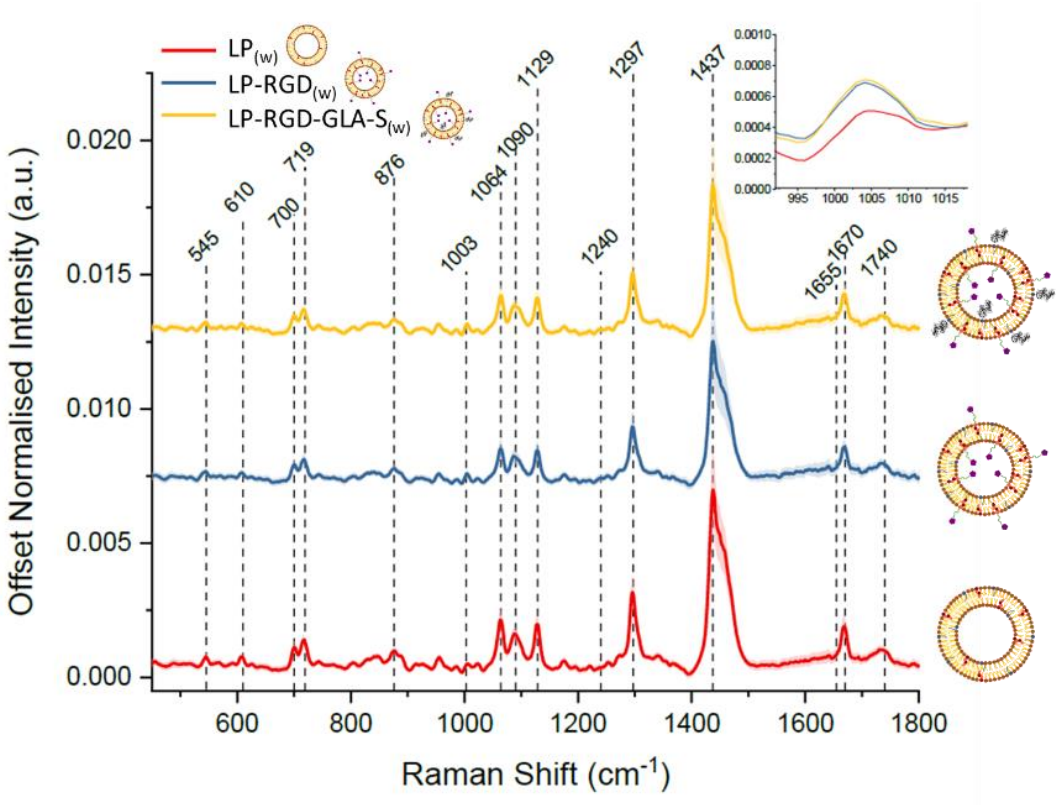


Figure II.1. SPARTA® annotated overview of nanoliposomes in water. SPARTA® measurements overview shown as mean ± standard deviation for $LP_{(w)}$ (n = 199, red), LP-$RGD_{(w)}$ (n = 162, blue) and LP-RGD-GLA-$S_{(w)}$ (n = 177, yellow). Insert shows a close up of the spectral region between 990 and 1020 cm^{-1}. One production bacth of each nanoliposomal system was tested. Annotated peaks are highlighted and assigned in ***Table II.2***.

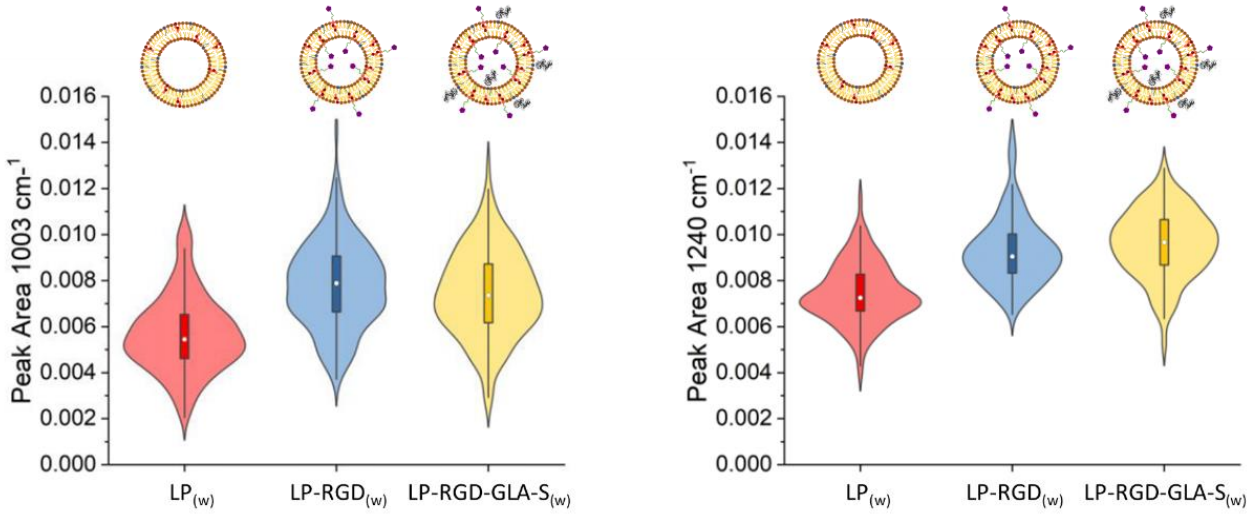


Figure II.2. Detection of RGD targeting ligand using SPARTA®. The targeting ligand peak area at 1003 cm^{-1} (left, phenylalanine peak) and 1240 cm^{-1} (right, amide peak) were extracted for all of the individual normalized nanoliposome spectra obtained by SPARTA®, shown here as a violin plot superposed onto a box plot. Comparison of unfunctionalized ($LP_{(w)}$) and functionalized ($LP\text{-}RGD_{(w)}$ and $LP\text{-}RGD\text{-}GLA\text{-}S_{(w)}$) formulations. One production bacth of each nanoliposomal system was tested.

Table II.2. Primary nanoliposome peak assignment.

POSITION	ASSIGMENT
545	Cholesterol
610	Cholesterol
700	Cholesterol
719	Lipid headgroup C-N stretch
876	Lipid choline headgroup stretch
1003	Amino acid (Arginine)
1064	C-C trans stretch
1090	C-C gauche, C-N stretch
1129	C-C trans stretch
1240	Amide, peptide (C-N, N-H)
1297	CH_2 twist
1437	CH_2, CH_3 deformation (overlapping)
1655	Amide, C=O / C=C
1670	C=O / C=C
1740	C=O

II.2.2. The influence of glucose on SPARTA® measurements and particle properties

The main objective of this subsection was to assess the impact of the glucose 5 % (w/v) solution on the properties of nanoliposomes, as well as, on SPARTA® measurements. As control, glucose 5 % (w/v) solution without presence of nanoliposomes was measured by SPARTA® following the procedures described on ***Chapter 7, Section 7.4.5.8***, and the mean spectrum obtained is shown in ***Figure II.3***. Glucose molecules showed Raman signals, with

peaks at 1067, 1124, 1366 and 1657 cm^{-1}, which might potentially interfere with subsequent particle measurements. However, this mean background signal, obtained from 20 spectral acquisitions of the glucose 5 % (w/v) solution, was subtracted during the data pre-processing of the next SPARTA® measurements carried out with nanoliposomal formulations containing glucose 5 % (w/v).

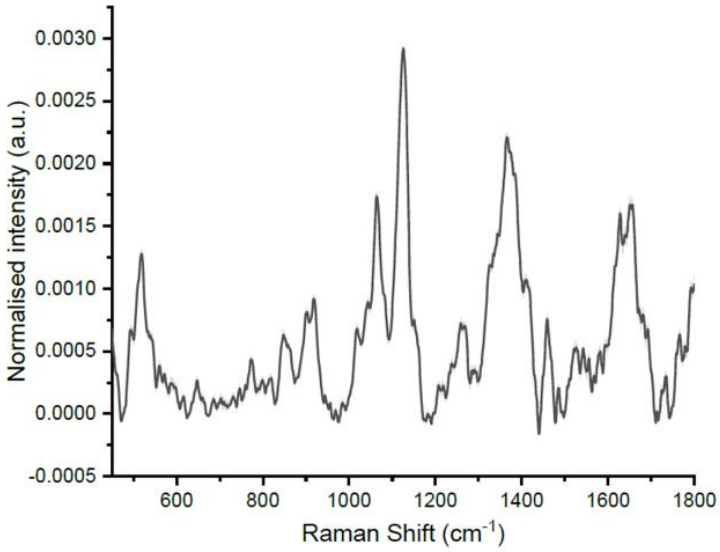


Figure II.3. SPARTA® measurements of glucose solution. Mean Raman spectra ± standard deviation of 20 solution spectra of glucose 5 % (w/v) solution, acquired at the same 10 second acquisition time as particle spectra.

To investigate the feasibility of performing SPARTA® measurements of nanoliposomal formulations in presence of glucose molecules, the nanoliposomal formulations prepared in water and studied in section II.2.1, were compared with the nanoformulations, $LP_{(gluc)}$, and LP-RGD-GLA-$S_{(gluc)}$, which are gathered in *Table II.1*, and were prepared equally at the same theoretical lipid concentration (9 mg/mL) in glucose 5 % (w/v), but differing on the presence of chol-PEG_{400}-RGD and GLA-S. Nanoformulations were measured by SPARTA® following the procedures described on *Chapter 7, Section 7.4.5.8*.

Comparing the results of the mean Raman spectra measured by SPARTA® in nanoformulations with and without glucose presence, relatively little change in the Raman signatures related to glucose addition was observed. The presence of glucose did not hinder the identification of the chol-PEG_{400}-RGD based on the 1003 cm^{-1} peak area (*Figure II.4* inset, and *Figure II.5*), with both LP-RGD-GLA-$S_{(gluc)}$ and LP-RGD-GLA-$S_{(w)}$, which contained the targeting moiety with and without glucose, having higher peak area than the unfunctionalized $LP_{(gluc)}$ and $LP_{(w)}$. The 1003 cm^{-1} peak area distributions obtained were relatively similar in the presence or absence of glucose, although glucose-containing LP-RGD-GLA-$S_{(gluc)}$ demonstrated a slightly higher peak area when comparing its mean of 0.0114 ± 0.0015 to the one of 0.0096 ± 0.0016 from LP-RGD-GLA-$S_{(w)}$. The detected glucose signal was

low in this Raman shift around 1003 cm^{-1}, what suggested a slightly higher functionalisation for the containing LP-RGD-GLA-$S_{(gluc)}$ nanoliposomes prepared in glucose buffer in contrast to the LP-RGD-GLA-$S_{(w)}$ nanoliposomes purified in water. Nevertheless, more batches must be analysed to statistically confirm that hypothesis. The distributions of the 1240 cm^{-1} peak were less clearly distinguishable between functionalised and unfunctionalized conditions, due to the probable interfering of glucose signals encountered in this region, which might be masking the functionalisation detection from the 1240 cm^{-1} peak.

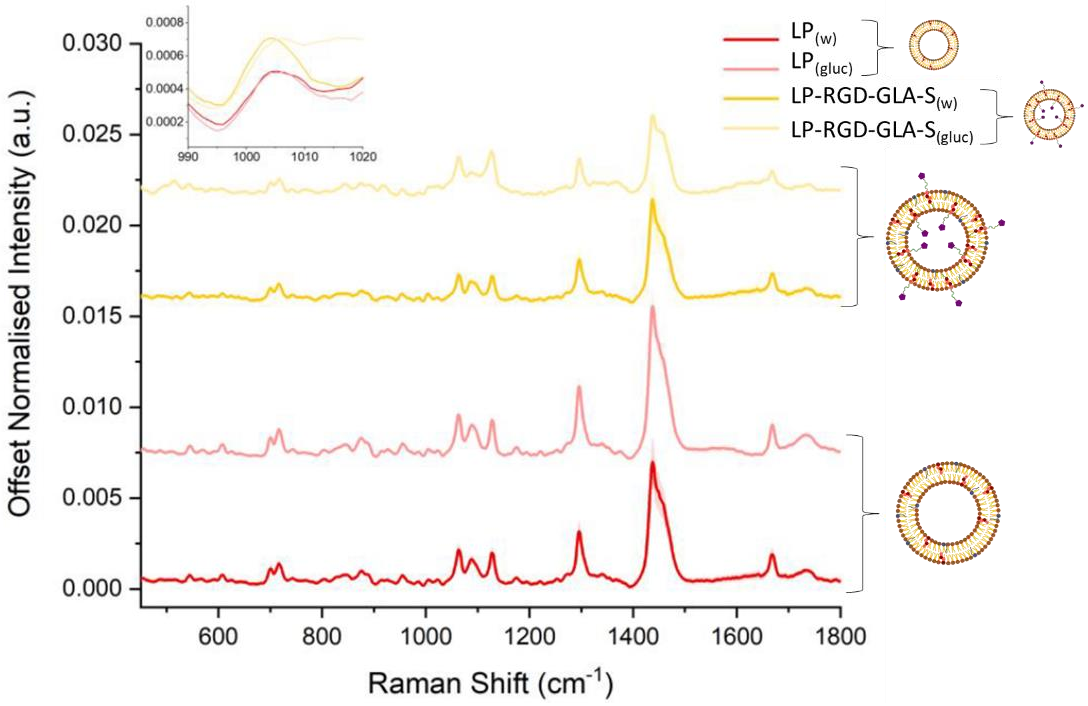


Figure II.4. SPARTA® overview of nanoliposomes prepared in water and glucose solution. SPARTA® measurements overview shown as mean ± standard deviation of $LP_{(w)}$ (n = 199, red), $LP_{(gluc)}$ (n = 154, light red), LP-RGD-GLA-$S_{(w)}$ (n = 177, yellow) and LP-RGD-GLA-$S_{(gluc)}$ (n = 146, light yellow). Insert shows a close up of the spectral region between 990 and 1020 cm^{-1}. One production bacth of each nanoliposomal system was tested.

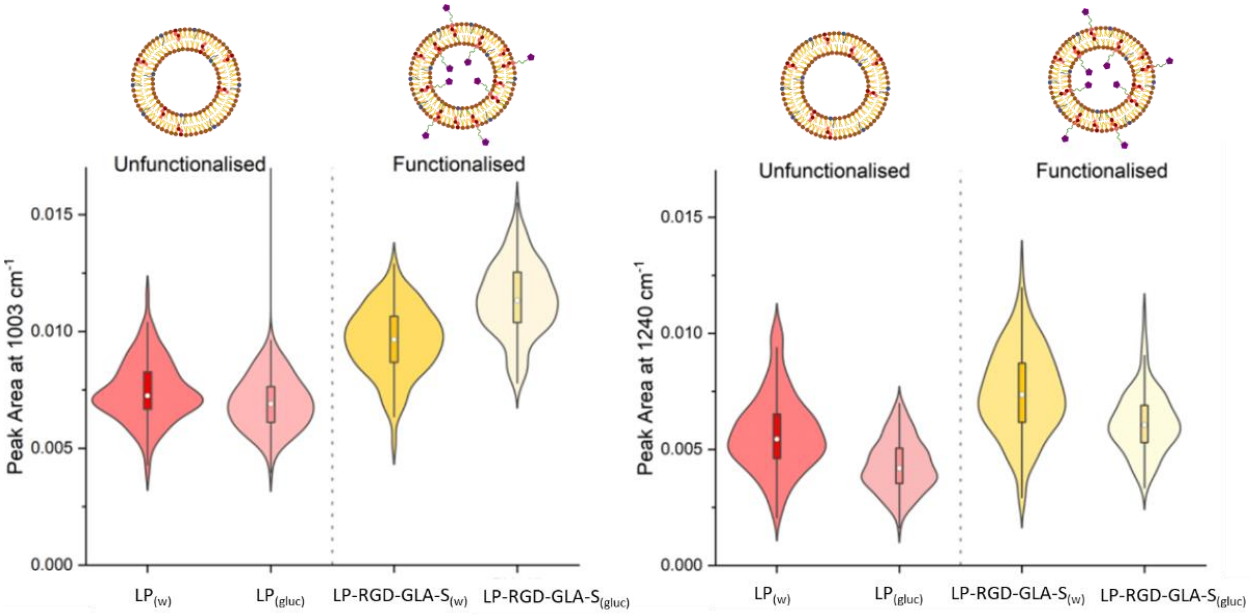


Figure II.5. Impact of glucose solution on SPARTA® detection of chol-PEG_{400}-RGD targeting moiety. The targeting ligand peak area at 1003 cm^{-1} (left) and 1240 cm^{-1} (right) was extracted for all of the individual normalised nanoliposome spectra obtained by SPARTA®, shown here as a violin plot superposed onto a box plot. Comparison of unfunctionalized ($LP_{(w)}$ and $LP_{(gluc)}$) and functionalized (LP-RGD-GLA-$S_{(w)}$ and LP-RGD-GLA-$S_{(gluc)}$) formulations in presence or absence of glucose. One production bacth of each nanoliposomal system was tested.

II.3. Summary

The preliminary analysis carried out by SPARTA® measurements evidenced consistent lipid and cholesterol ratios across all the liposome nanoformulations tested, and indicated proper batch-to-batch reproducibility. Besides, it was demonstrated the possible detection of chol-PEG_{400}-RGD targeting ligand through peaks at 1003 and 1240 cm^{-1}. In presence of glucose molecules, this targeting moiety was also detected through peak at 1003 cm^{-1}. However, the low GLA-S concentrations analyzed were not capable to be detected by the SPARTA® measurement parameters employed. Further investigation must be done to try to detect Raman signal from GLA-S enzyme.

In this way, SPARTA® approach demonstrated to be a potential technique for the accurate characterization of the integration efficiency of chol-PEG_{400}-RGD within liposome bilayer. Future studies using calibration curves might be useful to quantitatively determine the amount of chol-PEG_{400}-RGD molecules integrated in liposome membranes and batch-to-batch heterogeneity and reproducibility, but also to follow their leakage rate under storage conditions.

II.4. References

1 Penders J, Pence IJ, Horgan CC, *et al.* Single Particle Automated Raman Trapping Analysis. *Nat Commun* 2018; **9**: 4256.

III

FIELD FLOW FRACTIONATION COMBINED WITH MULTI-ANGLE LIGHT SCATTERING (FFF-MALS) FOR THE QUALITY CONTROL OF NANOPHARMACEUTICALS

III.1. Introduction to field flow fractionation-based methodologies

Liposomes are vesicles composed of lipid bilayers of amphiphilic character, which present large flexibility regarding size, number of membranes, composition or functionalization. These properties turn liposomes into suitable drug delivery systems for nanopharmaceutical purposes. The understanding and characterization of any nanoparticle delivery platform are critical for the identification of CQAs and to be successfully developed as nanopharmaceuticals. Examples of common CQAs required to monitor during liposome research, formulation, manufacturing and quality control are particle size distribution, shape, morphology, drug encapsulation and distribution, and stability. However, several conventional methods have limitations on population resolution, giving only an average value of the global particles that make up the formulation, and they are often not able to conserve the integrity of nanosystems[1,2].

Field flow fractionation (FFF) non-destructive methodologies (patented in 1966 by J. Calvin Giddings) are ideal for the complete separation of delicate particles from a broad size range (from 1 nm to 10 µm) which can be dispersed into a wide variety of solutions. In contrast to column separation techniques (e.g. size exclusion chromatography), FFF techniques present reduced system backpressure and minimal shearing due to the absence of a stationary phase. In this case, the gentle separation of particles is carried out by an external force field perpendicularly disposed to the open channel. Depending on the nature of the separation field, different FFF-based methodologies can be subclassified (***Table III.1***) as thermal FFF, sedimentation FFF, magnetic FFF,

electrical FFF, and flow FFF; each one of which is useful to analyze the distinct physicochemical properties used as the basis of separation[2].

Table III.1. Classification of FFF techniques and their respective external force field employed, as well as, the physicochemical property analysed as the particle separation basis.

FFF subclasses	External force field	Physicochemical property
Thermal FFF (ThFFF)	Thermal gradient	Soret coefficient
Sedimentation FFF (SeFFF)	Gravity or Centrifugal force	Effective mass (density)
Magnetic FFF (MgFFFF)	Magnetic field	Magnetic properties
Electrical FFF (ElFFF)	Electric field	Electrophoretic mobility
Flow FFF (FlFFF)	Cross flow	Diffusion coefficient

Flow FFF approaches can be used with channels of different geometrical shapes or manners of crossflow application, obtaining the diverse formats of symmetric flow FFF (SF4), asymmetric flow FFF (AF4), or hollow fiber flow FFF (HF5). Among them, AF4 has demonstrated to be the most versatile and permissive in size separation range, and hence, the most employed for the research community[2].

III.1.1. Operating principle of AF4 and applications

When using the AF4 approach, the fractionation of particles regarding their size and diffusion is performed in the mobile liquid phase that flows through a separated thin channel, thanks to the application of a perpendicular crossflow through a semi-permeable membrane, which is capable of counterweight the particle diffusion (***Figure III.1***). This situation allows a quicker diffusion, velocity and elution of small particles than large ones, and the subsequent well-resolved separation of mainly monodisperse particle populations according to size. The separation zone inside the channel is basically defined by a spacer of designated thickness able to influence the parabolic flow profile of the mobile liquid phase containing the nanoparticles. Moreover, the semi-permeable membrane across which the crossflow passes also contribute to the partial retention of analytes, and therefore, to the particle separation. Once the sample is injected into the separation channel, and before sample elution, a step of sample relaxation is required to concentrate the particles at a certain point before their separation. Nowadays, there exist two types of channel for these purposes: focusing and hydrodynamic relaxation. Focusing relaxation is employed in the conventional AF4 channels to relax the sample close to the membrane thanks to a focusing flow, although the risk of sample aggregation or sticking to the membrane causes material loss and colloidal particle instability. However, in order to avoid such limitations, hydrodynamic relaxation is used for the newer frit inlet channel or dispersion inlet channel[2,3] (***Figure III.1***).

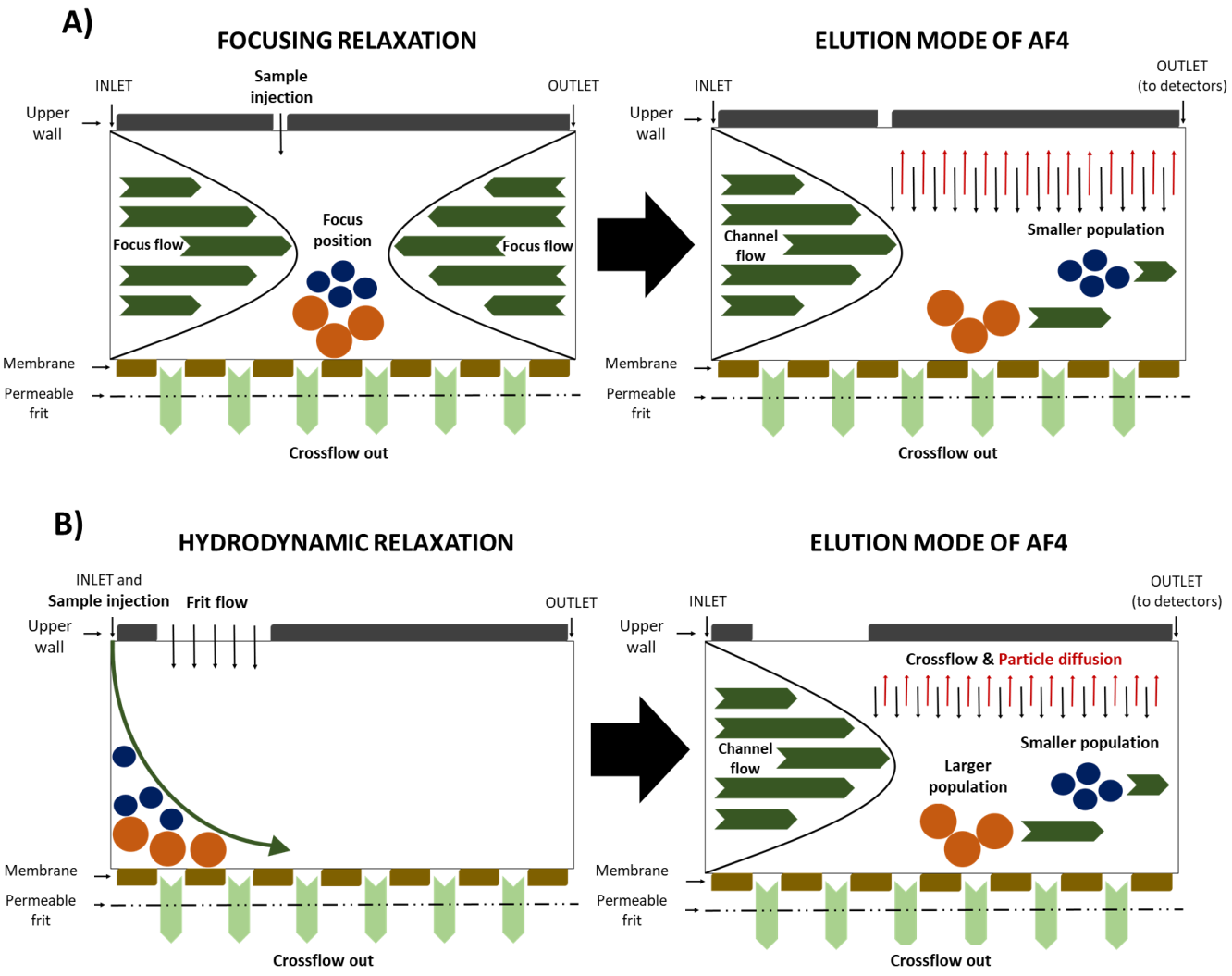


Figure III.1. Schematic representation of sample relaxation and elution steps for asymmetric flow FFF (AF4) when using A) focusing relaxation in conventional AF4 channels or B) hydrodynamic relaxation in frit inlet or dispersion inlet channels. Adapted from[2,3].

AF4 is an elution methodology that can be coupled to multiple detectors in tandem capable of providing the measurement of several CQAs (e.g. size, molar mass, mass concentration, shape factor and/or composition) of the size-resolved populations. Detectors to be used are: i) MALS capable of determining the molar mass, good quality root mean square radius between 10 – 500 nm (also denominated as the radius of gyration (R_g) which is calculated according to *Eq. III.1*), and the particle concentration which can be derived from the scattered intensity when there are higher than 10^7 particles/mL; ii) DLS for the measurement of Stokes radius (also named as hydrodynamic radius (R_h)) in an accurate range of 0.5 – 300 nm when coupled at FFF techniques in a maximum flow rate of 0.5 mL/min. Together with MALS, DLS can be useful to determine the particle shape and morphology by the ratio R_g/R_h; iii) UV, iv) refractive index (RI), and v) fluorescence detectors (FLD) are extensively used for determining the analyte concentration from samples with distinct intrinsic properties[2,3].

$$R_g = \sqrt{3/5} \cdot R_s$$

(*Eq. III.1*)

Where R_S is the geometric radius of a solid sphere.

In this direction, the combination of FFF elution approaches together with light scattering detectors (e.g. MALS and DLS) and concentration detectors (UV, RI and FLD), permits a deep and complete characterization of structuration and quantitative measurements of complex drug delivery systems which have been well-resolved according to their size. The commonest CQAs described in the literature that are possible to be monitored with these approaches include size distribution, shape and morphology, particle stability, drug encapsulation, and drug release or leakage[2,3].

III.2. Development of an AF4-MALS-dRI methodology for the characterization of GLA-loaded nanoliposomal formulations

In the frame of this thesis, a research period abroad was carried out in the group of Dr. Ivana Vinković Vrček from the Institute for Medical Research and Occupational Health (IMI) located in Zagreb (Croatia) with the aim to investigate the feasibility of measuring GLA-loaded RGD-targeted liposomes by AF4-MALS-dRI approach. The main purpose of the stay was to develop a method based on AF4-MALS-dRI to simultaneously detect the GLA-S enzyme and RGD-targeted liposomes. In this way, the size, morphology and structuration of both together with the GLA-S release from liposomal membranes might be monitored in different conditions to explore a wide range of CQAs characterizations.

For this initial stage of development, intermediate prototypes of GLA-free and GLA-loaded liposomes described in *Table III.2*, were prepared by DELOS-susp following the procedures described in *Chapter 7, Sections 7.4.1*. Details on the production of all nanoliposomal formulations used for the present study can be found in *Chapter 7, Table 7.7*. Non-encapsulated GLA-S protein was also tested by AF4-MALS-dRI to identify the elution time of this enzyme.

Table III.2. Intermediate prototypes of liposomes fabricated using the DELOS-susp technique, and GLA-S enzyme produced using CHO cultures, used for measurements of AF4-MALS-dRI methodologies.

Nanoliposomal system ID	Membrane composition (theoretical molar ratio)	Loaded GLA version	[A] $[lipid]_{theoric}$ (mg/mL)	[B] $[GLA]_{TGX}$ (µg/mL)	Size (nm)	PdI	ζ-potential (mV)	Storage media
LP-RGD_int	**DPPC:Chol:Chol-PEG_{400}-RGD (10:6.5:0.5) MKC = 0.04mg/mL**	None	1.2	0	147.1 ± 2.8	0.20 ± 0.01	46.9 ± 1.0	5 % EtOH + 1.2 % DMSO (v/v) in water
LP-RGD-GLA-S_int	**DPPC:Chol:Chol-PEG_{400}-RGD (10:6.5:0.5) MKC = 0.04mg/mL**	GLA-S	1.2	25 ± 1	151.9 ± 1.3	0.20 ± 0.01	40.2 ± 0.5	5 % EtOH + 1.2 % DMSO (v/v) in water
GLA enzyme version	**Production cell line – expression method**	**-**	**[A] $[lipid]_{theoric}$ (mg/mL)**	**[B] $[GLA]_{TGX}$ (µg/mL)**	**Size (nm)**	**PdI**	**ζ-potential (mV)**	**Storage media**
GLA-S*	Chinese Hamster Ovary (CHO K1) – Stable clone	-	0	3500 ± 100	9.3 ± 0.2	0.32 ± 0.02	-0.8 ± 0.2	Mannitol, sodium phosphate monobasic monohydrate, sodium phosphate dibasic heptahydrate

* Enzyme version provided by LeanBio SL. [A] Lipid concentration of all nanoliposomal formulations refers to the theoretical total amount of membrane components added to the DELOS-susp HPV. [B] GLA-S concentration was assessed by SDS-PAGE and TGX densitometry.

Instrumentation and data analysis

All the AF4-MALS-dRI measurements were carried out using an Eclipse separation system (Eclipse NEON FFF; Wyatt Technology Europe GmbH, Dernbach, Germany) coupled online to a dRI detector (G7162A, Agilent Technology, Böblingen, Germany) and an 18-angle static light scattering detector MALS (DAWN HELEOS II, Wyatt Europe, laser wavelength 658 nm). A dispersion-inlet channel (Wyatt Technologies, Dernbach, Germany) with a 350 µm plastic spacer was used, and a regenerated cellulose membrane with a cut-off of 10 kDa served as the accumulation wall (Wyatt Technologies, Dernbach, Germany). The mobile phase (10 mM PBS + 0.02% sodium azide) used for AF4-MALS-dRI analysis was previously filtrated through VacuCap 60 Vacuum Filtration Devices - 0.1 µm (4631, Pall Corporation, Portsmouth, UK).

Root-mean square radius (R_g or rms radius) and molar mass of samples were calculated by the Astra software version 8.1.2. (Wyatt Europe, Dernbach, Germany) using the Zimm fit model for the analysis of the GLA-S enzyme and the Berry fit model for the analysis of liposomes. R_g is defined by the equation ***Eq. III.1***, while molar mass can be determined if the specific refractive index increment (dn/dc) and concentrations of a solute are known. In this study, the theoretical lipid concentration of liposome samples was 1.2 mg/mL, while the concentration of GLA-S was 3.5 mg/mL. dn/dc values of 0.160 and 0.185 for phospholipids and proteins in water have been used, respectively[4].

Additional information about the instrumentation, the sample preparation procedure and data analysis is explained in more detail in ***Chapter 7, Section 7.4.5.9***.

III.2.1. Development of the A4F-MALS-dRI protocol for the detection of nanoliposomes

The nanoliposomal formulations used in this study, LP-RGD_int and LP-RGD-GLA-S_int, which are gathered in ***Table III.2***, were prepared equally at the same the theoretical lipid concentration (1.2 mg/mL) in 5 % EtOH and 1.2 % DMSO (v/v) in water, but differing on the presence of the GLA-S enzyme. The development of a methodology based on AF4-MALS-dRI was explored to characterize both, LP-RGD_int and LP-RGD-GLA-S_int nanoliposomes, following the procedures described in ***Chapter 7, Section 7.4.5.9***.

AF4-MALS-dRI is a technique highly sensitive to pressure changes, so it commonly gives an initial void peak caused by sample injection into the system. The higher the volume of injected samples leads to increased intensity of the void peak. Furthermore, crossflow is the key parameter that influences the elution time of particles when using AF4-MALS-dRI methods. A huge variety of elution gradients, types of channels and thickness of spacer employed to measure liposome-based formulations have been already published[3,5–7]. Therefore, we investigated various elution gradients using different crossflows to detect empty LP-RGD_int (without GLA-S presence) by AF4-MALS-dRI.

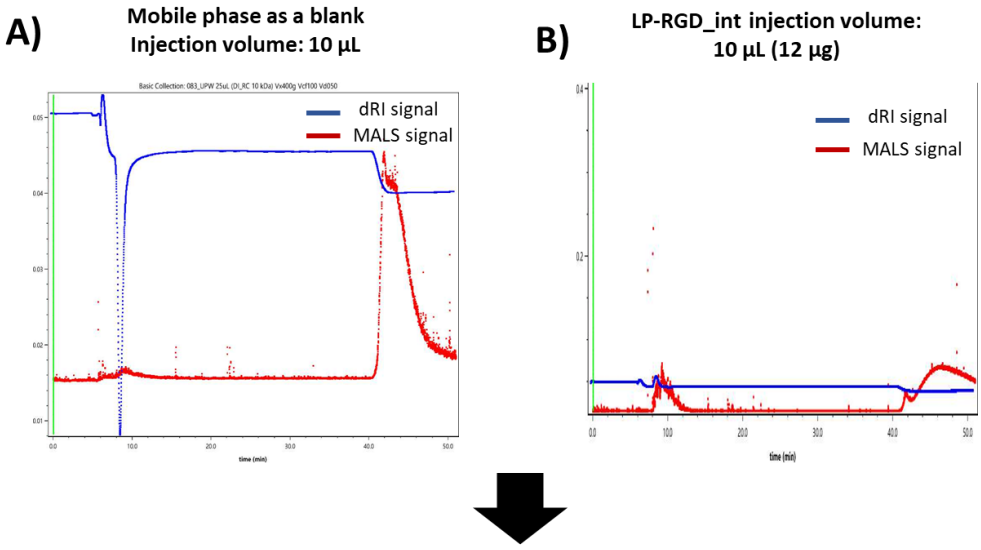
Impact of crossflow variation on fractogram peaks resolution

Initially, LP-RGD_int nanoliposomal formulation containing a theoretical lipid concentration of 1.2 mg/mL, as well mobile phase used as blank, was tested using similar conditions from previously published paper Moon *et al.*[5]. The main peak of LP-RGD_int nanocarriers was not visible within the runtime dispersion-inlet channel until the crossflow has been stopped (***Figure III.2***). In these cases, only two void peaks generated by pressure fluctuations occurring after sample injection and the sudden crossflow stopping, have been detected. During the last step of 10 min without crossflow, large particles and aggregates can also be removed from the dispersion-inlet channel.

However, large nanoparticles are easily eluted when employing lower crossflows[2,3]. Following other reported methodologies for liposomes[6,7], a linear decrease of the crossflow from 1 to 0 was employed to investigate the LP-RGD_int elution. Besides the broad peak that corresponds to LP-RGD_int when crossflows reached 0.5 mL/min, this condition also demonstrated a huge void peak when crossflow was 0 mL/min at the end of the fractogram, interfering with the peak of interest (***Figure III.3 A***).

After several trials with reduced crossflows (from 0.5 to 0.1 mL/min), a promising condition was found (and detailed in ***Figure III.3 B***) with sharper main peak of LP-RGD_int nanovesicles at 13.5 min, using a constant crossflow of 0.1 mL/min. In this new separation method, we added an additional step to minimize the intensity and interferences of the final void peak. This method still needed further optimization due to the interference of the initial void peak with the peak of liposomes. Therefore, we modified a previous method by adding a longer

initial step in order to delay the elution of the main peak (*Figure III.3 C*). In addition, to avoid abrupt changes in pressure, a linear gradient was prolonged which led us to the final method (*Figure III.4*). As we can see from all spectra, the small amount of lipid mass used in studies (6 – 12 µg) could not be detected by dRI detector. Therefore, molar mass of the liposomes cannot be calculated reliably. However, for such large complexes, the molar mass is not so much of interest and only R_g values will be provided. According to Hupfeld *et al.*[6] dRI was capable to detect concentrations of liposomes as long as the sample load was higher than 100 µg. To overcome the lack of sensitivity they suggested the dye method[8]. Higher concentrations should be also tested to determine the limit of detection (LOD) and limit of quantification (LOQ) of dRI detector.

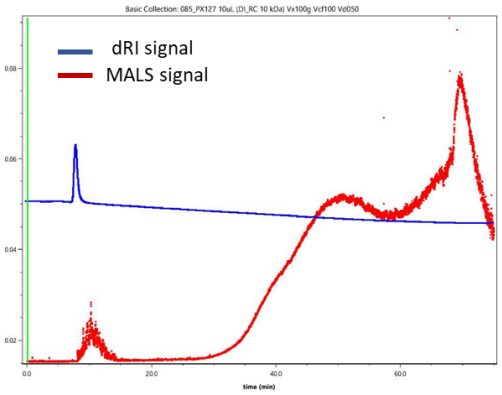


Injection flow (mL/min)	0.1
Channel flow (mL/min)	1

MODE	STEP DURATION (min)	XF START (mL/min)	XF stop (mL/min)
Elution	5	4	4
Elution + injection	35	1	1
Elution + injection	1	1	0
Elution + injection	10	0	0

Figure III.2. MALS and dRI fractograms obtained from the analysis of A) blank sample containing only mobile phase (10 mM PBS + 0.02% sodium azide; injection volume of 10 µL) and B) empty LP-RGD_int liposomes (injection volume of 10 µL, corresponding to an injection mass of 12 µg). Liposomal peak not eluted/detected with the expected elution conditions (constant crossflow at 1 mL/min) tested detailed on the corresponding table inside the figure.

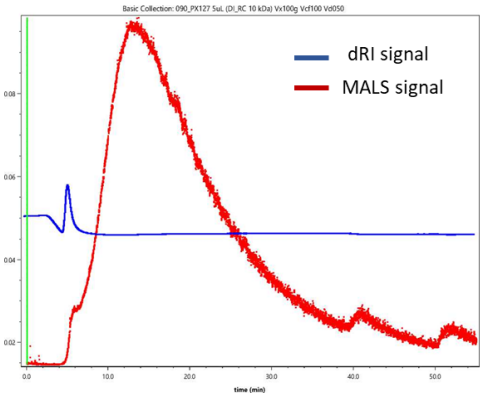
A) **LP-RGD_int injection volume: 10 µL (12 µg)**



FIRST AF4-MALS-dRI METHOD THAT ALLOWED LP-RGD_int ELUTION AND DETECTION

Injection flow (mL/min)	0.1		
Channel flow (mL/min)	1		
MODE	**STEP DURATION (min)**	**XF START (mL/min)**	**XF stop (mL/min)**
Elution	5	1	1
Elution + injection	65	1	0
Elution + injection	5	0	0

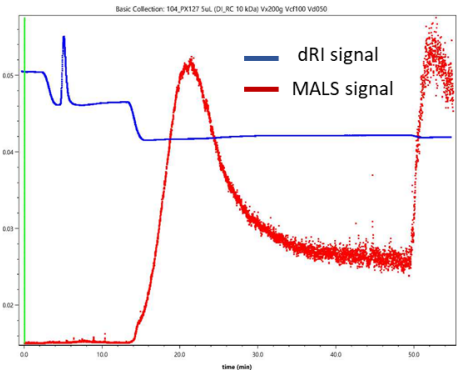
B) **LP-RGD_int injection volume: 5 µL (6 µg)**



IMPROVED AF4-MALS-dRI METHOD FOR THE INDIVIDUAL DETECTION OF LP-RGD_int

Injection flow (mL/min)	0.1		
Channel flow (mL/min)	1		
MODE	**STEP DURATION (min)**	**XF START (mL/min)**	**XF stop (mL/min)**
Elution	2	1	1
Elution + injection	2	1	0.1
Elution + injection	35	0.1	0.1
Elution + injection	1	0.1	0.05
Elution + injection	10	0.05	0.05
Elution + injection	5	0	0

C) **LP-RGD_int injection volume: 5 µL (6 µg)**

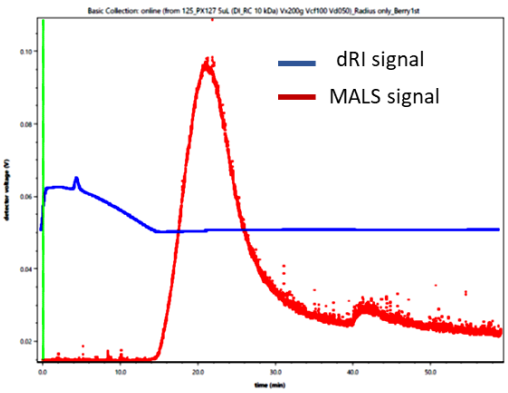


MODIFIED AF4-MALS-dRI METHOD TO DELAY THE ELUTION OF THE PEAK OF LP-RGD_int

Injection flow (mL/min)	0.2		
Channel flow (mL/min)	1		
MODE	**STEP DURATION (min)**	**XF START (mL/min)**	**XF stop (mL/min)**
Elution	2	2	2
Elution + injection	1	2	1
Elution + injection	10	1	1
Elution + injection	1	1	0.1
Elution + injection	35	0.1	0.1
Elution + injection	1	0.1	0
Elution + injection	5	0	0

Figure III.3. Evolution of AF4-MALS-dRI fractograms and elution conditions to improve the resolution and symmetry of LP-RGD_int peak using injection volumes of 5 – 10 µL (meaning a respective lipid injection mass of 6 – 12 µg). A) Elution conditions based on a linear crossflow decrease from 1 to 0 mL/min to estimate the better crossflow conditions to achieve well-resolved liposomal populations. B) Improved elution conditions for the elution of LP-RGD_int nanovesicles in a sharper peak using a constant crossflow of 0.1 mL/min. C) Modified elution conditions by adding a longer initial step in order to delay the elution of the main peak and avoid the interference of the initial void peak with the peak of LP-RGD_int liposomes. Detailed elution conditions of each method are detailed on the respective tables within the figure. The small amount of lipid mass used in all studies (6 – 12 µg) could not be detected by dRI detector.

LP-RGD_int injection volume: 5 µL (6 µg)



BEST OPTIMIZED AF4-MALS-dRI METHOD TO DATE, FOR THE INDIVIDUAL DETECTION OF LP-RGD_int

Injection flow (mL/min)	0.1
Channel flow (mL/min)	1

MODE	STEP DURATION (min)	XF START (mL/min)	XF stop (mL/min)
Elution	2	2	2
Elution + injection	2	2	2
Elution + injection	10	2	0.1
Elution + injection	35	0.1	0
Elution + injection	10	0	0

Figure III.4. Final optimized AF4-MALS-dRI method to obtain well-resolved populations of RGD-targeted liposomes. MALS and dRI fractograms obtained from LP-RGD_int nanovesicles (injection volume of 5 µL, and injection mass of 6 µg) using the optimized elution conditions compiled in the pointed table inside the figure.

Comparison of empty LP-RGD_int and biomolecule-conjugated LP-RGD-GLA-S_int liposomes

According to the manufacturer recommendations, FFF combined with MALS and quasi-elastic light scattering (QELS) are promising tools to characterize the drug encapsulation capacity of liposomes[1]. The key parameters that can provide this information are the R_g obtained from the MALS detector, and the hydrodynamic radius (R_h) from the QELS detector. When R_g is plotted against R_h, their slope yields the inner structure of liposomes. Slope values near to 1.0 mean spherical shell structure, meanwhile lower values (e.g. 0.75) represent solid spherical structures of uniform density. However, the AF4 equipment used for the characterization of LP-RGD_int has only coupled a MALS and dRI detector. Manufacturer instructions also indicate that distinct encapsulation degrees between liposomal formulations can be identified from MALS signals by obtaining non-overlaid R_g values between them. Moreover, filled liposomes normally present a more rigid spherical structuration resulting in the obtaining of sharper peaks in MALS-based fractograms, while empty liposomes have a more moldable structure which often bring about broad peaks in MALS fractograms[1].

With this in mind and using the previous conditions for empty LP-RGD_int nanovesicles, herein GLA-S-loaded liposomes (named as LP-RGD-GLA-S_int) were also examined by AF4-MALS-dRI. It can be observed that for better resolution of GLA-S loaded liposome signal we had to increase the injected mass in comparison with empty liposome (*Figure III.5 A*). Both spectra present a void peak that appeared after the crossflow reached 0 mL/min which could reflect the presence of elongated and big structures. CryoTEM micrographs (*Figure III.5 B*) also confirmed RGD-targeted liposomes destabilization and formation of such elongated, large and multivesicular nanoformulations after being incubated in PBS 100 mM for 30 min at room temperature (results described in *Chapter 5, Section 5.4.2.1* of this thesis). Interestingly, this peak was significantly higher in the case of GLA-S-

loaded liposomes. To avoid potential liposome destabilization during the runtime, different mobile phases should be tested. Moreover, GLA-S-loaded liposomes showed a slightly broader peak in comparison to empty ones which is contrary to expectations. This can be explained by the higher distribution of GLA-S molecules to the outer surface of the bilayer than the inner lumen which cause a slight deformation of the spherical-like shape of empty liposomes. More quantitative measurements from the same and different batches of empty and GLA-S-loaded nanoformulations should be tested to confirm this hypothesis.

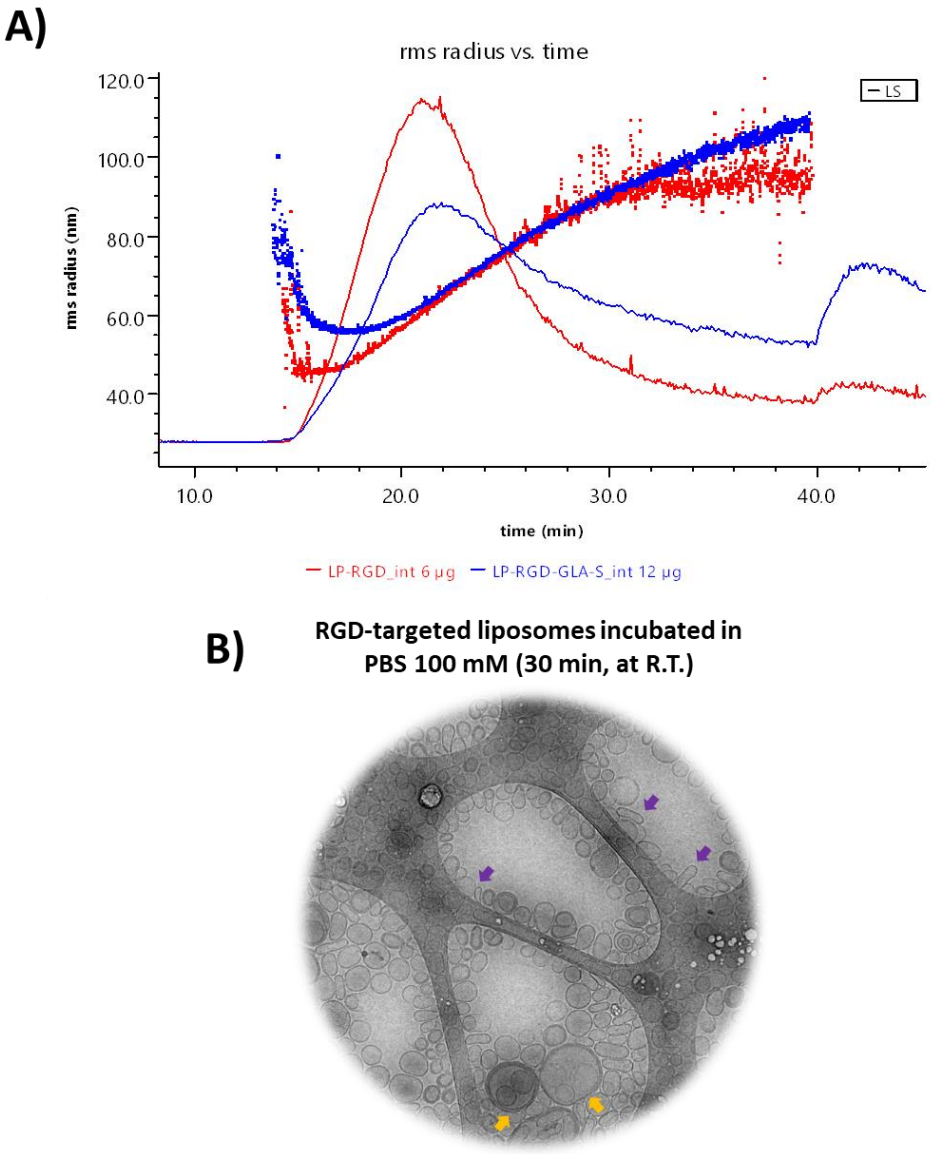


Figure III.5. A) Comparison of MALS peaks of empty LP-RGD_int liposomes (red colored; 6 µg injected), and GLA-loaded LP-RGD-GLA-S_int liposomes (blue colored; 12 µg injected), using the final method. B) CryoTEM imaging of RGD-targeted liposomes after their incubation for 30 min at room temperature in PBS 100 mM buffer. Legend: R.T. means room temperature.

In ***Table III.3***, the R_h and PdI of the nanovesicular formulations obtained by DLS analysis are compared with R_g obtained by AF4-MALS-dRI. The R_h of nanoliposomal formulations (from 147.1 to 151.9 nm) was larger than the R_g (from 74.6 to 85.5 nm). This discrepancy may result from the combined measurement of the hydration shell on the nanovesicle surfaces and the scattering light generated from media, since DLS technique is based on the batch measurement of static scattering from samples (which can contain nanoparticles of different sizes and morphologies), in contrast to AF4-MALS-dRI based on dynamic nanoparticle scattering measurement (where different nanoparticle populations have been separated by size and shape).

Table III.3. Comparison of nanoliposomal parameters obtained using different analyses: R_h and PdI values by DLS analysis, and R_g/nm values by AF4-MALS-dRI.

Nanovesicular sytem ID	R_h (nm)	PdI	R_g (nm)
LP-RGD_int	147.1 ± 2.8	0.20 ± 0.01	74.6
LP-RGD-GLA-S_int	151.9 ± 1.3	0.20 ± 0.01	85.5

Once we determined the key fractionation parameters, we then examined the loading capacity of AF4-MALS-dRI. Different amounts of LP-RGD-GLA-S input samples ranging from 6 to 96 µg were tested in order to investigate the minimal amounts of samples required for AF4 (***Figure III.6***). It was evidenced that there was an additional peak when the injection mass was ≥ 12 µg that eluted at around 10 min. This peak could result from GLA presence since GLA as a small molecule will elute earlier than liposomes. This should be confirmed by comparison of empty and GLA-loaded liposome spectra. Inputs of 6, 12 and 24 µg yielded almost identical fractionation profiles and rms radius determinations for liposomes, indicating comparable fractionation resolution and robust signal detections. However, if we confirm that additional peak results from the GLA enzyme, a liposome mass of 24 µg should be used in further studies. Contrary, when the amount of input increased to 96 µg signal intensity increased especially in the case of the unidentified peak. dRI signal was only present for this peak under these conditions. The rms radius of liposome was not able to be calculated in this case. However, a lower amount of liposomes should be tested in further studies to determine the LOQ of AF4-MALS-dRI.

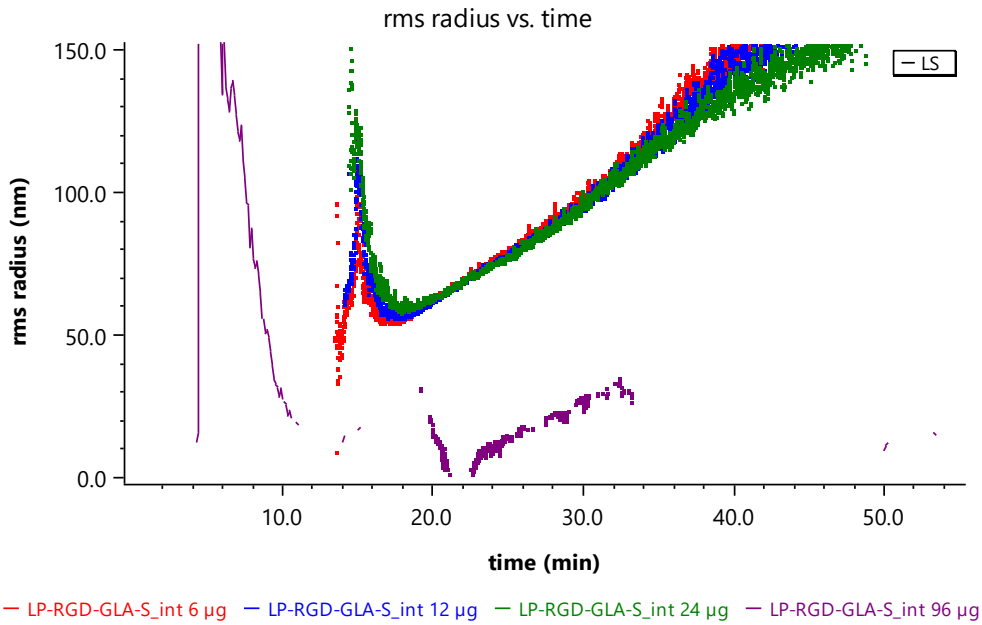
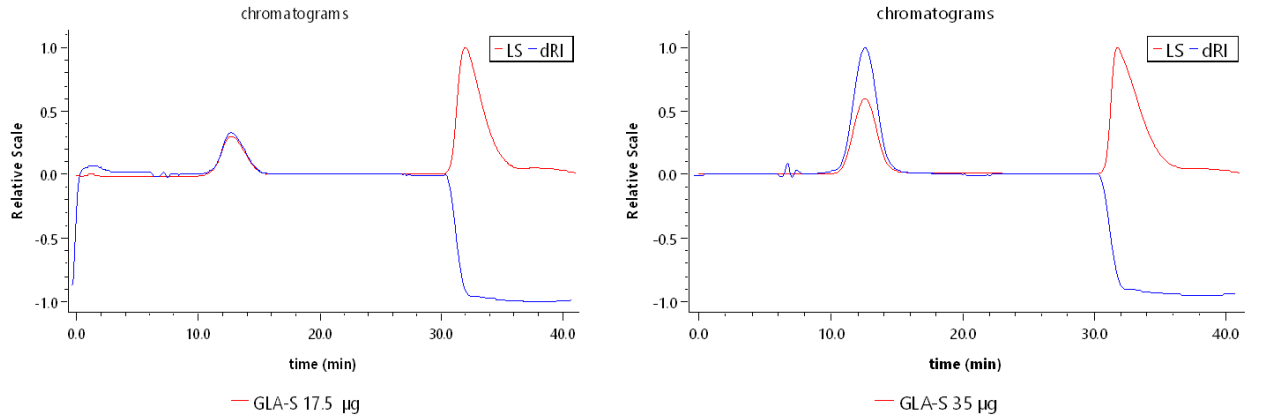


Figure III.6. Comparison of MALS fractograms from LP-RGD-GLA-S_int formulation analyzed in a range of injection masses from 5 to 80 µL (corresponding to theoretical lipid injection mass between 6 – 96 µg).

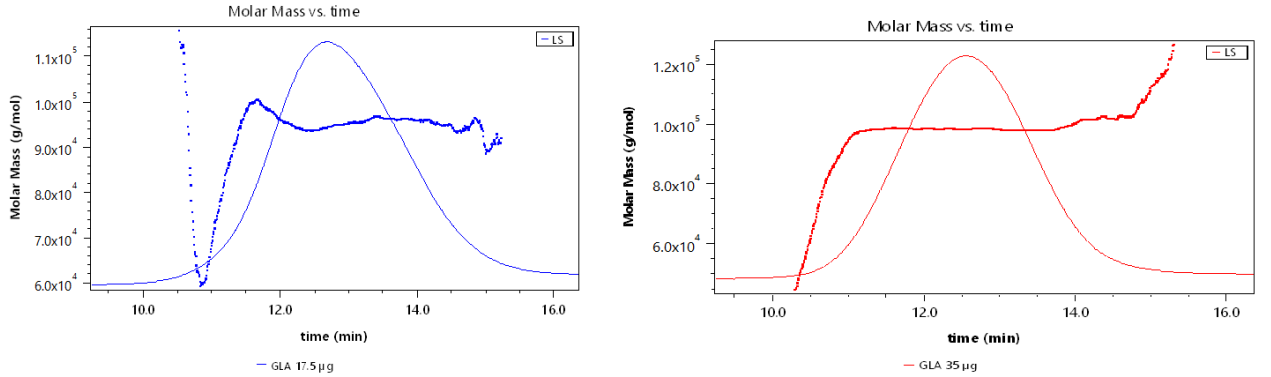
III.2.2. Development of the AF4-MALS-dRI protocol for the detection of GLA-S enzyme

Additionally, the AF4-MALS-dRI technique was used for the detection of the naked GLA-S enzyme version gathered in *Table III.2*. As previously described in *Chapter 3, Section 3.4.* of this thesis, GLA-S is primarily a homodimeric protein of about 10 nm characterized by DLS[9]. Normally, elevated crossflow is required to delay the elution time of small particles with higher diffusion, in order to be well-resolved from the initial void peak. The GLA-S molecules were eluted at 13 min, being well-resolved from the void peak that eluted at 6 – 8 min (*Figure III.7 A*). After diverse trials, the AF4 conditions summarized in *Figure III.7 B* allowed a proper signal-to-noise ratio of GLA-S for injection volumes of 5 and 10 µL (corresponding to a GLA-S injected mass of 17.5 and 35 µg, respectively). After the analysis by Astra software, the main peak of GLA-S corresponds to the expected homodimeric structure with a molar mass of approximately 100 kDa. However, if zooming the MALS signal and after the baseline correction, a second peak or shoulder at 17 min emerged (*Figure III.8*). This peak could represent a small second population of tetrameric or pentameric GLA-S (the mass fraction of this oligomer is below 1 %). This was clearer when analyzing 35 µg of the enzyme. The big peak obtained after 30 min might correspond to aggregates or contaminants capable of eluting after stopping the crossflow, or only to the artificial void peak generated by the crossflow shutdown.

A)



B)



C)

Injection flow (mL/min)	0.1		
Channel flow (mL/min)	1		
MODE	**STEP DURATION (min)**	**XF START (mL/min)**	**XF stop (mL/min)**
Elution	5	3	3
Elution + injection	25	3	3
Elution + injection	1	3	0
Elution + injection	10	0	0

Figure III.7. A) MALS and dRI fractograms obtained from GLA-S enzyme (injection volumes of 5 or 10 µL, and respective injection mass of 17.5 or 35 µg). B) Calculated molar mass and signal-to-noise ratio after data analysis of 17.5 µg (left and blue graph) or 35 µg (right and red graph). C) Detailed table of the elution conditions used for GLA-S analysis by AF4-MALS-dRI (GLA-S elution time of 13 min).

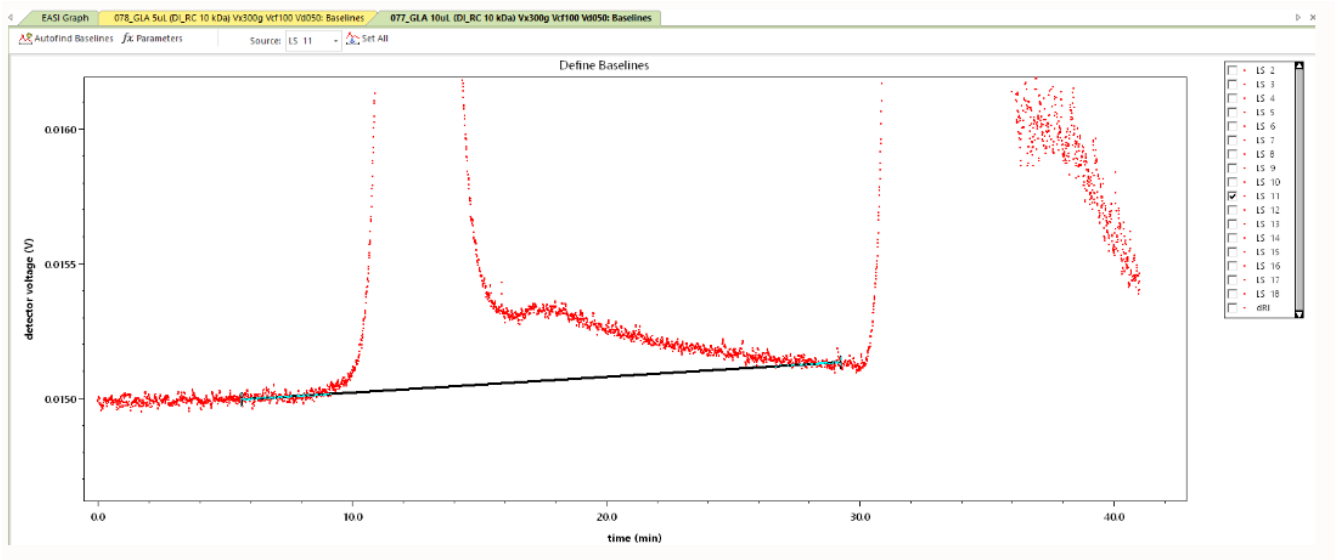


Figure III.8. Zoomed GLA-S peak (35 µg), showing a small population of tetramers/pentamers.

Interestingly, the GLA-loaded liposome intermediate prototype (LP-RGD-GLA-S_int) contains a maximal theoretical concentration of GLA-S around 25 µg/mL in a nanovesicular formulation with a theoretical lipid concentration of 1.2 mg/mL (approximated GLA:lipid ratio (m/m) of 1:48). GLA-S was diluted to 25 µg/mL in mobile phase, and analyzed by AF4-MALS-dRI using the previously developed method (***Figure III.7 C***). Injection volume was 5 µL which corresponds to the injection mass of 0.0125 µg. This result points out the necessity of two different injection volumes usage for accurately analyzing both analytes with good signal-to-noise ratio, due to the high difference between lipid and protein concentration in LP-RGD-GLA-S formulations. For this reason, both methods developed during this study will hopefully provide the possibility of individual monitoring of both analytes (GLA-S and RGD-targeted liposomes) present in LP-RGD-GLA-S formulations.

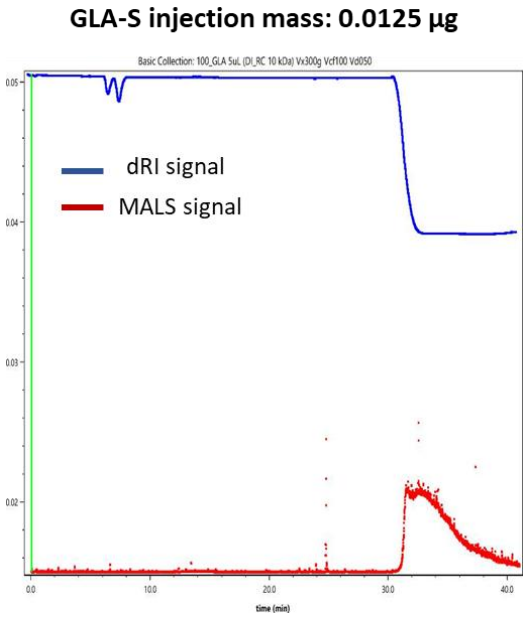


Figure III.9. Fractograms demonstrating the non-detection of GLA-S signal from MALS or dRI detectors when analyzing 0.0125 µg of enzyme.

So far, a methodology based on AF4-MALS-dRI has been developed for the detection of GLA-S enzyme. This method may be useful for characterizing diverse batch productions of GLA enzymes and monitoring their quality. Nevertheless, further method development has to be directed to find the LOD and LOQ of both, GLA-S and RGD-targeted nanovesicles, in order to design the possibility of performing binding experiments between GLA-S molecules and liposome bilayers, or to evaluate the possibility of detecting the GLA-S from more concentrated liposomal prototypes.

III.3. Summary

Collaborative work carried out in the group of Dr. Ivana Vinković Vrček from the Institute for Medical Research and Occupational Health (IMI) located in Zagreb (Croatia), yielded two analytical methods based on the FFF-MALS technique for the detection of GLA-S enzyme and RGD-targeted liposomes. The developed methodology will provide the possibility of investigating size and morphology between liposomal nanoformulations differing in composition, as well as investigate the supramolecular organization of different GLA enzyme versions (presence of monomer, dimer, tetramer or other structural conformations) and their probable aggregation under storage or other specific conditions.

III.4. References

1 Wyatt Technology Corporation. Liposome Characterizatio by FFF–MALS–QELS. Appl. Notebook-09-01-2011, Vol. 0, issue 0. 2012. https://www.chromatographyonline.com/view/liposome-characterizatio-fff-mals-qels (accessed Oct 2, 2023).

2 Bian J, Gobalasingham N, Purchel A, Lin J. The Power of Field-Flow Fractionation in Characterization of Nanoparticles in Drug Delivery. *Molecules* 2023; **28**: 4169.

3 Parot J, Caputo F, Mehn D, Hackley VA, Calzolai L. Physical characterization of liposomal drug formulations using multi-detector asymmetrical-flow field flow fractionation. *J Control Release* 2020; **320**: 495–510.

4 Nobbmann U. Refractive index increment dn/dc values - Materials Talks. Malvern Panalytical. 2013. https://www.materials-talks.com/refractive-index-increment-dndc-values/ (accessed Sept 21, 2023).

5 Hee Moon M, Park I, Kim Y. Size characterization of liposomes by flow field-flow fractionation and photon correlation spectroscopy Effect of ionic strength and pH of carrier solutions. *J Chromatogr A* 1998; **813**: 91–100.

6 Hupfeld S, Moen HH, Ausbacher D, Haas H, Brandl M. Liposome fractionation and size analysis by asymmetrical flow field-flow fractionation/multi-angle light scattering: influence of ionic strength and osmotic pressure of the carrier liquid. *Chem Phys Lipids* 2010; **163**: 141–7.

7 Yohannes G, Jussila M, Hartonen K, Riekkola ML. Asymmetrical flow field-flow fractionation technique for separation and characterization of biopolymers and bioparticles. *J Chromatogr A* 2011; **1218**: 4104–16.

8 Hupfeld S, Ausbacher D, Brandl M. Asymmetric flow field-flow fractionation of liposomes: 2. Concentration detection and adsorptive loss phenomena. *J Sep Sci* 2009; **32**: 3555–61.

9 Garman SC, Garboczi DN. The molecular defect leading to fabry disease: Structure of human α-galactosidase. *J Mol Biol* 2004; **337**: 319–35.